CATALYSIS

VOLUME II

FUNDAMENTAL PRINCIPLES (PART 2)

Edited by

PAUL H. EMMETT

Gulf Research and Development Company's Multiple Fellowship
Mellon Institute, Pittsburgh, Pennsylvania

Contributing Authors

Henry Eyring
Hugh M. Hulburt
W. B. Innes
Edward L. King
Ransom B. Parlin
Merrill B. Wallenstein
Ahlborn Wheeler
Bruno J. Zwolinski

BOOK DIVISION
REINHOLD PUBLISHING CORPORATION

Publishers of Chemical Engineering Catalog, Chemical Materials Catalog, "Automatic Control," "Materials & Methods"; Advertising Management of American Chemical Society

430 Park Avenue, New York

First Printing, January 1955
Second Printing, December 1961

Library of Congress Catalog Card Number 54-6801

Printed in the United States of America
THE GUINN CO., INC.
New York 14, N. Y.

PREFACE

As pointed out in the preface to Volume I of this series, the key position that catalysis occupies in modern industry and the progress being made toward making catalysis more of a science and less of an art both tend to make this an appropriate time for summarizing, in an orderly fashion, all that is known in regard to the theory and practice of catalysis. The present series represents such an attempt.

The fundamental principles and theories of both heterogeneous and homogeneous catalysis are included in the first two volumes of the series. In Volume I, an effort was made to include a consideration of some aspects of the art of catalysis as well as a presentation of the fundamental principles. To this end, a considerable amount of new material was included relative to catalyst supports and methods of catalyst preparation. The favorable reception of Volume I has encouraged us to follow a similar procedure in Volume II. Accordingly, discussions of modern concepts as to the nature of and mode of action of porous solid catalysts is flanked by a large number of tables comprising a systematic but arbitrary arrangement of catalysts according to the type of reaction being catalyzed.

This second volume of the series, in completing the presentation of fundamental catalytic principles, stresses the measurement of pore distribution; the influence of pore distribution on the kinetics, temperature coefficient, and specificity of reactions on solid catalysts; the nature of the catalyst surface and of the adsorbed material on the catalyst surface; and, finally, the general theories of heterogeneous catalysis. It also contains an extensive and detailed presentation of the general nature of homogeneous catalysis and of the factors that influence the behavior of homogeneous catalytic systems.

In successive volumes, various subdivisions into which it has become customary to divide catalytic work will be treated, including: hydrogenation and dehydrogenation; synthesis of hydrocarbons, ammonia, methanol, and higher alcohols; alkylation, isomerization, polymerization, cracking, hydroforming, hydrocracking, and hydrodesulfurization; and finally, oxidation, hydration, dehydration, halogenation, and miscellaneous reactions. The discussion of each of these topics will comprise a presentation of published factual matter as well as ideas and theories as to the mechanism of the reactions involved. Attention is focused on the catalysts and catalytic reactions and not on the engineering or economic characteristics of the processes. It should be noted, too, that the present series does not include a discussion of enzymes, the biochemical catalysts that are essential to life itself.

The editor, at this point, wishes to express his indebtedness to the editors of the various technical journals and books for permission to reproduce figures and tables from their various publications. He is especially appreciative of permission given by the Academic Press, Inc. to one of the authors to quote extensively from one of his previous articles published in Volume III of "Advances in Catalysis."

As pointed out in the preface of Volume I, the success of a series of this type must depend largely on the efforts of the individual contributing authors. The editor is grateful for the fine cooperation that has been obtained from the authors for these first two volumes. It is hoped that their authoritative summary of the present status of our knowledge of catalysis will be a useful review for those now working in the field, and a thought-provoking challenge to those who are only now becoming interested in the subject.

PAUL H. EMMETT

Pittsburgh, Pa.
December 1, 1954

CONTENTS

CHAPTER 1

CLASSIFICATION OF HETEROGENEOUS CATALYTIC VAPOR PHASE REACTIONS

W. B. Innes

Stamford Research Laboratories, American Cyanamid Company, Stamford, Conn.

This chapter might be considered as an addition (1942–1952) to the excellent beginning made by Berkman, Morrell and Egloff[1] in catalytic reaction classification. Systematic arrangement enables an orderly concise presentation of the large amount of literature on vapor phase heterogeneous catalysis and makes generalization much easier.

In considering how best to classify catalytic reactions, it was concluded that this should be governed by the type of bond change, the reaction mechanism, the type of catalyst active for the reaction and the nature of the product. The number of distinct reaction classes has decreased somewhat in recent years as it has become apparent that many reactions previously thought to be different in nature have a similar mechanism and, hence, should be grouped in one class. For example, cracking, alkylation, isomerization, hydrogen transfer and polymerization are now generally thought to usually proceed via a carbonium ion mechanism and, hence, they can be classified in one group. Hydrogenation-dehydrogenation reactions comprise another large group which now appears to have more in common than was previously realized. The primary classes are listed below.

(1) Acid catalyzed reactions
(2) Hydrogenation-dehydrogenation
(3) Oxidation
(4) Hydration-dehydration
(5) Halogenation-dehalogenation
(6) Combined dehydrogenation-dehydration
(7) Isotope exchange
(8) Miscellaneous

Progress in catalysis during the past ten years appears to have strengthened the hypothesis of unstable surface compound intermediates as a general explanation of heterogeneous catalytic action, and has also shed light on their nature. This can be said to be true of almost any reaction class that can be mentioned. In hydrogenation reactions unstable surface hydrides appear to function in this manner, while in the case of oxidation catalysts the catalysis has been related to the ability of the surface to give and take oxygen by virtue of different oxidation states. In the case of acid catalyzed reactions, the ability of the surface to accept and donate protons appears prerequisite. Dehydration-hydration catalysts form surface compounds with water.

Thermodynamic factors are very important in many catalytic reactions and, hence, this information has been presented where available. Heats of reaction are for gas phase reactions at 25°C and are taken primarily from the tabulations of Rossini *et al*[2].

ACID CATALYZED REACTIONS

Cracking

The term cracking has attained rather broad usage so that it encompasses the fission or splitting of any hydrocarbon in such a way that a carbon-carbon bond is ruptured. In the most common reaction, the cracking of paraffins, the main reaction is one of dealkylation according to the general equation:

$$R_1CH_2—CH_2—R_2 \rightleftharpoons R_1CH{=}CH_2 + R_2H$$

leading to the formation of an olefin and a lower paraffin. Cracking generally leads to a variety of products since primary products may in turn undergo further splitting and various carbon-carbon bonds may be involved. Catalysts active for splitting carbon-carbon bonds also appear to have activity for splitting carbon-hydrogen bonds[3].

Although dealkylation is endothermic (*ca.* 20 Kcal/mol), equilibrium is generally favorable at near atmospheric pressure and temperatures in excess of about 300°C because of entropy considerations resulting from the gain in molecular number. Because of subsequent reactions such as polymerization and hydrogenation, the net heat effect in the cracking of gas oil is small[4]. At low conversion it is endothermic while at high conversions it is exothermic.

Although cracking can occur by a free radical mechanism at elevated temperatures and be accelerated by nonacidic surfaces such as charcoal, best activity per unit surface with less light gas and coke production is attained with acidic type catalysts which are capable of proton transfer[5]. In fact, Tamele[6], Thomas[7] and Hansford[8] have been able to correlate activity with acidity. There appears to be general agreement that a carbonium-ion type mechanism is involved and that the latter is formed by simple addition of a proton from the surface in the cracking of olefins and aromatics. Several different views have been advanced as to how carbonium ions are formed from paraffins and naphthenes. Thomas[7] postulates thermal cracking to an olefin plus methane or other lower hydrocarbon. The olefin can then pick up a proton from an acidic surface to become a carbonium ion. Greensfelder, Voge and Good[5] postulate the removal of hydride ions to give carbonium ions. The rules governing the rearrangements of carbonium ions leading to cracking and conversion of normal to isoparaffins are discussed at length by the above authors. Beta cleavage relative to the carbonium ion is the primary step leading to cracking. Thomas[7] gives the following example:

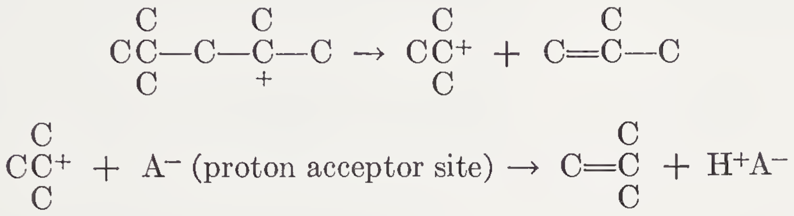

$$C\underset{C}{\overset{C}{C}}—C—\underset{+}{\overset{C}{C}}—C \rightarrow C\underset{C}{\overset{C}{C}}{}^{+} + C{=}\overset{C}{C}—C$$

$$C\underset{C}{\overset{C}{C}}{}^{+} + A^{-} \text{ (proton acceptor site)} \rightarrow C{=}\underset{C}{\overset{C}{C}} + H^{+}A^{-}$$

High Boiling Petroleum Fractions

The cracking of gas oil or even higher boiling petroleum fractions has assumed such extreme economic importance in the past decade that it equals thermal cracking in production capacity and far overshadows any other catalytic process. The cracking capacity in the United States now totals about two million bbls/day[9] and the cracking catalyst consumption is about 500 tons per day. Expansion under way is expected to further increase the total by 20 per cent in the next three years. The importance of cracking is further attested to by the large amount of recent literature on the subject which is discussed below under the headings of catalyst types. Included in the literature are a number of excellent general review articles[10-17] on catalytic cracking.

The Caterole process developed in England[18, 19, 20] for oil processing combines cracking with aromatization by operating at 1200°F with supported iron and copper catalysts.

Synthetic Silica-Alumina Catalysts. These catalysts can be regarded as the reaction product of silica gel and alumina (10 to 30 per cent). They were generally adopted for the first cracking units and have maintained their leading position despite the introduction of other catalysts. They are manufactured in powder form (ground or spray dried) for fluid cracking units[21] or in bead[22] or pellet form for the Houdry, Theromofor or Houdriflow units. A qualitative comparison of commercial fluid silica-alumina catalysts with other types is given in Table 1.*

The physical and chemical nature of synthetic silica-alumina catalyst has been extensively studied[23, 24, 25]. There is much evidence that the

---

* See section on carriers in Volume I for a quantitative comparison of physical properties.

Table 1. Comparison of Various Commercial Type Catalysts for Gas Oil Cracking[4]

	Synthetic Gel Catalysts		Natural Catalysts	
	silica-alumina[5]	silica-magnesia	montmorillonite	halloysite
Initial activity	excellent	excellent	good	poor
Steam stability	fair +	excellent	good	fair +
Thermal stability	good	fair	fair	good
Attrition resistance[3]	good[1]	good[1]	fair−	fair+
Ease of regeneration[6]	good	poor	good	fair
Gasoline yield	fair	excellent	good	good
Isobutane yield	excellent	poor	fair	good
Sulfur resistance	excellent	excellent	poor[2]	good

[1] Depends largely on particle size distribution and shape. Microspheroidal grades are excellent.

[2] Due to iron content which is activated by sulfur compounds, resulting in high gas and coke production. Can be minimized by use of steam.

[3] Fluid catalyst. Improves with usage.

[4] According to findings of the American Cyanamid Co. Stamford Research Laboratories, field reports and published literature.

[5] 12 per cent Al_2O_3 (stability increases with alumina content).

[6] Determined by C yield as well as by ease of burning off the carbon.

active component is a surface compound or complex resulting from the reaction of surface silicic acid and alumina. This complex, unlike either alumina or silica gel, has the properties of a strong surface acid, but there are different views as to its exact nature. Physically, the structure of fresh silica-alumina catalyst is probably similar to its silica gel precursor which apparently can be considered as an aggregation product of corpuscular silica particles with a diameter of about 50 Å joined at points of contact by chemical bonds (Si—O—Si). The degree of this bonding between colloidal particles in the hydrogel form, which apparently is favored by increased time, temperature and pH of silica gel aging, appears to determine the shrinkage on drying and the resultant porosity of the xerogel[25]. Increased porosity appears to lead to increased catalyst stability and decreased attrition resistance, other things being equal.

The extensive literature given in Table 2 covers many facets of silica-alumina catalyst preparation and usage including:

(1) The use of different raw materials.
(2) The addition of various promoters.
(3) Methods of obtaining desirable physical shapes and sizes.
(4) Manufacturing variables.
(5) Effect of cracking variables.
(6) Alumina/silica ratio.

TABLE 2. CRACKING OF HIGH BOILING PETROLEUM FRACTIONS

Silica-Alumina Catalysts (Synthetic)

Author	Chem. Abstracts	Ref.	Product or Subject
Ahlberg, J. E., and Thomas, C. L.	**41**, 7727	U.S. 2,428,257	diatomaceous earth
	39, 4450	U.S. 2,369,001	pelleting, extrusion
	39, 5456	U.S. 2,382,951	aluminum chloride
American Cyanamid Co.	**44**, 2146	Brit. 626,455	manufacturing process
		Brit. 680,747	manufacturing process
Ardern, D. B., Newton, R. H., and Barcus, G. L.	**39**, 3417	*IEC*, **37**, 546 (1945)	chemistry of cracking
Archibald, R. C., May, N. C., and Greensfelder, B. S.	**46**, 10593	*IEC*, **44**, 1811 (1952)	effect of temperature, space velocity
Ashley, K. D., and Jaeger, A. O.	**45**, 2608	Brit. 644,322	spray drying
	43, 9299	U.S. 2,478,519	aging of gel
Ashley, K. D., and Innes, W. B.	**41**, 853	U.S. 2,411,820	hydrogel filtration
	43, 2414	*JPCC*, **52**, 1364 (1948)	sodium contamination
Baker, M. O., Chesnutt, S. D., and Wier, T. P.		*IEC*, **44**, 2857	control of structure
Ballod, A. P., Patsevich, I. V., Feldman, A. S., and Frost, A.V.	**45**, 7861		effect of alkalies
Bates, J. R.		U.S. 2,463,508	manganese oxide promoter
	42, 2093	U.S. 2,429,981	manufacturing process and sodium removal
	40, 451	U.S. 2,375,757	
Bilisoly, J.	**43**, 3188	U.S. 2,459,987	high alumina mixed with silica-magnesia
Bitepazh, Y. A.	**42**, 21		activity vs. exchange kinetics
Blanding, F.		*IEC*, **45**, 1186	
Bodkin, E. A.	**43**, 9299	U.S. 2,480,628	sodium removal
Bond, G. R., Jr.	**41**, 4304	U.S. 2,417,054	berylia promoter
Brown, C. O., and Wainwright, R. B.		*CE*, **59**, #11, 148 (1952)	how they work best
Chapman, C., and Hendrix, H.	**43**, 5887	U.S. 2,470,142	drying prior to addition of alumina
Church, J. F.	**44**, 5040	U.S. 2,500,801	ex porous glass
Clark, I. T., and Harris, E. E.	**44**, 5040	*JACS*, **74**, 1031 (1952)	cracking of rosin
Connolly, G. C.	**43**, 7608	U.S. 2,474,888	aluminum trihydrate
	39, 3422	U.S. 2,363,231	bismuth promoter
	37, 2559	U.S. 2,301,257	coprecipitated catalyst
	43, 843	U.S. 2,448,960	drying before washing
Davison Chem. Corp.		Brit. 661,157	sulfate removal
Corner, E. S., and Kearby, K. K.	**45**, 1761	U.S. 2,529,283	magnesia promoter
Duffy, B. J., Jr., and Hart, H.		*CEP*, **48**, 344 (1952)	metals poisoning
Forrester, R. A.	**46**, 1248	U.S. 2,488,718	reactivation with HCl, Cl
Gibbs, F. C., Jr., Baird, B. M., and Brosamer, R. J.	**43**, 1932	U.S. 2,456,268	from partially dried silica gel

Table 2—*Continued*

Author	Chem. Abstracts	Ref.	Product or subject
Glassbrook, C. I., and Hansford, R. C.	**44**, 2676	U.S. 2,484,284	electric and magnetic fields during gelation
	42, 351	U.S. 2,428,798	
Greensfelder, B. S., Voge, H. H., and Good, G. M.	**44**, 2211	*IEC*, **41**, 2573 (1949)	thermal *vs.* catalytic
Hagerbaumer, W. A., and Lee, R.	**41**, 7713		coke combustion
Hemminger, C. E.	**44**, 247	U.S. 2,481,841	recycling fines
Hoekstra, J.	**45**, 2191	U.S. 2,532,497	oil drop method
Hogge, A. C., Jr.	**42**, 4740	Brit. 596,616	yields
Houdry, E.		U.S. 2,580,429	porcelain rod carrier
Hunter, J. B.	**43**, 8664	U.S. 2,477,373	use of bicarbonate
Hunter, E. A.	**43**, 6338	U.S. 2,472,830	from silica-magnesia
		U.S. 2,582,254	reactivation
Keating, G. H.	**41**, 576	U.S. 2,410,558	extrusion
Kimberlin, C. N., Jr.	**45**, 8168	U.S. 2,552,323	prevention of aggregation by freezing
	46, 666	U.S. 2,570,063	partial agglomeration
Lee, E. C., and Thomas, C. L.	**40**, 7600	U.S. 2,406,613–4	zirconia promoter
Makarov, S. K., and Kaliko, M.	**41**, 6697		water vapor poisoning
Marisic, M., and Schmitt, A.	**41**, 6682	U.S. 2,419,272	bead catalyst
Marisic, M.	**38**, 5577	U.S. 2,456,072	lime promoter
	40, 709	U.S. 2,387,596	methods of preparation
McKean, R. A., and Grandey, L. F.		*CEP*, **46**, 245 (1950)	T. C. C. variables
Meadow, J. R.	**42**, 7974	U.S. 2,430,724	reactivation
Milliken, T. H.	**44**, 2147	U.S. 2,487,065	powder addition
	45, 2120	U.S. 2,533,278	bead catalyst
Mills, G. A.	**44**, 3244	*IEC*, **42**, 182 (1950)	heavy metals
		PR, **32**, #2, 125 (1953)	
Mills, G. A., and Hindin, S. G.	**45**, 5394	*JACS*, **72**, 5549 (1950)	oxygen exchange
Mills, G. A., and Shabaker, H. A.	**46**, 243	*PR*, **30**, 9, 97 (1951)	steam stability
Oblad, A. G., Milliken, T. H., Jr., and Mills, G. A.	**45**, 8337		chemistry and structure
Oborin, V. I.	**42**, 5750		catalyst comparison
Olsen, C. R., and Sterba, M. J.	**44**, 826	*CEP*, **45**, 692 (1949)	effect of temperature
Pardee, W. A., and Elliott G.	**44**, 2146	U.S. 2,493,896	ex organic Silica compounds
Pardee, W. A.	**46**, 3257	U.S. 2,579,123	reactivation by silica addition

TABLE 2—*Continued*

Author	Chem. Abstracts	Ref.	Product or Subject
Paushkin, Ya., and Lipatov, Yu.	**45**, 6371		BF_3 promoter
Payne, J. W., Simpson, T. P., and Butzner, J. I.	**43**, 1930	U.S. 2,453,585	sodium removal
Payne, J. W.	**44**, 384	U.S. 2,483,372	sink-float separation
Pelzer, H.	**46**, 247	U.S. 2,507,220	HF
Pierce, J. A., and Kimberlin, C. N., Jr.	**43**, 1506	U.S. 2,454,942	spheroid agglomeration
	42, 9101	U.S. 2,448,460	microspheres from emulsions
Peet, N.	**45**, 10567	U.S. 2,472,723	heavy metal removal
Plank, C. J.	**46**, 10821	*AC*, **24**, 1304 (1952)	simple pH test for activity
	41, 7730	U.S. 2,428,741	HF, H_3PO_4, BF_3
Plank, C. J., and Drake, L. C.	**42**, 436	*JCS*, **2**, 399 (1947)	pore structure
Read, D., Jr.	**42**, 7022	U.S. 2,435,158	spray drying
Rescorla, A. R., Ottenweller, J. H., and Freeman, R. S.		*AC*, **20**, 196 (1948)	catalyst testing
Ries, H. E., Jr., Johnson, M. F. L., and Melik, J. S.	**43**, 6897	*JPCC*, **53**, 638 (1949)	adsorption isotherms
Ruthruff, R. F.	**42**, 2092	U.S. 2,430,249	C. *vs.* yields
	42, 2092	U.S. 2,430,784	partially ox. feedstock
Ryland, L.	**46**, 246	U.S. 2,565,886	high alumina
Ryland, L., and Tamele, M. W.	**43**, 5181	Brit. 616,307	high alumina
	43, 5583	U.S. 2,469,314	high alumina
See, M. J., and Bailie, J. C.	**43**, 1930	U.S. 2,455,445	hydrogel deglomeration
Schexnailder, R. E., Jr.		U.S. 2,582,722	bead catalyst
	43, 7162	U.S. 2,472,834	use of lime
Shabaker, H. A., and Milliken, T. H.	**44**, 1690	U.S. 2,489,333	clay carrier
Stright, P. and Danforth, J. D.		*JPC*, **57**, 488 (1953)	effect of LiOH
Shell Development Co.	**41**, 6702	Brit. 586,945	microspheres via kerosene
Schlesman, C. H.	**43**, 1884	U.S. 2,457,091	supersonic effect on setting of hydrogel
Snyder, J. A.	**45**, 10564	U.S. 2,481,253	heavy metal removal with CCl_4, HCl, Cl_2
	46, 1248	U.S. 2,488,744	
Standard Oil Development Co.	**44**, 2746	Brit. 628,420	from silica-magnesia
	42, 7520	Brit. 601,679	use of steam
	41, 7733	Brit. 589,868	
	44, 774	Brit. 623,578	oil emulsion
	41, 3268	Brit. 581,632	from aluminum hydrate

Table 2—*Continued*

Author	Chem. Abstracts	Ref.	Product or Subject
Thomas, C. L., and Lee, E. C.	**42**, 4724	U.S. 2,439,994	zirconia promoter
	39, 609	U.S. 2,347,648	zirconia promoter
Thomas, C. L., and Ahlberg, J. E.	**40**, 2612	U.S. 2,395,153	from $AlCl_3$
	36, 1349	U.S. 2,329,307	
	38, 857	U.S. 2,326,706	by hydrolysis
Thomas, C. L.	**43**, 3604	U.S. 2,462,236	from $AlCl_3$, wash after drying
Titova, A. N.	**42**, 729		nature and mechanism
Topchieva, K. V., Battalova, Sh., and Panchenkov, G. M.	**45**, 7860		alumina-silica
Voorhies, V.		U.S. 2,459,903	deglomeration of gel particles
Veltman, P. L.	**40**, 4510	U.S. 2,400,446	$AlCl_3$, AlF_3 promoters
Warner, B. R.		U.S. 2,579,133	reactivation by boria impregnation
Webb, G. M., and Ehrhardt, C. H.	**42**, 9138	*PP*, **2**, 5 (1947)	catalyst properties
Webb, G. M., and Moehl, R. W.	**46**, 2282	U.S. 2,484,258	NH_3 treatment of dried catalyst
Zabor, R. C , and Emmett, P. H.	**46**, 2786	*JACS*, **73**, 5639 (1951)	*n*-paraffin adsorption

AC = Analytical Chemistry
CE = Chemical Engineering
CEP = Chemical Engineering Progress
IEC = Industrial and Engineering Chemistry
JACS = Journal of the American Chemical Society
JCS = Journal of Colloid Science
JPC = Journal of Physical Chemistry
JPCC = Journal of Physical & Colloid Chemistry
PP = Petroleum Processing
PR = Petroleum Refiner

Synthetic Silica-Magnesia Catalysts. Silica-magnesia catalysts can probably be regarded as the surface reaction products of silica gel and magnesia (20 to 40 per cent). They have never found extensive commercial usage despite considerable research and important advantages (Table 3). This can be attributed primarily to poor regeneration properties. Unlike silica-alumina catalysts, silica-magnesia catalysts do not develop an appreciably increased pore diameter during usage. The resultant fine pore structure may account for the poor regeneration properties.

The silica-magnesia complex despite the alkaline nature of magnesia does have acidic properties[6] although it appears to be a weaker acid than silica-alumina. In aqueous solution a slightly alkaline pH is obtained due probably to the presence of small amounts of "free" MgO. Titration with acid in water indicates that the complex does not begin to decompose until a pH below about 6.5 is realized. The acid properties can be more readily demonstrated in nonaqueous mediums and by its ability to chemisorb organic bases at elevated temperatures[6, 26].

Literature on silica-magnesia catalysts is summarized in Table 3. It appears from this that a crucial step in preparing this catalyst is the reaction between silica gel and magnesia. Considerable time, elevated temperatures, and control of pH so that insoluble magnesium hydroxide does not form all appear to be of importance.

Natural Cracking Catalysts. Along with synthetic silica-alumina cracking catalysts, natural cracking catalysts of similar composition find wide commerical usage. These are mainly derived from montmorillonite and halloysite clays which are acid treated to activate them (exchange other surface cations for hydrogen ions). Physical properties of the commercial products manufactured by the Filtrol Corporation are given in the section on carriers in Volume I. Good and bad features of clay catalysts are listed in Table 1. Literature is given in Table 4.

Other Catalysts. A variety of other materials show activity for cracking. These include silica-zirconia, silica-titania, fluorides or fluoborates on silica-alumina or alumina carriers, etc. The fluoride catalysts have definite advantages such as high initial activity but tend to be slowly volatilized[27]. Recent literature is given in Tables 5 and 6.

The Cracking of Pure Hydrocarbons. The literature on the subject (Table 7) is largely limited to the extensive studies of Greensfelder and Voge[28-32], as well as the earlier work of Egloff, Morrell, Thomas and Bloch[33, 34]. The cracking of numerous paraffins, olefins, naphthenes and aromatics over silica-alumina and silica-zirconia-alumina catalysts was studied. Generalizations from their work are as follows.

(1) Carbon-carbon bond ruptures are selective so that cracked products seldom have fewer than three carbon atoms.

(2) Comparison of catalytic cracking of paraffins with thermal cracking indicates the former to be 5 to 60 times as rapid, the ratio increasing with molecular weight.

(3) Lower saturated hydrocarbons are not appreciably isomerized or cracked under usual cracking conditions.

(4) Olefins are much more easily cracked than paraffins and also readily undergo isomerization and coke formation under cracking conditions. Diolefins and aromatic olefins are even more readily cracked, saturated, polymerized and converted to coke.

(5) Naphthenes are quite susceptible to catalytic cracking, the rate increasing with molecular weight and being about 1000 times that of

TABLE 3. CRACKING OF HIGH BOILING PETROLEUM FRACTIONS
Silica-Magnesia Catalysts

Author	Chem. Abstracts	Ref.	Product or Subject
Ahlberg, J. E., Baral, L. L., and Tongue, T. O.	**46**, 6372	Brit. 666,380	heat treatment
Bailie, J. C.	**39**, 4457	U.S. 2,380,489	fluosilicic acid
Bailie, J. C., and See, M.	**39**, 4455	U.S. 2,378,530	U, Mo, W promoters
	38, 3821	U.S. 2,343,295	extrusion, thoria
Braithwaite, D. G.		U.S. 2,582,099	bead catalyst
Conn, A., Meehan, W. F., and Shankland, R. V.	**44**, 5085	*CEP*, **46**, #4,176 (1950)	commercial performance
Corner, E. S.	**45**, 8756	U.S. 2,470,411	hot aging then drying
Davison Chemical Corp.		Brit. 666,380	manufacturing, heat treatment
Ehrhardt, C. H.	**44**, 7056	U.S. 2,507,627	ammonium phosphate
Hunter, E. A., and Kimberlin, C. N., Jr.	**43**, 7162	U.S. 2,472,831 U.S. 2,472,833	metal sulfate promoter
Kimberlin, C. N., Jr., and Bilisoly, J.	**45**, 7346	U.S. 2,551,014–5	metal oxide promoter
La Lande, W. A.	**39**, 1518 **44**, 4666	U.S. 2,350,280 U.S. 2,451,564	pelleting
Marisic, M. M.	**45**, 2661	U.S. 2,528,767	drying bead catalyst
Nelson, K. J.	**45**, 8756	U.S. 2,470,410	mixing and heating
Pardee, W. A., and Montgomery, C. W.	**42**, 9154	U.S. 2,441,974	lime promoter
Pitzer, E. C.	**39**, 4457	U.S. 2,369,074	lanthanum promoter
Pryor, J. N.	**44**, 7525	Brit. 635,993	catalyst preparation
		U.S. 2,565,627	coprecipitation
Pier, M., v. Füner, W., and Free, G.	**38**, 858	U.S. 2,326,800	boric acid promoter
Ries, H. E., Jr., Johnson, M. F. L., and Melik, J. S.	**43**, 6897	*JPCC*, **53**, 638 (1949)	adsorption isotherms
Richardson, R. W., Johnson, F. B., and Robbins, L. V., Jr.	**43**, 8656	*IEC*, **41**, 1729 (1949)	pilot plant testing
Standard Oil Development Co.	**44**, 5499 **39**, 2398	Brit. 634,182 Brit. 556,711	alumina promoter
Thomas, C. L.	**42**, 7020	U.S. 2,432,634	catalyst preparation
Webb, G. M., and Moehl, R. W.	**45**, 2191	U.S. 2,532,525 U.S. 2,611,738	use of ammonium salts
Webb, G. M., Moehl, R. W., and Murray, M. J.	**45**, 4438	U.S. 2,546,031 U.S. 2,544,869	use of ammonium salts
Webb, G. M.		U.S. 2,605,237	catalyst preparation

CEP = Chemical Engineering Progress
IEC = Industrial and Engineering Chemistry
JPCC = Journal of Physical & Colloid Chemistry

TABLE 4. CRACKING OF HIGH BOILING PETROLEUM FRACTIONS

Natural Catalysts (Clays)

Author	Chem. Abstracts	Ref.	Product or Subject
Ahlberg, J. E., and Thomas, C. L.	**39**, 4450	U.S. 2,369,001	extruded
Bodkin, E. A., and Johnson, J.	**43**, 9428	U.S. 2,480,627	reactivation
Conn, A. L., and Brackin, C. W.	**43**, 8656	*IEC*, **41**, 1717 (1949)	S and steaming
Dart, J. C., Savage, R. T., and Kirkbride, C. G.	**43**, 3181	*CEP*, **45**, 102 (1949)	regeneration
Fawcett, E. W., and Haresnape, J. N.		U.S. 2,582,976	H_2S treatment
Gary, W. W.	**42**, 5629	U.S. 2,440,743	manganese promoter
	43, 4004	U.S. 2,464,127	acid activation
	42, 7946	U.S. 2,446,273	use of sludge acid
	41, 6034	U.S. 2,423,309	extrusion
Gary, W. W., and Secor, R. B.	**42**, 1033	U.S. 2,430,289	use of NH_3
	43, 370	U.S. 2,449,891	use of NH_3
	42, 9154	U.S. 2,432,746	use of NH_3
Grenall, A.	**44**, 2211	*IEC*, **41**, 1485 (1949)	acidity *vs.* heat
Hickey, J. H.	**44**, 2675	U.S. 2,484,828	acid treatment
Hornaday, G. F.	**46**, 1752	U.S. 2,494,556	S poisoned catalyst testing
Johnson, P. H. and Stark, C. P.		*IEC*, **45**, 849	
Kuryndin, K. S.	**43**, 6185		turpentine on kaolin
Mills, G. A., and Cornelius, E. B.	**46**, 1748	U.S. 2,495,751	iron removal
	44, 2145	U.S. 2,489,309	kaolin, iron removal
Mills, G. A.	**45**, 10565	U.S. 2,485,626	acid treatment of kaolin
	43, 8129	U.S. 2,477,639	
Mizimo, S.	**44**, 10442		heat treatment
Oulton, T. D.	**42**, 6069	U.S. 2,440,756	alum activation
	43, 3180	*JPCC*, **52**, 1296 (1948)	pore size
Owen, J. J.	**42**, 4316	U.S. 2,438,431	acid treatment in reducing atmosphere
Pierce, J. A., and Kimberlin, C. N., Jr.	**43**, 1506	U.S. 2,454,942	bead catalyst from clays
Secor, R. B.	**43**, 6403	U.S. 2,470,872	pelleting, etc.
	42, 7028	U.S. 2,432,822	preconditioning fluid catalyst
Shabaker, H. A.	**46**, 1752	U.S. 2,504,158	Florida kaolinite
	43, 8129	U.S. 2,477,664	activation procedure
	44, 2146	U.S. 2,489,332	iron removal
	46, 2283	U.S. 2,474,868	steam treatment of kaolin
Shabaker, H. A., Mills, Geo. A., and Denison, R. C.	**43**, 4843	U.S. 2,466,046 to U.S. 2,466,052	iron removal
Spicer, W. E., and Pierce, J. A.	**43**, 8662	U.S. 2,445,370	activation procedure
Thomas, C. L., Hickey, J., and Stecker, G.	**44**, 7050	*IEC*, **42**, 866 (1950)	chemistry

CEP = Chemical Engineering Progress
IEC = Industrial and Engineering Chemistry
JPCC = Journal of Physical & Colloid Chemistry

TABLE 5. CRACKING OF HIGH BOILING PETROLEUM FRACTIONS
Silica-Zirconia Catalysts

Author	Chem. Abstracts	Ref.	Subject or Product
Bates, J. R.	**44**, 4239	U.S. 2,454,369	BeO promoter
	46, 3258	U.S. 2,580,641	catalyst preparation
		U.S. 2,580,644	catalyst preparation
Blue, R. W.	**44**, 833	U.S. 2,481,493	SiO_2/ZrO_2 ratio
Bond, G. R., Jr.	**42**, 7000	U.S. 2,444,913	coprecipitated cat.
Connolly, G. C.	**39**, 2398	U.S. 2,366,491	silica gel impregnation
Kanhofer, E. R.	**42**, 8458	U.S. 2,438,560	catalyst preparation
Lee, E. C.	**39**, 5456	U.S. 2,382,239	catalyst preparation
Marisic, M. M., and Griest, E. M.	**42**, 9156	U.S. 2,442,774	catalyst preparation
	43, 3231	U.S. 2,461,089	bead preparation
Milliken, T. H., Jr., and Mills, G. A.	**43**, 8665	U.S. 2,477,638	acid treatment
Milliken, T. H., Jr., and Welinsky, I. H.	**43**, 3161	U.S. 2,456,721	hydrogel aging

thermal cracking. Final products are largely determined by secondary reactions.

(6) Wholly aromatic compounds such as benzene, biphenyl and naphthalene are practically inert under cracking conditions, whereas alkyl aromatics are readily cracked next to the ring to produce benzene, etc., the ease of cracking increasing with size of the alkyl group.

An interesting comparison of catalysts for cetane cracking[231] helps explain yield differences in gas oil cracking.

Alkylation

The term alkylation as generally employed denotes the replacement of a hydrogen atom in an organic compound by an alkyl radical. The classic method for carrying out alkylation is by means of the Friedel-Crafts reaction. In recent years alkylation has commonly been accomplished by reaction with an olefin as exemplified below by the alkylation of paraffin and aromatic hydrocarbons.

$$\text{(1)} \qquad \text{iso } C_4H_{10} + C_4H_8 \rightleftharpoons \text{iso } C_8H_{18} + 22 \text{ Kcal}$$

$$\text{(2)} \qquad C_6H_6 + C_2H_4 \rightleftharpoons C_6H_5C_2H_5 + 25 \text{ Kcal}$$

Equilibrium data[35] for these reactions are summarized below.

°K	$\text{Log}_{10} K$ Reaction (1)	$\text{Log}_{10} K$ Reaction (2)
300	5.7	12
500	0	4.3
800	−3.3	0
1400	−4.8	−2.5

Table 6. Cracking of High Boiling Petroleum Fractions

Miscellaneous Catalysts

Author	Chem. Abstracts	Ref.	Subject or Product
Bailey, W. A.	**40**, 1014	U.S. 2,377,744	boria-alumina-alkali
Bailey, W. A., and Greensfelder, B. S.	**40**, 451	U.S. 2,375,725	boria-silica-alumina
Bates, J. R.	**39**, 1044	U.S. 2,349,243	zirconia phosphate
	39, 3918	U.S. 2,378,904	alumina-zirconia
	46, 1244	U.S. 2,464,205	silica-alumina-berylia
Bond, G. R., Jr., and Mills, G. A.	**42**, 7017	U.S. 2,435,196	berylium phosphate
		U.S. 2,449,050	cerium phosphate
Connolly, G. C.	**39**, 3918	U.S. 2,364,949	alumina zirconia
	40, 2614	U.S. 2,396,641	tungsten oxide
	41, 6702	U.S. 2,424,152	boria-titania
	42, 7948	U.S. 2,445,346	boria-titania
	38, 4788	U.S. 2,340,935	berylia-alumina
		U.S. 2,341,363	berylia-alumina
Cook, L. W.	**40**, 4206	U.S. 2,398,819	aluminum fluoride-boria
Danforth, J. D.	**41**, 7727	U.S. 2,425,087	boria-titania
Darling, S. M.	**44**, 2224	U.S. 2,449,061	oxyfluorides
Garrison, A. D.	**44**, 317–8	U.S. 2,483,130–1	silicon fluoride
	41, 7726	U.S. 2,425,463	silicon fluoride
Greensfelder, B., Voge, H. H., and Good, G. M.	**44**, 2211	*IEC*, **41**, 2573 (1949)	carbon, alumina, silica
Grosse, A. V., and Mattox, W. J.	**39**, 4748	U.S. 2,381,820	chromia-silica gel
Hughes, E. C., and Darling, S. M.	**46**, 1751	U.S. 2,493,761	alkaline earth fluorides
	45, 9849	U.S. 2,466,706	fluoborates
Hunter, E. A.	**46**, 1670	U.S. 2,570,058	magnesia
Kimberlin, C. N., Jr.	**43**, 8076	U.S. 2,477,695	silica gel
Krieger, K. A., and Heinemann, H.	**43**, 2422	U.S. 2,457,566	bauxite
Marisic, M. M., and Griest, E. M.	**43**, 5133	U.S. 2,467,089	zirconia gel
Marisic, M. M.	**41**, 7724	U.S. 2,428,715	carbon
Mathy, E. V., and Helmers, C. J.	**46**, 4781	U.S. 2,564,268	boria-phosphate
Mathy, E. V.		U.S. 2,480,494	SnO_2-Al_2O_3
McGrew, E. H.	**40**, 7600	U.S. 2,377,093	alkali phosphate
Mills, G. A.	**44**, 3246	U.S. 2,453,152	silica-urania
	43, 9428	U.S. 2,446,547	thorium phosphate
N. V. de B. P. M.	**44**, 5091		boria-alumina
	43, 4792		boria-alumina
Oborin, V. I., and Lebedeva, N. V.	**41**, 7086		silica-chromia
Pardee, W. A., and Montgomery, C. W.	**42**, 9154	U.S. 2,441,974	magnesia-lime
Pitzer, E. C.	**38**, 1350	U.S. 2,328,846	HF-Al_2O_3
See, M. J., and Bailie, J. C.	**38**, 1100	U.S. 2,328,103	vanadia
Stowe, J. M., Marshall, E. E., Nickel, L. L., and Greenwood, R. S.	**42**, 9138	*PP*, **3**, 317 (1948)	alumina plus SiO_2, B_2O_3, fluosilicic acid
Young, D. W.	**38**, 3820	U.S. 2,349,911	titania-silica
West, J. P.		U.S. 2,584,405	silica-boria with Al_2O_3 or MgO

IEC = Industrial and Engineering Chemistry
PP = Petroleum Processing

TABLE 7. CRACKING OF PURE HYDROCARBONS

Silica-Alumina Catalyst

Author	Chem. Abstracts	Ref.	Agent being Cracked, etc.
Bloch, H. S. and Thomas, C. L.	**38**, 6529	*JACS*, **66**, 1589 (1944)	cycloolefins, paraffins
Clark, I. T., and Harris, E. E.		*JACS*, **74**, 1031 (1952)	rosin
Corrigan T. E., Garver, J. C., Rase, H. F., and Kirk, R. S.		*CEP*, **49**, 603 (1953)	cumene, kinetics
Cullinane, N. M., and Chard, S. J.	**42**, 7751	*JCS*, 804 (1948)	methanol and naphthalene
Dixon, J. K.	**41**, 6580	U.S. 2,422,165	diaryl substituted paraffins
Egloff, G., Morrell, J. C., Thomas, C. L., and Bloch, H. S.		*JACS*, **61**, 3571 (1939)	aliphatics
Kagan, M. Ya., and Savachenko, R.	**44**, 2914		mesityl oxide
Kutz, W. M.	**44**, 9985	U.S. 2,515,237	2-ethylnaphthalene
Maslyanskii, G. N., and Berlin, T.	**41**, 5289		cyclohexane
Obolentsev, R. D., and Gryazev, N.	**46**, 32		isopropylbenzene
	44, 9224		isopropylbenzene
Schmerling, L.	**45**, 341	U.S. 2,527,529	polyalkyl aromatics
Thomas, C. L., Hoekstra, J., and Pinkston, J. T.	**39**, 283	*JACS*, **66**, 1694 (1944)	alkyl aromatics
Topchieva, K. V., and Panchenkov, G. M.	**45**, 1858	cf. *CA*, **46**, 4340.	cumene
Topchieva, K. V., Battalova, Sh., and Panchenkov, G. M.	**45**, 7860		decahydronaphthalene
	46, 813		effect of catalyst comp.
Voge, H. H., *et. al.*		WPC, IV (1951)	many

Miscellaneous Catalysts

Author	Chem. Abstracts	Ref.	Catalyst	Agent being Cracked, etc.
Berg, L., Kindschy, E. O., Reveal, W. S., and Saner, H. A.		*CEP*, **47**, 469 (1951)	HF-Al_2O_3	alkyl aromatics
Greensfelder, B. S., and Voge, H. H.	**39**, 4445	*IEC*, **37**, 514 (1945)	SiO_2-ZrO_2-Al_2O_3	paraffins
	39, 5443	*IEC*, **37**, 983 (1945)		olefins
	40, 699	*IEC*, **37**, 1038 (1945)		naphthenes
Greensfelder, B. S., and Good, G. M.	**40**, 1010	*IEC*, **37**, 1168 (1945)	SiO_2-ZrO_2-Al_2O_3	aromatics
Haensel, V., and Ipatieff, V. N.	**37**, 4706	*IEC*, **35**, 632 (1943)	alumina	cyclohexane
Hansford, R. C.	**41**, 6392	*IEC*, **39**, 844 (1947)		butane

Table 7—*Continued*

Author	Chem. Abstracts	Ref.	Catalyst	Agent being Cracked, etc.
May, D. R., Saunders, K. W., Kropa, E. L., and Dixon, J. K.	**45**, 9990		kaolin	diarylethanes
Moldavskii, B., and Bezedel, L.	**41**, 4779		clay	alkyl aromatics
Roberts, R. M., and Good, G. M.	**45**, 9492	*JACS*, **73**, 1320 (1951)		cumene
Schmerling, L., and Ipatieff, V. N.	**39**, 1174	U.S. 2,349,834	$ZnCl_2$-Al_2O_3	dialkyl aromatics

CEP = Chemical Engineering Progress
JACS = Journal American Chemical Society
IEC = Industrial and Engineering Chemistry
JCS = Journal of Colloid Science
CA = Chemical Abstracts
WPC = World Petroleum Congress

It will be noted that paraffin alkylation is favored only at relatively low temperatures while the equilibrium for alkylation of aromatics is favorable up to 800°K.

Alkylation of isobutane with olefins was widely used during World War II to produce high octane material for aviation gasoline and many new "alkylate" installations are presently under construction. The isobutane and olefins are usually derived from the catalytic cracking of gas oil. Although some work has been done on vapor phase processes (Table 8), liquid phase acid catalysts (HF and H_1SO_4) are commonly used. Under conditions normally employed with HF and H_2SO_4 catalysts (40 to 100°F and 100 to 500 psi), *n*-butane passes through the reactor substantially unchanged although alkylation equilibrium is even more favorable for *n*-butane than for isobutane.

The alkylation of aromatics is equally as important industrially as the alkylation of isoparaffins and vapor phase catalytic processes were widely used during World War II[36] to make cumene (isopropyl benzene), a very high octane blending constituent. Equipment and catalysts used for polymerization of olefins can also be used under similar conditions for the alkylation of benzene with propylene. Favorable equilibrium at higher temperatures makes the alkylation of aromatics with olefins easier to carry out in the vapor phase than paraffin alkylation, although the liquid phase process with aluminum chloride catalyst (70 to 100°C, 12 atm) is also commonly employed. The effect of temperature, pressure, space velocity and benzene/propylene ratio with a phosphoric acid-kieselguhr catalyst has been discussed by McAllister[36]. Cumene has recently assumed im-

Table 8. Alkylation

Author	Chem. Abstracts	Ref.	Catalyst	Principal Product
Given, P. H., and Hammick, D.	**44**, 1429	*JCS*, 1779 (1949)	SiO_2-Al_2O_3	ethyl benzene
Gorin, M. H., Kuhn, C. S., Jr., and Miles, C. B.	**40**, 5909	*IEC*, **38**, 795 (1946)		mechanism
Ipatieff, V. N., and Pines, H.	**44**, 1137	U.S. 2,480,268	clay	bicyclo alkyl aromatics
Khmel'nitskii, Yu. L., Doladugin, A. I., Guseva, A. V., and Kropacheva, M. V.	**41**, 7086		H_3PO_4	alkyl benzene
Kosak, A. I., and Hartough, H. D.	**43**, 2644	U.S. 2,458,519	SiO_2-Al_2O_3	acetyl thiophene
Lavroskii, K.,and Mikhnovskaya, A. A.	**41**, 3283		clay	aromatic alkylate
	43, 4644		SiO_2-Al_2O_3	*n*-butyl aniline
Layng, E. T.	**41**, 2745	U.S. 2,414,206	copper phosphate	propylbenzene
Mamedaliev, Yu. G.	**42**, 6331		clay	aromatic alkylate
Moldavskii, B., and Bezedel, L.	**41**, 4779		clay	aromatics
Mavity, J. M.	**42**, 5049	U.S. 2,436,480	$H_4P_2O_7$	alkyl benzenes
Ohta, N.	**44**, 9226		$2H_3PO_4$-SiO_2	$C_3H_7C_6H_4OH$, etc.
Schmerling, L., and Ipatieff, V.	**39**, 1174	U.S. 2,349,834	$ZnCl_2$	alkyl benzene
	38, 977	U.S. 2,329,858	$MgCl_2$	alkyl aromatics
Schulze, W. A., and Stoops, C.	**44**, 8949	U.S. 2,514,419	SiO_2	alkyl phenols
Stand. Oil Development Co.	**41**, 6702		$AlCl_3$	catalyst preparation
Thomas, C. L., and Haensel, V.	**43**, 680	U.S. 2,448,160	SiO_2-Al_2O_3-ThO_2	alkyl benzene

JCS = Journal of Colloid Science
IEC = Industrial and Engineering Chemistry

portance as a raw material for making both phenol and acetone by the hydroperoxide process[37].

About half of the benzene produced is now alkylated to make ethyl benzene which is subsequently dehydrogenated to styrene[37]. Aluminum chloride, silica-alumina and supported phosphoric acid catalysts have been successfully used for this reaction although silica-alumina does not appear to have achieved wide commerical usage because of coke deposition. Moisture content of the feed must be carefully controlled to prevent dehydration or softening of kieselguhr supported phosphoric acid catalyst.

The older literature on alkylation is summarized by Berkman, Morrell, and Egloff[38]. The Unit Processes reviews on the subject have been written by Shreve[39-42]. Ipatieff and Schmerling[43] have covered the theory of iso-paraffin alkylation. Commerical aspects are reviewed by Mrstik, Smith and Pinkerton[44] and by Sherwood[37] (alkylation of aromatics). Recent literature on vapor phase catalysts is given in Table 8.

The effectiveness of acid catalysts for alkylation reactions indicates that carbonium ion mechanisms are involved. This subject has been discussed by Remick[45] who indicates the following steps for benzene alkylation:

$$R'CH{=}CH_2 + H^+ \rightarrow R'CH{-}CH_3^+ {=} R^+$$

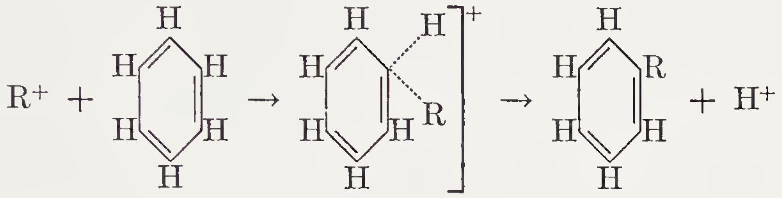

Isomerization

There are a great many isomeric compounds and, therefore, many isomerization reactions. Some of the more important types are listed below:

(a) *n*-butane ⇌ isobutane + 2.0 Kcal
(b) 1-butene ⇌ cis-2-butene + 1.7 Kcal
(c) *n*-butene ⇌ isobutene + 3.6 Kcal
(d) ethylbenzene ⇌ *o*-xylene − 2.6 Kcal
(e) ethylene oxide ⇌ acetaldehyde + 24 Kcal
(f) methylcyclopentane ⇌ cyclohexane + 3.9 Kcal

The older literature on the subject is well covered by Berkman, Morrell and Egloff[46]. More recently the field has been reviewed with reference to paraffin isomerization by Pines[47], Simons[48] and Gunness[49]. Isomerization as a Unit Process has been reviewed by Perry[50].

The conversion of straight chain to branched chain hydrocarbons is by far the most important type of isomerization reaction because of the much higher octane number of the latter. This reaction occurs during catalytic cracking of gas oil and naphtha reforming in addition to the primary dehydrogenation and dealkylation reactions, and accounts to a major extent for the high octane number of the product. Besides this, isomerization of pure *n*-butane and *n*-pentane has assumed considerable industrial importance[50]. A United States isobutane production rate of 50,000 bbl/day was achieved in 1945. The isoparaffins are subsequently alkylated to give high octane isoparaffins in the gasoline range. Although this reaction like alkylation is usually carried out in the liquid phase, the vapor phase process has not been entirely neglected (Table 9). Low temperatures (80 to 150°C), moderate pressures (10 to 20 atm), with a supported acid-promoted aluminum chloride are commonly used. Equilibrium is generally less favorable at high temperatures though the temperature coefficient and heats of reaction are low. Equilibrium constants for the reaction of *n*-butane ⇌ isobutane

TABLE 9. ISOMERIZATION

Aluminum Chloride Catalysts

Author	Chem. Abstracts	Ref.	Principal Reaction Product
Ipatieff, V. N., and Pines, H.	**39**, 531	U.S. 2,348,700	isobutane
Jones, H. H.	**44**, 7057	U.S. 2,506,720	isobutane
Meyers, C. O.	**43**, 844	U.S. 2,450,764	isobutane
Sachanen, A. N., and Caesar, P. D.	**39**, 3922	U.S. 2,376,509	isobutane
DeSimo, M., and McMillan, F. M.	**41**, 3287	Brit. 582,138	isoparaffins
Solomon, E., and Rubin, L. C.	**40**, 7539	U.S. 2,406,477	catalyst prep.
Sutton, M., and Nysewander, C.	**39**, 5458	U.S. 2,382,815	isoparaffins
Standard. Oil Dev. Co.	**39**, 707	Brit. 554,315	paraffins
Voge, H. H.	**40**, 600	U.S. 2,385,555	methyl cyclopentane
Warrick, H. R., and Watson, G. W.	**38**, 4956	U.S. 2,346,527	isobutane

Miscellaneous Catalysts

Author	Chem. Abstracts	Ref.	Catalyst	Product
Burgin, J.	**41**, 6271	U.S. 2,422,884	B_2O_3	isopentane
Cheltsova, M. A., and Petrov, A. D.	**39**, 1129		$ZnCl_2$	tetramethyl ethylene
CIBA Ltd.	**44**, 9591	Swiss, 264,593	Al, Mg	camphene
Clark, A., Matuszak, M., Carter, N., and Cromeans, J.		*IEC*, **45**, 803 (1953)	MoO_2-Al_2O_3	isopentane
Fawcett, E. W. M.	**42**, 7029	Brit. 601,202	$CuHPO_4$	isobutene
Fowler, G. W., and Fitzpatrick, J. T.	**42**, 583	U.S. 2,426,264	Li_3PO_4	allyl alcohol
Gallaway, W. S., and Murray, M. J.	**42**, 8150	*JACS*, 70,2584 (1948)	silica gel	olefins
Greensfelder, B. S., Archibald, R. C., and Fuller, D. L.	**41**, 7714	*CEP*, **43**, #10 (1947)	MoO_2-Al_2O_3	isoparaffins
Hay, R. G., Coull, J., and Emmett, P. H.	**44**, 1786	*IEC*, **41**, 2809 (1949)	Al_2O_3	2-butene
Hoekstra, J.	**44**, 5581	U.S. 2,502,565	$MgCrO_4$-SiO_2-Al_2O_3	high octane gasoline
Hokkaido Art. Pet. Co.	**43**, 2216		$ZnCl_2$	isobutylene
Howes, D. A., and Fawcett, E. W. M.	**40**, 5442	U.S. 2,394,927	NiW sulfide	isoparaffins
Ipatieff, V. N., and Monroe, G. S.		U.S. 2,538,248	Ni	
Jacobs, E., and Lunsted, L.		U.S. 2,600,654 –5	chromic oxide complex	allyl alcohol
Keith, P. C.	**41**, 3286	U.S. 2,415,890	SiO_2-Al_2O_3	isobutane

TABLE 9—*Continued*

Author	Chem. Abstracts	Ref.	Catalyst	Product
Levina, R. Ya., Viktorova, E. A., and Eikhfeld, V. I.	**43**, 6153		Cr_2O_3-Al_2O_3	olefins
Lundsted, L., and Jacobs, E.	**44**, 1128	U.S. 2,479,632	Cr_2O_3	allyl alcohol
Maslyanskii, G. N.	**39**, 454		MoS_2	methyl cyclopentane
Murray, M. J.	**44**, 2226	U.S. 2,487,978	alk. earth halides	
Ohta, N.	**44**, 9224 **44**, 9226		SiO_2-Al_2O_3	isobutene
Simons, J. H.		AIC II, 197 (1951)	HF	many
Standard Oil Dev. Co.		Brit. 555,288	B_2O_3-Al_2O_3-SiO_2	monoolifins
Stahly, E. E., and Laughlin, K. C.	**39**, 2182	U.S. 2,361,508	AlX_3	promoters
Thomas, C. L., and Bloch, H. S.	**38**, 6087	U.S. 2,352,416	thoria silica gel	isoolefinic gasoline

JACS = Journal American Chemical Society
CEP = Chemical Engineering Progress
IEC = Industrial and Engineering Chemistry
AIC = Advances in Catalysis, Academic Press, New York

as given by Rossini[51] are reproduced below:

Temp, °C	0	100	300	600
$\log_{10} K$	0.6	0.4	−0.1	−0.5

Rossini also gives equilibrium concentrations of C_8 aromatics from 200 to 1600°K and Haensel[52] points out that all forms of catalytic processing of these compounds give an equilibrium distribution. *m*-Xylene is favored particularly at low temperatures. The ethyl benzene fraction varies from 0 to 25 per cent in the temperature range 0 to 1600°K. Hay, Coull and Emmett[53] give equilibrium distributions for the normal butenes in a fundamental study of the chemical engineering of double bond migration. Storch, Golumbic and Anderson[54] give equilibrium data for pentanes, pentenes and hexanes.

Although acid-type catalysts are generally used for isomerization, the work of Ciapetta *et al.*[55] indicates that even better conversions of normal to isoparaffins are obtained when both hydrogenation and acidic sites are present. This is perhaps not surprising since carbonium ions are probably more readily formed from olefins than paraffins and the "hydrogenation sites" can at least momentarily convert paraffins to olefins.

Polymerization and Depolymerization

A limited definition of polymerization is utilized. Only reactions where identical or isomeric monomer units combine without splitting out products are considered to be in this category. Polycondensation reactions are not included. Depolymerization is, of course, the reverse process.

Vapor phase polymerization processes are relatively few because of the high boiling point of most polymerizates. They are exothermic reactions favored by low temperatures and high pressures. Most vapor phase polymerizations are carried out at 100 to 1500 psi and 100 to 300°C. A number of excellent reviews on the subject have been written[56-62, 228].

In recent years the catalytic polymerization of normally gaseous olefins to high octane gasoline has been of considerable importance to the oil industry. Butylene polymerization to produce codimer which was hydrogenated to give hydrocodimer was a process widely used during the war to manufacture aviation gasoline blending components[60]. Feedstocks containing other olefins as well as the butenes are now commonly used for making high octane gasoline by this method. Equilibrium data for the reaction $n\ C_4H_8 + i\ C_4H_8 \rightleftharpoons C_8H_{16}$ are given below[63].

Temp, °K	300	400	500	600	800
$\log_{10} K$	7.4	3.0	1.1	−0.4	−2.2

Agents for polymerization are almost all classed as acidic as is true also for cracking, alkylation and isomerization. This has lent strong support to the view that a carbonium ion mechanism is usually involved in all of these. According to this theory, the function of the catalyst is to supply and receive protons. Whitmore's[64] explanation is that a catalyst proton adds to the olefin double bond. This carbonium ion then adds to the double bond of another olefin to form a larger complex. The latter can then return a proton to the catalyst and become a dimer or polymerize further. The promotional effect of transition group elements is not readily explainable though Clark[65] suggests that they increase surface acidity.

Recent literature on vapor phase polymerization is summarized in Table 10.

Hydrogen Transfer

Reactions of this type involve rupture of a carbon-hydrogen bond and transfer of the hydrogen atoms or protons to other molecules. Thomas[66] appears to have been the first to focus attention on this type of reaction. Examples are:

(a) 2 cyclohexene $\rightleftharpoons$ benzene + cyclohexane
(b) $C_2H_4 + C_4H_{10} \rightleftharpoons C_2H_6 + C_4H_8 + 2.6$ Kcal
(c) cyclohexane + 3 acetone $\rightleftharpoons$ benzene + 3 isopropanol + 8.4 Kcal
(d) cyclohexane + 3 ethylene → benzene + 3 ethane + 49 Kcal

Table 10. Polymerization

Author	Chem. Abstracts	Ref.	Subject or Product
Phosphoric Acid Catalysts			
Cane, R. F.	**38**, 1465		rapid activity determination
Ciapetta, F. G., Macuga, S. J., and Leum, L. N.	**43**, 1713	*IEC*, **40**, 2091 (1948)	butylene
Corson, B. B., and Brady, L.	**43**, 5419	Brit. 616,260	ethyl benzene
Galle, R. R., and Parfanovich, B. N.	**41**, 4768		isobutylene polymers
Ipatieff, V. N., and Schaad, R. E.	**39**, 2485	*IEC*, **37**, 362 (1945)	heptenes and heptanes
Kyowa Chem. Ind. Co	**43**, 3576		catalyst preparation
Langlois, G., and Walky, J.		*PR*, **31**, #8, 79 (1952)	improved process
Mattox, W. J.	**41**, 6703	U.S. 2,422,692	isobutane
Mavity, J. M.	**45**, 1273	U.S. 2,525,145	catalyst preparation
Schaad, R.	**45**, 3156	U.S. 2,537,283	butene trimers
Schmerling, L.	**43**, 5640	U.S. 2,470,190	olefin polymers
Stadtherr, J.	**43**, 1559	U.S. 2,456,338	olefin polymers
Stewart, M. M., and Moore, F. J.	**42**, 7520	U.S. 2,446,619	olefin polymers
Silica-Alumina Catalysts			
Johnson, G. C., and Fawcett, F. S.	**40**, 6047	*JACS*, **68**, 1416 (1946)	nonenes
Obolentsev, R. D.	**43**, 6151		isobutylene
Offutt, W. C.	**44**, 11081	U.S. reissue 23,254	isobutylene
Quigg, H. T.	**42**, 4338	U.S. 2,439,021	high boiling hydrocarbon
Thomas, C. L.	**39**, 2965	*IEC*, **37**, 543 (1945)	olefin polymers

Miscellaneous Catalysts

Author	Chem. Abstracts	Ref.	Catalyst	Product or Subject
American Cyanamid Co.	**43**, 2381	Brit. 602,816	$BaCl_2$, $CaCl_2$ on C	cyanuric chloride
Anderson, J.	**39**, 5457	U.S. 2,381,481	fluoboric, fluosilicic acid	olefin polymers
Bailey, G. C., and Reid, J.	**39**, 4887	U.S. 2,381,198	Ni on kieselguhr	olefin polymers
Bond, G. R., Jr.	**45**, 342	U.S. 2,527,522	Ce phosphate	gasoline
Burroughs, S.	**43**, 1605	U.S. 2,455,225	fullers' earth	resin formation

Table 10—*Continued*

Author	Chem. Abstracts	Ref.	Catalyst	Product or Subject
Franklin, L. U., and Dunlay, E. E.	**39**, 5460	U.S. 2,383,642	clay	depolymerization of olefins
Freed, W. V.	**44**, 4921	U.S. 2,492,693	alk. metal	pentene + heptene
Hertzel, S. J., and Kennedy, R. M.	**43**, 5640	U.S. 2,470,166	$NiO-Al_2O_3-SiO_2$	ethylene polymers
Hickinbottom, W. J.	**40**, 4282		BF_3, $AlCl_3$	olefin polymer
Hughes, E. C., and Stine, H. M.	**44**, 3700	U.S. 2,494,510	Cu fluoborate, Cu pyrophosphate on alumina	propylene polymers
Ipatieff, V. N.	**41**, 4802	U.S. 2,419,142	$ZnO-Al_2O_3-CuO$	isophorone, mesitylene
McAllister, S. H., Anderson, John and Peterson, W. H.	**43**, 2763	U.S. 2,460,303	Co	C_5 olefins
Moorc, F. J., and Stewart, M. M.	**44**, 7340	U.S. 2,507,864	$NiO-Al_2O_3-SiO_2$	diolefins
Phillips Petroleum Co.	**43**, 5788	Brit. 619,231	$NiO-Al_2O_3-SiO_2$	olefin polymers
Rudakov, G. A., and Gulyaeva, L. I.	**41**, 114		clay	polyterpenenes
Steegmuller, F.	**44**, 6712		many	polymers of C_2H_2,C_2H_4 etc.
Steffens, J. H., Zimmerman, M. U. and Laituri, M. J.	**43**, 4839	*CEP*, **45**, 269 (1949)	Cu pyrophosphate	propylene, butylene polymers operating variables
Warner, A. J., and Talbot, T. H.	**43**, 1059	U.S. 2,450,027	fuller's earth	alkyl styrene dimer

IEC = Industrial and Engineering Chemistry
JACS = Journal of the American Chemical Society
PR = Petroleum Refiner
CEP = Chemical Engineering Progress

Heats and free energies are generally low and depend on the individual case.

As is evident from Table 11, relatively little has been published on this subject. Very interesting papers by Blue and Engle[67] on the use of silica-alumina catalysts (varying SiO_2/Al_2O_3 ratio) for both hydrogen transfer and deuterium-hydrogen exchange have appeared recently. It would appear from this work that acidic type catalysts such as silica-alumina cracking catalysts are active for reactions of this type and that a carbonium ion mechanism is usually involved. Greensfelder, Voge, and Good[68] give the

Table 11. Hydrogen Transfer

Author	Chem. Abstracts	Ref.	Catalyst	Product or Subject
Bartlett, P. D., *et. al*	**38**, 5793	*JACS*, **66**, 1531 (1944)	AlX_3	Me_3CH, etc.
Blue, R. W., Hohn, V. C. F., Regier, R. B., and Heckelsberg, L. F.,		*IEC*, **44**, 2710	SiO_2-Al_2O_3	granule size
Blue, R., and Engel, C.	**45**, 2759	*IEC*, **43**, 494 (1951)	SiO_2-Al_2O_3	paraffin + aromatic
Cade, G.	**45**, 341	U.S. 2,527,529	alumina	monoalkyl aromatics
Folkins, H. O., and Thacker, C.	**40**, 1877	U.S. 2,391,146	Cr_2O_3-Al_2O_3	ethyl benzene
Gorin, M. H., Gorin, E., Sharp, L. G. and Welinsky, I. H.	**40**, 5236	U.S. 2,401,865	clay	butane
Ipatieff, V. N., and Grosse, A. V.	**37**, 6673	U.S. 2,322,025	Ce, Mo, V	$C_2H_6 + C_5H_{10}$
Kagan, M., and Flid, R.	**40**, 6950 **40**, 6950		palladium Cr_2O_3-Al_2O_3	benzene, kinetics
Kleiderer, E. C., and Kornfeld, E. C.	**43**, 191	*JOC*, **13**, 455 (1948)	nickel	dehydrocholesterol
Plate, A. F.	**40**, 3409		V_2O_3-Al_2O_3	cyclopentadiene
Shcheglova, N., and Kagan, M.	**44**, 916		platinum	benzene
Thomas, C. L.	**38**, 6529	*JACS*, **66**, 1586 (1944)	SiO_2-Al_2O_3	general

IEC = Industrial and Engineering Chemistry
JACS = Journal of the American Chemical Society
JOC = Journal of Organic Chemistry

following example in case of hydrogen transfer from a cycloparaffin to an olefin:

$$(CH_3)_2C{=}CH_2 + H^+ \text{ (acid site)} \rightarrow (CH_3)_3C^+$$

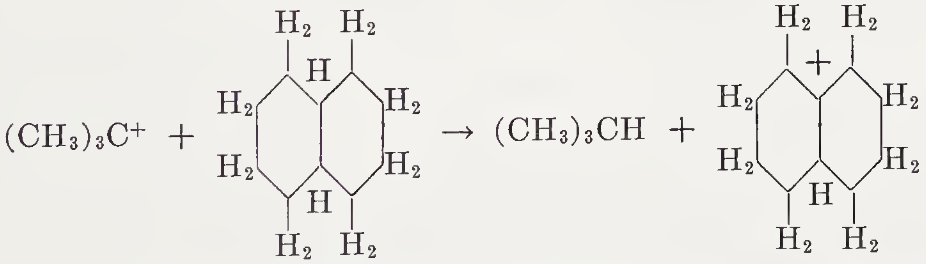

The hydrogen donor may then lose a proton to the catalyst to become a less saturated molecule. Silica-alumina compositions showing relatively high activity for hydrogen deuterium exchange were relatively inactive for hydrogen transfer. However, it will be noted from other literature on the subject that elements active for hydrogenation such as Pt are also active for hydrogen transfer.

HYDROGENATION-DEHYDROGENATION

In this class of reactions are included all of those in which hydrogen is a reactant or product in which a hydrogen-hydrogen bond is broken or formed with the exception of reactions in which both H_2 and H_2O are reactants or products (for example, the synthesis of butadiene from ethyl alcohol). Hydrogen transfer reactions not involving a hydrogen-hydrogen bond are classified with the acid catalyzed group. The different reaction types are listed below.

(1) Carbon-carbon bond saturation or the reverse (aromatics excepted).
(2) Hydrogenation of aromatics and aromatization.
(3) Hydrogenation or dehydrogenation of oxyorganic compounds.
(4) Hydrogenolysis of carbon-oxygen or nitrogen-oxygen bonds and the reverse reactions.
(5) Hydrogenation of oxides of carbon and the reverse reactions.
(6) Hydrodesulfurization.
(7) Ammonia synthesis and decomposition.

A very large amount of literature has appeared on the subject in recent years. Important recent work of a general nature is listed below:

1. Dowden, D. A., "The Theoretical Basis of Heterogeneous Catalysts," *J. Chem. Soc.*, **1950,** 242.
2. Laidler, K. J., "The Mechanism of Surface Reactions Involving Hydrogen," *J. Phys. & Colloid Chem.*, **55,** 1067, 1077 (1951).
3. Eley, D. D., "Mechanism of Hydrogen Catalysis," *Quarterly Review, London*, **3,** 209 (1949).
4. Adkins, H., and Shriner, R. L., "Catalytic Hydrogenation and Hydrogenolysis," 2nd Ed. Vol. 1, Henry Gilman, New York, John Wiley & Sons, Inc., 1945.
5. Foster, A. L., "Importance of Hydrogenation Catalysis to Refining Technique," *Oil Gas J.*, **44,** 23, 109 (1945).
6. "Hydrogenation Catalysts," P. B. Report 16,782.
7. Johnson, A. W., "Recent Advances in Reduction and Hydrogenation," *Sci. Progress*, **37,** 512 (1949).
8. Jones, D. G., and Taylor, A. W., "Selective Hydrogenation," *Chemistry & Industry*, **1951,** 1075.
9. Boudart, M., "Electronic Chemical Potential in Chemisorption and Catalysis," *J. Am. Chem. Soc.*, **74,** 1531 (1952).
10. Beeck, O., "Catalysis and Hydrogen Adsorption on Metals," "Advances in Catalysis," Vol. II, New York, Academic Press, Inc., 1950.
11. *Discussions of the Faraday Society No. 8* (1950):
    (a) Beeck, O., "Hydrogenation Catalysis," p. 118.

(b) Beeck, O., and Ritchie, A. W., "The Effect of Crystal Parameter on Hydrogenation and Dehydrogenation," p. 159.
(c) Schwab, G. M., "Alloy Catalysts in Dehydrogenation," p. 166.
(d) Dowden, D. A., and Reynolds, P. W., "Some Reactions over Alloy Catalysts," p. 184.
(e) Garner, W. E., "Adsorption and Catalysis on Oxide Catalysts," p. 211.
(f) Steiner, H., "Notes on Oxide Catalysts for Hydrocyclization," p. 264.

12. Storch, H. H., Golumbic, N., and Anderson, R. B., "The Fischer Tropsch and Related Syntheses," New York, John Wiley & Sons, Inc., 1951.

Older work is reviewed in the following references:

13. Williams, E. C., and de Simo, M. "Catalytic Dehydrogenation of Oxyorganic Compounds," "Twelfth Catalysis Report," Chap. VII, New York, John Wiley & Sons, Inc., 1940.
14. Williams, E. C., and Beeck, O., "Hydrogenation of Hydrocarbons," "Twelfth Catalysis Report," Chap. X, New York, John Wiley & Sons, Inc., 1940.
15. Berkman, S., Morrell, J. C., and Egloff, G., "Catalysis," New York, Reinhold Publishing Corp., 1940.
16. Ipatieff, V. N., "Catalytic Reactions at High Pressure and Temperature," p. 1, 166, New York, The Macmillan Co., 1936.
17. Smithells, N. J., "Gases and Metals," New York, John Wiley & Sons, Inc., 1937.
18. Adkins, H., "Reactions of Hydrogen with Organic Compounds Over Copper-Chromium Oxide and Nickel Catalysts," University of Wisconsin Press, 1937.

On the basis of work referred to above, particularly that of Beeck, it appears that active catalysts for reactions involving hydrogen can be separated into three groups which are best discussed separately, namely:

(1) Transition group and bordering metallic elements
(2) Transition group oxides or sulfides
(3) Other oxides.

Metals. Several generalizations can be made although it should be realized that thermodynamic, geometric, and selectivity and poisoning factors peculiar to the reaction in question must also be considered.

(1) The catalyst must be capable of forming chemical bonds with one or both of the reactants (chemisorption) but maximum activity is realized when the bonding is not too strong and the products of the reaction are still readily released. Too strong adsorption of one component at the expense of the other might also lessen reaction rate. Heats of adsorption of hydrogen appear to parallel those for olefins.

(2) The strength of bonding with hydrogen increases with an increase in the number of vacant *d* orbitals as shown below in Table 12. However, catalytic activity commonly reaches a maximum at about one vacant *d* orbital/atom so that the elements Co, Ni, Rh, Pd, Ir and Pt are generally the most active metals for reactions involving hydrogen, although there are many exceptions as discussed under the heading of selective hydrogenation.

TABLE 12. PERIODIC ARRANGEMENT OF CATALYTIC ELEMENTS FOR REACTIONS INVOLVING HYDROGEN

	V	Cr	Mn	Fe	Co	Ni	Cu	Zn
Vacant *d* orbitals[4]	5–7	4–5	3–5	2–4	1–3	0–2	0–1	0
Heat of H_2 ads.[1]		43		33		31	9[3]	very low
$\log_{10}k^2$		−4.0		−3.0		−2.9		
	Cb	Mo	Ma	Ru	Rh	Pd	Ag	Cd
Vacant *d* orbitals	5–6	4–5	3–4	2–3	1–2	0–2	0	0
Heat of H_2 ads.[1]					28	27	low	low
$\log_{10}k^2$					−0.1	−1	inactive	
	Ta	W	Re	Os	Ir	Pt	Au	Hg
Vacant *d* orbitals	5–7	4–6	3–5	2–4	1–3	0–1	0	0
Heat of H_2 ads.[1]	47	43				28	low	low
$\log_{10}k^2$	−4	−4				−2.0	inactive	

[1] Initial heat of adsorption of hydrogen in Kcal/mol from data of Beeck *et al.*[69]

[2] K = rate constant for hydrogenation of ethylene, data of Beeck *et al.*[69]

[3] Data of Ward.[70]

[4] Higher figures are usual handbook values. The lower figures are obtained if all outer electrons drop back to *d* orbitals. According to Dowden,[71] nickel has 0.6 vacant *d* orbitals in the solid state.

(3) The adsorptive and in some cases the catalytic properties of alloys of these metals can be estimated from the average number of vacant *d* orbitals. When elements with no vacant *d* orbitals but with free electrons are alloyed with metals having vacancies, the electrons may fill empty orbitals of the latter component. Catalytic and adsorptive properties are affected accordingly.

(4) The number of unfilled *d* orbitals per atom decreases with increased hydrogen sorption and the electrons derived from the hydrogen may be shared. Hence, heats of adsorption and catalytic properties may also be affected by the degree of hydrogen sorption.

Transition group oxides. Elements with a large number of vacant *d* orbitals such as V, Cr, Cb, Mo, Ta and W are relatively inactive for reactions involving hydrogen, probably because of their strong adsorption for reactants and/or reaction products. Although their lower oxides or sulfides are reasonably stable under hydrogenation conditions, partial reduction to a near metallic state might occur at the surface. If so, electrons from the residual oxygen would be expected to lessen the strong adsorption by filling some of the empty orbitals so that adsorption and catalytic properties would be similar to elements with fewer empty orbitals. This may explain why MoO_2 and Cr_2O_3 are quite active for most reactions involving hydrogen, whereas metallic Mo and Cr are inactive.

Taylor[72] has suggested that the activity of transition group oxides for reactions involving hydrogen was related to their tendency to form metal excess or metal deficient structures (relative to stoichiometric amounts). Such lack of stoichiometry accounts for their behavior as semi-conductors. The great influence of small amounts of impurities on electrical conductivity can be cited as being similar to the effect of small amounts of impurities on catalytic activity. However, no very convincing mechanism or experimental correlation appears to have been offered for a hypothesis of this nature as applied to reactions involving hydrogen.

Other oxides. A slight activity for reactions involving hydrogen is shown by other compounds such as alumina. However, in most cases this can be attributed to iron or other impurities. The relatively low activity shown by pure alumina has been explained by Dowden[71] on the basis of a proton exchange mechanism via cation defects. It is very susceptible to poisoning by water vapor.

Carbon Bond Saturation or the Reverse

(a) $H_2 + H_2C{=}CH_2 \rightleftharpoons CH_3{-}CH_3 + 33\ \text{Kcal}$
(b) $H_2 + CH \equiv CH \rightleftharpoons CH_2{=}CH_2 + 32\ \text{Kcal}$
(c) $2H_2 + CH_2{=}CH{-}CH{=}CH_2 \leftrightarrows CH_3{-}CH_2{-}CH_2{-}CH_3 + 57\ \text{Kcal}$

As a result of the high heat values, dehydrogenations of straight chain hydrocarbons are only favored at temperatures in excess of at least 600°C. Equilibrium constants from the data of Rossini[73] are tabulated below in Table 13.

The most important reaction of this class, economically, is butadiene synthesis from butenes which are usually obtained by butane dehydrogenation. The need for synthetic rubber made from butadiene during World War II resulted in intensive research in this field as indicated in Table 14. This development is reviewed in recent literature[74-76].

TABLE 13. EQUILIBRIUM DATA FOR THE HYDROGENATION OF OLEFINS

$\log_{10} K_p$

Normal Olefin	25°C	200°C	400°C	600°C	800°C
C_2	17.6	8.9	3.9		
C_3	15.2	7.2	2.7		
C_4	15.4	7.3	2.8		
C_6	15.2	7.2	2.7		
C_8	15.2	7.3	2.9	0.7	−1.0
C_{10}	15.2	7.2	2.8		

Table 14. Hydrogen Addition to Multiple Bonds or the Reverse

Author	Chem. Abstracts	Ref.	Product or Subject
		Chromia Catalysts	
Amos, James L.		U.S. 2,603,610	styrene
Balandin, A. A., *et al.*	**42**, 6218		butadiene
Blue, R. W., Holm, V. C. F., Regier, R. B., Fast, E., and Heckelsberg, L. F.		*IEC*, **44**, 2710 (1952)	effect of grain size
Dixon, J. K.	**40**, 1174	U.S. 2,387,836	dimethyl styrene
Dodd, R., and Watson, K. M.	**40**, 4941		pilot plant design
Frey, F. E.	**43**, 5030	U.S. 2,465,016	C_2 to C_5 olefins
Ghosh, J. C., Guha, S. R., and Roy, A. N.	**42**, 4036		styrene
	42, 3245		butadiene
Haas, F. E.	**39**, 5422	U.S. 2,384,737	methacrylonitrile
Hanson, G. H., and Hays, H. L.	**42**, 4803	*CEP*, **44**, 431 (1948)	butenes ex butane Phillips plant
Hays, H., and Dolezal, E.	**44**, 5086		butenes ex butane
Houdry, E., and Shabaker, H. A.	**40**, 5066	U.S. 2,399,678	butadiene
Houdry, E.	**41**, 6272	U.S. 2,423,029	butadiene
Kiddoo, G.		*CE*, **58**, #9, 169 (1952)	butylenes, commercial process
Mattox, W. J.	**40**, 3460	U.S. 2,395,058	butadiene
Mavity, J. M., Zetterholm, E. E., and Hervert, G. L.		*IEC*, **38**, 829 (1946)	styrene
Mitsukuri, J., and Shinbo, M.	**44**, 6875		butadiene, etc.
Mond, A. L.	**37**, 4930	Brit. 546,709	butadiene
Owen, J. R.	**44**, 4167	U.S. 2,499,675	pelleted catalyst
	44, 2004	U.S. 2,483,929	BeO promoter
	42, 442	*JACS* ,**69**, 2559 (1947)	surface area *vs.* catalyst activity
Parker, R., and Huffman, H. C.	**42**, 1049	U.S. 2,426,118	berylia silica promoter
Roy, A. N.	**42**, 3246		water poisoning
Standard Oil Development Co.	**42**, 3206	Brit. 595,457	butadiene
Thomas, C. L.	**39**, 4079	U.S. 2,377,113	butene
Varga, J., and Freund, M.	**45**, 1332		butylene
Visser G. H.	**40**, 6950		effect of structure
Yamazaki, G.	**44**, 1125		dehydrog. of paraffins

TABLE 14—*Continued*

Author	Chem. Abstracts	Ref.	Product or Subject
		Iron Catalysts	
Beckberger, L. H., and Watson, K. M.	**42**, 2919	*CEP*, **44**, #3 229 (1948)	butadiene, kinetics
Corson, B. and Webb, G.	**44**, 4667	Brit. 632,291 U.S. 2,614,996	butadiene styrene
Davies, E. P., and Eggertsen, F. T.	**43**, 5135	U.S. 2,461,147	butadiene (extr. cat.)
Emmett, P. H., and Gray, J. B.	**38**, 5133	*JACS*, **66**, 1338 (1944)	hydrog. of olefins
Fulton, S., and Kearby, K.	**40**, 719	U.S. 2,383,643	butadiene
Gaylor, P. J.		*PP*. **8**, 735	ethylene mfr.
Gutzeit, C. L.	**43**, 370	U.S. 2,449,295	butadiene
Kiddoo, G.		*CE*, **58**, #9, 160 (1952)	styrene
Kearby, K. K.	**42**, 198	U.S. 2,426,829	styrene
	44, 3874	*IEC*, **42**, 295 (1951)	butenes
	42, 198	U.S. 2,426,829	butadiene
	41, 4800	U.S. 2,418,888	butadiene
Kleiber, C. E., Campbell, D. L., and Stines, D. E.	**41**, 2426	U.S. 2,414,876	butadiene
Meinert, R. N., and Vesterdal, H. G.	**45**, 1156	U.S. 2,518,354	butadiene
Morrell, C., and Slotterbeck, O. C.	**43**, 680	U.S. 2,449,004	PhCMe:CH_2
N. V. de B. P. M.	**43**, 5410		butadiene
Nickels, J. E., Webb, G. A., Heintzelman, W., and Corson, B. B.		*IEC*, **41**, 563 (1949)	ethyl styrene
Oliver, E., and van Berg, C.	**43**, 2764	U.S. 2,459,449	butadiene
Standard Oil Development Co.	**42**, 356	Brit. 587,151	butadiene
Sumerford, S. D.	**42**, 7312	U.S. 2,436,616	
		Nickel Catalysts	
Baker, L., and Bernstein, R.		*JACS*, **73**, 4434 (1951)	mechanism
Burford, W., and Frazer, J.	**39**, 1350	*JACS*, **67**, 331 (1945)	ethane
Corson, B., and Webb, G.	**43**, 5788	U.S. 2,470,092	olefins
dePauw, F., and Jungers, J.	**44**, 915		ethylene, ethane
Doumani, T., and Deering, R.		U.S. 2,600,379	styrene

Table 14—*Continued*

Author	Chem. Abstracts	Ref.	Product or Subject
Dowden, D. A.		*IEC*, **44**, 949 '52	theoretical aspects
Eucken, A.	**44**, 3342		olefins
Hougen, O. A., and Watson, K. M.	**41**, 2286	Chem. Proc. Prin., III, p. 943	isooctane, kinetics
Kazanski, B., and Bulanova, T.	**43**, 589		pentane
Kwan, T.	**43**, 7802		sulfided catalysts
Levering, D., Morritz, F. L. and Lieber, E.	**44**, 5199	*JACS*, **72**, 1190 (1950)	platinic chloride
Ogawa, E., Tada, M., and Okuno, T.	**44**, 7637		magnetization
Ohe, H.	**42**, 6735		ethylene
Sherburne, R., and Farnsworth, H. E.	**45**, 6912	*JCP*, **19**, 387 (1951)	ethane
Sheridan, J.	**39**, 2967	*JCS*, 133 (1945)	ethylene, ethane
Shiwa, T.	**44**, 1524		ethylene
Smith, H. A., Alderman, D. M., Jr., Shacklett, C. D., and Welch, C. M.	**44**, 2354	*JACS*, **64**, 3769 (1942)	Raney Ni, aging and area
Standard Oil Development Co.	**44**, 774	Brit. 623,595	Raney Ni from Si
Starkey, F., and Bremner, J. G.	**43**, 4700	Brit. 608,540	tetrahydrofuryl alc.
Taylor, T., and Dibeler, V.	**46**, 30	*JPCC*, **55**, 1036 (1951)	paraffins and olefins
Tokunaga, T.	**44**, 3002		olefins
Tsutsumi, S.	**43**, 5610		saturated oil
Ueno, S., and Anzai, R.	**43**, 5210		saturated oil
Voorhies, A.	**42**, 356	U.S. 2,428,692	isobutane and isopentane
Wilson, J. N.		Petroleum Div. Abs. (Sept. 1952)	mechanism
Platinum Group Catalysts			
Haensel, V.	**43**, 2746	U.S. 2,456,633	H_2PtCl_6-SiO_2 gel
Jones, M. C. K.	**42**, 8456	U.S. 2,440,673	paraffins
Kawamoto, O., and Furukawa, K.	**44**, 1524		ethylene
Minachev, Kh., and Shuikin, N. I.	**44**, 7785		alkanes, etc.
Rosenblatt, E. F.		U.S. 2,475,155	deposition on carrier by hydrolysis

TABLE 14—*Continued*

Author	Chem. Abstracts	Ref.	Product or Subject
Sheridan, J., and Reid, W. D.		*JCS*, 2962 (1952)	ethylene, Rh and Ir
Shiwa, T.	**44**, 1524		ethylene
Shur, A. S., and Demenev, N.	**45**, 5501		
Lonza Elek.	**43**, 5030	Swiss Pat. 241, 650	ethylene
Tamaru, K.	**46**, 2384		ethylene, ethane
	45, 2298		ethylene
Vvedenskii, A. A., Dobronravov, R. K., and Frost, A. V.	**40**, 6950		cyclohexane
Yamanaka, T.	**45**, 1857		Hg, Pb inhibition
	42, 6629		ethylene
Alumina Catalysts			
Mond, A. L.	**41**, 6897	Brit. 572,045	styrene
Schulze, W. A., and Hillyer, J. C.	**44**, 1628	U.S. 2,485,927	butadiene
Schulze, W., Hillyer, J., and Drennan, H. E.	**39**, 4887	U.S. 2,380,876	1-3-butadiene
	39, 4080	U.S. 2,377,579	butadiene
	39, 3299	U.S. 2,367,622–3	butadiene
Wood, W. H., and Capel, R. G.		*IEC*, **37**, 1148 (1945)	styrene
Calcium Nickel Phosphate Catalysts			
Britton, E., and Dietzler, A.	**42**, 6106	U.S. 2,442,319	butadiene
	43, 2382	U.S. 2,456,367	butadiene
Britton, E., Dietzler, A., and Noddings, C. R.	**46**, 1668	*IEC*, **43**, 2871 (1951)	butadiene
Heath, S. B.	**45**, 3965	U.S. 2,542,813	butadiene
Copper Catalysts			
Jones, D. G.	**44**, 3030	Brit. 621,744	side chain hydrogenation
Kagan, M., and Fridman, S.	**44**, 917		olefin *vs.* benzene
Kearby, K. K.	**41**, 2886	U.S. 2,407,373	butadiene
McCabe, C. A., and Halsey, G. D., Jr.		*JACS*, **74**, 2732 (1952)	ethane
Miyake, R.	**44**, 352		oil hydrogenate
Stroupe, J. D.	**43**, 5653	*JACS*, **71**, 569 (1949)	x-ray diffraction study $CuO\text{-}Cr_2O_3$

Table 14—*Continued*

Author	Chem. Abstracts	Ref.	Product or Subject
Weizman, C.	**43**, 7950	Brit. 572,821	diolefins
Wynkoop, R., and Wilhelm, R.	**44**, 6713	*CEP*, **46**, 300 (1950)	ethylene (catalyst size)
Cobalt Catalysts			
Reynolds, P. W., and Donaldson, J. W.	**44**, 5499	Can. 461,114	Foraminate Co-Al
Rubinshtein,. A. M., and Pribytkova, N. A.	**45**, 5010		alpha *vs.* beta Co
Stiles, A. B.	**46**, 664	U.S. 2,570,882	sintered pelleted catalyst
Molybdena Catalysts			
Cheney, L. C.	**44**, 4512	Brit. 608,969	biotin
Claussen, W. H., and Wellman, H. B.	**42**, 1415	U.S. 2,432,286	coprecipitated ex $AlCl_3$
N. V. de B. P. M.	**43**, 5039		dehydrogenation of hydroaromatics
Miscellaneous Catalysts			
Komarewsky, V. I., Bos, L. B., and Coley, J. R.	**42**, 2500	*JACS*, **70**, 428 (1953)	V_2O_5-Al_2O_3
Sherwood, P. W.		*PP*, **8**, 902 (1953)	ZnO-Cr_2O_3-Al_2O_3 for styrene mfr.

IEC = Industrial and Engineering Chemistry
CEP = Chemical Engineering Process
CE = Chemical Engineering
JACS = Journal of the American Chemical Society
JCP = Journal of Chemical Physics
JCS = Journal of the Chemical Society
JPCC = Journal of Physical & Colloid Chemistry
PP = Petroleum Processing

The thermodynamics of butene dehydrogenation has been studied by Rossini[73] ($\text{Log}_{10}\ K = 1$ at 727°C). The most generally used catalyst "1707"* developed for this purpose[75] has a Fe_2O_3-MgO-K_2O composition. The reaction is carried out at 650° or higher in the presence of steam to prevent carbon deposition and to lower partial pressures. The kinetics have been studied by Beckberger and Watson[77]. The iron might be considered as the

---

* Developed by the Standard Oil Co. of New Jersey.

active agent, magnesia the binder and carrier, while the function of the potassia is to catalyze the reaction of steam with incipient coke. Chromia-alumina catalysts are generally used for converting butanes to butenes[78].

More recently The Dow Chemical Co. has introduced for butadiene synthesis a calcium nickel catalyst[79] which is claimed to be more efficient than "1707" and which was possibly originally developed for another dehydrogenation reaction of great economic consequence[80-81], the dehydrogenation of ethyl benzene to styrene. For this latter reaction, "1707" and ZnO-Cr_2O_3-Al_2O_3 catalysts[226, 227] are also used.

In general, there appears to be no great preference in choice of hydrogenating element for reactions of this class, though the more active catalysts find greater favor as seen from Table 14.

Hydrogenation of Aromatics and Aromatization

(a) $C_6H_6 + 3H_2 \rightleftharpoons C_6H_{12} + 49$ Kcal naphthene formation
(b) $C_6H_6 + 4H_2 \rightleftharpoons C_6H_{14} + 60$ Kcal paraffin formation
(c) $C_6H_6 + 3H_2 \rightleftharpoons C_6H_{12} + 30$ Kcal olefin formation

The large demand for aromatics for explosives, chemical intermediates, and high octane motor fuel components has made these dehydrogenation reactions of great economic importance. In particular, "naphtha reforming" in which a C_7 petroleum fraction is passed over a catalyst at about 500°C with recycled hydrogen under pressure was an important wartime method for making toluene[81]. It has also received much attention in recent years as a means of solving the aromatics shortage and upgrading straight run gasoline to a high octane, sulfur-free product. New processes of this nature have been developed by Universal Oil Products Co.[82-86] (Pt-Al_2O_3-AlF_3 pellets), Atlantic Refining Company[87, 88] (Pt-SiO_2-Al_2O_3 pellets), Houdry Process Corp.[89, 90, 97] (catalyst nature not revealed), Kellogg Co.-Standard Oil Co. of New Jersey, Standard Oil Co. (Indiana)[91-93] (fluid MoO_3-Al_2O_3), Socony Vacuum Co., and the Standard Oil Co. of Ohio[94] (Cr_2O_3-Al_2O_3 beads). These processes[229, 230] convert naphthenes to aromatics but leave the paraffins substantially unchanged except for isomerization of normal to branched chain compounds. The nonaromatization of the paraffins can be attributed in part to equilibrium considerations. Hydrogen recycle and high pressures are utilized to minimize carbon formation but these operating conditions also repress aromatization of paraffins. Processes employing Pt catalysts appear to give higher gasoline yields at 70 to 90 octane levels, while MoO_3 appears to give better yields above 90 octane. The higher octane ceiling for MoO_3 probably can be attributed to the more favorable equilibrium for aromatization at the conditions commonly used with MoO_3 *vs.* those used for Pt (250 psi, mol ratio H_2/hydrocarbon = 2–4, temp. = 930°F, for MoO_3 *vs.* about 500 psi,

Table 15. Equilibrium Constants* for Aromatization Reactions

Toluene Formation

Reactant	100°C	200°C	300°C	400°C	500°C	600°C
methyl cyclohexane	−10	−4	0.7	3.0	5.3	7.5
n-heptane	−12	−5	0.3	2.9	5.5	8.0
n-heptene	−3.0	−0.5	1.3	2.5	3.8	4.5

* $\log_{10} K_p$

mol ratio H_2/hydrocarbon = 5–10, temp. = 900°F for Pt). Although higher temperatures increase reaction rate and give more faovrable equilibrium, an upper limit is dictated because of reduced liquid yields. This is caused by hydrocracking to gaseous products.

Reactions for the hydrogenation of aromatics are fairly exothermic as indicated above. However, loss in molecular number leads to a decrease in entropy so that aromatization, the reverse of aromatic hydrogenation, is favored at temperatures in excess of about 300°C. Equilibrium constants given by Rossini[95] are tabulated in Table 15.

The effect of molecular weight on the equilibrium of naphthene conversion as reported by Fowle, Bent, and Masologites[88] is shown in Table 16. The effect of hydrogen pressure on equilibria for methyl cyclopentane and n-heptane conversion to toluene is given by Greensfelder, Archibald and Fuller.[96]

A large amount of literature on aromatization reactions has appeared in recent years as indicated in Tables 17 and 18. Chromium oxide, molybdena and platinum catalysts are most widely used.

Hydrogenation and Dehydrogenation of Oxyorganic Compounds Without Water Addition or Elimination

(a) $CH_3CH_2OH \rightleftharpoons CH_3CHO + H_2 - 12\text{ Kcal}$

(b) $2C_2H_5OH \rightleftharpoons CH_3COOC_2H_5 + 2H_2 - 2.4\text{ Kcal}$

(c) $CH_3CHOHCH_3 \rightleftharpoons CH_3COCH_3 + H_2 - 14\text{ Kcal.}$

Table 16. Naphthene-Aromatic Equilibrium

Mol % Aromatic*

Temp. (°C)	C 6	C 7	C 8
400	4	14	72
450	14	46	87
500	64	87	97
550	90	97	100

* Computed for 500 psig and 10/1 H_2/hydrocarbon mol ratio.

TABLE 17. AROMATIZATION AND THE REVERSE WITHOUT HYDROGEN RECYCLE

Author	Chem. Abstracts	Ref.	Product or Subject
Chromia Catalysts			
Edson, K. C.	**41**, 4808	U.S. 2,419,342	BaO_2 promoter
Layng, E. T.	**41**, 7738	U.S. 2,423,328	magnesia promoter
Luyten, L., and Vlieghere, R.	**37**, 5307		benzene
Nametkin, S. S., Khotimskaya, M. I., and Rosenberg, L. M.	**42**, 3339		aromatization of cycloaliphatics
Obolentsev, R. D., and Usov, Yu. N.	**42**, 1570		olefins and aliphatics
Taylor, H. S., and Fehrer, H.	**38**, 3289	U.S. 2,336,783	nickel promoter
Taylor, H. S., Fehrer, H., and Turkevich, John	**39**, 407	U.S. 2,357,271	zinc oxide promoter
Varga, J., Rabo, G., and Zalai, A.	**45**, 10022		K_2O promoter
Visser, G. H.	**44**, 7636		toluene (K_2O promoter)
Nickel Catalysts			
Adkins, H., Rae, D. S., Davis, J. W., Hager, G. F., and Hoyle, K.	**42**, 2247	*JACS*, **70**, 381 (1948)	diphenyl
Chitwood, H. C., Fitzpatrick J. T., Fowler, G. W., and Freure, B. T.		*IEC*, **44**, 1696 (1952)	phenols-alkali sulfate promoter
Flid, P., and Kagan, M.	**45**, 4124		benzene
Gwynn, M. H.	**44**, 663	U.S. 2,481,921	naphthenes
Herbo, C., and Hauchard, V.	**41**, 4368		cyclohexane
	40, 4941		cyclohexane
Herbo, C.	**44**, 9785		alcohols, cyclohexane
Hill, F. N., and Selwood, P. W.	**43**, 8831	*JACS*, **71**, 2522 (1949)	cyclohexane
Nicolai, J., Martin, R., and Jungers, J. C.	**44**, 419		cyclohexane
Sillar, S.	**44**, 1136		phenol
Tanida, S.	**42**, 330		cyclohexane
	41, 4368		MoO_3 and W_2O_5
Ugnade, H. E., and McLaren, A. D.	**38**, 957	*JACS*, **66**, 118 (1944)	naphthenic alcohol
Voorthuijsen, J., and Engel, W. F.	**43**, 3453		methylcyclohexane

Table 17—*Continued*

Author	Chem. Abstracts	Ref.	Product or Subject
		Molybdena Catalysts	
Roberts, R. M., Eggertsen, F. T. and Greensfelder, B. S.	**44**, 4168	U.S. 2,498,709	zinc nitrile promoter
Russell, A. S., and Stokes, J. J., Jr.	**40**, 6945	*IEC*, **38**, 1071 (1946)	effect of surface area
	42, 4437	*IEC*, **40**, 520 (1948)	heat stability
Smith, J. O., Jr.	**41**, 6702	U.S. 2,424,636	zirconia promoter
		Platinum Group Catalysts	
Frost, A., and Lapin, Y.	**42**, 6630		benzene
Gryaznov, V. M.	**45**, 4540		cyclohexane
Kagan, M., and Scheglova, N.	**44**, 1313		benzene
Lapin, Y., and Frost, A.	**41**, 4027		benzene
Musaev, I., and Gal'pern, G.	**42**, 1484		cyclohexane
Novikov, S. S., *et al.*	**44**, 916		benzene
Shuikin, N. I., *et al.*	**44**, 8872		aromatics
	42, 4437		benzene
	45, 10020		benzene

Other Catalysts

Author	Chem. Abstracts	Ref.	Catalyst	Product
Burk, R. E., and Hughes, E. C.	**37**, 6877	U.S. 2,321,006	Cu	aromatics
Holder, C. H., and Welty, A. B., Jr.	**40**, 2290	U.S. 2,392,738	Co, MoO$_3$	aromatics
Hull, Washington	**40**, 4860	U.S. 2,401,246	Cr$_2$O$_3$-NiO, Fe$_2$O$_3$	*p*-cymene
Ipatieff, V. N., and Haensel, V.	**40**, 600	U.S. 2,386,957	ZnO-CuO	aromatics
	42, 7330	U.S. 2,444,509		
Isobe, H., Tanaka, K., and Yabuki, S.	**43**, 7911		Fe	benzene
Komarewsky, V.	**37**, 387		Co	cyclohexane
Midzugichi, J., and Yagi, Y.	**41**, 4483		Cu	hydronaphthalene
Minachev, Kh. M., *et al.*	**45**, 3698		Co	cyclohexane
Plate, A. F., and Tarasova, G.	**44**, 8215	*UOPB*, **27**, #19	V oxides	aromatics
Soc. des usines Chimiques Rhone-Poulenc	**43**, 1813		Cu	pyrazine

IEC = Industrial and Engineering Chemistry
JACS = Journal of the American Chemical Society
UOPB = Universal Oil Products Co. Bulletin

Table 18. Hydroforming* (Aromatization with Hydrogen Recycle)

Author	Chem. Abstracts	Ref.	Subject
		Chromia Catalysts	
Archibald, R., and Smith, A. E.	**38**, 1871	U.S. 2,331,292	Bayer alumina carrier
Ahlberg, J. E.	**39**, 3421	U.S. 2,374,404	zirconia promoter
Black, J. F.	**43**, 7222	U.S. 2,474,214	zinc aluminate carrier
Blaker, D. G.	**38**, 6087	U.S. 2,351,094	alkaline promoter
Burk, R. E., and Hughes, E. C.	**37**, 386	U.S. 2,290,033	coprecipitated nitrates
	41, 5297	U.S. 2,401,334	S compounds
	38, 4424	U.S. 2,345,096	copper promoter
Greensfelder, B. S., Archibald, R. C. and Fuller, D. L.	**41**, 7714	*CEP*, **43**, 561 (1947)	fundamental study
Hibbard, R. R.	**40**, 2620	U.S. 2,395,048	from CrO_3
Hirsch, J. H.	**41**, 7729	U.S. 2,423,833	fluid catalyst
Huffman, H. C.	**41**, 855	U.S. 2,411,829	berylia promoter
Hughes, E. C.	**38**, 480	U.S. 2,323,868	coprecipitation
Hughes, E. C., Stine, H. M., and Darling, S. M.	**44**, 827	*IEC*, **41**, 2184 (1949) *IEC*, **44**, 572 (1952)	varying naphtha
Mavity, J. M.	**38**, 6087	U.S. 2,351,624	titania carrier
Payne, J. W., *et al*		*PE*, **24**, #6 C-10	thermofor reforming
N. V. de B. P. M.	**41**, 3592		aerogel
Standard Oil Development Co.	**37**, 6100	Brit. 547,246	peptized alumina carrier
Universal Oil Products Co.	**45**, 1759	Brit. 639,945	high mass velocity
Marisic, M. M.	**44**, 2676	U.S. 2,492,167	bead manufacture
		Molybdena Catalysts	
Arveson, M. H.	**40**, 7599	U.S. 2,371,599	fluid process
	40, 451	U.S. 2,372,165	fluid process
Bailie, J. C., Heard, L., and Shankland, R. V.	**40**, 6801	U.S. 2,404,024	Al_2O_3 from Al
Bailie, J. C., and Shankland, R. V.	**41**, 598	U.S. 2,408,724	Al_2O_3 from Al
Bloch, H. S., and Thomas, C. L.	**33**, 4450	U.S. 2,369,001	silica-alumina carrier
Belchetz, A.	**41**, 5295	U.S. 2,421,677	fluid process
Black, J. F.	**43**, 7222	U.S. 2,474,214	zinc aluminate
	43, 6818	U.S. 2,474,213	
Claussen, W. H., and Wellman, H. B.	**42**, 1415	U.S. 2,481,824 U.S. 2,432,286	use of graphite, coprecipitation

TABLE 18—*Continued*

Author	Chem. Abstracts	Ref.	Subject
Daussat, R. W., and Moak, O. W.	**44**, 5581	U.S. 2,502,930	high stability, extrusion with clay
Davidson, S.		U.S. 2,508,014	silica and zinc oxide promoters
Greensfelder, B. S., Archibald, R. C., and Fuller, D. L.	**41**, 7714	*CEP*, **43**, #10, 561 (1947)	reactions
Hill, L. R., Vincent, G. A., and Everett, E. F.	**40**, 6793		high octance fuel
Heard, L., Shankland, R. V., and.Bailie, J. C.	**38**, 4763	U.S. 2,345,600	Al_2O_3 from Al metal
Holder, C. H.	**39**, 5460	U.S. 2,386,050	effect of sulfiding
Huffman, H. C.	**42**, 7971	U.S. 2,437,531–2	
	42, 4340	U.S. 2,437,533	silica promoter
	41, 855	U.S. 2,411,829	berylia promoter
Kearby, K. K.		U.S. 2,556,280	CaO, MgO promoter
	43, 7161	U.S. 2,474,215	zinc aluminate carrier
Layng, E. T.	**44**, 2147	U.S. 2,487,564	silica promoter
Layng, E. T., and Suman, F. T., Jr.	**43**, 1561	U.S. 2,453,327	titania promoter
McGrath, H., and Hill, L. R.	**45**, 10557	Adv. Chem. Ser. No. 5, 39 (1951)	fluid hydroforming
McGrath, H.		*PR*, **30**, 12, 102 (1951)	fluid hydroforming
Mattox, W. J.	**42**, 4315	U.S. 2,438,569	removal of sulfate
Mavity, J. M.	**39**, 4467	U.S. 2,369,497	titania carrier
Meinert, R. N., and Holt, P.	**41**, 7094	U.S. 2,419,323	zinc aluminate
Murphree, E. V.	**43**, 389	U.S. 2,451,041	zinc oxide promoter
N. V. de B. P. M.	**43**, 8579		$Al(NO_3)_3$ for Na removal
Pirzer, E. C.	**41**, 7731	U.S. 2,423,947	from sodium aluminate
Smith, A. E., and Beeck, O.	**43**, 1931	U.S. 2,454,227	beta alumina
	43, 6762	U.S. 2,474,440	lithium oxide promoter
	41, 7066	U.S. 2,422,172	beta alumina
	41, 5269	U.S. 2,422,372	lime promoter
Smith, A. E.	**41**, 6702	U.S. 2,424,636	zirconia promoter
Shell Development Co.	**39**, 526	Brit. 555,046	Pt promoter
Spicer, W. E. and Watts, R.	**37**, 1594	U.S. 2,296,406	acetic acid peptization
Standard Oil Development Co.	**44**, 8102	Brit. 637,178	zinc aluminate carrier
	45, 3605	Brit. 613,463	zinc aluminate carrier
Tamele, M. W., Irvine, V. C., and Mahar, J. F.	**43**, 1931	U.S. 2,454,724	impregnated catalyst

TABLE 18—*Continued*

Author	Chem. Abstracts	Ref.	Subject
Thomas, C. L., and Morrell, J. C.	**42**, 7027	U.S. 2,444,965	kaolin promoter
Thomas, C. L.	**41**, 7728	U.S. 2,423,163	MoO_3, Al_2O_3 and rosin mix pelleted
Triggs, W. W.	**40**, 4510	Brit. 570,072	alumina from trihydrate
U. O. P.	**42**, 5629	Brit. 577,385	Al_2O_3 from $AlCl_3$
Webb, G. M., and Smith, M. A.	**39**, 3133	U.S. 2,371,087	magnesia promoter
Webb, G. M., *et al*		*PP*, **2**, 836 (1947)	coprecipitated catalyst
Welty, A. B., Jr.	**40**, 6801	U.S. 2,406,117	regeneration
	38, 2425	U.S. 2,333,500	reduction of catalyst
Welty, A. B., Jr. and Holder, C. H.,		U.S. 2,456,351	zinc spinel carrier, high temperature activity
	45, 9851	U.S. 2,459,480	alternate oxidation and reduction
	44, 832	U.S. 2,447,043	zinc oxide and lime promoter
Yule, L. T., and Bennett, R.	**43**, 841	*IEC*, **40**, 1995 (1948)	pilot plant
		Platinum Group Catalysts	
Anon.		*PR*, **32**, #6, 143	Sinclair process
Ciapetta, F. G.		U.S. 2,550,531 U.S. 2,589,189	catalyst preparation
Faulkner, C. S., *et al.*		*OGJ*, #29, 116 (1952)	commercial unit
Fowle, M. J., Bent, R. D., Ciapetta, F. G., Pitts, P. M., and Leum, L. N.	**45**, 10557	*Adv.C.S.*, #5, 76 (1951)	catalyst development
		PR, **3** #3, 86 (1951)	
		OGJ, **51** #3,181 (1952)	
Haensel, V.	**46**, 728	U.S. 2,566,521	Al_2O_3-HX-PtS catalyst
	43, 8664	U.S. 2,479,110	Al_2O_3-HX-PtS catalyst
	43, 8578	U.S. 2,479,109	Al_2O_3-HX-PtS catalyst
		U.S. 2,611,736	Al_2O_3-HX-PtS catalyst
		U.S. 2,611,749	Al_2O_3-HX-PtS catalyst
	46, 11664	U.S. 2,606,878	Al_2O_3-HX-PtS catalyst
Haensel, V., and Gerald, C.	**45**, 10567	U.S. 2,478,916	cracking catalyst carrier
Haensel, V., and Donaldson, G. R.		*IEC*, **43**, 2102	platforming
		PP, **8**, 236 (1953)	effect of paraffins
Heinemann, H., Shalit, H., and Brigg, W. S.		*IEC*, **45**, 800 (1953)	Houdriforming

TABLE 18—*Continued*

Author	Chem. Abstracts	Ref.	Subject
Kastens, M. L., and Sutherland, R.	**44**, 5085	*IEC*, **42**, 582 (1950)	benzene
Mills, G. A., Heineman, H., Milliken, T. H., and Oblad, A. G.		*IEC*, **45**, 134 (1953)	mechanism
Nelson, E. F.	**44**, 2737	*PE*, 21C, 422 (1947)	platforming
Peel, D. H.	**41**, 1700	Brit. 579,363	naphthene dehydrogenation
Teter, J. W., Borgerson, B. T., and Beckberger, L. H.		*PP*, **8**, #10, 2 (1953)	Sinclair process

Other Catalysts

Berg, Clyde		*OGJ* **51**, #46, 286	Hyperforming
Bryns, A. C.		U.S. 2,445,345	Co or MoO_2 on MgO
Cole, R. M.	**39**, 4457	U.S. 2,373,626	Fe
	43, 5709	U.S. 2,423,176	$WS_2 \cdot 3\ Ni_2S_3$
Danner, P. S., and Mithoff, R.	**37**, 5856	U.S. 2,315,506	WO_3
Komarewsky, V. I., and Erikson, T. A.		*JACS* **75**, 4082 (1953)	V_2O_5, cyclohexene
Nahin, P. G., and Huffman, H. C.	**44**, 8102	U.S. 2,510,189	Co-Mo, NiW
Owen, J. R.	**44**, 2004	U.S. 2,483,929	Cr_2O_3
Porter, F. W. B., and Haresnape, J. N.	**45**, 9849	Brit. 653,320	Cu molybdate
Shiffler, W. H., and Claussen, W. H.		U.S. 2,485,073	V_2O_5
Stine, H. M.	**46**, 4213	U.S. 2,584,756	Fe
Stormont, D. H.		*OGJ*, **51**, #46, 168 (1953)	activated carbon

IEC = Industrial and Engineering Chemistry
PP = Petroleum Processing
PE = Petroleum Engineer
OGJ = Oil and Gas Journal
Adv. C.S. = Advances in Chem. Series
IEC = Industrial and Engineering Chemistry
CEP = Chemical Engineering Progress
PR = Petroleum Refiner
JACS = Journal of the American Chemical Society

* See *IEC*, **45**, 1897 (1953) for a more complete listing of 1953 literature.

Reactions of this nature are commonly used for the synthesis of aldehydes, ketones and esters. A moderate amount of literature on the subject has appeared in recent years as indicated in Table 19. Earlier literature on the subject is reviewed by Williams and de Simo[98]. Recent work pertaining to the dehydrogenation of ethyl alcohol to acetaldehyde and of methanol to formaldehyde (metal gauze catalyst) is discussed by Church and Joshi[99] and by Hader, Wallace and McKinney[100], respectively. The Tennessee Eastman Corp., at Kingsport, Tennessee, is stated[101] to use the reaction as an intermediate in making acetic anhydride. The American two-step process for making butadiene from ethanol which accounted for 60 per cent of that produced according to Corson *et al.*[102] used, as the first step, the dehydrogenation of about half the alcohol to acetaldehyde. These dehydrogenation reactions are only slightly endothermic so that equilibrium is favorable at fairly low temperatures (over about 200°C) because of the greater entropy of the products.

The more active dehydrogenation catalysts are generally unsuitable because of selectivity considerations. Copper has proved to be the most satisfactory active agent and Church and Joshi[99] claim yields of acetaldehyde from ethyl alcohol in excess of 90 per cent.

Wojcik[103] has published an interesting study on the hydrogenation of furan to furfuryl alcohol.

Hydrogenolysis of Carbon-Oxygen or Nitrogen-Oxygen Bonds

(a) $\phi OH + H_2 \rightarrow \phi H + H_2O + 42$ Kcal
(b) $CH_3CHO + 2H_2 \rightarrow C_2H_6 + H_2O + 59$ Kcal
(c) $CH_3NO_2 + 2H_2 \rightarrow CH_3NH_2 + H_2O + 57$ Kcal
(d) $HCOOH + 2H_2 \rightarrow HCH_2OH + H_2O + 18$ Kcal
(e) $\phi NO_2 + 3H_2 \rightarrow \phi NH_2 + 2H_2O + 132$ Kcal

Reactions of this type are usually very exothermic and equilibrium is generally favorable in the forward direction at all temperatures. Earlier literature is reviewed by Adkins and Shriner[104], Ellis[105], and Berkman, Morrell and Egloff[106]. Recent literature on the hydrogenolysis of acids and esters is summarized by Boyle[107] while hydrogenolysis of nitro compounds (amination by reduction) is covered by Werner[108].

Reactions involving hydrocarbon formation are seldom economic, but during World War II work was done on the hydrogenolysis of phthalic anhydride as a method for toluene synthesis[109]. Alcohol syntheses from acids are fairly common but they are usually carried out in the liquid phase (chromite catalysts).

Liquid phase processes are nearly always used for the hydrogenolysis of nitroparaffins although there are a few exceptions (Table 20). Considerable work has appeared on vapor phase hydrogenolysis of nitroaromatics. Usage

Table 19. Hydrogenation and Dehydrogenation of Oxyorganic Compounds

Copper Catalysts

Author	Chem. Abstracts	Ref.	Product or Subject
Charles, E., and Robinet, P.	**44**, 6990	U.S. 2,504,497	acetic acid
Church, J. M., and Joshi, H. K.		*IEC*, **43**, 1806 (1951)	acetaldehyde
Davies, R. R., and Hodgson, H.	**37**, 5370	*JCS*, 1943, 282	aldehydes
Guinot, H. M.	**43**, 2218	U.S. 2,456,187	butanol
Ivankov, P. Ya.	**42**, 1561		esters from alcohols
Jones, D. G., Bremner, J., and Keeys, R. K.	**43**, 7049	Brit, 621,743	furfuryl alcohol
Katsuno, M.	**44**, 7761		acetone
	44, 8856		
	43, 1718		furfural alcohol
Kiddoo, G.		*CE*, **59**, #9, 163 (1952)	ketones
Lefrancois, P.	**39**, 663		furfural alcohol
Lel'chuk, S. L.	**40**, 5627		alcohol to esters
McNeil, E., and Charlton, F.	**44**, 7867	Brit. 636,743	acetone
Neish, A. C.	**39**, 2248		aldehydes, etc.
Reynolds, P. W., and Donaldson, J. W.	**44**, 5499	Brit, 634,097	acetone
Rubinshtein, A. M., and Pribytkova, N. A.	**46**, 9962		physical properties *vs.* activity
Stewart, M. M.	**40**, 4860	U.S. 2,400,959	furfuryl alcohol

Other Catalysts

Author	Chem. Abstracts	Ref.	Catalyst	Product or Subject
Agronomov, A. E.	**46**, 4341		ZnO	kinetics and preparation method
Arnold, H. R.	**42**, 4724	U.S. 2,439,880	W, Mo oxide	aldehyde and ketone
Csuros, Z., Zech, K., and Geczy, I.	**41**, 110		Pt, Pd, Rh	selective action
Friedman, L., and Turkevich, J.		*JACS*, **74**, 1669 (1952)	Pt, Pd, Rh	isopropyl alcohol
Guest H., and McNamee, R.		U.S. 2,575,404	Fe-Cu-Cr	phenyl methyl carbinol
Herbo, C.	**44**, 9785		Ni	alcohols
Komori, S.	**42**, 2228		Fe	unsat. higher alc.
Lukes, R. M., and Wilson, C. L.		*JACS*, **73**, 4790 (1951)	Ni	furfuryl alcohol, etc.
Mottern, H.		U.S. 2,586,694	MgO, ZnO, BeO	acetaldehyde
Natta, G., and Baccaredda, M.	**44**, 2011		Pt, Pd, Rh	CH_2O

TABLE 19—*Continued*

Author	Chem. Abstracts	Ref.	Catalyst	Product or Subject
		Other Catalysts—*Continued*		
Nightingale, I., and Radford, H. D.	**44**, 3462	*JOC*, **14**, 1809 (1949)	CuCr oxide	aromatic alcohol
Rubinshtein, A., and Kulikov, S.	**45**, 6031		TiO_2	acetaldehyde
Rubinshtein, A. M., and Pribytkova, N. A.	**40**, 6325		MgO	butylaldehyde
Schneider, H., and Mistretta, V.	**43**, 6650	U.S. 2,472,493	ZnO	ketone

JACS = Journal of the American Chemical Society
JOC = Journal of Organic Chemistry
IEC = Industrial and Engineering Chemistry
JCS = Journal of the Chemical Society
CE = Chemical Engineering

of aniline for aniline dyes and xylidines for blending with aviation gasoline (improves supercharged engine performance) makes this reaction type of considerable importance. During the war the Shell Oil Co.[110] operated a xylidine plant which had a daily capacity of one million pounds and the Standard Oil Co. of New Jersey[108] operated another large plant at Baton Rouge (MoO_2-charcoal catalyst). Xylene fractions from hydroforming operations were nitrated to give the feedstocks. Recently, announcement was made[111] of the construction of a fluid vapor phase catalytic unit for aniline synthesis. Fluid operation helps solve one of the major problems of hydrogenolysis reactions, temperature control. Copper, nickel and oxides or sulfides of Mo, W, Ni and V find favor for reactions of this type (Table 20).

Hydrogenation of Oxides of Carbon and the Reverse Reaction

In this category are included the many reactions of carbon oxides with hydrogen, including:

(a) Formaldehyde synthesis: $CO + H_2 \rightarrow HCHO + 1.9$ Kcal
(b) Methanol synthesis: $CO + 2H_2 \rightarrow CH_3OH + 24$ Kcal (350°C)
(c) Higher alcohol synthesis: $nCO + 2\,nH_2 \rightarrow C_nH_{(2n+1)}OH + (n-1)H_2O$
(d) Methane synthesis: $CO + 3H_2 \rightarrow CH_4 + H_2O + 52$ Kcal (350°C)
(e) Higher hydrocarbon synthesis: $nCO + (2n+1)H_2 \rightarrow C_nH_{(2n+2)} + (n)H_2O$
(f) Oxo process: $CO + H_2 + RCH = CH_2 \rightarrow RC_2H_4CHO$

It is unnecessary to consider carbon dioxide separately since it is readily converted to the monoxide by the shift reaction ($CO + H_2O \rightleftharpoons CO_2 + H_2$) which is discussed under oxidation reactions.

TABLE 20. HYDROGENOLYSIS OF NITROGEN-OXYGEN BONDS

Author	Chem. Abstracts	Ref.	Catalyst	Product or Subject
Anon.		P.B. 5,886 P.B. 81,279	Cu-C	aniline
Condit, P. C.	**44**, 1430	*IEC*, **41**, 1704 (1949)	MoS	aromatic amines
DeLargey, R. J., Okie., J. P., and Roberts, L. M.	**43**, 2415		MoS-WS-NiS	aromatic amine process
Grim, R. J.	**36**, 5415	*JPCC*, **45**, 234 (1941)	Cd_3Cu_2	aniline
Houghton, A. S., and Lowdermilk, F. R.	**44**, 3019	U.S. 2,489,886	Ni	aromatic amines
Kern, J. G.		P.B. 1,777	Cu-pumice	aniline
Nash, R. W.		P.B. 81,279	Cu-pumice	aniline
Reynolds, P. W.		Brit. 630,161	Raney Co-Zn	amines
Rohrer, C., Rooley, J. and Brown, O. W.	**45**, 4540	*JPCC*, **55**, 211 (1951)	Ni tungstate	*n*-propylamine
Scharmann, W. G., and Nelson, K. J.	**44**, 685	U.S. 2,481,245	MoS-C	aromatic amines
Seto, I., and Sakuyama, S.		*JSCI, Japan,* Suppl. Bind. 44, 93B–4 (1941)	Ni	aniline
Smith, N. A., and Bedoit, W. C.	**46**, 31	*JPCC*, **50**, 1085 (1951)	Pt	amines
Souders, M., Jr.	**43**, 3454	U.S. 2,458,214	Cu-Ni	xylidines
Standard Oil Development Co.	**42**, 6850	Brit. 599,252	WS	aromatic amines
Teeters, W. O.	**45**, 2504	U.S. 2,526,913	Ni	aromatic amines
Voorhies, A.		U.S. 2,445,713	MoS-WS-NiS	aromatic amines, fluid catalyst

Hydrogenolysis of Carbon-Oxygen Bonds

Billica, H., and Adkins, H.		*OS*, **29**, 24 (1944)	Raney Ni	catalyst preparation
Dunbar, R. E., and Arnold, R.	**40**, 1781		Cu CrO_2	aldehydes
Ford, T. A.		U.S. 2,607,807	Ru	alcohols
Griffith, R. H.	**41**, 1701	Brit. 557,818	Mo	toluene
Kapecki, A. F.	**44**, 9087	U.S. 2,512,653	chromia	long chain alcohols
Larson, A. T.	**41**, 5546	Brit. 575,380	chromites	ethylene glycol
Pardee, F. W.	**37**, 2744	U.S. 2,305,104	chromites	ethylene glycol
Schmidt, O.	**38**, 113	U.S. 2,322,095		alcohols
Standard Oil Development Co.	**44**, 774		Ni	Raney Ni from Si
	43, 681		MoS-WS-Cr_2O_3	fluid catalyst
Woodward, L. A., and Glover, A. T.	**42**, 2081		Mo	benzene

IEC = Industrial and Engineering Chemistry
JPCC = Journal of Physical & Colloid Chemistry
JSCI = Journal of the Society of Chemical Industry (Japan)
OS = Organic Synthesis

Older literature on the subject is summarized in the following references:

1. Berkman, S., Morrell, J. C., and Egloff, G., "Catalysis," pp. 682–693, New York, Reinhold Publishing Corp., 1940.
2. Lazier, W. A., "Hydrogenation of Oxides of Carbon," Twelfth Catalysis Report, National Research Council, New York, John Wiley & Sons, Inc., 1940.
3. Marek, L. F., and Hahn, D. E., "Catalytic Oxidation of Organic Compounds in the Vapor Phase," New York, Chemical Catalog Co. (Reinhold Publishing Corp.), 1932.

Recently the field has been reviewed by:

4. Storch, H. H., Golumbic, N., and Anderson, R. B., "Fischer-Tropsch and Related Synthesis," New York, John Wiley & Sons, Inc., 1951.
5. Hirst, L. L., "Chemistry of Coal Utilization," Vol. II, chap. 20, New York, John Wiley & Sons, Inc., 1945.

The direct synthesis of formaldehyde from CO and H_2 appears impractical because of low equilibrium conversion. Newton and Dodge[112] conclude that equilibrium conversion is 0.4 per cent at 200°C and 300 atm. Also, it is doubtful if a catalyst with sufficient selectivity could be found. However, at least one publication[113] on the subject has appeared in recent years.

The equilibrium for methanol synthesis is much more favorable and that for higher alcohols even more so although higher pressures are necessary for good yields. The latter are also obtained as by-products in hydrocarbon synthesis. Dodge[114] gives the following Kp values for methanol synthesis.

	$Kp \times 10^4$			
Temp (°C)	30 atm	100 atm	300 atm	700 atm
250	26.0	46.0	120.0	270.0
300	3.7	5.2	12.0	26.0
350	0.72	0.87	1.7	3.7
400	0.19	0.22	0.39	0.75
450	0.05	0.06	0.10	0.18

Storch, Golumbic, and Anderson[125] give the following comparisons for the synthesis of different alcohols at 327°C.

	$\log_{10} K$ eq.
ethanol	−1.85
propanol-1	−0.74
butanol-1	+0.34
hexanol-1	1.48

Synthetic methanol is of great industrial importance since the catalytic process has almost completely replaced wood fermentation and production in the United States is about 0.2 billion gallons per year[115]. Ammonia synthesis plants can be used for methanol synthesis without drastic changes since synthesis conditions are similar (*ca.* 3000 psi, 350°C). However, the heat of reaction for methanol synthesis is twice as high as for ammonia synthesis so it is customary with ammonia synthesis type converters to limit the carbon monoxide content of the synthesis gas to about 10 per cent so as to keep the temperatures under control.

A large amount of work was published[116-122] on this subject in the period 1928–1933 covering a period of intensive activity following the introduction of synthetic methanol by German producers in 1925. This work has recently been summarized by Storch, Golumbic and Anderson[125]. Recent literature, which has not added greatly to the picture, is given in Table 21. Selectivity is probably the greatest factor governing choice of a catalyst. By-products are primarily dimethyl ether and methane, etc., which are favored by high temperatures. Since methane formation is very exothermic, an upset in converter or local hot spot can readily cause temperatures to get out of control with consequent damage to the catalyst. Hence, catalysts active for the methanation reaction such as Ni are not used. Iron and cobalt catalysts may give higher hydrocarbons. Dehydrating agents such as alumina favor dimethyl ether formation. Alkaline agents favor higher alcohol production. Copper and zinc alone, or in combination, and combined with chromia, still appear to be most popular as seen from Table 21, though $ZnO\text{-}Cr_2O_3$ is claimed to be the best (good selectivity, activity, and resistance to S poisoning).

Catalysts for higher alcohol synthesis are generally similar to methanol catalysts except for incorporation of alkaline materials. Although industrial utilization of the process was reported by Graves[123] in 1931, further large-scale application does not appear to have transpired except for Fischer-Tropsch by-products. The subject has recently been reviewed by Anderson, Feldman and Storch[124].

Methane Synthesis and Reforming. The methane synthesis reaction, methanization, which is a special case of hydrocarbon synthesis has achieved only minor technical importance, including the following applications:

(1) Converting toxic CO to CH_4 in domestic gas and also enhancing the calorific value.

(2) Eliminating CO from hydrogen containing gases used for catalytic processes which are poisoned by carbon monoxide such as ammonia synthesis.

The reaction is favored at low temperatures[125].

Temp. (°C)	127	227	327	427	627	827
$\text{Log}_{10}\,K$ eq	15.6	10.1	6.3	3.6	−.1	−2.5

and elevated pressures.

Because of the importance of the reaction to gas producers, much published research has been carried out by the British and American gas

Table 21. Alcohol Synthesis and Decomposition

Author	Chem. Abstracts	Ref.	Product or Subject
		Copper Catalysts	
Hasegawa, S.	**44**, 2356		decomposition mechanism
Ipatieff, V. N., and Monroe, G. S.	**40**, 1140	*JACS*, **67**, 2168 (1945)	effect of CO_2 on syn.
Larson, A. T.		U. S. 1,844,857	fused catalyst
Nippon Chem. Ind. Co.	**44**, 1127		isobutanol
Seelig, H., and Marschner, R.	**42**, 4328	*IEC*, **40**, **583** (1948)	decomposition
Yamanaka, T.	**42**, 6628		poisoning, MgO promotor
		Zinc Oxide Catalysts	
Ghosh, J., Sastri, and Vedaraman, S.	**45**, 7406		adsorption studies
Larson, A. T.	**41**, 6680	U. S. 2,425,625	hydrogen
Lonza Elektrisitat, etc.	**43**, 6338		catalyst preparation
Mittasch, A.		U. S. 1,558,559 U. S. 1,569,775	higher alcohols
Shekhter, A. B., *et. al.*	**46**, 3839 **44**, 26	*CA* **44**, 7132 *CA* **45**, 10021	cat. properties and structure
Siller, C. W.	**37**, 2645	*JACS*, **65**, 431 (1943)	area *vs.* activity
Tamura, M., and Shida, S.	**46**, 4339		
Tomita, A.	**41**, 3353 **45**, 10023		effect of precipitant mechanism

Other Catalysts, Etc.

Author	Chem. Abstracts	Ref.	Catalyst	Product or Subject
Kyowa Chemical Enterprises	**44**, 1525		MnO_2	aliphatic alcohols
Francon, J.	**42**, 3426		Ni	HCHO
Kastens, M. L., Dudley, J. F., and Troeltzsch, J.	**43**, 1714	*IEC*, **40**, 2230 (1948)		commercial product
Williams, A. A.		*CE*, **55**, #1, 111 (1948)		industrial status

JACS = Journal of the American Chemical Society
IEC = Industrial and Engineering Chemistry
CE = Chemical Engineering
CA = Chemical Abstract

associations. City gas methane manufacture is carried out at 1 to 50 atm., about 20,000 space velocity and about 400°C. Problems encountered in this process are S poisoning, carbon lay down (450 to 600°C), C_{4+} hydrocarbon formation, and loss in activity resulting from poor temperature control because of the high heat of reaction. Nickel catalysts promoted with alumina are recommended by Dent *et al*[126]. Application in an ammonia synthesis plant, iron catalyst, is discussed by Shearon and Thompson[127].

The kinetics of the hydrogenation of CO to methane were studied by Akers and White[128] and Luyten[129]. Luyten reported that within limits, the rate obeyed the expression $r = k\ p_{H_2}^{.6}/p_{CO}^{.2}$. Binder and White[130] studied the hydrogenation of carbon dioxide. They concluded that a mechanism for which the slow step was the reaction of adsorbed carbon dioxide with two or more molecules of adsorbed hydrogen would explain their data on a nickel catalyst.

Of much greater and of fast growing industrial importance is the reverse reaction in which C_1 to C_4 hydrocarbons are "reformed" with steam to produce hydrogen and carbon oxides. The economics of producing ammonia or methanol from natural gas are more favorable than from coke, though the situation may be reversed if the cost of the former continues to rise. At gas costs of 20 cents/*M* cu ft and coke costs of $5/ton, costs are about equal[131]. At present, more hydrogen is made by this process than all others combined (over 80 per cent of the United States synthetic ammonia capacity[132]) and annual United States catalyst consumption, including that for new plants, is estimated at 500,000 lbs[132]. Reforming is also used in the gas industry to meet peak load requirements. Propane or other low-molecular weight hydrocarbons are reformed to give a mixture which is a good substitute for that normally supplied by the gas utility[133].

Reforming operations are generally carried out with the aid of nickel catalysts at 550 to 850°C, 0 to 20 psi pressure, steam/gas ratio 2–10, and a hydrocarbon space velocity of 200 to 2000. Since the reaction is very endothermic, it is necessary to supply large amounts of heat to the reactor. This can be done by heating with gas the 7-inch diameter tubes containing the catalyst[131] and letting the exit gas pass out through a central tube.

Catalyst problems are similar to those encountered in synthesis. Overheating of catalyst can readily occur if inlet feed is reduced too much without a corresponding reduction in heat input. This permanently deactivates commercial nickel catalysts if the temperature reaches about 1050°C probably because of loss in surface[134]. Nickel catalysts are poisoned by even very small amounts of sulfur gases (over about 4 ppm) but regain their activity when the poison is removed. Because of this and the common occurrence of sulfur in objectionable amounts, the Institute of Gas Technology has attempted to develop S-resistant catalysts. Sebastian and

TABLE 22. METHANE SYNTHESIS

Author	Chem. Abstracts	Ref.	Product or Subject
Nickel Catalysts			
Akers, W., and White, R.	**42**, 6085	*CEP*, **44**, 553 (1948)	kinetics with CO
Binder, G., and White, R.	**45**, 331	*CEP*, **46**, 563 (1950)	kinetics with CO_2
Booth, N., Jolley, L. J., and Tebboth, J.	**41**, 2228	Brit. 579,427	syn. cat.
Chakravarty, K., and Sarker, J. M.	**38**, 6178		alumina promoter
Dent, F. J., *et al.*	**43**, 2405		city gas manufacture
Gilkeson, M., White, R., and Sliepcevich, C.		*IEC* **45**, 460 (1953)	use of stainless steel
Itterbeek, A., and van Dingenen, W.	**36**, 6062		mechanism
Luyten, L.	**37**, 3662		kinetics
Luyten, L., and Jungers, J.	**41**, 2310		kinetics
Mayland, B., and Hays, G.	**43**, 7200	*CEP*, **45**, 452 (1949)	thermodynamics
Nicolai, J., d'Hont, M., and Jungers, J. C.	**41**, 4699		kinetics
Strickland-Constable, R. F.	**43**, 7666		mechanism
Yasuda, M.	**44**, 2715		use of waste catalyst

CEP = Chemical Engineering Progress

Riesz[135] found that prereduced nickel catalysts were poisoned more than those that were put on stream in the oxide form in the presence of the S-containing gas and that catalysts sulfided with elemental sulfur were even more resistant.

Aside from increasing methane equilibrium conversion and conversion rate, higher temperatures also increase the CO/CO_2 equilibrium ratio. The latter can be calculated from the shift reaction equilibrium constant values which are given elsewhere. At the temperatures normally used (700 to 900°C) equilibrium relative to the shift reaction is closely approximated with Ni catalysts. In syntheses employing both CO and H_2 such as alcohol and hydrocarbon synthesis, high temperatures (800 to 850°C) are used for the methane-steam reaction to obtain the desired ratio of H_2/CO while low temperature operation (700 to 750°C) is favored where only hydrogen and no carbon monoxide is wanted such as for ammonia synthesis.

The recent literature indicates that ethane, propane, and butane can be reformed as readily as methane over active Ni catalysts though the steam/hydrocarbon ratio should be increased to prevent coke formation.

Table 23. Methane Reforming

Author	Chem. Abstracts	Ref.	Subject or Product
Nickel Catalysts			
Arnold, M. R., Atwood, K., Baugh, H. M., and Smyser, H. D.		*IEC*, **44**, 999 (1952)	catalyst testing, etc.
Batchelder, H. K.	**41**, 5371		S-resistant catalysts
Hach, C.	**44**, 2715	U.S. 2,492,986	CO_2, Ni *vs.* Cu
Horsfield, S. W.	**42**, 8443		reforming in the gas industry
Ipatieff, V. N., Monroe, G. S., and Fischer, L. E.	**44**, 3221		low temperature H_2 prod.
King, J. D.	**38**, 4774	*GW* **121**, 18	review
	39, 2189	*GW*, **122**, 196 (1945)	review
Komatsu, S., and Kuraku, H.	**41**, 3267		nitrates of Mg + Ni
Murphree, E. V., Brown, C. L., and Gohr, E. J.		*IEC*, **32**, 1203 (1940)	
Murphy, E. J.	**40**, 6786		S-resistant catalysts
Ogura, T., and Nagai, H.	**43**, 1944		reaction with CO_2
Reed, R. M.	**40**, 5211		hydrogen production
Riesz, C. H., *et al.*		*IGT* Bull. #10	S poisoning
Riesz, C. H., *et al.*		*PE*, **24**, C-17	catalyst supports
Reitmeier, R. E., *et al.*		*IEC*, **40**, 620 (1948)	carbon deposition
Shapleigh, J. H.	**46**, 2271	U.S. 2,575,324	S-resistant catalyst
Sebastian, J., and Riesz, C.H.	**45**, 6828	*IEC*, **43**, 860 (1951)	S-resistant catalyst
Smith, W. M.	**44**, 11068	U.S. 2,522,468	synthesis gas
Standard Oil Development Co.	**44**, 11068	Brit. 641,945	synthesis gas prod.
Tuttle, H.A.		*CEP*, **48**, 272 (1952)	commercial process
Kuraku, H.	**41**, 3353		chromites, synthesis gas
	41, 2974		chromites
Murphree, E. V., Tyson, C. W., Campbell, D. L., and Martin, H. Z.	**41**, 7065	U.S. 2,425,754	Fe, fluid process

IEC = Industrial and Engineering Chemistry
GW = Gas World
IGT = Institute Gas Technology Bulletin
PE = Petroleum Engineer
CEP = Chemical Engineering Progress

Hydrocarbon Synthesis (Fischer-Tropsch)

This type of reaction has recently been so thoroughly covered by Storch, Golumbic and Anderson[136], Weil and Lane[137] and Pichler[138] that it seems unnecessary to add to it except for Table 24 which catalogs some of the recent literature. However, an interesting recent description of the Bureau of Mines Fischer-Tropsch plant by Kastens, Hirst and Dressler[139] is worthy of mention.

The Oxo Process (Hydroformylation)

The Oxo reaction is the catalytic addition of carbon monoxide and hydrogen to an olefin to form aldehydes containing one more carbon atom. The aldehydes are usually hydrogenated to alcohols in a second stage. First commercial development of the process is credited to the Germans (1940) who used it during World War II to convert olefinic Fischer-Tropsch products to alcohols. The latter were converted to detergents or plasticizers. Pressures of 20 to 250 atm. at temperatures of 125 to 200°C with the standard cobalt-thoria-kieselguhr Fischer-Tropsch catalyst were employed. The process has now been adopted in this country by the Standard Oil Co. (Indiana) and the Standard Oil Co. of New Jersey. The subject is discussed in Chapter V of Storch, Golumbic and Anderson's book and some of the recent literature is given in Table 25.

Hydrodesulfurization

Reactions of this type such as

$$C_2H_5SH + H_2 \rightarrow C_2H_6 + H_2S + 18 \text{ Kcal}$$

find considerable application[225] in converting the sulfur compounds in sour petroleum stocks to easily removable hydrogen sulfide. Sulfur compounds decrease the octane rating of leaded gasoline and are also corrosive. Many catalysts are severely poisoned by sulfur compounds and, hence, hydrodesulfurization and H_2S removal steps are often employed prior to the main catalytic process (for example, the reaction of natural gas with steam on Ni catalysts or naphtha reforming on Pt catalyst).

Dehydrogenation catalysts which are not appreciably poisoned by S constituents such as cobalt-molybdate, nickel-tungsten sulfide, zinc oxides and bauxite are commonly used. The recent literature is summarized in Table 26.

Ammonia Synthesis

The synthesis of ammonia from nitrogen and hydrogen ($\frac{1}{2}N_2 + \frac{3}{2}H_2 = NH_3 + 12$ Kcal) was one of the first significant catalyst applications and it

Table 24. Fischer-Tropsch*

Author	Chem. Abstracts	Ref.	Subject
		Cobalt Catalysts	
Anderson, R., Hall, W., and Hofer, L.	**42**, 8058	*JACS*, **70**, 2465 (1948)	catalyst properties
Anderson, R., Hall, W., and Krieg, A.	**43**, 3273	*JACS*, **71**, 183 (1949)	activities and surface areas
Bashkirov, A., Kagan, Y. B., and Kryukov, Y. B.	**45**, 7861		synthesis mechanism
Brotz, W., and Spengler, H.	**44**, 6249		physical structure
Clark, A.	**44**, 4655	U.S. 2,497,761	olefin recycle
Craxford, S. R.	**42**, 3648		chemistry of synthesis
	41, 262		promoter function
Craxford, S. R., and Poll, A.	**44**, 8086	*JCP*, **47**, 253 (1950)	catalyst reduction
Friedman, A. H.	**44**, 4656	U.S. 2,500,533	wax preparation
Ghosh, J., and Basak, N.	**42**, 5643		chromia promoter
Ghosh, J., Sastri, M. V. C., and Kini, K. A.		*IEC*, **44**, 2463 (1952)	adsorption of H_2O and CO
Hamai, S., Hayashi, S., and Shimamura, K.	**41**, 4367		promoters
Hofer, L., and Peebles, W.	**42**, 1483	*JACS*, **69**, 2497 (1947)	x-ray studies
Hofer, L., Peebles, W., and Bean, E. H.	**44**, 9223	*JACS*, **72**, 2698 (1950)	x-ray studies
Montgomery, C. W., and Weinberger, E.	**42**, 4437	*IEC*, **40**, 520 (1948)	product distribution
Mulford, R., and Russell, W. W.		*JACS*, **74**, 1969 (1952)	catalytic hydrogenation
Rubin, L. C., *et al.*		US. 2,615,035	fluid catalyst
Russell, W., and Miller, G. H.	**44**, 8616	*JACS*, **72**, 2446 (1950)	fluid catalyst
Schutza, H.	**43**, 6497		effect of water
Weller, S.	**42**, 1483	*JACS*, **69**, 2432 (1947)	kinetics
		Iron Catalysts	
Anderson, R. B., Seligman, B., Shultz, J. F., Kelley, R., and Elliott, M. A.		*IEC*, **44**, 391 (1952)	variables of synthesis
Anderson, R. B., Hofer, L. J., Cohn, E. M., and Seligman, B.	**45**, 6032	*JACS*, **73**, 944 (1951)	phase changes

Table 24—*Continued*

Author	Chem. Abstracts	Ref.	Subject
Anderson, R. B., Shultz, J. F., Seligman, B., Hall, W. K., and Storch, H. H.	**44**, 10299	*JACS*, **72**, 3502 (1950)	nitrides of iron
Ayres, E., Montgomery, C. W., and Hirsch, J. H.	**43**, 2401	*PR*, **27**, #11, 583 (1948)	side reactions
Bashkirov, A., *et. al.*	**45**, 7861		synthesis mechanism
Bilisoly, J. P.	**44**, 8092	U.S. 2,509,204	catalytic conversion
	44, 3701	U.S. 2,496,265	fluid catalysts
Braude, G., *et al.*	**42**, 7147		mechanism
Campbell, W., and Johnstone, H. F.		*IEC*, **44**, 1570 (1952)	iron-copper catalyst
Dickinson, N. L.	**44**, 1673	U.S. 2,481,089	mechanism
Early, J. C., and Kellner, H.		U.S. 2,609,345	regeneration
Eidus, Ya. T.	**39**, 4792		alkaline activator
Friedman, A. H., and Moran, J. N.	**44**, 1672	U.S. 2,488,530	solid hydrocarbons
Hemminger, C. E.	**45**, 8742	U.S. 2,560,344–5	process
Hall, C. C., Gall, D., and Smith, S. L.		*JIP*, **38**, #3 (1946)	comparison fixed and fluid bed techniques
Hall, W. K., Tarn, W. H., and Anderson, R. B.	**45**, 5907	*JACS*, **72**, 5436 (1950) *JPCC*, **56**, 688 (1952)	surface area, pore volume
Hawk, C., Stern, N., and Hofer, L.	**43**, 827	U.S. 2,449,071	catalyst preparation
Herbert, W.	**39**, 2636		activator
Hofer, L., Anderson, R. B., Peebles, W. C., and Stein, K. C.	**46**, 233	*JPCC*, **55**, 1201 (1951)	chloride poisoning
Hofer, L., and Cohn, E. M.	**44**, 8823	*AC*, **22**, 907 (1950)	thermomagnetics
Johnson, E. A.	**43**, 1551	U.S. 2,455,419	regeneration
Keith, P. C.	**43**, 5574	U.S. 2,470,216	motor fuel
Kodama, S., *et al.*	**43**, 2397 –2401		many variables
	43, 2412, 2413		adsorption of H_2 and CO
	44, 9135		many variables
Kolbel, H., Ackermann, P., Juza, R., and Tentschert, H.	**43**, 8117		mechanism
Kolbel, H., and Engelhardt, F.	**43**, 4828		mechanism
Kolbel, H., and Langheim, R.	**44**, 3235		mechanism

Table 24—*Continued*

Author	Chem. Abstracts	Ref.	Subject
Kummer, J. T., DeWitt, T. W., and Emmett, P. H.	**43**, 2080	*JACS*, **71**, 2081 (1949)	mechanism studies
Latta, J. E., and Walker S. W.		*CEP*, **44**, 173 (1948)	process
Lee, J. A.	**44**, 5075	*CE*, **54**, #10, 105 (1947)	fluid catalyst
Merkel, H.	**44**, 8564		thermomagnetics
Mosesman, M. A.	**43**, 6338	U.S. 2,470,748	catalyst preparation
Murphree, E. V., Tyson, C. W., Campbell, D. L., and Martin, H. Z.	**39**, 3900	U.S. 2,360,787	fluid process
Ogawa, T., Kimumaki, J., and Fujisaki, T.	**42**, 7011		properties
Ogorzaly, H. J.	**43**, 3175	U.S. 2,458,870	periodic hydrogenation
Pichler, H.	**43**, 7664		gasoline synthesis in the United States
Pichler, H., and Merkel, H.	**44**, 3696		chemical and magnetic properties
Roberts, G., Jr., and Phinney, J. A.	**41**, 4285	OGJ, **45**, 45, 72 (1947)	manufacture of gasoline
		OGJ, **43**, 47, 264 (1945)	fluid process
Ryan, P.	**39**, 4218		synthol process
	40, 2964		synthol process
Segura, M.	**43**, 8076, 9420		
Segura, M., McAdams, D. R., and Spicer, W. E.	**45**, 4430	U.S. 2,541,671	catalyst preparation
Scharmann, W. G.	**43**, 5928	U.S. 2,467,861	mixed catalysts
Shultz, J. *et al.*		*JACS*, **74**, 637 (1952)	composition changes
Standard Oil Development Co.	**43**, 8121	Brit. 621,902	catalyst preparation
Stewart, M. M.	**42**, 8430	U.S. 2,438,584	nonsintered Fe catalyst
U.S. Bureau of Mines	**43**, 2397	Rept. Inv. #4456 (1949)	1948 Report
Vesterdal, H. G.	**44**, 317	U.S. 2,471,129	promoters
Voorheis, A.	**43**, 9420	U.S. 2,479,439	fluidized catalyst
Walden, G. Pierce, J. A., and Segura, M. A.	**44**, 1673	U.S. 2,488,150	catalyst preparation and regeneration
Walker, S. W.	**44**, 1672	U.S. 2,485,945	fluid type catalyst
Nickel Catalysts			
Booth, N., Wilkins, E. T., Jolley, L. J., and Tebboth, J. A.	**43**, 2402		mechanism

TABLE 24—*Continued*

Author	Chem. Abstracts	Ref.	Subject
Chakravarty, K., and Chakravarty, P.	**41**, 1989		effect of K_2CO_3
Chakravarty, K.	**43**, 2853	*Nature*, **160**, 907 (1947)	x-ray diffraction
Cornuault, P.	**44**, 8213		adsorption phase
Kimberlin, C. N., Jr. and Schexnailder, R. E., Jr.	**44**, 2206	US. 2,488,128	silica microspheres as a carrier
Michel, A., Bernier, R., and LeClerc, G.	**44**, 7638		thermomagnetics
Perrin, M.	**43**, 26		reduction with H_2
Teichner, S.	**43**, 27		specific surface and reduction
Trambouze, Y., and Perrin, M.	**44**, 9783		catalyst composition
Trambouze, Y.	**44**, 7132		differential thermal analysis
Zaidenman, I., and Khomyakov, K.	**45**, 8336		thermal studies

Other Catalysts

Author	Chem. Abstracts	Ref.	Catalyst	Subject
Dewey, D. R.	**40**, 7557		$ZnO\text{-}Al_2O_3$, $ThO_2\text{-}Al_2O_3$	Kaiser Wilhelm Institute
Frankenburg, W. G.	**44**, 7046	U.S. 2,507,510	TiB	mechanism
Grahame, J. H.	**44**, 7516	U.S. 2,503,724	$ZnO\text{-}Al_2O_3$	mechanism
Kita, G.	**42**, 6091		$Fe_2O_3\text{-}CuO$	oil from CO and H_2
Pichler, H., and Ziesecke, K. H.	**44**, 814, 815		$ThO\text{-}ZrO_2$	high pressure synthesis of isoparaffins
	44, 7040	U.S. Bur. Mines Bull. #488 (1950)		the isosynthesis
Teichner, S.	**44**, 7635 **43**, 8830			kieselguhr supports

JACS = Journal of the American Chemical Society
JCP = Journal of Chemical Physics.
IEC = Industrial and Engineering Chemistry
PR = Petroleum Refiner
JIP = Journal of the Institute of Petroleum
JPCC = Journal of Physical & Colloid Chemistry
AC = Analytical Chemistry
CEP = Chemical Engineering Progress
CE = Chemical Engineering
OGJ = Oil and Gas Journal

* For a more complete listing of 1953 literature see *IEC*, **45**, 1976 (1953).

TABLE 25. OXO PROCESS

Author	Chem. Abstracts	Ref.	Subject or Product
Adams, C. E., and Burney, D. E.	**43**, 5032	U.S. 2,464,916	alcohols and aldehydes
Atwood, K.		*IEC* **45**, 1981	review
Bhattacharyya, S., and Rao, B.		*JSIR*, **11B**, #2, 80 (1952)	proprionaldehyde
Bureau of Mines		Proc. TOM 12.13.14, p. 137	alcohols, German process
Clark, W.	**43**, 3180		Esso, isooctyl alcohol
Hart, M., Hoog, H., and Weeda, K.	**45**, 2607	U.S. 2,529,236	catalyst reactivation
Kiddoo, G.		*CE*, **58**, #9, 149 (1952)	review
N. V. de. B. P. M.	**44**, 1526		process, alcohols and aldehydes
Roelen, O.	**44**, 8856		aldehydes
Sherwood, P. W.		*PE* **27**, #7, C-13	review
		PP **8**, 241 (1953)	review
Wender, I., Levine, R., and Orchin, M.	**44**, 2439	*JACS*, **71**, 4160 (1949)	mechanism

IEC = Industrial and Engineering Chemistry
JACS = Journal of the American Chemical Society
CE = Chemical Engineering
JSIR = Journal of Scientific and Industrial Research (India)
PE = Petroleum Engineer
PP = Petroleum Processing

continues to rank as one of the most important. Annual production of synthetic ammonia in the United States was 1,600,000 tons in 1949[140] and expansion completed or under way at the present time will increase this about 50 per cent[141]. Soil depletion, population increase and usage for war purposes insure an expanding demand for ammonia products. Details of a typical Haber-Bosch plant have recently been published[142]. A plant using the Claude process was described by Shearon and Thompson[143].

Surveys of the older literature have been made by Emmett[144] and by Berkman, Morrell and Egloff[145]. More recently the theoretical aspects have again been reviewed by Emmett[146] and by Fleming[147]. A booklet by Nielsen[148] lists 250 references.

The last ten years have not seen any fundamental change in catalysts or catalytic processes. A study of the thermodynamics of nitrogen and hydrogen at high pressures has recently appeared[149]. Promoted fused magnetite-type catalysts are still in general usage and a description of their manufacture and performance has been given by Bridger *et al*[150]. Their

Table 26. Hydrodesulfurization

Author	Chem. Abstracts	Ref.	Catalyst	Subject
Atwood, K.		*IEC*, **45**, 1985		review
Berg, Clyde		*PP*, Feb. 1952	Co molybdate	
Bonner, W. A.		*JACS*, **74**, 1033 (1952)	Ni	source of H_2
Brusset, H.	**43**, 2080		C	fuel gases
Byrns, A., Bradley, W. E., and Lee, M. W.	**37**, 6862	*IEC*, **35**, 1160 (1943)	Co molybdate	desulfurization of gasoline
Cole, R. M., and Davidson, D.	**44**, 2216	*IEC*, **41**, 2711 (1949)	W, Ni, S	
Darlington, F. H.	**44**, 5077		$MgSO_4$-ZnO	H_2S
Glushnev, V., and Vasilev, S.	**43**, 8125		H_3PO_4, ZnCl	desulfurization of gas
Griffith, R. H.	**44**, 7516	Brit. 636,560		
Hale, J. H., Simmons, M. C., and Whisenhunt, F. P.	**44**, 2212		Co-Mo, bauxite and alumina	desulfurization of crude oil
Haresnape, J. N., and Porter, F. W. B.	**44**, 11079	Brit. 632,195	Co molybdate	desulfurization of gasoline
Herglotz, H., and Lissner, A.	**44**, 10474		Co Raney	
Huffman, H. C.	**42**, 7971	U.S. 2,437,532	Co molybdate	
Nahin, P., and Huffman, H. C.	**45**, 10569	U.S. 2,486,361	Co-Mo, Ni-W	desulfurization reforming
Owen, J. J.	**43**, 7214	U.S. 2,468,510	Cu	
Sheffer, M.	**43**, 8578	U.S. 2,479,520	Cu	HCN, Cl_2, CO_2, SO_2 (acid gas removal)
Sands, A. E., Wainwright, H. W., and Egleson, G. C.	**44**, 9136	U.S. Bur. Mines Inv. No. 4699, 51 (1950)	Huff Cat.	organic S removal

PP = Petroleum Processing
IEC = Industrial and Engineering Chemistry
JACS = Journal of the American Chemical Society

long life (several years), and ruggedness have established their leading position. Considerable progress has been made relative to synthesis and decomposition kinetics on this type of catalyst which is discussed at length by Emmett[146]. Patents have recently been issued on catalysts claimed to be active at lower temperatures where equilibrium is much more favorable[151, 152]. Fluid bed operation, particularly with the aid of ultrasonic vibrations[153], also appears to offer promise for lower temperature and/or pressure synthesis. Nielsen[154] reports the catalyst thermostability to be increased by lime addition to a potassia-alumina promoted fused magnetite, whereas Uchida[155] claims that lime lowers the thermostability of an Fe-K_2O-Al_2O_3 catalyst. The latter work is very comprehensive, covering the variation of activity with composition for many catalysts.

Selective Hydrogenation

Since many organic compounds can be hydrogenated to more than one product, it is often necessary not only that other classes of reactions not occur, but also that only the desired hydrogenation or dehydrogenation reactions take place. This problem has received considerable attention and has been thoroughly considered by Adkins[156] as applied to liquid phase reactions on Ni and Cu-Cr_2O_3 catalysts. The selective action may involve:

(1) Hydrogenation of one functional group but not another.

(2) Hydrogenation or dehydrogenation to the desired product but not further reaction to undesired products. Selective action may be obtained by several approaches as discussed below.

Use of Optimum Contact Time. In cases in which the desired product is capable of undergoing further reaction, such as the partial hydrogenation of acetylene to ethylene, contact time is of extreme importance. The shorter the time of contact the less chance for further hydrogenation. Unconverted reactants can be recycled to obtain high yields but this is often impractical. Hence, it is important to have a catalyst which gives a narrow contact time distribution so that at optimum space velocity almost all molecules will have time enough to be converted but few will have time enough to react further.

Adjustment of Conditions for Thermodynamic Selectivity. By use of suitable temperatures and pressures it is sometimes possible to make the undesired reaction thermodynamically impossible while desired reaction is favored. For example, hydrogen may be made to react with acetaldehyde to give ethane rather than ethanol by the use of temperatures greater than 300°C where equilibrium is unfavorable for the latter reaction.

Choice of Catalyst and Conditions. The most commonly used approach is to find a catalyst which under some conditions will favor one reaction over the other. This technique is discussed at length by Adkins[156] (see Adkins' Table 58) in which the selective action of Ni and Cu-Cr_2O_3 catalyst for hydrogenating various functional groups is pointed out. Seldom is the nature of selective action clear, but certainly differences in catalyst and functional group geometry play an important role. Adkins has attributed the preferential activity of Cu-Cr_2O_3 for the hydrogenation of groups containing oxygen and the preferential activity of Ni for carbon-carbon unsaturation to selective adsorption.

Table 28, which is largely based on Adkins' work and on recent literature,

TABLE 27. AMMONIA SYNTHESIS AND DECOMPOSITION

Author	Chem. Abstracts	Ref.	Subject
Iron Catalysts			
Annable, D.		*CES* (*France*) **1**, 145 (1952)	Temkin equation application
Atwood, K.		*IEC* **45**, 1984	review
Bridger, G. L., Pole, G. R., Beinlich, A. W., Jr., and Thompson, H. L.	**41**, 5265	*CEP*, **43**, 291 (1947)	catalyst production and performance
Brill, R.		*JCP*, **19**, 1047 (1951)	rate equations
de Boer, J. H.	**46**, 1339		synthesis adsorption
Burnett J. A., Allgood H. Y., and Hall, J. R.		*IEC*, **45**, 1678 (1953)	catalyst stabilization
Cirilli, V.	**41**, 7215		alumina-silica promotion
Emmett, P. H., and Kummer, J.	**37**, 4958	*JPCC*, **55**, 337 (1951)	kinetics
Emmett, P. H.		See ref. 146, page 214.	review
Farrar, G. L.		*OGJ*, **51**, #32, 82 (1952)	ammonia plant
Grinevich, V. M.	**40**, 3576		raw materials
Hall, W. K., Tarn, W. H., and Anderson, R. B.	**45**, 5907	*JACS*, **72**, 5436 (1950)	surface areas, etc.
Khrizman, I., and Korneyiuchuk, G.	**38**, 5719		kinetics
Hein, L. B.		*PP*, **7**, 1462 (1952)	low pressure process
		CEP, **48**, 412 (1952)	synthesis at 350 atm.
Koppe, P.	**44**, 8067		Haber-Bosch at Leuna
Koyana, T.	**41**, 3356		decomp. of NH_3
Kummer, J. T., and Emmett, P. H.	**45**, 8335	*JACS*, **73**, 2886 (1951)	Co chemisorption
	45, 5502		hydrogen adsorption
Love, K. S., and Brunauer, S.	**36**, 3092	*JACS*, **64**, 745 (1942)	alkali promoter
Love, K. S., and Emmett, P. H.		*JACS*, **63**, 3297 (1941)	kinetics
McGeer, J. P., and Taylor, H. S.	**45**, 8337	*JACS*, **73**, 2743 (1951)	decomposition on Re
Maxwell, L., Smart, J. S., and Brunauer, S.	**45**, 8829	*JCP*, **19**, 303 (1951)	catalyst thermodynamics
McCartney, J. T.		*JAP*, **22**, 1441 (1951)	electron microscope studies
Nielsen, A., and Bohlbro, H.		*JACS*, **74**, 963 (1952)	triply promoted catalysts

TABLE 27—*Continued*

Author	Chem. Abstracts	Ref.	Subject
Peters, C.		Oppau Ammonia Lab. 3042–165 PBL 73594	effect of promoters
Richardson, C. N.	**44**, 4643	U.S. 2,500,008	ultrasonic effect
Sastri, M., and Srikant, H.	**45**, 7406		nitrogen adsorption
	45, 9993		hydrogen adsorption
Shearon, W. H., and Thompson, H. L.		*IEC*, **44**, 254 (1952)	1000 atm. process
Shima, G.	**45**, 5888	cf. *CA*, **46**, 8832	sintered catalyst
Shinbo, M.		*CEJ*, **16**, 147	diffusion
Slack, A. V., *et al.*		*CEP*, **49**, 393	TVA plant
Temkin, M. I., and Pyzhev, V. M.		*AP* (*USSR*), **12**, 327 (1940)	kinetics
Temkin, M. I.	**45**, 3699	*JPC* (*USSR*), **24**, 1312 (1950)	kinetics
Temkin, M. I., and Kiperman, S.	**45**, 1854 **42**, 2501		kinetics, high recycle
Thompson, H. L., *et. al.*		*CEP*, **48**, 9, 468 (1952)	1000 atm. process
Uchida, H., *et al.*	**46**, 2245	cf. *CA*, **46**, 2246	effect of promoters, etc.
Wilchinsky, Z. W.	**44**, 969	*AC*, **21**, 1182 (1949)	catalyst morphology
Yamaguchi, S.	**46**, 1855	*JPCC*, **55**, 1409 (1951)	x-ray study

Other Catalysts

Author	Chem. Abstracts	Ref.	Catalyst	Subject
Kiperman, S.	**42**, 5320		Ru	kinetics
Kiperman, S., and Granovaskaya, V.	**45**, 9346		osmium	kinetics on osmium
Kiperman, S., and Temkin, M. I.	**41**, 332		W	kinetics
	40, 6950		Mo	kinetics
McGeer, J. P., and Taylor, H. S.	**45**, 8337	*JACS*, **73**, 2743 (1951)	Re	kinetics
Miyazaki, S.	**45**, 7864		Pt, Ni	decomposition
	45, 6473		W, Mo	decomposition
Odelhog, S.	**43**, 1536	Brit. 609,756	Mg + Ni	300°C catalyst
	44, 10273	Brit. 640,170		
Souby, A., and Schiller, J. C.	**45**, 6355	U.S. 2,550,389	Ni, W sulfide	low temp. pres. syn.
Suzuki, S.		*JAP*, 277 ('51)	cyanide comp.	cat. prep.

CES = Chemical Engineering Science (France)
CEP = Chemical Engineering Process

TABLE 27—*Continued*

JCP = Journal Chem. Physics
JPCC = Journal of Physical and Colloid Chemistry
OGJ = Oil and Gas Journal
JACS = Journal of the American Chemical Society
PP = Petroleum Processing
IEC = Industrial and Engineering Chemistry
CEJ = Chemical Engineering (Japan)
AP (USSR) = Acta Physicochim
JPC (USSR) = Journal Physical Chemistry
AC = Analytical Chemistry
JAP = Journal of Applied Physics

shows in an approximate manner the relative activity and temperature requirements of different active agents for the hydrogenation and dehydrogenation of various functional groups. It must be realized, however, that promoters such as alkalies and physical factors such as surface area and pore structure also play an important role in selective action. Homologues may differ appreciably from the specific compounds tabulated. Selectivity with these limitations can be predicted from Table 28 by observing the temperatures at which the different functional groups react. For example, consider the problem of selective hydrogenation of styrene to toluene. For good yields, hydrogenation of the benzenoid ring and hydrogenolysis of carbon-carbon bonds must be avoided while operating at temperatures high enough to hydrogenate the double bond. According to the table, nickel at temperatures of 140 to 170°C, iron at 150 to 200°C and Cu-Cr_2O_3 at 160 to 240°C would be expected to do the job. As another example, the hydrogenation of benzaldehyde to benzyl alcohol may be considered. It appears that nickel would probably give low yields because the hydrogenolysis reaction to toluene occurs at about the same temperature. However, it seems as if Cu-Cr_2O_3 at 160 to 180°C would be satisfactory.

OXIDATION

Oxidation is defined herein as a reaction in which a transfer of oxygen is involved. Usually free oxygen is one of the reactants but alternatively, H_2O, etc., may act as carriers. Water may or may not be a reaction product. If free oxygen is involved, the breaking of an oxygen-oxygen bond must occur.

Older reviews of the subject are given in the following references:

1. Lewis, B., and von Elbe, G., "Combustion, Flames and Explosions of Gases," New York, The Macmillan Co., 1938.
2. Ellis, C. "The Chemistry of Petroleum Derivatives," Vol. I, (1934); Vol. II New York, Reinhold Publishing Corp., 1937.

TABLE 28. CATALYTIC ACTIVITY OF VARIOUS CATALYSTS FOR DIFFERENT HYDROGENATION REACTIONS

Reaction Type	hydrogenation of hydrocarbons				hydrogenation of aromatics				dehydro-cyclization		hydrogenolysis of carbon-carbon bonds[1] (hydrocracking)		hydrogenation of oxyorganics (carbonyls, etc.)				hydrogenolysis of carbon-oxygen bonds		hydrogenolysis of nitrogen-oxygen bonds	
Catalyst	$H_2 + H_2C{=}CH_2 \rightleftharpoons CH_3CH_3$				$\phi H + 3\ H_2 \rightleftharpoons C_6H_{12}$				$C_7H_{16} \rightarrow \phi CH_3 + 4\ H_2$		$RCH_3 + H_2 \rightarrow RH + CH_4$		$H_2 + CH_3CHO \rightleftharpoons CH_3CH_2OH$				$C_2H_5OH + H_2 \rightarrow C_2H_6 + H_2O$	$\phi CH_2OH + H_2 \rightarrow \phi CH_3 + H_2O$	$\phi NO_2 + 3H_2 \rightarrow \phi NH_2 + 2H_2O$	
	→		←		→		←						→		←					
	rank	temp.[2]	rank	temp.[2]	rank	temp.[2]	rank	temp.[2]	rank	temp.[2]	rank	temp.[2]	rank	temp.[2]	rank	temp.[2]	temp.[2]	temp.[2]	rank	temp.[2]
Pt	2	125	2		1	175	1	400	1	450	3	425	1	100	1	250				
Pd	1	120	1		1	175	1	400												
Ni	3	130	3		2	180	1	400	1	450	1	350	2	125	2	250	270	140	1	175
Fe	4	140	4		3	240	2	>320			2								2	185
Cu	6		6	600	5	295	5	450			5		4	175	4	300			4	245
Co															3	275				
$Cu\text{-}Cr_2O_3$	5	150	5		4	250	4	440				450	3	150			300	190	3	220
MoO_2							3	430	2	475	4									
Cr_2O_3									3	485										
Mn_2O_3															5	370				
V_2O_3	8	400		600			5	450												
WO_3	7	325																		

---

[1] Depends greatly on other substituents. Diketones undergo C—C cleavage at temperatures as low as 125°C. Primary alcohols hydrocrack on Ni at 250°C.

[2] Estimated approximate temperature (°C) required for substantial vapor phase reaction.

3. Groggins, P. H., "Unit Processes in Organic Synthesis," New York, McGraw-Hill Book Co., 1935.
4. Marek, L. F., "Twelfth Catalysis Report, National Research Council," New York, John Wiley & Sons, Inc., 1940.
5. Berkman, S., Morrell, J. C., and Egloff, G., "Catalysis," 533–549, New York, Reinhold Publishing Corp., 1940.
6. Marek. L. F., and Hahn, D. E., "Catalytic Oxidation of Organic Compounds in the Vapor Phase," New York, Chemical Catalog Co., (Reinhold Publishing Corp.), 1932.

Newer work of a general nature is given in the references below:

7. Marek, L. F., *Ind. Eng. Chem.*, **40,** 1685 (1948); **41,** 1892 (1949); **42,** 1718 (1950); **43,** 1990 (1951); **44,** 2052 (1952).
8. Lewis, B., and von Elbe, G., *Ind. Eng. Chem.*, **40,** 1590 (1948); **41,** 1851 (1949); **43,** 1925 (1951).
9. Karpacheva, S. M., and Rozen, A. M., "Oxygen Exchange Between Catalysts and Reactants," *Doklady Akad. Nauk. USSR*, **75,** 55 (1950).
10. "Kinetics of Oxidation Reactions," *Trans. Faraday Soc.*, **42,** 99–398 (1946).
11. Marek, L. F., "Oxidation," Groggins, P. H. "Unit Processes in Organic Synthesis," 3rd Ed., New York, McGraw-Hill Book Co., 1947.
12. Hatch, L. F., "Oxidation of Hydrocarbons, *Pet Ref.*, **32,** 123 (1953).

Theory

The ability to give and take oxygen appears to be a prime requirement for an oxidation catalyst. Elements that form relatively unstable oxides (surface or bulk compounds) which are capable of reacting with the material being oxidized, but yet can be regenerated by oxygen or by an oxygen carrier under reaction conditions, are generally active catalysts. These are invariably transition group elements (Group VIII) and subgroup I elements. Examples given in Table 29 include all the common oxidation catalysts.

Oxidation reactions are generally quite exothermic and irreversible. It

TABLE 29. POSSIBLE VALENCE STATES DURING CATALYSIS

Element	Reaction	Possible Higher Oxidation State	Possible Lower Oxidation State
Cu	$CO + \frac{1}{2}O_2 \rightarrow CO_2$	CuO	Cu
Ag	$C_2H_4 + \frac{1}{2}O_2 \rightarrow C_2H_4O$	Ag_2O	Ag
Pt	$4NH_3 + 5O_2 \rightarrow 4NO + 6H_2O$	PtO	Pt
V	$C_{10}H_8 + 4\frac{1}{2}O_2 \rightarrow C_6H_4(CO)_2O + 2CO_2 + 2H_2O$	V_2O_5	V_2O_4
Fe	$CO + H_2O \rightleftharpoons CO_2 + H_2$	Fe_3O_4	Fe
Mn	$CO + \frac{1}{2}O_2 \rightarrow CO_2$	MnO_2	Mn_2O_3
Ni	$C_4H_{10} + 6\frac{1}{2}O_2 \rightarrow 4CO_2 + 5H_2O$	Ni_2O_3 or NiO	NiO, Ni

is usually necessary to dilute the reactants greatly, use a fluidized bed, use small diameter catalyst tubes, etc., to prevent severe hot spots with resultant catalyst deterioration. Large pore catalysts are generally preferred for such reactions because of greater uniformity of contact time and consequent better selectivity. Some oxidation reactions are extremely rapid such as the oxidation of ammonia so that the relatively low surface area of platinum gauze is sufficient.

Types of Oxidation

Catalytic oxidation reactions involving free oxygen can be divided into the principal types listed below:

(1) Oxygen addition:

(a) $SO_2 + \frac{1}{2}O_2 \rightarrow SO_3 + 23$ Kcal

(b) $C_2H_4 + \frac{1}{2}O_2 \rightarrow C_2H_4O + 65$ Kcal

(c) $CO + \frac{1}{2}O_2 \rightarrow CO_2 + 67$ Kcal

(d) $CH_3CHO + \frac{1}{2}O_2 \rightarrow CH_3COOH + 68$ Kcal*

(e) $C_6H_6 + \frac{1}{2}O_2 \rightarrow C_6H_5OH + 50$ Kcal

(2) Oxygenolysis of carbon-hydrogen bonds:

(a) $C_2H_6 + \frac{1}{2}O_2 \rightarrow C_2H_4 + H_2O + 26$ Kcal

(b) $C_2H_5OH + \frac{1}{2}O_2 \rightarrow CH_3CHO + H_2O + 45$ Kcal**

(c) $CH_3OH + \frac{1}{2}O_2 \rightarrow HCHO + H_2O + 38$ Kcal***

(d) $\frac{1}{2}O_2$ + olefin ($> 3C$) → unsaturated aldehyde or ketone + H_2O

(e) aliphatic hydrocarbons + nO_2 → oxygenated hydrocarbons + nH_2O†

(3) Oxygenolysis of nitrogen-hydrogen bonds:

$5/4O_2 + NH_3 \rightarrow NO + 6/4H_2O + 56$ Kcal

---

* Tennessee Eastman Co. is stated to make 85,000 tons/year of acetic acid anhydride using this reaction as an intermediate step, though no statement is made as to whether it is carried out catalytically. Carbide & Carbon Co.'s new plant in Texas City produces acetic anhydride by direct catalytic oxidation of acetaldehyde at low temperature.[159]

** The vapor phase catalytic reaction has been studied by Michels and Keyes[162].

*** Used for the bulk of U.S. formaldehyde production (about 100,000 tons/year) of which about 60 per cent is used in plastics or resin manufacture.

† The direct oxidation of propane and other aliphatic hydrocarbons has assumed considerable importance with the erection of a plant in Bishop, Texas, by the Celanese Corp. of America and by McCarthy Chemical Co., in Winnie, Texas, but according to Marek[160] the process is noncatalytic.

(4) Partial oxidation involving both the oxygenolysis of carbon-carbon bonds and carbon-hydrogen bonds:

$$C_{10}H_8 + 4\tfrac{1}{2}O_2 \rightarrow C_6H_4(CO)_2O + 2CO_2 + 2H_2O + 440 \text{ Kcal}$$

(5) Complete combustion involving both the oxygenolysis of carbon-carbon bonds and carbon-hydrogen bonds††

(a) $C_2H_6 + 3\tfrac{1}{2}O_2 \rightarrow 2CO_2 + 3H_2O + 341 \text{ Kcal}$

(b) $C_2H_5OH + 3O_2 \rightarrow 2CO_2 + 3H_2O + 305 \text{ Kcal}$

(6) Oxygenolysis of sulfur-hydrogen and sulfur-carbon bonds:

(a) $H_2S + \tfrac{1}{2}O_2 \rightarrow S + H_2O + 90 \text{ Kcal}$

(b) $CS_2 + 4O_2 \rightarrow CO_2 + 2SO_3 + 310 \text{ Kcal}$

Catalysts for Direct Oxidation

Vanadium Catalysts. Applications of vanadium catalysts for the oxidation of naphthalene to phthalic anhydride and SO_2 to SO_3 are of such commercial importance that they have received more attention in recent literature (Table 30) than any other type oxidation catalyst. Yearly United States production of sulfuric acid by contact catalytic processes with vanadium catalysts totals about 6 million tons[168] while phthalic production is estimated to be 120,000 tons/year[169]. Little of the recent literature, however, is concerned with sulfuric acid catalysts although the capacity of contact plants employing vanadium catalysts has more than doubled in the period 1941–1952. Earlier literature on this subject is reviewed by Fairlie[169] and by Marek[170].

The manufacture of fluid vanadium oxide catalyst for the production of phthalic anhydride has been described by Hathaway and Myrick[171]. It is based on a German formulation[172] described in FIAT and BIOS reports. Yields of 80 per cent with a life of over ten years are claimed.

Platinum Catalysts. The most important commercial oxidation process using platinum (usually in the form of gauze at 800°C) is the oxidation of ammonia to nitrogen oxides[173]. A comprehensive mechanism study of this reaction was recently reported by Zawadski[174]. Usage of Pt for sulfur trioxide synthesis has lost ground to vanadium catalysts because of high cost and sensitivity to arsenic poisoning[21]. Michels and Keyes[162] have studied the oxidation of ethyl alcohol to acetaldehyde, etc., with a platinum-silica gel

†† Complete combustion is seldom carried out catalytically. However, recent developments indicate important catalyst applications. Sophia Berkman[163, 164] recently announced a practical gasoline engine with piston walls made out of catalytic material which serves to reduce engine knock. E. J. Houdry of the Oxy Catalyst Manufacturing Co.[165] and others[166, 167] have announced catalytic processes for combustion of hydrocarbon fumes which can be used for smoke and fume abatement as well as heat generation.

catalyst. E. J. Houdry[165] and the Catalytic Combustion Corp.[166, 167] have developed platinum catalysts and processes for the complete combustion of hydrocarbon fumes at about 260°C. Recent literature is summarized in Table 30.

Silver Catalysts. Silver catalysts are used without exception for the oxidation of ethylene to ethylene oxide. Although the process has not yet assumed important commercial stature[175], much research (Table 30) has been carried out and a large fluid bed unit is under construction[176]. McBee, Haas, and Wiseman[177] using a Ag on corundum catalyst reported optimum conditions to be 225 to 325°C, high air/ethylene ratio and small addition of ethylene dichloride to suppress other reactions. Plant design features for a proposed German plant have been published[178]. Another important process[179, 180] using silver catalysts but about which little has appeared in recent literature is the oxidation of methanol to formaldehyde.

Nickel Catalysts. Little application has been made of nickel oxidation catalysts except in cases of complete combustion. Examples are given in Table 30.

Copper Catalysts. Usage of copper catalysts appears to be pretty much limited to oxidation of carbon monoxide to dioxide and alcohols to aldehydes and ketones. The McCarthy Chemical Co. may have employed copper oxidation catalyst for converting methanol to formaldehyde[180, 181]. The Carbide and Carbon Chemicals Corp. use a copper catalyst and a halide poison for side reactions for making glyoxal from ethylene glycol[161]. R. V. Green[166] has developed a copper chromite catalyst for the complete combustion of organic fumes (260°C).

Manganese Catalysts. Manganese catalysts find applications similar to copper catalysts. They are very active for CO oxidation particularly when promoted with CuO and CoO (hopcalite catalysts). It appears that the unusual nature of manganese carbonate may be responsible for this high activity[182]. However, they are readily poisoned by water vapor for this reaction. Recent literature is given in Table 30.

Iron Catalysts. Iron catalysts find little commercial use for direct oxidation reactions. Their lack of more general application can possibly be attributed to poor selectivity.

Oxidation by Oxygen Carriers

Examples of vapor phase catalytic reactions of this type include,

$$\text{(a)}\quad CO + H_2O \leftrightharpoons CO_2 + H_2 + 9.8\ \text{Kcal. } (400°C)$$

$$\text{(b)}\quad P_4 + 16H_2O \leftrightharpoons 4H_3PO_4 + 10H_2 + 176\ \text{Kcal. } (700°C)$$

The Shift Reaction. Reaction (a), commonly known as the water gas shift reaction, is of considerable industrial importance. It is usually used

TABLE 30. OXIDATION

Author	Chem. Abstracts	Ref.	Subject
Olefin Oxides from Olefins			
Silver Catalysts			
Aries, R.	**43**, 8399	U.S. 2,477,435	catalyst preparation
Becker, S. B.	**42**, 923	U.S. 2,430,443	fluid catalyst
Becker, S. B., and Arveson, M. H.	**40**, 344	U.S. 2,376,987	butadiene synthesis
Carter, R. M.	**37**, 890	U.S. 2,294,383	alumina refractory
Cambron, A., and McKim, F.	**42**, 334	U.S. 2,426,761	from silver oxalate
		U.S. 2,562,858	ex. Ag-Ca alloy
Cook, G. A.		U.S. 2,530,509	Al-Fe catalyst
Finch, H., and Bergsteinsson, I.	**41**, 6577	Brit. 587,584	catalyst preparation
Finch, H. deV., and Bergsteinsson, I.	**41**, 6890	U.S. 2,424,085	deposition on carriers
Foster, A. L.		*PE*, **25**, #4, C-38 (1953)	fluid process
H.A.C. for S., and I. R.	**42**, 1034	Brit. 591,670	catalyst preparation
Jefferson Chemical Co.		U.S. 2,533,204	
Heider, R. L., and Stehman, C. J.	**43**, 3446	U.S. 2,458,266	alumina carrier
Heider, R. L.		U.S. 2,554,459	BeO carrier
Law, G. H.	**40**, 5445	Can. 435,242	process
Metzger, K.		Oppau Ammonia Lab. 1938 Repts. FIAT Film 18, Frames 5818–6488	Pt and Pd activity
McBee, E. T., Haas, H. B., and Wiseman, P. A.	**39**, 2736	*IEC*, **37**, 432 (1945)	catalyst preparation
McKim, F., and Cambron, A.	**44**, 2836		kinetics
Nevison, J. A., and Lincoln, R. M.	**44**, 2550	U.S. 2,491,057	temperature control
Reyerson, L., and Oppenheimer, H.	**38**, 6178	*JPCC*, **48**, 290 (1944)	catalyst preparation
Robertson, N. C., and Allen, R. T.		U.S. 2,587,841	BaO + ZnO promoter
Sears, G. W., Jr.		U.S. 2,615,899–900	fluid catalyst
Twigg, G. H.	**41**, 3354	*PRS*, A, **188**, 92 (1946)	mechanism
	41, 2385	*TFS*, **42**, 284 (1946)	mechanism
Wan, Shen-Wu		*IEC*, **45**, 234 (1953)	kinetics

Table 30—*Continued*

Author	Chem. Abstracts	Ref.	Subject
West, T. J., and West, J. P.	**43**, 9299	U.S. 2,479,833–5	catalyst preparation
	43, 4289	U.S. 2,463,228	catalyst preparation
Cook, G. A.		U.S. 2,530,509	Al-Fe catalyst
Sears, G. W., Jr.		U.S. 2,615,900	fluid catalyst
Carbon Dioxide from Carbon Monoxide Copper Oxide Catalyst			
Bowen, B. E. V., Howlett, J., and Wood, W. L.	**44**, 8628	*JSCI* (*London*), 69, 65 (1950)	removal of acetylene
Chitani, T., Nakata, S., and Kanome, A.	**41**, 4366		mechanism
Garner, W. E., Gray, T., and Stone, F.	**44**, 2355	*PRS, A*, **197**, 294 (1949)	kinetics
Kanome, A., and Chitani, T.	**41**, 2974		mechanism
Mooi, J., and Selwood, P. W.		*JACS*, **74**, 2461 (1952)	structure and activity
Murdock, R. E., Brooks, F. R., and Zahn, V.	**42**, 2208	*AC*, **20**, 65 (1948)	combustion catalyst
Rienäcker, G.	**44**, 1314		effect of additives
Schenck, R.	**44**, 10473		activation energies
Turovskii, G. Ya., and Vainshtein, F. M.	**45**, 8336		mechanism
Silver Catalysts			
Dubrisay, R., and Favart, M.	**46**, 1855		metallized carbons
Fainshtein, S. M.	**41**, 6121		mechanism
Ishiwatari, T., and Chitani, T.	**41**, 3354		mechanism at different temperatures
Johnson, W. T. M., and Krieger, K. A.	**45**, 1857	Brookhaven Conf. Rept. #4, 16, Jan. 1950	mechanism
Platinum Catalysts			
Higginbotham, B. M.	**41**, 3592	U.S. 2,418,175	gas ignition
Krauss, W.	**45**, 29		kinetics
Margolis, L., and Todes, O.	**41**, 4028		kinetics

Table 30—*Continued*

Author	Chem. Abstracts	Ref.	Subject
		Manganese Oxide Catalysts	
Dolique, R., and Galindo, J.	**38**, 2555		mixed catalysts
Mooi, J., and Selwood, P. W.	**45**, 2298		mechanism
Petitpas, T., Cheylan, E., and Mathieu, M.	**40**, 5986		catalyst structure
		Miscellaneous Catalysts	
Akamatsu, H., and Sato, K.	**44**, 7637		Fe catalyst, mechanism
Keier, N., and Roginskii, S.	**41**, 6801		ex nickel carbonate
Margolis, L.	**45**, 2578		V catalyst
Rienäcker, G.	**44**, 10473		ThO_2-CeO_2
		Sulfur Trioxide from Sulfur Dioxide	
		Vanadia Catalysts	
Agliardi, N.	**41**, 7197		activation, adsorption of SO_2 and O
Boreskov, G. K., Ritter, L. G., and Volkova, E.	**43**, 8251		heating-up temperature determination
Calderbank, P. H.		*CEP*, **49**, 585 (1953)	converter design
		JAC, **2**, 482 (1952)	mechanism
Collette, F., and Scheepers, L.	**44**, 7636		reaction rates
Hirai, T.	**42**, 6495		pressure drop
Krichevskaya, E. L.	**41**, 6121		kinetics
Shogam, S. M.	**40**, 4860		manufacturing
Sirotkin, G. S.	**43**, 2744		deterioration of catalyst
Topsøe, H., and Nielsen, A.	**42**, 7946		activation
		Iron Catalysts	
Boreskov, G. K., and Sokolova, T. I.	**40**, 5211		kinetics
Garbato, C.	**44**, 2716		entrained iron oxide catalyst
		Platinum Catalysts	
Chesalova, V. S., and Boreskov, G. K.	**46**, 9961		preparation method *vs.* activity and area

Table 30—*Continued*

Author	Chem. Abstracts	Ref.	Catalyst	Subject
Water Synthesis				
Bruns, B. P.	**45**, 6912		Ag, CuO	mechanism
Rosenblatt, E. F.		U.S. 2,582,885	Pt	catalyst preparation
Roginskii, S. Z., Tret'yakov, I., and Shekhter, A. B.	**44**, 1313		Pt	electron microscope study
Tamura, M., and Shida, S.	**44**, 1313		Pt	catalyst activity comparison
Tret'yakov, I.	**44**, 7638		Pt	"zonal changes"
Wendlandt, R.	**44**, 2711		Pt	mechanism
Oxidation of Alcohols to Aldehydes				
Bohmfalk, J. F., *et al.*		*IEC*, **43**, 786	CuO	glyoxal
Cozzi, D.	**38**, 4499		vanadia	mechanism
Distillers Co., Ltd.	**46**, 1669	Brit. 658,240	CuO and Se	catalyst preparation
du Pont	**42**, 1961	Brit. 593,837–8	$MgO-MnO_2-MoO_3$	catalyst preparation
Field, E.	**44**, 10967	U.S. 2,519,751	Mn oxide	catalyst preparation
Hull, D. C., and Quarles, J.	**43**, 7609	U.S. 2,475,965	Cu oxide	effect of variables
McNall		U.S. 2,532,930	Fe, Ag	ozone activation
Parker, P. T.	**43**, 8398	U.S. 2,477,321	CuO	German chemical industry
Saito, H.	**45**, 4541		Mn, Co, Fe, Ni, V oxides	comparison
Stiles, A. B.	**44**, 2548	U.S. 2,491,695	Bi Molybdate	manufacturing
Martinuzzi, E.	**42**, 8058		vanadia	variables
Oxidation of Ammonia to Nitrogen Oxides Platinum Catalysts				
Apel'baum, L., and Temkin, M. I.	**45**, 1856 **42**, 5321		wire gauze	low pressures, mechanism
Pirie, J. M.	**42**, 5175		Pt-Rh *vs.* Pt	German indust. study
Stand. Oil Dev. Co.	**41**, 6678	Brit. 586,131		fluid cat.
Tuszynski, K.	**44**, 10472			temp. and Sp. vel.
Union chimique de belge	**41**, 7688	Brit. 449,156		mechanism
Wagner, C.	**44**, 10472		gauze	conversion calcn.
Zawadzki, J.	**45**, 9987			mechanism

TABLE 30—*Continued*

Author	Chem. Abstracts	Ref.	Catalyst	Subject
Nickel Catalysts				
Atroshchenko, V. I., and Konvisar, V. I.	**42**, 6066			filter net disint.
Krauss, W.	**44**, 2711			low temp. studies
Iron Catalysts				
Bubb, L. P., and Scott, A. B.		*JACS*, **73**, 4422 (1951)		activity vs. area and susceptibility
Krauss, W.	**44**, 2711			mechanism
Miscellaneous Catalysts				
Kobe, K. A., and Hosman, P. D.	**42**, 6063	*IEC*, **40**, 397 (1948)	Mn Bi oxides	process
Krauss, W.	**44**, 2711		CoO, Mn, Bi_2O_3	mechanism
Morita, N.	**41**, 3356		Cr oxides	low temp. studies
Sasaki, K.	**46**, 2246		CoO	temp. and economics
Schmid, G., and Keller, N.	**44**, 8214		CoO	
Teter, J. W.	**40**, 1294	U.S. 2,392,107	CoO	
Zawadzki, J.	**45**, 9987		CuO-MnO_2 Fe_2O_3-Bi_2O_5-MnO_2 CuO-MnO_2-$CaCO_3$	mechanism

Oxidation of Naphthalene to Phthalic Anhydride

Vanadia Catalysts*

Author	Chem. Abstracts	Ref.	Product or Subject
Beach, L. K., and Connolly, G. C.	**43**, 6338	U.S. 2,471,853	mechanism
Becker, S.	**43**, 2236	U.S. 2,453,740	mechanism
Connolly, G. C.	**44**, 5499	U.S. 2,504,001	cat. prep.
Cooper, W. C.	**44**, 8022	U.S. 2,510,803	cat. prep.
Kinney, C. R., and Pincus, I.		*IEC*, **43**, 2880 (1951)	feedstock comparison
Levine, I. E.	**43**, 7510	U.S. 2,474,001	mechanism

TABLE 30—*Continued*

Author	Chem. Abstracts	Ref.	Product or Subject
Longwell, J. P.	**44**, 2561	U.S. 2,491,500	process
Porter, F.	**37**, 890	U.S. 2,294,130	phosphate promoter
Shreve, R., and Wellborn, R.	**37**, 2004	*IEC*, **35**, 279 (1943)	various cats.
Tomeo, M., and Serrallonga, J.	**42**, 7274		process
Welty, A. B.	**44**, 2022	U.S. 2,485,342	heat control
Ruthruff, R. F.	**41**, 7740	U.S. 2,425,398	fluid process
Anon.		*CW*, **70**, No. 8, 40 (1952)	fluid bed plants
Sherwood, P. W.		*PR*, **32**, #3, 111 (1953)	commercial practice
Oxidation to Maleic Anhydride Vanadia Catalysts			
Anon.		*CIW*, **68**, #13	
		CE, **60**, #7, 238	plant
Bretton, R. H., Wan, S., and Dodge, B. F.		*IEC*, **44**, 594 (1952)	C_4 oxidation
Morrell, C. E., Beach, L. K., and Cunningham, M. E.	**44**, 5905	U.S. 2,504,034	process
Shinoyama, H., and Baba, G.	**43**, 7506		process
Shmidl, A.	**43**, 7039	U.S. 2,474,334	catalyst activation
Miscellaneous Products Vanadia Catalysts			
Cislak, F. E., and Otto, M. O.	**43**, 1811	U.S. 2,456,380	nicotinonitrile
Gulbransen, E., and Andrew, K.	**45**, 1412		chem. properties
Imperial Chemical Industries	**44**, 8022	Brit. 638,031	preparation
Kiddoo, G.		*CE*, **59**, #9, 168 (1952)	phthalic anhydride from xylene
Pongratz, A.	**43**, 7803		sintering
Ridge, D., and Emblem, H.	**43**, 8074		preparation
Roellman, W. F.		U.S. 2,526,689	fluid catalyst
Schlesman, C. H., Denton, W. I., and Bishop, R. B.	**43**, 1805	U.S. 2,456,597	phenol, process
Schalya, V. V. *et al.*	**45**, 1855		mechanism
Vorozhtsov, N., and Gurevich, D.	**40**, 7538		preparation
Woodward, C. F., Badgett, C. O., and Willaman, J. J.	**38**, 3899	*IEC*, **36**, 540 (1944)	nicotinonitrile

* See text for further references on vanadia catalysts.

Table 30—*Continued*

Author	Chem. Abstracts	Ref.	Subject or Product
Silver Catalysts			
Dubrisay, R., and Favart, M.	**42**, 4436		benzoic acid
Pshezhetskii, S. Ya., and Kamentskaya, S. A.	**43**, 5272		acetone, kinetics
Schenck, R., Bathe, A., Keuth, K., and Suss, S.	**37**, 3659		preparation
Twigg, G. H.	**41**, 1920		oxygen chemisorption
Platinum Catalysts			
Butyagin, P., and Elovich, S.	**45**, 3229		propylene oxide, mech.
Butyagin, P., and Margolis, L.	**43**, 6565		cat. ox. of hydrocarbons
Michels, L. R., and Keyes, D. B.		*IEC*, **34**, 138 (1942)	ethanol oxidation
Schalya, V. V., *et al.*	**45**, 1855		mechanism
Copper Oxide Catalysts			
Andreev, E., and Kavtaradze, N.	**43**, 6898		phosphorous
Hearne, G. W., and Adams, M. L.	**44**, 2011	U.S. 2,486,842	acrolein
	43, 2222	U.S. 2,451,485	acrolein
Karpacheva, S. M., and Rozen, A. M.	**44**, 917		oxygen exchange
Ladisch, R., and Simon, A.	**37**, 2254		cat. prep.
Lel'chuk, S. L., and Belen'kaya, A.	**41**, 2071		aliphatic carboxylic acids
Manganese Catalysts			
Baker, G. A., and Hunter, W.	**43**, 5421	Brit. 616,330	ketone or carbinol
Corner, E. S., and Lynch, C. S.	**45**, 6824	U.S. 2,553,551	carbon monoxide
Jenness, L. G.	**44**, 2145	U.S. 2,486,530	preparation
Rodier, Mme. G., and Rodier, G.	**44**, 4764		magnetic properties
Usines de Melle	**43**, 669	Brit. 603,175	aliphatic acids
Karpacheva, S. M., and Rozen, A. M.	**44**, 917		oxygen exchange

TABLE 30—*Continued*

Author	Chem. Abstracts	Ref.	Subject or Product
Nickel Catalysts			
Church, J. M., and Lynn, L.	**44**, 9345	*IEC*, **42**, 768 (1950)	methyl methacrylate
Corner, E. S., McGee, R. V. J., and Lynch, C. S.	**44**, 7046	U.S. 2,507,502	oxygen carriers

Miscellaneous Catalysts

Author	Chem. Abstracts	Ref.	Catalyst	Subject
Butyagin, P., and Margolis, L.	**43**, 6565		C, $MgO\text{-}Cr_2O_3$	cat. ox. of hydrocarbons
Brinkmann, G.	**44**, 418		C	H_2O_2
Brown, O. W., and Frishe, W. C.	**42**, 1793	*JPCC*, **51**, 1394 (1947)	thallium oxide	
Dolique, R., and Galindo, J.	**38**, 2555		$MnO_2\text{-}CuO\text{-}CoO$	mixed catalysts
Griffith, R. H., and Newling, W.	**43**, 7212	Brit. 622,324	TiO_2 or TiS_2	cat. ox. of H_2S
Kreimer, G. S., and Vakhovskaya, M. R.	**44**, 1304		W and Ce C	H_2O
Margolis, L., and Todes, O.	**42**, 7148 **46**, 4342		Cu-Cr oxide	ox. of isooctane affect of poisons
Mottern, H., and Mistretta, V.	**43**, 2222		ZnO, Bi_2O_3	methyl heptenone
Mugdan, M., and Young, D. P.	**44**, 3888	*JCS*, 2988 (1949)	OsO_4, WoO_3	glycol
Nippon Vol. Oil Co.	**43**, 1433		TiO_2, ZrO_2	olefin
Winslow, E. C.	**44**, 26	*JCE*, **26**, 497 (1949)	cerium molybdate	benzaldehyde
Bohmfalk, J. F., McNamee, R. W., and Barry, R. P.	**45**, 6321	*IEC*, **43**, 786 (1951)	iron	glyoxal

JPCC = Journal of Physical & Colloid Chemistry
JCS = Journal of the Chemical Society
JCE = Journal of Chemical Education
IEC = Industrial and Engineering Chemistry
PRS = Proceedings of the Royal Society
TFS = Transactions of the Faraday Society
JSCI = Journal of the Society of Chemical Industry (London)
JACS = Journal of the American Chemical Society
AC = Analytical Chemistry
JAC = Journal of Applied Chemistry
CIW = Chemical Industries Week
CEP = Chemical Engineering Progress
CE = Chemical Engineering
CW = Chemical Week
PE = The Petroleum Engineer

as one step in the preparation of hydrogen which may be used for ammonia synthesis, Fischer-Tropsch synthesis, hydrogenation of organic compounds, metallurgical reductions, etc. Feed material may be "reformed" methane, water gas, producer gas, etc., plus steam (steam/gas ~ 2). A good description of catalyst manufacture and usage in an ammonia plant has been given by Bridger, Gernes and Thompson[183]. Present yearly catalyst consumption in the United States, including that for new plants, probably totals about 2,500 tons/year despite a catalyst life of several years.

Equilibrium data from work of Emmett and Shultz[184] are given below.

Temp, °C	450	500	600	700	800
K_p	7.1	4.8	2.7	1.6	1.25

Reed[185] gives the following empirical expression:

$$K_p = \frac{(CO_2)(H_2)}{(H_2O)(CO)} = .0202\, e^{(7350/^\circ F+400)}.$$

It therefore follows since reaction rates increase with temperature, that with other conditions constant there is a temperature of maximum conversion. This increases with space velocity and decreases with an increase in catalyst activity.

Earlier literature on the subject is summarized by Berkman, Morrell and Egloff[186]. Recent work is listed in Table 31. Although other elements have been investigated (ZnO, V_2O_5, chromates, TiO_2, Co_2O_3, NiO), and it has been claimed that fused copper-cobalt oxide is more active at low temperatures[187], nearly all recent work, including that concerned with commercial catalysts, deals with iron oxide promoted with chromia with or without a magnesia binder. The effect of the chromia promoter has been investigated by Chin Ri[188], Bridger, Gernes and Thompson[183] and Ivanovskii[189] who found it to increase activity or stability.

Little fundamental work on kinetics has appeared. Rigamonti and Agliardi[190] report the rate to be proportional to about $p_{CO}^{0.7}$ on zinc oxide. Atwood, Arnold and Appel[191] in an investigation concerned with the effect of pressure utilize an expression for iron catalysts which can be derived by assuming the rate to be proportional to $k_1 p_{CO} - k_2 p_{CO_2}$. Emmett[192] has pointed out that a possible mechanism for the reaction is the following:

$$\text{(a) } 4CO + Fe_3O_4 \rightarrow 3Fe + 4CO_2$$

$$\text{(b) } 3Fe + 4\ H_2O \rightarrow Fe_3O_4 + 4H_2$$

Chemical analysis of equilibrium catalyst indicates an iron valence state very close to Fe_3O_4 which would indicate that if the above mechanism is correct, reaction (b) is much more rapid than reaction (a) under test conditions[193]. The influence of surface area does not appear to have been in-

TABLE 31. OXIDATION BY OXYGEN CARRIERS

Author	Chem. Abstracts	Ref.	Subject
Shift Reaction Iron Oxide Catalysts			
Allgood, H. Y., *et. al.*		S. W. Reg. ACS Meet. (Oct. 1951)	S poisoning
American Magnesium Metals Corp.	**37**, 2525		catalyst prep.
Ashley, K. D., and Innes, W. B.	**46**, 1188		magnesia binder
Atwell, K., and Schroeder		CIOS Rept. 5/15/45	German preparation
Atwood, K., Arnold, M. R., and Appel, E. G.	**44**, 9137	*IEC*, **42**, 1600 (1950)	effect of pressure
Atwood, K., and Arnold, M. R.		*IEC*, **45**, 424 (1953)	effect of additives
Barkley, L. W., Corrigan, T. E., Wainwright, H. W., Sands, A. E.		*IEC*, **44**, 1066 (1952)	reverse reaction
B.I.O.S. Overall Report #1		P.B. 88981–5, p. 37	high pressure operation
Bridger, G. L., Gernes, D. C., Thompson, H. L.	**42**, 4723	*CEP*, **44**, 368 (1948)	catalyst development
Bureau of Mines		Report C7368	German preparation
Carter, A. G.	**43**, 840	Brit. 604,376	catalyst preparation
Christain, D., and Boyd, Paul, B., Jr.	**43**, 5133	*CE*, **56**, #5, 148 (1949)	catalyst comparisons
Dely, J. G.	**41**, 4626	U.S. 2,419,255	extruded cat. prep.
Faragher, W. F., and Horne, W. A.	**40**, 7535		brown oxide cat. prep.
French Patent 935,719	**44**, 292		fluidized bed
Gosselin, A.	**42**, 1190		high pressure operation
Ivanovskii, M. D., *et al.*		*JCI* (*USSR*), **12**, 37 (1934)	siderite catalyst
Kirillov, I. P., and Sirotkin, G. D.	**43**, 3599		catalyst preparation
N. V. de B. P. M.	**44**, 6054		copper magnesia cat.
Kul'kova, N. V., and Temkin, M. I.	**43**, 7308	*JPC* (*USSR*), 23, 695 (1949)	kinetics
Oppau Ammonia Lab.		P.B. 73,594	brown oxide, high pressure
Reed, R. M.	**39**, 5055	*PR*, **24**, 349 (1945)	comm. H_2 production
Ri, K. C.	**43**, 1945		effect of Cr_2O_3 content

Table 31—*Continued*

Author	Chem. Abstracts	Ref.	Subject
Roiter, V. A., Gaukhman, S. S., Pisarjhevskaya, N. P., and Gvaliya, T. M.	**40**, 4593		mechanism
Stowe, V. M.	**39**, 4204	U.S. 2,365,562	magnesia carrier
Rigamonti, R., and Agliardi, N.	**44**, 9784		kinetics, zinc oxide

Steam Phosphorus Reaction

Author	Chem. Abstracts	Ref.	Catalyst	Subject
Hein, L. B., Megar, G. H., and Striplin, M. M.	**44**, 9641	*IEC*, **42**, 1616 (1950)	Cu cat	pilot plant
Shultz, J. F., Tarbutton, G., Jones, T. M., Deming, M. E., Smith, C. M., and Cantelou, M. B.	**44**, 9641	*IEC*, **42**, 1608 (1950)	Pt, Pd, Cu	catalyst development
Brunauer, S., and Shultz, J. F.		*IEC*, **33**, 828 (1941)	phosphate rock	effect of catalyst

IEC = Industrial and Engineering Chemistry
CEP = Chemical Engineering Progress
CE = Chemical Engineering
JCI (USSR) = Journal of Chemical Industries (USSR)
PR = Petroleum Refiner
JCP (USSR) = Journal of Physical Chemistry (USSR)

vestigated but granule or pellet size seems to have a major effect on activity[191].

Side reactions do not complicate the shift reaction at atmospheric pressure and high steam/carbon monoxide rates but at low steam/gas ratios and high pressures, methane or other hydrocarbon synthesis might be expected. Other catalyst problems include sulfur poisoning, scaling, spalling, loss in active surface, etc.

Steam Oxidation of Phosphorus. Although this process has not assumed industrial importance, three interesting investigations on the subject have appeared in recent literature. Shultz[194] *et al.* found that Pt, Pd and Cu supported on aluminum or zirconium phosphate were highly active for the reaction at 650 to 700°C.

HALOGENATION AND DEHALOGENATION

All reactions involving gain or loss of halogen are classified in this group. Examples of the principal reaction types are listed below.

Direct Halogenation of Paraffins

$$CH_4 + Cl_2 \rightarrow CH_3Cl + HCl + 33\ \text{Kcal}$$

$$CH_4 + 2Cl_2 \rightarrow CH_2Cl_2 + 2HCl + 60\ \text{Kcal}$$

$$CH_4 + 4Cl_2 \rightarrow CCl_4 + 4HCl + 127\ \text{Kcal}$$

$$CH_4 + 4F_2 \rightarrow CF_4 + 4HF + 403\ \text{Kcal}$$

Chlorination of Paraffins with O_2 and HCl

$$C_2H_6 + HCl + \tfrac{1}{2}O_2 \rightarrow C_2H_5Cl + H_2O + 41\ \text{Kcal}$$

Deacon Process[195-198]

$$4HCl + O_2 \rightarrow 2Cl_2 + 2H_2O + 28\ \text{Kcal}$$

Temp, °K	50	100	300	500
$\log_{10} K$	130	50	13	5

Friedel-Craft Reaction

$$C_6H_6 + C_2H_5Cl \rightarrow C_6H_5C_2H_5 + HCl + 9\ \text{Kcal}$$

Halogen Reaction With Unsaturates

$$HCl + C_2H_3Cl \rightarrow CH_3{-}CHCl_2 + 16\ \text{Kcal}$$

$$HCl + C_2H_4 \rightarrow CH_3{-}CH_2Cl + 15\ \text{Kcal}$$

$$HI + C_4H_8 \rightarrow C_4H_9I + 19\ \text{Kcal}\ (430°\text{C})$$

$$C_2H_4 + Cl_2 \rightarrow C_2H_3Cl + HCl + 24\ \text{Kcal}$$

$$C_2H_2 + HCl \rightarrow CH_2{=}CHCl + 23\ \text{Kcal}$$

$$C_2H_2 + 2Cl_2 \rightarrow CHCl_2CHCl_2 + 87\ \text{Kcal}$$

$$C_2H_2 + 2F_2 \rightarrow CHF_2CHF_2$$

Halogenation of Aromatics

$$C_6H_6 + Cl_2 \rightarrow C_6H_5Cl + HCl + 30\ \text{Kcal}$$

$$C_6H_6 + 6Cl_2 \rightarrow C_6Cl_6 + 6HCl$$

$$C_6H_6 + 6F_2 \rightarrow C_6F_6 + 6HF$$

Halogenation of Oxygen Compounds and the Hydrolysis of Organohalides

$$HCl + C_2H_5OH \leftrightarrow C_2H_5Cl + H_2O + 4\ \text{Kcal}$$

$$HF + 3C_2H_5OH \leftrightarrow C_2H_5F + C_2H_5OC_2H_5 + 2H_2O$$

$$C_6H_5OH + HCl \leftrightarrow C_6H_5Cl + H_2O$$

Older literature on halogen reactions is reviewed by Berkman, Morrell and Egloff[199], as well as Williams and Vaughn[200]. Recent work is well summarized by McBee and Pierce[201]. Recent literature dealing largely with vapor phase processes is given in Table 32.

Vapor phase catalytic processes are seldom used for reactions of this class though the recent literature indicates a trend in this direction. The ease with which most halogenations can be carried out with or without photochemical aid makes catalysts unnecessary in most cases, although halogen carriers are frequently used especially for fluorination.

Of primary, but until recently of diminishing importance, is the Deacon process for chlorine manufacture now largely supplanted by electrolysis. In this process HCl and air or oxygen are passed over a copper chloride supported catalyst (pumice, tile, etc.) at 350 to 400°C. Only two references dealing with the heterogeneous Deacon process are listed in Table 32, although the availability of tonnage oxygen has sparked new interest[196, 197]. A very interesting article by Crawford[195] has recently appeared dealing with the catalytic vapor phase chlorination of organics by means of HCl and O_2.

Direct halogenation of hydrocarbons is readily accomplished without catalysts but vapor phase catalytic processes are sometimes used to obtain better control and selectivity for the desired product with lower temperature operation. Supported copper and silver halides are usually used. Heat dissipation is a major problem particularly in fluorinations necessitating the use of diluents, heat conductive carriers, etc. Another catalyst problem is catalyst deactivation due to polymeric material. The catalytic action of Hg and Cu for fluorination is explainable[203] on the basis of the following steps using benzene fluorination as an example.

$$2AgF + F_2 \rightarrow 2AgF_2$$
$$18AgF_2 + C_6H_6 \rightarrow C_6F_{12} + 6HF + 18AgF$$

Supported copper, zinc and mercury halide catalysts are commonly used for hydrochlorination reactions.

Interesting work has been published by Russian workers[204, 205] (Table 32) on the catalytic hydrolysis of chlorbenzene to phenol with silica gel and copper chloride-silica gel catalysts.

HYDRATION AND DEHYDRATION

This class of reactions is limited herein to those in which water is transferred, added or abstracted in which gaseous hydrogen is not involved. Dehydrations may be either intramolecular (e.g., dehydration of an alcohol) or intermolecular (e.g., ester formation). Liquid phase processes which are more generally employed for hydration reactions are not considered. A comparison of vapor phase with liquid phase processes is given

TABLE 32. HALOGENATION-DEHALOGENATION

Author	Chem. Abstracts	Ref.	Catalyst	Product or Subject
Arnold, C. W., and Kobe, K. A.		*CEP*, **48**, 293 (1952)		thermodynamics, Deacon process
Amaker, T.	**43**, 3463	U.S. 2,460,564	$ThCl_4$, $CuCl_2$	$ClC_6H_3(CO)_2O$
Barton, D., and Mugdan, M.	**44**, 8854	*JSCI* (*London*), **69**, 75 (1950)	$AgCl_2$	vinyl chloride
Belic, I.	**44**, 6824		Ag foil	$C_6H_6Cl_6$
Blumer, D. R.	**40**, 2599	U.S. 2,395,314		chlorine
Bordner, C. A.	**44**, 7863	U.S. 2,504,919	Fe, Cu	olefins
Boyd, T.	**43**, 2629	U.S. 2,446,124	HgX-CeX-HCl	ethyl chloride
Boreskov, G. K., and Dzis'ko, V. A.	**45**, 2759		silica gel	phenol
Bralley, J. A.	**43**, 5790	Brit. 617,335	Hg	ethyl chloride
Brown, H. T., and Gorin, E.	**42**, 1048	U.S. 2,425,861	silica-alumina	gasoline
Cady, G. H., Grosse, A. V., Barber, E. J., Burger, L. L., and Sheldon, Z. D.	**41**, 3745	*IEC*, **39**, 290 (1947)	AgF	fluorocarbons
Cass, O. W.	**42**, 4565	*IEC*, **40**, 216 (1948)	Cu, Ag, Bi	furfural derivatives
Cherniavsky, A. J.	**44**, 6875	Brit. 635,013	Zn, Al, Bi, Fe	$C_2H_4Cl_2$
Codignola, F., and Piacenza, M.	**44**, 1126		phosphoric acid	dihalopentane
Churchill, J. W.	**42**, 6840	U.S. 2,440,786	C	$C_2H_2Cl_4$
Cremer, E., and Baldt, R.	**44**, 8216		many	ethylene
Darragh, J. L.	**43**, 7041	U.S. 2,473,990	clay	chlorobenzene
Du Pont	**44**, 2543	Brit. 628,165	$AlCl_3$	$CClF_3$
Du Pont	**42**, 333	Brit. 590,381	HgO, CaF_2	vinyl fluoride
Dzis'ko, V. A., Vishnevskaya, A. A., and Chesalova, V.	**45**, 4123		silica gel	phenol
Eberle, J. F.	**44**, 319	U.S. 2,481,207	Cu	alkylate
Faith, W. L.	**39**, 2738	*IEC*, **37**, 438 (1945)	V_2O_5	maleic, fumaric acid
Foster, R. T.	**45**, 2865	Brit. 639,435	$CuCl_2$-Al_2O_3	ethyl chloride
Freidlin, L. K., *et al.*	**45**, 3228		silica gel	phenol
	45, 5502		silica gel	phenol
	42, 2241		silica gel	phenol
Gevaert Photo-Product.	**45**, 3966	Brit. 643,743	Hg salt	vinyl halides
Gorin, E. Fontana, C. M., Kidder, G. A.	**43**, 1714	*IEC*, **40**, 2128 (1948)	KCl, $CuCl_2$	methyl chloride
Gorin, M. H., and Gorin, E.	**44**, 1248	U.S. 2,488,083	silica-alumina	liquid hydrocarbons

TABLE 32—*Continued*

Author	Chem. Abstracts	Ref.	Catalyst	Product or Subject
Green, H. D., and Taylor, D. S.	**41**, 1697	U.S. 2,413,496	Na cyanide	acrylonitrile
Gutner, R., *et al.*	**41**, 2310		Cu	phenol
Hearne, G., and La France, D. S.	**43**, 663	U.S. 2,446,475	Cu salt	chloroprene
Hillyer, J. C.	**44**, 1127	U.S. 2,480,021	$HgCl_2 + CaCl_2$	vinyl halides
Horton, A. W.	**40**, 345	U.S. 2,385,444	C	chlorohexanes
Hughes, E. C., Veatch, F., and Elersich, V.	**44**, 8878	*IEC*, **42**, 787 (1950)	$CuCl_2$	methyl aniline
Imperial Chem. Ind.	**43**, 4685	Brit. 615,634	$ZnCl_2$	Cl compound
	42, 7312	Brit. 600,296	Hg salt	vinyl fluoride
Ipatieff, V. N., and Schmerling, L.	**42**, 582	U.S. 2,427,791	Ni	alkyl halide
Lazier, W. A.	**40**, 1864	U.S. 2,389,626	gold halides	vinyl chloride
Lonza, Elek.	**43**, 6644		$HgCl_2$	vinyl chloride
McKim, F., and Cambron, A.	**44**, 2836		Ag	ethylene oxide
Miller, H. S.	**43**, 1433	U.S. 2,448,110	$AgCl_2ThCl_4$	vinyl chloride
Miller, C. B., and Bratton, F. H.	**44**, 5374	U.S. 2,478,201	AlF_3	chlorofluorocarbons
Musgrave, W., and Smith, F.	**44**, 3876	*JCS*, 302 (1949)	AgF	fluorocarbons
Neimark, I. E., *et al.*	**45**, 9350		silica gel	phenol
Ohta, N.	**46**, 1855		silica gel, $CuCl_2$	phenol
Park, J. D., Sharrah, M. L., and Lacher, J. R.	**43**, 7407	*JACS*, **71**, 2339 (1949)	$CaSO_4$	chlorofluorocarbons
Patat, F., and Weidlich, P.	**43**, 6969		$HgCl_2$	vinyl chloride
Pie, P. F., Jr.	**36**, 5484	U.S. 2,280,928	C	carbon tetrachloride
Potter, C., and Baron, S.	**45**, 10018	*CEP*, **47**, 473, (1951)	C	phosgene
Ramage, A. S.	**42**, 6839	U.S. 2,441,287	Pb-Ag-Sb	ethylene dichloride
Randall, Merle	**46**, 520	U.S. 2,547,139	$CuCl_2$	C_2Cl_4 , $C_2H_2Cl_4$
Richardson, R. W., and Pierce, J. A.	**43**, 1160	U.S. 2,451,870	Cr, Mn, V oxides	chlorine
Riches, W. W.	**44**, 247	U.S. 2,482,289	Cu	reactivation
Schwabb, L. E., and Hoelscher, H. E.		*CEP*, **48**, 564 (1952)	alumina	propyl chloride
Stanley, H. M., and Philip, T. B.	**38**, 980	U.S. 2,329,795	$HgCl_2$-C	vinyl chloride

Table 32—*Continued*

Author	Chem. Abstracts	Ref.	Catalyst	Product or Subject
Stern, G., and Friedrichsen, W.	**36**, 779		MgX	alkyl halides
Thomas, C. A., and Morris, H. E.	**36**, 6546	U.S. 2,285,473	$FeCl_3$	isopropyl chloride
Van Atta, G. R., and Dietrich, W. C.	**43**, 7502	U.S. 2,466,340	$CoPO_4$	fatty acid derivative
Wibaut, J. P., Sixma, F. L. J., and Suyver, J. F.	**44**, 7296		$FeBr_3$, $FeCl_3$	$C_{10}H_7Br$
Young, R. B.		U.S. 2,590,810	$CuCl_2$, carbon	vinyl chloride

CEP = Chemical Engineering Progress
JSCI = Journal Society of Chemical Industry (London)
IEC = Industrial Engineering Chemistry
JACS = Journal of the American Chemical Society
JCS = Journal of the Chemical Society

by Aries[206]. Several reviews of the earlier work[207–210] and summaries of the recent work have been written[211–213].

Knowledge of equilibrium constants is of vital importance in hydration reactions since equilibrium conversions in excess of 90 per cent are rarely realized at ordinary conditions. For example, equilibrium constants for ethylene hydration to ethanol are[207]:

Temp, °K	298	400	500	600	700
10^3K_p	3080	260	15.5	2.4	0.6

For higher olefins, hydration equilibrium is less favorable[214] and consequently even lower temperatures must be used for hydration reactions. In general, intramolecular dehydrations are endothermic and high equilibrium conversion is obtained only at high temperatures and low pressures. Intermolecular dehydration equilibrium is not in general markedly affected by temperature or pressure.

A complicating factor in nearly all reactions of this class is the occurrence of competitive, secondary and side reactions. In the hydration of an olefin to an alcohol, for example, the olefin may also undergo polymerization and the alcohol may undergo dehydration to an ether or dehydrogenation to an aldehyde. A comprehensive study of selectivity (dehydrogenation *vs.* dehydration) in the case of ethyl alcohol and formic acid decomposition was carried out on a variety of catalysts by Schwab and Schwab-Agallides[215]. They concluded that the physical state of the catalyst was important as well as its chemical nature. Sintering or recrystallization was found to favor dehydrogenation.

Substantially all hydration-dehydration catalysts have in common a strong affinity for water. The prime example is alumina which has a water content of several per cent even at 600°C, which can be attributed to chemisorption. Alumina catalysts are usually used for the dehydration of alcohols (Table 32), and rate data of Brey and Krieger[216] indicate the following steps in the process.

(1) adsorption of reactant
(2) surface decomposition (rate controlling)
(3) rapid desorption of olefin
(4) desorption of water.

The affinity of the surface for water is probably related to the activation energy for the surface dehydration. They found that the activity per unit surface area for ethyl alcohol dehydration at 400°C declined rapidly with increasing temperature of pretreatment over 600°C. This might be explained on the basis of the heat treatment in some way rendering the surface less hydrophilic. This could be checked by water sorption studies.

Next to alumina in point of usage for reactions in this class comes phosphoric acid or acid salts on various inert carriers (Table 33). They also have a strong affinity for water. Other active catalysts include silica-alumina gel, various metal combinations with alumina, clays, etc. Combinations of silica gel with tantala, zirconia or hafnia proved most suitable[217, 218] for butadiene synthesis.

Among the reaction types that fall in this class are the following:

alcohol synthesis $CH_2{=}CH_2 + H_2O \leftrightarrow CH_3CH_2OH^* + 11$ Kcal

aldehyde synthesis $HC{\equiv}CH + H_2O \leftrightarrow CH_3{-}CHO + 40$ Kcal

ketone synthesis $2HC{\equiv}CH + 2H_2O \leftrightarrow CH_3{-}CO{-}CH_3 + CO_2 + 85$ Kcal

ester synthesis $CH_3OH + HCOOH \leftrightarrow HCOOCH_3 + H_2O + 5.6$ Kcal

alkyl aryl synthesis $ROH + \phi H \leftrightarrow R\phi + H_2O$

amine synthesis $CH_3OH + NH_3 \leftrightarrow CH_3NH_2 + H_2O + 5.7$ Kcal

amide synthesis $CH_3COOH + NH_3 \leftrightarrow CH_3CONH_2 + H_2O + 4$ Kcal

diene synthesis $CH_3CHO + C_2H_5OH \leftrightarrow CH_2{=}CHCH{=}CH_2 + 2H_2O - 13$ Kcal

Recent literature on the subject is summarized in Table 33.

DEHYDRATION-DEHYDROGENATION

Included in this group are reactions in which both water and hydrogen appear on one side of the equation. References on the subject are given in

---

* This reaction has assumed economic importance in recent years with a yearly synthetic ethanol production of 111 million gallons in 1949. However, only Shell Oil Co.'s Deer Park plant[219, 220], with an 18 million gal/yr. capacity, employs a catalytic process (phosphoric acid, 1000 psi).

TABLE 33. HYDRATION-DEHYDRATION REACTIONS

Author	Chem. Abstracts	Ref.	Catalyst
Butadiene Formation			
Corson, B. B., Jones, H. E., Welling, C. E., Hinckley, J. A., Stahly, E. E.	**44**, 3874	*IEC*, **42**, 359 (1950)	Si, Mg, Ta oxides
Greenberg, H.	**42**, 334	U. S. 2,426,678	phosphoric acid
Hale, W. J.	**42**, 7785	U. S. 2,441,966	alumina-magnesia
Ipatieff, V. N.	**39**, 4774	U. S. 2,373,153	magnesia
Kampmeyer, P. M., and Stahly, E.	**43**, 4213	*IEC*, **41**, 550 (1949)	tantala-silica
Nagai, H.	**43**, 5359		clay, phosphoric acid
Natta, G., and Rigamonti, R.	**42**, 5839		silica-magnesia
Seymour, G., and Fortess, F.	**42**, 7311	U.S. 2,444,538	phosphoric acid
Spence, L. U., Butterbaugh, D. J., and Kundiger, D. G.	**42**, 5463	U.S. 2,438,464	SiO_2, ThO_2, ZrO_2
Srinivason, R., and Hazra, G.	**43**, 7898		MgO-SiO_2
	44, 3433		MgO-SiO_2-Al_2O_3
Stahly, E., Jones, H. E., and Corson, B. B.	**43**, 1713	*IEC*, **40**, 2301 (1948)	tantala-silica
Workman, A. R.	**41**, 1694	U.S. 2,412,762	$ZrOCl_2$

Olefin Formation

Alumina Catalysts

Author	Chem. Abstracts	Ref.	Subject or Product
Antipina, T. V., and Frost, A. V.	**41**, 1539		Al_2O_3 ex $AlCl_3$
	46, 9377		adsorption on Al_2O_3 *vs.* activity
Feacham, C., and Swallow, H.	**42**, 5750	*JCS*, 267 (1948)	Al_2O_3 ex bayerite
Kunii, T., Nishimoto, N., Tanifuji M., and Airo, M.	**43**, 6217		isobutene
Laurent, P. A.	**43**, 6217	U.S. 2,468,764	amylene
Makishima, G.	**44**, 3002		ammonia ppt.
Rubinshtein, A., and Vasserberg, V. E.	**45**, 10020		effective surface

IEC = Industrial and Engineering Chemistry
JCS = Journal of the Chemical Society
JACS = Journal of the American Chemical Society
JSCI = Journal Society of Chemical Industry (London)

TABLE 33—*Continued*

Author	Chem. Abstracts	Ref.	Subject or Product
Schwab, G. M., and Schwab-Agallidis, E.	**43**, 6497	*JACS*, **71**, 1806 (1949)	selectivity
Walker, C. A.	**44**, 2911	*IEC*, **41**, 2640 (1949)	1-dodecene
Miscellaneous Catalysts			
Areshidze, Kh., and Tavartkiladze, E. K.	**43**, 6153		clay
Miller, H.	**42**, 1076	U.S. 2,428,673	tungsten oxide
Miller, H. S.	**39**, 3791	U.S. 2,377,026	silica-alumina
Misukuri, S., and Shinbo, M.	**44**, 7863		silica-alumina
Murray, K. E.	**41**, 4771		clay
Nagai, H.	**46**, 412		kaolin-Fe_2O_3-KOH and kaolin-H_3PO_4
Nojima, E.	**44**, 6875		phosphoric acid
Rubinshtein, A., and Kulikov, S.	**45**, 6031 **44**, 7632		titania titania
Shriver, L. C.		U.S. 2,399,395	titania
Alcohol Formation			
Anderson, John, Stager, R. M., Jr., McAllister, S. H.	**39**, 708	U.S. 2,359,459	phosphoric acid
Cheney, H. A., Dagley, R., Jr., and McAllister, S. H.	**42**, 3425	U.S. 2,434,394	$CuSO_4$-Al_2O_3
Deering, R. F.	**44**, 4923	U.S. 2,496,621	phosphoric acid
Deutsche Gold-und Silber-Scheideanstalt	**38**, 1245		Cu, Ag, Mn, W oxide-alumina
Gresham, W. F.	**44**, 9979	U.S. 2,511,467	Cd, Ag, Zn acetate
Reynolds, P. W., and Grudgings, D. M.	**43**, 8379	Brit. 622,937	tungsten oxide
Miscellaneous Products Alumina Catalysts			
Abe, Shiro	**41**, 6122		preparation
Antipina, T. V., and Frost, A. V.	**45**, 937		adsorption and kinetics
Appleby, W. G., Dobratz, C. J., and Kapranos, S. W.	**39**, 455	*JACS*, **66**, 1938 (1944)	heptene
Bentley, F. J. L.	**41**, 6681	Brit. 586,494	activation
Balandin, A., and Vasserberg, V.	**41**, 1539		isopropane

Table 33—*Continued*

Author	Chem. Abstracts	Ref.	Subject or Product
Brey, W. S., Jr., and Krieger, K. A.	**44**, 2709	*JACS*, **71**, 3637 (1949)	acetylene, heat treatment
DuPont	**44**, 7877	Brit. 635,853	anisole
	43, 3439	Brit. 610,172	vinyl cyanide
Eucken, A., and Wicke, E.	**42**, 7148		heavy water exchange
Feilchenfeld, Hans		*IEC*, **45**, 855	di-ethyl ether
Heinemann, H., Wert, R. W., and McCarter, W. S. W.	**44**, 1889	*IEC*, **41**, 2928 (1949)	acetals, nitriles, esters
Makishima, G.	**41**, 5371		acetylene
N. V. de B. P. M.	**44**, 5387		phenols
Redmon, B. C.	**44**, 7345	U.S. 2,485,510	acrylic acid, etc.
Rubinshtein, A. M., *et al.*	**46**, 9961		effective surface
Smith, E. F.	**43**, 3440	U.S. 2,456,599	methyl amine
Wicke, E.	**44**, 2357		oxide contacts

Clay Catalysts

Areshidze, Kh.	**43**, 5010		cyclohexene
I.S.O.C.R. Japan	**44**, 3006		vinyl cyanide
Nekrasov, A., and Krentsel, B.	**44**, 1006		diisopropyl ether

Phosphoric Acid Catalysts

Emerson, W.	**43**, 3461	U.S. 2,457,988	phenyl acetaldehyde
Erichsen, L.	**44**, 1429		ethyl benzene
Fallows, L., and Mellers, E.	**42**, 1032	U.S. 2,429,262	hydrogen cyanide
Gear, J. L.	**44**, 5379	U.S. 2,501,092	propylaldehyde
Mollerstedt, B.	**44**, 1528		acetaldehyde
Standard Oil Development Co.	**43**, 1058	Brit. 574,738	toluene
Yakubovich, A. Ya.	**41**, 4367		acetaldehyde

Silica-Alumina Catalysts

Bremner, J., and Jones, D. G.	**43**, 1795	U.S. 2,451,712	2,3-dihydropyran
Cullinane, N. M., Chard, S. J., and Meatyard, R.	**43**, 1019	*JSCI* (*London*) **67**, 232 (1948)	ethyl benzene
Mahan, J. E.	**43**, 8398	U.S. 2,476,500	amides
Topchieva, K., and Ballod, A.	**45**, 2760		acetone

TABLE 33—*Continued*

Author	Chem. Abstracts	Ref.	Catalyst	Products
Miscellaneous Catalysts				
Arnold, H. R., and Carnahan, J. E.		U.S. 2,591,493	metal molybdite	olefins, etc.
Brintzinger, H., and Mollers, A.	**43**, 2533		BeO, La_2O_3, Al_2O_3, ThO_2, TiO_2	tetrahydrafuran, CO_2
Balandin, A., and Egorova, N.	**44**, 8215		Cb and Ta oxides	
Broun, A. S., *et al.*	**38**, 2314		zinc oxide	acetone
Carter, A. G.	**43**, 5886	U.S. 2,470,688	alkali, MgO, etc.	$CO_2 + H_2O$
Du Pont	**43**, 3439	U.S. 2,417,068	silica gel	vinyl cyanide
Dai Nippon Celluloid Co.	**44**, 3515		$CuCl_2$-Al_2O_3	vinyl cyanide
Dyck, A. W. J.	**41**, 393		Fe_2O_3-ZnO	acetone
Gresham, W. F.	**42**, 6841	U.S. 2,439,426	Fe, Ni, Mn chromites	nitriles
Gershbein, L. L., Pines, H., and Ipatieff, V. N.	**42**, 1185	*JACS* **69**, 2888, (1947)	magnesia	$C_3H_6 + Me_2CO$ etc.
Kung, F.	**39**, 4085	U.S. 2,373,190	manganese oxide	vinyl cyanide
Kreps, S. I., and Nachod, F. C.	**43**, 8397	U.S. 2,477,380	exchange resins	*tert.* BuOH
Levesque, C. L., and Craig, A. M.	**42**, 2165	*IEC*, **40**, 96 (1948)	exchange resins	esters
Miller, Harry	**42**, 1076	U.S. 2,428,673	tungsten oxide	castor oil dehydration
Miyahara, Y., and Sano, I.	**44**, 9223		zinc oxide	mechanism
Nozu, R.	**44**, 3009		$CdCrO_4$, $CdMoO_4$, $Cd_3(VO_4)_2$ on clay	HCN, EtCHO, Me_2CO
Redmon, B. C., and Griffin, G. R.	**43**, 4288	U.S. 2,464,768	H_2SO_4, H_3PO_4	acrylic acid esters
Rode, T., and Balandin, A.	**41**, 1920		silica gel	water control
Rienacker, G., and Bade, H.	**37**, 2253		Cu	carbon dioxide
Reynolds, P. W., and Grudgings, D. M.		U.S. 2,536,768	tungsten oxide	
Schwab, G., and Schwab-Agallidis, E.	**39**, 4791		Cu-Ag, Cu-Ni alloys	carbon dioxide
Spangenberg, J. J.	**41**, 4028		TiO_2, ThO_2-ZrO_2	esters

TABLE 33—*Continued*

Author	Chem. Abstracts	Ref.	Catalyst	Products
Tekko Soc. Inc.	**44**, 4023		ZnO-Fe_2O_3	acetaldehyde
Topsøe, H.	**44**, 8363		Cd & Zn phosphates	acetaldehyde
Topsøe, H., and Nielson, A.	**44**, 1524		Cd Phosphate	vinyl ester
Usines de Melle	**41**, 7065	Brit. 589,709	BPO_4	tetrahydrofuran
Wicke, E.	**44**, 2357		zinc oxide	

Table 34. By far the most important example is the one-step synthesis of butadiene from alcohol

$$2C_2H_5OH \rightarrow C_4H_6 + 2H_2O + H_2 - 25 \text{ Kcal}$$

which is reputed to account for the bulk of USSR synthetic rubber. The development of this process has been attributed[221] to Lebedev dating back over twenty years. It is discussed by Corson, Jones, Welling, Hinckley and Stahly[221] who investigated several hundred catalysts for this application but found the two-step process in which part of the alcohol is first dehydrogenated to acetaldehyde to give higher butadiene yields.

Catalysts most suitable for this application are primarily dehydration agents combined with very mild dehydrogenation components. The exact composition of the so-called "Lebedev catalyst" used in the USSR has probably not been published. Equilibrium is favorable at elevated temperatures because of entropy considerations and best yields are realized at 400 to 425°C[221].

CATALYTIC EXCHANGE REACTIONS

Although exchange reactions in which isotopic elements are exchanged between compounds or otherwise participate in a reaction are of minor commercial interest, they provide a powerful tool for studying reaction mechanisms. Taylor[222] and Kummer and Emmett[223] have reviewed recent progress in this field. A recent symposium[224] on the use of isotopes in the petroleum chemistry included several papers on the subject. Mass and infrared spectroscopy and Geiger counters are commonly used to determine isotopic compositions. The literature is summarized in Table 35.

MISCELLANEOUS REACTIONS

There are many reactions that do not fall into the categories given above. In general their mechanisms are not well understood so that it appears

Table 34. Dehydration-Dehydrogenation

Butadiene Synthesis

Author	Chem. Abstracts	Ref.	Catalyst
Butterbaugh, D., and Spence, L. U.	**41**, 6272	U.S. 2,423,681	silica-magnesia
Butterbaugh, D., and Spence, L. U.	**42**, 9102	U.S. 2,447,181	silica-magnesia
Corson, B., Jones, H. E., Welling, C. E., Hinckley, J. A., and Stahly, E. E.	**44**, 3874	*IEC*, **42**, 359 (1950)	Si-Mg-Ta-oxides
Natta, G., and Rigamonti, R.	**42**, 5839		silica-magnesia
Rigamonti, R., and Russo, F.	**42**, 3309		silica-magnesia
Spence, L. U., Butterbaugh, D. J., and Kundiger, D. G.	**42**, 5463	U.S. 2,438,464	SiO_2-ThO_2, ZrO_2
Srinivason, R., and Hazra, G.	**44**, 3433		Mg-Si-Al oxides
	44, 1398		Si-Mg-Zr oxides
	43, 7898		silica-magnesia
Szukiewics, W.	**42**, 7785	Can. 448,963	silica-magnesia

Miscellaneous Products

Author	Chem. Abstracts	Ref.	Catalyst	Product
Dolgov, B., and Nizovkina, T.	**43**, 8252		copper	ethyl acetate
Gresham, W. F.	**42**, 7314	U.S. 2,443,420	Cu-Zn	ethyl cyanide
Hager, G. F.	**44**, 4499	U.S. 2,481,922	Ni-Cu-Cr_2O_3	cyclohexanol
Janz, G. J., *et al.*		*IEC*, **45**, 1343	Cr_2O_3-Al_2O_3	phenyl-pyridine
Kagan, M., *et al.*	**42**, 4515		zinc chromate	bivinyl
Lel'chuk, S., *et al.*	**42**, 4436		copper	esters
Takahashi, T., and Hikawa, F.	**43**, 5363		Mg-Mn oxides	butanol
Wagner, C. R.	**41**, 1235	U.S. 2,412,437	chromia alumina	vinyl cyanide
Hoog, H., and Engel, W.	**43**, 5426	Dutch 62,562	copper	C_6H_7N

TABLE 35. EXCHANGE REACTIONS

Reactants	Principal Products	Catalyst	Temp. (°C.)	Author	Chemical Abstracts	Ref.
Hydrogen Exchange**						
$H_2 + D_2$	HD	ZnO, $Fe\text{-}Al_2O_3\text{-}K_2O$		Taylor, H. S.	**44**, 7132	
$H_2 + D_2$	HD	$Ni\text{-}ThO_2$, $Ni\text{-}Cr_2O_2$	−195–0	Sadek, H. and Taylor, H. S.	**44**, 5199	
$H_2 + D_2$	HD	Fe + promoters		Kummer, J. T., and Emmett, P. H.	**46**, 8488	*JPC*, **56**, 258
$H_2 + D_2$	HD	$Fe\text{-}Al_2O_3\text{-}K_2O$	−195	Emmett and Kummer	**44**, 6711	cf. *CA* **45**, 550
$H_2 + D_2$	HD	SiO_2, Al_2O_3	150–300	Holm, V. C. F., and Blue, R. W.	**45**, 2759	*IEC*, **43**, 501*
para H_2	ortho H_2	W		Couper, A., and Eley, D. D.		*PRS*, **A211**, 536
para H_2	ortho H_2	S, Ni, Pt, Pd		Eley, D. D.	**43**, 26	*TFS*, **44**, 216
$CH_4 + 2\ D_2$	$CD_4 + H_2$	Ni	206–255	Kemball, C.	**45**, 331	*PRS*, **A217**, 376
$C_2H_2 + D_2$	cis $C_2H_2D_2$	Ni	−80	Douglas, J. E., and Rabinovitch, B. S.		*JACS*, **74**, 2486 (1952)
$C_2H_4 + D_2$	C_2H_3D	Ni	25	Douglas, J. E., and Rabinovitch, B. S.		*JACS*, **74**, 2486 (1952)
$CH_4 + CD_4$		$SiO_2\text{-}Al_2O_3$	345	Parravano, G., Hammel, E. F., and Taylor, H. S.	**42**, 7148	*JACS*, **70**, 2269 (1948)
$CH_4 + CD_4$		Ni	100–255	Wright, M. M., and Taylor, H. S.	**43**, 7802	
$CH_4 + CD_4$	CH_2D_2	ZnO, $Fe\text{-}Al_2O_3\text{-}K_2O$		Taylor, H. S.	**44**, 7132	
$C_2H_2 + C_2D_2$		Ni	25	Douglas, J. E., and Rabinovitch, B. S.		*JACS*, **74**, 2486 (1952)

$C_2H_4 + C_2D_2$	$C_2H_2D_2$	Ni		Douglas, J. E., and Rabinovitch, B. S.		*JACS*, **74**, 2486 (1952)
$C_2H_2D_2 + C_2H_2$	no change	Ni	25	Douglas, J. E. and Rabinovitch, B. S.		*JACS*, **74**, 2486 (1952)
$C_2H_3D + C_3H_6$	$C_2H_4 + CH_3—CHCHD$	Ni	45	Koizumi, M.	**46**, 1339 **41**, 2974	
2 MeCHDMe	$MeCH_2Me + MeCD_2Me$	$AlCl_3$-Al_2O_3		Beeck, O., Otvos, J. W., Stevenson, D. P., and Wagner, C. D.	**43**, 7897	*JCP*, **17**, 419 (1949)
$D_2 + NH_3$	NH_2D	Pt, Pd, Ni, W, Fe, Cu		Kemball, C.		*TFS*, **48**, 254 (1952)
$Me_3CD + Me_2(C^{13}H_3)CH$	$Me_3CH + Me_2(C^{13}H_3)CD$	$AlCl_3$-Al_2O_3		Wagner, C. D., Beeck, O., Otvos, J. W., and Stevenson, D. P.	**43**, 7897	*JCP*, **17**, 419 (1949)
$D_2 + C_6H_6 + H_2 + C_6H_{12}$		Pt, Cr_2O_3	160	Balandin, A. A., Kharina, Z. V., and Teis, R. V.	**41**, 4698	
$D_2O + —MOH$	$—MOD + H_2O$	SiO_2-Al_2O_3		Hansford, R. C., Waldo, P. G., Drake, L. C., and Honig, R. E.		*IEC*, **44**, 1108 (1952)
$C_4H_9D + MOH$	$C_4H_{10} + MOD$	SiO_2-Al_2O_3		Hindin, S.G., Mills, G. A., and Oblad, A. G.	**45**, 6371	*JACS*, **13**, 278 (1951)

TABLE 35—*continued*

Reactants	Principal Products	Catalyst	Temp. (°C.)	Author	Chemical Abstracts	Ref.
		Other Exchange Reactions				
$O_2^{16} + H_2O^{18}$	$H_2O + O_2^{18}$	αFe_2O_3, γFe_2O_3 Fe_2O_3-BiO	various	Morita, N.	**41**, 4366 **41**, 2974	
$CO + O_2^{18}$		CuO	300–550	Chitani, T., Nakata, S., and Kanome, A.	**41**, 4366	
$SO_2 + O_2^{18}$		Pt	300–500	Nakata, S., and Morita, N.	**41**, 4366	
$O_2^{18} + MO$	MO^{18}	Al_2O_3, ZnO	200–400	Karpacheva, S. M., and Rozen, A. M.	**46**, 3382	cf. *CA*. **45**, 1855
$O_2^{18} + MO$	MO^{18}	CuO, NiO + Co_3O_4	400–1000	Allen, J. H., and Lauder, I.	**43**, 8821	
$H_2O^{18} + MO^{16}$	$H_2O^{16} + MO^{18}$	Fe_2O_3, SiO_2, MnO_2		Karpacheva, S. M., and Rozen, A. M.	**44**, 917	
$H_2O^{18} + \frac{1}{2}O_2^{16}$	$H_2O^{16} + \frac{1}{2}O_2^{18}$	Cr_2O_3-Al_2O_3	350–470	Karpacheva, S. M., and Rozen, A. M.	**44**, 917	
$O_2^{18} + MgO$	MgO^{18}	MgO		Houghton, G., and Winter, E. R. S.	**44**, 3340	
$H_2O^{18} + M_xO_y^{16}$	$M_xO_y^{18} + H_2O^{16}$	SiO_2-Al_2O_3 SiO_2, Al_2O_3, act. clays	100	Mills, G. A., and Hindin, S. G.		*JACS*, **72**, 5549 (1950)
$N_2^{30} + N_2^{28}$	N_2^{29}	Fe-Al_2O_3-K_2O	500	Kummer, J. T., and Emmett, P. H.	**45**, 9346 **44**, 6711	*JCP*, **19**, 289 (1951)
$N_2^{31} + N_2^{28}$	N_2^{29}	ZnO, Fe-Al_2O_3-K_2O		Taylor, H. S.	**44**, 7132	
$NH_3 + ND_3$	NH_2D, NDH_2	ZnO, Fe-Al_2O_3-K_2O		Taylor, H. S.	**44**, 7132	
$CO + H_2 + C_2^{14}H_5OH$	radioactive hydrocarbons	Fe-Al_2O_3-ThO_2		Kummer, J. T., Podgurski, H. H., Spencer, W. B., and Emmett, P. H.		*JACS*, **73**, 564 (1951)

JACS = Journal of the American Chemical Society.
IEC = Industrial and Engineering Chemistry.
* cf. *IEC*, **44**, 107 (1952) (25 catalysts)
** For a more complete listing of 1952–53 literature see *IEC*, **45**, 1991 (1953)

CA = Chemical Abstracts
PRS = Proceedings of the Royal Society (London)
JCP = Journal of Chemical Physics

TABLE 36. MISCELLANEOUS REACTIONS

Principal Reaction Product	Principal Reactants	Catalyst	Author	Chemical Abstracts
Acids				
benzoic acid, etc.	phthalic acid	Al_2O_3	Spada, A.	**37**, 5384
Alcohols				
diacetone alcohol	acetone	$Ba(OH)_2$	Bruce, D. C.	**44**, 773
alcohols	alkyl sulfonic esters	Ni	Kenner, G. W., and Murray, M. A.	**44**, 565
xylenol	isophorone	Fe, Co, Cr	N. V. de B. P. M.	**44**, 5387
Aldehydes				
methyl vanillin	opianic acid	Cu, bronze	Weijlard, J., and Tischler, M.	**44**, 2558
Amines				
$Me_2C_6H_3NH_2$	NH_3 + isophorone	Al_2O_3	Ballard, S., and Winkler, L. E.	**41**, 2438
R_2NH	RNH_2	Al_2O_3	N. V. de B. P. M.	**44**, 7343
amines	H_2 + alcohol + NH_3	Ni, Cu	Nippon Chem. Ind.	**44**, 1129
amine	olefin + NH_3	Co	Teter, J. W.	**39**, 5253
amines		CoO	Teter, J. W.	**42**, 1034
Aromatics				
high octane hydrocarbons	F. T. oxygenated compounds	Al_2O_3	Grahame, J. H.	**43**, 2421
Esters				
methyl acetate	CO + MeOH	Co + Ag	Brooks, R. E.	**43**, 3443
alkyl acetate	$CH_2(CH_2OH)_2$	quartz	Olsen, S.	**44**, 1130
acrylic acid esters	β-propiolactone + alcohol	C	Steadman, T., and Feazle, C. E.	**43**, 5035

Table 36—*Continued*

Principal Reaction Product	Principal Reactants	Catalyst	Author	Chemical Abstracts
vinyl esters	acetylene + acetic acid	Zn or Cd	Staudinger, J. J. P., Coppock, P. D., and Hadley, D. J.	**41**, 2072
$HCO_2CH:CH_2$	$C_2H_2 + HCOOH$	zinc formate act. C	Ushakov, S. N., Arbuzova, I. A., and Rostovskii, E. N.	**43**, 567
Ethers				
aliphatic ether	isoolefin + alcohol	ion exchange resin	Leum, L. N., Macuga, S. J., and Kreps, S. I.	**44**, 652
Ketones				
ketones	ester + aromatic acid	ThO_2	Webb, J. L. A., and Webb, J. D.	**43**, 8367
Olefins				
isobutylene	acetone	SiO_2-Al_2O_3	Larine and Frost	**41**, 5093
Lactones				
betahydroxy carboxylic acid	aldehyde + ketone	clay	Young, F. G., and Fitzpatrick, J. T.	(1)
Nitriles				
HCN	$O_2 + CH_4 + NH_3$	Pt	Chretien, A., and Thomas, A.	**42**, 6495
HCN	$CH_4 + NH_3 + O_2$	Pt	Green, H. D.	**39**, 5055
HCN	$NH_3 + O_2 + CH_4$	Pt-Ir gauze	Houpt, A. G., and Smith, C. W.	**44**, 4642
HCN	$Ch_4 + NH_3 + O_2$	Pt gauze	Merrill, D. R., and Perry, W. A.	**43**, 9396
EtCN	$EtCHO + NH_3$	Co, Cu, Zn	Gresham, W. F.	**43**, 1433
aliphatic nitriles	tertiary olefin oxide + NH_3	CuO	Mahan, J. E.	**44**, 7342

Table 36—*Continued*

Principal Reaction Product	Principal Reactants	Catalyst	Author	Chemical Abstracts
acetonitrile	propylene + NH_3	Al_2O_3	Mahan, J. E.	**42**, 2613
acetonitrile	$C_2H_2 + NH_3$	$ZnO\text{-}Al_2O_3$	Standard Oil Development Co.	**42**, 2983
propionitrile	NH_3 + iso BuOH	Ag, Cu	Spence, L. U., Butterbaugh, D. J., and Robinson, F. W.	**38**, 3296
PhCN		MoO_3, W_2O_5	Caldwell, H., and Chapman, H. D.	**43**, 3439
PhCN	PhMe + O_2 + NH_3	V_2O_5	Cosby, J. N., and Erchak, M., Jr.	**44**, 6885
aromatic nitriles	NH_3 + methyl cyclohexane + O_2	$V_2O_5\text{-}MoO_3$	Erchak, M., Jr.	**44**, 3024
vinyl cyanide	C_2H_2 + HCN	$NaKCO_3$	Du Pont	**44**, 3006
vinyl cyanide	C_2H_2 + HCN	sodium cyanide	Green, H., and Taylor, D. S.	**41**, 1697
vinyl cyanide	C_2H_2 + HCN	sodium cyanide	Harris, C. R., and Sharples, W. C.	**41**, 2072 **41**, 4802
vinyl cyanide	C_2H_2 + HCN	Cu + cuprous salt	Imp. Chem. Ind.	**42**, 2269
vinyl cyanide	C_2H_2 + HCN	ZnO	Nippon Nitrog. Fert.	**44**, 3006
vinyl cyanide	C_2H_2 + HCN	Zn-Cd	Schulze, W., and Mahan, J. E.	**41**, 7409
vinyl cyanide	C_2H_2 + HCN	Cd, Mg, ZnO	Spence, L. U. and Haas, F. O.	**40**, 595
nitriles	HCN + tetrahydrofuran	H_3PO_4, char.	Codignola, F., and Piacenza, M.	**44**, 2014
nitriles	substituted aromatic + NH_3	MoO_3	Denton, W., and Plank, C.	**44**, 10728
nitriles	substituted aromatic + NH_3	$NiPO_3$	Denton, W., and Bishop, R. B.	**44**, 1138
nitriles	olefin + NH_3	$Fe_2(MoO_3)_3$, $Fe_2(WO_3)_3$	Denton, W., and Bishop, R. B.	**44**, 4022
nitriles	olefin + NH_3	Co, Ni	Teter, J. W.	**44**, 1128

TABLE 36—*Continued*

Principal Reaction Product	Principal Reactants	Catalyst	Author	Chemical Abstracts
		Other Nitrogen Compounds		
RCONHR	$RCN + RNH_2 + H_2O$	$SiO_2\text{-}Al_2O_3$	Mahan, J. E.	**43**, 8398
$PhNO_3$	$HNO_3 + C_6H_6$	phosphates	Rout, A. E.	**41**, 6897
		Sulfur Compounds		
$H_2S + CO_2$	$S + CO + H_2O$	NiS, CoS	Dönges, E.	**43**, 2532
CS_2, H_2S	$CH_4 + S$	$SiO_2\text{-}Al_2O_3$	Folkins, H. O., and Miller, E.	(2)
acetyl thiophene	$\underline{SCH{=}CHCH{=}CH}$ + Ac_2O	$SiO_2\text{-}Al_2O_3$	Kosak, A., and Hartough, H. D.	**43**, 2644
mercaptans	olefins + H_2S	$SiO_2\text{-}Al_2O_3$	Lyon, L. P., Jr.	**42**, 3425
butadiene + S	butene + SO_2	Cu	Stone, and Korpi,	**41**, 6575
thiophene + H_2S	diolefin + H_2S	Al_2O_3	Wadley, E. F.	**44**, 11181
mercaptan	2 pinene thiol + 2 pentene	Se	Walling, C.	**43**, 2219
		Paraffins		
CH_4	C_2H_5OH	Ni, Cu	Ipatieff, V. N., Monroe, G. S., Fischer, L. E., and Meisinger, E. E.	**44**, 537

1. U.S.P. 2,580,714
2. U.S.P. 2,565,215

best to classify this literature simply on the basis of principal reaction products as given in Table 36.

Acknowledgment

Permission of the American Cyanamid Co. to publish data obtained by the Stamford Laboratories is gratefully acknowledged.

References

1. Berkman, S., Morrell, J. C., and Egloff, G., "Catalysis," New York, Reinhold Publishing Corp. (1940).
2. Rossini, F. D., Wagman, D. D., Evans, W. H., Levine, S., and Jaffe, A., Natl. Bur. Standards Circ. 500, Washington, D. C. (1952).
3. Blue, R. W., and Engel, C., *J. Ind. Eng. Chem.*, **43,** 494, 501 (1951).
4. Dart, J. C., and Oblad, A. G., *Chem. Eng. Progr.*, **45,** 110 (1949).

5. Greensfelder, B. S., Voge, H. H., and Good, G. M., *Ind. Eng. Chem.*, **41**, 2573 (1949).
6. Tamele, M. W., *Discussions Faraday Soc.*, **8**, 270 (1950).
7. Thomas, C. L., *Ind Eng. Chem.*, **41**, 2564 (1949).
8. Hansford, R. C., *Ind. Eng. Chem.*, **39**, 849 (1947); "Advances in Catalysis," Vol. IV, New York, Academic Press, Inc., 1952.
9. Haensel, V., Sterba, M. J., *Ind. Eng. Chem.*, **43**, 2020 (1951).
10. Haensel, V., and Sterba, M. J., *ibid*, **40**, 1660 (1948).
11. Haensel, V., and Sterba, M. J., *ibid*, **41**, 1914 (1949).
12. Haensel, V., and Sterba, M. J., *ibid*. **42**, 1739 (1950).
13. Heinemann, F., *Petroleum Refiner*, **27**, No. 5, 273 (1948).
14. Boyd, J. H., *Chem. Ind.*, 594 (1948).
15. Sittig, M., *Petroleum Refiner*, **29**, Nos. 6, 8, 10, 11 pp. 9, 199, 130, 125 (1950); **31**, No. 9, 263 (1952). *Petroleum Processing*, **4**, 274 (1949).
16. Thomas, C. L., Anderson, N. K., Becker, H. A., and McAfee, J., *Petroleum Refiner*, **22**, No. 11, p. 95 (1943).
17. Murphree, E. V., Fischer, H. G., Gohr, E. J., and Sweeney, W. J., *Petroleum Refiner*, **22**, No. 11, 87 (1943).
18. *Chem. Ind.*, **60**, 226 (1947).
19. Gaylor, P. J., *Petroleum Processing*, **1**, No. 4, 261 (1946).
20. *Petroleum Refiner*, **28**, No. 4, (1949).
21. *Chem. Eng.*, **58**, No. 11, 218, No. 12, 224 (1951).
22. Porter, R. W., *Chem. & Met. Eng.*, **53**, No. 4, 94 (1946).
23. Ries, H. E., "Advances in Catalysis," Vol. IV, New York, Academic Press, Inc., 1952.
24. Webb, G. M., and Ehrhart, C. H., *Petroleum Processing*, **1**, 5 (1947).
25. Ashley, K. D., and Innes, W. B., *Ind. Eng. Chem.*, **44**, 2857 (1952).
26. Milliken, T. H., Mills, G. A., and Oblad, A. G., *Discussion Faraday Soc.*, **8**, 279 (1950).
27. Sittig, M., *Petroleum Refiner*, **29**, No. 10, 130 (1950).
28. Greensfelder, B. S., and Voge, H. H., *Ind. Eng. Chem.*, **37**, 514 (1945).
29. Greensfelder, B. S., and Voge, H. H., *ibid*, **37**, 983 (1945).
30. Greensfelder, B. S., and Voge, H. H., *ibid*. **37**, 1038 (1945).
31. Greensfelder, B. S., Voge, H. H., and Good, G. M., *Ind. Eng. Chem.*, **41**, 2573 (1949).
32. Greensfelder, B. S., *Advances in Chem. Ser. No. 5*, 3–12 (1951).
33. Egloff, G., Morrell, J. C., Thomas, C. L., and Bloch, H. S., *J. Am. Chem. Soc.*, **61**, 357 (1939).
34. Bloch, H. S., and Thomas, C. L., *J. Am. Chem. Soc.*, **66**, 1589 (1944).
35. Rossini, F. D., "Chemical Thermodynamics," New York, John Wiley & Sons, Inc., 1950.
36. McAllister, S. H., Anderson, J., and Bullard, E. F., *Chem. Eng. Progr.*, **43**, 189 (1947).
37. Sherwood, P. W., *Petroleum Refiner*, **32**, No. 1, 97 (1953).
38. Berkman, S., Morrell, J. C., and Egloff, G., "Catalysis," New York, Reinhold Publishing Corp., 1940.
39. Shreve, R. N., *Ind. Eng. Chem.*, **40**, 1565 (1948).
40. Shreve, R. N., *ibid*. **41**, 1833 (1949).
41. Shreve, R. N., *ibid*, **42**, 1650 (1950).
42. Shreve, R. N., *ibid*, **43**, 1908 (1951).

43. Ipatieff, V. N., and Schmerling, L., "Advances in Catalysis," Vol. II, New York, Academic Press, Inc., 1950.
44. Mrstik, A. V., Smith, K. A., Pinkerton, R. D., *Advances Chem. Ser. No. 5*, 97–108 (1951).
45. Remick, A. E., "Electronic Interpretations of Organic Chemistry," New York, John Wiley & Sons, Inc., 1949.
46. Berkman, S., Morrell, J. C., and Egloff, G., "Catalysis," New York, Reinhold Publishing Corp., 1940.
47. Pines, H., "Advances in Catalysis," Vol. I, New York, Academic Press, Inc., 1948.
48. Simons, J. H., "Advances in Catalysis," Vol. II, New York, Academic Press, Inc., 1950.
49. Gunness, R. C., *Advances in Chem. Ser. No. 5*, 109–119 (1951).
50. Perry, S. F., *Ind. Eng. Chem.*, **42,** 1715 (1950); **40,** 1624 (1948).
51. Rossini, F. D., "Chemical Thermodynamics," New York, John Wiley & Sons, Inc., 1950.
52. Haensel, V., *Ind. Eng. Chem.*, **43,** 2021 (1951).
53. Hay, R. G., Coull, J., and Emmett, P. H., *Ind. Eng. Chem.*, **41,** 2809 (1949).
54. Storch, H. H., Golumbic, N., and Anderson, R. B., "The Fischer-Tropsch and Related Syntheses," New York, John Wiley & Sons, Inc., 1951.
55. Ciapetta, F. G., Pitts, P. M., and Leum, L. N., Petroleum Div. Abstracts, A.C.S. Meeting, Sept. 1952.
56. Winding, C. C., Unit Processes Review, Sept Issues of *Ind. Eng. Chem.* (1948–51).
57. Berkman, S., Morrell, J. C., and Egloff, G., "Catalysis," pp. 600–629, New York, Reinhold Publishing Corp., 1940.
58. Burk, R. E., National Research Council, Twelfth Catalyst Rept., p. 180, New York, John Wiley & Sons, Inc., 1940.
59. Steffens, J. H., Zimmerman, M. U., and Laituri, M. J., *Chem. Eng. Progr.*, **45,** 269 (1949).
60. Ipatieff, V. N., and Schaad, R. E., *Ind. Eng. Chem.*, **37,** 362 (1945).
61. Schmerling, L., and Ipatieff, V. N., "Advances in Catalysis," Vol. II, p. 71, New York, Academic Press, Inc., 1950.
62. Langlois, G. E., Petroleum Div. Abstracts, A.C.S. Meeting, Sept. 1952.
63. Rossini, F. D., "Chemical Thermodynamics," New York, John Wiley & Sons, Inc., 1950.
64. Whitmore, F. C., *Chem. Eng. News*, **26,** 668 (1948).
65. Clark, A., Petroleum Div. Abstracts, A.C.S. Meeting, Sept. 1952.
66. Thomas, C. L., *J. Am. Chem. Soc.*, **66,** 1586 (1944); *Ind. Eng. Chem.*, **41,** 2564 (1949).
67. Blue, R. W., and Engle, C. J., *Ind. Eng. Chem.*, **43,** 494, 500 (1951).
68. Greensfelder, B. S., Voge, H. H., and Good, G. M., *Ind. Eng. Chem.*, **41,** 2573 (1949).
69. Beeck, O., *Discussions Faraday Soc.*, **8,** 118 (1950).
70. Ward, A. F., *Proc. Roy. Soc.*, **A133,** 506 (1931).
71. Dowden, D. A., *Ind. Eng. Chem.*, **44,** 984 (1952).
72. Taylor, H. S., *Discussions Faraday Soc.*, **8,** 9 (1950).
73. Rossini, F. D., "Chemical Thermodynamics," New York, John Wiley & Sons, Inc., 1950; American Petroleum Institute Research Project 44, National Bureau of Standards.
74. Russell, R. P., Murphree, E. V., and Asbury, W. C., *Trans. Am. Inst. Chem. Engrs.*, **42,** 1 (Feb. 25, 1946).

75. Kearby, K. K., *Ind. Eng. Chem.*, **42,** 295 (1950).
76. Thornton, D. P., *Natl. Petroleum News*, **36,** No. 9, R211 (1944).
77. Beckberger, L. H., and Watson, K. M., *Chem. Eng. Progr.*, **44,** 229 (1948).
78. Hanson, G. H., and Hays, H. L., *Chem. Eng. Progr.*, **44,** 431 (1948).
79. Britton, E. C., Dietzler, A. J., and Noddings, C. R., *Ind. Eng. Chem.*, **43,** 2871 (1951).
80. Ghosh, J. C., Guha, S. R. D., and Roy, A. N., *Petroleum*, **10,** 236 (1947).
81. Mavity, J. M., Zetterholm, E. E., and Hervert, G. L., *Ind. Eng. Chem.*, **38,** 829 (1946).
82. Marshall, C. H., *Chem. Eng. Progr.*, **46,** 313 (1950).
83. Nelson, E. F., *Oil Gas J.*, **47,** No. 49, 95 (1949).
84. Haensel, V., and Sterba, M. J., *Ind. Eng. Chem.*, **40,** 1660 (1948).
85. Haensel, V., and Donaldson, G. R., *Ind. Eng.*, *Chem.* **43,** 2102 (1951).
86. Haensel, V., and Berger, C. V., *Petroleum Processing*, **6,** 264 (1951).
87. Fowle, M. J., Bent, R. D., Ciapetta, F. G., Pitts, P. M., and Leum, L. N., *Advances in Chem. Ser. No. 5*, 76–82 (1951).
88. Fowle, M. J., Bent, R. D., and Masologites, G. P., 17th Mid-Year Meeting, American Petroleum Inst., May 1952.
89. Ardern, D. B., and Dart, J. C., *Advances in Chem. Ser. No. 5*, 13–29 (1951).
90. Heinemann, H., Schall, J. W., and Stevenson, D. H., *Oil Gas J.*, 166 (Nov. 15, 1951).
91. McGrath, H. G., and Hill, L. R., *Advances in Chem. Ser. No. 5*, 39–57 (1951).
92. Murphree, E. V., *Advances in Chem. Ser. No. 5*, 58–59 (1951).
93. Seebold, J. E., Bertetti, J. W., Snuggs, J. F., and Bock, J. A., Preprint American Petroleum Inst. Proc. 17th Meeting, May, 1952.
94. Hughes, E. C., Stine, H. M., Strecker, H. A., Eastwood, S. C., Gutzeit, C. L., Stover, W. A., and Wantuck, S. J., *Ind. Eng. Chem.*, **44,** 572 (1952).
95. Rossini, F. D., "Chemical Thermodynamics," New York, John Wiley & Sons, Inc., 1950.
96. Greensfelder, B. S., Archibald, R. C., and Fuller, D. L., *Chem. Eng. Progr.*, **43,** 561 (1947).
97. Burtis, T. A., and Noll, H. D., *Petroleum Eng.*, **24,** No. 6, C39 (1952).
98. Williams, E. C., and de Simo, M., "Twelfth Catalysis Report, National Research Council," New York, John Wiley & Sons, Inc., 1940.
99. Church, J. M., and Joshi, H. K., *Ind. Eng. Chem.*, **43,** 1804 (1951).
100. Hader, R. N., Wallace, R. D., and McKinney, R. W., *Ind. Eng. Chem.*, **44,** 1508 (1952).
101. Zabel, H. W., *Chem. Ind.*, No. 8, 217 (1948).
102. Corson, B. B., Jones, H. E., Welling, C. E., Hinckley, J. S., and Stahly, E. E., *Ind. Eng. Chem.*, **42,** 359 (1950).
103. Wojcik, B. H., *Ind. Eng. Chem.*, **40,** 210 (1948).
104. Adkins, H., and Shriner, R. L., "Catalytic Hydrogenation and Hydrogenolysis," 2nd Ed., Vol. I, Henry Gilman, New York, John Wiley & Sons, Inc., 1945.
105. Ellis, C., "Hydrogenation of Organic Compounds," 3rd Ed., New York, D. Van Nostrand Co., Inc., 1930.
106. Berkman, S., Morrell. J. C., and Egloff, G., "Catalysis," New York, Reinhold Publishing Corp., 1940.
107. Boyle, C. J., *Ind. Eng. Chem.*, **42,** 1707 (1950).
108. Werner, J., *Ind. Eng. Chem.*, **40,** 1576 (1948); **41,** 1831 (1949); **42,** 1661 (1950); **43,** 1917 (1951).
109. Griffith, R. H., Brit. Patent 577,816.

110. De Largey, R. J., Okie, J. P., and Roberts, L. M., *Chem. Eng.*, **55,** No. 10, 124 (1948).
111. *Chem. Week*, **70,** No. 25, 10 (1952).
112. Newton, R. H., and Dodge, B. F., *J. Am. Chem. Soc.*, **56,** 287 (1934).
113. Francon, Jacques, *C. A.*, **42,** 3426 (1948).
114. Dodge, B. F., "Chemical Engineering Thermodynamics," New York, McGraw-Hill Book Co., 1944.
115. Kastens, M. L., Dudley, J. F., and Troeltzsch, J., *Ind. Eng. Chem.*, **40,** 2230 (1948).
116. Storch, H. H., *J. Phys. Chem.*, **32,** 734 (1928).
117. Frolich, P. K., Davidson, R. L., and Fenske, M. R., *Ind. Eng. Chem.*, **21,** 867 (1929).
118. Frolich, P. K., and Cryder, O. S., *Ind. Eng. Chem.*, **21,** 867 (1929).
119. Fenske, M. R., and Frolich, P. K., *Ind. Eng. Chem.*, **21,** 1052 (1929).
120. Brown, R. L., and Galloway, A. E., *Ind. Eng. Chem.*, **21,** 310 (1929).
121. Lewis, W. K., and Frolich, P. K., *Ind. Eng. Chem.*, **20,** 285 (1928).
122. Dodge, B. F., and Newton, R. H., *J. Am. Chem. Soc.*, **55,** 747 (1933).
123. Graves, G. D., *Ind. Eng. Chem.*, **23,** 1381 (1931).
124. Anderson, R. B., Feldman, J., and Storch, H. H., *Ind. Eng. Chem.*, **44,** 2418 (1952).
125. Storch, H. H., Golumbic, N., and Anderson, R. B., "The Fischer-Tropsch and Related Syntheses," New York, John Wiley & Sons, Inc., 1951.
126. Dent, F. J., Mognard, L. A., Eastwood, A. H., Blackburn, W. H., and Hebden, D., *Gas Research Board, Comm.* **GRB20,** 103 pp. (1945).
127. Shearon, W. H., and Thompson, H. L., *Ind. Eng. Chem.*, **44,** 254 (1952).
128. Akers, W., and White, R., *Chem. Eng. Progr.*, **44,** 553 (1948).
129. Luyten, L., *C. A.*, **37,** 3662 (1943).
130. Binder, G., and White, R., *Chem. Eng. Progr.* **46,** 563 (1950).
131. Tuttle, H. A., *Chem. Eng. Progr.* **48,** 272 (1952).
132. Arnold, M. R., Atwood, K., Baugh, H. M., and Smyser, H. D., *Ind. Eng. Chem.*, **44,** 999 (1952).
133. Horsfield, S. W., *C. A.*, **42,** 8443 (1948).
134. O'Boyle, C. J., *Ind. Eng. Chem.*, **42,** 1705 (1950).
135. Sebastian, J. J., and Riesz, C. H., *Ind. Eng. Chem.*, **43,** 869 (1951).
136. Storch, H. H., Golumbic, N., and Anderson, R. B., "The Fischer-Tropsch and Related Syntheses," New York, John Wiley & Sons, Inc., 1951.
137. Weil, B. H., and Lane, J. C., "Synthetic Petroleum from the Synthine Process," New York, Chemical Publishing Co., Inc., 1948.
138. Pichler, Helmut, "Advances in Catalysis," Vol. IV, New York, Academic Press, 1952.
139. Kastens, M. L., Hirst, L. L., and Dressler, R. G., *Ind. Eng. Chem.*, **44,** 450 (1952).
140. *Chem. Eng. News*, **28,** 3106 (1950).
141. *Chem. Eng.*, **59,** No. 2, 176 (1952).
142. *Chem. Eng.*, **58,** No. 8, 174 (1951).
143. Shearon, W. H., and Thompson, H. L., *Ind. Eng. Chem.*, **44,** 254 (1952).
144. Emmett, P. H., Chapter VIII in "Fixed Nitrogen," Edited by H. A. Curtis, p. 150, New York, Chemical Catalog Co., Inc. (Reinhold Publishing Corp.) 1932.
145. Berkman, S., Morrell, J. C., and Egloff, G., "Catalysis," New York, Reinhold Publishing Corp., 1940.
146. Emmett, P. H., "Colloid Chemistry," Vol. VI, Edited by J. Alexander, New York, Reinhold Publishing Corp., 1946.

147. Fleming, H. W., *Ind. Eng. Chem.*, **43,** 1983 (1951).
148. Nielsen, A., "An Investigation of Promoted Iron Catalysts for the Synthesis of Ammonia," Jul. Gzellerups Forlag, Copenhagen. 1950.
149. Sage, B. H., Olds, R. H., and Lacey, W. N., *Ind. Eng. Chem.*, **40,** 1453 (1948).
150. Bridger, G. L., Pole, G. R., Beinlich, A. W. Jr., and Thompson, H. L., *Chem. Eng. Progr.*, **43,** 291 (1947).
151. Odelhog, S. O., Brit. Patents 640,170, 609,756.
152. Souby, A. M., and Schiller, J. C., U. S. Patent 2,550,389.
153. Richardson, C. N. U. S. Patent 2,500,008.
154. Nielsen, A., and Bohlbro, H., *J. Am. Chem. Soc.*, **74,** 963 (1952).
155. Uchida, H., Shima, G., Todo, N., and Okawa, K., *C. A.*, **46,** 2245 (1952).
156. Adkins, Homer, "Reactions of Hydrogen," Madison, University of Wisconsin Press, 1937.
157. Jones, D. G., and Taylor, A. W., *Chem. Ind.*, 1075 (1951).
158. Rideal, E. K., and Taylor, H. S., "Catalysis in Theory and Practice," p. 279, New York, The Macmillan Co., 1926.
159. Zabel, Z. W., *Chem. Ind.*, 217 (1948).
160. Marek, L. F., *Ind. Eng. Chem.*, **40,** 1637 (1948).
161. Bohmfalk, J. F., Jr., McNamee, R. W., and Barry, R. P., *Ind. Eng. Chem.*, **43,** 786 (1951).
162. Michels, L. R., and Keyes, D. B., *Ind. Eng. Chem.*, **34,** 138 (1942).
163. *Chem. Eng. News*, **30,** 338 (1952).
164. *Chemical Week*, **70,** No. 5, 28 (1952).
165. *Chemical Week*, **70,** No. 23, 45 (1952).
166. *Chem. Ind. Week*, No. 15, 30 (1951).
167. *Chem. Eng. News*, **29,** 1252 (1951).
168. Kastens, M. L., and Hutchinson, J. C., *Ind. Eng. Chem.*, **40,** 1340 (1948).
169. Fairlie, A. M., "Sulfuric Acid Manufacture," New York, Reinhold Publishing Corp., 1936.
170. Marek, L. F., "Twelfth Catalysis Report, National Research Council," p. 166, New York, John Wiley & Sons, Inc., 1940.
171. Hathaway, N. E., and Myrick, O. D., *Chem. Ind.*, 581 (1949).
172. Nash, Roy W., PB 81279 FIAT Report 649.
173. Green, S. J., "Industrial Catalysis," Ernest Benn, Ltd., London (1928).
174. Zawadzki, J., *Discussions Faraday Soc.*, **8,** 140 (1950).
175. McClellan, P. P., *Ind. Eng. Chem.*, **42,** 2403 (1950).
176. *Chem. Eng. News*, **30,** No. 48, 5104 (1952).
177. McBee, E. T., Haas, H. B., and Wiseman, P. A., *Ind. Eng. Chem.*, **37,** 432 (1945).
178. Vaughn, W. E., and Goepp, R. M., Jr., FIAT Report 875 (1947).
179. Olive, T. R., *Chem. Eng.*, **56,** No. 2, 130 (1949).
180. Neidig, C. P., *Chem. Ind.*, No. 8, 214 (1947).
181. *Chem. Eng.*, **56,** No. 1, 132 (1949).
182. Petitpas, T., Chelen, E., and Mathieu, M., *C. A.*, **40,** 5986 (1946).
183. Bridger, G. L., Gernes, D. C., and Thompson, H. L., *Chem. Eng. Progr.*, **44,** 363 (1948).
184. Emmett, P. H., and Shultz, J. F., *J. Am. Chem. Soc.*, **52,** 268 (1930).
185. Reed, R. M., *Trans. Am. Inst. Chem. Engr.*, **41,** 453; *Petroleum Refiner*, **24,** 349 (1945).
186. Berkman, S., Morrell, J. C., and Egloff, G., "Catalysis," p. 775, New York, Reinhold Publishing Corp., 1940.
187. White, E. C., and Shultz, J. F., *Ind. Eng. Chem.*, **26,** 95 (1934).

188. Ri, K. C., *J. Soc. Chem. Ind. (Japan)*, **45,** 1713 (1942).
189. Ivanovskii, M. D., *J, Chem. Ind. (U.S.S.R.)*, **12,** 37 (1934).
190. Rigamonti, R., and Agliardi, N., *C. A.*, **44,** 9784 (1950).
191. Atwood, K., Arnold, M. R., and Appel, E. G., *Ind. Eng. Chem.*, **42,** 1600 (1950).
192. Emmett, P. H., in "Colloid Chemistry," Vol. VI, p. 214, Edited by J. Alexander, New York, Reinhold Publishing Corp., 1946.
193. Unpublished data, Stamford Research Laboratories, American Cyanamid Co.
194. Shultz, J. F., Tarbutton, G., Jones, T. M., Deming, M. E., Smith, C. M., and Cantelou, M. B., *Ind. Eng. Chem.*, **42,** 1608 (1950).
195. Crawford, R. M., *Chem. Eng. Progr.*, **46,** 483 (1950).
196. Arnold, C. W., and Kobe, K. A., *Chem. Eng. Progr.*, **48,** 293 (1952).
197. Johnstone, H. F., *Chem. Eng. Progr.*, **44,** 657 (1948).
198. De Benedictis, Aldo, and Luten, D. B., U. S. Patent 2,448,255.
199. Berkman, S., Morrell, J. C., and Egloff, G., "Catalysis," New York, Reinhold Publishing Corp., 1940.
200. Williams, E. C., and Vaughn, W. E., "Twelfth Catalysis Report," p. 240, New York, John Wiley & Sons, Inc., 1940.
201. McBee, E. T., and Pierce, O. R., *Ind. Eng. Chem.*, **40,** 1611 (1948); **41,** 1882 (1949); **42,** 1694 (1950); **43,** 1974 (1951).
202. *Ind. Eng. Chem.*, **39,** 359–434 (1947).
203. Cady, G. H., Grosse, A. V., Barber, E. J., Burger, L. L., and Sheldon, Z. D., *Ind. Eng. Chem.*, **39,** 290 (1947).
204. Dzis'ko, V. A., Vishnevskaya, A. A., and Chesalova, V. S., *C. A.*, **45,** 4123 (1951).
205. Freidlin, L. K., Neimark, I. E., Fridman, G. A., and Sheinfain, R. Y., *C. A.*, **45,** 5502 (1951).
206. Aries, R. S., *Can. Chem. Process Ind.*, **32,** 1004 (1947).
207. Hawk, B. S., and Lazier, W. A., "Twelfth Catalysis Report," Chap. VIII, New York, John Wiley & Sons, Inc., 1940.
208. Ellis, E., "The Chemistry of Petroleum Derivatives," Vol. II, New York, Reinhold Publishing Corp., 1937.
209. Berkman, S., Morrell, J. C., and Egloff, G., "Catalysis," p. 549, New York, Reinhold Publishing Corp., 1940.
210. Ipatieff, V. N., "Catalytic Reactions at High Pressures and Temperatures," p. 60, New York, The Macmillan Co., 1936.
211. Heinemann, H., Wert, R. W., and McCarter, W., *Ind. Eng. Chem.*, **41,** 2928 (1949).
212. Emmett, P. H., in Alexander's "Colloid Chemistry," Vol. VI, p. 214, New York, Reinhold Publishing Corp., 1946.
213. Tapp, W. J., *Ind. Eng. Chem.*, **40,** 1619 (1948); **42,** 1698 (1950).
214. Storch, H., Golumbic, N., and Anderson, R. B., "The Fischer-Tropsch and Related Syntheses," New York, John Wiley & Sons, Inc., 1951.
215. Schwab, G. M., and Schwab-Agallides, E., *J. Am. Chem. Soc.*, **71,** 1806 (1949).
216. Brey, W. S., Jr., and Krieger, K. A., *J. Am. Chem. Soc.*, **71,** 3637 (1949).
217. Corson, B. B., Jones, H. E., Welling, C. E., Hinckley, J. A. and Stahly, E. E., *Ind. Eng. Chem.*, **42,** 359 (1950).
218. Kampmeyer, P. M., and Stahly, E. E., *Ind. Eng. Chem.*, **41,** 550 (1949).
219. Zabel, H. W., *Chem. Ind.*, No. 2, 212 (1949).
220. *Chem. Eng.*, **56,** No. 8, 109 (1949).
221. Corson, B. B., Jones, H. E., Welling, C. E., Hinckley, J. A., and Stahly, E. E., *Ind. Eng. Chem.*, **42,** 359 (1950).
222. Taylor, H. S., *J. chim. phys.*, **47,** 1225 (1950).

223. Kummer, J. T., and Emmett, P. H., *J. Phys. & Colloid Chem.*, **55,** 337 (1951).
224. ACS Meeting, Division of Petroleum Chemistry, Physical and Inorganic Chemistry, Sept. 1950.
225. Hoog, H., Klinkert, H. G., and Shaftsma, A., *Petroleum Refiner*, **32,** 5, 137 (1953).
226. Sherwood, P. W., *Petroleum Processing*, **8,** 102 (1953).
227. Boundy, R. H. and Boyerm, R. F., "Styrene, Its Polymers, Co-polymers and Derivatives," New York, Reinhold Publishing Corp., 1952.
228. Langlois, G. E., *Ind. Eng. Chem.*, **45,** 1470 (1953).
229. Bramston-Cook, H. E., *Chem. Eng. Progr.*, **48,** 381 (1952).
230. Weber, G., *Oil Gas J.*, **51,** 51, 131 (1953).
231. Gladraw, E. M., Kress, K. W., and Kimberlin, C. N. Jr., *Ind. Eng. Chem.*, **45,** 142 (1953).

CHAPTER 2

REACTION RATES AND SELECTIVITY IN CATALYST PORES

Ahlborn Wheeler

*Polychemicals Department, E. I. du Pont de Nemours & Company, Inc., Wilmington, Delaware**

Introduction

During the last fifteen years a major advance in catalysis has been our greatly increased knowledge concerning the physical structure of solid catalysts. On the one hand, techniques such as x-ray and electron diffraction have aided in elucidating structure on an atomic scale. On the other hand, a variety of new techniques have been developed which elucidate the gross physical structure of typical catalysts. These latter techniques have shown that solid catalysts in general contain a network of interconnecting very fine pores and that this network of fine pores, because of its immense surface area, is the seat of catalyst activity. The total surface area, distribution of sizes and total volume of these pores can now be determined by routine methods. Along with these experimental developments has come a corresponding theoretical development in interpreting the role of this pore structure in determining catalyst performance. Thus, in a very slow reaction, reactants can diffuse to the center of the catalyst pellet before they react. Such a slow reaction will use the entire internal surface area of the catalyst. On the other hand, in the case of a very active catalyst containing small pores, a reactant molecule will react (due to collision with pore walls) before it can diffuse very deep into the pore structure. Such a fast reaction for which diffusion is slower than reaction will use only the outer pore mouths (outer peripheral layer, say 0.1 mm thick) of a catalyst pellet. An important result of the theory is that when diffusion is slower than reaction, all the important kinetic quantities such as activity, selectivity, temperature coefficient, and kinetic reaction order become dependent on the pore size and pellet size with which a catalyst is prepared. This is because pore size and pellet size determine the degree to which diffusion affects reaction rates.

---

* Present address: Houdry Process Corp., Marcus Hook, Pa.

Since almost all catalysts contain a highly developed pore structure, and since these pores can influence all the important aspects of catalyst behavior, it well behooves both experimenter and theoretician to take these effects into account. Two important conclusions which the following treatment leads to are:

1. Fundamental studies aiming at intrinsic "chemical" reaction kinetics should be carried out at temperatures low enough and on catalyst granules small enough so that diffusion effects in pores are not important. A simple criterion for this is given later.
2. For practical studies seeking to improve catalyst performance, simple calculations given later can predict quite accurately whether a change in pore size or pellet size will improve activity and selectivity. Unlike many aspects of heterogeneous catalysis, the effect of pore structure on catalyst behavior can be put on quite a rigorous basis, making predictions from the theory relatively accurate and reliable.

The purpose of this chapter is to develop the physical and mathematical picture of reactions in catalyst pores. We first discuss some generalities concerning the pore structure and especially some experimental techniques for investigating this structure. We next consider the mechanism of transport in catalyst pores. Finally, we treat our main problem; diffusion accompanied by reaction in porous catalysts, and deductions which can be made from these calculations. As compared to our earlier review[1], we have tried to simplify and clarify the treatment. Those thoroughly familiar with earlier work in this field may find the following sections of particular interest: (a) a section in which for the first time we treat pressure and temperature gradients in single catalyst particles from a unified viewpoint, and in which we also include some new aspects of hydrogenation kinetics; and (b) a section in which for the first time we discuss from an over-all viewpoint the determination of pore size distribution by low temperature adsorption (work of Shull[2]; Barrett, Joyner and Halenda[3]; and Wheeler[7]).

THE IMPORTANCE AND ORIGIN OF CATALYST PORE STRUCTURE

External vs. Internal Surface Area

Since heterogeneous catalysis is a surface phenomenon, high internal surface area is a necessity for almost all solid catalysts of practical importance. Even though the very small external surface of a catalyst granule were immensely active, its activity would soon be destroyed by the merest trace of catalyst poisons. Accordingly, nonporous catalysts are virtually unknown commercially and are rarely used, except for highly academic studies under scrupulously "clean" conditions. High temperature oxidation reactions (e.g., ammonia or sulfur dioxide oxidation) on wire gauze are an apparent exception, but there is good evidence (e.g., Hurt[4]) that these reactions are not truly heterogeneous, the gauze acting as an initiator for gas-phase reaction chains. Also the conditions are extremely favorable (high temperature, oxidizing environment) for the removal of catalyst poisons.* Even though a rapid reaction uses only the outer peripheral layers of a porous catalyst pellet, the surface area available in this outer shell is immense compared to the external surface. For example, it is easy to compute that for a porous catalyst of modest internal surface area (say, 20 sq meters/gm) the area contained in the peripheral layer only 0.1 mm thick is about 4,000 times the external area. Thus, even this thin outer shell will contain an activity and resistance to poisons several thousand fold greater than the external surface. In the past it has been a subject of controversy just how much of the internal surface area was available to a reaction in a given practical case. A main purpose of this chapter is to answer just this question.

Origin of the Pore Structure

High porosity in catalysts arises naturally from a number of preparatory procedures, and the success of a given catalyst preparation is in no small part dependent on success in creating high porosity and high internal surface area. The three most important mechanisms by which porosity is produced are as follows:

(1) In precipitated catalysts, the precipitate is first formed as very minute particles which later "flock" together to give a porous mass, with the ill-fitting initial particles loosely cemented together.

(2) A second factor is the elimination of water or other compounds under the action of heat. Thus, ignition of alumina hydrate or of fresh "wet" silica gel causes a marked rearrangement of the solid structure which leaves a high surface area product. Preferred methods of preparing metal catalysts (e.g., nickel) often involve precipitation as carbonate followed by ignition to oxide. No doubt the elimination of CO_2 during ignition causes increased porosity and surface area in such catalysts.

(3) Finally, chemical attack to remove certain constituents is a common way to create porosity. Thus fused iron oxide catalysts for ammonia synthesis are nonporous before reduction, but after reduction with hydrogen both porosity and high surface area are produced. In this case oxygen removal is accompanied by rearrangement of the compact mass of fused iron oxide crystallites into a porous mass of ill-fitting iron crystallites. Activated carbons of immense internal surface area are prepared by the corrosive attack of high temperature steam and/or oxygen on vegetable

---

* Probably an even more important factor to be considered in connection with ammonia oxidation over platinum is the marked roughening of the gauze during the initial period of operation to produce a surface area much greater than that of the original smooth gauze.

structures (wood or coconut shells) or on coke. Raney-type metal catalysts are prepared in high surface area form by attack of alkali on aluminum-containing alloys.

EXPERIMENTAL METHODS FOR INVESTIGATING PORE STRUCTURE

For a particular catalyst material we are interested in (a) the average pore size and pore size distribution of the material, (b) the total surface area of all pores, and (c) the manner in which these fine capillaries are "hooked up," one to the other, to give the over-all structure. An important reason for investigating the pore structure by a variety of techniques is to use a variety of data in testing any proposed model of the pore structure. Once we have a satisfactory model which correlates considerable physical data we can then use this model with confidence to predict new data, concerning various properties such as catalyst performance. Several important methods for studying the pore structure will now be discussed.

Surface Area and Pore Volume

Surface area determination, preferably by the gas adsorption (BET) method gives the total surface area of the pore walls, including roughness on an atomic scale. The surface area per gram which we designate by S_g, combined with the pore volume per gram, V_g, gives a measure of the average pore size, as described below. Surface area measurements have been reviewed extensively elsewhere[5].

Measurement of pore volume per gram, V_g, may be carried out by several techniques. The simplest procedure is to boil a weighed sample of granular catalyst in an appropriate liquid such as water, carbon tetrachloride or cyclohexane. After the mixture is cooled, the liquid is decanted, and the catalyst is superficially dried and weighed. The weight increase divided by the density of the liquid gives the volume of liquid absorbed into the pore structure. Possible errors are caused by failure of boiling to eliminate all air from the pore structure and by an arbitrary element in deciding just when the pellets are superficially dry. The method however gives rapid and reasonably accurate results, but is not easily applicable to fine powders, since the point at which these are superficially dry is difficult to determine.

A more accurate method which gives additional data is the so-called mercury-helium method. Here a bulb of accurately known volume, V_b, is filled with catalyst. The total dead space in the bulb is determined with helium, this being the sum of the gross dead space between catalyst pellets plus the pore volume within the pellets. The helium is now pumped out and the volume of mercury necessary to fill the bulb is determined. Since mercury does not wet most catalyst materials it will fill the gross dead space but will not enter the catalyst pores. Thus, the difference between the helium dead space, V_d, and the mercury dead space equals the pore volume. The helium dead space measurement also determines the true chemical density, ρ_t, of the material. Experimentally,

$$\rho_t = \frac{w}{V_b - V_d}$$

where w is the weight of the catalyst, and V_d is the volume of the dead space as measured by helium. From the pore volume and chemical density two equivalent quantities may be calculated: the particle density of the catalyst, ρ_p (i.e., the density of a single catalyst pellet) and the "porosity" of the material θ (i.e., the fraction of the volume of a given pellet which is pore space). The relation between these four quantities is:

$$\frac{1}{\rho_p} - \frac{1}{\rho_t} = V_g = \theta/\rho_p \tag{1}$$

Experimentally it turns out that the porosity θ for many catalysts is roughly 0.5, meaning that a catalyst pellet is usually about one-half pore space. A rough but useful picture is that the volume of a bulb or reactor filled with typical catalyst is about one-quarter pore space, one-quarter solid catalyst and one-half gross dead space between catalyst granules.

Pore volume data can be combined with surface area measurements to calculate an average pore size. Thus, if pores are assumed to be cylindrical (with smooth walls and no intersection with other pores) the average pore radius is given by:

$$\bar{r} = 2V_g/S_g \tag{2}$$

since the total surface area per gm would be $2\pi rL_g$ and the pore volume would be $\pi r^2 L_g$, where L_g is the pore length per gram. Surface roughness could make Eq. (2) give too low values, while intersections with other pores would cause too high values. Experimentally it appears these two opposing sources of error just about cancel, as average pore radii calculated from Eq. (2) agree well with other estimates. This is discussed in more detail later in this chapter. Table 1 contains surface area, pore volumes and mean pore radii (radii calculated from Eq. (2)) for some typical catalyst materials. We note that pore radii for many important catalysts are in the range 10 to 200 Å.

Determination of Pore Size Distribution by Low Temperature Adsorption Measurements

Early Work. Experimentally the easiest method for determining pore size distribution in the important range of 10 to 200 Å is by interpretation

Table 1. Surface Area, Pore Volume and Mean Pore Radii for Typical Catalyst Materials[1]

Catalyst	S_g, m²/gm	V_g, cc/gm	r, Å	Ref.
Activated carbons	500–1500	0.6–0.8	10– 20	9
Silica gels	200– 600	~0.40	15–100	9
S_1O_2-Al_2O_3 cracking catalysts	200– 500	0.2–0.7	33–150	9
Activated clays	150– 225	0.4–0.52	~100	9
Activated alumina ("Alorco")	175	0.388	45	9
Kieselguhr ("Celite" 296)	4.2	1.14	11,000	9
Fe-Synthetic NH_3	4–11	~0.12	200–1,000	25*
Porous plate (Coors 760)	1.6	0.172	2,150	9
Pumice	0.38	—	—	25*
Fused copper catalyst	0.23	—	—	25*

* Ref. 25, p. 298.

of the sigmoid-shaped adsorption isotherms obtained when a condensable vapor is adsorbed on a porous solid. Due to capillary condensation in the pores, the amount adsorbed is greater than would be observed on nonporous materials of the same surface area. Since the amount of capillary condensation at a given pressure depends on pore size, proper interpretation can lead to quite accurate pore size distribution estimates. It is usually advisable to use nitrogen at liquid nitrogen temperature for pore distribution measurements, since accurate surface area values can then be calculated from the same data and since there is a larger background of experience for nitrogen as an adsorbate than for other gases. The experimental method consists of first measuring an adsorption branch of the isotherm in which the pressure is increased from low pressures up to the saturation pressure (1 atmosphere for N_2 at -195.6). At the saturation pressure the whole pore structure is filled with capillary condensation, so that the volume adsorbed at this point gives a measurement of the total pore volume. A desorption branch is now traced by lowering the pressure in small increments. The desorption branch lies higher than the adsorption branch, due to causes discussed in detail by Dr. Ries in Volume I, Chapter 1 of this treatise. Dr. Ries also discussed the general theory of capillary condensation, so we do not repeat this. It will suffice to say that capillary condensation occurs because the vapor pressure over a concave meniscus (formed by liquid in a pore) is lower than that of the bulk liquid, and this lowering is given by the Kelvin equation:

$$-R_gT \log P/P_0 = \frac{2\sigma V}{r_m} \tag{3}$$

when R_g is the gas constant; P, the vapor pressure of the meniscus; P_0, the vapor pressure of the bulk liquid; σ, the surface tension of the liquid;

V, the molal volume of the liquid; and r_m, the radius of the meniscus. Applied to nitrogen at −195.8°C, this means, for example, that a meniscus of 30 Å radius has a vapor pressure only about 72 per cent as large as bulk liquid nitrogen. The liquid condensed in a capillary is of course in equilibrium with its meniscus, and hence is under a very large tension (negative pressure) equal to $2\sigma/r$ or about 100 negative atmospheres for 30 Å pores.

As early as 1914 Anderson[6] suggested that the Kelvin equation could be used to determine pore sizes. Anderson assumed that all of the adsorption was due to capillary condensation. He further assumed that at a given pressure on the desorption branch of the isotherm all pores smaller than the corresponding Kelvin radius were filled by capillary condensation. Thus, if we use Eq. (3) to convert from pressure to pore radius, we can replot the isotherm as volume adsorbed (calculated as volume of liquid) vs. radius. With Anderson's assumptions, this is a plot of volume of pores smaller than r, vs. pore radius r. Hence, the slope of such a plot at any point is equal to the frequency of pore sizes of this radius. It is easy to show that although this procedure gave results of the right order of magnitude, it yielded pore sizes that were too small by a factor of about two. For example, the surface areas back-calculated from these pore size distributions are too high by a factor of about two. Also the shape of the pore size distribution function for various materials is most strange and "unnatural" looking.

Recent Developments. To remedy these deficiencies, in 1945 the writer (Wheeler[7]) devised an improved theory which took into account the effects of multilayer adsorption. Two new assumptions were made. In the first place, it was assumed that at any point on the desorption branch of the isotherm, all pores larger than a certain radius R_c were covered with an adsorbed multilayer of thickness t, whereas all pores smaller than R_c were filled by capillary condensation. Secondly, since all unfilled pore walls have an adsorbed layer of thickness t on them, it was assumed that the radius of the meniscus in a filled pore, where it joins a larger pore, will not be the pore radius R_c but a smaller radius $R_c - t$. In other words, under conditions of adsorption we are not dealing with pores of the true physical radius R_c, but with pores whose radii have been effectively diminished by the thickness of the adsorbed multilayer. Thus, the writer argued that the Kelvin equation applies not to the actual pore radius but to the effective radius of the "inside tube" left after multilayer adsorption has taken place. The maximum true pore size R_c which will be filled by capillary condensation at a pressure P is then given by:

$$R_c = t + \frac{2\sigma V}{R_g T \log P_0/P} \tag{4}$$

which is obtained by substituting $(R_c - t)$ for r_m in the Kelvin equation, and solving for R_c. If the multilayer thickness t is known as a function of pressure, then Eq. (4) tells us that at a given pressure P all pores smaller than R_c will be filled with liquefied adsorbate held by capillary condensation. We further assume that the thermodynamic equilibrium implied by Eq. (3) is established on the desorption branch of the isotherm.

With these assumptions, the equation for the adsorption isotherms can be developed as follows. The volume V_a adsorbed at any point on the isotherm, computed as liquid volume, is given by:

$$V_a = V_c + V_m \tag{5}$$

where V_c is the volume of capillary condensed liquid in pores smaller than R_c, V_m is the volume of adsorbed multilayers on pores larger than R_c, and R_c is given as a function of pressure by Eq. (4).

We next introduce the pore size distribution function $L(R)dR$ defined as the length of pores (per gram of catalyst) which have radii in the range R to $(R + dR)$. Thus to be practical, for R in angstrom units, the function $L(30)$ for a particular catalyst would give the length of pores per gram of catalyst having radii in the range 29.5 to 30.5 Å. With this definition the volume $V_c(< R_c)$ of all pores having radii less than R_c is given by:

$$V_c(<R_c) = \int_0^{R_c} \pi R^2 L(R)\, dR \tag{6}$$

while the surface area and pore length in pores larger than R_c are given respectively by:

$$S(>R_c) = \int_{R_c}^{\infty} 2\pi R L(R)\, dR \tag{7}$$

$$L(>R_c) = \int_{R_c}^{\infty} L(R)\, dR \tag{8}$$

Going back to the equation for the isotherm, Eq. (5), we see that V_c, the volume of condensed liquid in capillaries is by definition $V_c(< R_c)$ and so is connected to the pore size distribution function by Eq. (6). V_m, the volume of the adsorbed multilayer, calculated as liquid volume, is for a single cylindrical pore, the volume of a cylindrical shell of outside radius R and inside radius $R - t$, or is $\pi\ [R^2 - (R - t)^2]L(R)$. Multiplied out, this is $\pi(2tR - t^2)L(R)$. Hence, the volume of multilayer adsorption on all pores larger than R_c is the integral of this, or:

$$V_m = t \int_{R_c}^{\infty} 2\pi R L(R)\, dR - \pi t^2 \int_{R_c}^{\infty} L(R)\, dR \tag{9}$$

$$= tS(> R_c) - \pi t^2 L(> R_c) \tag{10}$$

Putting these expressions for V_m and V_c back into Eq. (5) gives the equation of the isotherm:

$$V_a = V_c(< R_c) + tS(> R_c) - \pi t^2 L(> R_c) \qquad (11)$$

This equation states that the volume adsorbed at any pressure is equal to the capillary condensed volume $V_c(< R_c)$, plus the volume of multilayer adsorption of thickness t on the "free surface area" of capillaries not filled by capillary condensation, less a correction term which takes into account the fact that pores are cylindrical so that the volume of a layer of thickness t on an area S is not tS but is smaller than this.

The isotherm may also be written compactly in terms of $L(R)$ as:

$$V_g - V_a = \int_{R_c}^{\infty} \pi(R - t)^2 L(R)\, dR \qquad (12)$$

where V_g is, as defined above, the total pore volume per gram. Equation (12) states that the pore volume not filled is simply the sum of the volume of all the "inside tubes" of unfilled pores which are covered with multilayer adsorption. Equations (11) and (12) are of course mathematically identical as is discernible by expanding $(R - t)^2$ in Eq. (12) and then using Eqs. (6), (7) and (8). We note that Anderson's original method corresponds to Eq. (11) or (12) with t set equal to zero.

If t, the multilayer thickness, is known as a function of pressure, then R_c is also known as a function of pressure from Eq. (4). Since V_a and V_g are experimentally measured, only the pore size distribution function $L(r)$ remains as an unknown in Eq. (12), or in its equivalent Eq. (11). Since $L(R)$ occurs under the integral sign, Eq. (12) is an integral equation for $L(R)$ and hence is difficult to solve by simple analytical methods. Several methods of determining $(L(R))$ are however applicable. The writer's original method[7] was to assume a pore size distribution function $L(R)$. The isotherm was calculated for this assumed distribution function and compared with the experimental data. This method was later improved and extended by Shull[2]. Recently Barrett, Joyner and Halenda[3] have shown that a piecewise numerical integration of Eq. (12) may be carried out, without making assumptions concerning the shape of the pore size distribution function. The writer will briefly describe a new solution in closed analytical form which should be capable of yielding accurate results with very little work. These various approaches are described below.

(1) *Early Wheeler-Shull Method:* The writers interest in this problem was originally aroused by some excellent experimental work carried out under Drs. M. Tamele and H. Byck in the Colloid Department of Shell Development Company. A set of fifteen silica gel samples had been prepared covering a complete spectrum of average pore size from 7 to 77 Å, as judged

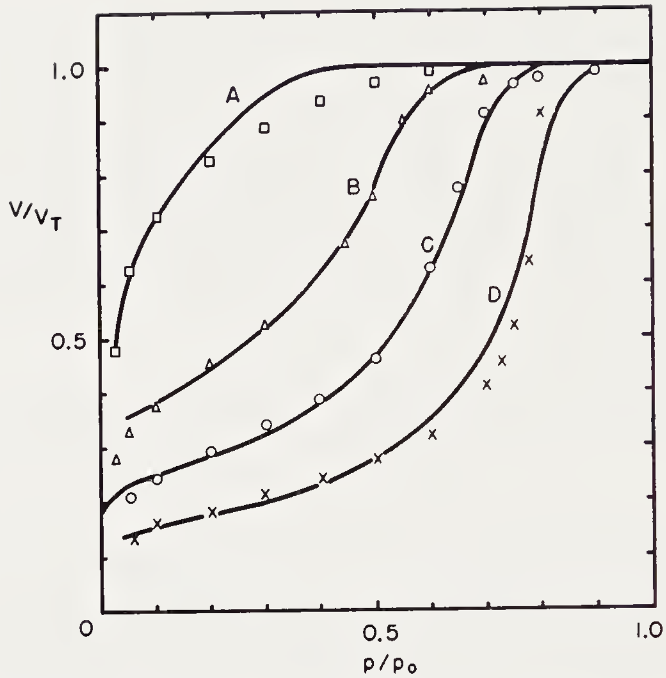

FIG. 1. Isotherms for the adsorption of nitrogen at −195°C on four silica gels: Comparison between theory and experiment: Curves are calculated for Gaussian distribution of pore sizes ($\beta = 2$). Points are experimental. Experimental values of $\bar{r}$ for curves A, B, C, D, are respectively 9.6, 18.7, 28, 50 Å. Values of $\bar{r}$ used for calculated isotherms are respectively 10, 17, 30, 50 Å

by Eq. (2). Low temperature adsorption isotherms using N_2 at −195.8°C were measured for all gels. When plotted on the reduced plot V_a/V_g vs. P/P_0, the fifteen isotherms (desorption branches) formed a complete family of curves in that there was no crossing of isotherms and a number of gels with the same values of $2\ V_g/S_g$ had identical reduced plots (even though V_g and S_g taken separately were different). The advantage of using the reduced plot (i.e., V_a/V_g as ordinate) is clearly that the absolute frequency of pore sizes is cancelled out, and only the relative frequency determines the reduced isotherm. The foregoing data suggested that all gels might have the same general shape of pore size distribution. Four isotherms of the family of fifteen are shown in Figure 1. The writer therefore devised the preceding theory and set about to test it with this silica gel data. He decided to assume several shapes for $L(R)$ in Eq. (12), and to compare the isotherms calculated purely theoretically with the experimental data. A decision had to be made concerning the dependence of multilayer thickness on pressure. Here two choices were possible. Data on physical adsorption of N_2 on nonporous materials (e.g., TiO_2 pigment, glass spheres, etc.), give one consistent curve for t vs. P/P_0 as shown in

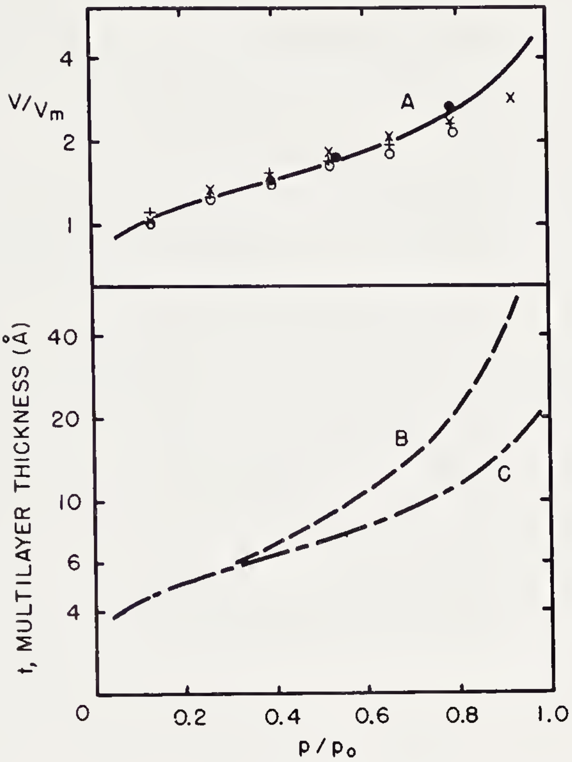

FIG. 2. Multilayer thickness as obtained for large crystals and as calculated from BET theory.[2] "Curve A—Experimental values of the number of adsorbed layers (V/V_m) for crystalline materials of large crystal size; Curve B—Multilayer thickness for N_2 calculated from BET theory; Curve C—Multilayer thickness curve derived from Curve A."[2]

Figure 2, which is taken from Shull's paper[2]. The uppermost curve gives the number of adsorbed layers vs. P/P_0 for various nonporous adsorbents, while the bottom curve converts this to thickness in Å using 4.3 Å per layer of nitrogen. As one choice, one could therefore use such a composite curve to relate P/P_0 to thickness t. A second logical choice is to use a curve lying higher than the empirical curve of Figure 2. The writer originally argued that multilayer adsorption in small pores should be larger than on plane surfaces due to the proximity of adjacent pore walls and to surface tension effects from the cylindrical meniscus formed by the adsorbed layer. He therefore arbitrarily chose the BET equation with $C = \infty$, shown as the middle dotted curve in Figure 2. Shull[2] later pointed out that this was a poor choice since the BET equation mainly lies higher than the empirical curve at high values of P/P_0 (large pore region) whereas actually it should lie higher at low values of P/P_0 and asymptotically approach the empirical curve for high P/P_0. The writer agrees with Shull, and believes the preferable choice is to use the Halsey[8] equation, which, applied to nitrogen, is:

$$t(\text{Å}) = 4.3 \left[\frac{5}{\ln P/P_0} \right]^{1/3} \tag{13}$$

This agrees with the empirical curve almost exactly for $P/P_0 > 0.5$ and thus is a useful extrapolation and computational formula. Also, it has the desirable characteristic of being a little above the empirical curve for low P/P_0. t computed from Eq. (13) is given for selected P/P_0 values in Table 2. The table also contains values of r_m computed from Eq. (3). The sum $t + r_m = R_c$ shown in the table is then the critical radius, that is, the largest pore size which is filled at a pressure P/P_0. Thus, the first step in the computation is to construct Table 2.

Next, two types of pore size distribution function $L(R)$ were assumed, namely a Gaussian or "probability" shape.

$$L(R) = A_G \exp -\beta^2 \left(\frac{R}{R_0} - 1 \right)^2 \tag{15}$$

and a Maxwellian shape:

$$L(R) = A_M \left(\frac{R}{R_0} \right) e^{-R/R_0} \tag{16}$$

Here R_0 is the most probable pore radius, on a length basis while A_G and A_M are dimensionless numbers giving the absolute frequency but not the relative frequency of pore sizes. For the Gaussian distribution β is a parameter of sharpness, $\beta = 2$ giving moderately sharp distribution, $\beta = 5$ giving very sharp distributions. The Maxwellian distribution is not symmetrical about the most probable pore radius, and has a long "tail" containing many pores larger than the most probable pore size. The "average" pore radius defined by $\bar{r} = 2V_g/S_g$ is connected to the most probable

TABLE 2. MULTILAYER THICKNESS t AND CRITICAL RADIUS Rc AS A FUNCTION OF PRESSURE (UNITS, ANGSTROMS, FOR t, r_m, Rc)

P/P_0	t	r_m	$R_c = t + r_m$
0.1	5.55	4.15	9.7
0.3	6.92	7.94	14.9
0.5	8.30	13.8	22.1
0.7	10.4	26.7	37.1
0.8	12.1	42.7	54.7
0.9	15.5	91.0	106.5
0.95	19.8	188	208
0.97	23.4	312	335

radius R_0 by simple equations obtained by integration of (15) and (16). These equations are:

$$\bar{r} = R_0\left[1 + \frac{1}{2\beta^2}\right] \equiv \frac{2V_g}{S_g} \tag{16}$$

for the Gaussian distribution and

$$\bar{r} = 3R_0 \equiv 2V_g/S_g \tag{17}$$

for the Maxwellian distribution. If the total pore volume for a catalyst has been measured, and it has been ascertained that the pore size distribution follows a Gaussian (or Maxwellian) distribution, then Eq. (16) or (17) can be looked upon as determining the surface area S_g in terms of the pore volume and distribution parameters. This obviously provides a check on the whole method, since this surface area computed from the distribution of pore sizes should agree with the BET surface area.

The parameters A_M and A_G may also be eliminated in terms of the total pore volume V_g by the equations:

$$A_G = \frac{V_g\beta}{\bar{r}}\left[1 + \frac{1}{2\beta^2}\right]^2 \tag{18}$$

$$A_M = \frac{9V_g}{2\pi(\bar{r})^3} \tag{19}$$

The method of computing a theoretical isotherm proceeds as follows: Using, for example, the Gaussian distribution with $\beta = 2$ and $R_0 = 30$ Å, we first compute $V_c(< R_c)$, $S(> R_c)$ and $L(> R_c)$ from Eqs. (15), (6), (7), and (8) at selected values of R_c. These are calculated by purely mathematical integration of Eqs. (6), (7), and (8) and all these will contain the undetermined factor A_G. For each value of R_c there is a corresponding value of t and of P/P_0 which Table 2 gives. Thus, to compute a given point on the isotherm we fix R_c (hence t and P/P_0), and substitute the corresponding values of $V_c(< R_c)$, $S(> R_c)$, $L(> R_c)$, and t into Eq. (11). This gives the volume adsorbed as a definite number times the undetermined factor A_G. Since A_G is proportional to the total pore volume V_g as given by Eq. (18), and since we have fixed R_0 (and hence $\bar{r}$, by Eq. 16), we can compute V_a/V_g as an absolute function of R_c. Using Table 2 to convert from R_c to P/P_0 we can compute the exact reduced isotherm (V_a/V_g vs. P/P_0) for the Gaussian distribution with given β and R_0. In this way a complete family of isotherms for the Gaussian distribution with $\beta = 2$ was computed, each isotherm having a different value of the mean pore radius (R_0 or $\bar{r}$). Four members of the family are shown as the curves in Figure 1. This purely calculated family agreed remarkably with the experimental family, the points of Figure 1 being experimental. In addition, the experimental and theoretical $\bar{r}$ values of the matching curves agree to better than ± 10 per cent. This means that given the pore volume, one obtains values for the surface areas of the gels calculated from the Gaussian pore size distribution which agree with the BET areas to within the practical absolute accuracy of either method.

In summary, the writer showed that, using the proposed theory, a large family of silica gels all had approximately a Gaussian distribution of pore sizes with the sharpness parameter $\beta = 2$. The fact that the BET thickness t rather than the preferred values of Table 2 were used will not change the calculated curves significantly for the small pored gels (Curves A, B, C). Using the preferred smaller thickness would improve the agreement for Curve D, since the calculated values lie higher than the experimental values.

Shull[2] next published several improvements and extensions. As described earlier he suggested that the empirical multilayer thickness was preferable to the BET thickness. Secondly, he extended the calculations to the Gaussian distribution with $\beta = 5$ and published complete sets of calculated isotherms for the Gaussian ($\beta = 2$ and 5) and Maxwellian distributions. Thirdly, he showed how an experimental isotherm which does not fit any calculated curve can be resolved into a sum of two distributions. Shull preferred to plot his calculated isotherms as what is essentially a plot of $\log (V_g - V_a)/V_g)$ vs. R_c. For comparison with an experimental isotherm, the experimental one is plotted as $\log (V_g - V_a)$ vs. R_c, and compared with the calculated curves. The writer is not clear as to the advantage of this method over the reduced isotherm V_a/V_g vs. P/P_0, since a value for the total pore volume is needed in either case, and is always automatically obtained due to the nature of the experimental method. A minor improvement in Shull's calculated plots would be to attach to each the values of $\bar{r} = 2V_g/S_g$ instead of R_0 (the most probable pore radius) since $\bar{r}$ is much more closely related to experiment. $\bar{r}$ is connected to R_0 by Eqs. (16) and (17).

(2) *Barrett-Joyner-Halenda Method*: An important advance in the technique of solving Eq. (12) was made by Barrett, Joyner and Halenda[3]. They introduced the idea of performing a numerical stepwise integration which starts a high pressure end of the isotherm. Rather than starting with Eq. (12) their basic equation was arrived at by intuitive reasoning and therefore contains a fair number of approximations. We therefore start afresh and describe a somewhat more exact version of their general method, which we then compare with their treatment.

If Eq. (12) is differentiated with respect to R_c and then the infinitesimal increment dR_c replaced by a finite increment ΔR_c, we obtain:

$$\Delta V = \pi(R_c - t)^2 L(R_c)\Delta R_c + 2\pi(\Delta t) \int_{R_c}^{\infty} (R - t)L(R)\, dR \tag{20}$$

This equation says that at any point on the desorption branch of the isotherm if the pressure is lowered say by a small increment Δp, then a volume ΔV will be desorbed which is the sum of two effects: (1) pores in the radius range ΔR_c corresponding to Δp will be emptied except for a multilayer thickness t left on the pore wall; (2) all larger pores will suffer a thinning Δt of their adsorbed multilayers. The experimental isotherm is plotted as volume adsorbed vs. R_c, and the graph is then divided into a large number (10 or 20, say) of vertical strips by lines at equally spaced values of R_c. ΔV for each strip is the change in volume adsorbed over this increment of R_c. For each strip all quantities in Eq. (20) are known except for $L(R)$ and the integral which involves $L(R)$. R_c and t are the average or midpoint values of R_c and t for the strip. Thus, if the value of the integral were known, we could solve Eq. (20) for the value of $L(R)$ at the midpoint of each strip. The method of solution is to obtain a good value for the integral by the following accumulation procedure: At the high pressure end of the isotherm will be a final strip containing the volume of all pores larger than the value of R_c at the last vertical line, say from $R_c = 100$ Å to $R_c = \infty$. We idealize these largest pores into a single pore of one fixed arbitrary size, say 110 Å. Since we assume there are no larger pores than this one, the integral in Eq. (20) is zero for the last strip, and hence the volume of this largest pore, $\pi R^2 L(R)$, is obtained by solving Eq. (20) with the integral neglected:

$$\pi R^2 L(R) = (\Delta V)_1 \frac{R^2}{(R - t)^2} \tag{21}$$

when R is the presumed radius of the largest pore (e.g., 110 Å), $(\Delta V)_1$ is volume increment in the last strip and t is the adsorbed layer thickness on 110 Å pores. Solution of Eq. (21) gives $L(110)$ or the length of the largest pores which have been idealized into one large pore of radius 110 Å. We now go to the next to last strip and approximate the integral in Eq. 20 by the single value of $(R - t)L(R)$ for the largest pore. This enables us to solve Eq. (20) for the length (or volume) of pores in the next to last strip. This process is continued, the integral in Eq. (20) being evaluated by accumulating the values of $(R - t)L(R)$ for all previous strips. Thus, the general solution for the volume of pores in any strip is given by:

$$R^2 L(R)\Delta R = \frac{R^2}{(R - t)^2}(\Delta V) - \frac{R^2}{(R - t)^2} 2\pi\Delta t \sum (R - t)L(R)\Delta R \tag{22}$$

where the summation goes over all previously calculated strips. Equation (22) is simply a rearrangement of Eq. (20), with summation substituted for integration.

Barrett, Joyner and Halenda's intuitive equation is somewhat different from Eq. (22), the term $R^2/(R - t)^2$ being neglected before the second term on the right, and t being neglected under the summation sign. Thus their equation is:

$$R^2L(R)\Delta R = b\Delta V - \Delta tS_g(> R) \tag{23}$$

whereas the exact equation is:

$$R^2L(R)\Delta R = b\Delta V - b\Delta tS_g(> R) + b2\pi t\Delta tL(> R) \tag{24}$$

where $b = R^2/(R - t)^2$. Neglecting the "b" factor before $(\Delta t)S_g(> R)$ and omitting the last term in Eq. (24) are partially compensating errors, but the $S_g(> R)$ term is always more important. The result is that Eq. (23) should give somewhat too high values for the pore size distribution function, especially at the small pore end where both b and $S_g(> R)$ are large. In spite of this minor defect, Barrett, Joyner and Halenda have obtained pore size distributions using Eq. (23) which agree very well with data from the mercury porosimeter method to be described in the next section. In the writer's opinion, in using the Barrett, Joyner and Halenda piecewise integration method the full Eq. (24) should be used, because equations of the form (23) can be solved by a more rapid, more exact method described in the next paragraph.

(3) *A New Method of Solution:* Since the term in Eq. (11) involving t^2 is small (also the corresponding term containing $t\Delta t$ in Eq. (24)) the following method of solution suggested itself to the writer while writing this manuscript. This is an analytical solution for equations of the type of Eq. (23). If the last term in Eq. (11) is dropped and the resulting equation is differentiated with respect to R_c, the result is:

$$\frac{dV_a}{dR_c} = \pi R_c(R_c - 2t)L(R_c) - \frac{\partial t}{\partial R_c} S(>R_c) \tag{25}$$

Since the derivative of $S(> R_c)$ is just $2\pi R_cL(R_c)$ this equation can be written

$$f'(x) = \tfrac{1}{2}(x - 2t)\frac{dy}{dx} - \frac{dt}{dx}y \tag{26}$$

where we write x for R_c and y for $S(> R_c)$, and $f'(x)$ is dV_a/dR_c which is the slope of the V_a vs. R_c plot. This is a simple linear differential equation for y, and so can be solved exactly for y as a function of $f'(x)$ and dt/dx. It turns out we can avoid ever taking slopes, the result being that one graph plus a few minutes with a planimeter effects a rapid and accurate solution. The details follow: The solution of Eq. (26) is:

$$y \equiv S(>R_c = [g(R_c)]^{-1} \left[\int_{R_c}^{\infty} g(x) \frac{2}{x - 2t} \frac{dV_a}{dx} \, dx \right] \tag{27}$$

where

$$g(x) = \text{exp.} - \int_0^{R_c} \frac{dt}{dx} \frac{2}{x - 2t} \, dx \tag{28}$$

Both $g(x)$ and the product of this with $2/(x - 2t)$ are computed and tabulated once and for all. The integral in $g(x)$, (see Eq. 28) is simply the area under a plot of $2/(x - 2t)$ vs. t. The integral in Eq. (27) is just the area under a plot of $g(x)[2/(x - 2t)]$ vs. $V_a(x)$. We thus start with a "master table" which we use for all calculations applying to nitrogen at −195.8°C. This table contains values of t, $2/(R_c - 2t)$, $g(R_c)$ and [$g(R_c)$ times $2/(R_c - 2t)$] all at selected values of R_c and hence at selected values of P/P_0. To apply to a given experimental isotherm we add to the table the experimental values of V_a, the volume adsorbed, at the selected R_c values. We now plot $[g(R_c) \times 2/(R_c - 2t)]$ as ordinate vs. V_a as abscissa and take the area under this curve with a planimeter from each tabular V_a value out to the end of the curve to the right. This area is the value of the bracket in Eq. (27) at the value of R_c corresponding to the V_a value chosen. This area is then divided by the tabular value of $g(R_c)$ at this R_c value. Thus a calculation to get 10 points for the pore size distribution function involves 1 plot, ten planimeter areas and ten multiplications, or less than one hours work. The result is the "cumulative" distribution function on a surface area basis, $S_g(> R_c)$. From many standpoints this is the most desirable quantity to calculate, since the total surface area ($S_g = S(> 0)$) is automatically calculated (to be compared with the BET value) and from $S_g(> R_c)$ the amount of surface contained in pores of a given size range can be told at a glance. Other noncumulative distribution functions such as $\pi R^2 L(R)$ (which Barrett, Joyner and Halenda compute) or $L(R)$ can be obtained from $S(> R_c)$ by tabular or graphical differentiation.

Two refinements in this treatment are possible. For example the first solution given by Eq. (27) can be considered a first approximation. From this the last term on the right in Eq. (11) (which has been neglected so far) can be computed and subtracted from the experimental values of V_a. The computation of $S_g(> R_c)$ from Eq. (27) is then repeated using these corrected values for V_a. Alternatively before any computation is started, an approximate correction (for the last term on the right of Eq. (11)) may be subtracted, this correction being based on a Gaussian or Maxwellian shaped distribution of the same $\bar{r}$ value as the experimental isotherm. By comparing the experimental isotherm with Shull's calculated curves, the most appropriate correction can be judged. Thus Shull's curves should be supplemented by a set of curves giving for each the value of the last term on the right of Eq. (11) in units of V_a/V_g. These curves rise to a maximum at an R_c value of about 0.7 $\bar{r}$. The absolute correction at the maximum amounts to about 8 per cent of the total pore volume for Gaussian or Maxwellian distributions of $\bar{r} = 20$ Å, and about 3 per cent of the total pore volume for $\bar{r} = 50$ Å.

Critique of Low-Temperature Adsorption Method for Pore Size Distribution. In summary the general method we have outlined contains the following assumptions: (1) that on the desorption branch of the isotherm we have thermodynamic equilibrium so that the modified Kelvin equation applies. The adsorption branch is not in equilibrium since super-saturation is probably necessary to fill a pore with capillary condensed liquid. (2) A tacit assumption is that each pore space must be connected with at least one larger pore, since otherwise the smaller pore cannot empty at the proper pressure. (3) That the meniscus radius is that of the inside tube formed by multilayer adsorption. (4) That pores are cylindrical. (5) That the surface tension of liquid nitrogen is the same in small pores as in bulk. These five assumptions are all capable of improvement, at the expense of complicating the theory. However, the existing theory which proceeds from these assumptions gives results in good agreement with two other methods, the BET method for surface areas and the mercury porosimeter method, (see next section). In addition, these assumptions have a simplifying effect on the experimental data, showing that many pore size distributions are of a logical probability type shape. We thus justify our assumptions a posteriori since they give a logical result in agreement with other data.

Determination of Pore Size Distribution by Mercury Porosimeter Method. A second approach to the determination of pore size distribution is the mercury porosimeter method developed by Ritter and Drake[9]. Although experimentally more difficult than the low temperature physical adsorption technique, this method has the advantage that large pores (> 300 Å) can be measured. The main disadvantage is that a very high pressure apparatus is necessary for determining small pores in the 10 to 40 Å range. Since mercury does not "wet" most catalyst materials it will not go into the pore structure unless forced in under pressure. If the contact angle between mercury and solid catalyst is θ, then the surface tension force tending to keep mercury out of a pore of radius r is $-2\pi r\sigma \cos\theta$, where σ is the surface tension. (Complete nonwetting corresponds to a contact angle of 180°, or $\cos\theta = -1$). If the mercury is under a pressure p, then a force $\pi r^2 p$ will tend to drive it into the pore, where πr^2 is the cross-sectional area of the pore. If these two opposing forces are equated we get the equation:

$$p = \frac{2\pi\sigma \cos \theta}{r} \tag{28}$$

for the pressure necessary to force mercury into a pore of radius r. Presumably the contact angle varies some for different materials, but Ritter and Drake settle on 140° as a good practical average. With this assumption, the pressure to fill pores of 10,000 Å radius is 100 psi.; to fill 1,000 Å pores, 1,000 psi.; and to fill 100 Å pores, 10,000 psi. An apparatus going to 100,000 psi. will fill 10 Å pores. The method consists in contacting an evacuated sample of catalyst with liquid mercury, and then observing the contraction in mercury volume as a function of pressure, due to the disappearance of mercury into the pore structure. The data are plotted as volume of mercury forced into the capillaries vs. pore radius; Eq. (28) is used to convert from pressure to radius. This is a plot $V_c(> R)$ (the volume of pores larger than R) vs. R, so that the slope is equal to the pore size distribution function on a volume basis $\pi r^2 L(r)$. Ritter and Drake[9] measured the distribution of macropores (larger than 100 Å) for a variety of materials such as cracking catalysts, activated carbons, activated clay and diatomaceous earth. The presence of a large number of macropores in activated carbon is of especial interest, showing this material to have an exceedingly broad pore distribution containing many pores from circa 10 Å all the way up to 100,000 Å. For other materials no particular generalization can be made except that the distributions appear to be reasonably sharp with most of the pore volume in pores in the range 50 per cent smaller to 50 per cent larger than the $\bar{r}$ value, where $\bar{r} = 2V_g/S_g$.

The assumptions and potential errors in the mercury porosimeter method are about the same as in the low temperature adsorption method. The main assumptions are (a) that each pore is connected to at least one larger pore, for a bottleneck pore completely surrounded by smaller pores would not fill with mercury according to Eq. (28), but would fill at a higher pressure corresponding to the diameter of the smaller pores; (b) that pores are cylindrical; (c) that mercury has a contact angle of 140° and (d) that the surface tension of mercury in small pores is the same as in bulk.

In conclusion, for determination of pore size distribution of catalysts it appears that an ideal combination is to use a relatively low pressure (say up to 10,000 psi.) mercury porosimeter for macropore measurements plus low temperature physical adsorption measurements for the smaller pores. More work needs to be done to show that the two methods give consistent and similar results, the work of Joyner, Barrett and Skold[28] being one of the few cross-checks available at the present time.

A Working Model of the Pore Structure

In order to correlate catalytic reaction rates with pore structure we need a working model which will allow us to compute diffusion rates into a catalyst pellet from a minimum of easily obtained physical data. Ideally diffusion rates should be measured experimentally for each type of catalyst, but in practice such measurements are seldom carried out. Our practical objective is to set up a model from which diffusion rates can be calculated from surface area and pore volume measurements alone.

In summary, the foregoing experimental methods tell us (a) that pores are interstices between the ill-fitting crystallites or other building blocks which make up the catalyst, (b) although catalyst pores certainly are not cylindrical, a useful picture can be made in which they are treated as cylinders, with possibly rough walls and with many intersections with other pores. Since, in a catalytic reactor, molecules can enter the pellet only through pores on the external pellet surface, we need a value for the number of such external pores, as well as the average radius and length of each pore.

We first get a good value for the number of pore mouths per unit external surface as follows: First, the external surface of a catalyst pellet (as well as any imaginary internal surface) is made up of a fraction θ of voids which are pore mouths, plus a fraction $(1 - \theta)$ of solid catalyst. It is easy to show (e.g., Wheeler[1]) that this fraction θ must be equal to the "porosity" or volume fraction of voids in the whole pellet. Thus the total number of pore mouths must be equal to the total area of pore mouths divided by the area per mouth. If pores ran exactly at right angles to the surface, the area per mouth would be πr^2 where r is the average pore radius, and the total number of pore mouths per cm^2 external surface would be $\theta/\pi r^2$. But it is a very specialized assumption to assume that randomly directed pores run at right angles to a given surface. Instead we shall assume that on the average they run at about 45°, since some pores will run at almost right angles but others will run almost parallel to the surface. Hence, the area of intersection of an average pore with the surface will be $\sqrt{2}$ larger or $(\sqrt{2}\pi r^2)$ since a cylinder of radius r intersects a plane in an ellipse of area πr^2 sine α, where α is the angle between the plane and the axis of the cylinder (45° in this case). Adding this up, we find that *the number of pore mouths per unit external surface of catalyst pellet is approximately* $\theta/(\sqrt{2}\pi r^2)$ where r is the average pore radius. We note that by the "direction of a pore" we mean the direction of the "streamlines" along which molecules will flow through the pore structure.

If we use this value for n_p the number of external pore mouths per cm^2 external area, then the total number of pore mouths for a given pellet is $n_p S_x$ where S_x is the external surface area per pellet. If we assign an average length L per pore, we now can write two equations which equate the pore volume ($n_pS_x\pi r^2L$) and the surface area contained in the n_pS_x pores to the experimental pore volume and surface area. These two equations can be looked upon as determining the average pore length L and average radius $\bar{r}$ in terms of the experimental pore volumes and surface areas. These equations yield:

$$L = \frac{V_p}{S_x}\sqrt{2} \tag{29}$$

$$\bar{r} = \frac{2V_g}{S_g}(r.f.)(1 - \theta) \tag{30}$$

where V_p is the volume of the catalyst pellet and ($r.f.$) is the roughness factor for the pore walls. Equation (29) says that the average pore length for this model is equal to $\sqrt{2}$ times the volume to external surface ratio for the pellet. For catalyst pellets in the shapes of spheres or cubes and for cylinders whose diameter equals their length, the volume to surface ratio turns out to be $a/6$ where a is the pellet size: that is the diameter of the sphere, the side of the cube or the length of the cylinder. Thus for almost all practical shapes of catalyst particles we can assume that the average length of a typical pore is approximately $a\frac{\sqrt{2}}{6}$ where a is the particle size. We emphasize that this length is the one to be used for the catalytic case, where all external faces of a catalyst pill are bathed in gas. For experiments in which we measure the permeability of a single pellet to gas flow after sealing off the side of the pellet, then S_x in Eqs. (4a), (4b), (4d) refers only to the area of one end of the pellet, and equation (4d) shows that the pore length to be used in this case is $\sqrt{2}$ times the length of the pellet. The factor $\sqrt{2}$ corresponds to the devious path a molecule must travel in flowing through the pellet.

Equation (30) is simply a more accurate version of Eq. (2) in which possible roughness of pore walls and intersections with other pores are taken into account. The term $(1 - \theta)$ on the right side of Eq. (30) arises since pore walls are not all solid but contain many intersections with other pores. Here we assume that the pore wall like any other surface is made up of a fraction θ of voids (intersections) and a fraction $(1 - \theta)$ which is solid and hence contributes to the internal surface area. The derivation of Eqs. (29) and (30) is described in somewhat more detail elsewhere (Wheeler[1]). We note from Eq. (30) that the ratio $2V_g/S_g$ is equal to the "average" pore radius only when ($r.f.$) $(1 - \theta)$ is equal to unity. Since the porosity θ for most material is equal to about 0.5 and since a roughness factor of 2.0 is reasonable for most materials, it is likely that $2\,V_g/S_g$ is a physically meaningful average pore radius for most materials.

In summary, we have a model which enables us to compute the average pore length, radius, and number of pores from the three easily determined experimental qualities: pellet size, internal surface area per gram and pore volume per gram.

MECHANISM OF DIFFUSION AND FLOW IN CATALYST PORES

We now consider the problem of how reactant molecules are transported into and within the porous structure of a catalyst granule. Three mechanisms are possible. By far the most important mechanism is diffusion. Diffusion is the random process by which molecules flow from points of high concentration to points of lower concentration in the absence of total pressure differences. By sheer probability more molecules are moving (by their random kinetic motions) away from a region of high concentration than are moving toward it, so that a net flow occurs. A diffusion coefficient D is defined by saying that if a concentration gradient dC_A/dx of reactant exists at a surface of area S, then the net number of molecules which cross this surface by diffusion is:

$$\frac{dn}{dt}\text{ (molecule per sec.)} = SD\,\frac{dC_A}{dx}$$

The units of D are cm^2/sec. We discuss the various kinds of diffusion in catalyst pores later in this section. A much less important mechanism of transport in catalyst pores is by forced flow due to pressure differences within the granule. These differences can arise for example due to "volume change" in a gas phase reaction. Thus in hydrogenation or polymerization reaction the "volume contraction" due to reaction can cause the interior of a catalyst pellet to be at a lower pressure than the exterior. Hence there will be a forced flow of reactants into the pellet due to this pressure difference. Also, gross pressure gradients can exist across a catalyst pellet due to pressure drop in a reactor. Thus the up stream end of a pellet in a flow reactor is at a slightly higher pressure than the down stream end. This can conceivably cause a forced flow of reactant right through the pore structure of the pellet. However, calculations (Wheeler[1], Thiele[11]) show that both of these types of forced flow are relatively unimportant as compared to diffusion. The essential reason for this is that forced flow of the Poiseuille or stream-lined type is proportional to the fourth power of the pore radius, and hence is very slow in pores of 100 Å or so commonly encountered in catalysts. Thus in macro sized tubes, 1 mm or larger in diameter, we rightfully think of diffusion as being much slower than forced flow, but in tubes 10^5 times smaller, the relative rates of these processes invert, due to the r^4 term in Poiseuille's Law. For present purposes we, therefore, neglect the effect of forced or mass flow in catalyst pellets. A third specialized type of transport in small pores is two-dimensional migration in adsorbed layers on the pore wall. A number of studies have shown that this may be very rapid under the rather specialized conditions where thick physically adsorbed layers of reactant are formed. Some of these studies are described in an earlier review (Wheeler[1]). The recent work of Carman[10] is also noteworthy in this connection. However, since at present the writer knows of no catalytic reaction for which it is necessary to invoke surface migration to explain observed reaction rates, we neglect this mechanism in the present treatment.

We now return to diffusion and consider the two important types of diffusion which are possible in small pores. Our objective is to derive a formula for the diffusion coefficient in a given catalyst pellet from a knowledge of pore volume and surface area alone. Two main types of diffusion are possible in small pores: (a) Knudsen or molecular diffusion which will occur whenever the mean free path between intermolecular collisions is large compared to the pore diameter and (b) ordinary or "bulk" diffusion which occurs when the mean free path is small compared to the pore diameter. In general Knudsen diffusion occurs for all gas phase reactions carried out at one atmosphere pressure on catalysts whose pores are about 200 Å in radius or smaller. Under these conditions the mean free path between gas-phase collision is about 1,000 Å for typical molecules. Hence, after a collision with the pore wall, a reactant molecule will fly to another wall before having a collision with a second molecule. Intermolecular collisions may thus be neglected, and a molecule travels within the pore by a series of "random flights" interrupted by collisions with the pore wall. The "resistance" to diffusion is due to the fact that, after collision with the pore wall, the molecule is just as apt to reverse its direction as it is to proceed in the direction of its previous flight. In 1909 Knudsen showed from his studies of flow in fine capillaries at low pressures that this must be due to each collision with the wall being actually a very brief period of adsorption in which the molecule loses its momentum to the solid surface. After this brief instant of adsorption the molecule evaporates from the surface at a completely random angle. Knudsen showed that under these conditions the diffusion constant per unit cross-sectional area of pore is given by:

$$D_K = \tfrac{2}{3} r\bar{v} = 9.7 \times 10^3 r \sqrt{\frac{T}{M}} \frac{\text{cm}^2}{\text{sec}} \qquad (31)$$

where r is the pore radius in cm, $\bar{v}$ is the average molecular velocity, T is the temperature in °K and M is the molecular weight. We use the subscript K with D in Eq. (31) to denote the Knudsen diffusion coefficient. Thus D_K is proportional to pore radius. Numerical values for molecules of ordinary weight at ordinary temperature range from 0.01 cm^2/sec for pores of 10 Å radius up to about 10 cm^2/sec for pores of 10,000 Å radius. Since molecules travel completely independently in Knudsen diffusion or flow, the flow is independent of total pressure and depends only on partial pressure differences of the diffusing species. This means that in small pores at 1 atmosphere pressure we never have to correct gas diffusion rates into a catalyst for forced flow due to "volume change" in reaction, since Knudsen diffusion is independent of total pressure differences within the pellet which have been set up by the reaction.

The second type of diffusion possible in catalyst pores is ordinary "bulk diffusion." Whenever the mean free path between intermolecular collision is small compared to the pore radius, molecules will strike each other much more frequently than they strike pore walls. Hence the "resistance" of pore walls may be neglected, and the ordinary bulk value D_B of the diffusion coefficient will hold. In practice the mean free path is smaller than pore radius in three important cases: (a) all liquid phase reactions on all catalysts (b) high pressure reactions operating above 100 atmospheres or so on all catalysts (c) low pressure (1 atm.) gas reactions on catalysts containing very large pores, say 5,000 Å or larger. For these three cases the bulk value of the diffusion coefficient D will pertain. This may be looked up in the literature or calculated by the semiempirical method of Gilliland[12].

Thus in theory one should calculate the mean free path in a catalytic gas-phase reactor and compare it to the average pore radius in order to determine whether Knudsen or bulk diffusion is operative. In practice the formula given below effectively does this automatically and gives a smooth transition between the two types of flow as pressure or pore size is increased. The formula we suggest for the diffusion coefficient D in pores of any size at any gas pressure is:

$$D = D_B(1 - e^{-D_K/D_B}) \tag{32}$$

The physical meaning of this formula is as follows: Elementary kinetic theory gives for the bulk diffusion coefficient in a mixture of molecules of similar mass and molecular diameter the formula $D_B = \frac{1}{3} \bar{v} \lambda$ where λ is the mean free path. Thus the ratio D_K/D_B is exactly the ratio of pore diameter $(2r)$ to the mean free path λ. When this ratio is large the exponential term in Eq. (32) is zero, and we have bulk diffusion, $D = D_B$. When this ratio is small (0.2 or less) expansion of the exponential in a power series gives $D = D_K$, so that Eq. (32) automatically gives the correct type of diffusion and a smooth transition between the two types at any pore size or pressure. We illustrate Eq. (32) by computing the diffusion coefficient of hydrogen (in $H_2 - N_2$ mixture) in 50 Å pores at 30 atmospheres pressure, 200°C. Using Eq. (31) for D_K we find the Knudsen diffusion coefficient for

H_2 in 50 Å pores is $7.43_1 \times 10^{-2}$ cm²/sec at 473°K. For the bulk diffusion coefficient, International Critical Tables gives the value $D_0 = 0.674$ cm²/sec for 1 atmosphere, 0°C, $H_2 - N_2$ mixtures. For other pressures and temperatures we use the approximate formula for gases:

$$D_B = D_0 \left(\frac{T}{273}\right)^{1.75} \frac{1}{P(\text{atms})} \tag{32a}$$

and find $D_B = 5.84 \times 10^{-2}$ cm²/sec at 30 atmospheres, 473°K. Substituting these values for D_K and D_B in Eq. (32) we find $D = 5.32 \times 10^{-2}$ cm²/sec in 50 Å pores, 200°C. We note that for this problem diffusion is in the transition range between Knudsen and bulk diffusion, since D_B and D_K are about of the same magnitude, meaning that mean free path and pore diameter are of the same magnitude. The form of Eq. (32) is purely intuitive and no doubt will be improved as accurate experimental data accumulate.

Our next problem is to compute the diffusion coefficient D_c within an actual catalyst granule. This will be simply the diffusion coefficient for a single pore times the number n_p of pores per unit surface of pellet which we computed in the last section ($n_p = \theta/\sqrt{2}\pi r^2$), times a factor $1/\sqrt{2}$ since pores on the average run at about 45° to a given surface. That is, only a factor $1/\sqrt{2}$ of the concentration gradient normal to the surface is operative in the direction of the pore axis, or alternatively molecules must travel $\sqrt{2}$ farther than the bee-line normal to a surface, due to deviousness of the pore structure. Putting this all together we get:

$$D_c = \tfrac{1}{2}\theta D \tag{33}$$

where D_c is the over-all diffusion coefficient within a porous catalyst pellet, θ is the porosity and D is the diffusion coefficient for a single catalyst pore, given by Eq. (32). Equation (33) says that the diffusion coefficient in a porous pill is smaller than that for the pores which make up the pill due to two factors: (a) only a fraction θ of the pill is open structure, the remaining fraction $(1 - \theta)$ being solid (b) a factor of approximately ½ arises due to the deviousness of the pore structure, since the factor $\sqrt{2}$ comes in twice: once in the number of pores per unit area and again because each pore runs at an angle of about 45° to a given surface.

Thus in Eqs. (33) and (32) we have a complete theory of the diffusion coefficient in porous catalysts. The only experimental data necessary are surface areas and pore volumes in order to compute the average pore radius and porosity. There is little accurate experimental data on pure diffusion through materials of know pore size with which to compare the theory. Earlier experimental work has been described in the writers' earlier review, (Wheeler[1]) and is in substantial agreement with the theory. More recent unpublished work by Dr. Weisz of the Socony Vacuum Laboratories further corroborates the essential correctness of Eqs. (32) and (33), although detailed comparisons are not yet available. A drastic test of the theory is that, when applied to an actual catalytic reaction, it shall give predictions in agreement with experiment. So far, as described in later sections, no major discrepancies have arisen. The main cases in which major breakdown of our simple theory would be expected are: (a) gas phase diffusion within catalysts having a large number of "main artery" macropores leading to much smaller pores. In particularly unfavorable cases this should lead to a peculiar mixture of "bulk diffusion" in macropores plus Knudsen diffusion in small pores, which the theory does not contemplate (b) a porous solid which had many bottle-neck pore spaces cut off by very small pores would behave in a peculiar manner, as diffusion in and out of these bottle-neck spaces would be ruled not by an average pore radius but by a much smaller effective radius.

Concerning experimental techniques of measuring diffusion rates within catalyst particles, two main methods are possible: (a) the sides of a cylindrical pellet are sealed off and the two flat faces are contracted with two different gases, say by flowing pure nitrogen past one face and pure CO_2 past the other face. The rate of steady state diffusion through the pellet is determined by analysis of the two gas streams for "contamination" by the other component. This method has been used by Wicke[13] and by Weisz[14]. (b) A second method is to first fill the pore structure with one component (either gas or liquid) followed by measuring the rate of efflux of this component into a second component. For example Blue and his co-workers[15] have introduced this method for gases by filling the pore structure of catalyst granules with radioactive butane. The rate of efflux of radio-butane into a flowing stream of ordinary butane is then measured. Eagle and Scott[26] have applied the method to liquids. Although experimentally somewhat simpler, this "efflux method" has the disadvantage that adsorption-desorption effects on the catalyst surface can conceivably complicate the results for materials of high surface area. Since it is not a steady state method, the somewhat complicated equations for nonsteady state diffusion must be used in interpreting the results.

We purposely say very little about the mechanism of "forced flow" (under a pressure head) in catalyst granules because we believe this has little role in catalytic reaction rates. Measurement of forced flow rates through single catalyst pellets can give interesting information concerning the nature of the pore structure, but in the writers opinion diffusion rate measurements are much more meaningful. An exception to this is the case of materials (e.g., silica gels) having only small pores so that Knudsen flow is operative. Here measurement of the forced flow rate also measures the

Knudsen diffusion coefficient since Knudsen "forced flow" and Knudsen diffusion are identical.

REACTION RATES ON POROUS CATALYSTS

So far we have considered the nature of the pore structure and the mechanism of transport in catalyst pores. We now turn to our main problem namely that of diffusion in pores accompanied by reaction. Our objective is to obtain an equation for the rate of reaction on a porous catalyst which is sufficiently active so that the concentration of reactant within the pellet is lower than in the gas phase surrounding the pellet. Or stated another way, our objective is to determine the "fraction of internal surface area available" to a given reaction. We shall find a number of important results. In particular we shall find that the pore structure can affect all the important kinetic quantities, such as activation energy, order of reaction, selectivity and poisoning effects.

The physical picture we wish to make is shown in Figure 3 which shows two adjacent catalyst pellets in say a flow reactor. We see the catalyst pellets as a random network of small pores, and we greatly enlarge the diameter of one pore for illustrative purposes. Between our catalyst pellets in the most general case a turbulent gas stream will be flowing. A typical reactant molecule will be swept, by the turbulent flow, into a quiescent gas layer near the external catalyst surface. Our molecule will then diffuse more slowly through this quiescent layer, and will next start to diffuse into the catalyst pore structure, as shown by the zig-zag path. Now if our catalyst is relatively inactive and if diffusion in the pore structure is fast, a reactant molecule will be able to diffuse deep into the pore structure before it reacts. Such an inactive catalyst will show a uniform concentration of reactant as we make a traverse across the gas stream into the pore structure. This uniform concentration is shown as the horizontal dotted line (labelled Case I) in the graph at the bottom of Figure 3. Here we plot concentration of reactant vertically against distance from center of gas stream. Distances on the horizontal scale correspond with the picture above, so that $x = 0$ is the center of the gas stream, while x_s corresponds to the external edge of the catalyst pellet.

In contrast to an inactive catalyst, if our catalyst is highly active with small pores, a reactant molecule will react (due to collisons with pore walls) before it can diffuse very deep into a pore. This is shown in Figure 3 by a white ball turning into a black ball after a few collisions with the active pore wall. For such a catalyst only the external pore mouth will be useful since the center of the pellet is full of inert product molecules. For this active catalyst we will get the dome-shaped curve shown as Case II. Concentration of reactant falls rapidly to zero at some point a short distance

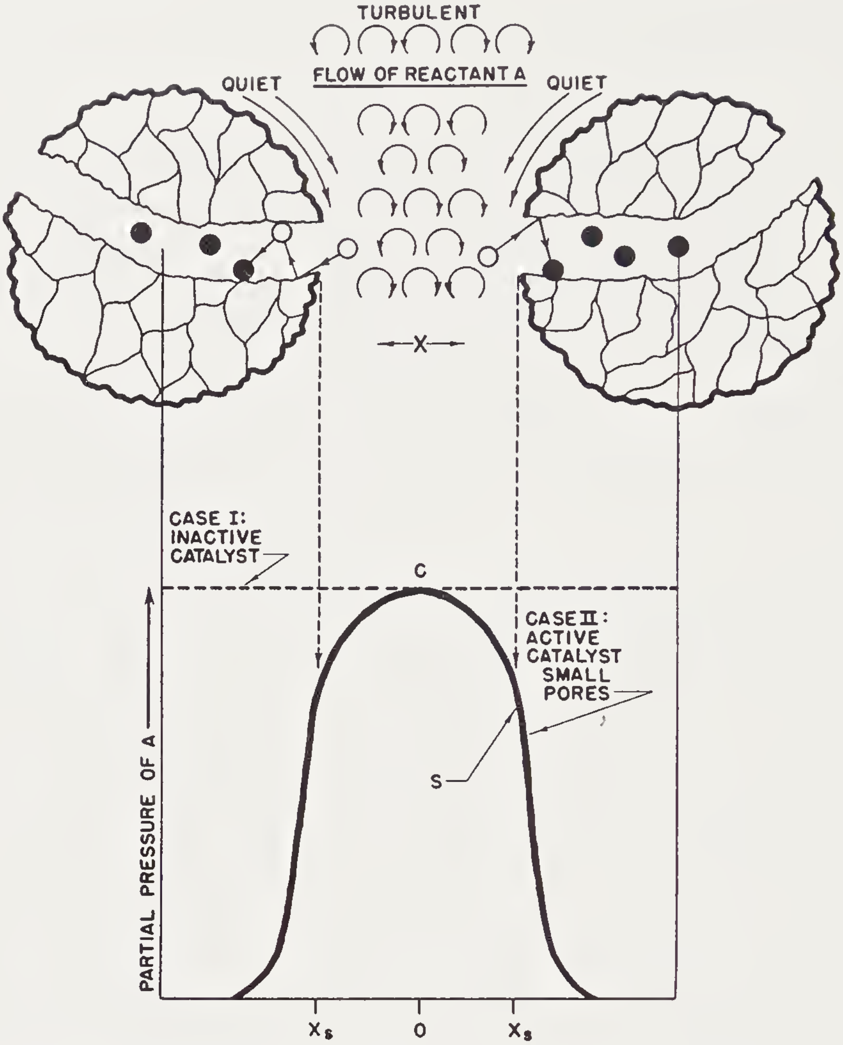

Fig. 3. Diffusion from flowing gas stream to and into catalyst pills. Upper part of figure is a pictorial representation of two catalyst pills; lower part is a plot of reactant concentration for a traverse through the gas stream into the catalyst pills. The dotted horizontal line shows constant reactant concentration for an inactive catalyst. The dome-shaped curve shows fall in concentration with an increase in the value of x due to reaction for an active catalyst with small pores.

within the pellet. We say that such an active catalyst has only a small fraction of its internal surface available to the reaction. For a highly active catalyst we may have not only a concentration drop within the catalyst pellet, but there may also be a concentration gradient between the main gas stream and the external catalyst surface, since diffusion to the catalyst in the quiescent gas layer may not be able to keep up with fast reaction. This is illustrated in Case II by the initial falling branch of the curve between points C and S, and is discussed further on pages 150–151.

The important point we wish to make is that for Case II (active catalyst, small pores) reaction kinetics will be quite different than for Case I. For Case I we measure the true intrinsic kinetics; for Case II we do not. It is important in any experimental situation to know which case we are dealing with. We now show how this can be done, and we also examine the kinetics of Case II.

Derivation for Spherical Catalyst Particles

We first give a rigorous derivation for a first order reaction on a spherical catalyst pellet, and later show how, by a model of the pore structure, this may be generalized to granules of any shape. Consider a porous spherical particle of radius R and imagine a spherical shell within the particle contained between the two spheres of radius r and $(r - dr)$. The equation to be solved for steady state diffusion into the pore structure accompanied by reaction is that the inward flow of reactant into the spherical shell less the flow out of the shell must be equal to the rate of reaction on the catalyst contained within the spherical shell. If diffusion is the main means of transport, then the inward flow rate through the sphere at r is:

$$4\pi r^2 D_c \frac{dC_A}{dr} \tag{34}$$

where $4\pi r^2$ is the area of the sphere, D_c is the diffusion coefficient in the catalyst particle (i.e., that experimentally observed by diffusing gas or liquid through a single catalyst pellet) and C_A is the concentration of reactant. The differential of Eq. (34) is the flow into the spherical shell less the flow out of the shell. The mass of catalyst contained within the shell is $(4\pi r^2\, dr)\rho_p$, where ρ_p is the particle density of the catalyst. The surface area of catalyst contained in the shell is therefore $(4\pi r^2\, dr)\rho_p S_g$ where S_g is the conventional surface area per gram. Hence the rate of reaction within the spherical shell is $(4\pi r^2\, dr)\rho_p S_g k C_A^n$ where k is the intrinsic catalyst activity per unit (internal) surface area for a reaction of the n^{th} order and C_A is the concentration of reactant A. The fundamental equation to be solved is therefore that the differential of Eq. (34) is equal to the last expression for the reaction rate. After a little rearrangement this becomes for a first order reaction:

$$\frac{d^2C_A}{dr^2} + \frac{2\, dC_A}{r\, dr} = \frac{9h^2C_A}{R^2} \tag{35}$$

where

$$h = \frac{R}{3}\sqrt{\frac{\rho_A S_g k}{D_c}} \tag{36}$$

Here R is the radius of the spherical catalyst pill. We solve Eq. (35) with the boundary conditions that (1) $C_A = C_A^0$ at $r = R$ and (2) $dC_A/dr = 0$ at $r = 0$. The first condition means that we fix the concentration of reactant at the surface of the pellet. The second means that there is no diffusion through the center of the pellet since this is a point of symmetry. The solution is

$$\frac{C_A}{C_A^0} = \frac{R}{r}\left(\frac{\sinh 3h \frac{r}{R}}{\sinh 3h}\right) \tag{37}$$

where sinh is the hyperbolic sine function, $\frac{1}{2}(e^{+x} - e^{-x})$. Equation (37) shows how the concentration of reactant C_A falls with distance within the pellet. We see that the fall in concentration depends only on the dimensionless parameter h (defined by Eq. 36) and on the reduced distance r/R. The concentration at the center of the pellet ($r = 0$) is $C_A^0\ 3h/(\sinh 3h)$. For h small (less than about 0.2), this is approximately C_A^0 (since $\sinh 3h \cong 3h$ for h small). Thus for $h < 0.2$, diffusion is fast enough as compared to reaction so that the whole pellet is available, the concentration of reactant at the center of the pellet being approximately the same as at the pellet surface. For h equal to about 1.5 or greater Eq. (37) shows that the concentration of reactant at the center is less than one-tenth that at the pellet surface, since reaction is rapid compared with diffusion.

The total reaction rate on the single pellet can be obtained either from the diffusion rate of reactant into the pill, $4\pi R^2 D_c(dC_A/dr)_{r=R}$ or by integrating the rate in a spherical shell $(4\pi r^2\, dr)\rho_p S_g k C_A$ over the pill using Eq. (37) for C_A. The result in either case is:

$$\text{Rate (per pellet)} = 4\pi R^2 C_A^0 \sqrt{\rho_p S_g k D_c}\left[\frac{1}{\tanh 3h} - \frac{1}{3h}\right] \tag{38}$$

where tanh is the hyperbolic tangent function.

Since $4\pi R^2$ is the external area of the catalyst granule, S_x, and since $\rho_p = \theta/V_g$ (equation 1) and $D_c = \frac{1}{2}\theta D$, Eq. (33), Eq. (38) may also be written:

$$\text{Rate (per pellet)} = S_x \theta C_A^0 \sqrt{\frac{kD}{\bar{r}}}\left[\frac{1}{\tanh 3h} - \frac{1}{3h}\right] \tag{39}$$

where $\bar{r} = 2\, V_g/S_g$ and θ is the "porosity" of the pellet.

To obtain the "fraction of surface area available" to the reaction, we note that if the internal surface area of the pellet were completely available to the reaction (i.e., if reactant concentration were uniform throughout the pellet) then the rate would be:

$$\left(\frac{4\pi}{3} R^3 \rho_p\right) S_g k C_A^0 \tag{40}$$

where the parenthesis is simply the mass of the pellet (i.e., volume times density). Dividing the actual rate Eq. (38) by the completely available rate, Eq. (40), gives f the "fraction of surface available":

$$f = \frac{1}{h}\left[\frac{1}{\tanh 3h} - \frac{1}{3h}\right] \tag{41}$$

We see this depends only on the dimensionless parameter h, defined by Eq. (36).

Reaction on Catalyst Granules of Arbitrary Shape

Before discussing the above results we shall first show that the solution for the rate in the form of Eq. (39) is also a very good approximation for catalyst pills of arbitrary shape, as well as for spherical granules. To do this we first solve the equation for reaction accompanied by diffusion in a single pore, and use the model of the pore structure described on pp. 132–133 for granules of any shape. This solution has been described in detail elsewhere (Wheeler[1]) so that we give only a brief summary here. It turns out that for a single pore of length L the fraction of surface available works out to be:

$$f = \frac{1}{h_1} \tanh h_1 \tag{42}$$

where h_1 is defined by:

$$h_1 = L\sqrt{\frac{2k}{rD}} \tag{43}$$

Here r is the pore radius, L is the pore length and D is the diffusion coefficient in this size pore. If we now use our model of the pore structure described on pp. 132–133 for the number and average length of pores in a pellet of external area S_x, we get for the rate per pellet:

$$\text{Rate (per pellet)} = S_x \theta C_A^0 \sqrt{\frac{k}{rD}}\,[\tanh h_1] \tag{44}$$

We see that this differs from Eq. (39) only in the form of the bracket at the far right, and h_1 rather than h appears in Eq. (44). Calculation shows that these two brackets are numerically almost identical functions of h and h_1.

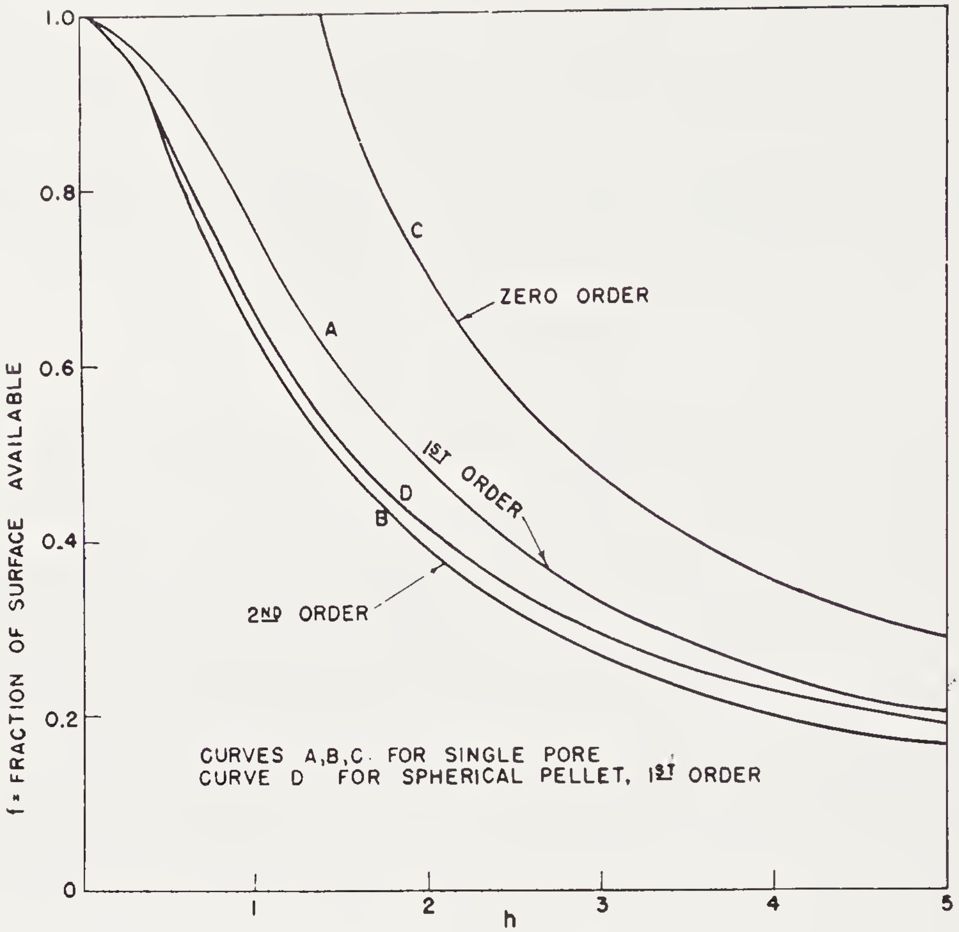

FIG. 4. "Dependence of fraction of surface available on the parameter h.[1] For $h > 5$, f is equal to $1/h$ for curves A and D, is equal to $\sqrt{2/h}$ for curve C and takes the value $\frac{1}{h}\sqrt{\frac{2}{3}}$ for curve B."[1]

In Figure 4 Curve D we plot Eq. (41), f vs. h, for spherical granules and in Curve A we plot Eq. (42), f vs. h_1, for a single pore. The fact that these two curves lie very close to each other shows visually that the brackets in Eqs. (44) and (39) are almost identical functions of h (or h_1) since f is just these brackets divided by h (or h_1). We still must compare the definition of h and h_1. To do this we use our model of the pore structure for D_c as it appears in Eq. (36). Since $D_c = \frac{1}{2}\theta D$ and since $\rho_p = \theta/V_g$, the definition of h in Eq. (36) becomes:

$$h = \frac{2R}{3}\sqrt{\frac{S_g}{2V_g}\frac{k}{D}} \tag{45}$$

for spherical pellets. Now if we used our value for the pore length from Eq. (29), $L = \frac{V_p}{S_x}\sqrt{2}$, and substitute this in the definition of h_1 Eq. (43) we obtain:

$$h_1 = 2\frac{V_p}{S_x}\sqrt{\frac{k}{rD}} \tag{46}$$

for pellets of arbitrary shape. Since the volume to surface ratio for spheres is $R/3$, Eqs. (45) and (46) are identical if the average pore radius occurring in (46) is taken to be $\bar{r} = 2\,V_g/S_g$. We have thus shown that Eqs. (44) and (39) are virtually identical, if our model of the pore structure is used, even though the equations were derived by quite different mathematics. This gives us confidence that Eq. (44) is a high approximation for particles of arbitrary shape and that the definitions of h and h_1 given by Eqs. (36), (43), (46), are all virtually identical. From an experimental standpoint the most general definition of h is:

$$h = 2\frac{V_p}{S_x}\sqrt{\frac{S_g}{2V_g}\frac{k}{D}} \tag{47}$$

obtained from (46) by the substitution $r = 2\,V_g/S_g$.

Theoretical Equation for Conventional First Order Rate Constant

So far we have derived a rate expression for the activity of a single catalyst pellet. It is convenient to describe the experimental activity of a catalyst by computing the rate constant *per unit volume* of reactor. Therefore, to compare with experiment we convert Eq. (44) (or its equivalent Eq. 39) into the activity per unit volume by multiplying by the number of pellets per unit volume of reactor. This number is $\rho_B/V_p\rho_p$ where ρ_B is the bulk density of catalyst in the reactor and V_p is the actual volume per pellet so that the denominator is the weight per pellet. The result is that: Rate (per unit bulk reactor volume, moles/sec.) =

$$\tfrac{1}{2}(S_x/V_p)^2\rho_B V_g D C_A^0[h \tanh h] \tag{48}$$

Since for almost all practical shapes of pellets (e.g., spheres and cylinders whose length equals their diameter, etc.) the external surface to volume ratio is $a/6$ where a is the granule size (i.e., diameter of sphere or cylinder), we can put Eq. (48) with any one of the three following forms:

Rate (per unit bulk reactor volume, moles/sec.)

$$= \frac{6}{a\sqrt{2}}\rho_B\sqrt{V_g S_g k D}\,[\tanh h]C_A^0 \tag{49}$$

$$= \frac{18}{a^2}\rho_B V_g D[h \tanh h]C_A^0 \tag{50}$$

$$= \rho_B S_g k\left(\frac{\tanh h}{h}\right)C_A^0 \tag{51}$$

Eqs. (49), (50), and (51) are all equivalent where the definition of h given in Eq. (47) is used to convert from one form to the other. By definition the theoretical first order rate constant is exactly any one of the three Eqs. (49–51) with C_A^0 deleted.

We thus are in a position to determine the fraction of surface available in a given practical reaction from the value of the experimentally observed rate constant, as follows: If we equate the experimental rate constant $k_{\text{exp.}}$ to the theoretical one, using Eq. (50) we obtain:

$$k_{\text{exp.}} = \frac{18}{a^2} \rho_B V_g D(h \tanh h) \tag{52}$$

which can be rearranged to:

$$(h \tanh h) = \frac{k_{\text{exp.}}}{k_D} \tag{53}$$

where

$$k_D = \frac{18}{a^2} \rho_B V_g D \tag{54}$$

Since all quantities in k_D are known (Eq. 32 is used for D) or can be easily measured experimentally, we simply compute a numerical value for k_D in a given case, take the ratio of $k_{\text{exp.}}$ to k_D and then use Eq. (53) to compute h. The fraction of surface available can then be read off Figure 4. In practice we do not need to compute h since the relation between f, the fraction of surface available, and $k_{\text{exp.}}/k_D$ can be computed once and for all. This relation is shown by the curve of Figure 5. Mathematically this curve is simply a plot of $(\tanh h)/h$ vs. $(h \tanh h)$.

Second Order and Zero Order Reactions

So far we have considered only first order reactions. Calculations by Thiele[11] show that second order reactions behave similarly to first order in that the fraction of surface available is still given to good accuracy by:

$$f = \frac{\tanh h_2}{h_2}$$

where h_2 now has the same definition as before (Eqs. 45, 46, or 47) except that k (the first order constant) under the square root sign is replaced by $k_2 C_A^0$ where k_2 is the intrinsic second order rate constant per unit surface area and C_A^0 is as usual the concentration of reactant at the pellet surface. This means that in general for a second order reaction in a flow reactor the fraction of surface available is smaller at the inlet-end than at the outlet,

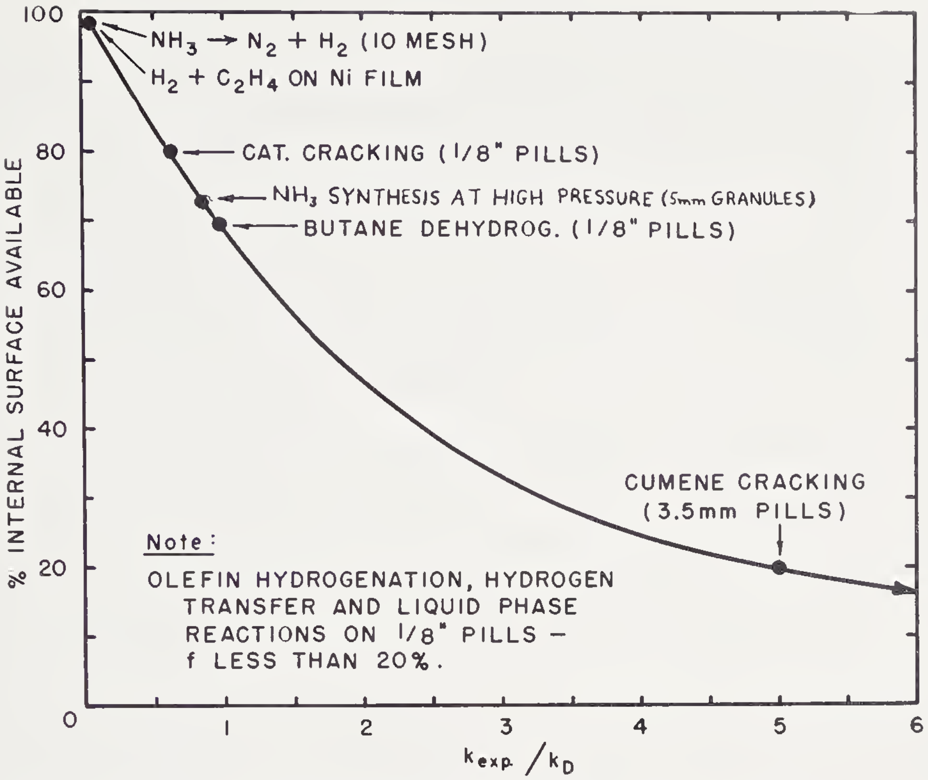

FIG. 5. Dependence of fraction of surface available on the ratio $k_{\text{exp.}}/k_D$, computed from $f = (\tanh h)/h$, $k_{\text{exp.}}/k_D = h \tanh h$.

since the concentration of reactant and hence h_2 changes down the tube. The rate equation for a second order reaction (per unit bulk volume of reactor, analogous to Eq. 49) is:

Rate, second order reaction, per unit bulk volume =

$$\frac{6}{a\sqrt{2}}\, \rho_B \sqrt{V_g S_g k_2 D}\, [\tanh h_2]\, C_A{}^{3/2}$$

This shows that fast second order reactions ($h_2 > 2$) become $\frac{3}{2}$ order. Thus rapid second order reactions should not be observed on porous catalysts, since they would become $\frac{3}{2}$ order. Alternatively, slow reactions observed to be second order at low temperatures should become $\frac{3}{2}$ order at high temperatures where the catalyst is more active.

Zero order reactions are an interesting special case discussed earlier by the writer (Wheeler[1]). Here the fraction of surface available remains constant at unity up to a value of $h_0 = \sqrt{2}$ and then falls off for larger volumes of h_0. Here h_0 is the zero order h, defined as for first order except that k, the first order rate constant, is replaced by k_0/C_A^0, k_0 being the zero order intrinsic rate constant. Figure 4 shows the fraction of surface available f vs. h for zero and second order reactions.

Kinetics of Fast Reactions on Porous Catalysts

We have written the rate expressions Eqs. (49–51) in three equivalent forms since each form illustrates a different point. Equation (51) shows that when h is small (inactive catalyst, large pores) true kinetics will be observed just as if the internal surface area was spread out on a plane surface. This is because for h small, $\tanh h \cong h$ so that the rate becomes $\rho_B S_g k C_A^0$ which is the rate for a plane surface of area $\rho_B S_g$ which is the catalyst area per unit volume of reactor. The most interesting form is Eq. (49). Here for h larger than about 2.0 (active catalyst, small pores), $\tanh h$ can be set equal to 1.0. The rate on such an active catalyst now is inversely proportional to pellet size, "a," and is proportional to the square root of the intrinsic catalyst activity, constant, k. Thus only one-half the true activation energy will be observed, since diffusion is cutting down on the true temperature coefficient of reaction. Reaction rate is no longer proportional to internal surface area but has a slightly complex dependence on this as follows: Under conditions of bulk diffusion (D independent of pore radius) Eq. (49) shows that fast reactions will be proportional to the square root of both surface area per gm. S_g, and pore volume V_g. However for Knudsen diffusion in catalyst pores (small pores, moderate or low gas pressure) D will be proportional to average pore radius $\bar{r}$. Since $\bar{r} = 2\, V_g/S_g$, the surface area S_g just cancels in Eq. (49) for Knudsen flow, and catalyst activity is proportional to pore volume V_g only. Thus catalyst activity can be either strictly proportional to internal surface area (slow reaction), proportional to the square root of internal surface area (fast reaction, bulk diffusion), or independent of internal surface area (fast reaction, Knudsen diffusion). Independent of the type of diffusion, all fast reactions rates on small pores ($h > 2$) will be proportional to the *external* surface area of catalyst granules, since pore mouths only are useful, and for this reason the rate becomes inversely proportional to catalyst pellet size, Eq. (49).

To clarify our definitions of the rate constants k, $k_{\text{exp}.}$ and k_D we make the following remarks: k is the intrinsic first order rate constant per unit catalyst surface area, defined by the statement that whenever a concentration C_A of reactant A is in contact with one sq cm of catalyst surface, a reaction rate of kC_A molecules (or moles) per second will be observed. The dimensions of k are cm/sec; k depends in general exponentially on temperature. $k_{\text{exp}.}$ is the conventional first order rate constant per unit volume of reactor, calculated from experimental data from:

$$k_{\text{exp}.} = \frac{1}{\tau} \log \frac{1}{1 - \alpha} \tag{55}$$

where τ is the contact time and α is the fraction reacted. The units of $k_{\text{exp}.}$

are $\sec.^{-1}$, and $k_{\text{exp.}}$ is the inverse of the contact time which gives 63 per cent conversion. k_D is purely a defined quantity which arose naturally from the mathematical equations. Physically it is the inverse of a diffusion time, since the average time it takes for a molecule to diffuse a distance x is x^2/D. Thus $\frac{a^2}{18D}$ is just the average time it takes a molecule to diffuse a distance $\frac{a}{6}\sqrt{2}$, which is just the average pore length our model gives. The product $\rho_B V_g$ occurring in k_D is the pore volume per cc of reactor. Hence the ratio $k_{\text{exp.}}/k_D$ can be written physically:

$$k_{\text{exp.}}/k_D = \frac{\text{Diffusion time into pore of average length}}{\text{Contact time for 63\% conversion}} \tag{56}$$

Thus when the diffusion time is short compared to the reaction time, internal surface is completely available as shown by Figure 5. When diffusion time is long compared with reaction time, then only a small fraction of surface will be available.

The dependence of reaction order on pore structure is of interest. From what has been described, it follows that first order reactions do not change their order, but second order and zero order reactions on active porous catalysts move one-half an order toward first order (i.e., second order becomes $\frac{3}{2}$, zero order becomes $\frac{1}{2}$ order). Physically this is because diffusion is an essentially first order process, so that the effect of diffusion into porous catalysts is to make the reaction tend toward first order. Since the rate of a rapid reaction on a porous catalyst is proportional to the square root of the diffusion coefficient (e.g., Eq. 49), there will be a further dependence on total pressure for gas phase reactions under conditions of bulk diffusion. Thus if the total pressure is doubled for a first order reaction on a catalyst with large pores, it might spuriously appear that the reaction were not first order, since the rate would not double but would go up only by $\sqrt{2}$ due to a depressing effect on the bulk gas phase diffusion coefficient.

PRESSURE AND TEMPERATURE GRADIENTS IN SINGLE CATALYST PELLETS

An interesting aspect of our theory is that large temperature and pressure gradients are predicted within single catalyst particles under conditions commonly met with in practice. We first treat the somewhat simpler phenomena of pressure gradients, and a corollary to this which applies to hydrogenation reactions.

Pressure Gradients in Single Catalyst Pellets

We have shown that drastic partial pressure gradients (e.g., given by Eq. 37) can exist in active catalyst pellets. We now show that total pressure gradients also can be expected. If we consider a spherical catalyst granule in which diffusion is the main means of transport, the concentration gradient of reactant within the pellet at a distance r from the center of the pellet, is given by

$$4\pi r^2 D_A \frac{dC_A}{dr} = \text{reaction rate of } A \text{ inside the sphere at distance } r \tag{57}$$

from the pellet center.

Let us assume that the reaction is stoichiometrically given by $A \rightarrow qB$ where q is the number of product molecules formed per molecule of A reacted. Then in a steady state the number of molecules of B formed which must diffuse outward through the spherical surface a distance r from the center must be q times the reaction rate of A within the sphere. Hence we get the equation that

$$D_A \frac{dC_A}{dr} = -\, qD_B \frac{dC_B}{dr} \tag{58}$$

which connects the concentration gradient of B with that of A. Thus if Eq. (58) is integrated, we get:

$$C_B(r) - C_B^0 = q \frac{D_A}{D_B} [C_A^0 - C_A(r)] \tag{58a}$$

which states that the concentration increase in B, (taken from a distance r from the center to the exterior surface) is equal to qD_A/D_B times the concentration decrease in A (taken from the surface of the pellet to the same point a distance r from the center). From Eq. (58) the total concentration of reactant plus product at a point within the pellet may be computed as:

$$C_A(r) + C_B(r) = \frac{D_A}{D_B}\, q\left[C_A^0 - C_A(r)\right] + C_B^0 + C_A(r) \tag{59}$$

Equation (59) applies strictly only under conditions of Knudsen diffusion, since under conditions of bulk diffusion a streamlined mass flow will superimpose on diffusion. Under these conditions of Knudsen flow, $D_A/D_B = 1/\sqrt{q}$ due to the mass relationship between reactant and product molecules. If the catalyst pellet is located in the inlet end of the reactor where $C_B^0 = 0$ then we get for the fractional increase in total concentration of molecules at a point within an active pellet (where C_A has fallen to zero), the result that:

$$\frac{C_T}{C_A^0} = \sqrt{q} \tag{60}$$

where C_T = the total concentration = $C_A + C_B$. For a gas phase reaction (pressure proportional to total concentration), Eq. (60) shows that the total pressure at the center of an active catalyst pellet is larger or smaller than at the exterior surface depending on whether q is greater or less than unity. Thus for a cracking reaction in which four fragments are formed ($q = 4$), the pressure at the center of an active pellet should be twice as large as in the external gas stream. Likewise in a polymerization reaction in which quadrimer is formed, the pressure would be one-half as great at the center as at the surface.

Kinetics of Ethylene Hydrogenation on Metals

An interesting corollary to these considerations comes from considering a rapid hydrogenation reaction ($A + B \rightarrow C$) under conditions of Knudsen diffusion which is expected for most metallic catalysts at 1 atmosphere pressure. For definiteness we consider ethylene hydrogenation. Since the Knudsen diffusion coefficient of ethylene is a factor $\sqrt{28/2} = 3.74$ slower than for hydrogen, the concentration gradient of ethylene at any point in a catalyst pellet must be 3.74 times as great as the gradient of hydrogen. This means that, starting with an equimolar mixture of H_2 and C_2H_4, within an active catalyst pellet the concentration of ethylene will fall to zero at a point where the hydrogen concentration has fallen by only about 27 per cent. Hence the interior of an active pellet is filled with hydrogen and ethane, and suffers from ethylene "starvation." If a higher concentration of ethylene is now used in the feed stream, the reaction can now penetrate deeper, before all the ethylene is reacted. This would thus give a pseudo-dependence on ethylene pressure which should be observed on active porous catalysts, but not on thin metallic films or on inactive porous catalysts.

This can all be worked out mathematically for Knudsen flow, and hinges on finding the distance within a pellet at which the ethylene concentration falls to zero, due to its slower diffusion. In short, the effective fraction of surface available depends on the ratio of ethylene to hydrogen, and increases with ethylene pressure up to a ratio of 3.74. Detailed calculations show that a pseudo-square root dependence on ethylene pressure should be expected on active porous catalysts, even though the true kinetics were independent of ethylene concentration.

Temperature Gradients Within Single Catalyst Particles

We now show that temperature gradients up to 100° can be expected within single catalyst pellets if they are poor heat conductors (nonmetallic) and are catalyzing a rapid exothermic (or endothermic) reaction. We consider a spherical granule and consider an imaginary spherical surface within the granule a distance r from the center. Within this spherical surface there will be a certain rate of reaction and the amount of heat generated within this sphere will be H times the reaction rate where H is the molal heat of reaction and the rate is in moles per second, say. Now in a steady state all this heat must pass out through the imaginary spherical surface. By the laws of heat conduction, therefore, the temperature gradient at the imaginary surface is given by

$$-4\pi r^2\lambda \frac{dT}{dr} = H \times \text{rate} \tag{61}$$

where λ is the heat conduction coefficient for the catalyst. The left side of (61) is the rate at which heat passes out through the imaginary spherical surface. The right side is the rate of heat generation within the imaginary sphere. Now since Eq. (57) holds for the concentration gradient of reactant, we divide (61) by (57) and get:

$$-\frac{dT}{dr} = \frac{HD}{\lambda}\frac{dC_A}{dr} \tag{62}$$

This equation may be integrated from the exterior surface to the center of the granule to give the total temperature change within the granule as a function of the total concentration change of reactant. The result is:

$$T_c - T_s = \frac{DH}{\lambda}(C_s - C_c) \tag{63}$$

where T_c and C_c are temperature and concentration at the center, T_s and C_s are temperature and concentration at the external surface. For a rapid reaction on active catalyst with small pores, $C_c = 0$, so that Eq. (63) gives the total temperature rise within the granule in terms of measurable quantities. As a practical application of Eq. (63) we consider an olefin hydrogenation reaction ($H \cong 30{,}000$ cal/mole) going on a kieselguhr or alumina supported catalyst containing pores about 200 Å in radius. If the concentration in the gas phase C_s is about 10^{-4} moles/cc (i.e., about 1 atmosphere pressure) and the Knudsen diffusion coefficient $D \cong 0.1$ cm/sec on 200 Å pores, then we compute:

$$T_c - T_s = \frac{0.1 \times 30{,}000}{\lambda} \times 10^{-4} = \frac{0.3}{\lambda} \tag{64}$$

λ, the coefficient of heat conduction for porous solids of the oxide type is somewhat uncertain, but appears to be about 3×10^{-3} cals/cm^2/sec/°C according to Lange's "Handbook of Chemistry and Physics." Thus Eq. (64) would predict about 100°C temperature rise within the catalyst pellet. Obviously experimental measurement of this rise is desirable. We note that metallic catalysts have high values of λ, and so we do not expect large temperature gradients within metal catalysts.

We note that although Eq. (63) gives the exact total temperature rise, the form of the temperature profile within the granule must be obtained by solving the differential equation of heat conduction analogous to Eq. (35). This equation is:

$$\lambda \frac{d^2T}{dr^2} + \frac{2}{r} \lambda \frac{dT}{dr} = -H\rho_p S_g k C_A \tag{65}$$

for a first order reaction which must be solved simultaneously with Eq. (35). Here in general k depends on T exponentially, and this presents mathematical difficulties. For k independent of T, Eq. (65) can be solved easily. In fact for this case, Eq. (62) shows the gradient of T is proportional to the gradient in C_A, which can be immediately computed from Eq. (37). Qualitatively the temperature gradient is sharpest near the periphery of the granule. For an exothermic reaction which penetrates only a short distance (say 0.1 mm), the whole center of the pellet will be at a uniform high temperature, with a sharp temperature drop near the periphery of the catalyst pellet.

Comparison with the Work of Thiele and Others

Thiele[11] first solved the equations for simultaneous diffusion and reaction within a porous catalyst pellet, obtaining essentially Eqs. (35), (37), (41), and (42). His physical picture of the pore structure was however rather specialized, so that his result is not described in quantities as directly experimentally observable as ours. Thiele's definition of h is also dimensionally different from ours. In terms of our symbols, his h is:

$$h_T = \sqrt{\frac{2k}{rD}} \tag{66}$$

where the subscript T implies Thiele. Thiele's modulus h then has the dimensions of an inverse length, as compared to our dimensionless quantity. Weisz[14] has used still other symbols for our h and f. Weisz uses the Greek symbol φ for our h, and η for our fraction of surface available, f. Thiele and Hougen and Watson[16] have called our fraction of surface available f the effectiveness factor, EF.

After deriving Eq. (63), the writer found that Damkohler[17] had considered this problem some years earlier. We call your attention also to the interesting recent work of Amundson[27] in this field. For example Smith and Amundson[27] have considered the reversible reaction A $\rightleftharpoons$ B on porous catalysts.

COMPARISON OF THEORY WITH EXPERIMENT (APPLICATION TO PRACTICAL REACTIONS)

So far our theory has predicted that on active catalysts containing small pores (for which $h > 2$) reaction rates should (a) become strongly dependent (inversely) on catalyst granule size (b) the apparent activation energy should fall off to one half its low temperature value (c) the order of the reaction and effect of total pressure should become different than for plane surfaces or for inactive catalysts at low temperatures. We now compare these predictions with experimental data on a number of reactions. We treat all reactions as if they were simple first order, as calculation shows this causes but small errors.

Catalytic Cracking of Gas-Oils

The writer has previously discussed this reaction in some detail (Wheeler[1]) so we give only a brief summary here. An abundance of experimental data shows that at 500°C cracking of gas oil on typical silica-alumina catalysts is slow enough to be independent of diffusion effects, since relatively large pills (say ⅛ in.) and fluid bed operation give roughly similar performance. We predict this result as follows, by computing the ratio of $k_{\text{exp.}}$ to k_D. The experimental value for $k_{\text{exp.}}$ at 500°C is close to 0.17 sec.$^{-1}$, corresponding to a liquid hourly space velocity of 4.0 vols of liquid gas oil per volume of reactor per hour which gives about 50 per cent conversion. (This value of $k_{\text{exp.}}$ is based on a liquid density of 0.774 and molecular weight corresponding to cetane.) k_D defined by Eq. (54) is calculated as follows: For ⅛-in. pills we take for the granule size $a = 0.31$ cm. At 1 atmosphere pressure in the small pores of about 30 Å radius found in silica aluminas, the diffusion will be pure Knudsen diffusion with $D = 5.3 \times 10^{-3}$ cm^2/sec for a large molecule of the molecular weight of cetane. For $\rho_B V_g$ we take the value 0.25 since this is simply the pore volume per unit volume of reactor. With these values k_D works out to be 0.24 sec^{-1} and the ratio $k_{\text{exp.}}/k_D = 0.17/0.24 = 0.70$. Figure 5 shows this corresponds to 77 per cent of the surface available for ⅛-in. pills, so that fixed bed performance on ⅛-in. pills should agree quite well with fluid bed performance on much smaller particles, in agreement with experiment. We note that at higher temperatures where $k_{\text{exp.}}$ is say five times higher than at 500°C, then reaction rate should begin to depend strongly on pellet size, since here only about 30 per cent of the surface area would be available ($k_{\text{exp.}}/k_D \cong 3.5$) with $h = 3$. This predicted result is confirmed by the data of Archibald, May and Greensfelder[18] who find the expected inverse dependence of activity on mesh size at 550 to 630°C. In this temperature range the catalyst is 5 to 30 times more active than at 500°C, as judged by the space velocities necessary to give 50 per cent conversion.

Cumene Cracking

Prater, Weisz and Lago[19] have studied catalytic cracking of isopropyl benzene on a variety of granule sizes of silica alumina, from 380 to 420°C. This reaction is much faster than gas-oil cracking. The experimental results show that at 420°C although small granules of 0.0112 cm diameter are completely available to the reaction, granules 0.35 cm in diameter are only 20 per cent available. We show that our theory predicts just this result. The experimental values for k_{exp}. are 4.5 sec.$^{-1}$ on 0.0112 cm granules and 0.905 sec^{-1} on 0.35 cm granules. We now calculate k_D for these two sizes. Prater *et al.* do not give the average pore size of their catalyst, but we estimate this as 20 Å radius from the measured surface area of 349 sq m per g. This gives a Knudsen diffusion coefficient of $D = 4.7 \times 10^{-3}$ cm^2/sec. Taking $\rho_B V_g$ as 0.25, we compute $k_D = 180$ sec.$^{-1}$ for 0.0112 cm granules. This gives $k_{\text{exp}}./k_D = 0.02$, or using Figure 6 a fraction of surface available in excess of 99 per cent, in agreement with experiment for the small granules. For the larger granules k_D works out to be 0.18, so that $k_{\text{exp}}./k_D = 0.90/.18 = 5$, corresponding to 20 per cent of surface available, in fortuitously excellent agreement with experiment. We would thus predict that the apparent activation energy on the small particles would be twice that for the larger granules. Prater *et al.* also verify this experimentally.

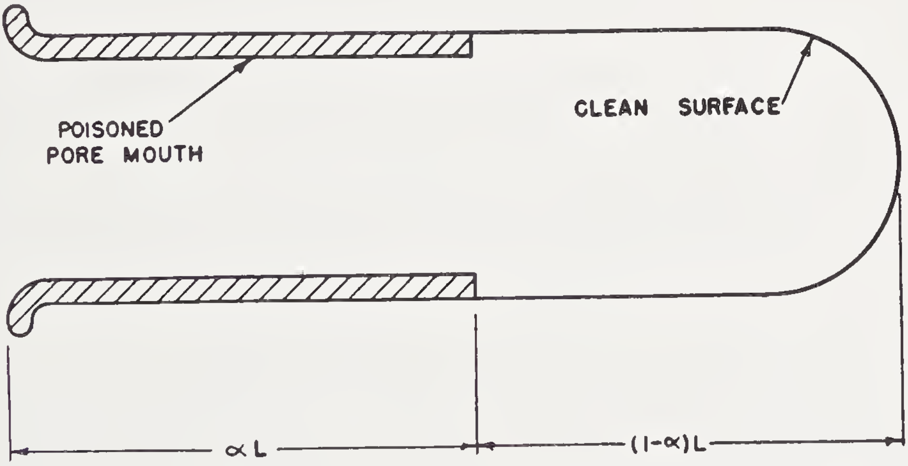

FIG. 6. Schematic representation[1] of the preferential adsorption of poison near the mouth of a pore. α is the fraction of the pore of length L covered with poison.

Ammonia Decomposition

This reaction was discussed earlier by the writer (Wheeler[1]). The data of Love and Emmett[20] show that pellets up to 10 mesh in size are completely available to the reaction in the temperature range 387 to 467°C on singly promoted iron catalysts at 1 atm. pressure. We predict this since their observed $k_{\text{exp.}}$ is never more than 1 to 2 sec.$^{-1}$ while k_D works out to be about 16 sec.$^{-1}$ for 10 mesh pellets, assuming Knudsen flow in pores of 230 Å radius. Thus $k_{\text{exp.}}/k_D$ is about 0.06, or the fraction of surface available for 10 mesh pellets is 98 per cent, in agreement with the results of Love and Emmett.

Ammonia Synthesis

In ammonia synthesis at conventional pressures of about 300 atmospheres, diffusion in catalyst pores is surely of the bulk type. In our earlier discussion of this reaction (Wheeler[1], p. 304) we derived the approximate equation for 5 mm granules:

$$\begin{aligned} h \tanh h &= k_{\text{exp.}}/k_D \\ &= 3.3 \times 10^3 \, [F.R., \text{ moles/cc/sec}] \log \frac{1}{1 - \alpha_c} \end{aligned}$$

where $F.R.$ is the feed rate of nitrogen in moles/cc/sec and α_c is the fractional approach to equilibrium. This equation corresponds to bulk diffusion of nitrogen-hydrogen mixtures assuming the diffusion coefficient is inversely proportional to the pressure. Conventional operation of ammonia synthesis (Larson and Tour[21], Nielsen[22]) appears to correspond to about 50 per cent approach to equilibrium at a feed rate of nitrogen of about 0.1 to 0.4 moles of nitrogen per cc *per hour*. This gives a value of $k_{\text{exp.}}/k_D$ of 0.06 to 0.25, meaning the fraction of surface available should be 80 per cent or greater for even the most active ammonia synthesis catalysts. This result is in good agreement with the data of Larson and Tour[21] who find activity independent of granule size. (We wish to thank Dr. A. Nielsen of the Haldor Topsøe Laboratories for pointing out a numerical slip at the bottom of page 304 of our earlier discussion, (Wheeler[1]). The borderline space time yield corresponding to 80 per cent surface available should read 11 g of NH_3 per cc of catalyst per hour, not 0.79 g.)

Ethylene Hydrogenation on Evaporated Metal Films

This reaction was considered in detail in the earlier discussion (Wheeler[1]). In agreement with experiment it was concluded that very active thin nickel films 2.2×10^{-4} cm thick were 98 per cent available to ethylene-hydrogen-mixtures at 23°C ($h = 0.23$). We note, however, that films 10 times thicker

(2×10^{-3} cm) or even thin films at a higher temperature (above 125°C) would not be completely available. Thus diffusion can effect the rate on even very thin films in the higher temperature range when their activity is exceedingly high.

Hydrogen Transfer from Decalin to Butylene

Blue *et al.*[15] have studied the rapid reaction of hydrogen transfer from decalin to isobutylene at 342°C on silica alumina TCC beads containing pores of an average radius of 24 Å. Their essential result is that 5 mm beads have only a small fraction of surface available to the reaction, since they are about 8 times less active than 40–60 mesh catalyst. 40–60 mesh catalyst has most of its internal surface available since particles twice as large (20–40 mesh) are only about 10 per cent less active. This result is predicted by the theory as follows: For 0.5 mm beads operated at a coke level of 1 per cent by weight, $k_{\text{exp.}}$ is 0.75 sec^{-1}, k_D works out as 9.1×10^{-2} sec^{-1} for Knudsen flow in 24 Å pores on 0.5 cm beads. The ratio $k_{\text{exp.}}/k_D$ is thus 8.2, corresponding to only 12 per cent of surface available for the large beads, in excellent agreement with Blue's result that 60-40 mesh granules are about 8 times more active than the large beads. We furthermore calculated in agreement with experiment that the 40–60 mesh granules should be almost completely available, as follows: The ratio $k_{\text{exp.}}/k_D$ for 0.5 mm granules corresponds to a value of $h = 8$ for this size bead. Since 40–60 mesh granules are 16 times smaller, the value of h for these small granules will be 16 times smaller or about 0.5. This corresponds (Figure 4) to about 93 per cent of surface available, in agreement with experiment.

Butane Dehydrogenation

Blue *et al.*[15] in the above paper also investigate butane dehydrogenation on 12 per cent chromia-alumina at 530°C. This is a "borderline reaction" since 3.2 mm pellets are only about 30 per cent less active than granules 10 times smaller, so that the large granules must have about 70 per cent of their internal surface available. Our theory predicts the somewhat larger value of about 90 per cent availability for 3.2 mm granules as follows: $k_{\text{exp.}}$ for these pellets is about 0.58 sec^{-1} corresponding to a contact time of 1.2 seconds for 50 per cent approach to equilibrium. The pore size is given by Blue *et al.* as 110 Å radius. Thus k_D is 1.85 sec^{-1} assuming Knudsen flow. The ratio $k_{\text{exp.}}/k_D$ is 0.31, corresponding to 90 per cent of surface available. The discrepancy between the experimental value of 70 per cent and the calculated value of 90 per cent can be due to (a) errors in the theory (b) blocking of pores by the chromia impregnated on the catalyst which would make k_D smaller (c) experimental factors in research such as by-passing of the larger pellets due to their diameter (3.2 mm) being sizeable as compared with the reactor tube diameter (about 13 mm internal diameter). In any case, both theory and experiment show the reaction to the "borderline" with diffusion effects just beginning to be of importance.

Other Studies

Decrease in the apparent activation energy due to diffusion within catalyst pores has been found by Wicke and Brotz[23] for ortho-para hydrogen conversion on nickel and for methanol decomposition on zinc oxide. They also verified that, under conditions of bulk diffusion, inert gas and increase in total pressure should depress the rate by an inverse square root law. Bokhoven and Hoogshagen[24] found diffusion in catalyst pores to cause the apparent activation energy to decrease in the higher temperature range for the water gas reaction on Fe_2O_3-Cr_2O_3 catalysts and for ammonia synthesis on iron catalysts at one atmosphere pressure.

Effect of Diffusion (Mass Transfer) to the Surface of the Catalyst

As discussed in connection with Figure 3, for a very active catalyst diffusion through the gas phase to the catalyst pellets may be slow enough so that the concentration of reactant at the external catalyst surface may be smaller than in the main gas stream. For such a case the catalyst appears to be less active than it really is, so that the experimental rate constant, apparent fraction of internal surface available, and other kinetic quantities are not the true ones, but are dependent on flow conditions (turbulence etc.) in the reactor. It is thus important in the case of very active catalysts to know when diffusion to the catalyst is important. Engineering data are at hand to determine this (e.g., Hougen and Watson[16]) but these correlations appear to be seldom used by catalytic chemists. We have derived a simplified criterion from the engineering data which a chemist can use in a few moments. The engineers measure experimentally a "rate constant" for diffusion k_G per unit external surface of catalyst pills. They find this quantity depends on a large number of quantities, especially on granule size, flow rate, molecular weight of flowing fluid, viscosity, diffusivity, etc. By making certain rough assumptions we can simplify their result into a rough but useful equation. We arrive at the conclusion that the conventional first order rate constant per unit volume of reactor (usual units, $\sec^{-1}$) for a reaction completely limited by diffusion to the catalyst is approximately:

$$k_\infty = 10 \sqrt{\frac{V_L}{\bar{M} a^3 P_T}} \text{ (sec.}^{-1}\text{)} \tag{67}$$

where V_L is the linear velocity of flowing gas (computed on the basis of an empty reactor), $\bar{M}$ is the average molecular weight of the flowing gas, a is the pellet size and P_T is the total reactor pressure in atmospheres. V_L and a should be expressed in cm/sec and cm, respectively. The main assumptions used in deriving the above equation from the engineers correlation are that all gases have the same viscosity and the same Schmidt number. These assumptions are good to a factor of about two. k_∞ as given by the above equation gives the first order rate constant for an infinitely active catalyst for which reaction rate is limited completely by diffusion to the external catalyst surface. Thus a criterion that mass transfer (diffusion) to the catalyst surface is not affecting reaction rate is that the experimentally observed rate constant should be smaller than k_∞ by a factor of about 10.

A further deduction is that Eq. (49) (which connects the experimentally observed rate constant with the catalyst structure and intrinsic activity) needs modification to take mass transfer into account. We propose the following modification to be used whenever $k_{\text{exp.}}$ is comparable with k_∞ in magnitude:

$$k_{\text{exp.}} = \frac{\left\{\dfrac{6\rho_B}{a\sqrt{2}} \sqrt{V_g S_g k D} \tanh h\right\}}{1 + \{\ \} \left(10 \sqrt{\dfrac{V_L}{\bar{M} a^3 P_T}}\right)^{-1}} \tag{68}$$

Here the bracket { } stand for the quantity in this bracket in the numerator, while the parenthesis in the denominator is k_∞. The meaning of Eq. (68) is that for a catalyst of very great intrinsic activity (k very large), the quantity in the numerator will be very large, so that the term unity can be neglected in the denominator. The numerator would then cancel the same term in the denominator, so that $k_{\text{exp.}} = k_\infty$ as desired. On the other hand when k_∞ is much larger than $k_{\text{exp.}}$, the denominator can be neglected and we recover Eq. (49). An important use of Eq. (68) is to compute the true intrinsic activity k and the fraction of surface available for a very active catalyst for which diffusion to the catalyst is affecting the observed rate.

REACTION RATES ON POISONED CATALYSTS—(APPARENT SELECTIVE POISONING)*

In the study of catalysis, the manner in which catalyst poisons affect activity is a matter of considerable importance. In investigations of the poisoning effect it is usual to add increasing amounts of poison to a catalyst material, and plot the per cent of activity left after adding poison against

---

* Except for a few minor word changes and corrections, the next two sections are taken almost verbatum by Dr. Wheeler from his earlier publication in Vol. III of "Advances in Catalysis." We wish to thank the Academic Press for permission to quote this portion of his previous article directly.

per cent of catalyst surface poisoned. If this curve is linear (i.e., if activity is halved by poisoning half the surface) the poison is termed "non-selective." If, however, poisoning 10 per cent of the surface causes the activity to drop by a factor of say five, the term "selective poisoning" is applied. In the past it has been common to attribute "selective poisoning" to preferential adsorption of poison on active centers which make up only a small fraction of the surface. Our purpose is to show that "selective poisoning" should also be observed for porous catalysts having completely homogeneous surfaces, if one assumes that poisons are rapidly and tightly adsorbed so that they stick on pore mouths (i.e., on the outer periphery of a catalyst pellet) rather than being homogeneously distributed into the interior of the pellet. Even when the poison is homogeneously distributed throughout the pellet, we do not expect poisoning curves to be linear for fast reactions. We shall show that a number of different shapes of poisoning curves are possible, depending on the location of poison, on pore size and on catalyst activity. We first consider poisons which are homogeneously distributed throughout a pellet. For clarity we limit our discussion to first order reactions.

Homogeneous Adsorption of Poison

If the poisoning molecule (e.g., carbon monoxide) must make many collisions with the catalyst surface before adsorption can occur, then poisoning molecules will have the opportunity to diffuse deep into the catalyst pellet before being "cleaned up" by the pore walls. Such poisons will be evenly distributed along the wall of a typical pore. If a fraction of the pore surface α is poisoned, the simplest assumption is that the intrinsic activity k of the pore wall decreases to $k(1 - \alpha)$, that is linearly with the fraction poisoned. The activity of the whole pore, or whole pellet, is not directly proportional to $k(1 - \alpha)$ for a fast reaction, but for first order reactions is proportional to $h \tanh h$, as given by Eq. (50). For a poisoned pore we find h by substituting $k(1 - \alpha)$ for k in Eq. (43):

$$h = L\sqrt{\frac{2k(1-\alpha)}{rD}} = h_0\sqrt{1-\alpha}$$

when h_0 is the value of h for the unpoisoned pore. The ratio F of activity of poisoned pore to unpoisoned is thus:

$$F = \frac{\text{Rate poisoned}}{\text{Rate unpoisoned}} = \frac{h_0\sqrt{1-\alpha}\tanh(h_0\sqrt{1-\alpha})}{h_0 \tanh h_0} \qquad (69)$$

When h_0 is small (surface completely available) this ratio becomes $1 - \alpha$, since the hyperbolic tangent terms become equal to their arguments. This, of course, is the usual "classical case" of non-selective poisoning. When h_0

is very large (say 100, surface only about 1 per cent available) over most of the poisoning curve the hyperbolic tangent terms will equal unity and we find

$$F = \sqrt{1 - \alpha} \text{ (for } h \text{ large)} \tag{70}$$

This equation shows that for fast reaction in which poison is distributed homogeneously, activity will fall less than linearly with poison concentration. This type of poisoning might be called "antiselective". Physically this occurs because the reaction uses more of the internal surface of the less active poisoned catalyst. That is, the slower reaction on a poisoned catalyst penetrates deeper into the catalyst pellet, because of the decreased value of h. In Figure 7, Curve B and Curve A, we plot the poisoning curves for these two limiting cases: h_0 very large and h_0 very small. For intermediate values of h_0, intermediate curves would be obtained. We next consider the

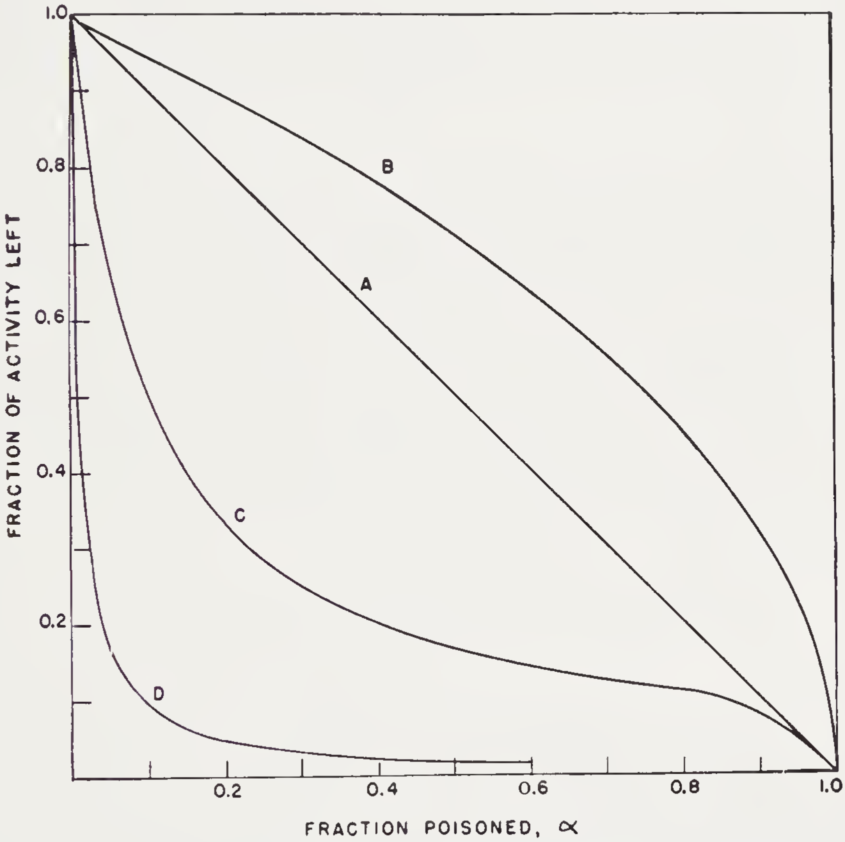

FIG. 7. Types of poisoning curves to be expected for porous catalysts. Curve A is for a nonporous catalyst or for a porous catalyst in which h_0 is very small and poison is distributed homogeneously. Curve B is for homogeneous adsorption of poison with h_0 large (Eq. 69). Curves C and D are for preferential adsorption of poison near the pore mouth. For curve C, $h_0 = 10$ and for curve D, $h_0 = 100$ (Eqs. 70, 73).

case where poison is selectively adsorbed on the outer periphery of the catalyst particle.

Reaction with Poisoned Pore Mouths

Since many catalysts, especially the reduced metals, are excellent "getters" for active poison molecules, in many cases we can expect poison molecules to be adsorbed in an immobile condition after a very few collisions with a catalyst surface. For this case when a small amount of poison is added, the outer pore mouths will become completely poisoned, with the inner recesses of the catalyst particle completely clean. With successive addition of poison, progressive poisoning down a pore will occur. If a pore of length L has sufficient poison added to cover a fraction α of its surface, then the length αL nearest the mouth will be completely poisoned, and a length $(1 - \alpha)L$ beyond this will be clean (see Figure 6). Thus molecules must diffuse through the length αL before reaching active surface. We now show that diffusion through this poisoned mouth can be, in the case of a fast reaction, a very slow process which can become rate determining, and hence addition of a small amount of poison can cut down activity by a large factor.

Looking at Figure 6, we assume that the concentration of reactant at the pore mouth is C_0, and we wish to find the rate of reaction in a pore which has its initial length αL poisoned. We assume transport of reactant through the poisoned portion to be by diffusion. Under steady state conditions this will occur with a linear concentration gradient $\frac{\Delta C}{\Delta L} = \frac{C_0 - C_1}{\alpha L}$ where C_1 is the (unknown) concentration at the end of the poisoned region. The rate of this diffusion through the poisoned length αL must equal the rate of reaction in the clean region of length $(1 - \alpha)\ L$. Thus the equation which determines C_1 is for a first order reaction:

$$\pi r^2 D \frac{C_0 - C_1}{\alpha\ L} = \pi r C_1 \sqrt{2rkD} \tanh [h_0(1 - \alpha)] \tag{71}$$

where the left-hand side is the rate of diffusion through poisoned part of the pore and the right hand side is rate of reaction on the clean part. As before h_0 is the value of h for the unpoisoned pore, so that $h_0(1 - \alpha)$ is the value of h for the unpoisoned portion of length $L(1 - \alpha)$. Solving Eq. (71) for C_1 and putting this value back into the left side of Eq. (71) gives for the desired rate in the poisoned pore:

$$\text{Rate} = \frac{[\pi r \sqrt{2rkD} \tanh h_0 (1 - \alpha)] C_0}{1 + \alpha h_0} \tag{72}$$

This rate observed in the poisoned pore divided by that in a clean pore is:

$$F = \left[\frac{\tanh h_0 (1 - \alpha)}{\tanh h_0}\right] \frac{1}{1 + \alpha h_0} \tag{73}$$

For active catalysts with small pores (h_0 large), $h_0(1 - \alpha)$ will be much larger than 2.0 so that the bracketed term becomes equal to one, and we get:

$$F = \frac{1}{1 + \alpha h_0} \quad (\text{For } h_0(1 - \alpha) > 2) \tag{74}$$

This equation shows that a very large drop in activity can be caused by a small amount of poison. For example, if we cover only 10 per cent of a catalyst surface with poison ($\alpha = 0.1$), this can cause the activity to drop, not by 10 per cent, but by 91 per cent, if say h_0 were 100. (That is if $h_0 = 100$, $\alpha = 0.10$, then $F = \dfrac{1}{1 + 10} = 0.09$ so only 9 per cent of original activity is left, and hence 91 per cent has been lost). The physical cause of this effect is that the unpoisoned catalyst was using only the outer periphery of the pellet (the outer 1 per cent since $h = 100$, and the fraction of surface available is approximately the inverse of h). Poisoning the outer 10 per cent of the catalyst surface has destroyed the original site of the reaction, and has forced the reactants to diffuse deeper into the pellet before they are able to reach the active parts of the catalyst. The slower rate of diffusion over this larger distance has caused the observed rate to drop severely. In Figure 7 (lower curves) we plot the poisoning curves for such catalysts in which the poison is selectively adsorbed on the pore mouths. Each curve is for a different value of h_0, the value of h for the unpoisoned catalysts.

The temperature coefficient of reaction on such poisoned catalysts will be markedly lower than on unpoisoned catalysts, as is discernible from the rate Eq. (72). For large h_0 (greater than about 20) and for moderate amounts of poisoning ($\alpha = 0.2$ to 0.9), then the hyperbolic tangent term in Eq. (72) will always be about unity, and in the denominator 1.0 may be neglected as compared with αh_0. For such poisoned catalysts the rate becomes:

$$\text{Rate} = \pi r^2 \left(D \frac{C_0}{\alpha L}\right) \tag{75}$$

which is simply the rate of diffusion through the poisoned pore mouths under the maximum available gradient $C_0/\alpha L$. Since diffusion is rate determining, the temperature coefficient on such poisoned catalysts will be very low indeed, and the apparent activation energy will drop to zero.

In summary, the temperature coefficient on catalysts with poisoned pore mouths will behave as follows: (a) Over the lowest temperature in which reaction is measurable the true activation energy will be measured. This is because reaction will be so slow (k so small) that unpoisoned surface will be completely available to reaction and diffusion through the poisoned pore mouth will not be rate controlling. This is reflected in Eq. (72) by the range in which h_0 is so small (considerably less than 1.0) that h_0 can be neglected as compared with 1.0, and tanh $h_0(1 - \alpha)$ can be set equal to $h_0(1 - \alpha)$, (b) As the temperature and hence the reaction rate is increased, the temperature coefficient will fall off for two reasons. First, diffusion rate through the poisoned pore mouths will begin to be too slow to support the fast reaction on the unpoisoned portion of the catalyst and secondly a decreasing portion of the unpoisoned surface area will be available for reaction. This is reflected in Eq. (72) by αh_0 and $h_0(1 - \alpha)$ both becoming of the order of unity or slightly larger, (c) when the temperature is raised sufficiently so that the catalyst becomes very active (k very large), the reaction will be completely controlled by diffusion rate through the unpoisoned pore mouth, and the temperature coefficient will drop to zero. This is reflected in Eq. (72) by both αh_0 and $(1 - \alpha)h_0$ being both much larger than 1.0. Some of the various possible activation energy plots which might be expected for a catalyst with 11 kcal true activation energy are given in Figure 8. The reaction is assumed to operate in the range 200 to 450°K, both the true activation energy and operating range being taken to approximate those for ethylene hydrogenation on nickel. Various shapes are obtained depending on the value h_{200} assumed for the unpoisoned catalyst at 200°K and depending on the fraction of surface poisoned. The formula used to compute the curves is that the rate at a temperature T°K is given, in arbitrary units, by:

$$\frac{y \tanh [(1 - \alpha)yh_{200}]}{1 + \alpha y h_{200}}$$

$$\text{when } y = \exp \frac{11{,}000}{2R} \left(\frac{1}{200} - \frac{1}{T}\right)$$

It appears from Figure 8 that depending on pore size and on condition of poisoning, any value of the activation energy plot may be observed between the limits of observing the correct intrinsic activation energy over the whole temperature range (top curve) to observing practically zero activation energy over the whole range. These considerations emphasize that fundamental investigations aiming at true activation energies should use carefully purified feeds and small catalyst pellets containing large pores only. The falling off of activation energies to almost zero in the high temperature region has been observed in a number of reactions (e.g., ethylene hydrogenation). Poisoning of catalyst pore mouths offers one likely explana-

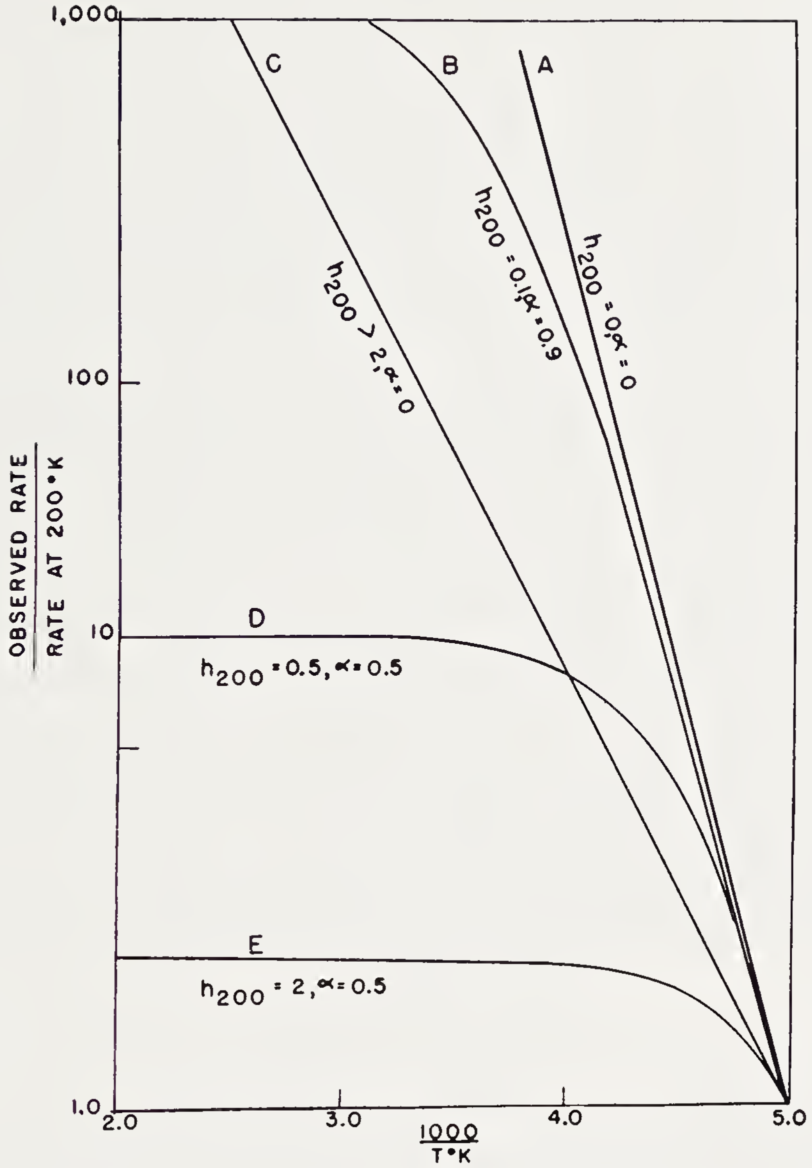

FIG. 8. "Effect of poison and pore size on apparent activation energy. Plots of observed reaction rate vs. 1/T for a hypothetical catalyst having 11,000 kcal. intrinsic activation energy (e.g., nickel in ethylene hydrogenation) but prepared with different pore sizes and poisoned to varying extent with poison preferentially adsorbed near the pore mouth. Curve A: large pores, no poison. Curve B: fairly large pores, 90% poisoned ($h_{200} = 0.1, \alpha = 0.9$). Curve C: Small pores, no poison. Curve D: Moderate size pores, 50% poisoned ($h_{200} = 0.5, \alpha = 0.5$). Curve E: Small pores, 50% poisoned ($h_{200} = 2, \alpha = 0.5$). The horizontal portions of D and E correspond to diffusion controlled reaction."[1]

tion for this, although other explanations connected with the adsorption characteristics of the reactants are also possible. It appears that a necessary and sufficient experimental criterion that intrinsic activation energies are being measured, uncomplicated by pore structure effects, is that catalyst activity and activation energy should be independent of catalyst pellet size.

EFFECT OF PORE STRUCTURE ON CATALYST SELECTIVITY

So far we have considered the effects of pore structure on the general characteristics of catalytic reaction rates. We have seen that pore structure can strongly affect the activity, the temperature coefficient, the kinetic order of the reaction and the poisoning characteristics of the catalyst. We now shall show that pore structure can markedly influence catalyst selectivity.

As a preliminary we wish to distinguish sharply between three different types of catalyst selectivity, since each type is affected quite differently by the pore structure. For convenience we designate the three fundamentally different types of selectivity by Type I, Type II and Type III.

Type I Selectivity in Catalyst Pores

We often need a catalyst which is highly reactive toward one particular compound in a mixture but relatively inactive toward a second component. Thus a selective catalyst which will hydrogenate olefins in the presence of aromatics, leaving the aromatics unchanged, is an illustration of Type I selectivity. Alternatively we might want a catalyst which will dehydrogenate six membered rings (e.g., cyclohexane) but which will not dehydrogenate five membered rings (cyclopentane). Thus Type I selectivity involves the relative rates of reaction of two different types of compounds on the same catalyst. This type of selectivity may be defined by the reaction scheme:

$$A \xrightarrow{k_1} B + C$$

$$X \xrightarrow{k_2} Y + Z$$

which means that molecule A (e.g., cyclohexane) reacts with rate constant k_1 (e.g., to give benzene and hydrogen), whereas on the same catalyst molecule X (e.g., cyclopentane) reacts with rate constant k_2. If we assume that both reactions are first oder and that k_1, k_2 are the over-all rate constants per g (or per cc) of catalyst, then the rate equations which govern reactor performance are:

$$\frac{-dA}{dt} = k_1A \tag{76}$$

$$\frac{-dX}{dt} = k_2X \tag{77}$$

If we divide (76) by (77) and integrate we obtain an equation describing the selectivity of catalyst performance:

$$\alpha_A = 1 - (1 - \alpha_x)^S \tag{78}$$

where α_A and α_x are the fractions of A and X reacted and S is the ratio k_1/k_2. Thus the per cent of A reacted at a given level of conversion of X depends only on the ratio S. We term this ratio of rate constants the selectivity factor S since it determines the selectivity of the catalyst. We note in passing that if experiments are carried out at different contact times, then a plot of log $(1 - \alpha_A)$ vs. log $(1 - \alpha_x)$ should be a straight line of slope S if the assumed first order kinetics are valid for a particular reaction.

The important point we now wish to make is that the ratio of bulk rate constant k_1/k_2 (and hence the selectivity) depends not only on the intrinsic selectivity of the catalyst, as it would be observed on an ideally flat surface, but also on the pore structure, as given by Eq. (49). For example the bulk rate constant k_1 is not necessarily proportional to the intrinsic activity constant k_A for the reaction $A \rightarrow B + C$ but according to Eq. (49) is proportional to:

$$\sqrt{k_A} \tanh h_A$$

where h_A is given by:

$$h_A = L\sqrt{\frac{2k_A}{rD_A}}$$

It follows that the observed selectivity factor is equal to:

$$S = \frac{k_1}{k_2} = \sqrt{\frac{k_A D_x}{k_x D_A}} \frac{\tanh h_A}{\tanh h_X} \tag{79}$$

where k_A and k_x are the intrinsic rate constants for $A \rightarrow B + C$ and $X \rightarrow Y + Z$, respectively. For a catalyst of moderate activity with large pores, h_A and h_X will be small and the intrinsic selectivity factor

$$S = \frac{k_A}{k_x} \text{ (for } h \ll 1) \tag{80}$$

will be observed. This follows from the property of the hyperbolic tangent that $\tanh h \cong h$ when h is small. Thus when h is small (large pores, moderate activity) the true intrinsic selectivity will be observed, just as if the catalyst area were contained in a plane surface. On the other hand if the catalyst has small pores h_A and h_B will be large (greater than unity) and for this case

$$S = \sqrt{\frac{k_A D_x}{k_x D_A}} \text{ (for } h \gg 1) \tag{81}$$

Equation (81) follows from (79) since tanh $h \cong 1$ when $h \gg 1$. Thus a catalyst prepared with very small pores can be expected to have a selectivity factor equal approximately to the square root of the selectivity factor observed for the same catalytic material prepared with very large pores. The physical reason for this is that only a small fraction of catalyst surface is available to the faster of the two reactions while a larger fraction is available to the slower reaction. Thus small pores tend to weaken Type I catalyst selectivity by retarding a fast reaction to a larger extent than a slow reaction. Providing no catalyst poisons are present, it appears that this decrease of selectivity can proceed no further than the square root relation given by Eq. (81). For example if $A \rightarrow B + C$ were intrinsically nine times faster than $X \rightarrow Y + Z$, we would observe the first reaction to be only three times faster on a catalyst containing very small pores.

If, however, tightly adsorbed catalyst poisons are present it is easy to show that small pores can completely destroy Type I selectivity. On p. 154, paragraph 2, we showed that poisons preferentially adsorbed on the pore mouth can reduce the rate of a fast reaction to the rate of diffusion through the poisoned pore mouth. Since diffusion rates of similar molecules are about the same, we could expect the rates of $A \rightarrow B + C$ and $X \rightarrow Y + Z$ to be reduced to about the same level on catalysts with poisoned pore mouths, regardless of their intrinsic relative rates. Thus the combination of tightly adsorbed poisons and small pores can completely destroy Type I catalyst selectivity, causing reaction rates to be diffusion controlled.

In conclusion when dealing with selective reactions of Type I, maximum selectivity should be observed with catalysts containing large pores using reactants which are as free of poisons as possible. In the treatment given above we have assumed that poison molecules are equally efficient in destroying the reaction sites.

Type II Selectivity

Type II selectivity is characterized by parallel (or simultaneous) reactions of a single reactant species. Here the reactant molecule A can be converted into either the "desired" product B or an undesired product C, symbolized by the reaction scheme:

$$\begin{tikzcd} C & \\ A \arrow[u, "k_2"] \arrow[r, "k_1"] & B \end{tikzcd}$$

For example, ethanol can be either dehydrogenated to acetaldehyde or dehydrated to ethylene. Likewise ethylene may be oxidized to either ethylene oxide or to carbon dioxide plus water. A selective catalyst will promote one reaction at the expense of the other.

If the two competing reactions are of the same kinetic order (e.g., first order), then the catalyst pore structure will not affect Type II selectivity. This is because at each point in the pore structure the two reactions will go at the same relative rate, k_1/k_2, independent of the partial pressure of A. Hence the yield of the desired product B will be $k_1/(k_1 + k_2)$, independent of the catalyst pore size. (We define yield here as the number of moles of B formed per mole of A reacted.) If, however, the two reactions are of different kinetic order, then selectivity may depend on pore size, since the decrease in partial pressure of A within the pore structure will affect the two competing reaction rates differently. The concentration of reactant A will decrease markedly within the catalyst pore structure for a rapid reaction on a catalyst with small pores. If the reaction $A \rightarrow B$ were first order with respect to A, and if the reaction $A \rightarrow C$ were second order, then the lower concentration of A existing in the catalyst interior would cause the rate of the second order reaction to fall markedly, thus favoring $A \rightarrow B$ at the expense of $A \rightarrow C$. In this case a catalyst with small pores should give better yields of B than a catalyst with larger pores. Using a catalyst with small pores is somewhat equivalent, in Type II selectivity, to lowering the total reactor pressure in the case of a catalyst with no pores since in either case the effective partial pressure of A surrounding the site of reaction is lowered.

It follows that a practical rule for Type II selectivity is that: if operating a reactor at low pressures of reactant gives better yields than higher pressures, then catalysts with small pores should further improve the yields of desired product. On the other hand, if high pressure operation gives improved selective yields, then catalysts with small pores should be avoided.

Type III Selectivity (Unstable Intermediate)

Perhaps the most common and important type of selective reaction is that in which the desired product is an unstable intermediate which can react further to give undesired by-products. The reaction scheme for Type III selectivity is:

$$A \xrightarrow{k_1} B \text{ (desired)} \xrightarrow{k_2} C$$

Good selectivity depends on the rate constant k_1 being much larger than k_2. A technically important example of Type III selectivity is the dehydrogenation of butylene to butadiene. Butadiene is highly unstable and can polymerize and crack to coke and other undesirable by-products. A second example is the hydrogenation of acetylene to ethylene. Ethylene is unstable since it can further be hydrogenated to ethane. Many organic oxidation reactions are typical examples of Type III selectivity since the desired intermediates readily react further to oxides of carbon and water. Type III selectivity can usually be clearly distinguished from Type II since in the former the yield of desired intermediate B decreases markedly with per cent of A reacted, while in Type II selectivity yield of B is independent of per cent A reacted.

We now compare the performance of nonporous catalysts with the selectivity expected for porous catalysts in Type III reactions. Referring to the Type III reaction scheme given above, we note that if k_1 and k_2 are the intrinsic rate constants per unit internal surface, then on a plane surface the yield of B for first order kinetics would be determined by the equations:

$$\frac{-dA}{dt} = k_1 A \tag{82}$$

$$\frac{dB}{dt} = k_1 A - k_2 B \tag{83}$$

Here A and B are the concentrations of A and B at a point in the reactor. Dividing (83) by (82) we get:

$$\frac{-dB}{dA} = 1 - \frac{1}{S}\frac{B}{A} \tag{84}$$

when S is the selectivity factor k_1/k_2. Integration of (84) gives the conversion to B as a function of per cent A reacted:

$$\alpha_B = \frac{S}{S-1}(1 - \alpha_A)\left[(1 - \alpha_A)^{-[1-(1/S)]} - 1\right] \tag{85}$$

where α_B is the fraction of initial A converted to B, α_A is the fraction of A reacted and S is the selectivity factor k_1/k_2. The yield of B, that is the moles of B formed per mole of A reacted, is α_B/α_A and hence is obtained by dividing Eq. (85) by α_A. Equation (85) applies to nonporous catalysts reacting according to first order kinetics for reactions without volume change. In Figure 9, top curve, we use Eq. (85) to calculate the per cent conversion to B vs. per cent A reacted for a selectivity factor of $S = 4.0$. A maximum conversion of 62 per cent to B is observed at about 80 per cent conversion of A. The yield of B at this point is the ratio of these two numbers, or 62/80 = 78 per cent.

The foregoing result holds only for nonporous catalysts since Eqs. (82) and (83) assume that the bulk concentration of A and B at a point in the reactor are the same as those at the catalyst surface. With a porous catalyst granule, however, the concentrations of A and B within the granule are in general different from the concentrations at the external catalyst surface. The reactant A will diffuse into the pore structure where it will be reacted to

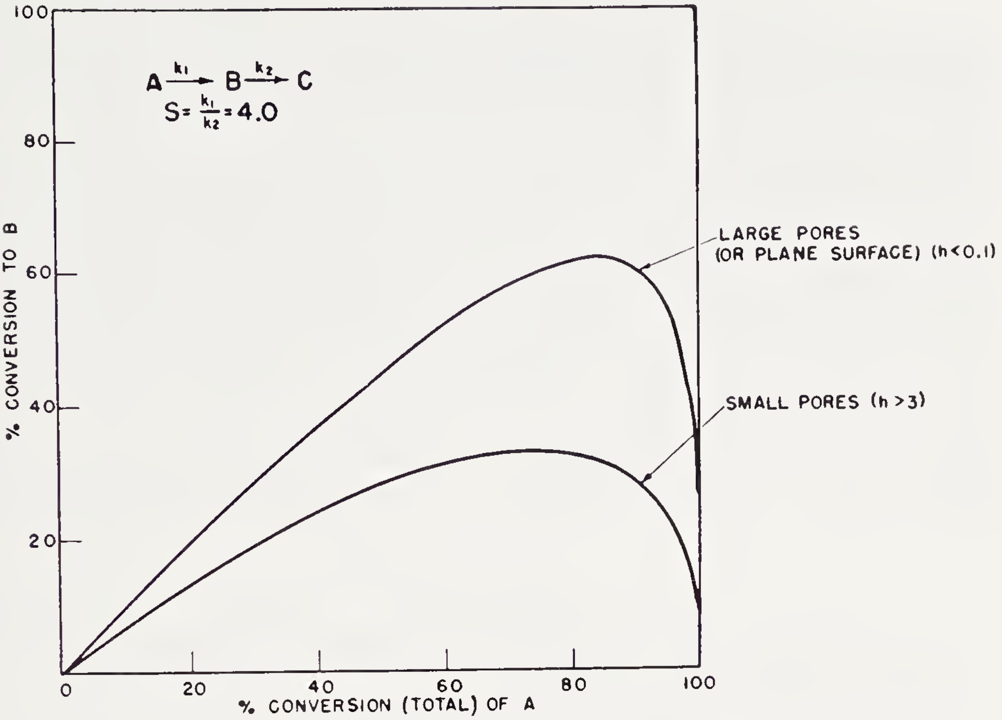

FIG. 9. "Effect of pore size on yields of unstable intermediate in Type III selectivity; A→B→C. Curves are calculated using Eq. (85) for large pore case, Eq. (87) for small pore case, with $S = 4.0$."[1]

the unstable intermediate B. An unstable molecule B formed within a pore must make many random collisions with the pore walls before it escapes out of a pore mouth into the gas phase. Thus while trying to "find its way out" of the pore structure, the intermediate B has a high probability of degenerating into the undesired product C. We can thus expect catalysts with small pores to give poorer yields of an unstable intermediate than will the same material prepared in a nonporous condition.

The decreased yields (due to unstable intermediate "getting lost" so to speak, in the pore structure) can be quantitatively calculated as described in the earlier review (Wheeler[1], p. 318). The calculations show that for active small pores, Eq. (84) for the differential yield of B at a point in the reactor must be replaced by:

$$-\frac{dB}{dA} = \frac{\sqrt{S}}{1+\sqrt{S}} - \frac{1}{\sqrt{S}}\frac{B}{A} \tag{86}$$

Integration of (86) gives the integrated conversion to B for the whole reactor, which replaces Eq. (85):

$$\alpha_B = \frac{S}{S-1}(1-\alpha_A)\left[(1-\alpha_A)^{-[1-(1/\sqrt{S})]} - 1\right] \tag{87}$$

Equation (87) shows, for highly porous catalysts, how the conversion to B depends on fraction of A reacted for various values of the intrinsic selectivity factor $S = k_1/k_2$. In Figure 9, lower curve, we plot α_B vs. α_A for $S = 4$. Thus Figure 9 gives a direct comparison between the performance of porous and nonporous catalyst. For the porous catalyst (lower curve) the maximum conversion to B is only 33 per cent (at about 75 per cent conversion of A) with a yield of B of only 44 per cent. This is to be compared with the 62 per cent conversion to B with a yield of 78 per cent obtained with nonporous catalyst of the same intrinsic selectivity. It thus appears that the pore structure can cut down on yields in Type III selectivity by a factor of about two. The above data is for a selectivity factor of 4.0.

Calculation with other values of the selectivity factor ranging from 1.0 to 10 show that in all cases the yield loss of B due to pore structure is about a factor of two.

References

1. Wheeler, A., "Advances in Catalysis," Vol. III, pp. 250–326, New York, Academic Press, Inc., 1950.
2. Shull, C. G., *J. Am. Chem. Soc.*, **70,** 1405, (1948).
3. Barrett, E. P., Joyner, L. G., and Halenda, P. P., *J. Am. Chem. Soc.*, **73,** 373, (1951).
4. Hurt, D. M., *Ind. Eng. Chem.*, **35,** 522, 1943.
5. Emmett, P. H., "Catalysis," Vol. I, Chapter 2, New York, Reinhold Publishing Corp., 1954.
6. Anderson, J. S., *Z. physik Chem.*, **88,** 191, (1914).
7. Wheeler, A., report #S-9829 circulated to the PAW "Recommendation 41 Group" of the Petroleum Industry, June 1945; presented at AAAS Gordon Conference on Catalysis, 1945 and 1946.
8. Halsey, G. D., *J. Chem. Phys.*, **16,** 931, (1948).
9. Ritter, H. L., and Drake. L. C., *Ind. Eng. Chem., Anal. Ed.*, **17,** 787, (1945).
10. Carman, P. C., and Roal, F. A., *Proc. Roy. Soc.*, (*London*), **209,** 35, (1951).
11. Thiele, E. W., *Ind. Eng. Chem.*, **31,** 916, (1939).
12. Gilliland, E. R., *Ind. Eng. Chem.*, **26,** 681, (1934).
13. Wicke, E., *Angew. Chem.*, **19,** 57, (1947).
14. Weisz, P. B., described at 1953 Gordon Conference on Catalysis, New London, N. H.
15. Blue, R. W., Holm, V. C. F., Regier, R. B., Fast, E., and Heckelsberg, L., *Ind. Eng. Chem.* **44,** 2710, (1952).
16. Hougen, O. A., and Watson, K. M., "Chemical Process Principles," Vol. III, Chapter 20, New York, John Wiley & Sons, Inc., 1947.
17. Damkohler, G., *Z. Phys. Chem.*, **A193,** 16, (1943).
18. Archibald, R. C., May, N. C., and Greensfelder, B. S., *Ind. Eng. Chem.*, **44,** 1811, (1952).
19. Prater, C. D., Weisz, P. B., and Lago, R. M. presented before Kansas City ACS Meeting, March 1954, Paper #84, Div. Phys. and Inorg. Chem.; also to appear in "Advance for Catalysis," Academic Press.
20. Love, K. S., and Emmett, P. H., *J. Am. Chem. Soc.*, **63,** 3297, (1941).

21. Larson, A. T., and Tour, R. S., *Chem. & Met. Eng.*, **26,** 647, (1922).
22. Nielsen, A., and Bohlbro, H., *J. Am. Chem. Soc.*, **74,** 963, (1952); also Nielsen, A., Monograph published by J. Gjellerups Forlag, Copenhagen, 1950. (An investigation on Promoted Iron Catalysts for the Synthesis of Ammonia.)
23. Wicke, E., and Brotz, W., *Chemie Ing. Tech.*, **21,** 219, (1949).
24. Bokhoven, C., and Hoogshagen, J., *J. Chem. Phys.*, **21,** 159, 1953.
25. Brunauer, S., "Physical Adsorption," Princeton University Press, 1945.
26. Eagle, S. E., and Scott, J. W., *Ind. Eng. Chem.*, **42,** 1287, (1950).
27. Amundson, N. R., presented at Gordon Conference on Catalysis, June 1953; also Smith, N. L., and Amundson, N. R., *Ind. Eng. Chem.*, **43,** 2156, (1951).
28. Joyner, L. G., Barrett, E. P., and Skold, R. E., *J. Am. Chem. Soc.*, **75,** 3155, (1953).

CHAPTER 3

THE NATURE OF CATALYTIC SURFACES

Hugh M. Hulburt

Chemical Construction Corp., New York, N.Y.

INTRODUCTION

Although the phenomenon of contact catalysis was recognized early in the development of modern chemistry, a fundamental understanding of its nature has been one of the latest developments in chemical theory and is even yet not completely attained. Involving as it does the most specific properties of solid surfaces, heterogeneous catalysis has only in recent years begun to yield to systematic inevestigation based on all of the allied branches of chemistry and physics which have to do with solids, and their interactions with molecules.

This chapter will comprise a survey of present knowledge of the nature of solid surfaces (especially catalytic ones) from the standpoint of a consistent electronic theory. This theory is far from firmly established in its details. Nevertheless the concepts presented here should prove useful in organizing old knowledge and in stimulating new experiments and extensions of theory.

ELECTRONIC STRUCTURE OF SOLIDS

Classification of Solids

Seitz[31] has classified crystalline solids into the following five empirical types: (a) metals, (b) ionic crystals, (c) valence crystals, (d) semiconductors, and (e) molecular crystals. Of these, metals and semiconductors appear most frequently as active agents in heterogeneous catalysis, although ionic crystals (alumina) and valence crystals (silicon carbide) are common as catalyst supports. As might be expected, these empirical types have typically different electric structures; we shall discuss them separately after establishing a few very general theorems.

The solids whose electronic structure we shall discuss are typically crystalline, that is, they consist of ordered aggregates of atoms, molecules or ions. The units of these aggregates will be termed in general *leptons*[18] when no deeper characterization of their nature is intended. To be sure, many important catalytic materials have no detectable crystalline structure, e.g., the synthetic alumino-silicate cracking catalysts. The similarity of their catalytic properties to those of chemically similar crystals leads us to postulate that the lack of X-ray pattern arises from the smallness of the crystallite rather than from a truly random arrangement of leptons. The persistence of characteristic complex ions of the metals even in solution lends emphasis to the importance of the coordination complex as a structural unit, even in "amorphous" materials. One may expect in the amorphous solids to find the same kinds of coordination complexes as in well crystallized modifications of the same materials. For this reason, the structures of known crystals, even if not themselves catalytic, are worthy of study.

Among the metals, it is becoming increasingly evident that even supported metals are usually microcrystalline. Here also, the study of larger crystals will be rewarding insofar as principles of the behavior of solids can be established. It cannot be assumed, however, without careful investigation that the properties of crystal surfaces are quantitatively correlated with the bulk properties of the ordered aggregates beneath.

Energy Levels in Periodic Potentials

The fundamental properties of any crystal must follow from the behavior of the nuclei and electrons of which it consists. The positively charged atomic cores, by definition, occupy lattice sites in a regular geometrical arrangement. To a good approximation, their vibratory motion can be treated independently of the much faster motion of the valence electrons. We consider the nuclei to be in fixed positions, therefore, and proceed to discuss the motion of the valence electrons in the periodic electric potential field arising from the lattice of positive charges. Any practical calculation must involve a further simplification of this picture. We suppose that it is legitimate to discuss the motion of any one electron separately in the average field of the nuclei and all the other electrons. The average field chosen must, of course, be consistent with the average charge distribution found as a result of the theory. This agreement is found by successive trials, and the resultant potential (still periodic) is the *self-consistent field,* first introduced by Hartree[15].

We thus deal initially with the motion of each electron in the average field of the balance of the system. The simple superposition of these motions gives a first approximation to the behavior of the complete system. This degree of approximation is inherent in every present-day theory of multi-electron systems.

The properties of an electron in the self-consistent field are described by a wave function or *orbital* which is the solution of a partial differential equation derivable from the Schrödinger equation for the complete system. This equation, *the Hartree-Fock equation*, is slightly different for each quantum state of the electron. Furthermore, each orbital depends upon all the other orbitals, since these determine the self-consistent field. Thus we are presented with a complex interlocking set of equations which can be solved only by numerical methods. Nevertheless, certain general properties of the solutions, or *orbitals*, can be demonstrated without complete integration.

The first of these is the existence of discrete energy levels. Not only are the possible energy states of a given electron discrete in energy, but in a system of several electrons, no more than two can occupy the same orbital (*Pauli Principle*), and double occupany is possible only if the electrons have antiparallel spins. The periodicity of the lattice determines the general nature of the energy distribution of the orbitals. It is this periodicity which causes the energy levels to group themselves into *bands*, within which the levels are very closely spaced, separated by gaps sometimes amounting to several hundred kilocalories. The number of levels in each band is an integer multiple of the number, N, of unit cells in the volume of crystal under consideration. For metals, with one atom per unit cell, there are as many levels per band as atoms in the system. With two atoms per unit cell, there will be $2N$ levels per band.

Labels for Bands and Band Orbitals. In designating energy bands it is customary to refer them to the corresponding levels in the discrete atoms from which the solid crystal might be considered to be assembled. Thus, $1s$ atomic orbitals interact to give rise to the $1s$ band of the solid, etc. This point of view is most appropriate, of course, when the interaction is small. The bands are then narrow and well separated. As the leptons approach, a given electron comes into the field of more and more nuclei and the range of energies in the band widens. At sufficiently close approach, adjacent bands may "overlap," i.e., orbitals arising from the interaction of $2p$ atomic orbitals may have a lower energy than the highest energy orbitals arising from $1s$ atomic orbitals. In such a case, a relabelling of the bands might be desirable, but not enough detailed knowledge of the energy level system is now at hand to warrant such a change.

Within a band, the orbitals may be shown to take the form

$$\Psi_k = X_k^{(r)} e^{2\pi i k \cdot r} \tag{1}$$

where r is the position vector which locates the electron whose coordinates are x, y, z; $X_k^{(r)}$ is a function with the periodicity of the lattice, and k is a wave-number vector related to the momentum components of the electron by the Broglie relations:

$$p_x = hk_x \; ; \qquad p_y = hk_y \; ; \qquad p_z = hk_z \tag{2}$$

where h is Planck's constant. It is readily shown that the momentum vectors p, or the wave-number vectors k, may have only certain discrete magnitudes and orientations, and hence, when plotted in p-space, terminate on discrete points of a lattice called the *reciprocal lattice*. Thus we may identify any particular band orbital (often called a *Bloch function*) by citing the value of k. These values play the role of quantum numbers.

In accordance with the customary interpretations of wave functions, the probability charge distribution of an orbital is given by

$$\rho_k^{(r)} = \Psi_k^{*(r)}\Psi_k^{(r)} \tag{3}$$

$$\rho_k^{(r)} = X_k^{*(r)}X_k^{(r)} = |X_k^{(r)}|^2 \tag{4}$$

These quantities give the probability that an electron be found in a unit volume in the neighborhood of r.

If $X_k^{(r)}$ is, to a rough approximation, considered constant, the Bloch function, Eq. (1), becomes the wave function of a free electron whose energy (all kinetic, since the potential must be constant for a *free* electron) is

$$\epsilon(k) = \frac{h^2k^2}{2m} = \frac{p^2}{2m} \tag{5}$$

Thus we find directly the interpretation of k in terms of momentum. When the electrons are not free, the dependence of the energy upon k becomes more complex, since now potential energy must be included. We may still write, however,

$$p_x = \frac{m}{h}\frac{\partial\epsilon}{\partial k_x}, \qquad \text{etc.} \tag{6}$$

Characteristic Energy Curves. These results lead us to refer to four different types of graph to describe the properties of crystals, which we shall call the *energy characteristics*. The first is a plot of energy *versus* lattice parameter (Figure 1). This plot describes the spread and eventual overlap of bands as the constituent leptons approach each other.

The second characteristic is a plot of energy *vs.* r, position in the crystal. This is usually superposed on a plot of potential energy (or self-consistent field) for reference, and r is usually taken in a plane containing the ion-cores (Figure 2).

The third characteristic is a plot of the energy level density *vs.* energy in a given band. The level density is the number of levels per unit of energy change. We note in Figure 3 that this density is far from uniform, but rises to a maximum below the upper band limit, then falls rapidly to zero at the top of the band. More detailed discussion will follow.

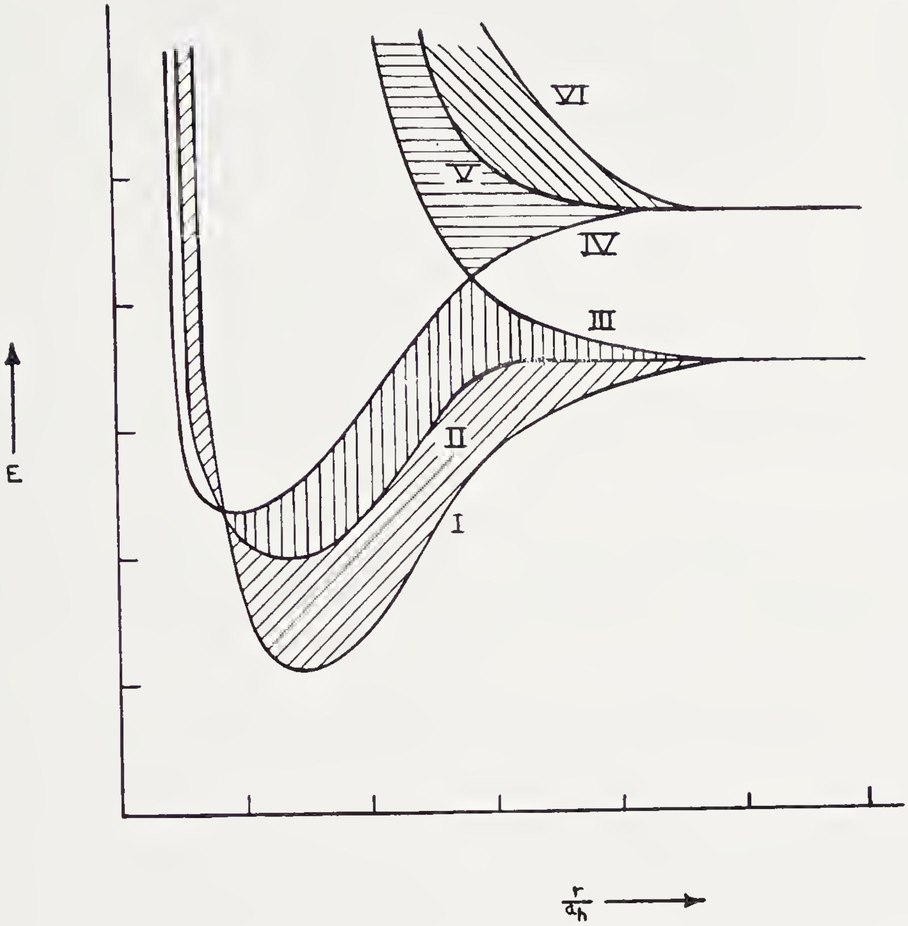

FIG. 1. Energy *versus* lattice parameter. The six valence electrons in a diamond lattice give rise to bands which broaden and eventually overlap as the leptons approach each other.

The fourth characteristic is a plot of energy *vs.* momentum or wave-number, k. This is a surface in four-dimensional space, since k has three components. It is usually given as a section in two-dimensions (Figure 4). For free electrons, every such slice is a parabola, but when the periodic potential is taken into account, the gaps shown in Figure 4 arise and correspond, of course, to the forbidden energy bands.

Brillouin Zones. The same information can be presented in a different way if we plot surfaces of constant energy in k-space (three-dimensional). The energy jumps now occur on specific surfaces of the reciprocal lattice, which for nearly free electrons enclose a polyhedron, but are not planes of constant energy. The points lying on this polyhedron each yield two values of the energy, namely the upper limit of one band and the lower limit of the next. All other points not on such a boundary yield a unique value of the energy, $\epsilon(k)$. These polyhedra are called *Brillouin zones* and the bounding planes are *zone boundaries.* Each point within a zone has coordinates

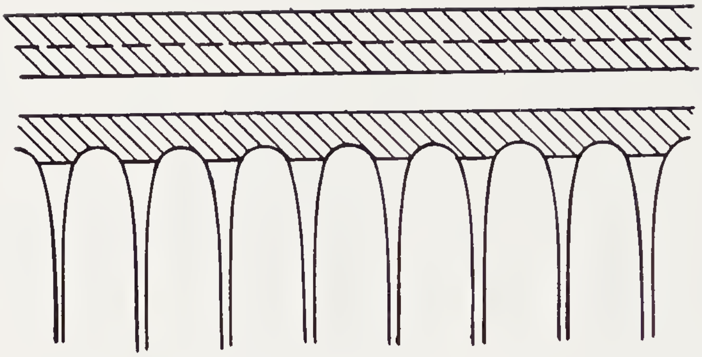

Fig. 2. Energy *versus* position. The allowed energy bands of the electron (shaded regions) are shown superposed on a plot of the potential energy of an electron as it moves along a line of atom cores.

k_x, k_y, and k_z, and hence corresponds to a particular band-orbital. There are thus N points in each zone if there are N orbitals (states) per band.

The shape of the zone boundary can be deduced from the symmetry of the crystal lattice without knowing $X_k^{(r)}$. To every set of parallel lattice planes, there is a radius vector which is perpendicular to the set and whose length is equal to the reciprocal of the distance between successive planes of the set. This vector locates the corresponding point of the *reciprocal lattice.* For every direct lattice one can thus construct a reciprocal lattice in terms in which electron momenta are described as vectors. Thus, the Bloch function for free electrons, Ψ_k, describes motion parallel to some set of lattice planes associated with k in the reciprocal lattice. The existence of zone boundaries means that certain lattice planes cannot be traversed by free electrons. If they are directed against these planes from the outside, they will be reflected in accordance with the well-known Bragg reflection for X-rays and for electrons. Hence the zone boundaries are associated experimentally with highly reflecting lattice planes.

When a nearly free electron moves inside the crystal, every change of direction constitutes a transition in k, and hence a transition from one band-orbital to another. Throughout the lower range of energies, these transitions of direction can always occur without a change of energy, but near the zone boundaries, certain such directional transitions will be forbidden. If attempted, the electron would be reflected internally, just as are externally incident electrons. Thus certain lattice planes are not accessible to electrons near the top of the band.

Periodic Boundary Conditions. All of the above considerations are most easily formulated mathematically if we assume that the potential energy and wave-functions take the same values at $r = L$ as at $r = L$, where L is large relative to the side of a unit cell. In particular, the shapes of the *zone* boundaries are most easily deduced from the symmetry of the

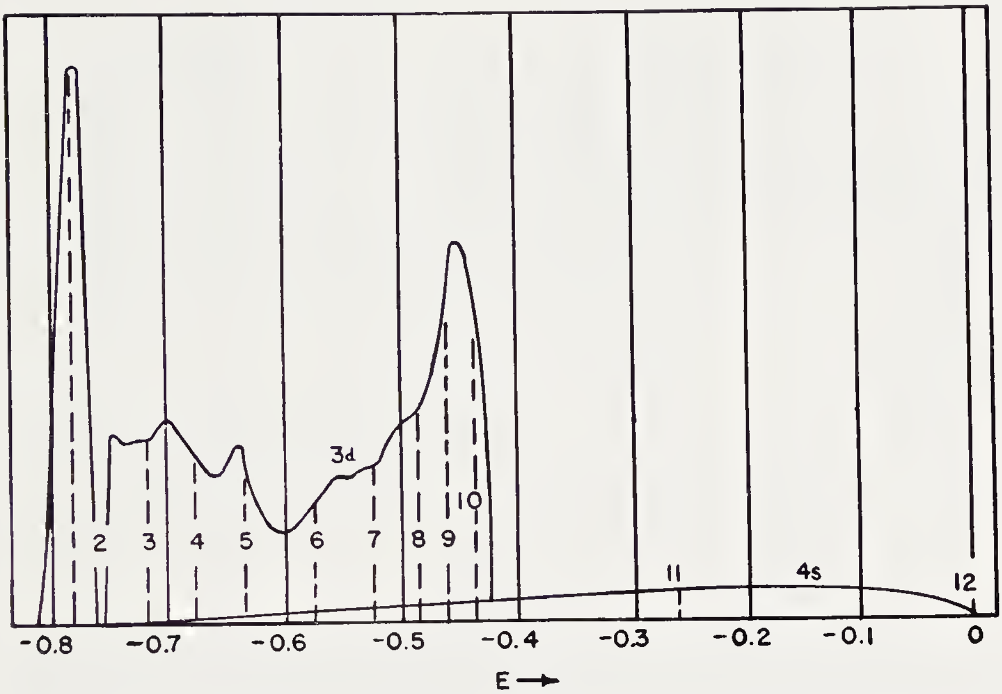

Fig. 3. Energy level density in the iron group metals. The vertical lines designate the limit to which the levels are filled in elements having the indicated number of electrons. The d-band is not quite filled in nickel (10 electrons). (After Slater.)

direct lattice in this case. Such a boundary condition means physically that we do not distinguish the state of surface leptons from those in the interior of the lattice. For most properties of solids, this neglect is not serious, but for catalysis it is of prime importance. However, since it seems likely that surface leptons can be treated as a two-dimensional lattice, all of the qualitative properties discussed so far pertain equally well to this two-dimensional case. In a later section we shall give more detailed consideration to the relationship of surface states to volume states.

Lattice Imperfections. Real crystals are distinguished from ideal crystals by the imperfect periodicity of the self-consistent field in which the electrons move. These deviations are termed *lattice imperfections* and arise from several causes.

It was shown by Wagner[49] and Schottky that the free energy of a crystal containing a number of unoccupied lattice sites, or *vacancies*, is lower than that of a perfect crystal with all sites occupied. The displaced leptons may be found on the surface leaving vacancies (Schottky defects) in the interior, or in interstitial sites (Frenkel defects), leaving vacancies on the surface. This introduction of vacancies raises the potential energy of the crystal, but also increases the entropy, since the number of states of equal energy associated with different locations of the vacancy is enormously greater than the single state possible for a perfect crystal. There will thus be an

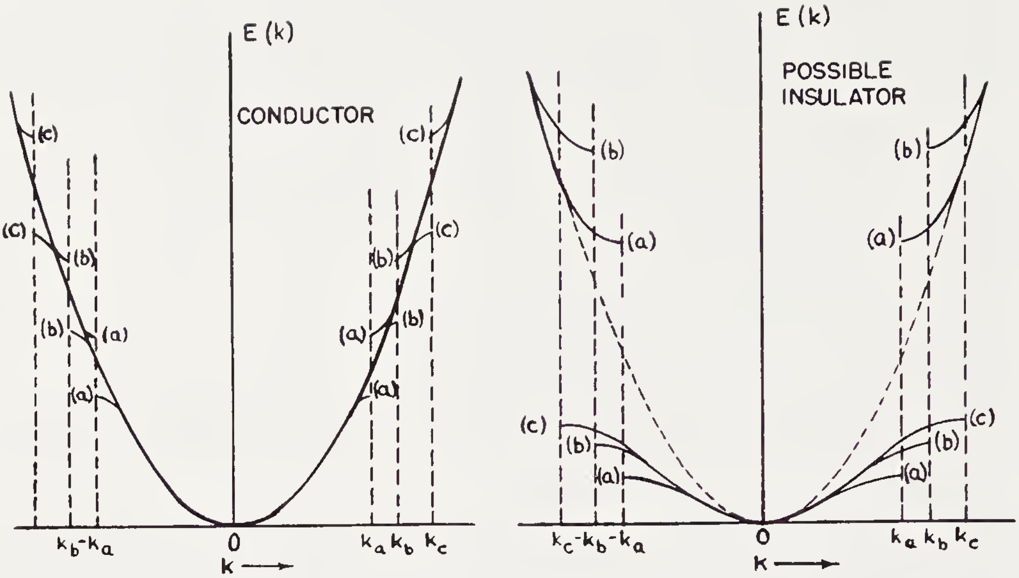

FIG. 4a

FIG. 4. Energy *versus* momentum or wave number.

(a) Overlapping bands. This plot shows the energy as a function of the momentum wave number, k, along lines through the origin of k space in three prominent directions, a, b and c. The zone boundary occurs at k_a, k_b and k_c. Note that in the first zone the curves approach k_a, k_b and k_c from the left and in the second zone from the right. Thus, the second zone has a lower energy at k_a than the first zone has at k_b.

(b) Non-overlapping zones. The energy gap is so large that every level of the first zone lies below every level of the second zone. (After Seitz.)

equilibrium number of vacancies which will give a minimum free energy to the crystal.

Imperfections may also be associated with *impurities*. That is, regular (or interstitial) lattice sites may be occupied by leptons chemically different from those in the perfect crystal. Solid solutions present examples of this sort. The potential energy in the neighborhood of the foreign lepton is different from that near a lepton of the host crystal and the perfect periodicity is disturbed. In ionic crystals, substitution of an ion of different valence from the host, e.g., ferrous for ferric, has the same kind of effect.

These two types of imperfection consist of a perturbation of the ideal periodic potential energy which extends over several unit cells of the lattice. For such a case, Wannier[50] and Slater[40] have shown how the effect of the perturbation can be calculated if the unperturbed levels are known. Physically, their result means that the electrons in the perturbed lattice move as if their unperturbed energy were all kinetic, and the perturbation were the only potential energy. Thus the total energy can be found in this approximation by simply adding the perturbation potential to the unperturbed energy. In Figure 5a we see such a plot for the case in which the charge on one lepton has been increased over that of the host. The unper-

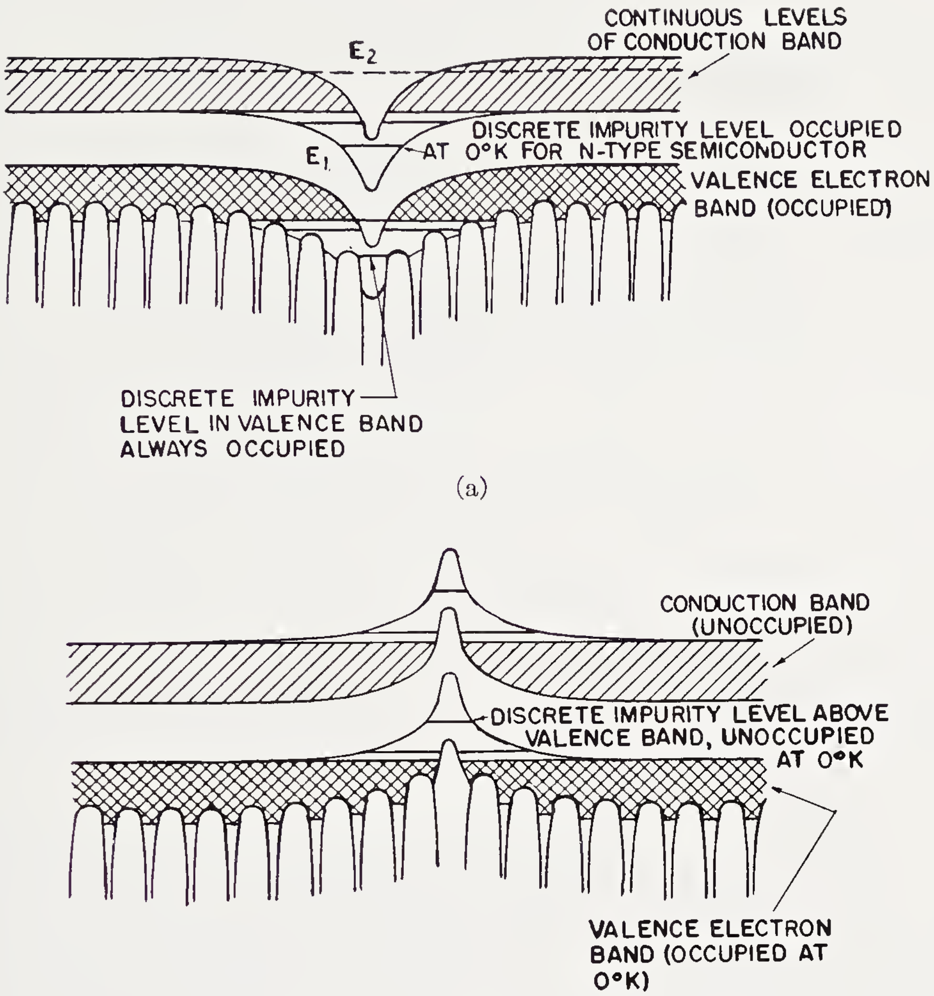

(a)

(b)

Fig. 5. (a) Energy levels in the vicinity of an impurity atom in an N-type semiconductor; (b) Energy levels in a P-type semiconductor.

turbed total energy does not vary with position through the crystal, whereas the perturbation is a Coulombic potential centered on the foreign lepton. In addition, the energy level distribution is modified. One or more of the levels of the perfect crystal may become separated from the band and appear as discrete levels with orbitals localized near the impurity and energies lying below those of the unperturbed orbitals they replace. This localized level is very like the hydrogenic orbital one would expect in the Coulombic potential field if it were present alone. Since, in general, too shallow a potential well does not permit a state with negative energy relative to that of the completely dissociated system, a localized level does not occur if the perturbation is too weak, even though the energies of electrons in the continuous band are lower near to the impurity.

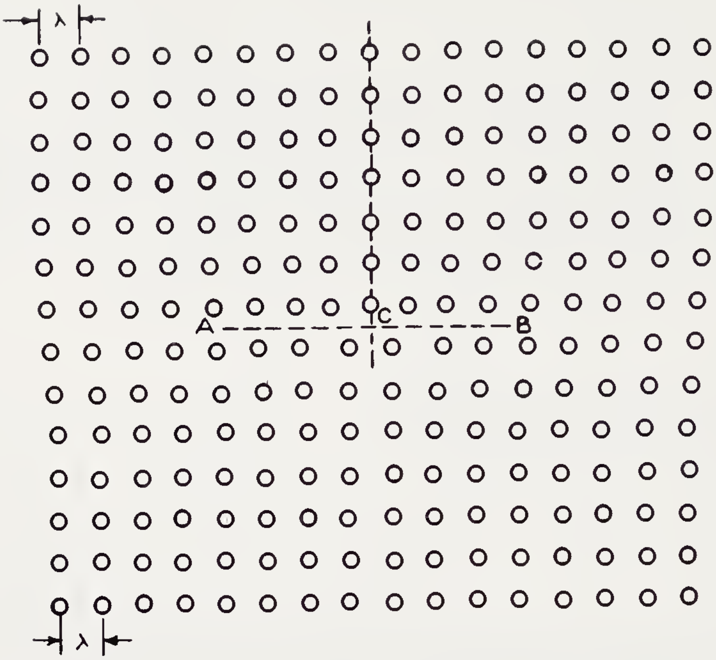

FIG. 6. Atom arrangement in the vicinity of an edge dislocation. The dislocation line is perpendicular to the plane of the figure at C. There is one more lattice plane above AB than below.

In this approximation, the perturbation is assumed to leave the lattice distances unaltered. Other types of lattice defect, however, are characterized mainly by an abrupt change in lattice parameter or crystal symmetry. A *dislocation* consists essentially of a region in which an extra lattice plane has been crowded in, as shown in Figure 6. The abrupt change in lattice parameter as one crosses the dislocation line is evident. Crystal *grain boundaries* involve at least a change in the orientation of the lattice as one crosses a certain plane. At *phase boundaries*, of course, an entirely new lattice symmetry is encountered. *Surfaces* may also be looked upon as abrupt changes in crystal symmetry, since the potential energy field has a one-sided symmetry which terminates at the surface. Because of this asymmetry in the potential, the lattice spacing may be different in the surface layer of atoms from that in the bulk of the crystal, both in directions perpendicular and parallel to the surface plane. On this account, we shall discuss surface states in more detail in a later section.

The theory of sudden changes in lattice parameter is not so far advanced as for mild perturbations. James[19] has treated the one-dimensional case in detail and shows how localized orbitals can arise with energies possibly different from the allowed energies in either ideal lattice. The extension of these ideas to a more realistic model has not yet been made. Qualitatively, however, the existence of localized orbitals with energies forbidden in the ideal crystal must be considered likely at any of the lattice defects just cited, in which there is a sharp change in crystal symmetry or lattice parameter.

These localized levels are formed at the expense of the continuous band. Hence, in crystals with bands filled, the defect levels will be filled also. If perchance the defect level from an upper empty band has a lower energy than the top of the lower filled band, it may be occupied, leaving a vacancy in the band-orbitals. Thus conduction through the bulk of the crystal can be associated with the filling of localized defect orbitals. Examples of this sort of behavior are still conjectural, but may occur in some semiconductors to be mentioned in later paragraphs.

Metals and Insulators. Since we can assign no more than two electrons to any one orbital, yet have one or more electrons per lepton of crystal to dispose of, it is clear that many levels in a band must be occupied in the ground state of the crystal. When successive bands do not overlap and there are just enough electrons to fill some band exactly, it will require considerable energy to excite an electron to the next higher band. As we have seen, any change of motion in the lattice involves a transition to another orbital; hence in a filled band, no electronic conductivity can exist. In the alkali metals, however, we have an example in which only one electron per atom is contributed to an *s*-band capable of holding two electrons per atom. In such a case, conductivity can occur because transitions are possible with very small expenditures of energy.

At this point we make our first and major distinction between classes of crystals. Those with completely filled bands just above which is a forbidden band of energies are *insulators* or *semiconductors*. Those with incompletely filled bands are *metals*. We shall discuss them separately because of the wide diversity of their properties in consequence of their different electronic structure.

METALS

Energy Level Density

Free Electron Model. The thermodynamic properties of electrons in metals can be evaluated statistically only after the energy level distribution is known. Present knowledge is only fragmentary, but suffices to establish qualitative trends. For perfectly free electrons, every value of the momentum at constant energy is equally likely within a band and the energy level density is readily computed as

$$g(\epsilon)\,d\epsilon = \frac{4\pi V(2m^*)^{3/2}}{h^3}\,\epsilon^{1/2}\,d\epsilon \tag{7}$$

where V = volume of crystal
m^* = effective mass of the electron
h = Planck's constant
ϵ = energy level measured from the bottom of the band.

For truly free electrons, m^* is equal to m, the actual electronic mass. In real crystals, however, this simple result is only a rough approximation but can be made adequate in some cases by empirically adjusting m^*. In Figure 7, the level density indicated by soft X-ray emission spectra is given for typical metals. It is evident that the free electron approximation is subject to large corrections in the case of overlapping, nearly full and narrow bands.

Fermi-Dirac Distribution. The number n_i of electrons having energy ϵ_i, there being $g_i(\epsilon_i)$ orbitals with this energy is

$$n_i = g_i/[e^{+(\epsilon_i - \mu)/kT} + 1] \tag{8}$$

according to Fermi-Dirac statistics. The parameter μ is a characteristic of the distribution known in the theory of solids as the *Fermi level*; it is identical with the Gibbs free energy per electron, or *chemical potential* of the electron in the metal[24]. Since the energy levels in Eq. (8) are very closely spaced, we can treat the distribution as continuous within a given band with good accuracy. Thus, the number of electrons with energy in the range dn to $n + dn$ is

$$dn = g(\epsilon)\, d\epsilon/[e^{+(\epsilon - \mu)/kT} + 1] \tag{9}$$

The value of μ is fixed by the requirement that integration of Eq. (9) (or summation of Eq. (8)) yields the total number of electrons in the metal, N.

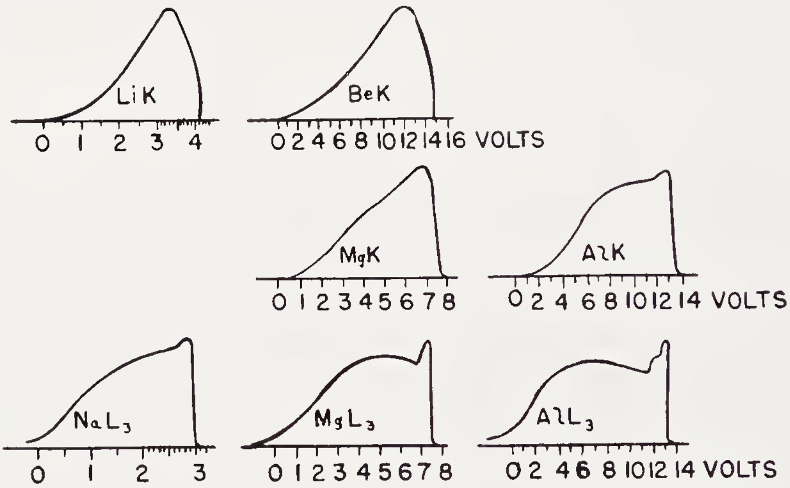

FIG. 7. Soft X-ray emission spectra of several metals. (After Skinner.)

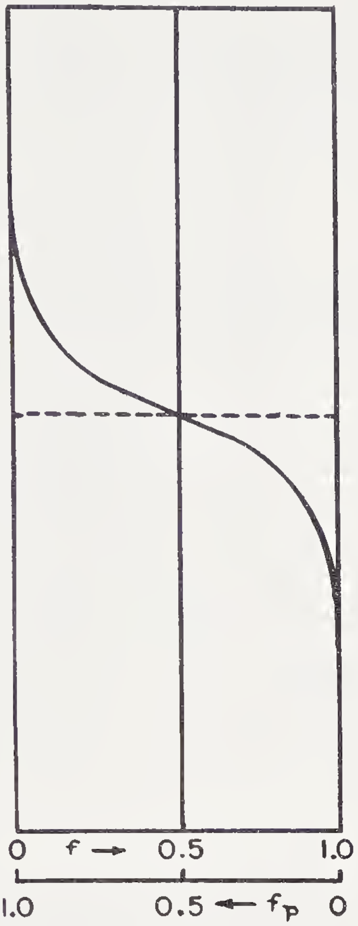

FIG. 8. Fermi distribution. The ordinate is $(E - \mu)/kT$. The abscissa is $f = 1/[1 + \exp(E - \mu)/kT.]$

$$N = \int_0^\infty \frac{g(\epsilon)\, d\epsilon}{e^{+(\epsilon-\mu)/kT} + 1} \tag{10}$$

Figure 8 is a plot of Eq. (9) at several temperatures. At absolute zero, all levels up to an energy μ are filled and all higher levels are empty. At higher temperatures, however, there is thermal excitation of electrons into higher levels. Quantitative calculation, however, shows that the numbers of excited electrons are small at laboratory temperatures; the value of μ/kT is then ordinarily large.

For orientation as to magnitudes, the results for free electrons will be quoted. At 0°K,

$$\mu = \mu_0 = \frac{h^2}{2m^*}\left(\frac{3n_0}{8\pi}\right)^{2/3} \tag{11}$$

where

$$n_0 = N/V = \text{the electron density}$$

The mean energy is

$$\bar{\epsilon}_0 = \tfrac{3}{5}\mu_0 \tag{12}$$

For most transition metals, μ_0 is about 5–7 e.v., or 100–150 kcal/mole of electrons. At higher temperatures, assuming $\mu_0 \gg kT$, one finds approximately

$$\mu = \mu_0\left[1 - \frac{\pi^2}{12}\left(\frac{kT}{\mu_0}\right)^2\right] \tag{13}$$

$$\bar{\epsilon} = \bar{\epsilon}_0\left[1 + \frac{5}{12}\pi^2\left(\frac{kT}{\mu_0}\right)^2\right] \tag{14}$$

It is evident that at almost all catalytic conditions, both μ and $\bar{\epsilon}$ are nearly independent of temperature in metals with electrons far from the upper band limit. In semiconductors, however, where nearly full bands are involved, the chemical potential will be found more sensitive to experimental conditions.

Band Structure of Metals

Brillouin Zones. Most metals crystallize in close-packed lattices with either cubic or hexagonal symmetry. In Figure 9 are shown the first two zones in the face-centered cubic (cubic close-packed) lattice. The associated *reciprocal* lattice is body-centered cubic, and the first two Brillouin zones in this case are shown in Figure 10. For the hexagonal lattice, the first two zones for nearly free electrons in the direct lattice are shown in

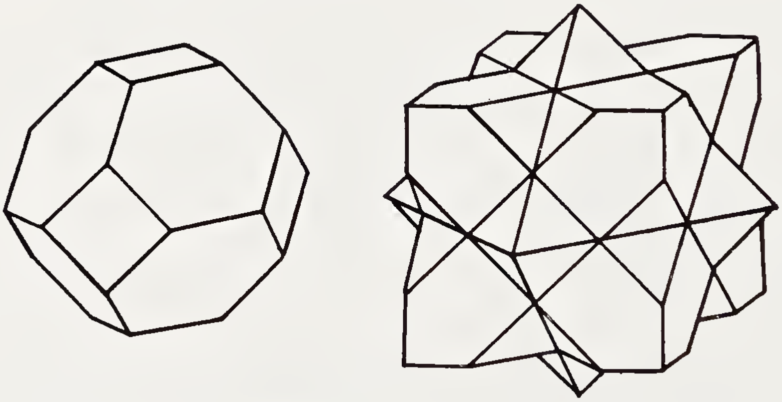

FIG. 9. The first and second Brillouin zones for a face-centered cubic lattice. (After Seitz.)

Figure 11. These figures are plots in momentum space of those surfaces on which energy jumps occur. Thus electrons having momentum components which would fall outside the zone surface must lie in the second band. To every point in the first zone there corresponds an orbital with specified momentum components. Since the orbitals are periodic in momentum space, there also exist orbitals having momenta greater than those between multiples of $\hbar k$, which lie in the higher bands (and zones). Hence it is possible to superpose the second zone point-for-corresponding-point on the first by simple translations of its parts. Thus all of the properties arising from zone structure can be deduced from a knowledge of the first zone alone. For nearly free electrons, the zone surfaces are planes, but as the interaction of electrons with the lattice increases, the surfaces deviate from the planar. The space part, $X_k^{(r)}$, of the band-orbital, is now no longer constant in r, but varies in magnitude over the unit cell. In the opposite limit, known as the *tight binding* approximation, the atoms of the metal are so far apart that $X_k^{(r)}$ is nearly independent of k and looks like an atomic orbital. The

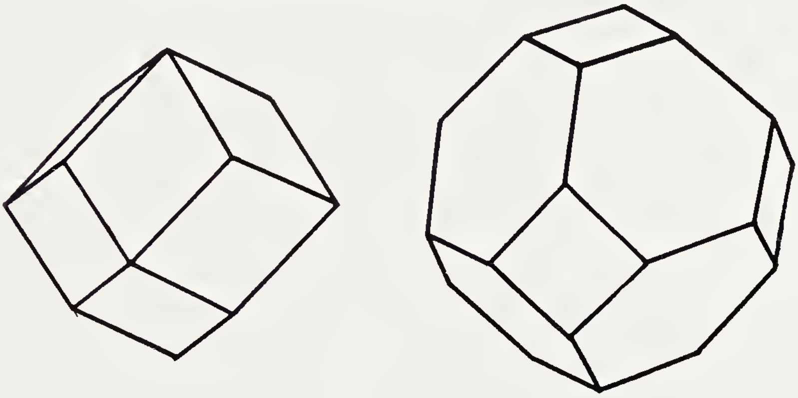

FIG. 10. The first and second Brillouin zones for a body-centered cubic lattice. (After Seitz.)

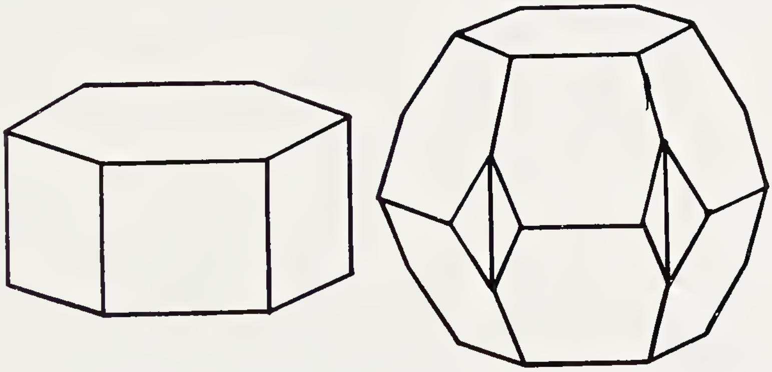

FIG. 11. The first and second Brillouin zones for a close-packed hexagonal crystal. The second zone is not unique and may be drawn in many different ways. (After Seitz.)

energy is then nearly independent of k and the zone structure appears only in higher approximations.

Analogy to Molecular Structure. These two extremes correspond in molecular theory to the *molecular orbital* and *valence-bond* theories, respectively. One may show by this correspondence that one complete zone of orbitals arises from each electronic atomic orbital of the free atoms. In alkali metals, it is usually supposed that the inner-core electrons occupy atom-like orbitals, whereas the valence electrons (one per atom) occupy band-orbitals. Since there is one such orbital per atom, each accommodating two electrons, the s-band of the alkalies is only half filled. In the alkaline-earth metals, the s-band should be filled and no conductivity would be observed if there were an appreciable energy gap between s- and p-bands. The observed conductivity requires us to suppose that, in fact, the s- and

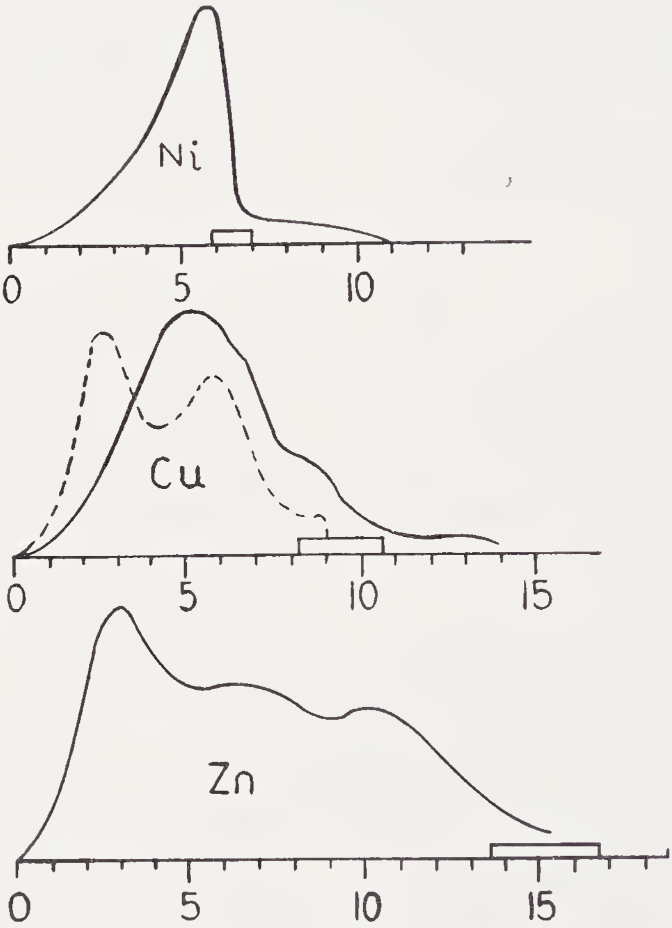

FIG. 12. Soft X-ray emission of nickel, copper and zinc as determined by Farineau. The band structure of zinc is entirely different from that of nickel and copper. The theoretical curve of Krutter for copper indicates the approximate nature of these calculations.

p-bands overlap in energy. The overlap in *k*-space may be only partial, however. This means that motion in some lattice planes will be more probable than in others. The markedly lower conductivity of the alkaline earths as compared to alkalies supports this view.

In the transition metals, of most interest for catalysis, the valence electrons occupy, *d*, *s*, and *p* orbitals in the free atoms which give rise to *d*, *s* and *p* bands in the metal. These bands undoubtedly overlap, though the precise details have not yet been worked out. Since, in general, band width increases with overlap of the atomic orbitals, we may expect the *d* band to be narrower than the *s* and *p* bands, due to the fact that the *d* electrons lie closer to the nucleus and interact less with each other than do the *s* and *p* electrons. The *d*-band contains 10 N states, whereas the *s* and *p* bands contain only 8 N states in all. Hence the density of states in energy must be much higher in the *d*-band than in the *s*-*p* band.

The soft X-ray emission arising upon electron bombardment of metals results when conduction electrons fall into the holes created when the impinging electrons eject orbital electrons from the inner K or L shells of the ion-cores. Since the terminal state of this transition is the same for all electrons, the spread in frequency arises from the spread in energy of the conduction electrons. The intensity of the emission at any frequency is thus a measure of the number of conduction electrons occupying band-orbitals of the corresponding energy. Certain secondary influences complicate this simple interpretation, but the general features of the energy level density must be given by these X-rays emission bands.

In Figures 7 and 12, the experimental results of O'Bryan and Skinner[28] for light metals and of Farineau[10] for copper, nickel and zinc are shown. The high intensity midway in the copper and nickel emission bands is probably to be associated with the high density of levels in the *d*-band. A determination of the highest occupied levels in the band requires a careful interpretation of the low-intensity tail which cannot yet be given unambiguously.

Computed Energy Level Distributions. Several attempts have been made to calculate level-density curves from quantum theory. The computational exigencies necessitate considerable approximation even in the self-consistent field treatment and the errors introduced in this way cannot yet be evaluated. At present, however, these computations are scarcely less reliable than direct experimental evidence and thus deserve a detailed review.

The first investigation of the interaction of *d*, *s* and *p* bands was made by Krutter[21] in the case of copper. He divided the lattice into cells, each containing one Cu^+ ion. The band-orbital for the entire metal is a periodic repetition of the pattern within each cell. An approximation to the self-consistent field within the cell was made by using the field derived for the

$3d^9 4s$ configuration, using atomic orbitals derived by Hartree for the free copper atoms. Figure 3 gives the resulting energy-level distribution, and the point to which the band would be filled by 1, 2, · · · ·, 12 valence electrons per atom. The dotted line in Figure 12 reproduces this same curve and shows that quantitative agreement with X-ray emission data is not attained, although the general features are accounted for.

Slater [41] has discussed the properties of the transition metals using Figure 3, on the assumption that the level density is roughly the same in the iron group metals as it is in copper. Thus, in nickel, we should expect the *d*-band orbitals to be not quite all filled. This permits some unpaired *d*-electrons

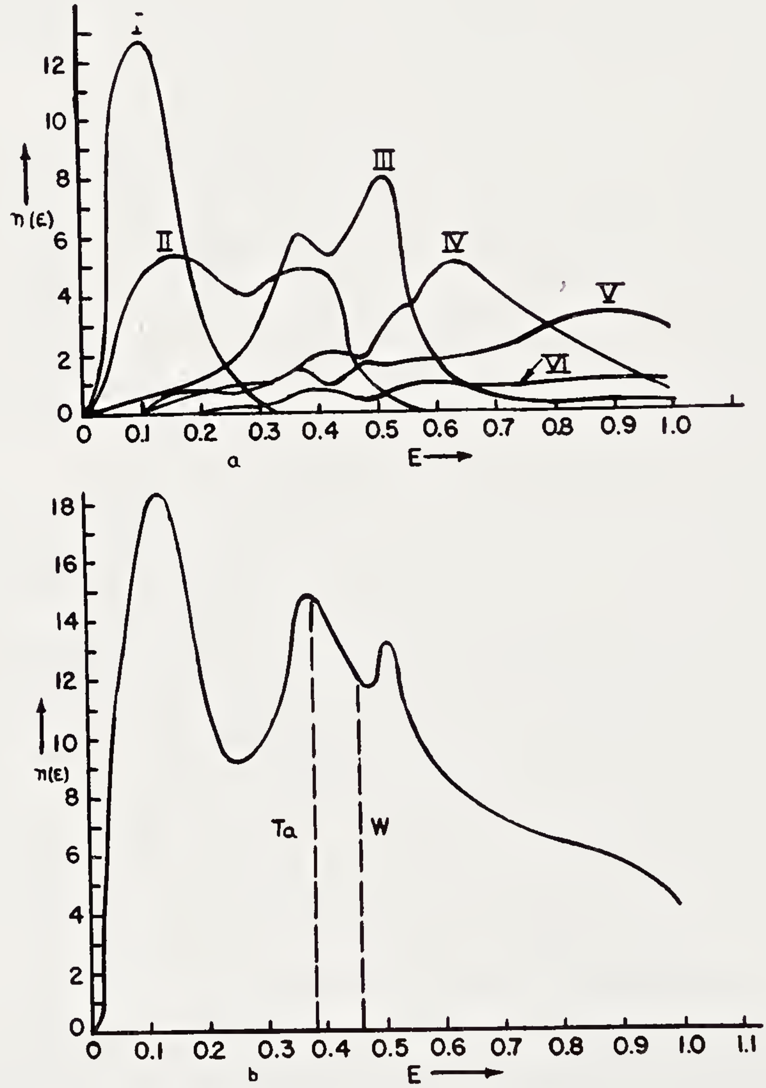

FIG. 13. Energy level density calculated for the five *d*-zones and one *s*-*p* zone of tungsten. (After Manning and Chodorow.)[23]

and accounts for the paramagnetic behavior of nickel, as well as of cobalt and iron.

Manning and Chodorow[23] have made a similar calculation for tungsten. This metal has a body-centered cubic lattice, whereas copper is close-packed (face-centered). The inner 5*f* electron atomic orbitals are assumed to be undistorted in the solid, and only the 6*s*, 6*p* and 6*d* orbitals are considered to overlap in the conduction band. The initial charge distribution was used to compute a new, very nearly self-consistent field. The resulting energy level distribution curve is shown in Figure 13. In this approximation, the six atomic orbitals give rise to six zones of overlapping energy. Five of these arise from *d*-orbital overlap (Curves I to V), and one from *s*-*p* orbital overlap (Curve VI).

More recently Wohlfarth[54] has completed a new calculation for nickel, with results differing in detail from those of Krutter. In particular, a narrower band was found, principally because the self-consistent field was more exactly approximated.

The most accurate theoretical treatment to date is that of Löwdin[22] for sodium. He has computed the following lattice parameter and cohesive energy in the ground state with high accuracy starting with no empirical data beyond the values of the fundamental constants, *e*, *m*, *h*, etc. The extension of his methods to excited states and to overlapping bands is yet to be accomplished, however.

	Calc.	*Exp.*
Cohesive energy (kcal/mole)	24.7	26
Lattice parameter (Å)	3.69	3.67

Properties of Metals

The principal properties of metals can be discussed in terms of the qualitative energy level distributions and band systems just presented. Conductivity, magnetic susceptibility and cohesive energy are the principal properties of interest to catalysis. In addition, the surface properties are of primary importance, including surface energy, surface potential, electron emission phenomena (thermionic, photoelectric and field emission), and chemisorptive activity. We shall discuss these in turn.

Conductivity. The most characteristic physical property of a metal is its electrical conductivity. This has long been associated with the mobility of electrons through the metallic lattice. On the band theory, we see that mobility under external fields is possible only for electrons in partially empty bands, since motion involves a change in direction of the electron relative to the origin of a unit cell and hence implies a transition from one momentum state to another. This is impossible unless vacant orbitals are available. In an ideal rigid lattice, the conductivity should be infinite, since the mobile electron can range unimpeded throughout the lattice. In reality, however, the nuclear vibrations of the lattice provide transient distortions of the lattice regularity, and hence fluctuations in the energy of the conduction orbitals. These give rise to energy barriers to the electron's progress, and hence account in part for the resistance of real metals. Other, more stable lattice imperfections, such as foreign atoms, vacancies, dislocations, and grain boundaries also pose energy barriers to the motion of the conduction electrons. Since conductivity is little influenced by the surface conditions of a metal, it will not be discussed in further detail here.

Magnetic Properties of Metals. *Band Theory.* The magnetic susceptibility has been an important property in guiding the development of the theory of the metallic bond. This is because it is determined chiefly by the number of unpaired electrons in the ion cores and hence gives a useful index of the number of electrons which occupy band-orbitals and are shared throughout the lattice. The coexistence at the moment of three distinct theories of paramagnetism in metals, however, indicates the present inconclusive state of our understanding.

A small metallic crystal, when placed in an inhomogeneous magnetic field, experiences one of three possible forces: (1) a weak repulsion by the field (i.e., a force driving it to regions of lower magnetic field strength); such a metal is *diamagnetic*; (2) a weak attraction; such a metal is *paramagnetic*; (3) a strong attraction; such a metal is *ferromagnetic.* The maximum couple exerted on a magnet in a uniform field of unit intensity is its *magnetic moment*, and the magnetic moment per unit volume of a substance is called its *intensity of magnetization*, I. Experiments indicate that in paramagnetic and diamagnetic materials, the intensity, I, is proportional to the field, H. The ratio $I/\mathrm{H} = \kappa$ is called the *magnetic susceptibility.* Diamagnetic susceptibilities are negative; paramagnetic susceptibilities are positive. Ferromagnetic substances show susceptibilities which increase strongly with field strength at low fields, but eventually reach a constant asymptotic saturation value. The susceptibility of a ferromagnetic is also a function of the previous magnetic history of the material. The *susceptibility per unit mass* is usually denoted $\mathrm{X} = k/\rho$; the *atomic or molar susceptibility* is $\mathrm{X}_M = kM/\rho$ where M is the atomic or molecular weight and ρ is the density of the material.

Since classical electrodynamics shows that every closed electric circuit is associated with a magnetic moment equal to the current multiplied by the area enclosed by the circuit, it is natural to seek an explanation for the magnetic properties of matter in terms of the orbital electron currents within the atoms composing it. The observed magnetic intensity is then the resultant of the atomic moments. Goudsmit and Uhlenbeck[2], however, showed that each electron possesses an intrinsic moment in addition to that associated with its orbital motion. This intrinsic moment is customarily associated with so-called *electron spin*, since a charged spherical shell spinning about an axis would indeed have a magnetic moment.

The hydrogen atom in its n^{th} energy state consists of one electron in a circular orbit about the nucleus at radius a_n. The angular momentum of such an electron is:

$$p_\phi = ma_n^2\omega = nh/2\pi$$

where m = electron mass and ω = angular velocity. Bohr's atomic theory gives the quantum form on the right. But the magnetic moment is:

$$\mu_n = \frac{\pi a_n^2}{2}\cdot\frac{e}{c}\cdot\frac{\omega}{2\pi} = \text{(area of orbit)} \times \text{(current in e.m.u.)}$$

Substituting for a_n from the quantum condition:

$$\mu_n = \frac{nhe}{4\pi mc}$$

The natural unit of magnetic moment is thus the *Bohr magneton*:

$$\mu_{\text{B}} = he/4\pi mc = 9.273 \times 10^{-21} \text{ erg/oersted}$$

The *spin magnetic moment* of the electron turns out to be $\pm 1\mu_{\text{B}}$. This result is irreconcilable with the observed accompanying half quantum of angular momentum on any mechanical model and it is generally agreed that the spin moment arises in reality from a poorly understood relativistic effect in the theory of the electron.

Diamagnetism arises chiefly from the orbital electronic motion of the substance and is usually apparent only when paramagnetism is absent. In solids, the orbital electrons are not free to respond to an external magnetic field of modest strength because of their considerable mutual interactions. The field then has no effect on the resultant magnetic moment of the solid, and the orbital contribution to magnetic susceptibility is said to be *quenched.*

Orbital motion can never give rise to paramagnetism. We must look to the electronic spins for the source of this effect, since these can contribute a permanent moment which will be enhanced by the application of an external field. Thus, if the lowest energy state of the system is one in which electrons occur in singly occupied orbitals with parallel spins, there will be a resultant paramagnetic moment.

It is also possible for the spins to be arranged on a lattice so that nearest neighbors are antiparallel. Such a substance is said to be "antiferromagnetic." Since the entropy of such an arrangement is greatly enhanced by a somewhat imperfect pairing, such substances should have a small permanent moment and will behave paramagnetically. As the temperature is raised, the degree of disorder is increased, and the resultant moment passes through a maximum, since a completely random array will have a lower moment, but higher energy than a partially ordered one. The rather strong paramagnetism of the nonferromagnetic transition metals is attributed by some to antiferromagnetism, and its weak temperature dependence is taken to indicate that the maximum moment is attained near room temperature. In ferromagnetics, however, the moment declines uniformly with temperature increase, since the maximum moment occurs in the completely ordered state.

The chief factor which determines the difference in energy between this state and a nonmagnetic state in which orbitals are doubly occupied by electrons with antiparallel spins is the electrostatic interaction of the electrons and nuclei.

The collective electron, self-consistent field is especially helpful in understanding why a magnetic state may have lower energy than a nonmagnetic one. The energy of the system may be computed by taking first the Coulombic interaction of all pairs of particles, electrons and nuclei averaged over the electronic orbitals. This, however, counts the interaction of each electron with itself. This "Coulombic" energy must, therefore, be corrected by subtracting the energy of a charge distribution equivalent in magnitude to one electronic charge and localized in the neighborhood of the electron in question. This is the "exchange charge" and the correction is the "exchange energy." It is negative, since it serves to lower the energy of the entire system. In virtue of the Pauli Exclusion Principle, this exchange interaction occurs only between electrons of the same spin, since they cannot occupy the same orbitals and must therefore, avoid each other in space. A similar, but usually smaller, correction, called the "correlation energy," must be made for the interaction of electrons of opposite spin.

It is now clear that every pair of electrons of the same spin will contribute an "exchange integral" tending to lower the energy of the system. This integral is the average interaction energy of the electron with the excess positive charge in its neighborhood, averaged over its orbital. We should expect that when several orbitals of the same energy are available, they will each be singly occupied so far as possible, since this provides the maximum number of exchange integrals. In atoms, this principle is known as Hund's Rule of Maximum Multiplicity.

In a metal, the kinetic energy of the electrons is least when each orbital is doubly occupied, with zero resultant spin. However, the potential energy is reduced, as we have just seen, by putting some of these electrons into higher orbitals where they can have parallel spins. We should expect in some cases, therefore, that the loss in kinetic energy will be more than compensated by such a transfer, and a paramagnetic (or ferromagnetic) state will result. Detailed computations[42, 55] show that in nickel this is the case even in the absence of an external magnetic field. Presumably the other ferromagnetic metals will be accounted for similarly. In other cases, the energy of transfer may be low enough that it can be provided by the action of an external magnetic field. In the absence of the external field, no such transfer can occur. In these cases, the metals are paramagnetic, but not ferromagnetic.

Since the exchange energy depends upon the interaction of conduction electrons, it will not vary greatly from one metal to the next in a transition series. The possibility of ferromagnetism then depends chiefly on there being levels available at not too high an energy. In narrow *d*-bands, the level density is high and the energy increment per electron promotion is much less than in broad bands. Since band width increases with overlap of atomic orbitals, we should expect the tendency to ferromagnetism to increase as we pass to the right in the periodic table from titanium to nickel, since the increasing nuclear charge makes the *d*-shells shrink and so overlap less in the metal. Thus, in titanium, the interatomic distance is 2.65 times the diameter of the 3*d* shell, whereas in nickel this factor is 3.69. In this way we gain a consistent explanation of magnetic properties on the band theory.

The precise magnitudes of the resultant moments cannot be predicted as yet, but are known experimentally. When a ferromagnetic substance is saturated magnetically, each atom is independently oriented with its moment aligned with the imposed field. The resultant moment in magnetons per atom is equal to the average number of unpaired electrons per atom. For the iron series, we find the moments:

$$\text{Fe} = 2.21; \qquad \text{Co} = 1.716\ ; \text{Ni} = 0.606$$

Since the 3*d*, 4*s*, and 4*p* bands overlap in these metals, it is generally assumed that these moments indicate a population in the *s*-band of .22, .72 and .61 electrons per atom, respectively, leaving the same number of holes in the narrow *d*-band. This band will be occupied by 7.78, 8.28 and 9.39 electrons, respectively. Of these, five in each case will have the same spin, leaving the observed numbers of unpaired spins in the *d*-band. The stability of this unbalanced configuration is explained along the lines suggested above. The *s*-electrons, however, occupy a much broader band, and the promotion necessary to uncouple their spins is too great to be compensated by the reduction in potential energy. The *s*-electrons therefore contribute a negligible amount to the net moment, on this view.

If, for example, nickel is alloyed with manganese, the net result is to substitute an atom with three less *d*-electrons for a nickel atom. This should increase the average number of holes in the d-band and the average magnetic moment of the alloy should increase by three magnetons per Mn atom. This is as observed, and other alloy systems behave similarly, with the exception of Fe-Ni, in which Ni appears to add no magnetic carriers to the iron-rich alloy.

Dowden[8] has suggested that the catalytic activity of metals and alloys is associated with these d-band positive holes. Dilke, Eley and Maxted[7] have detected a decline in the magnetic susceptibility of high-area palladium upon chemisorption of dimethyl sulfide. The detailed consideration of these and similar phenomena will be given in the next chapter.

Pauling's Valence Bond Theory. The two alternative treatments of metallic binding take a viewpoint closer to the valence-bond theory of molecular binding. Pauling[29] begins with electron-pair bond-orbitals between adjacent pairs of atoms, entirely analogous to the bond in H_2. However, the number of bonded pairs (ligands) exceeds the possible number of electron-pairs by several fold in most metals. If each atom has twelve ligands, each contributing one valence electron (as in sodium), there will be six electron-pair bonds to be assigned to the twelve positions. This assignment can be made in $12!/6!\,6! = 924$ different ways, each of which corresponds to one possible orbital, all of which have the same energy. In such a case, there will be strong resonance between the possible bond configurations. To account for electron mobility, it is necessary to postulate that ionic states also contribute to this resonance, since only through these can there be a net transfer of charge. The mathematical complexity of the wave-functions assumed in this approach is so great as to forestall even the roughest direct calculations as yet. However, certain approximate relations in earlier resonance theory between bond length, resonance energy and number of resonating species have been extended empirically by Pauling to the case of the metals.

He supposes the resonating pair-bonds to be responsible for the cohesive energy and the bond distances, whereas the ionic forms ("unsynchronized resonance") permit electron transport properties, such as conductivity. The number of electrons per atom disposed in pair bonds is assumed to be the same as in normal chemical compounds, e.g., one for sodium, two for calcium, etc. In the transition elements of the sixth, seventh and eighth groups, as well as in the first and second B subgroups, special valence assumptions must be made and multiple valencies are postulated. Of the nine dsp valence orbitals available in atoms of this group, up to six are supposed to be occupied by bonding pairs, two remain as nonbonding atomic d-orbitals and one is available for ionic resonance, the "metallic orbital." In nickel, Pauling postulates[29] two hexavalent atomic configurations: Ni-A: $3d^6 4s4p^3$; Ni-B: $3d^7 4s4p^2$. The empty p-orbital in Ni-B is the metallic orbital. In each case, six electrons are shared in covalent bond formation,

TABLE 1

Sc 20 (3)	Ti 27 (4)	V 35 (5)	Cr 39 (6, 3)	Mn 40.1 (6, 4)	Fe 40.7 (5.78)	Co 39.5 (6)	Ni 40.0 (6)
Y 19 (3)	Zr 31 (4)	Cb 39 (5)	Mo 43(6)	Tc 46 (6)	Ru 50 (6)	Rh 50 (6)	Pd 46 (6)
Lu 19 (3)	Hf 29 (4)	Ta 39 (5)	W 43 (6)	Re 46 (6)	Os 49 (6)	Ir 49(6)	Pt 44 (6)

The figures in parentheses indicate the valencies assigned.

leaving two unpaired *d*-electrons in Ni-A, and none in Ni-B. The resonance mixture of A and B in the ratio 30:70 accounts for the magnetic moment as well as for an average valence of 5.78 which fits into the correlation of valence with bond length. In this way, the observed magnetic moment and bond length are used to fix the proportions of each resonance form and the valence assignment.

The six bonding orbitals of Ni-A are d^2sp^3, whereas in Ni-B, they are d^3sp^3. These are presumed to hybridize in the metal, giving ⅓ *d*-character to Ni-A and 3⁄7 *d*-character to Ni-B, or 40 per cent *d*-character to the 30:70 resonance mixture. In Table 1 we quote Pauling's results[29] for percentage *d*-character in the transition metal bands.

The case of iron is significant in that no hexavalent form alone can be made to agree with the observed magnetic moment since it could have at most a magnetic moment of $2\mu_B$. A mixture of 78 per cent hexavalent d^3sp^3, 22 per cent quinquevalent d^2sp^3, in each case including one empty metallic orbital, is assumed by Pauling. There are, however, several alternative formulations which give very nearly the same magnetic moment and bond length if one is permitted arbitrary non-integer valencies.

In no case except iron, however, must a non-integer valence be assumed as well as a non-integer average *d*-orbital occupancy. Pauling's valence numbers are close to or identical with those used in ionic and covalent compounds of the metals but can hardly be said to be established on any theoretical grounds. The true physical significance and even the uniqueness of the per cent *d*-character are very obscure in this picture. Its use in correlating catalytic reaction rates will be discussed in a later section.

If Pauling's ideas are translated into the language of band-theory, we should expect the overlapping *d*, *s*, *p* bands to be split into two subbands, of which Pauling's valence electrons, up to six in number, occupy the lowest and do not contribute to the net magnetic moment. The remainder occupy a higher, essentially atomic, band-orbital which would be very narrow indeed, and in which the rule of maximum multiplicity would be observed.

This view would predict a nearly constant band width for all transition metals, and accounts for the difference in magnetic properties in terms of the difference in energy of the valence band and the narrow magnetic band. This latter cannot fill before Fe is reached in the periodic table, if Pauling's valencies are adopted.

A clear decision cannot be made between these two views in the absence of direct experimental evidence as to the shapes of the conduction bands in the transition metals. It must be granted, however, that the band theory is at present capable of semiquantitative theoretical results which cannot be matched by Pauling's formulation.

Zener's Empirical Theory. Zener[56] has recently proposed a third interpretation of the magnetic properties of metals. His view point is intermediate between the extreme collective-electron picture of band theory and the extreme valence bond theory. As in the latter, it is necessary to postulate a number of empirical hypotheses not yet deduced in rigorous fashion from the Schrödinger equation. These principles refer to the interaction between the incomplete *d*-shells of neighboring atoms in Group IV A and higher.

(1) The spin correlation between electrons in the incomplete *d*-shell of a single atom is essentially the same in the solid as when the atom is in the isolated gaseous state. By Hund's Rule, this gives the incomplete *d*-shell the highest possible net electron spin.

(2) The exchange integral between *d*-shells of adjacent atoms has always the same sign as in the H_2 molecule. Thus the direct interaction between adjacent *d*-shells will give the lowest resultant energy when their net spins are antiparallel, leading to an anti-ferromagnetic configuration, i.e., one in which the permanent magnetic moments are aligned so far as possible in antiparallel pairs throughout the lattice.

(3) The spin of an incomplete *d*-shell is strongly coupled to the spin of the conduction electrons. This is analogous to the strong spin coupling (Russell-Saunders) between 3 *d* and 4*s* electrons in the isolated atoms.

(4) The *d*-shell electrons distribute themselves among the atoms so as to maximize the total number of pairs of electrons having like spin within the individual atoms.

Fundamentally, each of these principles is justified by showing that it lowers the energy of the solid when operating independently of the others.

Principle (1) is valid whenever the energy of reversing the spin of one electron in the atom is large in comparison with the width of the *d*-band, for then bands arising from this excited atomic state will not overlap the normal *d*-band. Thus, the difference in energy between quintet Cr and triplet Cr (with only one unpaired *d*-electron), is 2.5 e.v., more than twice the estimated *d*-band width in Fe and in W. Principle (2) is purely empirical, but is not contradictory to any other properties of matter.

Principle (3) is evident in isolated atoms, as we have seen, in which the lowest energy state is that in which a single outer *s* electron has its spin parallel to that of the *d*-shell. The energy to reverse this coupling diminishes from 0.93 e.v. in Mn to 0.39 e.v. in Ni[2] and is proportional to the overlap between the *s* and *d* orbitals. When the isolated atoms condense to the metal, the *s* electrons are much more confined. In the free atom, only about one third of the *s*-electron density lies within the sphere equal to the atomic volume of the atom in the metal. Thus, the *d*-*s* coupling will be about three times greater in the metal than in the free atom. Fairly accurate charge distributions are known for the transition metal atoms by means of which this increase can be computed quantitatively.

When the free atoms are condensed to metal, all or part of the *s* electrons become the conduction electrons of the metal. As such, they interact with each other both electrostatically and magnetically. We have seen that electrons with parallel spins must occupy separate band-orbitals and hence automatically avoid each other. Their electrostatic repulsion is thus less and the total energy lower than if the spins were antiparallel. This paramagnetism of free electrons, corrected for all other terms in the electronic interaction which lead to a reduced repulsion ("correlation energy"), tends to induce ferromagnetism.

A completely ordered antiparallel arrangement of adjacent spins is not possible in the face-centered cubic or hexagonal close-packed lattices, but can be attained in the body-centered cubic lattice, in which every atom can be surrounded by nearest neighbors of opposite spin. One should expect, therefore, that antiferromagnetism is associated with body-centered cubic crystals. These, according to Zener's principles, will be those with larger *d*-shells, giving more interaction by principle (2). In turn, this leads to the transition elements of lower atomic number in each period. It is precisely these metals, from Ti to Fe, Zr to Mo, Ta and W, which occur in body-centered cubic modification. Recent investigations[25] have shown that of these Cr is indeed antiferromagnetic, although the case for V is doubtful.

In the case of tungsten, with two *s* electrons per atom going into the conduction band, Hsu[17] has calculated the binding energy in terms of the interaction of nearest and next-nearest 5*d* shells in the antiferromagnetic body-centered cubic lattice. Four types of interaction contribute to the binding energy:

(1) C_{ab}, the Coulombic electrostatic interaction of adjacent *d*-shells (bonding);

(2) $2V_{ab}$, the electrostatic interaction of conduction electrons and adjacent cores (bonding);

(3) K_{ab}, the electronic kinetic energy increase due to interaction between adjacent cores (anti-bonding);

(4) X_{ab}, the exchange interactions between electrons of the same spin on adjacent cores (bonding).

The binding due to the two conduction electrons in the *s*-band is very small in comparison to C_{ob} for tungsten. In fact, for mercury, which also has two electrons in the *s*-band, the 5*d*-shells are so small and overlap so little that the first three terms above are negligible. The *s*-band contribution to the cohesive energy is thus measured by binding energy of mercury, which is very small compared to tungsten. This view ascribes the cohesion of tungsten almost entirely to the Coulombic interaction of W^{++} ions in a body-centered lattice with each other and with the conduction electron-cloud in which they are embedded. If nearest neighbors have parallel spins, the net repulsion $K_{ab} + X_{ab}$ between nearest neighbors is 62 per cent larger than when spins are antiparallel because of the greater promotion required to accommodate electrons of parallel spin in overlapping orbitals. Thus the antiferromagnetic state is associated with markedly lower kinetic energy in the *d*-shell.

Principle (4) is required to understand the fact that iron, contrary to the above expectations, is ferromagnetic in the body-centered cubic-lattice, and nonferromagnetic in the face-centered cubic modification. Zener supposes that in iron the *d*-shell overlap is strong enough to induce an antiferromagnetic alignment of spins in both phases. However, in the body-centered cubic lattice, the bonding exchange interaction of the electrons can be increased by transferring some electrons to adjacent atoms. This makes possible a larger average number of pairs of electrons of the same spin per atom, whose interaction, by Hund's Rule, lowers the total energy. Thus in two isolated atoms of iron, with seven *d*-electrons, there will be two electrons per atom with unpaired, say (−) spins. If, however, two electrons are transferred from one atom to the other, there will be four electrons in one atom with, say (−) spin and none in the other. The interactions of the five electrons per atom with (+) spins is identical in each case, but, by the transfer, we have produced six pair-interactions between the four electrons of (−) spin, or three per atom instead of the one pair per atom in the normal case. This amounts to treating iron as a mixture of conduction electrons and cores of Fe^{+++} and Fe^{-} instead of $2Fe^{+}$. The transfer increases the electrostatic repulsions between next nearest neighbors, but Zener estimates this increase to be less than the gain in exchange energy. If the Fe^{+++} are located at the center of the unit cell, with the Fe^{-} at the corners with antiparallel spins, the average magnetic moment is 2.0 μ_B. The remaining 0.22 μ_B observed is easily accounted for by the polarization of the conduction electrons themselves. That is, the ground state for the *s*-band will have 0.61 electrons per atom of one spin and 0.39 of the other, rather than 0.50 of each, as in paramagnetic metals.

This charge transfer process must be a dynamic one, since no permanent polarization of b.c.c. Fe is observable by neutron diffraction studies. It thus takes on some of the features of Pauling's resonating A and B structures, but is more directly related to independently observable quantities.

The magnetic properties of alloys of metals in the first transition period are also consistent with this interpretation. Experiments show that the change in saturation magnetic moment per atom per unit increase in electrons per atom is one Bohr magneton. This change is an increase until the average moment reaches 2.5 μ_B, and thereafter becomes a decrease. On the strict band model, each lattice site (or cell) is occupied by the same number of electrons regardless of nuclear charge. Thus, substitution of atoms of atomic number less than iron results in a decrease in the average number of electrons. On Zener's theory, the positive ion cores have a complete half-shell of *d*-electrons, so the depletion will be at the expense of the negative ion cores, thus increasing the number of unpaired electrons and the magnetic moment by unity. Addition of atoms of atomic number greater than iron will result in electrons being added to the positive ion-cores after the *d*-shells on the negative ions are filled. This will, of course, decrease the magnetic moment. If the charge transfer is supposed to occur independently between atoms of each kind in the alloy, rather high charges are acquired by the alloying atoms. Thus, for vanadium, with 4 *d*-electrons per atom in the alloy, three less than iron, there would be V^{-4} and neutral V cores arising from the transfer of electrons so as to give one set of cores 5 *d*-electrons and the other 9, as in iron. It is likely that these excessively charged anions transfer charge to adjacent iron anions. Since these have parallel moments and incomplete *d*-shells, no change in moment results. In iron-nickel alloys, however, the nickel ions would be Ni^{+++++} and Ni^{+}. The charge transfer required to diminish the electrostatic repulsions must come from the Fe^{-}, but entails a reversal of spin and consequent change in moment. In fact, if we have Ni^{+++} instead, the two electrons transferred from Fe^{-} precisely cancel the increased moment of $2\mu_B$ per nickel atom predicted by the strict band theory. In fact, the observed increase in moment per added nickel atom is zero in iron alloys, and this anomaly on the band theory has here an easy explanation.

One further example of the application of this theory is the ferromagnetism induced in f.c.c. iron by reaction with nitrogen to form the interstitial compound Fe_4N in which the nitrogen atom occupies the center of the unit cube. We now suppose each nitrogen to acquire three electrons from neighboring iron atoms in the cube face, giving Fe^{++} ions in the faces and Fe^{+} ions in the cube corners, with N^{---} ions in the center. The removal of an electron from the *d*-shell of Fe is assumed to permit enough contraction of the *d*-shells to destroy the antiferromagnetic coupling with second nearest neighbors. Thus face-center atoms remain antiferromagnetically coupled with corner atoms, but are ferromagnetically coupled with each other. The net spin is thus that of the three face atoms less that of one corner atom, or $(12 - 3)\mu_B/4 = 2.22\mu_B$, as observed.

The similarities to Pauling's picture are to be noted. Both focus attention on the atomistic nature of metals. Zener, however, uses crystal orbitals, rather than resonating valence bonds, to describe the s-band of conduction electrons and postulates the same number of conduction (valence) electrons as in band theory. He thus retains the good account of electron transport properties achieved in the band theory. In the d-band, however, he considers the electrons as nearly localized between adjacent leptons, whereas band theory considers them to be shared throughout the lattice. The quantitative work suggests, however, that the interaction between d-shells is largely Coulombic, and that the exchange resonance characteristic of the covalent bond is of minor importance. This is in striking contrast to the molecular binding postulated by Pauling in which the exchange resonance presumably predominates. This difference presumably arises because the more uniform charge distribution in metals permits better screening of nuclear repulsions than in molecules. Coulombic electrostatic forces between electrons and nuclei *per se* are thus more effective in binding than in molecules. While the comparison of binding energies of tungsten and mercury supports the idea that here the s-electrons contribute very little to the binding, the same does not necessarily hold for the iron group, where Ni has only 4 kcal more binding energy than Cu. Here the exchange contributions of the conduction electrons to the net binding may be much higher. In addition, the increased overlap of the d-shells will increase the relative importance of exchange binding forces between them.

The interaction of the first three principles is well illustrated in Zener's calculation of the Weiss inner field in iron, cobalt and nickel. Here it is supposed that the atomic elementary magnetic moments interact to generate an effective field, H_{eff},

where
$$\begin{aligned} H_{\text{eff}} &= H + WI \\ H &= \text{external applied field} \\ I &= \text{intensity of magnetization} \\ W &= \text{Weiss constant} \end{aligned} \tag{15}$$

Then the energy of interaction between the elementary magnetic moments is: $E = -\frac{1}{2}I(H_{\text{eff}} - H)$ or

$$E_{\text{spin}} = -\tfrac{1}{2}WI^2 \text{ per cm}^3. \tag{16}$$

If S_d is the mean component along the direction of magnetization of the magnetic moment (or spin) of each incompleted-shell (in Bohr magnetons),

$$\begin{aligned} E_{\text{spin}} &= -\tfrac{1}{2}W'S_d^2 \text{ per atom} \\ W' &= N\mu_B^2 W \end{aligned} \tag{17}$$

W' is thus the magnetic interaction energy per atom per unit moment.

From theory, this same energy is given by:

$$E_{\text{spin}} = \tfrac{1}{2}\alpha S_d^2 - \beta S_d S_c + \tfrac{1}{2}\gamma S_c^2 \tag{18}$$

where S_c is the mean net magnetic moment of the conduction electrons.

The first term is the energy of interaction of the moments of the d-shells. The coefficient α is proportional to the direct electron exchange interaction between adjacent d-shells and, by principle (2), diminishes as the d-shells become separated but does not change sign. It is assumed to be positive. A large spin interaction stabilizes the ground state, so that α serves to increase the cohesive energy also.

The second term is the coupling energy between conduction electrons and d-shell electrons. The coefficient β is likewise proportional to the electron exchange integral between s and d electrons. It will be taken as positive, the explicit negative sign indicating that this effect counteracts the direct d-shell coupling. In the isolated iron atom, the state $3\ d^7$ for the core has a spin of $3\mu_B$. The remaining $4s$ electron may have parallel or antiparallel spin, and these states differ by 0.624 e.v. in the atom. This represents twice the interaction energy, giving $-\beta_0 S_d S_c = 0.312$, or ($S_d = 3$, $S_c = 1$), $\beta_0 = .104$ e.v. However, as noted previously, this coupling is increased in the solid by the increased overlap. so that $\beta = \beta_0/f = 3.28\beta_0$, if Hartree functions for iron are used.

The third term is the direct coupling between the conduction electrons. By Hund's Rule, the energy (binding) is increased when the spin is increased, so that γ is positive. This spin maximization involves an increase of the average electronic kinetic energy, which for free electrons amounts to: $\gamma_{kL} = \dfrac{10}{9}\bar{\epsilon}_k/V$

where $\bar{\epsilon}_k$ = average kinetic energy

v = number of conduction electrons per atom.

However, this energy increase is partly compensated by the tendency we have noted of electrons in different orbitals to avoid each other. This reduces the estimated electronic repulsion and lowers the total energy. For free electrons, this "correlation exchange energy" can be computed and the net result is to diminish the kinetic energy term by about half. Table 2 summarizes the calculations for Fe, Co and Ni.

TABLE 2

Configuration	Fe $3d^74s$	Co $3d^84s$	Ni $3d^94s$
β_0	0.104	0.125	0.148
β	0.34	0.41	0.48
γ_{ke}	7.8	5.5	5.9
γ_{ex}	−5.5	−2.7	−3.0
γ	2.3	2.8	2.9
β^2/γ	.050	.060	0.81
W'	.028	.036	.065
α	.022	.024	.016

The spin energy is minimized when $S_c = \beta/\gamma S_d$, or

$$E_{\text{spin}} = \tfrac{1}{2}\{\alpha - \beta^2/\gamma\} S_d^2$$

Hence we find:

$$W' = \beta^2/\gamma - \alpha \tag{19}$$

For ferromagnetism, W' is positive; for antiferromagnetism, W' is negative. Thus we find that α, measuring the d-shell overlap, is very small in Fe, Co and Ni, and that β^2/γ gives nearly quantitative agreement with observation.

Closer inspection shows that the differences in Weiss constant on this theory arise primarily from β_0, since γ is quite insensitive to valence and the ratio β/β_0 was taken equal to 3.28 for all three metals. The increase in β_0 as we pass from Fe to Ni occurs chiefly because of the added density in the d-shell, which leads to stronger exchange interaction. With increasing nuclear charge, the d-shell shrinks somewhat also but this effect is not great since the overlap with adjacent d-shells is small in any case. The same effect results, in the band theory, in a higher average density of states in the d-band as it fills, as shown in Figure 3. The numerical estimates furnished by Zener's theory are not yet matched by band theory calculations, however.

It is evident that Zener's theory follows the qualitative notions of strict band-theory very closely, but departs from it in treating the d-shell by the atomic orbital method. This affords a more immediate numerical computational scheme and has permitted correlation of an impressive number of subtle structural features of metals and alloys with their magnetic properties. It is distinctive in suggesting that all paramagnetism in metals is in fact antiferromagnetism. This is a point susceptible of direct confirmation by neutron diffraction studies, and will be of crucial importance in testing the validity of Zener's approach.

Heavy Transition Metals. The heavier transition metals are paramagnetic, but not ferromagnetic. This may be associated with an antiferromagnetic lattice in Zener's picture, or with a zero net moment in the absence of a field on Slater's development of band theory. In either case, the d-shells overlap much more than in the cases of Fe, Co and Ni, lending to a much broader d-band on the band theory and to a stronger antiferromagnetic interaction on Zener's theory. As shown in Hsu's calculations for tungsten, the electrostatic interactions may be much more strongly bonding in the antiferromagnetic state.

Band theory computations on tungsten[13] also show a marked d-band binding, with a much wider d-band than in the case of the iron group and negligible binding in the s-p band. This means that the exchange energy gained by uncoupling conduction electron spins will not repay the increase in kinetic energy required, and the ground state will remain nonmagnetic. An applied field, however, can provide this uncoupling energy, and paramagnetism results. However, this explanation is purely qualitative. The uncoupling energy should also be reflected in the electronic specific heat of these metals, but the estimates from this data do not agree with those from magnetic susceptibility. This indicates an important weakness in the present stage of development of this theory.

By studying the change in saturation moment of ferromagnetic alloys with the heavier transition metals, one is led to attribute similar valences to them as to the iron group. In palladium, the paramagnetic susceptibility drops to zero when 0.65 atoms of hydrogen per atom of palladium have been dissolved in it. This is taken to indicate that 0.65 holes in the d-band have thus been filled. However, when high area palladium is exposed to hydrogen, the susceptibility falls initially at a rate which would bring it to zero at an atom ratio of 1Pd to 2H[35]. This seems to indicate a marked influence of the crystallite size on the electronic binding of the finely divided metal.

Surface Properties of Metals. Among the more accessible physical properties of surfaces are those related to electronic emission phenomena, namely, the contact potential and work function. Since these quantities are measures of the free energy change in the process of transporting an electron from one conductor to another, or from vacuum to conductor, respectively, it is evident that they are closely related to the electronic structure of the interior cells of the solid as well as to that of the surface cells. The utility of these quantities and the frequent confusion in their discussion warrants a careful definition and discussion of them here.

We consider first[16] an isolated portion of a conductor with sensibly uniform properties, temperature and chemical composition, containing n

electrons. We may then define the *electrochemical potential*, $\bar{\mu}$, as

$$\bar{\mu} = (\partial F/\partial n)_{T,v} \tag{20}$$

where F is the Helmholtz free energy.

Thus if a small number of electrons, δn, are brought from infinity and added isothermally to the system, the work done on the electrons is equal to $\bar{\mu}\delta n$ minus the free energy of the gaseous electrons at infinity. More generally, for a composite system of several phases, the electrochemical potential in the i^{th} phase, μ_i, is defined as

$$\bar{\mu}_i = \left(\frac{\partial F}{\partial n_i}\right)_{T,V,n_{k\neq i}}, \tag{21}$$

where n_i is the number of electrons in the i^{th} phase.

Since a change, $\Delta\Phi$, in the electrostatic potential, Φ of a body requires work $-e\Delta\Phi$ on each electron in that body, the change in $\bar{\mu}$ is also $-e\Delta\Phi$. Since such a change in potential might occur in transferring charge from the interior to the surface of the body, we see that $\bar{\mu}$ is a function of the state of the surface as well as of the interior. Insofar as the state of the surface is characterized by its charge distribution, we may segregate its effect by defining the *chemical potential*

$$\mu = \bar{\mu} + e\Phi \tag{22}$$

where μ is now a function only of the temperature and the internal state of the body.*

For a system in equilibrium, the free energy change accompanying a transfer of charge from phase 1 to phase 2 must be zero. That is,

$$\bar{\mu}_1 = \bar{\mu}_2 \tag{23}$$

If the electronic energy is measured from a zero for electrons at rest at infinity, the Fermi-Dirac distribution determines the probability $P\ (\epsilon)$ that an electron occupy a state of energy;

$$P(\epsilon) = 1/[\exp\{(\epsilon - \bar{\mu})/kT\} + 1] \tag{24}$$

Thus the electrochemical potential, $\bar{\mu}$, is the pertinent parameter (often called the *Fermi level*) in the energy distribution of electrons[11]. For all

---

* This formulation is modified in the usual way when the surface contributes an appreciable share to the total free energy. We then add to the total free energy of the bulk that excess contributed by the surface, $\gamma\, d\sigma$, where γ is the surface tension and $d\sigma$ is the element of surface area.

processes involving electron transfer to solids, therefore, the electrochemical potential is of paramount interest.

The *true work function*, φ, of a uniform surface is defined as

$$\varphi = \Phi_a - (\mu/e) = \Phi_c - \Phi_a - (\mu/e) \tag{25}$$

Where Φ_a = electrostatic potential of an electron in the vacuum just outside the surface

Φ_c = electrostatic potential inside the conductor.

Here $\Phi_c - \Phi_a$ changes by $4\pi\Delta$ when the dipole moment per unit area of the surface changes by Δ. The chemical potential, μ, however, is a volume property and is independent of the surface structure. For this reason, μ/e is sometimes called the *inner work function.* Since all thermodynamic definitions presuppose a system of uniform properties, the surface in question here must be such a system, such as a single face of a perfect crystal.

Just outside a conducting surface an electron is acted on by an attracting force, the *image force*, derived from the *image potential*, $e/4x$, where x is the distance from the surface. Since this represents the average potential energy of an electron in the field of the surface, it is the quantum self-consistent field for a free electron outside a conductor, and should be derivable from the wave-functions of the surface cells of the crystal. If the crystal is an insulator of effective dielectric constant K_1, the image potential is $(e/4x)(K_1 - 1)/(K_1 + 1)$. For semiconductors, values intermediate between this and that for a metal will be found. The appropriate value of K_1 is that associated with the surface layer of solid of thickness x, and hence is itself a function of x except for metals. An effective potential of this sort is often called a *motive*, i.e., a quantity whose gradient at any point gives $1/e$ times the force on an electron at that point.

When two conductors are connected, electrons flow from one to the other until a state of equilibrium is reached (at constant temperature). In such a case, the electrochemical potentials of the two conductors must be equal. By Eq. (25), then

$$\varphi_2 - \varphi_1 = \Phi_{a_1} - \Phi_{a_2} \tag{26}$$

Thus there is a potential difference between a point in the vacuum just outside conductor 1 and a point in the vacuum just outside conductor 2. This difference is the *contact potential difference*, discovered by Volta. Since this is a measurable quantity, it affords a direct empirical evaluation of differences of the true work functions of two conductors.

A second experimental quantity is the current emitted at constant temperature from a conductor subjected to a saturating collecting field. This is given in the case of a uniform emitting surface by the Richardson-

Dushman equation:

$$j = A(1 - \bar{r}_v)T^2 \exp [(\bar{\mu} + eM_v)/kT] \tag{27}$$

Where j = current (amp/cm^2)
$\bar{r}_v$ = fraction of impinging electrons reflected at the conductor surface which return across a reference plane outside the metal.
M_v = electrostatic potential or *motive*, at the reference point outside the metal.
$A = (4\pi mk^2e/h^3) = 120$ amp cm^{-2} deg^{-2}

In Eq. (27) the current j is measured at a particular plane outside of and parallel to the surface, at which the motive is M_v . Any change of M_v due to a new choice of this plane induces a compensating change in $\bar{r}_v$, so that j is in fact independent of the particular plane chosen. Thus we see how a direct evaluation of the electrochemical potential can be derived from empirical determinations of the thermionic emission current.

In practice, however, only rarely is the surface uniform, and the theoretical equation needs modification if a "patchy" or nonuniform emitting surface is used. Thus surface heterogeneities have a direct experimental consequence in the shape of the thermionic emission curve, since they result in a strong dependence of the motive, M_v , on position. The reflection coefficient, $\bar{r}_v$, is also affected, since this measures the fraction of electrons impinging on the conductor surface from the outside which would be reflected past the reference plane. An independent evaluation of this function requires knowledge of the details of the dependence of the motive on position, i.e., of the potential fields near the surface.

For moderate collecting field, one can define an *apparent work-function*

$$\varphi^* = -\frac{k}{e}\frac{d}{d(1/T)} \ln (j/T^2) \tag{28}$$

and an *apparent emission constant*, A^*, by

$$\ln A^* = -\frac{e}{k}\frac{d\varphi}{d\varphi} - \left(\frac{T}{1 - \bar{r}}\right)\frac{d\bar{r}}{dT} + \ln [A(1 - \bar{r})] \tag{29}$$

Empirically, these quantities are often nearly constant and may be related to the observed emission current by

$$j = A^*T^2 \exp [-e\varphi^*/kT] \tag{29a}$$

Studies on clean metal surfaces have provided ample evidence for nonuniformity consisting of the juxtaposition of different crystal planes in a polycrystalline surface. Nichols[27] has made quantitative measurements of the thermionic emission from a single crystal tungsten wire, and finds definite maxima for emission normal to the 111, 114, 116 planes, with minimal for the 110, 112, 100 planes. These correspond to a variation in work function of at least 0.3 e.v. and maybe as high as 1 e.v.

Similar conclusions can be drawn from emission patterns obtained by cold fields and photoelectric excitation of single crystals, as well as from studies on the effect of adsorbed foreign substances on these properties and on the contact potential, which will be discussed in detail below. It is remarkable that the emission patterns of the thermionic effect are identical with those found in cold field emission.

The theoretical interpretation of all these effects is concerned with the rate at which electrons escape from metal into the vacuum outside under the influence of thermal agitation, radiation, and/or external electrostatic fields. This electron transfer must occur over or through a potential energy barrier. When the external electrostatic field is weak, this barrier is governed chiefly by the work-function of the metal and quantum mechanical tunnelling is negligible. At moderate fields, the barrier height begins to be a marked function of the field strength and at high fields it is so low that the tunnel-effect accounts for most of the emission. Since experimentally the work function is found to be relatively insensitive to temperature changes, it will be sufficiently precise for our purposes to discuss its value at absolute zero. Here internal energy and free energy coincide and we have

$$e\varphi = -\left(\frac{\partial U}{\partial n}\right)_{V,\,{}^\circ K} - e\Phi_a \tag{30}$$

Where Φ_a = electrostatic potential just outside the crystal face
U = energy of the lowest quantum state of a crystal containing n electrons.

The term U is determined chiefly by the electronic structure of the interior cells of the metal, but includes also the contributions of surface cells. When these have asymmetrical charge distributions, a surface dipole moment results, and thus do surface impurities and lattice defects affect the work function.

It has been found essential in calculating theoretical values of the work function to include the "correlation energy" of the electrons. Thus, it is not sufficient to suppose that the electrons are moving independently in a self-consistent field. They tend to avoid each other to a greater degree than this approximation predicts. We have already seen that electrons of like spin must avoid each other because the Pauli principle requires a point of zero charge density between them. The resulting reduction of potential energy is the "exchange energy." However, electrons of unlike spin also avoid each other. For free electrons, Wigner has calculated the resultant reduction in energy ("correlation energy") as about ⅓ to ½ the exchange energy, the ratio decreasing at higher electrons densities. For partially bound electrons, as in *d*-bands, this correlation energy has not been computed, but is probably not greatly different than for free electrons.

The work function is thus seen to be a function of the energy of an interior electron as well as of the surface dipole moment. The relative importance of these two terms is difficult to assess, since neither has yet been accurately evaluated either by theory or unambiguous experiment. However, the observed changes in contact potential and work function induced by adsorption of foreign substances suggest strongly that the surface term has large if not major importance.

SEMICONDUCTORS

General Description

Nonmetals, salts and oxides have been classified according to the mechanism of their electrical conductivity into ionic conductors, in which the current is carried by the migration of constituent ions through the lattice, and semiconductors, in which the current is carried by the migration of electrons. The magnitude of the electrical conductance of these substances varies over an enormous range, but at moderate temperatures is usually much less for ionic conductors than for semiconductors, which in turn are much poorer conductors than metals.

The band theory, as we have seen, relates electronic conduction to incompletely filled bands. In metals, these are readily accounted for. In oxides and salts, however, there is usually an even number of electrons per lepton and the larger lattice spacing than in metals makes overlapping of bands unlikely. These substances should not conduct by electronic motion, and, indeed, their conductivity is usually many-fold less than for a typical metal. Nevertheless, it is not negligible and increases rapidly as the temperature rises. It is extremely sensitive to the presence of traces of foreign leptons in the lattice, and, contrary to metals, is usually increased by contamination. Clearly, a new structural feature not of importance in metals is playing a decisive role in these substances.

Wilson[53] proposed that lattice imperfections constitute this new factor. In the ideal nonmetallic structure, each lattice point is occupied by the proper lepton to preserve the complete symmetry of the crystal. Lattice imperfections occur wherever this symmetry is broken: (1) at grain boundaries or dislocations, where the lattice parameters undergo an abrupt change; (2) at lepton vacancies in the ideal lattice; (3) at interstitial leptons; (4) at points where foreign leptons occupy regular or (5) interstitial lattice sites. At any lattice imperfection, the ideal periodicity of the potential energy of an electron in the lattice is perturbed, and the difference between the actual potential energy and that of the ideal periodic lattice may be treated in theory as a perturbation. One expects, therefore, a modification of the energy level distribution and of the charge distribution "caused by" the perturbation of the lattice imperfection. Usually, an isolated imperfection produces a local disturbance in the ideal charge distribution and an energy level in the forbidden range of the ideal crystal. This level is usually referred to as a "localized impurity (or imperfection) level." When the density of imperfections becomes high enough so that they interact, the new levels may not be completely localized, however, and the conductivity associated with them approaches metallic character.

Even in an ideal insulator crystal, however, conductivity will develop when an electron is excited from the normally filled valence band to the empty band above it. In this upper, or *conduction*, band it has high mobility. Moreover, the *positive hole* left in the valence band is mobile also and carries a current. The excitation energy for this process is too large in most cases to permit its experimental realization. However, silicon and germanium are believed to conduct by this process above 600°C. Such a semiconductor is said to be *intrinsic*.

When an interstitial atom is added to an ideal lattice, it furnishes one or more extra electrons to the lattice, but no new lattice site. There will thus be an energy level added to those of the ideal lattice for each added electron as well as a perturbation of the potential energy near the interstitial atom. These levels are usually in the forbidden range not far below the lowest level of the conduction band, which is ideally empty. Thus even at moderate temperatures the excess electron can be excited into the conduction band where it contributes to the conductivity. The "hole" in the interstitial atom, however, is ineffective in this case because too much energy is required to transfer electrons from normal valence bands to the localized level on the interstitial atom. Such a material shows conduction by negative carriers only and is called an N-type or metal-excess semiconductor.

The same result is found when an ion of algebraically lower charge is substituted for a normal ion of the ideal lattice. Again an extra electron is added, but no new lattice site. This electron goes into a localized level lying just below the conduction band, from which it is readily excited thermally into the conduction band.

The image of these cases occurs when an electron deficiency is introduced into the ideal lattice as, for example, by the substitution of a cation of higher charge in a normal cation site. This perturbation transfers one level from the valence band to the forbidden region just above it. Since there is one less than the ideal number of electrons, this level is empty in the ground state. However, at moderate temperatures, a valence electron can be excited into it if it lies not too far above the valence band. The imperfection level is localized, and the excited electron cannot contribute to conductivity, but the "positive hole" left in the valence band is mobile. Thus the crystal conducts with positive carriers having the mass and charge of electrons, called "holes." Such a conductor is called a p-type or metal *defect* conductor.

That electron vacancies should behave like positively charged masses under electromagnetic forces is readily demonstrated. For an electron near the top of an allowed band, the kinetic energy E_T is related to the momentum by the equation

$$E_{\mathrm{T}} - E_B = -(p_x^2 + p_y^2 + p_z^2)/2m^* \tag{31}$$

where E_B = energy of upper edge of the band. The electrodynamic force on an electron is given by

$$F = m^*\, d = -e(\mathcal{E} + v \times \mathrm{H}/c) \tag{32}$$

We note that the force on a positive charge is identical with the force on a negative charge of negative mass, and that the energy of an electron at the top of the band is the same as the energy of an electron of negative mass at the bottom of a band.

Now consider a full band and single out one electron in state S. The total current due to all electrons is

$$\sum_{i \neq s} - \frac{e}{V} v_i + \frac{-e}{V} v_s = 0 \tag{33}$$

Where v_i = velocity of an electron in state i
V = volume of the crystal
$-e$ = charge on an electron

Hence

$$\frac{e}{V} v_s = \sum_{i \neq s} \frac{-e}{V} v_i \tag{34}$$

The current associated with all but one electron in a full band is equal, but opposite in sign, to the current associated with the missing electron.

Thus we find that "holes" in a full band behave like positive charges of positive effective mass m^*. Both the sign of the current and the electromagnetic forces are correctly given by this convention. The alternative assumption of a negative charge with negative mass would satisfy Eqs. (31) and (32) but not the current equation (34).

Equation (31) assumes that the surface of constant kinetic energy is a sphere in momentum space. Near zone boundaries, this cannot be true, since the zone boundary is not spherical and the electron cannot traverse the boundary. The effective mass, m^*, must therefore be a function of the electronic momentum near the zone boundary. By Eq. (31),

$$\frac{\partial^2 E_T}{\partial p_x^2} = 1/m^* \tag{35}$$

Thus the curvature of the $E_T(p)$ surface is a measure of the effective mass. In semiconductors, ionic and valence crystals, the effective mass is not greatly different from the free electron mass, and this concept considerably simplifies the qualitative theoretical discussion.

Zinc oxide is a typical n-type semiconductor. The equilibrium crystal at temperatures above 0°K. contains more than one zinc ion per oxide ion, and has the formula $Zn_{1+x}O$. The excess zinc is present as interstitial ions, and the accompanying electrons occupy impurity levels just below the conduction band (see Figure 5b). It is believed that the equilibrium crystal has very few lattice vacancies in the case of zinc oxide, and at low temperatures the excess electrons move in orbitals localized around the interstitial ions. At higher temperatures, these electrons gain enough energy to escape from the interstitial ions and wander through the entire lattice, permitting conductivity. From the point of view of resonance, this conducting state is a resonance hybrid of all the structures which can arise from assigning the excess electron in turn to each of the zinc ions of the lattice. This viewpoint, although pictorial, is not numerically fruitful, however, because (1) the number of excess electrons is a function of the temperature, (2) the number of canonical structures is too large to compute with sufficient accuracy, and (3) neither the energy of a canonical structure nor the resonance energy can be computed at present.

In the case of the silver halides, there is a similar metal excess. However, the cations are appreciably mobile at temperatures above 200°C. in this case, and it is believed that this mobility is evidence for cation vacancies as well as interstitial atoms in the lattice.

In cuprous oxide, the opposite case occurs. Here the equilibrium crystal contains a certain number of cupric ions. Its formula is thus $Cu_{2-x}O$. To preserve charge equality in the bulk crystal, these cupric ions must be balanced by cuprous cation vacancies. In principle, such vacancies may occur either in the body of the crystal or on the surface, analogous to the possibilities in AgCl and ZnO. The ion mobility seems to indicate interior vacancies in the case of Cu_2O.

Energy Levels in Imperfect Crystals

We have noted that lattice imperfections result in departures from ideal symmetry of the potential energy of an electron in the lattice. Slater[43] has amplified a theorem due to Wannier[51] to justify a qualitative graphical scheme for discussing these perturbations and their effects. To arrive at the perturbed potential field, enough electrons are added to or subtracted from the actual structure to leave a structure in which the valence band is exactly filled. This structure will in general have excess positive or negative charges at certain lattice points. The potential energy of these *excess* charges is the perturbation energy in question.

Thus, in Figure 5a is shown the case in which a lepton carrying an excess electron is substituted in a normal position (e.g., P for Si in silicon). If the excess electron is abstracted from the structure, a positive charge on the donor lepton remains, but the valence band is still filled. The perturbation energy is thus the Coulombic energy of this positive charge. Conversely, if the lepton is deficient in electrons, a structure with a filled valence band would be negatively charged at the impurity lepton, and the potential energy diagram of Figure 5b would apply.

Wannier's theorem states that the excess electron (or hole) moves like a particle in the potential energy field consisting of the sum of the normal electronic (total) energy and the perturbation defined above. Thus one arrives at the potential fields indicated, which govern the motion of the excess electrons or holes.

In the case of *n*-type conductors, there is an excess electron per impurity lepton, and the impurity level is occupied (a donor level). It is now evident why this level is below, but near to the upper conduction band, since the perturbation should produce a hydrogen-like level with small ionization energy in the "depression" of the conduction band.

In the case of *p*-type conductors, the potential energy is raised near the impurity in the valence band and an empty discrete level is introduced (an acceptor level) just above the normal valence band.

A cation vacancy is a site of high potential energy for an electron. It thus acts like a *p*-type impurity and generates an empty acceptor level just above the top of the valence band. Similarly, an anion vacancy introduces an empty level just below the conduction band as well as localized level in the bottom of the valence band. Since this latter level is at lower than normal energy, it will be filled, leaving a hole at the top of the valence band.

In solid solutions, the resulting structures must be electrically neutral, but several types of lattice imperfection can be expected in favorable circumstances. These are conveniently arranged in cases.

Case I: Substitution of normal cation by one of lower positive charge.

- (A) Anion vacancies are introduced to compensate.
- (B) Interstitial normal cations are introduced to compensate.
- (C) Normal cations are oxidized to compensate.

Case II: Substitution of normal cation by one of higher positive charge.

(A) Cation vacancies are introduced to compensate.
(B) Interstitial anions are introduced to compensate.
(C) Normal cations are reduced to compensate.

Case I: bis. Substitution of normal anion by one of higher negative charge.

Case II: bis. Substitution of normal anion by one of lower negative charge.

These possibilities must be distinguished experimentally. The interstitial anions of Case II(B) have not been required to date to account for any semiconductor properties and will be ignored henceforth.

Interstitial cations will be favored over anion vacancies in Case I when the lattice is spacious enough to accommodate them without too much ion-repulsion. Thus in zinc oxide, the structure may be thought of as an interlinked system of edge-shared tetrahedra, such that every alternate tetrahedron of zinc ions contains an oxide at its center, and vice versa. In this case, the vacant tetrahedra are geometrically equivalent to the filled ones. Insertion of an interstitial ion is favored by the decrease in electrostatic energy due to the insertion of a positive ion in the midst of a tetrahedron of oxide ions, but this is compensated in part by the high energy level required to accommodate the extra electron. In nickel oxide, no such favorable sites exist for interstitial Ni^{++}, and the choice must lie between anion vacancies (I A) and valence induction (I C).

Verwey[46] has prepared substitutional solid solutions of Li_2O and Nb_2O_3 in nickel oxide, NiO. When Li^+ is substituted for Ni^{++} in the ideal NiO lattice, a local excess of electrons occurs. Of course, the accompanying extra oxide ion vacancies at the crystal surface provide the net charge compensation. However, in the interior these electrons occupy localized donor levels of the p-type associated with Li^+ cores. Such a configuration is readily oxidized by atmospheric oxygen, which takes up the electrons at the surface, forming oxide ions and surface cation vacancies. However, it is the nickel ions which lose their electrons. If the Li^+ were to be oxidized to Li^{++}, the perturbation would largely disappear and the entire ionization energy of Li^+ would be required to bring about the oxidation. If the perturbation remains, but the localized electron is transferred, the process will be exothermic since the $O^=$ band lies below the cation band. This is more favorable and implies that it is Ni^{++} which is oxidized.

An alternative structure would involve anion vacancies in the body of the lattice to compensate the Li^+. As we have seen, these would also introduce empty p-type levels in the valence band. The extra electrons will apparently be less well stabilized in these traps than by the surface oxidation.

This phenomenon, called *valence induction*, has also been observed by

Selwood in certain oxides deposited on high area supports of well-defined crystal structure, such as rutile.

In general, valence induction will occur when the oxidation of the normal cation requires less energy than the transfer of an anion to the surface from the interior. Since creation of an oxide ion vacancy decreases the charge at the vacant site by two units, whereas oxidation of Ni^{++} to Ni^{+++} increases it by one unit, it is evident that the purely electrostatic interactions will favor valence induction. In addition, the excess electron will be accommodated at a lower energy level by this configuration than in anion vacancies. Thus unless the oxidation potential of the normal cation is too high, valence induction will be preferred. Among the transition elements, this phenomenon should be expected frequently.

In Case II, interstitial anions are usually energetically prohibited. Moreover, the energy for reduction is frequently greater than for oxidation of the same normal ion, since some increase in size is to be expected and because the lower valence states are ordinarily less stable for ions like Ni^{++}. The usual case here will be II(A), in which cation vacancies are introduced to compensate the high-charged substituted cations. However, valence induction may also be expected in favorable cases.

Thus, Verwey fuses NiO with La_2O_3, and finds a markedly increased electrical conductivity, ascribed to the introduction of positive holes (the La^{+++} ions) and cation vacancies. In a similar experiment with ZnO, the situation is more complex because ZnO normally contains interstitial zinc ions. As Tl_2O_3 is dissolved in it, the cation vacancies introduced in equivalence to the Tl^{+++} ions trap the interstitial zinc atoms in normal sites. Thus the number of excess electrons is much reduced and the electrical conductivity falls. In addition, even without actual migration of the zinc atoms into the vacancies, one would expect their electrons, normally in *n*-type levels, to annihilate the holes introduced by the Tl^{+++}, since these are at lower energies.

When Nb_2O_5 is fused with TiO_2, either cation vacancies or valence induction of Ti^{+++} is to be expected. If valence induction occurs, oxygen is lost from the surface and a vacancy free crystal is left in which two types of impurity level are present. Associated with the Nb^{+5} is an *n*-type potential, with discrete level just under the conduction band. This level is filled by the electron associated with the Ti^{+++}. Conduction will occur by excitation of this electron to the conduction band and will be *n*-type. If valence induction does not occur, every four Nb^{+5} ions will be accompanied by a Ti^{+4} vacancy. The impurity level due to the Nb^{+5} is now empty, but that due to the cation vacancy gives rise to a positive hole in the valence band. In this case, conduction should be *p*-type.

Normal TiO_2 is an *n*-type semiconductor and probably contains Ti^{+3}

compensated by anion vacancies. Upon exposure to oxygen at 800 to 1000°C, it loses its dark color and its conductivity. However, TiO_2 containing Nb_2O_5 (~1 %) cannot be bleached nor does its resistance rise when so treated[52]. This leads one to suggest that the anion vacancies have disappeared and the reduced Ti^{+++} is stabilized by the Nb^{+5}. If, in addition to Nb^{+5}, Al^{+++} is incorporated in the rutile lattice, the resistance rises again. These lower charged cations must induce reoxidation of the Ti^{+3} to Ti^{+4}, as in Case I(C).

The precise relationship of these lattice imperfections to catalytic action is still conjectural. It should be realized that surface vacancies and defects only will be likely to be of primary significance. Even in Cases I(C) and II(C), in which valence induction avoids interior ion vacancies, the oxidation or reduction must involve loss or gain of surface ions and will give rise to surface defects. Wagner[47] has proposed that oxide vacancies may be important sites for adsorption and activation of hydroxyl groups. Of primary significance may be the fact that semiconductors are reservoirs for the receipt and supply of electrons from adsorbed matter on the surface. Thus, positive ions on the surface may be stabilized by the possibility of oxidizing or reducing an interior cation. In this respect, interior cation and anion vacancies may play a role in catalytic activity by affecting the energetics of this electron transfer process. The ready adaptability of the semiconductor surface to its environment has thus far forestalled a clear-cut demonstration of the connection between electronic structure and catalytic activity. It has proved difficult to carry out catalytic reactions on surfaces of known electronic structure. The molecules undergoing reaction seem to bring the surface to a steady state that is not independently controllable. More detailed discussion of these attempts will be given in a later paragraph.

Distribution of Energy States in Semiconductors

In an earlier section, the energy distribution of quantum states in conduction bands typical for metals was discussed. In semiconductors, this type of distribution, while applicable to the conduction band, is of less significance because of the relatively small numbers of conduction electrons. Of more interest is the number $N(E)$ of impurity levels of energy E to $E + dE$. This distribution is very narrow when the total number of impurities is small; that is to say, each impurity atom has about the same energy as every other of the same type, unless they are so numerous as to interact with each other. The schematic energy level distribution then has the appearance of Figure 14. Here we visualize a semiconductor with N_d donor impurity atoms per unit volume and N_a acceptor atoms. The top of the valence band is at energy E_v ; the bottom of the conduction band is at E_c . Donor and acceptor levels have energies E_d and E_a , respectively. Since the donor lepton has one more electron than the host lepton, the Wannier perturbation potential is negative, and the extra electron lies at a lower energy than those of the host atom. Thus for each donor atom, one state is removed from the valence band of the host and converted to a donor state at a lower level. These states will, of course, be fully occupied. The conduction band, however, is affected similarly. In this case, the impurity level will be occupied by the extra electron of the donor, even though the host conduction levels are empty.

Acceptor impurities, with one less electron than the host, contribute a positive Wannier perturbation, and an empty impurity level just above the host band. This is of importance only for the valence band in semi-conductors. Since this acceptor level may be reached easily by thermal excitation,

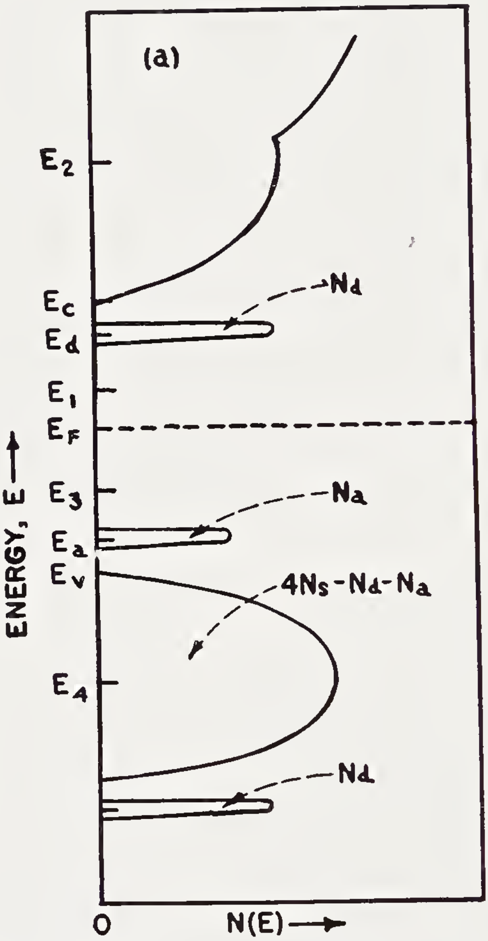

FIG. 14. Schematic energy level density in a semi-conductor. N_a, N_d and N_s are the densities of acceptors, donors and lattice sites, respectively. The upper band (conduction band) is largely empty. The lower (valence) band is nearly filled. The energy E_F, the Fermi level, is placed so that an electron has equal probability of being in a state above or below it.

it may be filled from the valence band, leaving a mobile "hole" in the valence band.

If the host crystal is supposed to have $4N_s$ states per unit volume in each band, the presence of N_d donors will create N_d donor levels below the host band. Similarly, N_a acceptors will create N_a acceptor levels above the host band. In total, there will remain $4N_s - N_a - N_d$ states in the host band.

For electrons in any system, the probability that a state of energy E be occupied, if it exists, is given by the Fermi-Dirac distribution:

$$f = 1/[1 + \exp (E - \mu)/kT] \tag{36}$$

where μ is Fermi level. We have noted earlier that μ may also be interpreted as the chemical potential of an electron in the system. We note that the probability that an electron have energy $E = \mu$ is $f = \frac{1}{2}$. However, there

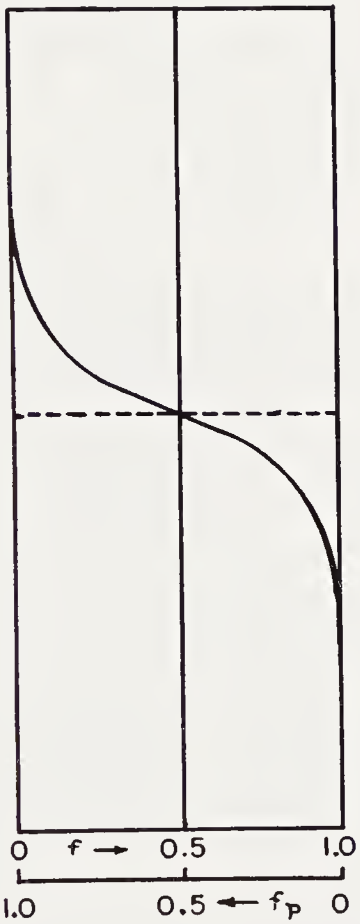

FIG. 15. Fermi distribution. The ordinate is $(E - \mu)/kT$. The abscissa is $f = 1/[1 + \exp (E - \mu)/kT$. This is the same as Fig. 8; it is repeated here for convenience.

TABLE 3

P = density of holes in valence band
P_a = density of holes bound to acceptors
$P_t = P + P_a$
N_d = density of donors
n = density of excess electrons in the conduction band
n_d = density of excess electrons bound to donors
$n_t = n + n_d$
N_a = density of acceptors
N_s = number of atomic sites per unit volume
N_c = effective density of states in the conduction band
N_v = effect density of states in the valence band

may be no actual level with this energy in the semiconductor. The temperature dependence of f is shown in Figure 15. For donor levels, it is easily shown that E is always enough higher than μ to justify the classical *approximation*

$$f \cong e^{-(E-\mu)/kT} \qquad (E - \mu \gg kT) \tag{37}$$

Similarly, when E is much smaller than μ:

$$f_p = 1 - f \cong e^{-(E-\mu)/kT} \qquad \left\{\begin{matrix} E < \mu \\ \mu \gg kT \end{matrix}\right\} \tag{38}$$

But if f is the fraction of available states occupied by *electrons*, then $1 - f$ is the fraction occupied by *holes*. Thus both electrons and holes have the Maxwell-Boltzmann distribution with respect to the departure from the Fermi level, μ.

To find the number of occupied states of energy, E, we must multiply the number of states, $N(E)$, by the probability $f(E)$. This involves computing the Fermi level as a function of the total number of electrons, the distribution of states, $N(E)$, and the temperature.

We introduce the nomenclature of Table 3. The equilibrium semiconductor is electrically neutral. This entails a relationship between the densities of donors, acceptors, electrons and holes. If the valence or coordination structure were completed, each donor would acquire a positive charge and each acceptor a negative charge. The excess charge would then be $N_d - N_a$. This must be offset by the excess holes and electrons, hence

$$N_d - N_a = n + n_d - P - P_a = n_t - P_t \tag{39}$$

The total number of electrons is

$$n_t = n + n_d = \int_{E_1}^{E_2} fN(E)\, dE \tag{40}$$

if the range E_1 to E_2 covers the donor states and the conduction band. Similarly,

$$P_t = P + P_a = \int_{E_3}^{E_4} f_p N(E)\, dE \tag{41}$$

where the energy range now covers the valence band and the acceptor levels. In view of Eqs. (37) and (38), we note that (40) and (41) are functions of μ and T only. Hence, for fixed temperature, Eq. (39) is satisfied for only one value of μ. This permits determination of the temperature dependence of the Fermi level, μ.

In evaluating Eq. (40), we make use of the fact that very few conduction electrons are present. Then $N(E)$ has the form cited earlier for free electrons, $N(E) = \gamma\pi P^3/3h^3$, and $E = E_c + P^2/2$ in the conduction band. This results in

$$n = 2\left(\frac{2\pi mkT}{h^2}\right)^{3/2} e^{-(E_c-\mu)kT} \tag{42}$$

and

$$N_C = 2\left(\frac{2\pi mkT}{h^2}\right)^{3/2} \tag{43}$$

The excess electrons bound to donors is

$$n_d = N_d e^{-(E_d-\mu)/kT} \tag{44}$$

since they are all at the same energy level, E_d.

Similarly, for bound and free holes,

$$P_a = N_a e^{-(\mu-E_a)/kT} \tag{45}$$

$$P = N_v e^{-(\mu-E_v)/kT} \tag{46}$$

$$N_v = 2\left(\frac{2\pi m_p kT}{h^2}\right)^{3/2} \tag{47}$$

where m_p = effective mass of a hole.

We may now survey the qualitative behavior of the Fermi level as the temperature is raised. At low temperature, all holes are filled and excess electrons are bound. Then

$$n_d = N_d - N_a \tag{48}$$

Some of the donor levels must be filled, and it follows that μ must lie only a few times kT below E_d since, at low temperatures, levels above

$E = \mu$ are nearly all empty. As the temperature rises and appreciable numbers of electrons are excited from donors to the conduction band, μ must fall, since n_t is constant. Eventually, nearly all the donor electrons are excited to the conduction band and

$$n \cong n_d - N_a \tag{49}$$

At this point $n_d \cong 0$, and hence μ must have fallen several kT below E_d. Further increase in temperature brings μ close enough to the mid-point between the bands so that appreciable numbers of holes are produced. The semiconductor is now said to be "intrinsic." At still higher temperatures, μ comes still more closely to $(E_c + E_v)/2$. Hence both electrons and holes increase in density exponentially with temperature. If μ were to be below the mid-point, electrical neutrality could not be maintained, for then holes would out-number electrons. In this range of intrinsic semi-conductivity,

$$n = N_d e^{-(E_c+E_v)/2kT} \tag{50}$$

$$p = N_a e^{-(E_c+E_v)2kT} \tag{51}$$

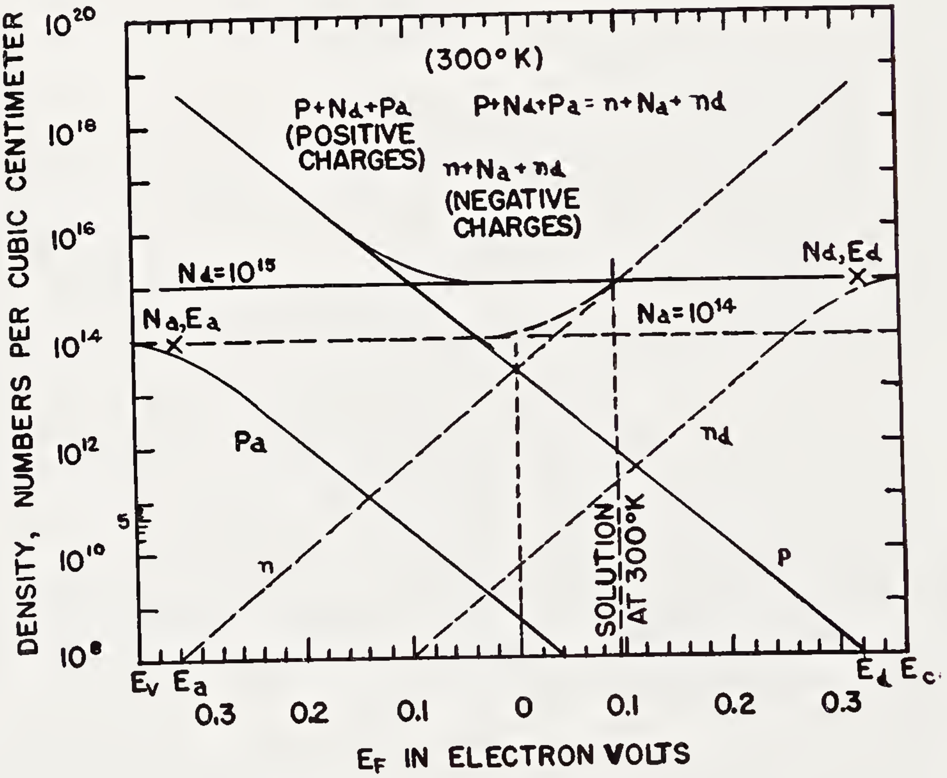

Fig. 16. Determination of Fermi Level as a function of acceptor density. For nomenclature see Table 3. (After Shockley.)

Because of the symmetry between holes and electrons, if $N_a > N_d$, μ lies just above E_a at low temperatures and rises gradually to the mid-point.

At fixed temperature, the graphical solution of Eq. (39), as in Figure 16, will illustrate the trend of μ with N_a and N_d. The density n, of free electrons increases exponentially with μ. The density, n_d, of bound electrons increases exponentially at first but approaches saturation at $n_d = N_d$. Similarly for the positive charges. At the point S, the total of the positive charges equals that of the negative charges and Eq. (39) is satisfied.

We note that as N_d approaches N_a from above, μ decreases. At still lower values $N_d < N_a$, μ approaches the value for which $n = p$, $\mu = \frac{1}{2} \times (E_c + E_v)$. We conclude that for n-type semiconductors at temperatures for which there is considerable dissociation of the *excess electrons* from their donors, the Fermi level decreases as the density of donors decreases, but does not fall below $\frac{1}{2}(E_c + E_v)$. For P-type semiconductors, at temperatures for which there are appreciable numbers of holes, μ lies near E_a and rises as N_a falls.

Electrical Conductivity and Catalytic Activity

These considerations will now be applied to a discussion of the relationship to be anticipated between electrical conductivity and catalytic activity of semiconductors. The electrical conductivity may be expressed as

$$\sigma = nev \tag{52}$$

where n = density of conduction electrons
e = electronic charge
v = electron mobility

The mobility, or velocity per unit field, in turn may be expressed in terms of a *mean free time* between collisions, called the relaxation time, τ.

It is readily shown that[36]

$$v = e\tau/m \tag{53}$$

where m = effective mass of a conduction electron. The mean *free path* between collisions is $l = v\tau$, if v is the mean velocity of a conduction electron.

The relaxation time τ depends upon the nature of the electron "collision." Lattice ions in thermal motion are always available, and are the dominant factor at high temperatures. Any lattice imperfection will interact with the conduction electrons and will contribute to τ. In impurity semiconductors, the impurities themselves are the chief obstacles at low temperatures. Lattice vacancies, dislocation and grain boundaries also make a contribution. The problem of calculating τ is thus a formidable one in theory. However, reasonable approximations exist for charged impurities[5a], neutral impurities[9] and lattice vibrations (called phonons)[37].

For thermal vibrations, $\tau = l/v$, and is a function of temperature and elastic constants of the crystal.

For charged impurities,

$$v_I = e\tau_I/M = \frac{8}{\pi}\sqrt{\frac{2}{\pi}}\,\frac{K^2(kT)^{3/2}}{N_I e^2 m^{1/2}} \ln\left[1 + \left(\frac{3KkT}{e^2 N_I^{1/3}}\right)^2\right] \tag{54}$$

where K = dielectric constant of the crystal
N_I = density of impurity ions.

For neutral impurities,

$$v_N = 8\pi^3 e^3 m/20kN_n h^3 \tag{55}$$

We note that the mobilities are inversely proportional to the density of scattering centers. The contribution of thermal motion is to decrease mobility at higher temperatures. The mobility through ionic impurities rises with temperature, and that through neutral atoms is temperature independent.

The major effect of temperature on conductivity is through n, the density of conduction electrons. This increases exponentially but with an "activation energy" which is temperature dependent. This complex behavior makes essential a careful consideration of temperature effects on semiconductor properties.

At low temperatures, the number of conduction electrons is much lower than the number of donors, and the activation energy of the conductivity is $E_d - E_c$. For if $n \ll n_d$,

$$n_d = N_d - N_a = fN_d \tag{56}$$

whence

$$f = (N_d - N_a)/N_d \tag{57}$$

But

$$f = 1/\{1 + \exp[(E_d - \mu)/kT]\} \tag{58}$$

or

$$E_d - \mu = kT \ln[(1 - f)/f] \tag{59}$$

This gives us

$$\mu = E_d + kT \ln[(N_d - N_a)/N_a] \tag{60}$$

We have seen that

$$n = N_c e^{-(E_c - \mu)/kT} \tag{61}$$

Using the result just obtained for μ, we find

$$n = N_c \frac{(N_d - N_a)}{N_d} e^{-(E_c - E_d)/kT} \tag{62}$$

Thus, when $N_d \gg N_a$, the conductivity is nearly independent of the density of donor impurities.

At higher temperatures, when donors are ionized in appreciable numbers, this simple result no longer holds true, for, as we have seen, the Fermi level itself falls as the temperature rises, as shown schematically in Figure 17. The apparent activation energy is then

$$\frac{d[(\mu - E_c)/kT]}{d(1/T)} = \frac{1}{k}\left[\mu - \frac{T\,d\mu}{dT} - E_c\right] = \frac{1}{k}(\mu^* - E_c) \tag{63}$$

where

$$\mu^* = \mu - T\frac{d\mu}{dT} \tag{64}$$

Reference to Figure 17 will show that at all temperatures above that for the maximum in μ, the apparent activation energy is less than $E_c - E_d$ and may even be negative. As the number of acceptors rises (or the number of donors falls) the initial slope becomes less, is zero when $N_d = 2N_a$, and becomes negative for smaller numbers of donors. The apparent activation energy thus rises and approaches $E_c - E_d$ as the number of donors falls. When there are no acceptors, $N_a = 0$, we have

$$n + n_d = N_d \tag{65}$$

$$nd = f(E_d)N_d \tag{66}$$

$$n = (1 - f)N_d \tag{67}$$

At low temperatures, $f \approx 1$, and $1 - f \rightarrow e(E_d - \mu)/kT$.

Since

$$n = N_c \exp[(\mu - E_c)/kT] \tag{68}$$

we find, equating the two expressions for n,

$$\mu = \frac{E_c + E_d}{2} + 2kT \ln(N_d/N_c) \tag{69}$$

or

$$n = \frac{N_d^2}{N_c} e^{-(E_c - E_d)/2kT} \tag{70}$$

Thus, when no acceptors are present, the low temperature activation energy is half the ionization energy of the impurity. Moreover, the conductivity now increases in proportion to the density of donors.

In most catalytic semiconductors, the density of donors or acceptors is

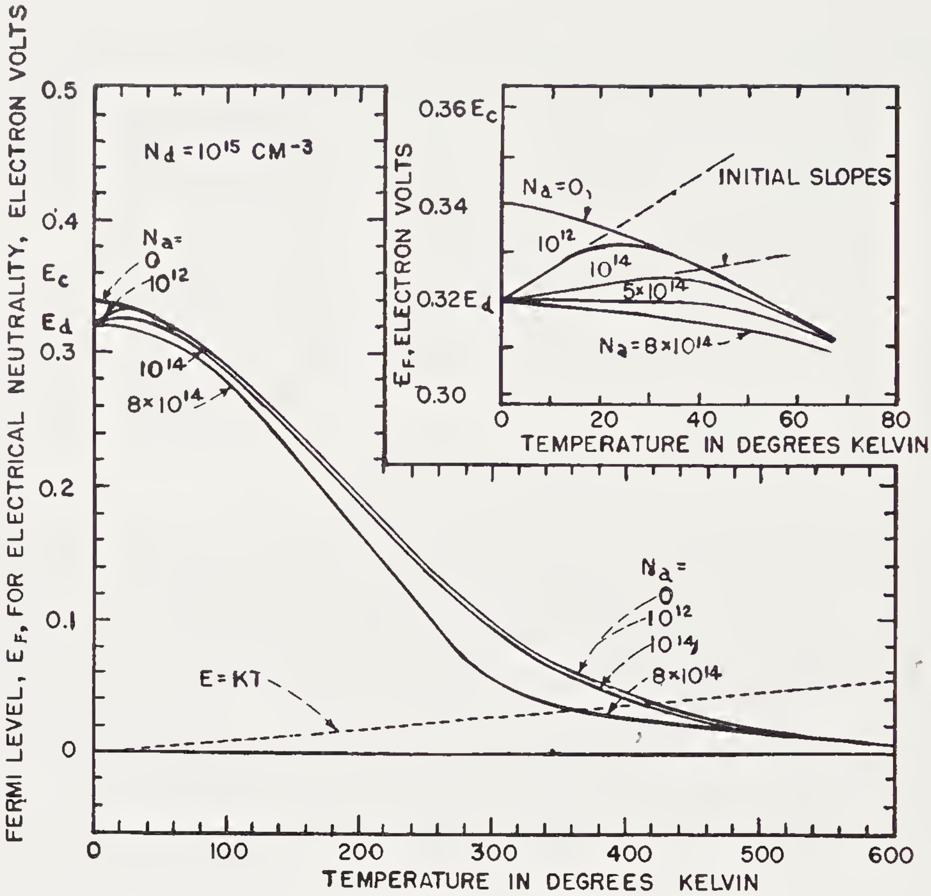

FIG. 17. Temperature dependence of the Fermi Level in a semi-conductor plotted for several acceptor densities. (After Shockley.) Nomenclature in Table 3.

determined by the atmosphere at the solid surface. For example, zinc oxide in the presence of one atmosphere pressure of oxygen is an *n*-type semiconductor. Presumably, the excess electrons arise from the spontaneous evolution of oxygen to leave a zinc-rich oxide. These extra zinc atoms may be supposed to occupy interstitial lattice sites, their valence electrons weakly bound with about $\frac{1}{20}$ the ionization energy of the free gaseous atom. The concentration of these atoms is a function of the oxygen pressure. We may write

$$\text{ZnO (solid)} \rightleftharpoons \text{Zn}^{++}\ \text{(i)} + 2e\ \text{(i)} + \tfrac{1}{2}\text{O}_2\ \text{(g)}. \tag{71}$$

If the atmosphere is modified by introducing N_2O, more readily adsorbable oxide ions are supplied by the reaction

$$\text{N}_2\text{O} + 2e\ \text{(i)} \rightleftharpoons \text{N}_2\ \text{(g)} + \text{O}^{-}\ \text{(ads.)} \tag{72}$$

analogous to the reverse of Eq. (71). The adsorbed gases, O_2 and N_2O, are thus playing the role of acceptors with such low-lying energy states that they are completely filled. Hence N_a is increased in the presence of N_2O. We have seen that this should cause the apparent activation energy for conduction to rise. However, the effect will not be marked unless $N_d < 2N_a$.

Consider now the effect of replacing zinc ions by gallium (Ga^{+++}) in the ZnO lattice. To maintain electroneutrality, there must be introduced one cation vacancy for every two Ga^{+++} ions. These vacancies will be filled in part by zinc atoms formed by the evaporation of more oxygen. However, the ionization potential of Ga^{++} is 50 per cent more than that of Zn^{+}. Hence we should expect that the excess electrons will be associated with the gallium preferably to the zinc. Thus, the number of donors will be proportional to the dissolved gallium and their energy will be somewhat lower than in pure zinc oxide.

An increase in N_a, by introducing N_2O, will now have less effect than on pure ZnO, since the number of donors is initially greater. Thus, the apparent activation energies will be increased much less by N_2O for the gallium-containing zinc oxide than for pure zinc oxide.

These facts make explicable the results of Wagner[48] who studied the decomposition of nitrous oxide over a zinc oxide semiconductor, both pure and containing gallium. The conductivity of the ZnO in oxygen was increased fifty-fold by dissolving gallium in it. The introduction of 10 per cent N_2O decreased the conductivity of pure ZnO about 30 per cent. The rate of decomposition of N_2O was found to be about 1.4 times faster when gallium was present, but the activation energy is about 7500 calories higher. No values for the conductivity of the gallium-containing catalyst in N_2O were reported. If it be assumed that the catalytic reaction is proportional to the density of conduction electrons, these observations agree qualitatively with the expectations outlined above. The pre-exponential factor must be about 60 times larger in the presence of 1 per cent Ga than in its absence, to be consistent with the activation energy and rate change. This is entirely consistent with the probable increase in the number of donors upon admixing gallium in this proportion. A similar explanation was given in less detail by Boudart[4].

It is now apparent that no simple correlation between catalytic activity and electrical conductivity should be expected, even when conduction electrons do control the rate of catalysis. In many cases, so many donors and acceptors are supplied by the reactants that the conductivity becomes very high. One must then speak of an *impurity band* of finite width, which may overlap the conduction band, as suggested by James[20]. Excitation now becomes very easy and the above theory must be modified to account for the interaction of impurity centers and "degeneracy" in the energy level distribution. It seems unlikely, however, that the supply of an electron can be rate-controlling under these conditions.

DISLOCATIONS

Although the concept of the dislocation was proposed by Prandtl in 1928 to account for the plastic deformation of solids, it is only in recent years that it has been realized how fundamental this type of crystal imperfection is for the understanding of many other crystal properties[39]. Seitz in particular has emphasized[32, 38] that dislocations may act as sources or sinks for an unlimited number of lattice vacancies or interstitial atoms. Moreover Frank has proposed[12] that spiral dislocations are the sites of crystal growth, and, hence, should be found on all major crystal faces. It is to be expected, then, that surface chemistry and catalysis must also consider the influence of this type of crystal imperfection on the physical and chemical properties of surfaces.

A picture of the most general type of dislocation is gained if the solid is supposed to be cut along some plane surface and a number of lattice planes removed from a disc inside some closed bounding curve. The cut faces are then rejoined and the gap where matter was removed is supposedly filled by elastic deformation of the two halves. The atoms inside the closed boundary of the disc will be in register except near the boundary itself, which constitutes a dislocation line. In our model, this line is closed, but it may also emerge at some crystal surface. Two types of surface defect may then result.

The Taylor-Orowan, or *edge dislocation*, produces in the surface a step of width equal to the number of lattice planes removed (Figure 18). In the interior of the crystal, this type of dislocation results from the insertion (or removal) of an extra lattice half plane (Figure 6). The crystal below the *slip plane*, AB, is in tension; above it, the crystal is in compression. The *dislocation line* is in the slip plane at C, perpendicular to the plane of the figure. It is evident that by a shift of one-half step in C toward B, the atoms above the slip plane are translated to the right. Because of the symmetrical position of the atoms about C, this shift can occur with very little activation energy, and the easy slip observed in metal crystals is accounted for, despite their high cohesive energies.

The second type of dislocation is the *Burgers*, or *screw* dislocation. In a crystal face, such a dislocation produces a spiral step (Figure 19). The dislocation line cuts the crystal face at C, and constitutes the screw-axis of the distorted crystal. In the interior, this line may be a closed loop of finite length and defines a region in which an extra lattice plane produces an elastic distortion of the nearly perfect crystal. In this case, motion of the dislocation in a direction parallel to its axis produces a shear in the crystal.

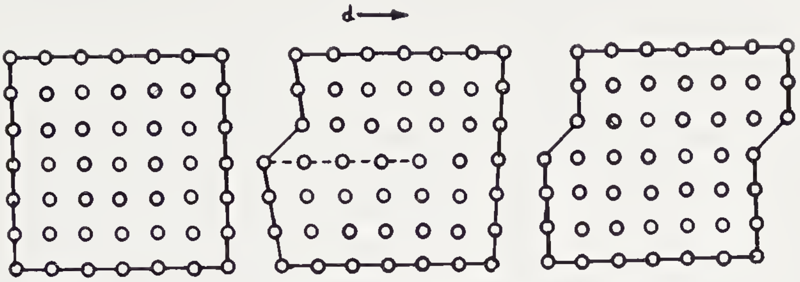

POSITIVE DISLOCATION

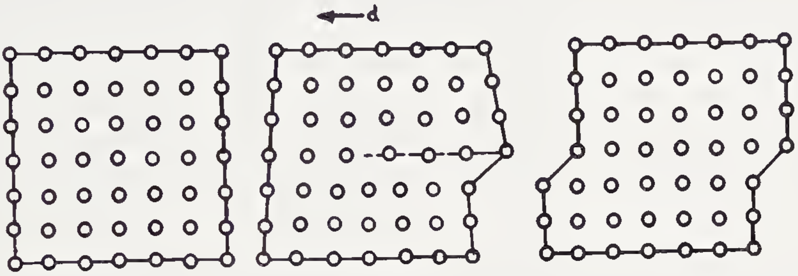

NEGATIVE DISLOCATION

FIG. 18. Taylor-Orowan or edge dislocations.

The general dislocation ring is characterized by the displacement vector (*Burgers vector*, *s*) of the atoms inside the ring relative to those outside. Thus, one can pass through undistorted unit cells along a path which completely encircles a dislocation line. This path can be described by the number of steps N_x, N_y, N_z, taken in each of three reference directions in the lattice. If equal numbers of steps are taken in the positive and negative directions in each case, one would return to his starting point if the lattice were perfect (Figure 18). If, however, this path encloses a dislocation (Figure 20), the loop will not close when $\Delta N_x = \Delta N_y = \Delta N_z = 0$. The vector required for closure is s, the Burgers vector. In Figure 20, this is illustrated for the Taylor-Orowan type of dislocation. The Burgers vector lies in the slip plane and is perpendicular to the dislocation. Reference to Figure 19 will show that for a screw dislocation, the Burgers vector is parallel to the dislocation line, but the slip plane is not uniquely defined. Clearly, in the general closed loop, the Burgers vector has a constant magnitude and direction for every path encircling the loop, but the direction of the dislocation is arbitrary. Thus the edge and screw dislocations are extreme types, with every intermediate angle possible between the Burgers vector, s, and the dislocation line. An extension of this reasoning shows that a dislocation line cannot terminate in the interior of a crystal. Hence, it either emerges at the surface (or at a grain boundary) or forms a closed loop in the interior.

The distortion of the lattice near a dislocation gives rise to a higher potential energy than in a perfect lattice. This energy, by elasticity theory, should be proportional to $| s |^2$. Estimates of its magnitude indicate that it may amount to as much as 1 e.v. per atomic length *along the line*[34]. The density of dislocation rings is usually stated in terms of the number of lines intersecting one square centimeter of area in the crystal. This ranges from 10^8 or 10^9 in good crystals to 10^{12} in cold-worked material. Thus, dislocations are separated on the average by 10^2 to 10^4 Å. The boundaries which characterize the mosaic structure of single crystals may be considered as a line of dislocations. The lattices on either side of the boundary are disoriented through a small angle such as may arise by the continued insertion of new planes (Figure 6). Thus the coherent scattering domains in X-ray analysis are bounded by planes of dislocations. The densities quoted are consistent with the estimates of the sizes of mosaic blocks from X-ray data. One should expect, then, that every crystal grain larger than 100 Å will have dislocations on its surface. In extreme cases, one atom per thousand in the surface is near a dislocation.

Their high energy of formation makes it certain that dislocations will not remain in true equilibrium in a nearly perfect crystal. They must form in some nonequilibrium process and persist only because of a very slow rate of destruction. The precise mechanisms of formation and destruction are very conjectural, but several reasonable theories can be proposed.

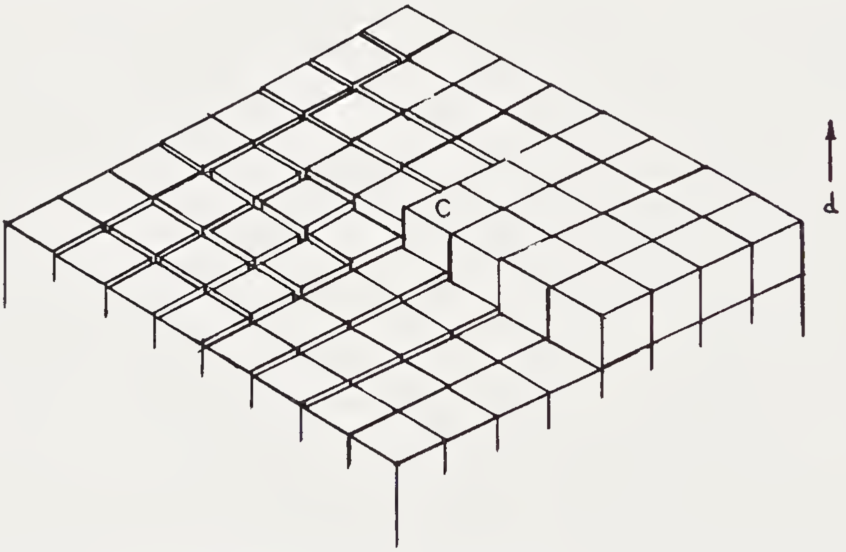

Fig. 19. Burgers or screw dislocation emerging at C on a crystal face. Each cube represents an atom. The screw dislocation generates a spiral step about the dislocation axis.

Seitz has pointed out that when lattice vacancies congregate in a single plane, a dislocation is generated by collapse of the crystal over the vacant area. Since as much as 1 per cent of the lattice sites may be vacant in crystals near the melting point, it is not unreasonable that, in condensation from melts, this mechanism may generate dislocations. Frank has proposed that all crystal growth is catalyzed by screw dislocations, the step in the surface furnishing the site of lowest free energy for addition of a lepton. Nucleation of crystal growth seems to require, on this theory, the formation of such a dislocation. The free energy of such a partially disordered nucleus is higher than that of an ideally ordered one, which in turn is higher than that of the saturated solution. As the ordering process sets in, however, it is likely that nuclei with dislocations will form in appreciable numbers at reasonable supersaturations. These can grow rapidly by deposition in the indestructible spiral step, whereas perfect faces, though of lower free energy, grow so much more slowly as to disappear. Thus all crystals which have grown in reasonable time (i.e., geologic ages or less) have dislocations.

Dislocations move under stress, either by simple translation parallel to the Burgers vector, or by diffusion of leptons in directions other than that of the Burgers vector. At high enough temperatures thermal motion may bring a dislocation line completely to the surface, where it disappears. More

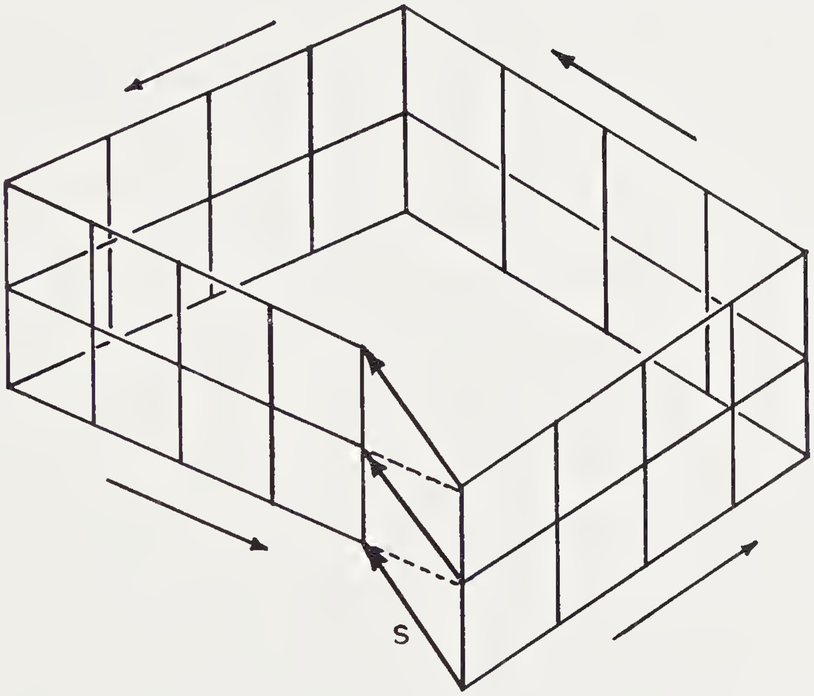

Fig. 20. Definition of the Burgers vector s. A path along lattice vectors encircling a dislocation fails to close by the vector s.

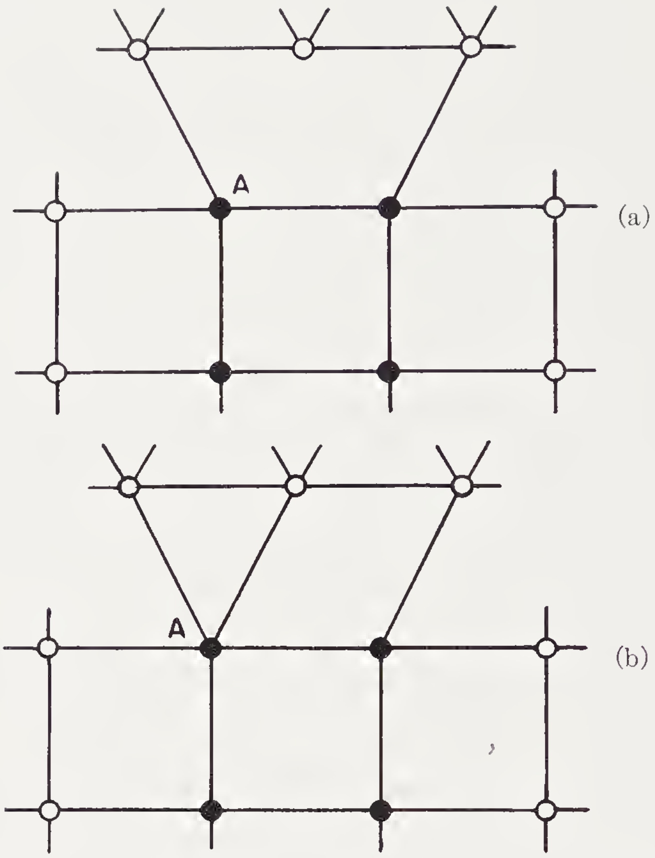

Fig. 21. Effect of coordination number on coherence at phase boundaries.

(a) Lines represent ligancy of each lepton. Atom A is not bound coherently to the upper phase and the normal ligancy of 5 is not possible for the middle lepton of the top row.

(b) By increasing the ligancy of A to 5, a coherent phase boundary is obtained and all the upper phase leptons have their normal ligancy.

likely, however, as Seitz has shown[33], is the "dissolving" of the dislocation into lattice vacancies, which wander away by diffusion. This is the reverse of one mechanism of formation, and is proposed to account for the increase in conductivity of ionic crystals in plastic flow, as observed by Gyulai[14]. Since these diffusional processes are very slow in solids[44], dislocations may be expected to have long lives under most circumstances.

On catalytic surfaces, it is possible that dislocations may afford sites for valence induction. Smith[44] has pointed out that at phase boundaries in which crystals of different coordination meet, coherent non-planar interfaces can occur by transferring some leptons to the coordination of the other. Thus in Figure 21a, where the lines represent the ligancy of the leptons, no coherent interfacial line can be drawn, and a dislocation must exist at the phase boundary. If, however, the ligancy of one of the four-coordinate atoms (Atom A) is increased to 5, the nonlinear coherent interface of Figure 21b is possible. Moreover, at interfaces between crystals of the same coordination, there are inevitably leptons of abnormal coordination at dislocations. The present writer suggests that the interfacial energy of such misfit regions can often be reduced by such a change in coordination. Thus phase and grain boundaries afford, at the dislocations which emerge there, sites where abnormal valencies can be induced by the stabilization of unusual coordination numbers. Mills, Millikan and Oblad[26] made a similar suggestion when they proposed "potential acid sites" at the phase boundaries between four-coordinate silica and six-coordinate alumina. It is possible that mechanical strain at the phase boundary can be relieved by a change in coordination when a hydrocarbon is adsorbed on the surface. A similar structure may make more explicit the "structural adsorption" which Cook, Pack and Oblad[6] postulated to precede all physical adsorption. The possible relationship of these notions to the "adlineation" theory of catalytically active surfaces proposed by Schwab and Pietsch[30] needs no further elaboration.

Smith has pointed out[45] that thin coherent films of oxide on a metal will probably have a nonplanar surface both on the metal and air sides so as to accommodate the change in ligancy of the metal in the two phases. This interface, moreover, has a lower free energy than a grain boundary in the metal itself. It seems very likely that the area-promoting effects of alumina in reduced iron catalysts may be associated with these observations. The lower interfacial energy of the metal-alumina interface would favor smaller crystallites, and the nonplanar interface would introduce many steps which should enhance catalytic activity by furnishing adsorption sites.

SURFACE STATES IN SOLIDS

The discussion thus far has concerned the electronic state of a solid, the entirety of which is made up of identical repeating units defined by a typical potential energy function. This assumption cannot be applied at the surface of a solid, for here the potential energy must rise asymmetrically to zero as an electron passes *out of the surface layer* into free space. Tamm[45] was the first to show, for a one-dimensional square well potential, that this abrupt termination of a lattice could give rise to permitted levels at energies forbidden to electrons in the interior lattice. The corresponding orbitals are localized at the surface, and decay exponentially with distance into the crystal. This surface-localized property will be taken as the defining characteristic of a *surface state.* When two-dimensional surface lattices are considered, it is found that these states exhibit band structures and the orbitals are delocalized in the surface, but do not penetrate the interior. Goodwin[13] and Shockley[39] have examined this more general case from two different points of view. Goodwin has approximated the surface orbitals by linear combination of free atomic orbitals. This "tight-binding" approximation is the more exact the smaller the overlap between atomic orbitals and can give only qualitative results for metals.

Very recently, Artmann[1] has reviewed and extended previous[52] work, using the "tight-binding" approximation. The following discussion is based largely on his publication.

The existence of surface levels and their qualitative character can be understood on the basis of simple perturbation and resonance theory. We have seen how the perturbation of adjacent cells splits the levels in any one of them into bands of levels separated by forbidden energy gaps. When bands overlap, the atomic orbitals which approximate the crystal orbitals must lie in the same energy range, at least in part. They are thus capable of hydridization. Thus when S and P orbitals have the same energy, four equivalent linear combinations can be found, two of which have greater bonding power than either pure S or pure P. These hybrids will be a more appropriate basic set of orbitals to use in describing the bonding in an atomic-molecular system.

We now consider a semi-infinite crystal with nonoverlapping bands. To some degree of approximation, its energy is equal to the sum of the energies of the electrons in each of the atoms, considered as isolated systems, diminished by the "exchange" or "delocalization" energy that arises because of the possibility of sharing electrons between all the cells of the crystal. If the potential energy in each isolated cell is the same, no surface levels can exist. If, however, the surface cells have higher energy than the rest because of the deformation of the potential energy at the surface, the electrons in these cells may occupy these higher levels, but be unable to escape into the interior, where such high energy is forbidden. We thus consider a surface state interacting with an interior state. If their unperturbed energies are sufficiently close, their interaction will be strong and the surface electrons are delocalized. If their unperturbed energies differ greatly, however, the surface electrons will be trapped in localized surface states.

When two (unperturbed) bands overlap in energy, even though there is no perturbation in the surface cells, surface states may arise. In this case, we should consider the exchange between cells in terms of the hybrid orbitals appropriate to the overlapping bands. Since these are superpositions of S and P orbitals in certain proportions, it is possible to find a combination which does not vanish in the surface cells, but also does not interact with the interior cells. Such an orbital is destroyed in the superposition of itself with the orbitals of the interior cells. These particular hybrids are surface state orbitals.

When the surface cell potential energy is exactly that of the interior cells, each pair of hybrids gives rise to a pair of surface states, one belonging to each of the overlapping bands. When there is a surface perturbation, however, both surface states belong to the upper band. This is because the higher energy surface states interact more strongly with the upper than with the lower of the overlapping bands.

We thus expect to find two sorts of surface levels. The first type, belonging to the lower band, arise when bands do not overlap and when the surface perturbation is strong. These are called *Tamm levels.* The second type occur when bands do overlap and the surface perturbation is weak. They are called *Shockley levels.* They belong to the upper band and lie below it. It is, of course, possible that these localized surface levels overlap the interior levels in energy in some cases, and this is not inconsistent with their localized nature.

A careful self-consistent field treatment shows that in a fully occupied band, the sum of the charge in interior states and in surface states (when they exist) is the same in *every* cell (interior and surface) of the crystal. This means that the electrons in surface states are abstracted from interior states of the *surface cells* only, and hence do not contribute a net negative charge to the surface. This conclusion is not rigorous for partly filled bands, but is still very nearly true, in the sense that the surface charge so acquired is very small.

The mathematical expression of these ideas is implicit in the work of Goodwin, Shockley and Artmann. However, the quantitative evaluation of the terms "strong" and "weak" perturbations is not as yet possible and the actual computations are prohibitively complex for any realistic crystal model. The qualitative ideas, however, are surely valid and useful.

Thus for a crystal of N_i interior atoms and $N_s = N - N_i$ surface atoms, there will be N states in all. If the surface states are Tamm states, the lower band will have N_i interior states and N_s Tamm states, with N states in the upper band. If the surface states are Shockley states, there will be N states in the lower band, N_s surface states and N_i states in the upper band. Artmann suggests that a Shockley surface band may in some cases overlap a filled interior band below it. In such a case, transitions to the surface band would be expected and volume electronic conductivity should result. Bardeen[3] has postulated a similar state of affairs in silicon and germanium to account for the fact that in silicon-metal contacts, the contact potential is independent of the work function of the metal. In this case, the semiconductor surface is supposed to have available a store of bound electrons in surface states which serve to screen the interior of the semiconductor and prevent a change of the interior space charge when the metal contact is made. Apart from some very hypothetical relations to catalysis to be made later, this phenomenon is the only experimental evidence for surface states to date.

These notions may be applied to the overlap of *d* and *s* bands in the transition metals. First, we suppose the *d* and *s* bands to interact strongly. Any surface states will be Shockley states, arising from the *s*-band and lying at intermediate energies, which probably overlap the interior band energies. Thus, as the crystallite size diminishes and the proportion of surface to interior atoms increases, surface states will be occupied at the expense of the *s*-band. As the *d*-*s* overlap diminishes, the Shockley states will rise in energy and eventually be absorbed in the upper band.

In the opposite case of a strong surface perturbation, surface states will be Tamm states and will arise only when *d*-*s* overlap is weak. In this case, they lie above and belong to the *d*-band. As crystallite size diminishes, the surface states cause the *d*-band to empty. One might, in the case of nickel, expect a full interior *d*-band with no unpaired spins when enough atoms are on the surface to abstract all of the empty *d*-band orbitals. The holes will have all been transferred to the surface when 0.3 interior orbitals per atom have been abstracted, or 6 per cent of the total number[5] of *d*-orbitals available. This ratio of surface to volume atoms is attained in a cube about 100 atoms on an edge. For iron, however, with 2.2 holes per atom, the interior *d*-band will need to lose 25 per cent of its orbitals to the surface before it becomes filled. This will occur in a cube approximately 25 atoms on an edge. For smaller particles, the surface states will be partially occupied. They lie somewhat higher in energy than the interior *d*-band, by an amount that increases with the *d*-*s* splitting in the isolated atom as well as with the strength of the surface perturbation.

Since there is at present no agreement as to the magnitude of *d*-*s*-*p* hybridization in metals, one cannot reach any satisfactory conclusion as to the nature of surface states, if any, which they may display. Even if Shockley states are assumed, the depletion of the *d*-band as particle size diminishes will be expected if one expects all available states to be filled up to the same energy level, since the surface states must be below the Fermi surface, and hence below the holes in the *d*-band. It is, of course, possible that no surface states exist in metals at all. Indeed, they do not seem to be required as yet to account for any observed properties.

References

1. Artmann, K., *Z. Physik.*, **131,** 244 (1952).
2. Bacher, R. F., and Goudsmit, S., "Atomic Energy States," New York, McGraw-Hill Book Co. Inc., 1932.
3. Bardeen, J., *Phys. Rev.*, **71,** 717 (1947).
4. Boudart, M., *J. Chem. Phys.*, **18,** 571 (1950).

5. Chapman, S., *Monthly Notices, R.A.S.*, **82,** 292–97 (1922).
5a. Conwell, E., and Weisskopf, V. F., *Phys. Rev.*, **69,** 258A (1946); **77,** 288 (1950).
6. Cook, M. A., Pack, D. H., and Oblad, A. G., *J. Chem. Phys.*, **19,** 367 (1951).
7. Dilke, M. H., Eley, D. D., and Maxted, E. B., *Nature*, **161,** 804 (1948).
8. Dowden, D. A., *J. Chem. Soc.*, **1950,** 242.
9. Erginsoy, C , *Phys. Rev.*, **79,** 1013 (1950).
10. Farineau, J., *Compt. Rend.*, **205,** 365 (1937).
11. Fowler, R. H., and Guggenheim, E. A., "Statistical Thermodynamics," Chap. II, Cambridge University Press, 1939.
12. Frank, F. C., *Discussions Faraday Soc.*, **1949,** 48.
13. Goodwin, E. T., *Proc. Camb. Phil. Soc.*, **35,** 205, 221, 232 (1939).
14. Gyulai, Z., and Tomka, P., *Z. physik.*, **96,** 350 (1935).
15. Hartree, D. R., *Proc. Camb. Phil. Soc.*, **24,** 89 (1928).
16. Herring, C., and Nichols, M. H., *Rev. Mod. Phys.*, **21,** 185 (1949).
17. Hsu, Y. C., *Phys. Rev.*, **83,** 975 (1951).
18. Hüttig, G., "Handbuch der Katalyse," Vol. VI, Edwards Bros., 1945.
19. James, H. M., *Phys. Rev.*, **76,** 1602, 1611 (1949).
20. James, H. M., and Ginzbarg, A. S., *J. Phys. Chem.*, **57,** 840 (1953).
21. Krutter, H. M., *Phys. Rev.*, **48,** 664 (1935).
22. Löwdin, P., *J. Chem. Phys.*, **19,** 1570, 1579 (1951).
23. Manning, M. F., and Chodorow, M. I., *Phys. Rev.*, **56,** 787 (1939).
24. Mayer, J. E., and Mayer, M. G., "Statistical Mechanics," p. 374 ff, New York, John Wiley & Sons, Inc., 1941.
25. McGuire, T. R., and Kriessman, C. J., Jr., *Phys. Rev.*, **82,** 774 (1951).
26. Mills, G. A., Millikan, H., and Oblad, A. G., in "Advances in Catalysis," Vol. III, (Edited by N. G. Frankenburg, V. I. Komarewsky and E. K. Rideal) New York, Academic Press, Inc., 1951.
27. Nichols, M. H., *Phys. Rev.*, **57,** 297 (1940).
28. O'Bryan, H. M., and Skinner, H. W. B., *Phys. Rev.*, **45,** 370 (1934).
29. Pauling, L., *Proc. Roy. Soc.*, **A196,** 343 (1949); Pauling, L. *Phys. Rev.*, **54,** 899 (1938).
30. Schwab, G. M., and Pietsch, E., *Z. physik. Chem.*, **121,** 189 (1926).
31. Seitz, F., "Modern Theory of Solids," New York, McGraw-Hill Book Co., 1940.
32. Seitz, F., *Phys. Rev.*, **79,** 723, 890, 1002, 1003 (1950).
33. Seitz, F., *Phys. Rev.*, **80,** 239 (1950).
34. Seitz, F., and Read, T. A., *J. Appl. Phys.*, **14,** 100, 170, 470, 538 (1941).
35. Selwood, P. S., personal communication.
36. Shockley, W., "Electrons and Holes in Semi-Conductors," Chap. 8, New York, D. Van Nostrand Co., 1950.
37. Shockley, W., *ibid.*, Chaps. 11, 17, 1950.
38. Shockley, W. "Imperfections in Nearly Perfect Crystals," Chaps. 1, 2, 3, 13, 14, New York, John Wiley & Sons, Inc., 1952.
39. Shockley, W., *Phys. Rev.*, **56,** 317 (1939).
40. Slater, J. C., *Phys. Rev.*, **76,** 1592 (1949).
41. Slater, J. C., *J. Appl. Phys.*, **8,** 385 (1937).
42. Slater, J. C., *Phys. Rev.*, **36,** 57 (1930).
43. Slater, J. C., *Phys. Rev.*, **76,** 1592 (1949).
44. Smith, C. S., "Imperfections in Nearly Perfect Crystals," Chap. 14, New York, John Wiley & Sons, Inc., 1952.
45. Tamm, I., *J. Phys. Z. Sowiet*, **1,** 733 (1942).

46. Verwey, E. J. W., Hayman, P. W., and Romeyn, F. C., *Chem. Weekblad.*, **44,** 705 (1948).
47. Wagner, C., *J. Chem. Phys.*, **18,** 69 (1950).
48. Wagner, C., *J. Chem. Phys.*, **18,** 70 (1950).
49. Wagner, C., and Schottky, W., *Z. physik. Chem.*, **B11,** 163 (1931).
50. Wannier, G. H., *Phys. Rev.*, **52,** 191 (1937).
51. Wannier, G. H., *Phys. Rev.*, **52,** 191 (1937).
52. Weyl, W. A., ONR Report 25.
53. Wilson, A. H., *Proc. Roy. Soc.* **A133,** 458 (1931); **134,** 277 (1931).
54. Wohlfarth, E. P., *Phil. Mag.*, **42,** 95 (1951).
55. Wohlfarth, E. P., *Phil. Mag.*, **40,** 703, 1095 (1949).
56. Zener, C., *Phys. Rev.*, **81,** 440 (1951); **82,** 403 (1951); **83,** 299 (1951); **85,** 324 (1952).

CHAPTER 4

NATURE OF COMPLEXES ON CATALYST SURFACES

Hugh M. Hulburt

Chemical Construction Corp., New York, N.Y.

While a considerable body of fact and theory has been accumulated on the bulk properties of crystalline solids, the state of knowledge and understanding of surfaces is much more fragmentary. The ill-defined, often transient, surface complexes which are intermediates in catalytic reactions are even less well understood. Nevertheless, the basic principles discussed in Chapter 3 have an application here also which it is now proposed to explore. Most of the interpretations are admittedly conjectural, yet, it is hoped, consistent with general physicochemical principles and provocative of further investigation.

In keeping with the distinction in chemical bond types, we shall first discuss complexes on pure and promoted metals and then complexes on oxides which are characterized by a high degree of ionic bonding and by semiconductor properties.

Nature of Surface Complexes on Catalyst Surfaces

The first question concerns the degree to which actual catalytic surfaces approximate the regular crystal lattice planes dealt with in theory. This is without question partly a matter of how the catalyst has been prepared. Considering here only "metals," we must discuss first the reduced bulk oxides, such as the iron synthetic ammonia catalyst, or a reduced cuprous oxide. It is very difficult in these cases to establish that the metallic surface is absolutely free of oxygen. Even though the stoichiometry of the reduction indicates its completeness with respect to iron (in the ammonia catalyst case), the presence of oxide promoters, such as alumina and alkali oxides, would bring a partial monolayer of combined oxygen into contact with the iron. Beeck[9] and co-workers have sought to avoid this possibility by preparing their metals by evaporation and condensation in vacuum or inert atmosphere.

Reduced oxides supported on kieselguhr, alumina and similar supports are even more subject to question than bulk metal catalyst, since it has been demonstrated[82] that oxygen is mobile on these supports at the temperatures required to reduce the catalysts.

The notorious difficulty in cleaning up bulk metal surfaces for work function determinations, even for refractory metals such as tungsten and tantalum, adds to one's suspicions concerning the usual catalysts. Probably least suspect are those prepared by the evaporated film technique and a few cases in which metal wires in an electron emission tube are cleaned by positive ion bombardment[22].

The state of the surface just after preparation may well differ from that attained in the course of a catalytic reaction. Very few of the studies to be described have been made on an actively catalyzing surface. Moreover, it is becoming more and more clear that the difference between these two states is not always negligible or predictable.

Ever since Taylor[64, 65] first proposed the "active point" concept to account for the extreme sensitivity of catalytic surfaces to poisons, the structural nature of these "points" has been under discussion. With the kinetic studies of Beeck[9] on evaporated metal films, the necessity of the concept came into serious question. Enough evidence is now at hand, however, to attempt a critical review and partial resolution of this question.

Classification of Complexes

The theoretical problem is to account for these variations in terms of the structure of the appropriate complex. It is helpful to consider the question of how one might attempt in principle to calculate the "true" energy of activation of a reaction (or the heat of adsorption). In either case, one takes the total energy to be the sum of the energies of appropriate sub-systems with negligible mutual interactions. These sub-systems will be called "energetic units." The question is now reduced to a decision as to how many surface (and sub-surface) atoms and how many adsorbate atoms have significant interaction energies in the activated complex (or adsorbed state) and thus comprise the energetic unit.

The adsorbate complexes are either single molecules, or a molecule and a set of interacting neighbors, which we will call a *neighborhood.*

The solid phase lepton complexes constitute reaction sites which may be distinguished by their crystal coordination as (1) plane-face leptons, with normal crystal structure through the surface face; (2) *edge* leptons, with normal crystal coordination in a *quadrant* adjoining the edge; (3) *corner* leptons, with normal structure in an *octant* adjoining the corner. Edges and corners may occur at solid-solid phase boundaries, as well as at solid-gas phase boundaries.

The various types of energetic units for surface-adsorbate systems may now be classified.

Type A: One adsorbate molecule + one surface site.
  (1) Adsorbate molecule + surface face.
  (2) Adsorbate molecule + edge.
  (3) Adsorbate molecule + corner.

Type B: More than one adsorbate molecule (neighborhood) + one surface site.
  (1) Neighborhood + surface.
  (2) Neighborhood + edge.
  (3) Neighborhood + corner.

Theories of Catalytic Mechanisms

We are now in a position to describe the chief theories of adsorption and catalysis in common terms. The oldest, Theory I, ascribes a distribution of activation energies to a variation in heats of adsorption plus a constant true activation energy for the reaction. The heat of adsorption is computed from a distribution of energetic units of Types A(1), A(2) and A(3) (the active points on a heterogeneous surface with non-interacting adsorbate). This distribution is supposed to include more and more of the lower energy units as the amount adsorbed increases. Taylor's original thoughts and the usual Langmuir-Hinshelwood formulation of surface kinetics, as well as Halsey's more recent developments[34] underlie Theory I.

Theory II, proposed by Roberts[54], postulates again a constant true activation energy, but a heat of adsorption computed from energetic units of Type B(1). The energy of the unit, however, varies with the structure of the neighborhood of adsorbate molecules, specifically with the average intermolecular distance, which decreases with amount adsorbed. In catalysis, this view has been advocated by Beeck[9]. An obvious variant supposes that several different crystal planes contribute B1 units of different energy. There is thus again a distribution of activation energies similar to that in Theory I.

Theory III, recently advanced by Boudart[14], proposes energetic units of Type A(1), in which the interaction energy between adsorbate and crystal face falls as the amount adsorbed increases. This is ascribed to a shift in the electronic levels of the solid as molecules donate or abstract electrons on adsorption. There is thus once more a distribution of activation energies (through heats of adsorption).

None of these theories has clearly considered the possibility that the "true" activation energy, as well as the heat of adsorption, is nonuniform over the surface, or a function of amount adsorbed. This factor is involved in the statement that the activated complex must not be too tightly bound to the surface, and that only the less tightly bound molecules are catalytically activated. In terms of activated complex theory, this means that in reaction preceded by adsorption, there must be a correlation between heat of adsorption and true activation energy, such that they increase together, at least in certain ranges. Since the apparent activation energy is given by

$$E_{\text{app}} = E_{\text{true}} - \lambda$$

where λ is the heat of adsorption, it is entirely possible for E_{app} to have quite a different distribution than λ for the same set of energetic units if E_{true} is not the same for all of them. The three theories cited all implicitly assume that λ varies (within a certain range) much more widely than the associated values of E_{true}. Outside this range, although λ may be large and the distribution of units such as to include significant contributions, the associated E_{true} are very large. Consequently E_{app} is so large for these units that, even though they are numerous, they contribute negligibly to the average reaction rate.

Thus, the hydrogen initially adsorbed with high heat on a bare nickel film must have a very high activation energy for surface reaction, since it appears not to be active toward small amounts of ethylene. With increased amount adsorbed, however, the activation energy falls and reaction becomes rapid between adsorbed hydrogen and adsorbed ethylene. At still higher coverage, the heat of adsorption falls more rapidly than the true activation energy and the reaction slows again.

Since adsorbed films form spontaneously in many instances, it is usually postulated that such an adsorption precedes activation and reaction on the surface. From this point of view, heterogeneity has been sought in the heat of adsorption. That the heat of adsorption falls as the amount adsorbed increases is abundantly clear[6, 8]. Unfortunately, adsorption measurements alone, being thermodynamic, do not distinguish between the mechanisms cited above. If it be supposed that adsorption is monomolecular and that the adsorbed leptons do not migrate over the surface, the volume adsorbed on each type of site is governed by a Langmuir isotherm:

$$V_i = \frac{S_i b_i p}{1 + b_i p} \tag{1}$$

where S_i = volume adsorbed on complete coverage of type i sites
b_i = adsorption coefficient for i^{th} type of site
The total volume adsorbed is then,

$$V = \sum_i \frac{S_i b_i p}{1 + b_i p} \tag{2}$$

This result is of little use when the individual b_i and s_i are unknown. However, Zeldowitch[85], Taylor and Halsey[66], Roginsky and collaborators[55, 56, 57] and Sips[61, 61a] have all contributed to the inverse problem of fitting Eq. (2) (or its counterpart for a continuous distribution) to experimental isotherms. The most significant result is that the commonly observed Freundlich isotherm arises from an exponential distribution of adsorption energies:

$$S_i = e^{-\Delta H_i/RT} \tag{3}$$

The isotherm resulting is

$$v(p) = [p/(p + a)]^{1/n} \tag{4}$$

where a and n are parameters depending upon the parameters of Eq. (3).

The uniqueness of this converse conclusion is open to question on purely computational grounds. Since the points of an empirical isotherm are subject to a statistical standard deviation, the distribution of adsorption energies derived from it will be subject to statistical errors also. In practice, some specific form for the distribution curve is assumed and its parameters adjusted to give the best fit. The problem is very similar to that of the determination of the energy levels of a molecule by inverting the statistical mechanical formula for its free energy,

$$G = -kT \ln \sum_i G_i e^{-E_i/RT} \tag{5}$$

which has been discussed by Blade and Kimball[13]. In particular, it becomes evident that such a method is powerless to reveal a discrete set of adsorption heats unless the adsorption isotherm shows a series of steps. When this is not the case, a continuous distribution of heats will be found, regardless of the physical reality. Such step-wise isotherms have occasionally been claimed[1, 10], but it is possible that faulty experimental technique may have been responsible for the observations.

Volkenstein[67] has shown in detail how the Freundlich isotherm can arise with uniform binding of adsorbate to the surface if adsorbed leptons interact with a logarithmic potential energy. When this energy is a repulsion, an activation energy for adsorption is found, which increases with surface coverage.

It is thus apparent that criteria other than adsorption isotherms must be found by which to relate heat of adsorption to surface structure.

It is likely that too little emphasis has been placed heretofore upon the structure and chemical nature of the particular catalysts used in experiments purporting to disclose a heterogeneous active surface or its absence. In a few instances, pure single phases are dealt with. These include the evaporated metal films and the thoroughly degassed metal wires as used by Roberts, Langmuir, Becker, Rideal and co-workers.

All supported or oxide promoted catalysts are heterophase and special consideration must be given to their constitution before a comparison with pure metals can be assumed valid. This group includes the extensively studied iron synthetic ammonia catalyst, the reduced nickel and copper catalysts studied by Taylor and his co-workers, and all commercial catalysts.

The reduced pure oxides and degassed powdered tungsten studied by Frankenburg constitute a third group which are potentially pure metals but for which the completeness of reduction is very difficult to establish beyond doubt.

HETEROGENEITY OF CATALYST SURFACES

The interpretation of experiments on chemisorption, activated adsorption and exchange rates must be made in the light of known or reasonable structures for the catalytic surface. For only a few catalysts has this difficult stage of the investigation been pushed very far. It is reasonably sure that the evaporated metal films consist of microscopic crystallites of pure metal, usually oriented at random and having relatively large passages through the aggregate.

Kummer[38] and Emmett have attempted to shed light on the nature of the energetic heterogeneity of the synthetic ammonia catalyst in a study of chemisorption of isotopic carbon monoxide. If radioactive CO is admitted first to the catalyst, followed by inactive CO, the latter should be adsorbed on the weaker sites, if such exist, and should desorb first upon subsequent pumping.

The catalyst was a promoted reduced iron oxide (2.26% Al_2O_3, 0.21% ZrO_2, 0.61% SiO_2), for which the nitrogen physically adsorbed as a monolayer had a volume of 114 cc and the chemisorbed monolayer of CO was 27.5 cc. Sintering the catalyst reduced these values to 108 cc and 19 to 21 cc, respectively. The catalyst was reduced for several hours at 500°C and evacuated overnight at this temperature before each run. The initial additions of CO were usually made at −78°C, after which many hours of evacuation followed at −78°, −30° or 0° to permit the gas to reach the most active points. The second fraction of CO was then added at −78° or −195°C. The sample was subsequently degassed by a collecting diffusion pump at successively higher temperatures, and each sample was analyzed for radioactivity. In all runs, a substantial immediate exchange between the two portions of adsorbed CO was evident in the appearance of radioactivity in the first portions collected upon degassing. When the second portion was added at −195°C after the first radioactive portion at

−78°C, this rapid exchange was much reduced. As the temperature of pumping increased the collected gas became increasingly radioactive. A similar trend, but less marked, was observed when both samples were added at −78°C. When the initial portion was adsorbed at −195°C, the immediate exchange with a second portion adsorbed at −195°C was rapid, in contrast to the rate of exchange at −195°C when the first portion was adsorbed at −78°C. This is ascribed by Kummer and Emmett to the larger initial heat of adsorption on a bare surface at −78°, as measured by Beebe and Stevens[7].

It is striking that addition of oxygen to a monolayer of chemisorbed CO at −78°C did not result in the displacement of CO into the gas, despite uptake of enough oxygen to oxidize about ten layers of iron atoms. The displacement observed on CO addition cannot, therefore, be attributed to the evolution of heat of adsorption, since oxygen adsorption is even more exothermic. Upon degassing at room temperature, some CO_2 was evolved, about one-sixth as much as the CO. The specific activity was the same for both gases, however.

These results do not seem to admit a simple explanation. Although about 50 per cent of the adsorbed CO exchanged rapidly with radioactive CO, it is much too simple an interpretation to conclude that 50 per cent of the surface is really "homogeneous" and devoid of "active points." The formation of surface complexes of CO_2 when O_2 was added cannot be ruled out, and would be analagous to the results of Garner and co-workers[28] on cuprous oxide.

Eischens[23] has studied the kinetics of this exchange reaction using a radioactive carbon monoxide over a reduced iron catalyst. In two runs, he reports three or four distinct periods of constant, but different, specific rates, which decline in successive periods in the ratios $\infty:89:7:1$ and $\infty:60:1$, respectively. Although the data are incomplete, they suggest a heterogeneity of at most four species of surface, each with its characteristic exchange rate.

Kummer and Emmett[39] have made a similar study of the exchange between N_2^{30} and N_2^{28} over the same catalyst (No. 423) as was used in their CO studies and, in addition, over a doubly promoted catalyst (No. 435) containing 0.8 per cent Al_2O_3 and 0.25 per cent K_2O. The exchange velocity was high over both catalysts, but was considerably faster over catalyst No. 423, which contained no alkali. This rapid exchange is in contradiction to earlier work of Joris and Taylor[35] who found very slow exchange at 450 to 500°C. More recent work by McGeer[47] has demonstrated that reduction of the catalyst had been incomplete in Joris and Taylor's work and that the exchange rate is extremely sensitive to traces of remaining oxygen. When hydrogen was passed over the catalyst in a horizontal boat (Joris and

Taylor), the reduction was insufficiently complete. A similar reduction in which gas passed vertically through the catalyst (Kummer and Emmett; McGeer) produced a high exchange activity. McGeer concludes that the iron atoms active in nitrogen exchange have an excess free energy of at least 8 kcal. Almquist and Black[2] had concluded from the effect of oxygen poisoning on ammonia synthesis that active surface iron atoms had excess free energies ranging as high as 11 kcal, in reasonable agreement with the later work.

Kummer and Emmett[39] found that isotopic mixing was uniform over the surface, as judged by experiments similar to those with CO previously described. Thus, at 500°C, the catalyst was first equilibrated with 6.8 cc of heavy N_2; then 7.6 cc of normal N_2 was added, giving a gas pressure of 74 mm. After 14 minutes, the gas phase was pumped off and its analysis was compared with that of the adsorbed nitrogen. No difference was noted. In a second run, at much lower pressures, the adsorbed gas was removed in two portions, which again had the same isotopic composition. Thus in this case there is no evidence for a nonuniform binding energy on different parts of the surface at temperatures at which the catalyst is active for ammonia synthesis. Presumably if such heterogeneity does exist, its detection in these experiments is prevented by a very rapid surface migration of the adsorbed nitrogen.

Joris and Taylor as well as Kummer and Emmett noted that the equilibrium heavy nitrogen content over the reduced catalyst was markedly lower than in the original added nitrogen. This apparent dilution is far too great to be explained by preferential adsorption of one isotope, and is accounted for by the presence of adsorbed normal nitrogen picked up from traces present in the hydrogen during reduction. This gas must have survived even 24 hours' pumping at 500°C.

A similar phenomenon was observed by Weber and Laidler[72] over a singly promoted catalyst (No. 631) in a study of the exchange of NH_3 and D_2. At 122°C, a mixture of deuterated ammonia was rapidly pumped off to a residual pressure of less than one micron. The reaction vessel was then closed off from the pumps and the rate of desorption of the mixed ammonia was found to be about 5×10^{-9} mole sec^{-1}. The isotope NH_3 was then added to give a pressure of 20 cm and the rate of desorption of the deuterated ammonias was found to be about 1.4×10^{-6} moles sec^{-1}, an increased rate of about 300-fold. Moreover, admission of ammonia to the catalyst increased the rate of desorption of deuterium by at least ten-fold. Similar behavior was noted in the desorption of ammonia at room temperature from the glyptal coated brass wave guide of the micro-wave spectrometer used for analysis of the ammonia-gas mixture.

Farkas and Farkas[26] observed a similar phenomenon in the exchange of

H_2 and D_2 on quartz at 720°C. For this case, the reaction $H_2 + D_2 \rightleftharpoons 2HD$ can occur readily and could account for the enhanced desorption of deuterium in the presence of hydrogen.

At the lower temperatures of Weber and Laidler's work, the exchange rates are too slow to account for the enhanced desorption rates and, in any case, cannot explain the effect of ammonia pressure on the rate of deuterium desorption. Kummer[37] has suggested that place exchange of molecules adsorbed on adjacent high energy and low energy sites, followed by desorption from the low energy sites, could account for Weber and Laidler's observations. A third explanation depends upon supposing the binding energy to decrease uniformly as the surface coverage increases.

Present data do not permit a decision between these two last alternatives. If enough were known about the surface mobility of adsorbed ammonia and deuterium molecules, perhaps the place-exchange hypothesis could be made more quantitative. In particular, it is not clear to what extent the reduced oxide promoter is involved in ammonia adsorption. The reduced catalyst consists of at least two solid phases[15], one being a very finely divided alumina, possibly retaining some unreduced iron. The possibility exists that this may bind ammonia very tenaciously, as do the alumino-silicates, for example, and yet permit fairly rapid surface migration. If one supposes that at each moment the total adsorbed ammonia is distributed in some equilibrium way between iron surface and alumina surface, but evaporates only from the iron surface, it is readily shown* that the rate of desorption should increase with total surface coverage. All that need be postulated is the mobility of adsorbed molecules over all of the surface, regardless of its heterogeneity or homogeneity.

Less direct evidence is offered by the measurements of Kwan and Izu[41] on the rate of chemisorption of hydrogen on reduced copper. They found a very slow reaction at 300 to 400°C with an activation energy of 20.5 kcal. Using the activated state theory to calculate the rate of formation[42] of an activated complex involving G metal sites per mole of H_2, it was found possible to reproduce the observed rate of adsorption within a factor of two under the assumption that every exposed copper atom in the (110) plane is equally efficacious. The known approximations in this sort of comparison are large enough to prevent a more precise quantitative check, but one can at least conclude for this case that a substantial fraction of the exposed surface was active in chemisorption.[40]

* Thus, if A is the gas adsorbed on alumina and F the amount adsorbed on iron, we may write the partition equilibrium as $A = KF$, whence

$$F = \frac{A + F}{1 + K} \tag{6}$$

PURE METALS

The extensive work of Beeck and co-workers on the behavior of hydrogen and ethylene on evaporated metal films has led them to the belief that the active surface is substantially uniform in properties and includes most of the exposed crystal planes. Nor does it now appear that these catalysts are peculiarly active. Emmett[24] has found rapid exchange between H_2 and D_2 on iron synthetic ammonia catalysts at −195°C. Sadek and Taylor[58] find the same reaction to be rapid on nickel-chromia at the same temperature. Wright[84] has found the same catalyst to be at least ten times as active as evaporated nickel films at −78°C for ethylene hydrogenation. In view of the difficulty and critical importance of attaining complete reduction of the catalyst, it may well be questioned whether the older work[50, 51] on catalyst poisoning, which gave rise initially to the concept of a relatively few "active points," may have been done on chemically heterogeneous and partially oxidized surfaces.

Field Emission Studies

Even as pure a metal surface as can be afforded by a well degassed tungsten point displays remarkable heterogeneity for electron emission as well as for adsorption of foreign gases[49]. A tungsten wire etched to a tiny point consisting of a single crystal develops when heated a nearly spherical surface. It thus exposes all the possible crystal planes. Upon applying an electric field of about 50,000,000 volts/cm, electrons are ejected from the point at room temperature and below and may be caught upon a fluorescent screen on a projection tube. A characteristic pattern of light and dark spots is thus obtained which displays the symmetry of the metallic lattice and shows great differences in the work function for emission from different planes.

When foreign leptons are adsorbed on this tungsten tip, changes occur in the emission pattern which are characteristic for the adsorbed species. It is obvious that barium, for instance, is preferentially adsorbed on the 110 plane and here greatly reduces its work function, resulting in enhanced emission from this plane. As the temperature of the wire tip is raised, the diffraction spots evident in the pattern become mobile, and the barium deposit is seen to spread more uniformly to other planes.

Especially striking is the adsorption of carbon residues from organic matter on just those planes of tungsten atoms on which a condensed ring lattice can be fitted with one tungsten atom in the center of each ring. As the temperature of the wire rises, this deposit "melts," only to reappear upon cooling. Films of alumina likewise are mobile at sufficiently high temperatures, but congeal preferentially on certain lattice planes as the temperature is lowered.

The field emission microscope has afforded the most direct evidence that lattice planes have specific properties, and one need seek no further for heterogeneity in reduced metals. Beeck, Smith and Wheeler[9] have demonstrated that these properties include their catalytic influence, at least in the case of nickel, and Becker[4, 5] has abundantly confirmed Müller's observations with the projection tube. The extension of this technique to specific catalytic problems has yet to be carried out, and it seems to offer great promise as an investigative tool.

Massive Single Crystals

The work of Gwathmey and co-workers[32, 33, 44, 45] with large single crystals of copper, nickel, cobalt and iron is equally significant.

Very similar observations are reported by Gomer[30, 31] for field emission from nickel points. The oxide and carbide structures observed seem to bear little resemblance to bulk phase structures. Klein[36] has studied the reaction of carbon on tungsten with oxygen on tungsten by observing field emission patterns and suggests that the breaking of W—O bonds is rate controlling. Here also reactivity can be associated with definite crystal planes. The reaction of carbon monoxide with nickel[45] to produce a carbon deposit on a large single crystal was found to proceed at least 1000 times faster on the (111) face than on the (110) or (100) face. This is in contrast to Gomer's[30, 31] observations on the field emission of carbon-contaminated Ni tips, which showed adsorption to be most persistent on the (110) plane and hardly discernible on the (111) plane. It is likely that the surface in Gwathmey's case was covered initially by at least a monolayer of oxygen. In Gomer's case, however, it was initially free of adsorbed matter. It is evident that any interpretation based naïvely on equality of lattice parameters or "fit" of adsorbed leptons on lattice planes must be considered with considerable caution.

That the adsorbent solid enters actively into the mechanism of some catalytic reactions is suggested by Gwathmey and Leidheiser's observations of the hydrogen-oxygen reaction on copper. As reaction proceeds, the surface of a single lattice plane of copper recrystallizes and develops a characteristic pattern visible under the microscope. This could occur only by extensive surface diffusion and is induced by the gaseous atmosphere. Hence one must conclude that metal atom mobility is a reality under these conditions.

PROMOTED METALS

Most commercial "metal" catalysts contain minor amounts of substances called *promoters*, found to increase the activity or selectivity of the metal toward certain substrates. In general, these promoters may be (a) metals reducible under the conditions used to activate the catalyst, or (b) metal oxides not reducible under these conditions. The nature of the resulting surface and the mechanism of promoter action may be quite different in the two cases.

Alloys

The first case results either in an alloy catalyst or a heterophase metal-alloy system. It is likely that effects on catalytic activity thus induced are to be ascribed to a change in the electronic structure of the metal. The series of investigations on alloy catalysts begun by Rienäcker[53] and continued by Schwab and co-workers[60] are consistent with the general viewpoint proposed by Dowden[20] and demonstrated by several workers since[11, 17, 21, 52, 63].

The typical reactions investigated include hydrogenation of olefins, aromatics and alkynes; and dehydrogenation of alcohols and formic acid. In most cases, the rate constants for the catalytic reaction can be correlated reasonably well with such functions of the electronic structure as (1) lattice parameter, (2) saturation magnetic moment, (3) "*d*-bond character," (4) hardness, (5) Hume-Rothery's electron density. However, a completely satisfactory study has not yet been made. In some cases, the metallic phase has not been established in comparing a series of alloys; in others, the surface areas have not been determined. Since Beeck's demonstration of the difference in activity of different crystal faces, it would seem essential to establish at least that no preferential crystal habit was developed in the series of alloys studied, but this has not been done.

The electronic structure of the ideal metal or alloy crystal is only one of the factors that determines the free energy of the activated surface complex. To assess its relative importance, one must compare a series of metals and alloys which present (a) the same crystallographic configuration to the reactants (differing at most in lattice parameter, but not in symmetry), (b) a known surface area and (c) a known density of dislocations at the surface (or at least equal densities). Under the circumstances, differences between catalysts can be ascribed with some confidence to the differences in the electronic binding between adsorbate and catalyst as influenced by the electronic structure of the ideal metal or alloy crystal. Needless to say, these conditions are not easy to satisfy. Some ambiguity must, therefore, remain in the interpretation of the data obtained thus far.

It is quite likely that the process of forming the metal or alloy results in imperfections in the ideal lattice structure, at least at the surface. With these are associated local perturbations of the electronic structure of the ideal lattice which may result in particularly stable surface complexes. Nearly all observers working with evaporated metal films or clean tungsten wires report high heats of adsorption for the initial increments of adsorbate, which fall more or less rapidly with surface coverage. However, it does not appear that this tenaciously bound adsorbate is always available for catalytic reaction. The process of ageing or "sintering" a metal catalyst undoubtedly involves the destruction of the least stable of these surface imperfections by recrystallization, migration of dislocations and grain growth. That similar results can be obtained by prolonged catalytic use is a matter of practical knowledge that has been particularly well demonstrated by Gwathmey's[18, 45] work on the hydrogen-oxygen reaction on single crystals of copper and nickel. Here the course of the catalytic reaction results in the development of particular crystal facets, and the addition of alloying metals such as zinc and silver markedly influenced the choice of facets. Moreover, the resulting surface is not that in equilibrium with the metal vapor or with hydrogen at 500° to 1000°C, for annealing under these conditions results in "polishing" the reaction roughened surface.

In the light of these and other related observations, one may reasonably question the significance of the initial heat of chemisorption of hydrogen for the rate of catalytic hydrogenation. Since it is abundantly clear that only in very special cases will a catalytic surface "hold still" during use, inferences with respect to catalytic properties drawn from the properties of unused, fresh surfaces must be received with considerable reserve.

The nature of the catalytic reaction also has an important bearing on the type of surface binding to be postulated. The small atom of hydrogen is easily accommodated in the interstices of any metal lattice, and it is reasonable to suppose that chemisorbed hydrogen is held in part as "alloy" in the surface layers. Thus organic substrates may be expected to prepare their own surfaces for catalytic reaction.

In a reaction like the oxidation of SO_2 on platinum, however, conditions may be somewhat different, for even a chemisorbed monolayer of oxygen cannot be expected to penetrate the platinum lattice. At the temperature of the reaction (400 to 500°C), however, the metal atoms may be mobile in the surface layers and the characteristic structures may be quite different from those present during hydrogenation at much lower temperatures. One is thus led to question the pertinence of kinetic data on $H_2 - D_2$ exchange at low temperatures, for example, to the problem of the nature of the adsorbed complexes in benzene hydrogenation at 100 to 200°C or in reactions not involving hydrogen activation.

Oxide Promoters

The second type of promoter for metals, unreducible oxides, almost certainly results in a hetero-phase catalyst. The most intensively studied catalysts of this sort are the iron synthetic ammonia catalysts promoted with alkali oxides and alumina. Since these are discussed in detail in Volume III only a summary treatment will be given here.

The catalyst is formed by reduction of a fusion of iron oxide (Fe_3O_4) with promoters, during which process considerable internal surface and pore volume develops. The role of alumina is partly, if not chiefly, to stabilize this porous structure. It is also claimed that some unreduced iron is retained in a γ-Al_2O_3-Fe_2O_3 phase, but whether this has any bearing on the catalytic activity is uncertain.

Alkalies, such as sodium, potassium, and rubidium have definite promoting effects. They must be accompanied in the catalyst by equivalent amounts of oxide ion, but it is not established in what phases the alkali oxide is to be found. Several possibilities exist. The alkali may be associated with the alumina and assist in stabilizing the γ-Al_2O_3 structure. Alternatively, it may be dispersed on the metal surface, where it may be thought of as relatively independent adsorbed alkali and oxide ions. This latter possibility is similar to the case of tungsten, on which alkalis are adsorbed as positive ions and oxygen as negative ions. These adsorbed layers have large effects on the work function for electron emission and attempts have been made to relate such effects to catalytic activity. The high sensitivity of the catalyst to poisoning by gaseous oxygen is consistent with this view, if one supposes the slow step in the catalytic reaction to be inhibited by a negative surface charge on the metal.

Emmett and co-workers have noted that the relative adsorption capacities of reduced iron catalysts for carbon monoxide and carbon dioxide at low temperatures are consistent with the relative numbers of exposed metal and alkali atoms as calculated on reasonable hypotheses concerning their dispersion. Comparison of a series of catalysts which differed only in the amount of alkali promoter showed[46] that, while the total surface decreased with increase of alkali, the specific activity for ammonia decomposition increased. Furthermore, the fraction of the surface covered by iron decreased as alkali was added, as did the fraction (by difference) covered by free Al_2O_3, the atom ratio Fe/Al_2O_3 in the surface remaining constant at $\sim$1.9 for a series of five catalysts. Alkali thus causes a decrease in the portion of the surface present as iron, and the fraction present as free aluminum oxide, but promotes ammonia decomposition.

The interpretation is complicated by the observation of a change in the apparent order of the reaction upon addition of alkali promoter in the temperature range from 350 to 440°C. The singly promoted catalysts (Al_2O_3 only) show zero temperature coefficient and promotion by hydrogen in this temperature region. As alkali is added, the temperature coefficient increases and the effect of hydrogen progressively declines, becoming an inhibition at the highest alkali contents. More data will be required to elucidate this complex behavior.

It is not impossible, of course, that the alkali and alumina exist partly as separate phases and partly as a surface layer of alkali aluminate. The alkali may function as a flux in the spreading of alumina on the iron surface[62]. It can thus promote grain growth and loss of area incidental to its specific effects on the catalytic reaction. Gwathmey's results on copper and nickel[45] suggest that such a surface layer might have a decisive influence on the type of lattice plane presented by the iron crystal facets during the catalytic reaction.

None of these speculations, however, can be said to have any firm experimental basis as yet.

OXIDE CATALYSTS

The nature of surface complexes on oxide catalysts is fully as speculative a question as for metals. The number of reasonable possibilities is enhanced by the likelihood that strongly polarized or ionic adsorbates can be stabilized on ionic lattices, so that all degrees of ionicity might be expected in the surface complexes on such catalysts. In addition, the ease of electron transfer over macroscopic distances in semiconductors makes it unnecessary that the active donor or acceptor centers in the surface be immediately adjacent to the adsorbate lepton. Theory thus presents little or no restriction on the postulated surface structures and one must resort to experimental means of distinguishing the possibilities.

Irreducible Oxides

The group of catalysts comprising silica gels and silica-aluminas contain no readily oxidizable or reducible ion. They show very small electronic conductivity[74]. As a group they are nearly inert toward hydrogenation by molecular hydrogen, but are active for hydration-dehydration, hydrocarbon cracking, isomerization and hydrogen transfer from cycloalkanes to aromatics and olefins. The very extensive investigations on the mechanisms of these hydrocarbon reactions[27] have resulted in the "carbonium ion" theory for these systems. The adsorbed hydrocarbon is here assumed to have the reactivity of a carbonium ion, although investigators differ in the degree of ionicity they are willing to assign to the carbon-catalyst bond. Since the principal features of the reactivity of carbonium ions are well-established in the chemistry of acid-base catalyzed homogeneous organic reactions, there is a reasonable basis for judging the merits of this theory. The solid catalyst is presumed to have the properties of a generalized acid and, indeed, far-reaching analogies can be drawn between silica-alumina catalysts and acid catalysts such as sulfuric acid, phosphoric acid and aluminum chloride.

Oxide ions on silica and silica-alumina catalysts exchange readily with boiling water[48] and with gaseous oxygen at 400 to 500°C[79, 82, 83]. This is evidence for a very mobile surface at the temperatures at which most oxide-catalyzed reactions occur. Under such circumstances, it is difficult to see how molecular fields determined by lattice symmetry can be determinative. However, nearest-neighbor complexes similar to those found in polar solvents may be stabilized by the polar field of the catalyst surface, even though specific surface coordination is not present[25]. The same situation is found in aqueous solutions, in which the non-specific molecular field of the solvent dielectric serves to stabilize ionic structures not found in the gas phase. From this standpoint, one would look to inorganic complex ions for the prototype of the surface complexes participating in catalytic reactions.

Reducible Oxides

A second large class of oxide catalysts comprises oxides with reducible or oxidizable cations, sometimes coprecipitated with or supported on nonreducible oxides (e.g., chromia-alumina). Many of these show semiconductor properties under catalytic conditions, and numerous conjectures have been made concerning possible connections of conductivity with catalysis as pointed out in Chapter 3; however, a simple, direct correlation does not seem to exist.

This group, in addition to the typical activities of the silica-aluminas, also have good hydrogenation and dehydrogenation activity when properly activated. If one extends the ionic mechanisms postulated for "acid" catalysts to this case, one is forced to postulate that these catalysts are capable of polarizing the hydrogen molecule to permit it to add ionically. Such polar mechanisms are well established for the homogeneous halogenation of olefins[80], in which the solvent acts as a polarizing agent in the double-bond, halogen activated complex. Similar behavior of the hydrogen molecule is much rarer, only two homogeneous catalytic hydrogenations being known at present. The first of these, the hydrogenation of quinone to hydroquinone in quinoline solution of cuprous acetate, was discovered by Calvin[16]. Hydrogen-deuterium exchange and ortho-para hydrogen conversion also proceed over this catalyst[75, 81]. The second example is the high pressure catalysis of butyraldehyde hydrogenation by cobalt hydrocarbonyl, proposed as a homogeneous reaction by Wender[76, 77].

In addition, there is considerable evidence that the "oxo" or hydroformylation reactions of olefins with carbon monoxide and hydrogen are homogeneously catalyzed by cobalt hydrocarbonyl[78]. The reduction of aqueous solutions of metal salts by hydrogen is well-known and, in some cases at least, is initiated homogeneously.

Thus it appears that hydrogen can be activated by isolated molecules or complex ions. In the light of these examples, the postulate of a similar activation by surface complexes in oxide catalyst is not completely unreasonable.

Semiconductors

The recent attempts to link catalytic and electrical properties of semiconducting solids have already been discussed in Chapter 3. The basic viewpoint can be summed up in the concept of the necessity for cooperative action of all the leptons of the crystal structure in providing the catalytic activated complexes. Thus, any properties which depend essentially upon the band theory of solids for their explication do not exist in systems consisting of only a few leptons. The alternative viewpoint is that at most a few ions or atoms are essentially involved in the activated complex. In this case, the structures and binding are qualitatively the same as are found in homogeneous gases, pure liquids or solutions. That the solid phases also have cooperative properties is, on this view, coincidental.

One may seek the significant catalytic properties of chromia-alumina in the type and magnitude of its semiconductivity[74], or one may consider the degree of oxidation of the surface as the significant variable[68, 69]. In the former case, one is led to consider properties of assemblies of many leptons in a surface, such as electronic barrier layers[73], surface potential and electronic conductivity. In the latter case, one is led to consider chemical entities, such as CrO_3, free or "adsorbed," stabilization of unusual catalytic complex ions by the surface environment, solid acids, and solid oxidants. The former picture considers the surface as homogeneous, at least in some average sense. The latter picture emphasizes variability in the reactivity of particular neighboring surface atoms. The former model draws on solid-state physics for its concepts; the latter refers to the chemistry of complex ions.

It is much too soon to do more than point out the two viewpoints. The decisive experiments are yet to be made. Moreover, as knowledge accumulates, probably neither simple picture will be found adequate, yet each will have its range of usefulness as a guide to future work.

The extensive work reported on the decomposition of nitrous oxide illustrates a partial meeting of these two views[3, 19, 43, 59, 70]. The initial step in this reaction appears to be the dissociative adsorption

$$N_2O + e \rightarrow N_2 + O^-_{ads} \qquad (7)$$

Here the electron is furnished by the catalyst and the singly charged oxide ion is retained on the surface. Subsequently, the two following steps may occur:

$$O^-_{ads} + O^-_{ads} \rightarrow O_2(g) + 2e \qquad (8)$$

$$O^-_{ads} + N_2O \rightarrow N_2 + O_2 + e \qquad (9)$$

The electrons are here returned to the catalyst.

When *p*-type semiconducting oxides undergo reaction (7), the loss of an electron creates a positive hole and should enhance the conductivity. This enhancement has been observed in the case of N_2O decomposition on nickel oxide[71]. The analogous adsorption of molecular oxygen on cuprous oxide and nickel oxide, even at room temperature produces a similar rise in conductivity[29]. These reactions are undoubtedly very fast at 200 to 300°C on *p*-type oxides. The desorptions, reactions (8) and (9), are somewhat slower than reaction (7), since added oxygen is observed to inhibit the decomposition.

With *n*-type oxides, the electrons are furnished by the donors and the adsorbed oxide ion can be considered as an electron trap. In general, however, the ionization energy of these trapped electrons is much less than that of the donors. Hence only at high temperatures will there be an appreciable number of adsorbed oxide ions possible. As the temperature rises, moreover, reaction (8) is accelerated more than (9). Hence more anion vacancies (or donors) are available at high temperatures.

This is consistent with the general observation[19] that *n*-type oxides show activity at temperatures above 600°C, whereas *p*-type oxides are active below 300°C. In the range 300 to 600°C, the ionic insulator oxides MgO, CaO and Al_2O_3 are active. For the latter group, the observations of rapid surface oxide exchange with gaseous oxygen[82] at these temperatures is evidence that there must be abundant anion vacancies in the surface. These sites will stabilize the adsorbed oxide traps very greatly and thus permit reaction (7) to occur.

The electron furnished by the catalyst in reaction (7) comes, of course, from some particular lepton in the lattice. In *p*-type oxides, it is usually the lattice cation that acts as the donor. From the chemical standpoint, this amounts to increasing its valence (oxidation). In *n*-type oxides, the interstitial excess atoms are the donors. In insulators, it is most likely that double negative oxide ions are the donors, since the cations are especially difficult to oxidize.

The question remaining is whether the donor needs to be in the surface or whether it can be in the interior of the crystal. The cooperative model is noncommittal on this question, but suggests that, since electronic conductivity in bulk is possible, that interior donors can supply electrons to the surface traps. Studies by Anderson and co-workers[12] on the response of the conductivity of sintered oxides to changes in the partial pressure of oxygen suggest that this is indeed the case.

On the other hand, Voltz and Weller[69] report a quantitative relation between activity of chromia and chromia-alumina for decomposition of hydrogen peroxide and the amount of excess oxygen, expressed as CrO_3, in the *surface*, as determined by iodometric titration, or by pH as compared with the pH of pure CrO_3 solutions. The amount of excess oxygen thus determined corresponds to less than a monolayer. There was no evidence of interior oxidation. These observations make it extremely unlikely that, in this case, interior cations contribute electrons to the activated complex.

The large *n*-type conductivities measured by Weisz on similar catalysts during dehydrogenation of cyclohexane at 480°C, may be chiefly in the surface layers. This suggests that the reacting atmosphere rapidly establishes an oxidation-reduction steady state in the surface which regulates the concentrations and kinds of sites active in the reaction being catalyzed. For decomposition of oxides (N_2O or H_2O_2) it is probably donors (or excess oxide) which are essential. For decomposition of hydrides (hydrocarbons) it is acceptors (or oxidized cations) which are essential. In either case, the donors (or acceptors) supply (or receive) electrons to (or from) the adsorbate, which thus constitutes a surface trap for electrons (or holes). In so doing, the adsorbate is chemically activated for the reaction in question. This reaction may proceed through steps having little to do with the electronic conductivity of the reacting catalyzed system. Thus, in Weisz's *n*-type chromia catalyzing dehydrogenation, it is likely that the donors active in conductivity are Cr^{+2} ions stabilized by adsorbed cyclohexane (or benzene). Once formed, however, they may not participate in the active complex beyond contributing to the polarizing of a surface hydrocarbon complex. With an oxidizing substrate, one would expect a high *p*-type conductivity in chromia during the catalysis.

It is apparent that much work remains to be done before any conclusion can be drawn concerning the nature of the catalyst surface or the complexes found thereon during catalytic reactions.

References

1. Allmand, A. J., Burrage, L. J., and Chaplin, R., *Trans. Faraday Soc.*, **28,** 218 (1932).
2. Almquist, J. A., and Black, C. A., *J. Am. Chem. Soc.*, **48,** 2814 (1926).
3. Amphlett, C. B., *Trans. Faraday Soc.*, **50,** 273 (1954).
4. Becker, J. A., *Bell System Tech. J.*, **30,** 907 (1951).
5. Becker, J. A., and Hartman, C. D., *J. Phys. Chem.*, **57,** 153 (1953).
6. Beebe, R. A., "Handbuch der Katalyze," Vol. IV, Berlin, J. Springer, 1943.
7. Beebe, R. A., and Stevens, N. P., *J. Am. Chem. Soc.*, **62,** 2137 (1940).
8. Beeck, O., Cole, W. A., and Wheeler, A., *Discussions Faraday Soc.*, **1950**, 314.
9. Beeck, O., Smith, A., and Wheeler, A., *Proc. Roy. Soc.* London, **A177,** 62 (1940).
10. Benton, A. F., and White, T. A., *J. Am. Chem. Soc.*, **53,** 3301 (1931).
11. Best, R. J., and Russell, W. W., *J. Am. Chem. Soc.*, **76,** 838 (1954).
12. Bevan, D. J. M., and Anderson, J. S., *Discussions Faraday Soc.*, **1950,** 238.

13. Blade, E., and Kimball, G. E., *J. Chem. Phys.*, **18,** 626 (1950).
14. Boudart, M., *J. Am. Chem. Soc.*, **74,** 3556 (1952).
15. Brill, R., *Z. Elektrochem.*, **38,** 669 (1932).
16. Calvin, M., *Trans. Faraday Soc.*, **34,** 1181 (1938).
17. Couper, A., and Eley, D. D., *Discussions Faraday Soc.*, **1950,** 172.
18. Cunningham, R. E., and Gwathmey, A. T., *J. Am. Chem. Soc.*, **76,** 391 (1954).
19. Dell, R. M., Stone, F. S., and Tiley, P. F., *Trans. Faraday Soc.*, **49**, 201 (1953).
20. Dowden, D. A., *J. Chem. Soc. (London)*, **1950,** 242.
21. Dowden, D. A., and Reynolds, P. W., *Discussions Faraday Soc.*, **1950,** 184.
22. Eggleton, A. E. J., *Discussions Faraday Soc.*, **1950,** 195.
23. Eischens, R. P., *J. Chem. Phys.*, **19,** 377 (1951).
24. Emmett, P. H., and Kummer, J. T., *J. chim. phys.*, **47,** 67 (1950).
25. Eyring, H., Hulburt, H. M., and Harman, R. A., *Ind. Eng. Chem.*, **35,** 511 (1943).
26. Farkas, A., and Farkas, L., *Trans. Faraday Soc.*, **31,** 821 (1935).
27. Frankenburg, W. G., Komarewsky, V. I., and Rideal, E. K., "Advances in Catalysis," Vols. III, IV, New York, Academic Press, Inc., 1951, 1952.
28. Garner, W. E., Gray, T., and Stone, F. S., *Proc. Roy. Soc.*, **A197,** 294 (1949).
29. Garner, W. E., Gray, T., and Stone, F. S., *Discussions Faraday Soc.*, **1950,** 246.
30. Gomer, R., *J. Chem. Phys.*, **21,** 293 (1953).
31. Gomer, R., and Spear, D. A., *J. Chem. Phys.*, **21,** 730 (1953).
32. Gwathmey, A. T., and Benton, A. F., *J. Chem. Phys.*, **8,** 569 (1940).
33. Gwathmey, A. T., and Benton, A. F., *J. Phys. Chem.*, **44,** 35 (1940).
34. Halsey, G., *J. Chem. Phys.*, **16,** 931 (1948).
35. Joris, G. J., and Taylor, H. S., *J. Chem. Phys.*, **7,** 893 (1939).
36. Klein, R., *J. Phys. Chem.*, **21,** 1177 (1953).
37. Kummer, J. T., personal communication.
38. Kummer, J. T., and Emmett, P. H., *J. Am. Chem. Soc.*, **73,** 2886 (1951).
39. Kummer, J. T., and Emmett, P. H., *J. Chem. Phys.*, **19,** 289 (1951).
40. Kwan,T., *J. Research Inst. Catalysis, Hokkaido Univ., Sapporo, Japan*, **1,** No. 2, 95 (1949).
41. Kwan, T., and Izu, I. *Catalyst*, **4,** 28 (1948).
42. Kwan, T., and Kujirai, M., *J. Chem. Phys.*, **19,** 798 (1951).
43. Laidler, K. J., in "Catalysis," Ed. by P. H. Emmett, Vol. I, pp. 146–148, New York, Reinhold Publishing Corp, 1954.
44. Leidheiser, H. Jr., and Gwathmey, A. T., *J. Am. Chem. Soc.*, **70,** 1200 (1948).
45. Leidheiser, H., Jr., and Gwathmey, A. T., *J. Am. Chem. Soc.*, **70,** 1206 (1948).
46. Love, K. S., and Brunauer, S., *J. Am. Chem. Soc.*, **64,** 745 (1942).
47. McGeer, J. P., Doctoral Thesis, Princeton Univ., 1949.
48. Mills, G. A., and Hindin, S. G., *J. Am. Chem. Soc.*, **72,** 5549 (1950).
49. Müller, E. W., *Physikal Z.*, **37,** 838 (1936).
50. Pease, R. N., *J. Am. Chem. Soc.*, **45,** 1196 (1923).
51. Pease, R. N., and Stewart, L., *J. Am. Chem. Soc.*, **47,** 1235 (1925).
52. Reynolds, P. W., *J. Chem. Soc. (London)*, **1950,** 265.
53. Rienacker, G., and Sarry, B., *Z. anorg. Chem.*, **257,** 41 (1948) and references cited there.
54. Roberts, J. K., *Proc. Roy. Soc. (London)*, **A161,** 141 (1937).
55. Roginsü, S. Z., *Compt. rend. acad. sci. U.S.S.R.*, **45,** 61, 194 (1944).
56. Roginsü, S. Z., *Compt. rend. acad. sci. U.S.S.R.*, **47,** 412, 478, 558 (1945).
57. Roginsü, S. Z., and Todes, O., *Acta Physicochim. U.S.S.R.*, **20,** 307, 695 (1945).
58. Sadek, H., and Taylor, H. S., *J. Am. Chem. Soc.*, **72,** 1168 (1950).

59. Schmidt and Keller, *Naturwissen*, **37,** 43 (1950).
60. Schwab, G. M., *Discussions Faraday Soc.*, **1950**, 166 and references cited there.
61. Sips, R., *J. Chem. Phys.*, **16,** 490 (1948).
61a. (Quoted in "Advances in Physical Chemistry," Ed. by. G. H. Rollefson and R. E. Powell, Vol. I, 277, Stanford, California, Annual Reviews, 1950).
62. Smith, C. S., in "Imperfections in Nearly Perfect Crystals," Ed. by W. Shockley, Chap 14, New York, John Wiley & Sons, Inc., 1952.
63. Stowe, R. A., and Russell, W. W., *J. Am. Chem. Soc.*, **76,** 319 (1954).
64. Taylor, H. S., *Proc. Roy. Soc.*, **A108,** 105 (1925).
65. Taylor, H. S., *J. Phys. Chem.*, **30,** 145 (1926).
66. Taylor, H. S., and Halsey, G., *J. Chem. Phys.*, **15,** 624 (1947).
67. Volkenstein, F. F., *J. Phys. Chem. U.S.S.R.*, **21,** 163 (1947).
68. Voltz, S. E., and Weller, S., *J. Am. Chem. Soc.*, **75,** 5227, 5231 (1953).
69. Voltz, S. E., and Weller, S., *J. Am. Chem. Soc.*, **76,** 1586 (1954).
70. Wagner, C., *J. Chem. Phys.*, **18,** 69 (1950).
71. Wagner, C., and Hauffe, K., *Z. Elektrochem.*, **44,** 172 (1938).
72. Weber, J., and Laidler, K. J., *J. Chem. Phys.*, **19,** 1089 (1951).
73. Weisz, P. B., *J. Chem. Phys.*, **21,** 1531 (1953).
74. Weisz, P. B., Prater, C. D., and Rittenhouse, K. D., *J. Chem. Phys.*, **21,** 2236 (1953).
75. Weller, S., and Mills, G. A., *J. Am. Chem. Soc.*, **75,** 769 (1953).
76. Wender, I., *J. Am. Chem. Soc.*, **72,** 4842 (1950).
77. Wender, I., Levine, W., and Orchin, M., *J. Am. Chem. Soc.*, **72,** 4375 (1950).
78. Wender, I., Sternberg, H. W., and Orchin, M., *J. Am. Chem. Soc.*, **75,** 3041 (1953).
79. Whalley, E., and Winter, E. R. S., *J. Chem. Soc. (London)*, **1950,** 1175.
80. Wheland, G. W., "Advanced Organic Chemistry," pp. 293–301, New York, John Wiley & Sons, Inc., 1949.
81. Wilmarth, W. K., and Barsch, M. K., *J. Am. Chem. Soc.*, **75,** 2237 (1953).
82. Winter, E. R. S., *Discussions Faraday Soc.*, **1950,** 231.
83. Winter, E. R. S., *J. Chem. Soc. (London)*, **1950,** 1170.
84. Wright, M., Quoted by Taylor, H. S., in "Advances in Physical Chemistry" (Edited by G. H. Rollefson and R. E. Powell), Vol. I, 277, Stanford, California, Annual Reviews, 1950.
85. Zeldowitch, J., *Acta Physicochim. U.S.S.R.*, **1,** 961 (1934).

CHAPTER 5

GENERAL THEORIES OF HETEROGENEOUS CATALYSIS*

Ransom B. Parlin, Merrill B. Wallenstein, Bruno J. Zwolinski, and Henry Eyring

Department of Chemistry, University of Utah, Salt Lake City, Utah

INTRODUCTION

Catalytic research has not, up to the present time, led to the recognition of anything which might be considered a "general theory of heterogeneous catalysis." The tremendous volume of published literature on this subject has made it difficult to coordinate the many facets of the field into a single unified set of principles which may be understood to govern the phenomenon of chemical reaction at a solid surface. Indeed, the exploration of such allied fields as the physics of the solid state, molecular structure and the quantum-statistical treatment of reaction rates rather leads one to the point of view according to which the concept of a general theory should be discarded entirely in favor of a limited set of entirely different treatments each appropriate to a particular combination of adsorbent and reactants, and possibly temperature, as well. In any case, it is becoming increasingly obvious that it does not suffice to show merely that experimental data obtained over a limited temperature and pressure range can be accurately explained by a specific model employing some particular kind of interaction or combination of interactions. Often many such models derived from entirely different points of view can be shown to be equally satisfactory under such circumstances, while they may all break down when applied to more comprehensive experimental measurements. The reason for this is of course two-fold: it may be that the mechanism of the reaction and the significant forces involved actually do change with, say, increased surface coverage, temperature and the like. Alternatively, it may be equally true that a model based on one particular type of interaction to the exclusion of others must be replaced by a more sophisticated picture before it can apply to the reaction in any general way. Probably both reasons are important to some extent in any but the simplest cases of contact catalysis.

---

* The authors wish to thank the Office of Naval Research for financial support of this work.

While a universal treatment of heterogeneous reactions is thus unlikely of accomplishment, it is generally recognized that the process can be divided into certain fundamental steps common to any catalytic reaction, and it is here proposed that these basic elementary processes be examined both from the point of view of their individual microcosm and as to their relationship to the global process of chemical transformation. It is hoped that there will emerge a kind of total unity, at least as regards the methods of treatment and the formulation of the theoretical picture appropriate to a given specific reaction.

It is an axiom that without adsorption heterogeneous catalysis does not exist; more recently this has been modified, in the main, to read, "without *chemical* (or *activated*) adsorption." Thus one fundamental step always involves the interaction of the reactant molecules or derivatives thereof with the surface (or possibly a modification of the surface produced by some prior adsorption). Many factors may be individually or simultaneously important in this interaction: the geometrical organization of the (active) sites for adsorption, the rate of the adsorptive process itself, the thermochemistry of the adsorbate binding, including its distribution over the geometrical surface, competitive and cooperative adsorption, mobility of the adsorbed species and many others. All of these considerations extend as well to the problem of desorption of the reaction products, but in general the latter analysis may be assumed to run parallel with the former. One most important aspect of the treatment of this part of the catalytic reaction lies in the breaking down of the experimentally observed energetics into those heats and entropies of adsorption and of activation which correspond to the molecular model chosen for the reaction. It is only in this way that the true worth of a particular microscopic elementary process or chain of processes can be evaluated. In particular, it will be shown that it is essentially impossible to distinguish with certainty between the effects of the entropy of activation (or the classical frequency factor of Arrhenius) and the number of surface sites active in the surface reaction proper. It is more nearly true that through the study of mechanism one may hope eventually to obtain an approximation to the magnitude of the active part of the catalyst surface.

There exists a considerable body of opinion to the effect that there are very few truly simple reactions, in the sense that reactants proceed to stable products in a single chemical act. This is attested to by the rapidly dwindling number of classically first and second order reactions in the gas phase, while the number of accepted third order reactions is presently about four. The vast majority of homogeneous gas- and liquid-phase reactions appear then to be step-wise sequences of elementary processes, possibly complicated by alternative, simultaneous chains leading to different products. Certainly in the case of heterogeneous reactions involving a solid surface it is most unlikely that any other case exists. It is also generally understood, however, that in most cases of practical interest one elementary step in the chain of events leading to reaction is slower, under given conditions, than any other, and this "slowest step" or "rate-determining" reaction is the process which must kinetically be treated in detail. Under these conditions, the other elementary processes may be considered as being in effective chemical equilibrium and treated as such. This assumption enjoys great popularity, since it makes many complex reactions amenable to mathematical analysis and appears to be justified *a fortiori* by the success which is attained through its use. This is not to say, of course, that exceptions do not occur; however, the treatment in these cases is generally apparent and can, usually with some difficulty, be carried through in a straightforward manner. A different sort of criticism has recently been raised with regard to this simplifying assumption which is peculiar to the field of heterogeneous catalysis. In dealing with the problem of the heterogeneity of the catalytic surface with respect to the heats of adsorption and activation for adsorption, Halsey has emphasized the fact that with a distribution of activity over the surface it becomes difficult to define the slow step in a reaction, and, indeed, different elementary processes may simultaneously be rate-determining at different adsorption sites. While this suggestion is not without merit, it seems profitable to continue to employ the simpler point of view, at least in those cases in which it appears to provide a satisfactory interpretation of the data at hand, since in the present state of our knowledge the more rigorous method of attack appears impossibly difficult.

The process of interpreting the mechanism of a catalytic process consists then in assuming a chain of events, choosing one as the rate-determining reaction and thus determining the expression for the over-all rate of the chemical reaction. The most profitable way of carrying this out appears to be through the use of the machinery of statistical thermodynamics and absolute reactions rates. The success of a particular assumption must lie in the faithfulness with which the model reproduces the time, temperature and pressure dependence of the observed rate law, and as pointed out above cannot be inferred from limited data. Of paramount importance in this treatment is the decision as to the nature of the activated complex, its structure, mode of formation and transformation into stable products. While it is still impossible to carry out a rigorous treatment of this problem, we can draw heavily on the accumulated experience gained from the semi-empirical treatments of homogeneous gas reactions which have been successful in permitting insight into the mechanisms of so many reactions.

These two phenomena are fundamental to any theory of heterogeneous catalysis: the interaction of the various molecules or fragments involved in the reaction with the solid surface, usually treated as chemisorption and desorption, and the interaction of one or more adsorbate-surface complexes in the surface phase to lead to reaction products. Either of these, it appears, may be rate-determining in specific instances, or it may be the case that in some reactions it is impossible to determine an elementary act which can be singled out as the slow step. In the latter case it does not now appear possible to carry out an analysis of the reaction mechanism: it is always true, however, that one must be prepared to find a changing mechanism for the same over-all reaction carried out under widely varying conditions, and only a most exhaustive experimental treatment of even the simplest reactions can lead to a generally acceptable theory.

Adsorption—Ideal Case

The adsorption of gases on solid surfaces has long been recognized as a factor of primary importance in the process of catalytic reaction at surfaces[70, 75, 79, 120, 121, 123]. It has not, however, been possible to develop a complete theory setting forth on a quantitative basis the actual role of adsorption in catalysis. Indeed, the factors important in determining the nature and amount of adsorption on a given surface are not yet fully understood. One of the problems which looms large in this picture is that of the nature of the surface itself. From the simplest viewpoint the surface of a catalyst may be considered as a collection of independent, uniform sites which can interact in some way with a molecule of adsorbate to form a surface layer. Further simplification may be achieved by assuming that molecules adsorbed next to each other on the surface do not interact to any appreciable extent. While such a model must be considered beforehand to be somewhat unrealistic it nevertheless provides a reasonable basis from which to work toward an understanding of the results of experiment. The development of the consequences of assuming such an ideal model of a surface will be the general problem of this section. Further discussions based on the more realistic models suggested by experimental facts will be considered subsequently. As it turns out there is little point in exhaustive comparisons of the mathematical consequences of the simplified model with the existing data in the case of adsorption since it cannot be said that most of the equations derived constitute even a fair approximation to quantitative reality. One should consider the deductions immediately following as an important qualitative picture of the general nature of adsorption. If, however, those sites which possess appreciable activity for a given reaction were to be sparsely distributed over the actual surface, and if all other sites are of negligible activity for the reaction in question, then it might be supposed that the active sites will behave as independent, equivalent adsorption centers, thus justifying the application of the treatment below. There appears to be a considerable weight of experimental evidence[162] in support of such an assumption.

Types of Adsorption

There are two quite distinct classes of adsorption phenomena which are distinguished by the terms physical and chemical adsorption. While experimental results had already suggested the existence of these types[15, 133, 135, 198, 200], the first theoretical discussion of their natures appears to have been presented by Lennard-Jones[124].

Physical or van der Waals adsorption is characterized by a relatively low value for the heat of adsorption (of the order of a few kilocalories) and the fact that it is readily and completely reversible. As Lennard-Jones showed it can be accounted for completely by the van der Waals or polar (nonchemical) forces which act between the surface and the adsorbate molecules.

Chemical adsorption, on the other hand, seems to arise from the actual formation of a chemical bond with the surface since the measured heats of adsorption are generally an order of magnitude higher than for physical adsorption. Many cases are known in which chemisorption does not begin until the temperature is raised above the point where physical adsorption ceases to be important. It then proceeds at a measurable rate from which an activation energy can be deduced. Taylor[195] has given the name "activated adsorption" to such cases. All adsorptions in which large amounts of heat are evolved are difficult to reverse, requiring a high temperature and low pressure of adsorbate before desorption begins to occur to an appreciable extent.

The difference between chemical and physical adsorption is illustrated by the potential curves in Figure 1. Here curve I represents the van der Waals interaction. As the molecule is brought up to the surface there is a small attraction at a relatively large distance from the surface which changes over to a repulsion at distances less than the equilibrium value. If it is possible for a chemical bond to form between the approaching molecule and the surface then a curve of the type II will exist. At the point where the two curves cross the molecule can change over from van der Waals to chemical or activated adsorption with no change in energy. The two adsorption heats are indicated by H_a and H_w while the activation energy for chemical adsorption is indicated by E.

There is a tendency on the part of some authors to view chemical and activated adsorption as two quite different types although the only real difference on which to base a distinction is the apparent presence or absence of an activation energy. It should be clear from Figure 1 that the difference is most likely one of degree rather than kind. The point where

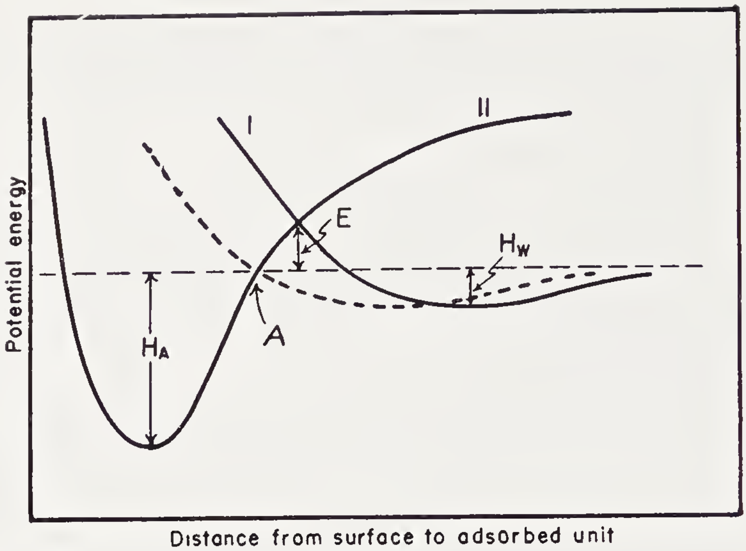

FIG. 1

the two curves cross will determine the nature of the chemical adsorption and whether or not there will be an activation energy. If, for example, the curves cross at a point A in the figure then chemisorption will occur rapidly even at very low temperatures. Examples of such cases are the adsorption of hydrogen on tungsten, nickel and other metals[55]; and also oxygen, nitrogen, and carbon monoxide[13, 20, 48, 164] on various metals at liquid air temperatures.

The fact that curve II lies above curve I at large distances implies the partial or complete dissociation of the molecule in the adsorbed state. The energy difference between the horizontal portions of the two curves represents the heat of dissociation or deformation which takes place during the adsorption. The curves themselves are in no way quantitative since the internuclear distances are not indicated on the diagram.

This picture of adsorption offers a ready explanation of the variation of the amount of adsorption with temperature which is frequently observed to behave as is schematically shown in Figure 2. This is exemplified by the experiments of Taylor and Williamson[200] on the adsorption of hydrogen on a mixture of MnO and Cr_2O_3. In these experiments it was found that the amount of adsorption decreased to a minimum at about 250°K and then as the temperature was raised further the adsorption increased, passing through a maximum at 500°K. On the basis of the two types of adsorption described it is clear that at temperatures such that kT is comparable to the heat of adsorption in the van der Waals layer the amount of this type of adsorption must become very small; while at temperatures where an appreciable fraction of the adsorbate molecules have energies comparable with the activation energy, chemical adsorption will begin to occur to an appreciable extent.

Also interesting is the fact that Figure 1 offers a qualitative explanation of the experimental observation that a slow change from physical to chemical adsorption can occur in some cases[199]. As long as the activation energy is not too high there will be a few molecules with sufficient kinetic energy to cross over to the chemically adsorbed state even at temperatures where physical adsorption still predominates.

With respect to the process of desorption only a few words are necessary. It is generally to be considered as the exact reverse of adsorption, the activation energy for desorption being the sum of the heat of adsorption and the activation energy for the adsorption process. This also implies of course that desorption of a physically adsorbed layer for which there is virtually no activation energy of adsorption will possess an activation energy for desorption just equal to the heat of adsorption. Usually, if a molecule in a chemisorbed layer gets enough energy to desorb it will leave the surface completely. It is possible however that special cases exist where the molecule can gain just sufficient energy to be transferred back to the physically adsorbed layer.

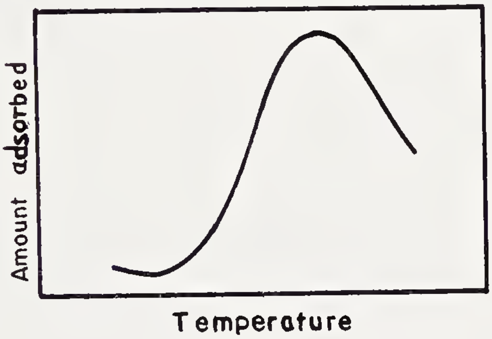

FIG. 2

Relative Importance of Physical and Chemical Adsorption to Catalysis

It may be stated with virtual certainty that no catalytic reactions ever occur on surfaces where neither reactant is chemisorbed. As evidence in support of this view one may note first that many catalytic reactions occur at higher temperatures by far than those at which physical adsorption of the reactants occurs. Secondly, even in those cases where the reaction occurs at temperatures in the region where physical adsorption might take place, it has been shown that one or more of the reactants undergo chemisorption at the same temperature. Third, the forces involved in physical adsorption are quite small as compared to the heats and activation energies of chemical reactions which often are an order of magnitude larger.

Even in the apparently exceptional case of the cracking of saturated hydrocarbons over solid catalysts where present techniques are unable to disclose any chemisorption at the cracking temperature one can only say that probably less than 1 part in 500 of the catalyst surface is covered by chemisorbed molecules. The demonstration of isotopic exchange between hydrogen of the hydrocarbon and the hydrogen or water of the catalyst is strong evidence of the existence of chemisorption.

It is, however, to be noted that physical adsorption may be important as a tool in elucidating the mechanism of catalysis, particularly in the field of surface area measurements, which has already been discussed in Chapters 1 and 2 of Vol. I and which will be discussed briefly below.

Physical Adsorption

In spite of the relative unimportance of physical adsorption to actual catalytic reactions, it seems advisable to deal briefly with the theoretical treatment of physical adsorption partly for purposes of orientation and partly to introduce in outline that part of the BET theory of physical adsorption which is important in conjunction with surface area measurements. Also, since this chapter purports to be a general review of past and present theories of catalysis it is necessary to mention those theories which have assumed that physical adsorption plays an important role.

The two theories of physical adsorption to be discussed in this section will, in line with our previous remarks, be those for which the physical model is a uniform adsorbing surface with no appreciable interaction between the adsorbed molecules. The first of these is concerned only with single layers of molecules or atoms.

Mobile Monolayers. Lennard-Jones[124] has shown theoretically and experimental studies have confirmed, that a solid surface presents a periodic potential field for an atom or molecule approaching the surface. In the simplest theory of a mobile film of molecules on a surface the assumption is made that this field is effectively uniform and enters the problem of an adsorbed monolayer only in that it restricts the motion of the molecules on the surface to two dimensions. The partition function for translation in two dimensions for a molecule of mass m is

$$l(T) = \frac{2\pi mkT}{h^2} \mathcal{A} \tag{1}$$

where $\mathcal{A}$ is the surface area and the other symbols have their usual significance. The complete partition function for a molecule in the surface layer may be written

$$f_a(T) = l(T)j(T)e^{\chi_a/kT} = \frac{2\pi mkT}{h^2} \mathcal{A}j(T)e^{\chi_a/kT} \tag{2}$$

where χ_a represents the potential energy of a molecule on the surface referred to the infinitely separated molecules as zero, and $j(T)$ is the partition function for the internal degrees of freedom of the adsorbed molecule assuming as usual that these degrees of freedom are the same in the adsorbed as in the gaseous molecule. The free energy of N_a adsorbed molecules is then

$$A_a = -kT \ln \frac{f_a(T)^{N_a}}{N_a!} = -kT \ln \frac{f_a(T)^{N_a} e^{N_a}}{N_a^{N_a}} \tag{3}$$

or

$$A_a = -N_a kT \ln \frac{2\pi mkT}{h^2} \frac{\mathfrak{a}}{N_a} j(T) e^{\chi_a/kT} - N_a kT \tag{4}$$

By a well known thermodynamic relation the two dimensional spreading pressure φ of the film is then

$$\varphi = -\frac{\partial A_a}{\partial \mathfrak{a}} = \frac{N_a kT}{\mathfrak{a}} \tag{5}$$

Equation (5) is the equation of state of a two-dimensional ideal gas. The effects of slight departures from nonideality of such a two-dimensional gas have been treated by Fowler[74].

From Eq. (4) the chemical potential of the adsorbed film is

$$\mu_a = \frac{\partial A_a}{\partial N_a} = -kT \left\{ \ln \frac{f_a(T)}{N_a} + 1 \right\} \tag{6}$$

while that for a gaseous molecule (ideal) is

$$\mu_g = -kT \left\{ \ln \frac{a(T)}{N_g} + 1 \right\}, \qquad a(T) = \left(\frac{2\pi mkT}{h^2} \right)^{3/2} V_g j(T). \tag{7}$$

At equilibrium

$$\mu_a = \mu_g$$

and consequently

$$\frac{f_a(T)}{N_a} = \frac{a(T)}{N_g}; \qquad e^{\chi_a/kT} \frac{\mathfrak{a}}{N_a} = \frac{(2\pi mkT)^{1/2}}{h} \frac{V_g}{N_g} \tag{8}$$

Defining

$$C_a = \frac{N_a}{\mathfrak{a}}, \qquad C_g = \frac{N_g}{V_g} = \frac{p}{kT}$$

gives

$$C_a = \frac{h e^{\chi_a/kT}}{(2\pi m)^{1/2}(kT)^{3/2}}\, p \tag{9}$$

Physical realization of such a surface film could only come at temperatures where $\chi_a \ll kT$ (under which condition the actual surface will appear as an essentially uniform potential) and at densities low enough so the assumption of no interaction between adsorbed molecules will hold.

Localized Monolayers. In localized adsorption the adsorbed molecules are held in fixed positions on the surface, one molecule at each adsorption site (or one per set of adsorption sites if more than one is required for each molecule). Again there is assumed to be no interaction between the adsorbed molecules, and the surface itself is assumed not to change properties when a molecule is adsorbed. The partition function of an adsorbed molecule under these conditions will be represented by

$$f_a(T) = e^{\chi_a/kT} j(T) \tag{10}$$

where now $j(T)$ includes all of the internal degrees of freedom of the adsorbed molecule as well as that vibrational degree of freedom gained from the loss of translational motion in the process of adsorption. χ_a is the potential energy of an adsorbed molecule in its lowest state referred to the infinite separation from the surface as zero.

Now let N_s be the number of adsorption sites on the surface of area $\mathcal{A}$ and N_a the number of adsorbed molecules in equilibrium with the gaseous adsorbate. Then $(N_s - N_a)$ is the number of empty sites. The complete partition function for the monolayer is then

$$g(N_a)\,[f_a(T)]^{N_a} \tag{11}$$

where $g(N_a)$ is the number of ways of distributing N_a molecules over N_s sites, one to a site. We have

$$g(N_a) = \frac{N_s!}{N_a!(N_s - N_a)!} \tag{12}$$

The free energy of the adsorbed layer is then

$$A_a = -kT \ln \frac{N_s!}{N_a!(N_s - N_a)!}\,[f_a(T)]^{N_a} \tag{13}$$

From this, using Stirling's approximation for the factorials, the chemical potential is

$$\mu_a = kT \ln \frac{N_a}{N_s - N_a} - \ln f_a(T) \tag{14}$$

and the absolute activity becomes

$$\lambda_a = e^{\mu_a/kT} = \frac{1}{f_a(T)} \frac{N_a}{N_s - N_a} \tag{15}$$

In the gas phase

$$\lambda_g = \frac{P}{kT} \frac{h^3}{(2\pi mkT)^{3/2} j(T)} \tag{16}$$

so that at equilibrium where $\lambda_a = \lambda_g$

$$\frac{1}{f_a(T)} \frac{N_a}{N_s - N_a} = \frac{P}{kT} \frac{h^3}{(2\pi mkT)^{3/2} j(T)} \tag{17}$$

Now let $N_a/N_s = \theta$, the fraction of the surface covered so that

$$\frac{\theta}{1 - \theta} = P \left\{ \frac{f_a(T)}{kT} \cdot \frac{h^3}{(2\pi mkT)^{3/2} j(T)} \right\} \tag{18}$$

or

$$\frac{\theta}{1 - \theta} = \frac{P}{P_{1/2}} \tag{19}$$

where

$$\frac{1}{P_{1/2}} = \frac{f_a(T)}{\dfrac{kT(2\pi mkT)^{3/2} j(T)}{h^3}} \tag{20}$$

which is just the equilibrium constant between adsorbed and gaseous molecules. Equation 19 can be rearranged to the form

$$\theta = \frac{P/P_{1/2}}{1 + P/P_{1/2}} \tag{21}$$

which is just Langmuir's well known adsorption isotherm. There are cases in which this isotherm is obeyed when applied to a physically or chemically adsorbed monolayer as long as the value of $P_{1/2}$ is used as an adjustable parameter, but it is seldom that the theoretical value and the experimental value of this parameter coincide[179]. The isotherm does not of course apply in any case involving the occurrence of multilayer adsorption.

BET Theory of Physical Adsorption. The original derivation of the BET theory[26] used a kinetic approach, carried out in much the same manner as Langmuir's derivation of his isotherm. More recently the derivation has been carried through from a statistical mechanical model[93] which seems to more clearly point up the assumptions and approximations involved. For that reason we shall outline briefly this approach for the simplest case in which capillary condensation is not considered.

The statistical model of the BET theory assumes the adsorption of the first layer consisting of X molecules, takes place on B localized sites per unit area of adsorbent and that A-X molecules are adsorbed on top of the X molecules in the first layer. Lateral interactions between molecules in the first as well as in higher layers are ignored. The potential energy of the molecules in the first layer is taken as $-\epsilon_s$ per molecule while for the second and higher layers this energy is $-\epsilon_L$ and is assumed to be the same as for the molecule in the liquid state. The partition function for the molecules in the first layer is then

$$j_s \cdot e^{\epsilon_s/kT}$$

while for those in the second and higher layers it is

$$j_L \cdot e^{\epsilon_L/kT}$$

The partition functions for the X molecules in the first layer and the A-X molecules in the higher layers are then

$$Q_s = \frac{B!}{X!(B - X)!} (j_s e^{\epsilon_s/kT})^X \tag{22}$$

$$Q_L = \frac{(A - 1)!}{(A - X)!(X - 1)!} (j_L e^{\epsilon_L/kT})^{A-X} \tag{23}$$

and the complete partition function for the system is

$$Q = \sum_{L=1}^{k} Q_s Q_L \tag{24}$$

Using the standard methods of statistical mechanics the equation

$$\frac{v}{v_m} = \frac{cx}{(1 - x)(1 - x + cx)} \tag{25}$$

can then be derived where

$$x = \frac{P}{P_0} = \frac{A - X}{A}, \qquad c = \frac{j_s}{j_L} e^{(\epsilon_s - \epsilon_L)/kT}, \qquad \frac{v}{v_m} = \frac{A}{B}$$

Equation (24) can be rearranged to the form

$$\frac{x}{v(1 - x)} = \frac{1}{v_m c} + \frac{(c - 1)x}{v_m c} \tag{26}$$

which, if the theory is correct, will clearly lead to a straight line if the left side is plotted against the relative pressure x. From the slope and intercept of this line the quantities v_m and c can be evaluated where v_m is the number of molecules required to form a complete monolayer on unit area of surface.

It is unnecessary to include a discussion of the validity of the BET theory as it concerns the whole problem of physical adsorption since this has been adequately taken care of elsewhere[50, 93] (see Chapter 1, Vol. I, of this series for references giving a critical discussion of the BET theory) and since in any case it is not strictly relevant to the problem of catalysis. The usefulness of Eq. (26) when applied to the data on low-temperature physical adsorption of inert gases, particularly nitrogen, lies in the value of the constant v_m which measures the surface area of the catalyst when multiplied by the area of a single molecule of the adsorbed gas. Several comparisons with other less convenient methods[3, 52, 91] have indicated that the BET method yields results which correspond quite closely to the actual physical area of the catalyst (see Chapter 2, Vol. I, of this series).

The importance of knowing the physical area of an adsorbent or catalyst is of course obvious. Such information is the first step in any process of determining the number and kind of sites on the surface which are responsible for chemisorption and catalytic reactions.

Physical adsorption and Theories of Catalysis. In 1929 Balandin[6] proposed what he called the "Multiplet Theory" in which he emphasized the importance of the geometric arrangement of those points of the surface which are active in the catalytic process being studied. In this connection he also pointed out the fact that strong (chemical) adsorption and high catalytic activity do not necessarily go hand in hand. The treatment postulates that there must in general be different kinds of active centers existing on the surface in a proper ratio and in suitable geometric organization. These organizations of active surface points are described as singlets, doublets, etc., depending on the number of bonds (existing in the reactant or possibly in the products) which may be simultaneously adsorbed upon them. If this adsorption is too strong, the surface is self-poisoned; if too weak, the probability of reaction becomes small. In addition, it is supposed that the surface sites function by "directing the valences of the adsorbed atoms" either toward each other in forming a new bond, or toward the atoms adsorbed on an associated member of the multiplet in breaking the bond. Such action would seem to imply a somewhat weak adsorption interaction, but nevertheless stronger than the van der Waals interaction of physical adsorption.

Rideal[162] has proposed a mechanism for the hydrogenation of olefinic compounds which assumes that the hydrogen is only adsorbed physically and in this condition reacts with a chemisorbed molecule of the olefin. Beeck[11], on the other hand, has proposed that the reverse is true, the ethylene in the van der Waals layer attacking chemisorbed hydrogen atoms.

Chemisorption

Chemical adsorption has already been adequately defined above; it is so called because it apparently involves actual chemical bonding of the adsorbate molecules to the surface. Because of the high values of adsorption heats the chemisorbed layer can be assumed to be essentially localized except perhaps at extremely high temperatures. The statistical treatment of this problem for the ideal case of a uniform surface and no interaction of the adsorbed molecules differs in no essential way from that just given for localized monolayers in physical adsorption. The potential energy of a molecule on the surface is different but this has no effect on the mathematical form. It is possible, however, to re-derive the equation in a slightly more sophisticated manner which extends the application of the equation, at least, formally, to a slightly more general case.

If we let f_s, f_1 and f_{1s} represent the partition function of an adsorption site, a gaseous molecule and an adsorbed molecule, respectively, then the quantity $(f_1f_s + f_{1s})$ represents the total number of possible states of a system consisting of a molecule and an adsorption site. Therefore

$$\theta = \frac{f_{1s}}{f_1f_s + f_{1s}} \tag{27}$$

is the fraction of molecules in the adsorbed state at equilibrium at a given temperature. This expression is equivalent to Eq. (21) as can be seen by rewriting (27) in the form

$$\theta = \frac{\dfrac{f_{1s}}{f_1f_s}}{1 + \dfrac{f_{1s}}{f_1f_s}} \tag{28}$$

and noting that

$$f_1 = \frac{kT}{p}\,\frac{(2\pi mkT)^{3/2}}{h^3}\,j(T) \tag{29}$$

This form of the Langmuir isotherm shows clearly the limit of applicability of the theory. The inclusion of the partition function for the surface sites both alone and in connection with the adsorbed molecule makes it unnecessary to assume that the surface site remains inert in the adsorption. The actual restrictions which must be obeyed are first that the surface must be uniform and second that there be neither induced changes in the sites as a result of the adsorption of a molecule on a neighboring site nor any cooperative interactions on the part of the adsorbed molecules. Thus it is possible to see that a theoretical calculation of the Langmiur constant according to Eq. (20) might be modified in certain cases to more closely agree with experiment. If there are several kinds of sites, a separate isotherm may be written for each of them and the results summed to give the over-all isotherm[120].

Polanyi[158] has pointed out that the Langmuir isotherm is not obeyed experimentally in most practical examples of adsorption measurements and that where it is obeyed the temperature dependence of its constants is not fulfilled. Polanyi's study included many cases of multilayer adsorption to which Langmuir's isotherm does not apply but even in unimolecular adsorption deviations are often found. For example, Palmer[149] measured the ratios of the adsorption coefficients on metals of mixtures of various gases with hydrogen. He found that this ratio, which should be a constant, is, with hydrogen as one of the gases, always too large in favor of hydrogen. This could be explained on the basis of a surface consisting of many different kinds of sites with varying activities (Hinshelwood[101]) or in view of the general behavior of hydrogen on metals, as chemisorption in whole or in part by the hydrogen.

The question then is whether or not such an isotherm can be of any value in applications to the problem of catalytic reactions. As will be seen later in this chapter this question is far from answered. There does, however, seem to be reason for supposing that it can be applied in some cases. The application of the Langmuir isotherm to, e.g., the analysis of rates of ethylene hydrogenation[65, 178] has shown that it is possible to fit the experimental data with constant values of the adsorption coefficients for experiments at a given temperature but at different initial pressures of reactants. Such results seem to indicate that in these cases the actual sites on the surface at which reaction takes place may be sufficiently dispersed and have energies lying in a sufficiently narrow band so that the conditions implicit in the isotherm are essentially fulfilled. In such a case of course the heats of adsorption deduced from the kinetic data would not necessarily bear any relation to the measured heats of adsorption of the single gases except that they will lie in the same range.

Rates of Adsorption. As has already been noted the type of chemisorption denoted by "activated" proceeds at a rate which is determined by an activation energy. At one time all chemical adsorption was thought to be characterized by an activation energy even though in some cases it might be small. Experiment has shown however that even at liquid air temperatures oxygen, nitrogen and carbon monoxide[20, 48] are rapidly chemisorbed on tungsten, a fact which indicates that if there is an activation energy for these gases on this metal it must be essentially zero. Even in those cases where an activation energy appears to exist care must be taken in its interpretation as a true activation energy since it may often be due to slow absorption into the lattice[12, 217] or to the displacement of previously adsorbed impurities[2, 164].

A few attempts have been made to calculate the activation energy for adsorption[183, 184] but the approximations involved are such that very little significance can be attached to the quantitative results. Their principal worth must be considered to lie in the indication they give regarding the geometrical requirements of the surface. In any event, our lack of a sufficiently detailed theory to allow precise calculations does not prevent a profitable theoretical investigation of the general nature of the reaction of gaseous atoms or molecules with surface sites.

In order to proceed beyond the broadest generalities regarding rates of adsorption from the point of view of an absolute calculation by the methods of Eyring, *et al.*, it is absolutely necessary either to know or to assume a specific unit molecular process as being rate determining. In adsorption, as well as in the actual catalytic reaction our information is usually not sufficiently detailed to allow any particular mechanism to be chosen as rate determining over all others that might be visualized although it may be possible to rule out certain ones as highly improbable on the basis of experimental evidence. Because of this situation it is useless to write down the rate equations for great numbers of possible cases: it does, however, seem worthwhile to briefly discuss one particular reaction in order to make clear what information is necessary, both experimental and theoretical before the method can successfully be applied. To this end we will consider the rates of adsorption and desorption for a gas which adsorbs without dissociation on a single adsorption site. For more detail regarding other mechanisms reference may be made to the work of Eyring *et al.*[80] or to the discussion in Chapters 3, 4, and 5 of Vol. I of this series.

The reaction of a single gas molecule with a single site on a uniform surface may be considered simply as a bimolecular reaction. The velocity of the reaction, according to absolute rate theory, is given by

$$v = c_g c_s \frac{kT}{h} \frac{f^\ddagger}{f_g f_s} e^{-\epsilon_s/kT} \tag{30}$$

where

c_g = the number of molecules per cc in the gas phase
c_s = the number of adsorption sites per cm^2 on the surface

and the f's are the partition functions per unit volume or area. ϵ_a is the activation energy for the adsorption of a single molecule at absolute zero. Equation (30) refers specifically to localized adsorption of single molecules or atoms on single sites of a uniform surface. If the surface is nonuniform in the sense that it may be considered as a number of surfaces consisting of different types of sites then the various quantities refer to suitable averages.

Given a set of data to which this equation can be applied, evaluation of the partition functions involved allows determination of the zero point energy. With this information it would be possible to determine the concentration of surface sites, c_s, which is the concern of many experimental investigations. Unfortunately our knowledge of $f^\ddagger$ and f_s is sketchy at best so that such an analysis leads only to an order of magnitude calculation of c_s. In any event, since it appears that essentially all surfaces are to some extent heterogeneous, it is probable that suitable information will not be forthcoming. As will be seen later, however, a similar line of reasoning in the case of catalytic processes may have a greater chance of success because the *effective* surface for reaction closely fulfills the requirement of uniformity.

Rate of Desorption. Desorption from a localized monolayer may be regarded as a unimolecular decomposition in which an adsorbed molecule acquires the necessary configuration and energy to escape from the surface. In this case the rate of the reaction may be written

$$v_d = c_a \frac{kT}{h} \frac{f^\ddagger}{f_a} e^{-\epsilon_d/kT} \tag{31}$$

where f_a is the partition function for the adsorbed molecules. Here again we have assumed a single adsorbed molecule to be desorbing from a single site.

As with the rate of adsorption this equation with a suitable set of data might yield valuable information concerning the concentration of chemisorption sites through evaluation of the quantity c_a at various degrees of surface coverage.

It is of interest to note that by equating the rates of adsorption and desorption and performing the obvious algebraic manipulations one recovers the Langmuir equation in the same form as Eq. (28). This further points up the fact that these equations deal only with the case of no surface interaction of the adsorbed molecules.

Competitive Adsorption and Poisoning for the Case of No Surface Interaction. For systems in which two or more gases are in contact with the same surface and in which both types of molecules can be adsorbed on the same kind of site the adsorption isotherm will be of the form:

$$\theta_1 = \frac{f_2 f_{1s}}{f_1 f_2 f_s + f_1 f_{2s} + f_2 f_{1s}} \tag{32}$$

or

$$\theta_1 = \frac{\dfrac{f_{1s}}{f_1 f_s}}{1 + \dfrac{f_{2s}}{f_2 f_s} + \dfrac{f_{1s}}{f_1 f_s}} \tag{33}$$

where the f's are the partition functions as before, the subscripts 1 and 2 corresponding to the different adsorbate species. The relative amounts of the surface covered by the two kinds of molecules will depend upon the magnitude of the standard free energies of adsorption. Rewriting (33) in the form

$$\theta_1 = \frac{K_1 p_1}{1 + K_1 p_1 + K_2 p_2} \tag{34}$$

one notes that at a given temperature, for large K_2

$$\theta_1 \approx \frac{K_1 p_1}{K_2 p_2} = K \frac{p_1}{p_2} \tag{35}$$

Cases displaying these qualitative aspects are to be found frequently in dealing with catalyst poisons, the poison often being so strongly adsorbed that it almost completely excluded the reacting gases from the surface. Maxted and his co-workers[131] as well as others have studied extensively the effect of various compounds in poisoning catalytic reactions, especially hydrogenation over metal catalysts. In this connection it is of interest to consider the effect on the rate of adsorption of having the catalyst surface partly covered with a poison. Again considering the simple case of single site adsorption of single molecules and assuming that the rate of adsorption of the poison is fast enough so that the equilibrium amount of poison is adsorbed in a time short compared with that of the reaction being studied, it is clear that Eq. (30) is applicable if the quantity c_s is now considered to be a function of the amount of poison present and its adsorption characteristics. Using the subscript p to denote the poison and letting L be the total number of adsorption sites per cm^2 of bare surface one obtains for c_s

$$L\theta_s = \frac{L}{1 + \dfrac{f_{ps}c_p}{f_p f_s} e^{\epsilon_p/kT} + \dfrac{f_{gs}c_g}{f_g f_s} e^{\epsilon_g/kT}} \tag{36}$$

where the concentration terms have been factored out of the partition functions f_g and f_p. Using this in Eq. (30) the expression for the rate of adsorption becomes

$$v = c_g \frac{L}{1 + \frac{f_{ps}}{f_p f_s} e^{\epsilon_p/kT} c_p + \frac{f_{gs}}{f_g f_s} e^{\epsilon_g/kT} c_g} \cdot \frac{kT}{h} \frac{f^{\ddagger}}{f_g f_s} e^{-\epsilon_a/kT} \tag{37}$$

Defining

$$A = \frac{f_{ps}}{f_p f_s}$$

and assuming the poison to be so strongly adsorbed that both unity and the last term in the deominator of Eq. (37) can be ignored gives

$$v = \frac{c_g}{c_p} \cdot \frac{L}{A} \cdot \frac{kT}{h} \frac{f^{\ddagger}}{f_g f_s} e^{-(\epsilon_a + \epsilon_p)/kT} \tag{38}$$

In this case the rate of adsorption varies inversely with the pressure of the poison and the heat of activation for adsorption is increased from ϵ_a to $\epsilon_a + \epsilon_p$ where ϵ_p is the heat of adsorption of the poison. Thus in order for a molecule of the desired gas to adsorb it must first displace a molecule of poison into the gas phase. It has been pointed out[80], however, that this change in the heat of activation will not cause as large a change in the rate of adsorption as might be expected due to a gain in entropy from the removal of an adsorbed poison molecule to the gas phase.

While these equations are interesting for their qualitative implications one must realize that present knowledge regarding the detailed nature of the molecular interactions involved and the lack of experimental data of a suitable kind precludes any immediate quantitative application. It also seems unwise for the time being to delve further into the realm of theoretical speculations based on any more sophisticated models of the chemical adsorption process.

Adsorption, Catalysis and Surface Geometry

Any detailed examination of the processes of adsorption and catalysis must of course include the question of the arrangement of the atoms in the surface of the catalyst. This is particularly true when one recognizes the possibility that in many cases the adsorption of a molecule on the surface may require more than a single atom of the surface. Under such circumstances it is natural to expect that the distances between the surface atoms and their orientations relative to each other must be of importance.

The first systematic attempt at correlating catalytic activity and crystal structure was carried out by Balandin[6, 7, 208] who considered the activity to depend solely on the geometric distribution and relative amounts of the active sites on the surface. In particular, he showed that in the case of the dehydrogenation of saturated six-membered rings over metal catalysts there is a definite and close correlation between activity and the ability of a particular metal to expose an octahedral face. Balandin emphasized that two factors are of great importance in determining the efficiency of a catalytic surface: the geometric distribution of adsorption centers and the actual spacings between them. To a considerable degree, more recent investigations have substantiated these predictions. Long, Frazer and Ott[127] investigated the hydrogenation of benzene over binary alloys of iron, cobalt and nickel and found these alloys to be active only when x-ray analysis showed them to be face-centered, with the concomitant possibility of exposing the preferred 111 crystal face. In addition, they found that the activity was proportional to the per cent of the face-centered structure present in such alloys as were composed of mixtures of structures, as in the case of iron-nickel mixtures. However, catalysts prepared from copper which was known to be face-centered were inactive presumably because hydrogen is not chemisorbed on this metal. Emmett and Skau[58] studied the hydrogenation of ethylene and benzene on iron catalysts and found the iron to be inactive toward benzene hydrogenation in spite of the fact that the surface area was high and the catalyst demonstrated considerable activity with ethylene, at temperatures as low as about −100°C. Thus it would appear that while the requirements postulated by Balandin for an effective surface are important, they cannot be considered necessary and sufficient.

Beeck and his co-workers have carried out an extensive program of investigation on the catalytic behavior of oriented and unoriented metal films which also points up the importance of the geometric arrangement of surface atoms. With an oriented platinum film in which the nonoctahedral crystal face is exposed, only about a tenth of the activity was found as when an unoriented film—which presumably exposed the octahedral face to some extent—was used[9]. Similarly, using nickel films in the hydrogenation of ethylene[13], orientation which presented the (110) plane gave five times the activity of the unoriented film. On the other hand, Beeck and Ritchie[10] have found that benzene hydrogenation (to cyclohexane) does proceed at a measurable rate on iron catalysts in which, they claim, the 110 plane is preferentially exposed even at 58°C, an observation which appears to be in conflict with the experiments mentioned above in which bulk catalysts were used.

The fact that there does seem to be this general correlation between the activity of a metal catalyst and the geometry of the interatomic spacing on the surface, together with the observations of numerous apparent exceptions in special cases points up the important restriction on the theory of

Balandin, often voiced by Beeck, that these geometric considerations can only be significant for a surface upon which the reacting species will adsorb. These same general conclusions have also been drawn from the calculations of Sherman and Eyring[183] and Sherman, Sun and Eyring[184] in their calculations of the activation energy for the adsorption of hydrogen on carbon and nickel.

ADSORPTION—NONIDEAL CASE

When one considers actual catalyst surfaces one finds that the process of adsorption, and hence of surface reaction, is complicated by one or both of two general phenomena: (1) different parts of the surface may appear to have different activities toward adsorption or (2) the adsorbed molecules may interact laterally so as to affect the probability of adsorption of neighboring molecules. While one or the other effect may predominate in a given case, it is generally difficult to distinguish between them without careful analysis of experimental data.

The situation is further complicated by the fact that the apparent heterogeneity of the surface may either be of an *a priori* nature or be induced by the interaction between the adsorbing molecules and the surface, even though the bare surface may be ideal in the sense referred to above. *A priori* heterogeneity may arise in a single component surface from the differing activities of those surface atoms at corners or edges, at the boundaries of incomplete layers or in the region of lattice imperfections. In the case of crystals composed of more than one species of atom different crystal faces may expose one kind of atom either exclusively (MoS_2 Griffith, Figure 8)[82] or preferentially (γ-Al_2O_3, 100 plane), and in any case, different crystal faces will expose planes of atoms with different spacings. Since it is possible to prepare surfaces in which only one crystal face is exposed only with the greatest difficulty, in general there will therefore be many regions differing both in their chemical nature and in geometric distribution of lattice sites. The surface of a multiphase solid will, of course be strongly heterogeneous because of the variation in composition of the several phases and particularly because of the presence of phase boundaries, in the region of which the surface atoms will be strongly perturbed. Finally, the accidental or intentional presence of impurities in a crystal will generally perturb the normal lattice and form isolated regions in which the activity of the surface will be substantially altered. Such foreign atoms have been observed to preferentially seek the surface, thus causing an effect considerably in excess of that which would correspond to their bulk concentration, but even those within the solid may be effective since their influence on lattice structure will be propagated through several atomic layers.

In certain cases, e.g., the dehydrogenation of butene to butadiene

(Owens[148]), it has been found that the activity of the catalyst is directly proportional to the apparent surface area as determined by the BET method. This is generally taken to mean that the total geometric surface is available to the reacting species and that all adsorption sites are equally active. While this interpretation is not unambiguous, these catalysts are probably the nearest approach to the ideal that one may expect.

A priori Heterogeneity

Some five years ago Taylor and Liang[197] reinvestigated the adsorption of hydrogen on zinc oxide, measuring the isobaric rate of sorption occurring upon an instantaneous change in temperature. These measurements were carried out in a temperature range in which the van der Waals adsorption could be shown to be negligible. The interesting result was obtained that upon passing to a higher temperature an instantaneous desorption took place, followed by a measurably slow readsorption of a somewhat larger volume of gas. This phenomenon was subsequently shown to be characteristic of a large variety of oxide and mixed oxide catalysts as well as certain metals, such as nickel and iron. It was suggested that the result could be explained by assuming the surface to be composed of regions of varying activity, with heats of adsorption and activation for the several regions such that an increase in temperature leads to a rapid desorption of gas from one region followed (isothermally) by a relatively slow adsorption on regions characterized by a higher activation energy. Upon lowering the temperature to its initial value the bare surface is rapidly recovered, the filled areas remaining covered because of the relatively high activation energy for desorption. Further studies on copper and its mixtures with magnesium and thorium[196], iron (doubly promoted with K_2O and Al_2O_3) and nickel[173] supported on kieselguhr, indicate the phenomenon to be general for catalysts prepared by the usual techniques. Sintering of the surface and the addition of small amounts of oxides of thorium and chromium had a marked effect on the activity of the catalyst for chemisorption and on the distribution of surface heterogeneities. A review of investigations dating from as early as 1930[193] indicates that in those cases in which it could be assumed or demonstrated that the adsorption was chemical rather than van der Waals these effects had already been noted.

It appears then that not only does the measurement of the total (BET) surface area of the catalyst not give a true indication of the surface area active in chemisorption at a given temperature, but in addition, this active area will in general not be the same at different temperatures. A catalytic surface must, according to this point of view, be characterized by a variety of regions each of which has its own area, and a heat and activation energy for chemisorption appropriate both to the surface itself and to the molecule being adsorbed. This conclusion is reflected in the work of Halsey and Taylor[90] in which the data of Frankenburg on the adsorption of hydrogen on tungsten powder were shown to be consistent with an exponential distribution of adsorption energies over the surface; Sips[186], who investigated the possibility of determining the nature of the distribution function from the adsorption isotherms; de Bruijn[36] in his discussion of the ammonia synthesis from the point of view of the heterogeneous surface, and others[34, 53, 54, 171, 194, 203, 219]. It is important to note also that according to this picture of the surface, adsorption studies at a temperature such that chemisorption is measurably slow do *not* provide information significant to catalysis at that temperature, although these studies may be important to the catalytic process at a higher temperature, where the rate of adsorption of those sites becomes fast enough to compete favorably with the surface chemical reaction.

Eucken[59, 60, 61, 62] has questioned the reality of these apparent *a priori* heterogeneities, holding that the same phenomenological results can be more simply explained in terms of lateral interactions of the adsorbed molecules (*vide infra*). Beeck, also, has questioned this point of view[11]; in particular he has demonstrated that in the case of an evaporated iron film, the surface covered by nitrogen is a constant fraction of the surface left bare by previously adsorbed hydrogen, viz:

$$\theta_N = 0.2(1 - \theta_H) \tag{39}$$

Thus, when one-fifth of the surface is covered by hydrogen, all of the *a priori* active centers should be covered, and no nitrogen at all should be chemisorbed, whereas actually about 16 per cent of the total surface is found to be covered upon sorption. Since no nitrogen at all is adsorbed when the surface is covered with hydrogen, the possibility of a second-layer coverage of hydrogen by nitrogen is excluded[9]. Others, notably Rideal[92], Roberts[164], Volkenstein[211] and Miller[141] have also emphasized the importance of adsorbate-surface and adsorbate-adsorbate interactions over that of active centers and at the present time the status of the latter is by no means clear. Certainly *a priori* heterogeneities exist, in a purely qualitative sense, and some variation in the activities of the several regions toward chemisorption must be assumed. The importance of these variations in the sorption process and in surface reactions involving the adsorbate-surface complex is still a question to be decided both in an absolute sense and as regards their significance relative to other types of interactions.

Another line of approach to the problem of active centers has been through the study of promoter action and the effects of catalyst poisons. The use of promoters in synthetic ammonia catalysts leads, in some cases to a decrease in the total area as measured by the low temperature adsorption method, but to an increase in the activity per unit area of considerable magnitude[51]. In general, small weight per cent additions of promoters are found to concentrate preferentially at the surface: this explains the relative magnitude of their effect on the catalytic activity but not, of course, the mechanism of activation. In a similar way, the addition of small quantities of foreign substances to the reacting molecules in the gas phase may reduce the efficiency of the catalyst surface to a marked degree. Poisoning of the surface in this manner may also be accomplished in some cases by the products of the surface reaction, as is the case in the dehydration of alcohols, and is normally attributed simply to an occupation of the active sites of reaction by an inactive molecule bound too tightly for ready desorption. On the basis of this picture, the action of such poisons can be interpreted in terms of the number of active sites, and comparison with the BET area indicates that, e.g., for a silica-alumina cracking catalyst[143] about 4 per cent of the total surface is active in the reaction. In this instance the poisons employed were such basic molecules as quinoline and other bases.

Other methods of investigation include the magnetic studies of Selwood and co-workers[181]. From considerations of the variation of the Weiss constant it can be inferred that when chromia is suspended on γ-alumina, for example, the active chromia is not homogeneously dispersed but must be isolated in microcrystals of from three to four atomic layers in thickness, and that only a small fraction of the alumina is covered[43, 44, 45, 182]. Loss of activity is accompanied by the spreading out of the chromia into the bulk of the alumina.

Any investigation into the question of heterogeneity which involves values of total surface area as measured by low-temperature van der Waals adsorption of gases such as nitrogen, argon, etc., must take cognizance of the possibility that some part of the measured area actually represents physical adsorption in regions not generally accessible to the reacting species in the chemical reaction. This is discussed in detail in Chapter 1[204, 218].

An extensive discussion of the influence of the atomic lattice characteristics of the surface on the rate of catalytic reactions, notably the hydrogenation of unsaturated hydrocarbons, has been presented by Beeck and collaborators in a series of papers (recently summarized[10] by Beeck) which indicates that even a pure metal in the form of a single crystal will exhibit a heterogeneity of surface arising from the difference in lattice dimensions characteristic of the various crystal faces exposed. Since a practical metal catalyst will generally be microcrystalline, this type of *a priori* heterogeneity would appear to be normal unless the adsorbate is exceedingly tolerant of the geometric nature of the surface.

Induction Effects

It has already been pointed out that the experimental data relating to surface heterogeneity can be interpreted equally well in terms of interactions between the various adsorbed atomic and molecular species concerned and the neighboring bare surface sites. In particular it is possible that the process of adsorption of a molecule or an atom is in itself responsible for the distortion of a region of the surface in such a way that subsequent adsorption may occur with a (usually) smaller heat and a different activation energy. This type of interaction has been termed "induced heterogeneity"[21] or simply "induction" and should be most important in the region of sparse coverage where lateral interactions of adsorbed molecules may be neglected.

Halsey[87] has discussed in some detail the noncooperative adsorption on an *a priori* heterogeneous surface using the formulation of Fowler[73] and demonstrated that the heat of adsorption will vary with the coverage of the surface approximately as

$$Q = -\chi_m \ln \vartheta \tag{40}$$

where for convenience the quantity ϑ has been defined in such a way that the coverage has the numerical value of unity when the adsorbate pressure equals the vapour pressure of the gas at the given temperature. χ_m is defined in terms of an exponential distribution of adsorption energies. i.e.,

$$N_\chi = ce^{-\chi/\chi_m}, \tag{41}$$

N_χ the number of sites of energy χ.

This result includes only the effect of the pre-existing distribution of adsorption energies and all interaction terms have been neglected. Thus it bears out the previous contention that cooperative phenomena are not required to explain the observed variations in the heat of adsorption with surface coverage and it seems probable that in the initial stages of the chemisorption process on most actual surfaces some such picture must be invoked. At the other extreme lies the contention that the surface is initially homogeneous, with all adsorption sites equivalent on the bare surface. In the case of nonmetallic adsorbents, Boudart[21] has emphasized the role of the electronic chemical potential in the sorption process. The surface is considered to be a two-dimensional semiconductor system and heats of adsorption and activation are considered from the point of view of the changes in the Fermi level of the surface which arise from changes in temperature and impurity concentration. The chemisorbed species will transfer an electron to the surface or receive one from it, depending on its electronegativity and thus act as a donor or an acceptor impurity according to the usual treatment of semiconductor theory[185]. An adsorbate of low electronegativity on a uniform surface will transfer in part an electron to the surface, which in this case will act as a simple defect or *p*-type semiconductor, forming a bond which is intermediate between the ionic and the covalent extremes. At constant temperature, the Fermi energy of the surface will then increase as the coverage increases, i.e., as the concentration of "donor impurities" increases, with a consequent decrease in the average strength of binding of the adsorbate molecules. In this way the differential heat of adsorption of such an adsorbate species will decrease as the surface becomes covered. Boudart points out that the Fermi energy is approximately proportional to the logarithm of the donor concentration: thus if the differential heat of adsorption is proportional to the Fermi energy, one again obtains the result given in Eq. (40) derived in terms of an exponential distribution of *a priori* sites of different energies.

A similar treatment of chemisorption on metal surfaces, again presumed completely homogeneous when bare, invokes the collectivization of the electrons bonding the adatom to the surface by the metallic conduction electrons[22]. This process has been discussed earlier[40, 100, 108, 144, 177] for the case of the dissolution of hydrogen in metals (e.g., palladium). It has also been noted[176] that with alloy catalysts the activation energy (for formic acid dehydrogenation) is proportional to the square of the electron concentration in the metal, as modified by the solute; this increase generally running parallel to the increase in both hardness and electrical resistance. In the treatment of Boudart[22], the chemisorption process consists of forming a number of metallic bonds with the surface, producing in consequence a double layer at the surface which is characterized in the aggregate by a dipole moment perpendicular to it. This layer will either increase or decrease the work function appropriate to the bare surface as well as the heat of adsorption of the sorbate, and, in fact, Boudart derives for the simple case of no dipole-dipole interactions the result

$$\Delta q = (n/2)\,\Delta\varphi, \tag{42}$$

Δq being the absolute change in heat of adsorption due to the double layer, $\Delta\varphi$ the change in work function and n the number of electrons involved in bond formation. It is to be noted that this effect on the heat of adsorption arises from the resonating-covalent or metallic bonds formed, and not from a simple polarization process; thus while a change in work function may be anticipated, no change in heat of adsorption can be expected in physical adsorption[138, 168].

Closely associated with the treatment of Boudart is that of Oblad, Cook and others[29, 30] and termed by them "structural adsorption." In general the surface of a solid will be in a strained configuration somewhere between the 'free radical" state, in which the lattice array is terminated by unbonded orbitals, and the equally high-energy condition in which all of these surfaces orbitals are saturated by the formation of (resonating) multiple bonds without dislocation of the lattice array. Thus a condition of disorder of the nuclei will arise at the surface as the atoms attempt to saturate these orbitals with a minimum alteration of the normal bond angles and this distortion will propagate inward from the surface to some extent. The presence of an adsorbed molecule or atom will provide a means of relieving this surface strain that is preferable to that obtaining at the bare surface, and it may be expected that this effect will be apparent at considerable distances from the site of adsorption.* This "first-order" strain in a pure solid is thought to be important primarily in the case of physical adsorption, since the energy associated with its release may be expected to be small. A "second-order" type is that associated with the presence of impurities at or near the surface, phase boundaries in mixed solids and lattice defects due to a nonstoichiometric lattice. Here the magnitude of the strain energy is much larger but is, of course, of considerably smaller lateral extent, and in this sense may be compared with the concept of active centers. However, it is to be noted that while the centers of maximum surface strain may be heterogeneously distributed, the cooperative effect by which the adsorption of one molecule aids, through the relief of local strain, in the adsorption of a neighboring one is still present, although direct interaction between adjacent molecules has not been invoked.

Lateral Interactions

As an alternative to the various descriptions of the catalytic surface which attribute either permanent or induced heterogeneity in activity to it, one may consider the possibility that adsorbate-adsorbate repulsions play an important role in the sorption process. Interactions are certainly important in physical adsorption, leading eventually to condensation of the gas molecules at high relative pressures, but here they are attractive. These attractive forces are long range and relatively nondirectional, but are too small to necessitate consideration in chemisorption, where the important interactions are of the order of magnitude of chemical bonds.

The simplest treatment of lateral interactions takes into account the electrostatic dipole-dipole repulsions of neighboring adsorbate molecules[122, 142, 164]: the energies required, however, to account for the large (ca. 40 kcal) changes in heat of adsorption observed cannot be accounted for in these terms[161]. An approximate quantum-mechanical calculation of the interaction between atoms fixed on a metallic lattice[24] has been carried out and indicates that the interaction energy should be inversely proportional to the distance between the atoms. Again the energies are low, of the order of

---

* Editors note: For experimental confirmation see recent paper by Yates[218a].

a few kcal, unless the atoms are in close juxtaposition, i.e., at nearly complete surface coverage. It has been pointed out by Boudart[22], however, that in certain cases, as for example the adsorption of metal atoms on a metal surface where the forces between adsorbate and surface closely resemble those between the adatoms themselves, the simple depolarization treatment may suffice and lateral interactions become important at moderate values of surface coverage.

Since many, if not most, catalytic reactions occur as the direct result of the interaction between adsorbed atoms and molecules, it is clearly of the greatest importance that this field be explored very thoroughly. While some progress has been made[72, 157, 167] the present state of our knowledge in this particular is very incomplete. For chemisorption itself, however, it is notable that repulsive forces between adsorbed molecules are only important at very high surface coverages, since the energies arising from these forces are small, and since, in addition, the effects attributable to them can adequately be explained in terms of other kinds of interactions.

Discussion

Chemisorption on nonideal surfaces involves three distinct processes: at low coverages adsorption takes place on those sites or regions of the surface which are most favorable, both from the point of view of the heat of adsorption and the energy of activation for the reaction, and in general the adsorbate molecules are statistically independent. Which sites actually satisfy the conditions which make them most favorable will be determined by the conditions of the experiment, especially the temperature, and the number and distribution of "good" sites on a particular catalyst at a given temperature will be strongly dependent upon the past history and method of preparation of the material. While adsorption may take place over a relatively large portion of the surface, the extent of the binding and the amount of deformation of the adsorbed molecule—and hence the tendency toward chemical activation—will vary from point to point as a direct consequence of this *a priori* heterogeneity.

In addition, the process of adsorption will perturb the surface and create new sites of greater or smaller activity even if the surface is initially homogeneous, and when the coverage is such that the adsorption of a molecule is no longer an unlikely event this effect may lead to a clustering of the adsorbate and an apparent heterogeneity. The cooperative nature of this interaction thus forces one to treat the surface as a dynamic system and its activity as a function not only of its previous history but also of its immediate conditions.

When the surface is nearly covered repulsive interactions between adsorbed molecules must finally become the determining factor in the process.

While relatively little is known about this type of interaction, there is no compelling evidence that it need be invoked in the range of temperatures and pressures commonly involved in normal usage. Lateral interactions of adsorbed molecules are, of course, the principle concern in the detailed treatment of surface reactions, but in the adsorption and desorption steps of the overall reaction it appears possible to neglect them without serious error.

It is not possible, at the present time, to assess properly the roles of these several phenomena in any general way. It appears that much more work will have to be done before our knowledge is sufficiently complete that any general treatment of either the thermodynamics or the kinetics of the chemisorption process on an arbitrary surface can be accomplished.

Energetics of Adsorption and Reaction

One of the fundamental problems in adsorption and surface reaction processes is the determination and interpretation of the energy changes which take place. As has been pointed out above, it is customary to distinguish between physical adsorption and chemisorption on the basis of the magnitude of the heats of adsorption, and to identify *activated* adsorption by the presence of an appreciable activation energy for the sorption process. It would appear that the fundamental distinction between the two former phenomena lies in the extent to which the adsorbing molecules interact with the surface atoms; a large energy of activation may generally be taken to imply that the entering molecules interact strongly with the surface whence it follows that activated adsorption is always chemisorption.

While there is not as yet universal agreement in the field of surface chemistry over the application of thermodynamics to adsorption data, certain rather obvious precautions may be mentioned at the outset. The true heat (or entropy, free energy, etc.) of *adsorption* must be carefully distinguished from the composite energy effects actually observed in sorption studies which may include heats of dissociation or reaction for the adsorbed species. Similarly, it is not always easy to distinguish the true activation energy in contact catalysis, since the observed effect may be the sum of the activation energy for the slowest process and heats of reactions for equilibrium steps in the over-all chain of events. The discussion on pp. 276–277 emphasized the fact that in certain cases involving extensive surface heterogeneity there may be no unique rate-determining process and hence the apparent measured activation energy cannot in such cases be identified with any particular reacting species.

In most cases, the observed energy effects are apportioned out to the several physical or chemical steps which appear in a particular model through the equilibrium and specific reaction rate constants of the derived rate expression. Extreme care in analysis is required before any considerable measure of confidence can be placed in a reaction sequence on the basis of reasonable magnitudes of these energies alone, since experience has shown that there usually exist several models which are equally satisfactory from this point of view. The same considerations apply equally to the question of identifying the entropies of reaction and activation for assumed reaction steps from a study of the temperature dependence of the over-all surface reaction, with, however, the added complication that the specific rate constant for the slowest process normally contains, either explicitly or implicitly, the specific area of the catalyst, or more generally the concentration of surface sites active in the catalytic reaction. This quantity cannot in most cases be determined independently in any way, since a given surface of constant true area is often found to exhibit different activities for different reactions and, indeed, at different temperatures for a given reaction.

Adsorption

Thermodynamics of Adsorption. Following Guggenheim[1, 83, 84, 85], we define a surface phase as the inhomogeneous region separating the homogeneous solid and gaseous phases. Since the pure solid itself is generally inert in adsorption it will be neglected in the considerations below. For *physical* adsorption it is possible to neglect as well the specific interactions of the adsorbed molecules with those atoms of the solid in the surface phase; under these conditions one may treat the system as a "pseudo one-component" system[98, 99, 210] and the variance of the system: gas-surface phase, becomes one or two, depending on whether the system is or is not closed to mass transfer. Thus with these assumptions, we may write for a closed system

$$dE = TdS - pdV = dE_g + dE_s \tag{43}$$

where the third term in the equalities[85] refers to the total internal energies of the gas and surface phases, respectively. Denoting molar quantities (equal to *partial* molar quantities in the one-component case) by bars, and assuming (1) $V_g \gg V_s$, (2) $\bar{E}_g$ a function of temperature alone, (3) $n_g + n_s =$ constant, and (4) constant surface area, Eq. (43) becomes

$$dE = n_g d\bar{E}_g + n_s d\bar{E}_s - (\bar{E}_g - \bar{E}_s)dn_s\,. \tag{44}$$

Choosing as variables the temperature and number of moles in the surface phase, Eqs. (43) and (44) may be expanded to give

$$dE = \left\{n_g \frac{d\bar{E}_g}{dT} + n_s \left(\frac{\partial \bar{E}_s}{\partial T}\right)_{n_s}\right\} dT + \left\{n_s \left(\frac{\partial \bar{E}_s}{\partial n_s}\right)_T - \bar{E}_g + \bar{E}_s\right\} dn_s \tag{45}$$

$$= \left\{T\left(\frac{\partial S}{\partial T}\right)_{n_s} - p\left(\frac{\partial V}{\partial T}\right)_{n_s}\right\} dT + \left\{T\left(\frac{\partial S}{\partial n_s}\right)_T - p\left(\frac{\partial V}{\partial n_s}\right)_T\right\} dn_s \quad (46)$$

Collecting terms, we may write

$$\begin{aligned} &\left\{n_g \frac{d\bar{E}_g}{dT} + n_s\left(\frac{\partial \bar{E}_s}{\partial T}\right)_{n_s} - T\left(\frac{\partial S}{\partial T}\right)_{n_s} + p\left(\frac{\partial V}{\partial T}\right)_{n_s}\right\} dT \\ &\quad + \left\{-T\left(\frac{\partial S}{\partial n_s}\right)_T + p\left(\frac{\partial V}{\partial n_s}\right)_T + n_s\left(\frac{\partial \bar{E}_s}{\partial n_s}\right)_T - \bar{E}_g + \bar{E}_s\right\} dn_s \end{aligned} \quad (47)$$

Under isothermal conditions the first term vanishes. Since n_s is an independent variable the coefficient of dn_s must also vanish; whence,

$$q \equiv -T\left(\frac{\partial S}{\partial n_s}\right)_T = -p\left(\frac{\partial V}{\partial n_s}\right)_T + \bar{E}_g - \bar{E}_s - n_s\left(\frac{\partial \bar{E}_s}{\partial n_s}\right)_T \quad (48)$$

where q is the differential isothermal heat of adsorption. Assuming the ideal gas law

$$V \approx V_g = \frac{n_g RT}{p} \quad (49)$$

and Eq. (48) takes the familiar form

$$q = \bar{E}_g - \bar{E}_s - n_s\left(\frac{\partial \bar{E}_s}{\partial n_s}\right)_T + RT + V_g\left(\frac{\partial p}{\partial n_s}\right)_T \quad (50)$$

Finally, if the adsorption takes place without external work (constant volume), the differential and integral heats of adsorption are obtained in the form,

$$\begin{aligned} q_d &= \bar{E}_g - \bar{E}_s - n_s\left(\frac{\partial \bar{E}_s}{\partial n_s}\right)_T \\ Q &= n_s(\bar{E}_g - \bar{E}_s) \end{aligned} \quad (51)$$

The corresponding expression for the adiabatic heat of adsorption may be derived in a similar fashion: from Eq. (43) one has

$$\begin{aligned} dE &= TdS - pdV \\ &= \left\{n_s\left(\frac{\partial \bar{E}_s}{\partial n_s}\right)_T + \bar{E}_s - \bar{E}_g\right\} dn_s + \left\{n_g \frac{d\bar{E}_g}{dT} + n_s\left(\frac{\partial \bar{E}_s}{\partial T}\right)_{n_s}\right\} dT \end{aligned} \quad (52)$$

Expressing the differentials dV and dT in terms of the independent set of variables S and n_s, one derives immediately

$$\left\{T - p\left(\frac{\partial V}{\partial S}\right)_{n_s} - \left[n_g \frac{d\bar{E}_g}{dT} + n_s\left(\frac{\partial \bar{E}_s}{\partial T}\right)_{n_s}\right]\left(\frac{\partial T}{\partial S}\right)_{n_s}\right\} dS$$
$$= \left\{p\left(\frac{\partial V}{\partial n_s}\right)_s + \left[n_g \frac{d\bar{E}_g}{dT} + n_s\left(\frac{\partial \bar{E}_s}{\partial T}\right)_{n_s}\right]\left(\frac{\partial T}{\partial n_s}\right)_S - \left[\bar{E}_g - \bar{E}_s - n_s\left(\frac{\partial \bar{E}_s}{\partial n_s}\right)_T\right]\right\} dn_s \tag{53}$$

For an adiabatic adsorption process, dS vanishes and using again the approximations of Eq. (49) one has

$$\left\{n_g \frac{d\bar{E}_g}{dT} + n_s\left(\frac{\partial \bar{E}_s}{\partial T}\right)_{n_s}\right\}\left(\frac{\partial T}{\partial n_s}\right)_S = -p\left(\frac{\partial V_g}{\partial n_s}\right)_S + \bar{E}_g - \bar{E}_s - n_s\left(\frac{\partial \bar{E}_s}{\partial n_s}\right)_T \tag{54}$$

The left hand side of Eq. (54) is the differential adiabatic heat of adsorption, $\mathring{q}_a$. The right-hand side can be transformed, using Eqs. (49, 51) to the form:

$$q_a = V_g\left(\frac{\partial p}{\partial n_s}\right)_T + RT + V_g\left\{\left(\frac{\partial p}{\partial T}\right)_{n_s} - \frac{p}{T}\right\}\left(\frac{\partial T}{\partial n_s}\right)_S + q_d \tag{55}$$

These quantities have been extensively discussed by, e.g., Hill[98, 99] and Everett[63] and Eq. (54) has been checked experimentally by Kington and Aston[112].

For the surface phase alone, one may write the expression

$$dE_s = TdS_s - pdV_s - \phi d\mathcal{a} + \mu_s dn_s \tag{56}$$

where

$$\phi \equiv -\left(\frac{\partial E_s}{\partial \mathcal{a}}\right)_{S_s, V_s, n_s}, \qquad \mu_s = \left(\frac{\partial E_s}{\partial n_s}\right)_{S_s, V_s, a} \tag{57}$$

Defining the Gibbs free energy for this phase as

$$F_s = E_s + pV_s - TS_s \tag{58}$$

or

$$dF_s = -S_s\, dT + V_s\, dp - \phi\, d\mathcal{a} + \mu_s\, dn_s \tag{59}$$

and specializing to constant surface area, the chemical potential is obtained in the form

$$d\mu_s = -\bar{S}_s\,dT + \bar{V}_s\,dp + \left(\frac{\partial\mu_s}{\partial n_s}\right)_{T,p} dn_s \tag{60}$$

In Eq. (60), $\bar{S}_s$ and $\bar{V}_s$ are the partial molar entropy and volume of the surface phase. For the gas phase

$$d\mu_g = -\bar{S}_g\,dT + \bar{V}_g\,dp \tag{61}$$

At equilibrium $d\mu_s = d\mu_g$ and Eq. (61) becomes, assuming $\bar{V}_g \gg \bar{V}_s$ and the gas phase ideal,

$$\frac{d\ln p}{dT} = \frac{\bar{H}_g - \bar{H}_s}{RT^2} + \frac{1}{RT}\left(\frac{\partial\mu_s}{\partial n_s}\right)_{T,p} \frac{dn_s}{dT} \tag{62}$$

This expression is normally used in the form

$$\frac{d\ln p}{dT} = \frac{q_{\text{st.}}}{RT^2} \tag{63}$$

i.e., at constant surface area and coverage: $q_{\text{st.}} \equiv \bar{H}_g - \bar{H}_s$ is defined as the isosteric heat of adsorption. To relate this quantity to the heats previously defined we note that

$$\begin{aligned} q_{\text{st.}} = \bar{H}_g - \bar{H}_s &= \left(\frac{\partial E_g}{\partial N_g}\right)_{T,p} + p\left(\frac{\partial V_g}{\partial n_g}\right)_{T,p} - \left(\frac{\partial E_s}{\partial n_s}\right)_{T,p} - p\left(\frac{\partial V_s}{\partial n_s}\right)_{T,p} \\ &\approx \bar{E}_g - \bar{E}_s - n_s\left(\frac{\partial \bar{E}_s}{\partial n_s}\right)_T + RT \\ &= q_d + RT \end{aligned} \tag{64}$$

For certain purposes it is convenient to define certain other thermodynamic functions particularly adapted to a discussion of surface phases: this aspect of the problem has been extensively treated by Hill, Everett and others in the references cited above. We note here only that in the present discussion the surface itself has been taken as inert, and the system as a whole treated as a pseudo one-component, two-phase system. While this is generally assumed satisfactory for physical adsorption, it will no doubt be necessary to modify the treatment for the case of chemisorption. Some progress is being made in this direction, notably by Hill, but a straightforward thermodynamic treatment of chemisorption does not now appear to be a particularly powerful tool. It may also be noted in passing that while the extension of the above equations to the case of multicomponent adsorption is formally easy, the resulting equations are not always as useful as in the case of the simpler systems.

In order to determine the various heats of adsorption experimentally, and generally to interpret the data of adsorption, it is necessary to obtain a relation between the surface coverage and the pressure of adsorbate gas, normally considered at constant temperature. There is, of course, no strictly thermodynamic argument which will explicitly determine such an isotherm, but it is possible to demonstrate the requirements which thermodynamics places upon the form of such a relationship. Considering again a one-component system we have for the surface phases

$$dE_s = T\,dS_s - p\,dV_s - \phi\,d\mathcal{A} + \mu_s\,dn_s \tag{56}$$

Using Euler's theorem and defining the (Gibbs) free energy as before in the form,

$$F_s = E_s + pV_s - TS_s \tag{58}$$

one derives immediately the expression

$$\begin{aligned} dF_s = -S_s\,dT + V_s\,dp - \phi\,d\mathcal{A} + \mu_s\,dn_s \\ = -\phi\,d\mathcal{A} - \mathcal{A}\,d\phi + \mu_s\,dn + n_s\,d\mu_s \end{aligned} \tag{65}$$

whence we obtain finally the result

$$d\mu_s = -\bar{S}_s\,dT + \bar{V}_s\,dp + (1/\Gamma)\,d\phi \tag{66}$$

where as usual the barred symbols refer to molar quantities and $\Gamma = n_s/\mathcal{A}$ is the surface coverage. For the gas phase

$$d\mu_g = -\bar{S}_g\,dT + \bar{V}_g\,dp \tag{67}$$

and at equilibrium, assuming constant temperature, the Gibbs equation for the isotherm is given as,

$$RT\,d\ln p = \frac{d\phi}{\Gamma} \tag{68}$$

(as usual, V_g has been assumed large compared with V_s and the vapor has been treated as ideal). Equation (68) must be the starting point for any "thermodynamic" derivation of adsorption isotherms, or alternatively for an experimental investigation of surface pressure, ϕ, from measured isotherms.

Volmer's derivation of the Langmuir isotherm can be described as follows. Assume the adsorbed phase to be a two dimensional imperfect gas with the equation of state,

$$\phi\left(\frac{1}{\Gamma} - \beta\right) = RT \tag{69}$$

Then Eq. (68) reduces to

$$d \ln p = \frac{d\Gamma}{\Gamma(1 - \beta\Gamma)^2} \tag{70}$$

which may be integrated to give the result

$$p = \frac{a\Gamma}{1 - \beta\Gamma} e^{1/(1-\beta\Gamma)} \tag{71}$$

a a constant of integration.

Taking the area occupied by a mole of adsorbed molecules as σ, this expression may be related to the fraction of the surface covered:

$$\Gamma = \frac{\vartheta}{\sigma} \tag{72}$$

$$p = \frac{a\vartheta}{\sigma\left(1 - \frac{\beta}{\sigma}\vartheta\right)} e^{1/(1-(\beta/\sigma)\vartheta)} \tag{73}$$

Expanding the exponential, assuming $\beta\Gamma = \frac{\beta\vartheta}{\sigma} \ll 1$ leads to the result,

$$\vartheta = \frac{\frac{\sigma}{ae} p}{1 + \frac{\beta}{ae} p} \tag{74}$$

which is of the Langmuir form. Taking p^* as the pressure at which the surface is, say, half covered permits evaluation of the constant a, leading to the equation,

$$\vartheta = \frac{\frac{\sigma}{2\sigma - \beta} \frac{p}{p^*}}{1 + \frac{\beta}{2\sigma - \beta} \frac{p}{p^*}} \tag{75}$$

Other degrees of approximation to the exponential in Eq. (73) lead to slightly different forms of the isotherm but these are not of great importance. The temperature dependence of the pressure coefficient in Eq. (75) resides in the standard pressure factor, related as usual to the heat of adsorption (isosteric) through the Clausius-Clapeyron equation.

Other thermodynamic restrictions upon the form of the adsorption isotherm have been discussed by Rushbrooke and Coulson[172]. Their argument is based upon consideration of a Carnot cycle but can be demonstrated in a somewhat more general form. We have for the closed system: gas plus adsorbate,

$$dE = TdS - pdV = dE_g + dE_s \tag{76}$$

Choosing as independent variables the temperature and pressure, we write,

$$\begin{aligned}\left\{T\left(\frac{\partial S}{\partial T}\right)_p - p\left(\frac{\partial V}{\partial T}\right)_p - \left(\frac{\partial E_g}{\partial T}\right)_p - \left(\frac{\partial E_s}{\partial T}\right)_p\right\} dT \\ + \left\{T\left(\frac{\partial S}{\partial p}\right)_T - p\left(\frac{\partial V}{\partial p}\right)_T - \left(\frac{\partial E_g}{\partial p}\right)_T - \left(\frac{\partial E_s}{\partial p}\right)_T\right\} dp = 0\end{aligned} \tag{77}$$

Since T and p are independent variables, both coefficients must vanish, whence, in particular,

$$T\left(\frac{\partial S}{\partial p}\right)_T - p\left(\frac{\partial V}{\partial p}\right)_T - \left(\frac{\partial E_g}{\partial p}\right)_T - \left(\frac{\partial E_s}{\partial p}\right)_T = 0 \tag{78}$$

It is convenient to specialize at this point in the following way: we assume the gas to be ideal and write for the equations of state and energy the expressions

$$pV_g = (N - N_s)kT \tag{79}$$

$$E_g = (N - N_s)\frac{kT}{\gamma - 1} \tag{80}$$

γ being as usual the (constant) ratio of specific heats. In addition it is assumed that the adsorbate energy is given by

$$E_s = -N_s W(T) \tag{81}$$

where W, the adsorption energy per molecule, is a function of temperature alone, i.e., independent of coverage. Then since with $V \approx V_g \gg V_s$, and

$$\left(\frac{\partial S}{\partial p}\right)_T \approx -\left(\frac{\partial V_g}{\partial T}\right)_p \tag{82}$$

Equation (78) becomes

$$\frac{kT^2}{p}\left(\frac{\partial N_s}{\partial T}\right)_p + \left\{kT + \frac{kT}{\gamma - 1} + W\right\}\left(\frac{\partial N_s}{\partial p}\right)_T = 0$$

or

$$\left\{\frac{W}{kT} + \frac{\gamma}{\gamma - 1}\right\} p \left(\frac{\partial N_s}{\partial p}\right)_T + T\left(\frac{\partial N_s}{\partial T}\right)_p = 0 \tag{83}$$

Eq (83) can (by assuming N_s separable in p and T) be shown to have solutions of the form

$$N_s(p, T) = N_s\left(\frac{p}{T^{\gamma/(\gamma-1)} \exp.\left\{-\int_T^{T_0} \frac{W}{kT^2}\,dT\right\}}\right) \tag{84}$$

It is to be noted that the criterion of thermodynamic consistency offered by Eqs. (83), (84) are only valid under circumstances in which the above simplifications are in order. The more stringent conditions obtained by, e.g., considering the heat of adsorption to vary with coverage. etc., are readily derived but cannot easily be applied.

Statistical Mechanical Treatment of Adsorption. While a thermodynamic discussion of adsorption and reaction has the great advantage of generality it suffers from the fact that specific solutions to the differential equations involved can only be obtained through the use of certain assumptions as to the microscopic nature of the system. Since such assumptions are necessary, it is convenient to apply statistical mechanical methods with which it is possible to see clearly and explicitly the nature of the molecular model assumed.

Considerable choice is available in choosing a model for the system: adsorbed gas, solid surface, gas phase. The previous discussion has been concerned exclusively with the special case in which the surface is assumed inert, and hence does not appear explicitly in the treatment except through its area, or number of sites available for adsorption, and through its influence on the chemical potential or activity of the adsorbed species. In actual fact, of course, it is well known that in chemisorption particularly the surface plays a role of considerable importance and must be reckoned as a distinct species. In addition, there is evidence to show that both the number and activity of the sites effective in catalytic adsorption, i.e., adsorption which leads to surface reaction, depend on both temperature and the extent of coverage in certain cases. Finally, the mobility of the adsorbed molecules has been shown to vary over a wide range, from completely localized adsorption with perturbations of the internal degrees of freedom of the adsorbate to what may best be described as a two-dimensional gas. We consider here some particular cases as illustrative of the current work in this direction.

If interactions between adsorbed molecules are completely ignored, and if the barrier to translation on the surface[165] may also be considered negligible the surface phase will correspond to a two-dimensional perfect gas, for which the partition function per molecule can be written,

$$f = \frac{2\pi mkT}{h^2} \mathcal{A} j(T) \tag{85}$$

where $\mathcal{A}$ is the area of the surface and $j(T)$ the partition function for the internal degrees of freedom of the molecule, including one extra vibration corresponding to the adsorption interaction. The consequences of this model have already been discussed (pp. 262–263) and shown to lead to the expression,

$$\phi = \frac{NkT}{\mathcal{A}} \tag{86}$$

for the spreading pressure (cf. Eq. (56)).

In cases of more practical interest the strength of the adsorption bond is weak and the barrier to translation small but the molecular interactions on the surface are not negligible. Here the area term in the translational partition function must as usual be replaced by a two-dimensional configuration integral over the coordinates of the molecules, and the resulting expressions are exactly analogous to the well-known treatment of imperfect gases[74, 94, 95]. While there is some evidence which indicates that mobile adsorption films on metals exist and may be catalytically important, the further development of the argument will not be carried out here.

The second principal model for the adsorbed film is that of the localized monolayer. Here the translational degrees of freedom of the gas molecule have been replaced by vibrations about some equilibrium position on the surface (in some cases rotational degrees of freedom have also been restricted or replaced by vibrations) and in general there is a potential energy w of interaction between the adsorbed molecule and the surface. Thus, the partition function per molecule on the surface will be of the form

$$f_{is} = e^{w_i/kT} j_{is}(T) \tag{87}$$

For complete localization there will be a combinatorial term, giving the number of ways of distributing N_{is} molecules of kind i over N_s surface sites, and the total partition function for the surface phase will be

$$\mathfrak{F} = \frac{N_s! \prod_i f_{is}^{N_{is}}}{\left(N_s - \sum_j N_{js}\right)! \prod_i N_{is}!} \tag{88}$$

Equation (88) gives for the chemical potential μ_{ks} of the kth species the result

$$\mu_{ks} = kT \ln \frac{N_{ks}}{\left(N_s - \sum_i N_{is}\right) f_{ks}} \tag{89}$$

This formulation leads, as shown previously, to the well known Langmuir expression for the adsorption isotherm.

In order to treat chemisorption, it is necessary to include in the formulation the effect of the adsorbate-surface interaction explicitly. Since the system is highly nonideal, this is extremely difficult to do in any general way and, in fact, no complete agreement exists as to the form of the partition function even in specific cases. The principal problem arises from the attempt to separate the total partition function into factors each of which are functions characteristic of a single molecule. When this is done it is possible to obtain immediately the chemical potential of each species and thence the equilibrium constant for adsorption or reaction. We may illustrate this process for a particular model in the following way: consider a surface phase consisting of N_{is} adsorbed molecules of species i, N_{is} covered surface atoms and N_o total surface atoms. Following Hill we assume that the number of sites active in adsorption at a given temperature is related to the geometric area through the equation:

$$B(T) = \alpha(T) \cdot \mathcal{A} \tag{90}$$

The partition functions (per molecule) for the various species may be defined as

$$\begin{aligned} f_{is} &= \left(\frac{kT}{h\nu_{is}}\right)^3 j_{is}(T) e^{\epsilon_{is}/kT} && \text{Adsorbed molecule} \\ f_i &= \left(\frac{kT}{h\nu_i}\right)^3 j_c(T) && \text{Covered surface site} \\ f_s &= \left(\frac{kT}{h\nu_0}\right)^3 j_c(T) && \text{Bare surface site} \end{aligned} \tag{91}$$

It has been assumed that the three translational degrees of freedom of the adsorbed molecule have been replaced by three vibrations of frequency ν_{is} and that the heat of adsorption is ϵ_{is}. $j_{is}(T)$ is the partition function for the internal degrees of freedom of the molecule and $j_c(T)$ that for the surface site. The total partition function for the complete surface phase is, then

$$\mathfrak{F} = \frac{B!}{\left(B - \sum_i N_{is}\right)! \prod_i N_{is}!} \left[\frac{kT}{hv_0} j_c^{1/3}\right]^{3\left(N_0 - \sum_i N_{is}\right)} \prod_i \left[\frac{kT}{hv_{is}} j_{is}^{1/3} e^{\epsilon_{is}/3kT}\right]^{3N_{is}} \prod_i \left[\frac{kT}{hv_i} j_c^{1/3}\right]^{3N_{is}} \tag{92}$$

$$= \frac{B!}{\left(B - \sum_i N_{is}\right)! \prod_i N_{is}!} f_s^{N_0 - \sum_i N_{is}} \prod_i (f_{is} f_i)^{N_{is}}$$

where the combinatorial term represents the number of distinguishable configurations on the surface. From the partition function one can immediately obtain the Helmholtz free energy and thence the chemical potential of the species in the usual way. Defining the absolute activity λ one has finally the result,

$$\lambda_{ks} \equiv e^{\mu_{ks}/kT} = \frac{f_s}{f_{ks} f_k} \frac{\vartheta_k}{\alpha - \sum_i \vartheta_i} = \frac{f_s}{f_k^*} \frac{\vartheta_k}{\alpha - \vartheta} \tag{93}$$

where f_k^* is the partition function of the adsorbate-surface complex and ϑ is the function of the available surface covered by all species of adsorbed molecules. The ϑ_k are defined by

$$\vartheta_k = \frac{N_{ks}}{\mathcal{A}} \tag{94}$$

It is now possible to derive other thermodynamic results directly: thus for the adsorption isotherm, since the absolute activity in the gas is given by

$$\lambda_{kg} = \frac{p_k}{\left(\frac{2\pi m_k kT}{h^2}\right)^{3/2} kT j_k} = \frac{p_k}{f'_{kg}} \tag{95}$$

we have at equilibrium,

$$\lambda_{ks} = \lambda_{kg}\,, \qquad \frac{\vartheta_k}{\alpha - \vartheta} = \frac{f_k^*}{f_s f_{kg}} p_k \tag{96}$$

again of the form of the Langmuir equation for multiple adsorption. Also, if species 1 and 2, say, are in chemical equilibrium with species 3 on the surface, the condition for equilibrium is

$$\lambda_{3s} = \lambda_{1s} \lambda_{2s} \tag{97}$$

which may be written in the form, using Eq. (93)

$$\frac{\vartheta_3(\alpha - \vartheta)}{\vartheta_1\vartheta_2} = \frac{f_s f_3^*}{f_1^* f_2^*} \equiv K(T) \tag{98}$$

where $K(T)$ is the (rational) equilibrium constant. The standard free energy is the free energy in the state in which

$$\vartheta_3^0\vartheta_s^0 = \vartheta_1^0\vartheta_2^0 , \qquad \vartheta_s = \alpha - \vartheta \tag{99}$$

and as usual may be defined in a variety of ways.

Even in the case of the single unimolecular surface coverage illustrated above the model cannot be considered either sufficiently general or satisfactory. Halsey[88] has treated the kinetics of adsorption in the case of a heterogeneous surface and Hill[97] has discussed the statistical thermodynamics of localized adsorption on heterogeneous surfaces. McMillan and Teller[137] and Hill[96] have extended the same type of treatment to multilayer adsorption as has Ono[146, 147] in a series of papers, but in every case it has only been found possible to include one of the several perturbing factors in each discussion. The very important problem of lateral interactions in chemisorption, of paramount interest in surface reactions, has been developed by Roberts[166, 167] and by Miller[139, 140] using the method of localized configurations in a manner similar to that employed by Peierls[156] and Bethe[17] in order-disorder theory and by Parlin and Eyring[150] and Cernuschi and Eyring[27] in the theory of liquids. The discussion includes both mobile and localized monolayers and excellent agreement is obtained between measured and calculated heats of adsorption for hydrogen on tungsten[163] and on nickel[14]. Using this treatment it is found that the heat of adsorption may be expected to depend in a strongly nonlinear way on the fraction of the surface covered in the case of a mobile film, while the dependence will be nearly linear for an immobile film. In some cases there is evidence that the type of adsorption changes from one to the other as the surface becomes saturated with consequent complication of the heat curve.

We defer further discussion of such specific models to a later section, since it does not appear possible to set down any general statement of the partition function of the adsorbed phase. It may perhaps be re-emphasized here that until it is possible to reduce the configurational partition function for semilocalized systems in some systematic way which will permit inclusion of the various types of attractions and repulsions known to be important every such treatment must be considered individually with respect to the data it is designed to represent.

From straightforward thermodynamic considerations we can write for the Gibbs free energy of a multicomponent system equations of the form

$$F = \sum_i N_i\mu_i = \sum n_i \left(\frac{\partial A}{\partial N_i}\right)_{T,V} = A - V\left(\frac{\partial A}{\partial V}\right)_{T,N_i} \tag{100}$$

The last of these equalities constitutes a partial differential equation for the Helmholtz free energy A, the solution of which sets certain purely thermodynamic conditions upon the possible functional dependence of this variable. We may obtain the general integral of Eq. (100) in the following way: choose as independent variables the temperature, volume and species concentrations, defined as

$$C_i = N_i/V \tag{101}$$

and substitute in the differential equation

$$V\left(\frac{\partial A}{\partial V}\right)_{T,N_i} + \sum_i N_i\left(\frac{\partial A}{\partial N_i}\right)_{T,V} = A \tag{102}$$

The relevant transformation equations are readily found to be

$$\begin{aligned} \left(\frac{\partial A}{\partial V}\right)_{T,N_i} &= \left(\frac{\partial A}{\partial V}\right)_{T,c_i} - \frac{1}{V}\sum c_i\left(\frac{\partial A}{\partial c_i}\right)_{T,V} \\ \left(\frac{\partial A}{\partial N_i}\right)_{T,V} &= \frac{1}{V}\left(\frac{\partial A}{\partial c_i}\right)_{T,V} \end{aligned} \tag{103}$$

whence Eq. (87) becomes,

$$V\left(\frac{\partial A}{\partial V}\right)_{T,c_i} = A \tag{104}$$

which may be written,

$$\left(\frac{\partial \ln A}{\partial \ln V}\right)_{T,c_i} = 1 \tag{105}$$

The most general solution to this equation is clearly

$$\begin{aligned} A &= V\phi, \\ \phi &\equiv \phi(T, c_1, c_2, \cdots, c_n) \end{aligned} \tag{106}$$

where ϕ is an arbitrary function of its argument. We note that in terms of the chosen variables the free energy can only have a linear dependence upon the volume of the system. In order to connect the thermodynamic result, (Eq. 106), with the formulations of statistical mechanics, we write

$$A = -kT \ln \mathfrak{F} = -kT \ln \left\{ Q \cdot \prod_i \frac{f_i^{N_i}}{N_i!} \right\} \tag{107}$$

where $\mathfrak{F}$ is the partition function for the whole assembly, composed of N_i molecules of species i. The f_i are functions of temperature alone and in general will be the partition functions per molecule for internal degrees of freedom (vibration and rotation) together with the translational partition function per unit volume (or area) when appropriate. Q is, in the case of an imperfect gas or liquid, the configurational partition function[74] and in general is a function of volume, temperature and the N_i's. From equations (106) and (107) it may readily be shown that

$$\begin{aligned} Q &= V^n e^{V\sigma} \\ \sigma &\equiv \sigma(T, c_1, c_2, \cdots, c_n) \end{aligned} \tag{108}$$

where N is the total number of molecules in the system. Also from Eqs. (108) and (106) it follows that

$$\phi(T, c_i) = -kT \left[\ln \prod_i \left(\frac{f_i e}{c_i} \right)^{c_i} + \sigma \right] \tag{109}$$

$$A = -kTV \left[\ln \prod_i \left(\frac{f_i e}{c_i} \right)^{c_i} + \sigma \right] \tag{110}$$

It may be noted that for a perfect gas, $\sigma = O$ and $Q = V^N$ as is to be expected. The utility of the development above lies in the fact that in terms of the function σ it is *formally* possible to define a quantity g_i such that for the total partition function we will have

$$\mathfrak{F} = \prod_i g_i^{N_i} = \prod_i \left\{ \frac{f_i e}{c_i} \; e^{\sigma / \sum_j c_j} \right\}^{N_i} \tag{111}$$

and $\mathfrak{F}$ has been split into terms each of which depend only upon the temperature and the various molecular concentrations, regardless of the lack of ideality of the assembly as a whole. The exponential term contains the concentrations of all of the various kinds of molecules and must be regarded as the contribution to the partition function for a given species of the molecular interactions.

From Eq. (111) the chemical potentials and the absolute activitiee of the various species are derived in the usual way as

$$\mu_k = \frac{1}{V} \left(\frac{\partial A}{\partial c_k} \right)_{T,V} = -kT \left[\ln \frac{f_k}{c_k} + \left(\frac{\partial \sigma}{\partial c_k} \right)_T \right], \tag{112}$$

$$\lambda_k = e^{\mu_k / kT} = \frac{c_k}{f_k} e^{-(\partial \sigma / \partial c_k)_T} \tag{113}$$

and the activities or fugacities by dividing the λ's by their values in some selected standard state, preferably one in which the terms in σ vanish or can be evaluated explicitly.

Certain other approaches to the calculation of adsorption heats may be mentioned briefly. Eley[46], assuming the adsorption bond to be of the covalent type, has used the procedure of Pauling[154, 155] to relate these heats to the heat of sublimation of the metal, the contact potential of the covered surface and the number of surface sites per unit area. In a number of cases (Cu, H_2 ; W, H_2) quite satisfactory agreement is obtained in the case of metal surfaces. Bremner[25] refers briefly to an application of molecular orbitals to the interaction between unsaturated molecules and metal surfaces in which the π-electrons tend to fill the vacancies in the *d*-band of the metal.

Kinetic Formulation

Recent investigations by some of the present authors[68] have led to the development of a somewhat different approach to the general problem of adsorption. This treatment is not restricted to adsorption phenomena, but applies quite generally within the framework of its assumptions to any process involving the reshuffling of a set of particles (electrons, atoms, molecules, etc.) among energy states. The method is equivalent to that introduced by van't Hoff and later used by Langmuir in connection with his well-known adsorption isotherm.

Consider a number n_i particles adsorbed on ω_i sites of a surface, leaving n_g free units in some volume V. For convenience, we assume the n_g gaseous molecules to behave as an ideal gas. At any instant, the bound particles are leaving the surface at a rate $n_i k'_i$. k'_i is the specific rate constant for desorption of a particle. The rate of adsorption from the free state is similarly obtained as the product of a specific rate constant k'_g and the number of sites available for adsorption. For the general case, this latter quantity requires some careful consideration. Consider first the case of unlimited adsorption on a given site: since any one of the n_i units is permitted to leave the site for the free state, microscopic reversibility requires that the reverse process must also be an allowable one. Thus each adsorbed particle must be counted as the equivalent of a site for condensation and the effective number of adsorption sites will be given as the sum of the ω_i *a priori* surface sites and the n_i adsorbed particles. The rate of condensation may then be written as $(\omega_i + n_i)\, n_g k_g'$. If, however, the surface site is saturated by d molecules, and p is the probability that any one of the sites *is* so saturated, thus removing a total of $(d + 1)$ candidates for adsorptions, we must write for the equilibrium rates an expression of the form

$$k'_i n_i = [\omega_i + n_i] n_g k'_g - p(d + 1)\omega_i n_g k'_g \tag{114}$$

or more simply, for a single kind of surface site,

$$n = \frac{\omega}{\dfrac{K}{n_g} - 1} \cdot \{1 - p(d + 1)\} \tag{115}$$

In this equation K is the equilibrium constant between the n adsorbed molecules and the n_g gas molecules, i.e., the ratio of k_i' to k_g'. Two important cases are apparent: for $d = \infty$, then $p = 0$ and

$$n = \frac{\omega}{\dfrac{K}{n_g} - 1} \tag{116}$$

while if $d = 1$, then $p = n/\omega$ and

$$n = \frac{\omega}{\dfrac{K}{n_g} + 1} \tag{117}$$

Equation (116) corresponds to unlimited adsorption in the idealized case for which the energy of adsorption remains constant, whether taking place on the surface or on a molecule already adsorbed. This has been shown[68] to be closely related to the phenomenon of condensation. Equation (117), based on the assumption that a site is saturated by a single molecule, clearly corresponds to monolayer adsorption and in fact is just the Langmuir isotherm. For a surface consisting of nonuniform sites, Eq. (117) may be modified by writing

$$n = \sum_i n_i = \sum_i \frac{\omega_i(E_i)}{\dfrac{K_i(E_i)}{n_g} - 1} \tag{118}$$

so that if the distribution function $\omega_i(E_i)$ for sites of different energies is known, n can be calculated. In the case of a continuous distribution, the summation in Eq. (118) is replaced by an integration and the function ω by $\omega(E)\,dE$. It should be remembered that in their present form the equations refer only to the case of no lateral interaction of adsorbed molecules: while it seems likely that the necessary formalism can be developed to include these effects, further study will be required in order to achieve any considerable degree of practical usefulness.

The general equation, (115), representing cases intermediate to those discussed above, gives the equilibrium number of molecules adsorbed at uniform energy on any surface for which the number of layers permitted is limited[69]. In order to use it, however, the probability, p, must be evaluated for specific instances. The necessary calculations are made in the following way: let $A(\omega, n, d)$ be the number of ways in which n objects can be placed on ω sites with no more than d on each site, and $A(\omega\text{-}1, n\text{-}d, d)$ the number of ways of arranging $n\text{-}d$ objects in ω-1 piles under the same restriction. The required probability is then

$$p = \frac{A(\omega - 1, n - d, d)}{A(\omega, n, d)} \tag{119}$$

The number $A(\omega, n, d)$ is quite easily shown to be just the coefficient of z^n in the expansion of the polynomial

$$(1 + z + z^2 + \cdots z^d)^\omega$$

This coefficient can also be shown to equal $(1/n!)$ times the nth derivative of this polynomial, evaluated at $z = 0$. Thus,

$$A(\omega, n, d) = \frac{1}{n!}\left\{\frac{d^n}{dz^n}(1 + z + z^2 + \cdots + z^d)^\omega\right\}_{z=0} \tag{120}$$

The probability p can then be expressed as

$$p = \frac{\dfrac{1}{(n-d)!}\left\{\dfrac{d^{n-d}}{dz^{n-d}}(1 + z + z^2 + \cdots + z^d)^{\omega-1}\right\}_{z=0}}{\dfrac{1}{n!}\left\{\dfrac{d^n}{dz^n}(1 + z + z^2 + \cdots + z^d)^\omega\right\}_{z=0}} \tag{121}$$

For large n and ω direct evaluation of Eq. (121) is not feasible, but methods of expressing p as a more easily evaluated function of its argument are presently under investigation.

Within the framework of the same general scheme that leads to Eq. (121) one can also find the equilibrium isotherm for adsorption into a crack or crevice between plane parallel walls which constitute ideal surfaces. We think of the system as shown in Fig. 3, where the walls are d units apart so

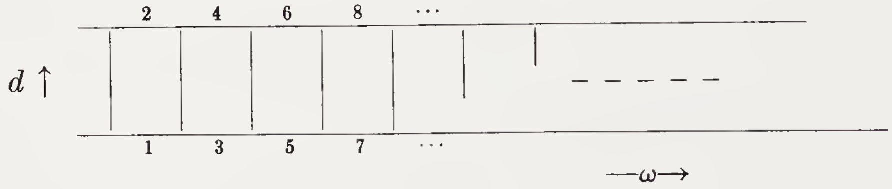

FIG. 3

that a maximum of d molecules can be adsorbed between any two opposed adsorption sites. The product of the generating functions for the two surfaces is

$$(1 + x + x^2 + \cdots)(1 + x + x^2 + \cdots) = \sum_{l=0}^{d} (l + 1)x^l \quad (122)$$

where $(l + 1)$ in each term of the series is the number of ways that l molecules can be put into the space between two sites. The coefficient of x^n in the expansion of

$$\left\{\sum_{l=0}^{d} (l + 1)x^l\right\}^{\omega/2}$$

is just the number of ways in which n molecules may be put into a crevice d units in width. This coefficient may be, as before, written

$$A(\omega, n, d) = \frac{1}{n!} \left\{\frac{d^n}{dx^n} \left[\sum_{l=0}^{d} (l + 1)\, x^l\right]^{\omega/2}\right\}_{x=0} \quad (123)$$

The probability p that one of these spaces between sites is filled is then

$$p = \frac{A(\omega - 2, d, n - d)}{A(\omega, n, d)} \quad (124)$$

The equation for n, the equilibrium number of adsorbed units is then, for this case,

$$n = \frac{\omega/2}{\dfrac{K}{n_g} - 1} \cdot \{2 - p(d + 1)\} \quad (125)$$

It should be emphasized that in all of the various cases considered above, the assumption has been made that lateral interactions are unimportant. The additional approximation that the surface sites are all alike can be removed whenever the distribution of adsorption energies is known. Within the framework of these approximations, Eq. (115) can be shown to be consistent with most of the well known treatments of adsorption equilibrium; for example, Eq. (115) is equivalent to the general form of the Brunauer-Emmett-Teller equation when the appropriate changes in variable are carried out. It will not, of course, be possible to correlate the formulation described here with adsorption isotherms in the derivation of which explicit attention has been paid to the changes in interaction energy with surface coverage. It is not only the "horizontal" interactions referred to above which introduce errors into the present treatment, but also the "vertical" changes in the heat of adsorption as one progresses from layer to layer. This latter effect has been approximately considered in the BET treatment through the constant c, and in several other discussions[5, 31, 37] through semi-empirical modifications of the theory.

Surface Reaction

The general expression for the specific rate constant for any reaction is

$$k' = \frac{kT}{h} K^{\ddagger} \tag{126}$$

where $K^{\ddagger}$ is related to the ordinary equilibrium constant between reactants and activated complex by

$$K_{\ddagger} = K^{\ddagger} \cdot \left\{ \left(\frac{2\pi mkT}{h^2} \right)^{1/2} \delta \right\} \tag{127}$$

and the term in brackets is the partition function for the degree of translational freedom corresponding to the reaction coordinate. These equilibrium constants usually refer to reactions of the form

$$\mathrm{A} + \mathrm{B} + \cdots \rightleftarrows (\mathrm{AB} \cdots)^{\ddagger}$$

where A, etc. may either be adsorbed molecules or molecules in the homogeneous phase above the surface. In terms of absolute activities the thermodynamic equilibrium expression is

$$\lambda_A \cdot \lambda_B \cdot \; \cdots \; = \lambda_{\ddagger} \tag{128}$$

Taking the ordinary activity as $a_i = \lambda_i / \lambda_i^0$, where λ_i^0 is the absolute activity of the ith component in its standard state, Eq. (128) may be written in the form,

$$K_{\ddagger} = \frac{a_{\ddagger}}{a_A a_B \cdots} = \frac{\lambda_A^0 \lambda_B^0 \cdots}{\lambda_{\ddagger}^0} \tag{129}$$

From the formulation Eq. (113) we have

$$\begin{aligned} K_{\ddagger} &= \frac{\dfrac{c_A^0}{f_A^0} e^{-\left(\frac{\partial\sigma}{\partial c_A}\right)^0} \cdot \dfrac{c_B^0}{f_B^0} e^{-\left(\frac{\partial\sigma}{\partial c_B}\right)^0} \cdot \cdots}{\dfrac{c_{\ddagger}^0}{f_{\ddagger}^0} e^{-\left(\frac{\partial\sigma}{\partial c_{\ddagger}}\right)^0}} \\ &= \left(\frac{c_A^0 c_B^0 \cdots}{c_{\ddagger}^0} \right) \left(\frac{f_{\ddagger}^0}{f_A^0 f_B^0 \cdots} \right) \exp. \left\{ \left(\frac{\partial\sigma}{\partial c_{\ddagger}} \right)^0 - \left(\frac{\partial\sigma}{\partial c_A} \right)^0 \cdots \right\} \end{aligned} \tag{130}$$

where the superscript zero denotes the value of the respective quantities in their standard states. If now we define the partition function per molecule per unit volume (or area) by

$$F_i' = \frac{f_i^0}{c_i^0} e^{\left(\frac{\partial\sigma}{\partial c_i}\right)^0} \tag{131}$$

we can write

$$K_{\ddagger} = \frac{F'_{\ddagger}}{F'_A \cdot F'_B \cdot \cdots} \tag{132}$$

and Eq. (126) with (127) gives for the rate constant the expression,

$$k' = \frac{kT}{h} \frac{F'_{\ddagger}}{F'_A F'_B \cdots} \tag{133}$$

Extracting the zero-point energy from the F' we have the alternative form,

$$k' = \frac{kT}{h} \frac{F_{\ddagger}}{F_A F_B \cdots} e^{-E_0/RT} \tag{134}$$

This latter expression is exactly the customary form of the absolute rate constant but with the difference that the partition functions are specified, once a standard state has been chosen, to be the product of temperature-dependent factors f, referring specifically to single molecules, and the exponential factor in σ representing the interactions of a given molecule with all of the other molecules in the system. If, as is not at all uncommon, the assumption is made that the molecules do not interact, then the latter factor becomes unity and for unit concentration as a standard state we have,

$$k' = \frac{kT}{h} \frac{f_{\ddagger}}{f_A f_B \cdots} e^{-E_0/RT} \tag{135}$$

Here the f's are usually approximated by vibrational partition functions when the reaction is between molecules bound tightly to the surface or, if A or B are gas molecules, by the ideal gas partition function per molecule.

It is clear from Eq. (130) that here as in homogeneous reactions the choice of standard state is entirely arbitrary provided only that it be explicitly stated. The usual choice for this standard state in surface reactions is that of unit concentrations of all species including the activated complex. While it is true that this choice corresponds to a completly unrealizable physical state in most cases[111], it is nevertheless the most convenient since it is in accord with the natural choice for the standard state for gases.

If a given reaction is studied in such a way that the variable being measured is one of those whose concentrations is rate determining, the rate constant thus determined will be that just discussed. The activation energy determined from this type of data is essentially that of Eq. (134) (the exact relation between E_0 and the classical activation energy has been investigated by several authors[80]). Unfortunately, the quantities measured in most catalytic rate determinations are not the ones involved in the rate determining step. The measured quantities are related to these through equilibrium constants which must be determined before the actual activation energy can be determined. This point has been discussed in some detail for the case of ethylene hydrogenation by the present authors[65]; for purposes of illustration we consider two simple cases here.

Certain unimolecular decompositions at catalytic surfaces can be described by a mechanism in which every adsorbed molecule is activated, i.e., the gas phase molecules are in direct equilibrium with the activated complex on the surface[114]. The velocity of such a reaction may then be written

$$v = k' c_g c_s \tag{136}$$

where

$$k' = \frac{kT}{h} K^{\ddagger} = \frac{kT}{h} \frac{F_{\ddagger}}{F_g F_s} e^{-E_0/RT} \tag{137}$$

The quantities F_f, F_g and F_s are just those defined in Eq. (131). The rate equation is then given by,

$$v = c_g c_s \frac{kT}{h} \frac{F_{\ddagger}}{F_g F_s} e^{-E_0/RT} \tag{138}$$

and the only energy appearing in the expression is the activation energy. The fact that in this case the complete system consists of two phases, gas and surface, offers no particular difficulty except that the concentrations are referred to the volume of the whole system. For such an assembly, the quantity σ may split into two nearly independent parts, one a function of temperature and the gas-phase concentrations and the other depending on the surface concentrations.

It is also reasonable to expect that other unimolecular decompositions at surfaces may proceed by the activation of an already adsorbed intermediate. In such a case the appropriate rate equation will be

$$v = n_{gs} \frac{kT}{h} \frac{F_{\ddagger}}{F_{gs}} e^{-E_0/RT} \tag{139}$$

where n_{gs} is the number of adsorbed molecules. To relate this rate on the surface to concentrations in the gas phase we assume equilibrium between gas and absorbed reactant and write

$$n_{gs} k'_{gs} = n_g (n_s - n_{gs}) k'_g \tag{140}$$

The left-hand side of Eq. (140) gives the rate of desorption of reactant and the right-hand side the corresponding rate of adsorption. The k's are the appropriate rate constants and n_g, n_s and n_{gs} the number of gas molecules, bare adsorption sites, and adsorbed molecules, respectively.

Putting in the appropriate expressions for the rate constants and cancelling similar terms one has

$$\frac{n_{gs}}{F_{gs}} e^{-E_0/RT} = \frac{n_g(n_s - n_{gs})}{F_g F_s} e^{-E_0'/RT} \tag{141}$$

Here E_0 and E_0' are the appropriate activation energies. This equation rearranges to

$$n_{gs} = \frac{K' n_g n_s}{1 + K' n_g} \tag{142}$$

where

$$K' = \frac{F_{gs}}{F_g F_s} e^{-(E_0 - E_0')/RT} \tag{143}$$

Equation (142) is of the form of the Langmuir isotherm but the resemblance is only formal since the F's contain, through the factors $e^{\left(\frac{\partial \sigma}{\partial c_i}\right)^0}$ all of the concentrations and, through them, n_{gs}. Equation (143) is thus not explicit for n_{gs} but does reduce to explicit form for the ideal cases in which either σ itself reduces to zero or its partial derivatives with respect to the concentrations are zero. Combining Eqs. (139) and (142) we have

$$v = \frac{K'}{1 + K' n_g} n_g n_s \frac{kT}{h} K^{\ddagger} e^{-E_0/RT} \tag{144}$$

or, extracting the zero point energy difference from K'

$$v = \frac{K n_g n_s}{(1 + K n_g e^{E_a/RT})} \frac{kT}{h} K^{\ddagger} e^{-((E_0 - E_a)/RT)} \tag{145}$$

Besides the cases for which this complete equation must be used as, for example, the decomposition of antimony hydride on an antimony surface[190], there are two limiting cases to be considered. If K is small, Eq. (145) reduces to

$$v = n_g n_s \frac{kT}{h} K K^{\ddagger} e^{-((E_0 - E_a)/RT)} \tag{146}$$

Since K being small means the surface is sparsely covered, n_s will be effectively constant and the rate will be of first order with respect to gas concentration. This equation shows the same dependence on gas concentration as Eq. (138) and in fact reduces to the form

$$v = n_g n_s \frac{kT}{h} \frac{F_\ddagger}{F_g F_s} e^{-((E_0 - E_a)/RT)} \tag{147}$$

when K and $K^\ddagger$ are replaced by their definitions. The appearance of E_a in the exponent will be impossible to confirm under experimental conditions for which Eq. (147) holds. If in a given case a decision is to be made at all between the mechanisms represented by Eqs. (138) and (147) the kinetic data must be extended through a very wide range of temperatures and gas concentrations.

The other limiting case occurs when K is very large compared to unity. Then Eq. (136) reduces to

$$v = n_s \frac{kT}{h} K^\ddagger e^{-E_0/RT} \tag{148}$$

and the rate becomes independent of the gas concentration. The activation energy found for this case will be the true activation energy. If it is possible, in a given reaction so to vary the experimental conditions that the kinetic law approximates both Eqs. (147) and (148) under different conditions then both E_0 and E_a can be evaluated easily. Systems which show the characteristics of these two limiting cases are known[114].

The examples just discussed are typical of the cases which arise in catalytic reaction studies. In most cases a reliable deduction of the mechanism requires the collection of data over the widest possible range of experimental conditions. It is the feeling of the authors that before an attempt is made to discuss a given reaction in terms of surface heterogeneity of the catalyst a sufficiently varied amount of data should be taken so that a mechanism based on the idea of an essentially uniform surface can first be shown to be incorrect. While this has undoubtedly been done in a large number of cases there are many reactions which might still yield to interpretation on the basis of analyses similar to that just discussed.

Nature of the Activated Complex

Theory and General Considerations

Without entering into a detailed discussion of the modern kinetic-thermodynamic-statistical treatment of chemical reaction theory, its ready applicability will be brought out by treating a typical contact catalytic process, namely, the hydrogenation of ethylene over a metal catalyst. Special emphasis will be placed on the use of potential energy surfaces which are so characteristic of the *activated complex* or *transition state* method of approach to the interpretation of chemical reactions whether they be homogeneous or heterogeneous in character. It is to be understood that the discussion will be centered on an understanding of the elementary steps in any catalytic phenomenon. The premise is made that in many favorable cases of catalysis there is only one important chain of reactions leading to the final products and this chain has one link which is responsible for the measured velocity of reaction. All others in the chain are assumed to be so much faster that practical chemical equilibrium is maintained at all other points in the chain. The complexity of many catalytic processes involving the cooperation of the various elementary reactions whether simultaneous or consecutive or both is not to be denied; consideration of certain of these complicating features is sometimes possible in specific cases and will then be included. It is felt, however, that a detailed discussion of these points will contribute little to any general theory of catalysis.

The absolute rate theory of reaction rates can very conveniently be divided into two stages: in the first stage one determines the energy of the reacting system consisting of the chemical species and the catalyst as a function of the relative configuration of the atoms and in the second one calculates the rate at which the kinetic system passes through the various intermediate configurations between the initial and the final state. The first part of the problem is pure quantal theory or the extension of the quantum mechanical valence theory to such configurations. The second part is the statistical mechanical calculation of the specific rate constant. F. London[126] in 1928 indicated how the methods of the still new quantum mechanics could be employed in calculating the energy of activation of chemical reactions which are termed "adiabatic" (or *adiabatisch-reversibel* as first given by Ehrenfest[42]) in the sense that they do not involve electronic transitions and occur on the same potential energy surface. With rather drastic approximations he obtained the following equation showing how the potential energy of a nonlinear system of three atoms with s electrons varied with their interatomic distances:

$$E = Q_{ab} + Q_{ac} + Q_{bc} - [\tfrac{1}{2}((J_{ab} - J_{bc})^2 + (J_{ab} - J_{ac})^2 + (J_{bc} - J_{ac})^2)]^{1/2} \qquad (149)$$

Here the Q's are coulombic integrals and the J's the customary exchange integrals and the potential energy is referred to the state of the separated atoms taken as zero. The usefulness of this equation in the construction of potential energy surfaces for the interpretation of chemical reactions was developed and extended by Eyring and Polanyi[64]. Since the London equation even in its approximate form involves quantities which can be completely evaluated only for the simplest system consisting of hydrogen atoms, they considered approximate solutions which led to the "semiempirical" method for the calculation of the energy of activation. This is aptly treated in a recent text[80] and the usefulness of the method is assessed in a paper by Hirschfelder, Eyring and Topley[102].

By proceeding to the second stage dealing with the statistical formulation of the specific reaction rate constant, the definition of an activated complex can be brought out. Actually Marcelin[128] in 1915 first recognized the existence of an "activated complex" or transition state for a chemical reaction when he clearly stated that *provided the chemical process does not disturb the equilibrium distribution* of the molecules, in phase space, the rate of a process is given by the rate at which molecules cross a critical surface in phase space.* Thus for each process there is an intermediate or critical configuration called the "activated complex" situated at the highest point of the most favorable reaction path on the potential energy surface, i.e., the path that requires the least expenditure of energy. This is shown in Figure 4 as a two-dimensional energy profile for the kinetic system, H and E being as usual the exothermicity of the reaction and the energy of activation, respectively.

It is apparent from this method of analysis for chemical reactions that it is not sufficient that the reacting molecules should collide with a certain mutual energy but it is necessary for the kinetic system to achieve a definite configuration as well. The activated configuration or the activated complex can be regarded as a normal molecule except that it possesses an extra degree of translational freedom along the reaction coordinate. This implies that the activated complex is a molecule which resists deformation, i.e., the potential energy increases with deformation in all directions except that one along the reaction coordinate. Whereas a normal nonlinear molecule possesses $3n$-6 normal modes of vibration, the activated complex has only $3n$-7, since along the one coordinate deformation leads to a breakdown or a transformation of the complex into a normal molecule or molecules.

In the application of the absolute theory of reaction rates to contact catalysis, the normal procedure is followed as in the treatment of all chemical reactions by assuming that the sites of the catalyst are to be considered as a reactant and treating the heterogeneous reaction as a homogeneous system in principle. If S_k is taken as the concentration of surface sites per square centimeter of the kth type and the customary assumption of an equilibrium involving the initial and the activated state

---

* The correctness of the equilibrium postulate in rate process has recently been studied by Kramers[113], Zwolinski and Eyring[221], Hulburt and Hirschfelder[106], Prigogine and Mahieu[159], and Takayanagi[191].

is made, the following equation can be written:

$$nC_i + mC_j + S_k \rightleftharpoons (C_{in}C_{jm}S_k)^{\ddagger} \rightarrow \text{Products} \tag{150}$$

where C_i and C_j represent the gaseous concentrations of the reactants. The subscripts n and m in the activated complex are used to denote any fragmentation of dissociation of the original reactants. The velocity of the reaction is then given by the concentration of activated complexes (treated as normal molecules by replacing the metastable degree of vibrational freedom by translational motion along the reaction coordinate) multiplied by the frequency of crossing the potential barrier at the saddle point,

$$\frac{1}{\delta q}\sqrt{\frac{kT}{2\pi m^{\ddagger}}}$$

and the transmission coefficient κ. κ is the chance that, having once crossed the barrier, the activated complex does not return. It follows, then,

$$v = \kappa(C_{in}C_{jm}S_k)^{\ddagger}\,\frac{(2\pi m^{\ddagger}kT)^{1/2}}{h}\,\delta q\cdot\sqrt{\frac{kT}{2\pi m^{\ddagger}}}\,\frac{1}{\delta q} \tag{151}$$

where δq is an arbitrary length at the saddle point. The expression simplifies to

$$v = \kappa(C_{in}C_{jm}S_k)^{\ddagger}\,\frac{kT}{h} \tag{152}$$

and since

$$K^{\ddagger} = \frac{(C_{in}C_{jm}S_k)^{\ddagger}}{C_i^n C_j^m S_k} \tag{153}$$

the specific reaction rate constant for the catalytic process is

$$k' = \kappa\,\frac{kT}{h}\,K^{\ddagger} \tag{154}$$

or

$$k' = \kappa\,\frac{kT}{h}\,\frac{F^{\ddagger}/\mathcal{A}}{\left(\frac{F_i}{V}\right)^n\left(\frac{F_j}{V}\right)^m\left(\frac{F_{S_k}}{\mathcal{A}}\right)}\,e^{-\epsilon_0/kT} \tag{155}$$

$$= \kappa\,\frac{kT}{h}\,\frac{f^{\ddagger}}{f_i^n f_j^m f_{S_k}}\,e^{-\epsilon_0/kT} \tag{156}$$

where the equilibrium constant for the activated state equilibrium is ex-

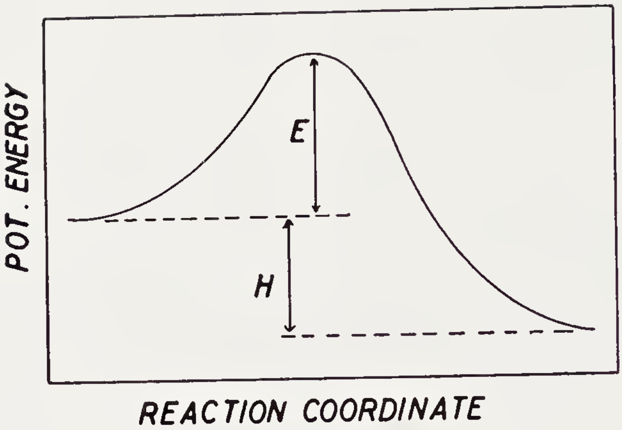

FIG. 4

pressed in partition functions defined per unit area and volume, respectively. The zero point energies have been separated from the vibrational part of the partition functions and put in the form of a Boltzmann factor. The ϵ_0 defines the *true* energy of activation at 0°K.

In adopting $K^\ddagger$ as our equilibrium constant (for activated complex with reactants) we are in fact adoping the convention that systems for which the positional coordinate normal to the potential barrier falls within the distance of one-half of $h/(2\pi m^\ddagger kT)^{1/2}$ on each side of the barrier are to be counted as activated complexes. Another way of saying the same thing is that h is the area in the phase space along the coordinate normal to the barrier and its conjugate momenta which is to be taken as belonging to the activated complex. The application of the activated complex or transition state theory to surface reactions has been carried out by Kimball[111], Tempkin[202], Eyring[118] and more recently by Laidler[115, 175].

With our definition of the equilibrium constant $K^\ddagger$, the customary tools and nomenclature of thermodynamics and statistical mechanics can be adopted in the treatment. To take into consideration the environment, activity coefficients are introduced with standard states for gases and solids defined according to the conventions of Lewis and Randall[125], whence the free energy of activation is given by

$$\Delta F^{0\ddagger} = -RT \ln K^\ddagger = -RT \ln \left[k_{\text{obs}} \cdot \frac{\gamma^\ddagger}{\gamma_i \gamma_j \gamma_S} \cdot \frac{h}{\kappa kT} \right] \qquad (157)$$

where k_{obs} is the observed specific rate constant in terms of the concentrations. The other relations are for the standard heat of activation,

$$\Delta H^{0\ddagger} = RT^2 \frac{\partial \ln K^\ddagger}{\partial T} \qquad (158)$$

for the standard entropy of activation

$$\Delta S^{0\ddagger} = \frac{\Delta H^{0\ddagger} - \Delta F^{0\ddagger}}{T} \tag{159}$$

and for the volume

$$\Delta V^{0\ddagger} = \frac{\partial \Delta F^{0\ddagger}}{\partial P} \tag{160}$$

As Guggenheim[86] has pointed out, the above relations involve certain small corrections, since the defined $K^\ddagger$ is expressed in concentration units instead of mole fractions. These corrections, however, are small and can be disregarded. As a matter of convenience the superscript zero will be dropped.

Some further general considerations of activated complexes in catalysis may be appropriate at this point. In the first place, many workers are prone to regard the accelerated rate that is observed in positive catalysis as being solely due to the heat of adsorption of the homogeneous activated complex on the surface of the catalyst (Figure 5). Although this may be true in some cases, where the acceleration in rate is brought about by the solvation of the activated complex, it appears more probable that a catalyst provides an entirely new path of reaction. This implies that the configuration and/or the composition of the activated complex on the surface does not even remotely resemble the complex for the homogeneous reaction.

For the moment let us assume* that the transmission coefficient κ is unity, as appears to be generally true for adiabatic reactions involving covalent molecules, and the concentration of the reactants is sufficiently low that an ideal case with unit activity coefficients can be taken; then the specific rate constant is

$$k' = \frac{kT}{h} e^{-\Delta F\ddagger/RT} \tag{161}$$

As to our above simplified expression for the specific rate constant, which formulation will be used in the remaining part of this chapter, it is seen that the standard entropy of activation can play a significant role in heterogeneous catalysis. Its effect will be reflected in the magnitudes of the classical frequency factor, A, in Arrhenius' empirical expression for the specific reaction rate constant. This simply re-emphasizes that not only the energy but also the configuration of the complex is to be considered. The impor-

* Born and Weisskopf[19] have formulated a mechanism of surface reactions based on the idea of quantum-mechanical tunneling through the potential barrier which would be reflected in values of κ less than unity. At the present time there is little evidence to indicate that such quantal effects could be important in catalysis.

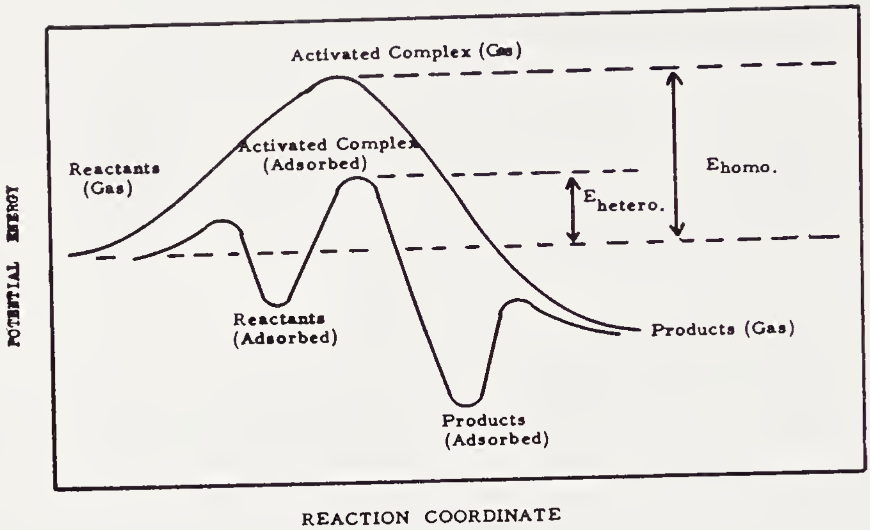

FIG. 5

tance of the entropy factor has been stressed by Beeck[11] and his co-workers in its relation to a general theory of heterogeneous catalysis.

A. E. Stearn[187] in discussing examples of *homogeneous* catalysis has stressed the relations of the two quantities $\Delta H^\ddagger$ and $\Delta S^\ddagger$ and also considered the influence of the catalyst in changing the activity coefficients of the reactants. Such an analysis will be presented briefly for it certainly is to be expected that similar considerations apply in *heterogeneous* processes. His thesis is that a catalyst may change the rate of reaction by becoming part of the activated complex or it may change the concentration of the activated complex by changing the activity coefficients of the reactants. The latter is a medium effect and the former a true catalytic effect providing that the catalyst does more than just simply solvate the activated complex. The translation of these concepts into the realm of heterogeneous processes is not new and has been discussed by many catalytic disciples; however, the specific interpretation in terms of the kinetic-thermodynamic quantities $\Delta H^\ddagger$ and $\Delta S^\ddagger$ may carry some additional merit. Though in *homogeneous* catalysis the two effects may act independently, it appears that *heterogeneous* processes require the concerted action of both these effects. The influence that these effects will have on a heterogeneous reaction are summarized in Table I for the two limiting cases of poor and good catalysts. The variations in the thermodynamic quantities are referred to the homogeneous reaction taken as a reference state. The second case of weak adsorption of reactants together with strong interaction of the activated complex with the catalyst is applicable in practically all cases of heterogeneous catalysis. Wherever negative catalysis has been observed, it is always possible to seek an explanation in terms of poisoning by impurities or inhibition of the reaction through adsorption of the reaction products.

TABLE 1

	$\Delta H\ddagger$	$\Delta S\ddagger$	$\Delta F\ddagger$	Catalytic effect
Strong solvation of reactants, weak interaction of activated complex with catalyst.	Increase	Compensating increase	No change	None
	Increase	Noncompensating increase	Larger	Negative
Weak adsorption of reactants, strong interaction of activated complex with catalyst	Decrease	Compensating decrease	No change	None
	Decrease	Noncompensating decrease	Smaller	Positive

In our generalization of the nature of the activated complex in contact catalysis, it was tacitly assumed that the complex would consist of the gaseous reactants and/or their fragments and the surface sites. This was written in the form of Eq. (150). Another possibility exists in which gaseous or adsorbed dissociation products are formed simultaneously with the activated complex, e.g.,

$$(n + p)C_i + (m + q)C_j + S_k \rightleftharpoons [C_{in}C_{jm}S_k]^{\ddagger} + pC_i + qC_j \qquad (162)$$

where p and q are integers. This situation appears to hold in the studies of Steinhardt[188, 189] on the deactivation of pepsin made in media of constant pH, where it was found that the velocity is proportional to the pepsin concentration and inversely proportional to the fifth power of the hydrogen-ion concentration. This is readily seen if the velocity is written

$$v = \frac{kT}{h} C^{\ddagger} \qquad (163)$$

but since the activated complex is given by

$$P \rightleftharpoons [P^{-5}]^{\ddagger} + 5H^{+1} \rightarrow \text{Products}, \qquad (164)$$

involving the ionization of five acid groups, then

$$K^{\ddagger} = \frac{C^{\ddagger}\gamma^{\ddagger}\mathcal{A}^{5}_{H^+}}{\mathcal{A}_p} \qquad (165)$$

in terms of activities, and it follows that

$$v = \frac{kT}{h} \cdot \frac{K^{\ddagger}}{\gamma^{\ddagger}} \cdot \frac{\mathcal{A}_p}{\mathcal{A}^{5}_{H^+}} \qquad (166)$$

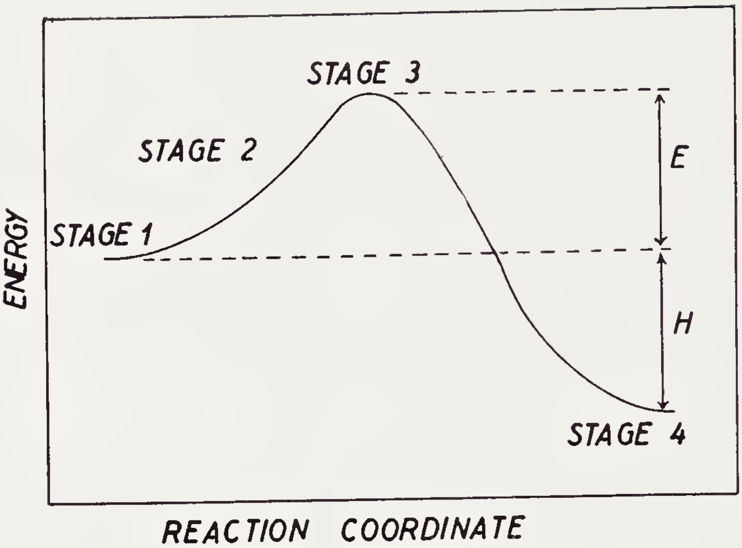

FIG. 6

in agreement with experiment[119]. Although at the present time there is little evidence in the field of contact catalysis to support the above mechanism for the formation of activated complexes, it is quite plausible that such mechanics could be important in hydrocarbon reactions occurring on cracking catalysts.

Recently C. A. Coulson[32] presented an admirable discussion of recent theories of chemical reactivity couched in the language of quantum mechanics which although limited to the noncatalytic reactivity of aromatic and conjugated molecules, which are much more amenable to computation, may be of interest with respect to catalyzed reactions. As shown in Figure 6, Coulson regards a chemical reaction as proceeding through four main stages. Of prime interest are stage 2, the polarized or perturbed state for the reacting system, and stage 3, the transition state where electronic rearrangements are so great that no longer can the two reacting systems be treated separately. He asks the question as to whether there is any *correlation between the mechanisms responsible for stages 2 and 3*. Stage 3 is of greatest interest, but it has been pointed out that calculations in this region are excessively difficult, obstructing one from drawing any general conclusions. However, if we assume that the polarized state (2) can be related to the static or nonreacting molecule and that stage 3 can be inferred by simple extrapolation, this can in many cases permit us to understand why a reaction favors one course over an alternative one. In a rather elegant manner, Coulson shows how the empirical rules of reactivity for aromatic and conjugated organic compounds established through the researches of R. A. Robinson, C. K. Ingold and A. Lapworth and their associates can be understood at least in a qualitative manner by calculations based on the polarized stage of the reaction path. The application and extension of these ideas to heterogeneous catalytic reactions in a detailed investigation would appear to bear fruitful consequences.

With respect to the shape and size of the activated complex the following considerations are relevant. In order to incorporate a foreign ion or molecule into a crystal (unless it is interstitial) it must be very near to the size of the unit it replaces. A 20 per cent difference in linear dimension usually precludes isomorphism. Likewise the new unit must either carry the same charge as the replaced unit or there must be additional substitutions which compensate for the charge. Interesting illustrations of the way these forces of containment prevent decomposition which otherwise would occur are exhibited by many crystals. Thus N_2O_5 in the gas phase or in solution decomposes rapidly at ordinary temperatures, while in the pure crystal there is no measurable decomposition. The expansion against the crystal forces necessary for formation of different shaped and usually expanded activated complexes entails a prohibitive expenditure of additional free energy of activation. In fact the preparation of pure crystals is a standard procedure for stabilizing many substances. The conditions for addition of a molecule to a surface are naturally far less stringent than for incorporation into the crystal interior. The fit being only along the interface we find the restrictions on shape much less severe. However, they are still very important, as is proved by the difference in rate at which optically active molecules are synthesized or destroyed on optically active enzymes. For two optical isomers, all the primary bonds are identical, so that only the external shape with its effect on secondary bonding causes the observed differences in free energy of activation. In living systems these free energy differences suffice to make only the *l*-amino acids appear. Since each factor of ten in the relative rates of two simultaneous reactions means a free energy of activation of about 1.3 kcal at room temperature, we see these shape forces must make free energy differences of around 2.6 kcal or more. Factors of a hundred-fold are of the utmost importance in catalyzed reactions so that any complete theory must take reactant and surface shapes into account. The fact that optical isomers sometimes crystallize in optically active and sometimes in racemic mixtures further emphasizes the critical nature molecular shape will have for formation of activated complexes.

Application of the Activated Complex Method to the Catalytic Hydrogenation of Ethylene

Whenever the subject of catalytic hydrogenation of olefins in a gas-solid system is brought up for discussion, the associated phenomena of exchange reactions, double-bond shift and *cis-trans* isomerization are immediately brought into the picture with the fond hope that a single specific mechanism can be found that will interpret the many results now available. As yet there is no general agreement as to the mechanisms of these reactions. Specifically, in the case of ethylene hydrogenation over metal catalysts, the following modifications have been proposed. Horiuti and Polanyi[103] suggested an associative mechanism, namely

$$C_2H_{4_{ads}} + H_{ads} \rightleftarrows [C_2H_{5_{ads}}]^{\ddagger} \rightarrow \text{Products}$$

for both hydrogenation and exchange, whereas A. Farkas favors a dissociative mechanism for the exchange

$$C_2H_{4_{ads}} \rightleftarrows [C_2H_{3_{ads}}]^{\ddagger} + H_{ads}$$

with a simultaneous addition of two hydrogen atoms or adsorbed molecular hydrogen to the adsorbed ethylene for the hydrogenation step. Recently, the authors[28, 65, 66, 216] after a careful investigation of the available kinetic data for the velocity of hydrogenation of both ethylene and propylene over a relatively wide range of values of temperature and pressure were led to a Langmuir-Hinshelwood type of mechanism. This is similar to A. Farkas' proposal[71] where the slow step involves interaction between the adsorbed species, with simultaneous addition of adsorbed hydrogen atoms or activated adsorbed molecular hydrogen. Except for minor details, the same conclusion was arrived at independently by K. J. Laidler[116]. In some recent appraisals of the problem, Laidler[129, 130] has elaborated his treatment and favors the catalytic production of ethane either by reaction between adsorbed ethyl radicals and adsorbed H atoms, or by dismutation between ethyl radicals adsorbed on neighboring sites. For the exchange he favors a unimolecular decomposition of an adsorbed ethyl radical to gaseous ethylene plus an adsorbed H atom. Similar ideas have been advanced by Stevenson, *et al.*[214, 215]. It is not the purpose of this section to unequivocally decide as to the correct mechanism involved in the system ethylene-hydrogen-solid catalyst, but rather to point out fundamental approaches to the general problem of understanding the kinetics of contact catalysis. The reader is thus referred to the excellent review of pertinent data and speculations on mechanisms of hydrogenation of olefins compiled by T. I. Taylor[201], and further amplified in Chapters 4 and 5 in Vol. I authored by K. J. Laidler.

At the outset, some additional comments and words of caution are in order with respect to all interpretations of kinetic data in terms of specific mechanisms. In all catalytic studies careful experimentation over wide ranges of all the independent variables is absolutely essential if the maximum amount of information is to be obtained from the kinetic data as to the nature of the activated complex. In addition, the authors found that kinetic studies for "constant volume" and "constant pressure" conditions as carried out by Toyama[206, 207], are especially helpful in the determination of the unknown parameters. In many cases the same analytical expressions in their dependence on pressure and temperature can be obtained for the velocities of processes involving different activated complexes. In such cases, it is necessary to resort to an examination of the energetics of the process, i.e., the magnitudes of the true energies of activation and the entropies and heats of adsorption of the reactants, to permit one to assign the correct critical configuration for the two reactions. If the available kinetic data are limited to narrow ranges of values for temperature and concentrations, one must proceed with caution in formulating mechanisms, for as the above authors[65] have shown, several kinetic models can readily reproduce the data. Similarly, the use of experimental energies of activation in the calculation of absolute rates of reaction which agree with the observed rates, or are of the right order of magnitude, does not constitute unequivocable proof for the correctness of the formulation.

Using the hydrogenation of ethylene as a typical example of a bimolecular gas-solid contact catalytic process, several formulations of velocity expressions will be written for the possible activated complexes that can arise in the critical step leading to the formation of ethane. This will demonstrate the mechanics of the method, and permit us to cite the contributions of several workers to our understanding of the theoretical aspects of contact catalysis.

As has been emphasized earlier in this section, it is believed that a slow step exists in a chain of events leading to the final products of a reaction permitting one to speculate about the nature of the activated complex that characterizes that particular elementary reaction step. Halsey[89], among others, has questioned this assumption particularly with respect to non-uniform surfaces. It is his thesis that if a sufficiently wide distribution function exists for the catalytically active sites, no group of sites can be selected and treated as effectively uniform. For the present considerations, however, the latter is assumed to be true so that a rate expression can be evaluated. It may not be out of place to again stress the nature of an activated complex in contrast to thermodynamically stable intermediates that appear to play prominent roles in many complex reaction systems. The latter can be identified with the "intermediate-compound" formation theory of catalysis popularized by Ipatieff[109] and co-workers. Its more recent application is found in the studies of dehydration of aliphatic alcohols on alumina. Balaceanu and Jungers[4] elucidate the mechanism by proposing ethyl ether as an intermediate which undergoes dismutation to form ethylene and alcohol.

Some additional assumptions are required to permit one to write explicit expressions for any catalytic process. Each of these have been questioned and contested by many workers from time to time; their general validity and applicability, naturally, rest on the successful interpretation of a variety of catalytic processes under diverse conditions of experiment. Besides our assumption of a rate determining step as given above, the following need to be made:

(1) Ideal catalytic surface, i.e., absence of heterogeneities of all kinds (see page 258).
(2) Neglect of volume phenomena such as solubility of reactants and products in catalyst.
(3) All transport processes are assumed to be rapid.
(4) Immobile adsorbed monolayers of reactants: no multilayer adsorption and adsorption obeys a Langmuir isotherm.
(5) Heats of adsorption are independent of surface coverage.
(6) Absence of poisoning of catalyst either by the main products of those resulting from secondary reactions, e.g., production of acetylene from ethylene during the hydrogenation.

With respect to points (4) and (6) some additional remarks need to be made. Most of the workers in the field now accept the idea that for a large fraction of known catalytic reactions adsorption of reactants or desorption of products is *not* the slow step in the catalysis. In certain instances, however, such as the exchange of nitrogen isotopes on iron[53, 136], or the synthesis and decomposition of ammonia[56, 220], the experimental data strongly suggest that the adsorption and desorption rates for the nitrogen molecule are rate-determining. The picture is also complicated by the very large effects arising from the presence, accidental or otherwise, of surface impurities. This is reflected in higher activation energies, since the activated displacement of surface contaminants will add the heat of adsorption of the latter to the true energy of activation for the process. This problem of surface contamination is of course, one of utmost importance in its own right, involving as it does all of the questions of promotion etc., so vital to industrial catalysis. Here again, another point needs to be emphasized, namely, the question of adsorption equilibria when surfaces are heterogeneous. Twigg[209] in some recent work on the catalytic hydrogenation and exchange reactions of ethylene over nickel catalyst supported on Kieselguhr pellets questioned the assumption that adsorption equilibrium through a Langmuir mechanism is achieved. This forced him to use Bodenstein's steady state treatment for his formulation of the activated complexes involved in hydrogenation and exchange. The correctness of the mechanism is debated by Laidler[129] since Twigg's mechanism leads to a constant rate instead of a maximum velocity at higher ethylene pressures.

Most reactions occurring at surfaces can be conveniently divided into two classes on the basis of their mechanism: when there is interaction between the chemical species adsorbed on adjacent surface sites, the Langmuir-Hinshelwood mechanism holds true, whereas, if an adsorbed species interacts with a molecule or atom in the gas phase, or in a secondary van der Waals layer, it is commonly referred to as the Rideal mechanism. The latter mechanism of a gaseous molecule bombarding a covered surface has been widely used by Balandin[8] and co-workers over a period of years. In the light of these mechanisms, the following activated complexes can regulate the hydrogenation scheme for ethylene:

Langmuir-Hinshelwood Mechanism

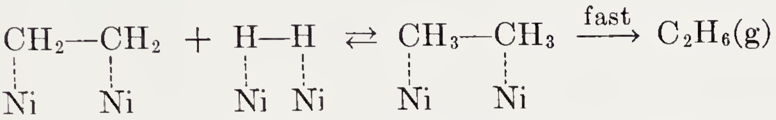

$$\underset{\text{Ni}}{\text{CH}_2}\text{—}\underset{\text{Ni}}{\text{CH}_2} + \underset{\text{Ni}}{\text{H}}\text{—}\underset{\text{Ni}}{\text{H}} \rightleftarrows \underset{\text{Ni}}{\text{CH}_3}\text{—}\underset{\text{Ni}}{\text{CH}_3} \xrightarrow{\text{fast}} \text{C}_2\text{H}_6(\text{g})$$

Here the activated complex is essentially a distorted ethane molecule formed by the interaction of the acceptor (subindex 1) and the molecular hydrogen (subindex 2). If the number of sites adjacent to an ethylene molecule is b, the probability that hydrogen and ethylene are adsorbed side-by-side will be

$$ab\sigma_1\sigma_2$$

where

a = number of sites per unit surface area of catalyst ($\sim 10^{15}$ sites/cm^2)
σ_1 = fraction of surface sites occupied by ethylene
σ_2 = fraction of surface sites occupied by hydrogen

Thus the rate of reaction will be given by

$$v = ab\sigma_1\sigma_2 k' \tag{167}$$

where k' is the specific rate constant that refers *explicitly* to the interaction between the two adsorbed species. This can be written as

$$k' = \frac{kT}{h}\,\frac{f^\ddagger}{f_{1s}f_{2s}}\,e^{-\epsilon^\ddagger/kT} \tag{168}$$

where

$\epsilon^\ddagger$ = energy of activation at 0°K
$f^\ddagger$ = partition function of activated complex per molecule per unit area
f_{is} = partition function for an adsorbed ith molecule per unit area.

A convenient procedure was developed by the authors[66] for finding the isotherms for the two reactant species. The fraction of sites covered by either of the two reactant molecules (competitive adsorption) will be given by the ratio of the chance that a molecule occupies a site to that for any other allowed state. In terms of partition functions,

$$\sigma_1 = \frac{f_{1s} f_2}{f_1 f_2 f_s + f_{1s} f_2 + f_{2s} f_1} \tag{169}$$

with a similar expression derived for σ_2, f_i being the partition function for a gaseous molecule per unit volume and f_s that for a bare site. Defining the equilibrium constants for adsorption as

$$K_i p_i = \frac{f_{is}}{f_i f_s} \tag{170}$$

where p_i is the partial pressure of component i, the velocity expression takes the form

$$v = ab \frac{K_1 K_2 p_1 p_2}{\left(1 + \sum_i K_i p_i\right)^2} k' \tag{171}$$

If noncompetitive adsorption is assumed, the velocity expression reduces to

$$v' = ab \frac{K_1 K_2 p_1 p_2}{(1 + K_1 p_1)(1 + K_2 p_2)} k' \tag{172}$$

a form generally used by Balandin[8].

Rideal Mechanism

For purpose of illustration, it will be assumed that only ethylene is adsorbed directly on a surface site and interacts with a hydrogen molecule in the gas phase or in a van der Waals layer as follows

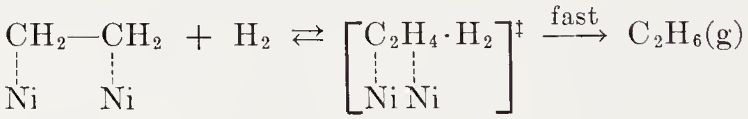

$$\underset{\mathrm{Ni}}{\mathrm{CH_2}}-\underset{\mathrm{Ni}}{\mathrm{CH_2}} + \mathrm{H_2} \rightleftarrows \left[\underset{\mathrm{Ni\;Ni}}{\mathrm{C_2H_4 \cdot H_2}}\right]^{\ddagger} \xrightarrow{\text{fast}} \mathrm{C_2H_6(g)}$$

Using the same notation, the velocity expression is

$$v = a\sigma_1 p_2 k' \tag{173}$$

or

$$v = a \frac{K_1 p_1 p_2}{(1 + K_1 p_1)} k' \tag{174}$$

where the specific rate constant is given by

$$k' = \frac{kT}{h} \frac{f^{\ddagger}}{f_{1s} f_2} e^{-\epsilon^{\ddagger}/kT} \tag{175}$$

Since all catalytic surface reactions require the activated adsorption of at least one chemical species, they should all show a maximum in the rate at some definite temperature and specified pressure. It can easily be shown that for a given ethylene pressure the rate is a maximum at

$$T_{\max} = \frac{Q_1}{R \ln \left\{ \dfrac{Q_1/q - 1}{A_1 p_1} \right\}} \tag{176}$$

for the Rideal mechanism. If K_2p_2 is neglected in comparison with K_1p_1, then from Eq. (171) for the Langmuir-Hinshelwood mechanism, the maximum in the rate will appear for a temperature

$$T_{\max} = \frac{Q_1}{R \ln \left\{ \dfrac{Q_1 + Q_2 - q}{Q_1 - Q_2 + q} \cdot \dfrac{1}{A_1 p_1} \right\}} \tag{177}$$

where the equilibrium and rate constants are defined as

$$K_i = A_i e^{Q_i/RT}$$

$$k' = Be^{-q/RT}$$

NATURE OF THE CATALYST

With the increasing understanding of the nature of the chemical bond, rapid strides were made during the middle thirties in the development of a unified theory of chemical reactions, principal emphasis being placed on gaseous systems. Along with this advance, it then became possible to move in the direction of a more complete interpretation of chemical action in heterogeneous sytems. While some details seem to be clarified by this application of homogeneous chemical kinetic theory to surface processes, one was primarily impressed by the inadequacy of our knowledge of the nature of catalytic action. As Professor Hugh S. Taylor pointed out in the 5*th* Spiers Memorial Lecture opening the Faraday Society Discussions on Catalysis, "The catalyst itself, rather than the reactions which occur on it, seems to be the principal objective for future research in the coming years." Even in the face of the vast amount of research carried out in this direction, our knowledge of the properties of solid catalysts is still not of the kind that will permit us to predict in any *a priori* fashion their specific catalytic action. In this section we will attempt to summarize some of the work pertinent to the types of catalysts and the relationships and correlations which have been found and to indicate some of the hypotheses used to describe the microscopic operation of the "mysterious forces of catalytic action" described by Berzelius. Some of the topics here summarized have already been treated in detail in Chapters 3, 4 and 5.

The development of reliable experimental methods for the determination of surface areas of solid materials by Harkins and Jura[91] and by Brunauer, Emmett, and Teller[26] helped immeasurably in correlating a considerable body of information on contact catalysis and established the importance of surface areas. An excellent summary and comparison of the methods was recently reported by Emmett[50]. In this connection, an often quoted calculation can readily be made to compare the velocity of a bimolecular reaction taking place in the gas phase with the corresponding velocity on a uniform surface. Thus one can readily show[117] that by making certain simple assumptions it is possible to arrive in a straightforward manner at the expression,*

$$\frac{v_{\text{het.}}}{v_{\text{hom.}}} = \frac{c_s}{f^{\ddagger}_{\text{hom.}}} e^{\Delta E/RT} \tag{178}$$

where ΔE is equal to $E_{\text{hom.}} - E_{\text{het.}}$, c_s is the concentration of sites on the smooth surface and $f_{\text{hom.}}{}^{\ddagger}$ is the partition function for the gaseous activated complex. Taking orders of magnitude for c_s and $f^{\ddagger}$ of 10^{15} sites/cm^2 and 10^{27} (for 1 cm^3), respectively, it follows that,

$$\frac{v_{\text{het.}}}{v_{\text{hom.}}} = 10^{-12} e^{\Delta E/RT} \tag{179}$$

This result appears to indicate a surprisingly slow rate for the surface reaction; however, the value of $\Delta E/RT$ is in many cases quite large, and, secondly, surface areas of ordinary catalysts may be of the order of 100 m^2/gm. Since the reaction is not limited to 1 sq cm, the latter can introduce a factor as large as 10^6 in favor of the rate of the surface reaction. Thus the older explanation of catalytic activity in terms of surface concentration alone is, as is well recognized, unsatisfactory.

The remarks which follow are limited to a consideration of the catalytic activity of solid materials in their pure state, with a very few exceptions. Mixtures of substances whether physical or chemical in nature (generally classified as *promoted* or *supported* catalysts) cannot be included in any general way within the framework of this discussion; alloys, however, exhibit some interesting properties which do lend themselves to our analysis and will be considered in a preliminary fashion. Similarly, primary processes such as capillary condensation and transport-controlled reactions in porous catalysts, though of fundamental importance in determining the activity of industrial catalysts, will here be omitted. The latter phenomena have been capably treated in a recent review article by Wheeler[218], and in Chapter 1.

---

* See also similar discussion in Vol. I of this series, page 234.

Classification of Solids

It may be useful to make a few rather obvious comments about our knowledge of the solid state before proceeding to a classification of solids. A far more satisfactory position is now held with respect to our understanding of true crystalline solids than with that of individual molecules. This has been brought about by two contributing concepts, namely: (1) geometrical properties of crystals and the refined experimental techniques of x-ray and electron diffraction have established unequivocally the structures of many solids; and, (2) quantum mechanical considerations become much simpler when one is permitted to introduce the symmetry properties of the crystal and through the discovery that coulombic rather than resonance or exchange forces play the predominant role in the cohesion of solids. In the case of catalytic activity, where interactions between molecules and surface forces of solids need to be understood, this problem presents untold mathematical complexities when treated by the methods of quantum mechanics.

Seitz, in his text "The Modern Theory of Solids," gives an empirical classification of types of solids which is convenient for our purpose. It is based on the general thermal, electrical, magnetic and chemical properties of solid substances and is given as:

(a) Metals
(b) Ionic crystals
(c) Valence crystals
(d) Semiconductors
(e) Molecular crystals

Transition regions exist between the types above, and actual solids often fall, of course, within these regions in their properties. Elements representative of all of the family sequences of the periodic table (with the obvious exception of the inert gases) can be found in various states of chemical aggregation among the good catalysts, and, with the exception of molecular crystals, examples of the other four ideal types of solids are known as catalysts. Molecular crystals with residual secondary or van der Waals forces can exert only very weak forces, and in general show little activity; the possibility remains, however, that irradiation in the ultraviolet or the Schumann regions could produce a sufficient number of metastable excited states to act as centers of catalytic activity. Those molecular crystals that do seem to function efficiently as catalysts bring about reactions that resemble processes in homogeneous systems involving the action of strong acids. It is, therefore, concluded that the sites in these cases which are responsible for the catalytic activity are strongly acidic (in the Lewis sense).

The straightforward, classical approach to the problem of finding empirical relations between the physical and chemical properties of catalysts and the kind and degree of chemical activity has borne little fruit, from the point of view of leading us toward a general understanding of the processes involved. This is principally a consequence of the fact that there is such a bewildering variety and number of such empiricisms in this field. An attempt at classification of catalysts and types of reactions may be found in Egloff's monograph on "Catalysis"[16] and also in Chapter 2 of the present volume. In a more specialized field, a rather complete discussion of the importance of surface geometry in catalytic reactions is given in two recent review papers[82, 208].

Catalytic Theories and the Nature of the Solid

Ionic Solids. These substances are distinguished by good ionic conductivity at high temperatures, and by good cleavage; furthermore they are characterized by being made up of a combination of highly electropositive and highly electronegative elements. The surface of an ionic crystal, with its checkerboard of electron acceptors (cations) and centers of high electron density may serve to bring about an incipient ionization in the activated complex on the surface. Such considerations have been advanced by, e.g., Eyring, Hulbert and Harman[67]. The importance of ionic mechanisms has been emphasized by Nyrop[145], although his model is generally considered conceptually incorrect (cf. Emmett and Teller[57]).

A number of ionic solids are capable of reacting heterogeneously with alcohols, acids or esters to produce simultaneously the dehydration and the dehydrogenation products. Since it does not appear that the free energies of activation for these two processes can differ by more than 1 to 2 kcal per mole, it seems probable that the nature of the activated complex is nearly independent of the size of the surface ions. Assume the following mechanisms for the decomposition of an alcohol, ROH, on a metal oxide, MO:

(a) $\mathrm{ROH} \rightleftharpoons \mathrm{R}^+ + \mathrm{OH}^-$ for dehydration, and
(b) $\mathrm{ROH} \rightleftharpoons \mathrm{RO}^- + \mathrm{H}^+$ for dehydrogenation,

with activation energies E' and E for (a) and (b), respectively. The difference in energies of activation for the two reactions, based on coulombic binding with the surface ions, is given approximately by the expresssion

$$E' - E \equiv \frac{ze^2(r_{\mathrm{R}^+} - r_{\mathrm{H}^+})}{(r_{\mathrm{R}^+} + r_{\mathrm{O}^=})(r_{\mathrm{H}^+} + r_{\mathrm{O}^=})} + \frac{z'e^2(r_{\mathrm{RO}^-} - r_{\mathrm{OH}^-})}{(r_{\mathrm{RO}^-} + r_{\mathrm{M}^{++}})(r_{\mathrm{OH}^-} + r_{\mathrm{M}^{++}})} + \delta E \tag{180}$$

where δE is an energy term which is independent of the surface, e is unit electrostatic charge, z and z' are the effective charges on the surface anions and cations respectively, and the r's are the ionic radii of the various species. Since most of the charge in the ion RO^- is located on the oxygen, we will have $r_{RO^-} \approx r_{OH^-}$, and the second term is small. In addition, if we neglect r_{H^+} in comparison with r_{R^+}, as will generally be permissible, Eq. (180) simplifies to the form,

$$E' - E = \frac{ze^2}{r_{O^=}(1 + r_{O^=}/r_{R^+})} + \delta E \tag{181}$$

From Eq. (181) it is apparent that in this approximation the cation of the addend does have a small effect, and this formulation would appear to be adequate to explain the small experimental differences observed in the activation energies. Such a treatment is similar to the older idea in which the catalyst acts as a polar solvent forming a two-dimensional ionic solution with the reactant (addend) and in this interpretation would seem still to warrant consideration.

One other point can be mentioned with respect to the class of pure ionic solids in their action as catalysts. Neglecting coulombic interactions for the moment, one would conclude that the most important centers of catalytic activity will probably be the cations of the solid, since the anions, with their full electronic complement, will not be expected to enter into chemical combination except under the most favorable conditions. Quantum mechanical exchange forces will then be associated almost entirely with the cations, which may utilize available p, d or f orbitals of proper energy. This is generally true of most of the heavier metals and particularly of the transition elements and inner transition elements with respect to d- and f-orbitals respectively.

Valence Crystals. Substances such as diamond, boron, silicon, germanium and gray tin, among the elements, and silicon dioxide, silicon carbide and boron nitride, to name a few among the compounds, are characterized by great hardness, lack of conductivity and large cohesive energies. Essentially, all of these substances represent giant inorganic polymers in which each atom exhibits its maximum valence, forming with its neighboring atoms primarily covalent bonds. Graphite, though an exception, is classified by Seitz as a valence crystal if attention is directed toward the chemical binding that exists in the layers of the crystal. With respect to the true three-dimensional covalent structures very little quantitative work has been carried out. Using a band theory approach, Kimball[110] has shown that while the $2s$ and $2p$ levels in the carbon atom do split in diamond into a total of eight bands (four of zero width) similar to the energy bands in metals, it appears that the four low-lying bands are completely filled and the four upper bands are empty. Further, the lowest of the empty bands lies above the highest filled band by an amount of energy in excess of the ionization potential of carbon. Since filled bands cannot contribute to electrical conductivity, and the unfilled levels are not accessible to the electrons below, the diamond crystal is a nonconductor. It seems probable that a similar situation exists generally with valence crystals, and this difficulty in promoting electrons for the purpose of facilitating the formation of substrate-surface complexes may be considered at least part of the explanation of their low catalytic activity. Where solids of the insulator type do act as catalysts (primarily for isomerization, cracking, hydration and dehydration reactions), they probably operate through a carbonium ion or a proton exchange mechanism. Roginskii[170] and Dowden[39] have classified catalysts on the basis of their electrical properties, and have suggested mechanisms of this type for the dielectric solids.

Daniels[35] has suggested that thermoluminescence may prove to be a useful tool for the investigation of catalytic activity, and Boyd and Hirschfelder[23] have considered thermoluminescence curves as measures of catalyst efficiency. If strains and lattice imperfections in the catalyst surface permit adsorbed molecules to interact chemically, they may also function as electron traps which can be emptied on heating. In some preliminary tests they found that a good aluminum oxide catalyst prepared by Homer Adkins gave considerably more thermoluminescence than a poor catalyst of the same material.

Semiconductors. A number of solids have an electrical conductivity behavior intermediate between metals and insulating materials. This behavior may be intrinsic, i.e., it may be exhibited by the substance in the pure state, or it may be induced by the presence of a (usually) minute quantity of some impurity. Conduction in an impurity semiconductor can be brought about either by freeing an electron from a discrete level to an empty band, in which case the conduction will be by the electron itself, or through promotion of an electron from a filled band to a discrete level. In the latter case the conduction is said to be by the "holes" left in the previously filled band. The two cases may be distinguished experimentally by the sign of the Hall coefficient, and are referred to as "n-type" or "p-type" conduction, respectively. If a filled band and an empty band in a pure solid are sufficiently close together (intrinsic semiconductor), there may be a temperature above which it is possible to promote electrons from one to the other, in which case a mixed type of conduction occurs in which both electrons and holes may contribute to the electrical conductivity. With the recognition of the fact that many oxides and sulfides which evidence good catalytic activity are simultaneously semiconducting has arisen an extensive interest in the properties of such substances. It seems reasonable to correlate the promotion of chemical reactions which involve electronic transitions with the electronic conductivity of these solids. Some excellent work along these lines has been carried out by Garner[76, 77, 78], Griffith[81], Bevan and Anderson[18], Parravano[151, 153], and Hüttig[107]. They show that the activity of semiconducting materials is associated with the electron levels and lattice defects arising from the impurity centers. Recently Parravano[152] in some studies on the rates of oxidation of carbon monoxide on several catalysts found a larger enhancement in rate occurring at the ferroelectric transition of the catalytic material. This further emphasizes the important role that surface energy states determined by the electrical properties of the catalyst play in determining catalytic efficiency.

In this same connection, Boudart[21] has considered a nonmetallic adsorbent to act as a two-dimensional semiconductor system, with the substrate playing the part of an acceptor or a donor in modifying the electron Fermi level of the adsorbate (*vide supra*). This specific influence which changes the electronic chemical potential of the adsorbent he refers to as "induction," and it is important both from the point of view of the modification of the surface caused by the reactants themselves and the changes in activity brought about by surface contaminants, which do not themselves enter into the catalytic reaction. From a somewhat different point of view, Volkenstein[212, 213] has also discussed the creation of new energy states or sites through interaction of the substrate with the adsorbent.

These same ideas of electron activity of the solid catalyst have been extended to promoter action and to poisoning. If one accepts the thesis that the rate of reaction depends on the concentration of holes and electrons in the surface layer of the adsorbent, which in turn depends on the surface concentration of poisons and promoters, a deeper insight into the detailed mechanism of catalysis is obtained. These concepts have been applied by Roginskii[169], Volkenstein[212] and Maxted[132, 134].

The use of magnetic susceptibility and nuclear relaxation methods for the investigation of promoted catalysts has been demonstrated to be a particularly effective approach and has been developed to a considerable extent by Selwood and his associates; a recent review[180] summarizes the advances in this field. (See also Chapter 8, Vol. I, of the present series.) These measurements yield information as to the oxidation (valence) states of paramagnetic ions supported on a catalytic surface, the interaction covalency and the degree of dispersion of supported paramagnetic catalysts. With this information one can speculate about the catalytic activity of these substances. Selwood finds striking evidence of the influence of valence induction on catalytic activity; in studies on the decomposition of hydrogen peroxide on supported oxides of manganese, a sharp maximum in the rate was found at an oxidation state corresponding to a valence of about 3.6. Now at low concentrations of manganese oxide supported on alumina, the valence induction effect causes manganese to exhibit a valence of 3, whereas at high concentrations, manganese has the normal valence of 4. Thus one concludes that a valence of 3.6 as observed for the maximum rate of decomposition of hydrogen peroxide implies that at least two adjacent manganese ions are involved in the reaction.

Metals and Alloys. The emphasis on the physics of the solid state as a mode of attack on the detailed mechanism of catalytic activity originated in the study of metal catalysts. Many workers have speculated on the correlation of the electron mobility of these substances with their catalytic activity. As ideas of metal structure evolved in terms of the new quantum theory, Rienäcker[160] in 1938 was one of the first to recognize that since the electron Fermi level of a metal was independent of temperature but strongly dependent on the presence of alloying elements, a study of alloy catalysts should prove fruitful in attempting to understand catalytic processes. This mode of attack has been extended by Schwab, Dowden, Eley and others, and has been recently reviewed with particular emphasis on the theoretical aspects of the problem by Dowden[38].

With regard to quantum mechanical studies of the electronic structure of molecules, two approximation methods are available, namely, the molecular orbital and the valence bond approaches. As applied to the metallic state they lead to the band theory (Brillouin zones) and the Pauling resonating-valence-bond theory approximations. From the band theory point of view, the electrons in the metal are confined to a potential box and a distribution function $G(E)$ for the density of electron levels can be determined. The seat of catalytic activity resides in the distribution of the electrons and the position of the filled electronic levels (the work function, ϕ) with respect to the electronic density and energy of the substrate. In contrast, according to Pauling's formulation of the resonating-valence-bond treatment, which is somewhat more appealing to the chemist, the emphasis is placed on the availability of atomic eigenfunctions for metallic bond formation. For the transition elements, hybridization of the available nine *s*, *p* and *d* type orbitals leads to three groups of orbitals: the "atomic" orbitals, principally of *d* character, the "bonding" orbitals or metal hybrid orbitals of the "$d^{2.56}sp^{2.22}$" type which largely determine cohesion (the number of electrons per atom is called the metallic valency) and the "metallic" orbitals, principally of the *sp* type. Comparison of this model with the properties of metals and alloys suggests that unfilled atomic orbitals are the seat of residual valency in the bulk metal and in turn of the catalytic activity.

Some application of these ideas may be noted. Schwab[176], in studies on the dehydrogenation of formic acid over homogeneous Hume-Rothery alloys (silver with metals of Groups II–V of the periodic table), offers evidence for the activation energy being proportional to the square of the electron concentration, and argues that the rate-determining step is the loss of two electrons from the formic acid molecule into the lowest unfilled level of the metal. In addition, he found that for intermetallic Hume-Rothery phases, the gamma phase shows a maximum activation energy and that there exists a striking parallelism between the resistance, the hardness and the catalytic activities of the alloys of copper and tin.

Couper and Eley[33] have shown how the energy of activation for the para-hydrogen conversion is increased when Pd is alloyed with enough Au just to fill up the holes in the *d* band of the former according to the band theory of metals. Dowden and Reynolds[41] studied, with a similar objective, the hydrogenation of styrene, the decomposition of methanol and the decomposition of formic acid on nickel-copper and nickel-iron alloys, observing that high catalytic activity appeared to be associated with partly empty *d* bands. The exceptional case of the decomposition of hydrogen peroxide is explained on the basis of the assumption that here the rate-determining process is the transfer of the electron from the metal to the substrate. Schuit[174] illustrates a correlation between the activation energy for the hydrogenation of ethylene and the valence-per cent *d*-character product where the latter is given by Pauling.

In this general area there is complete agreement only on the fundamental importance of the electronic states within the metal to catalysis: detailed mechanisms for these reactions are still open to question. The case of the hydrogenation or dehydrogenation of molecules on metal surfaces is, in many respects, a particularly poor one to use for purposes of illustration. The exact role of hydrogen in such reactions, indeed even its physical location during the process, is still a matter of considerable doubt. Opinions vary from the extreme situation in which the hydrogen molecule is not adsorbed at all, but attacks the sorbed reactant from the gas phase, to the opposite extreme in which the hydrogen atom exists as a solution in the bulk phase of the metal catalyst. The extent of this uncertainty in our knowledge here is well brought out in a general discussion among many of the principal workers in this field[47].

Concluding Remarks

The interpretation of the data obtained from catalytic processes thus requires information from three general areas: thermodynamics, kinetics and the ideas of structure. To a limited extent one is justified in drawing conclusions as to the efficiency of a catalyst on the basis of the thermochemistry of the adsorption and desorption steps or the entropy changes inherent in the organizational properties of the surface. The multiplet theory of Balandin[6] is an example of the importance of the latter effect, and has been discussed in an earlier section. In a subsequent paper[7], the same author has also discussed hydrogenation of different bonds over nickel surfaces from the point of view of their heats of formation. If one assumes that adsorption of a molecule leads to dissociation, partial or nearly complete, of some reactive bond, and that hydrogen is also adsorbed dissociatively, then it is shown that the hydrogenated products are in fact those for which the energy requirements are the least. For a rather extensive list of organic compounds containing carbon, oxygen, nitrogen, chlorine and bromine, Balandin demonstrates the considerable accuracy with which one can predict the products of the hydrogenation reaction. It is necessary to assume certain values for the heat of adsorption of various atoms to the nickel atoms in the surface, and to assign bond strengths to the various pairs of atoms in the reacting molecules. While some of these parameters are not acceptable by modern standards, the correlation is not radically affected by such corrections. However, the failure of such a treatment when applied more generally to this field points up the fact that the rate of reaction is only accidentally conditioned by these equilibrium, thermodynamic parameters. Balandin rightly points out that, at least in the cases considered in this paper, the principal function of the catalyst lies in its ability to weaken the bond which is about to be broken, and that in many cases this ability runs parallel to the strength of the binding of the participating atoms to the surface.

For many purposes, it is advantageous to consider the surface to be an active, rather than a passive participant in the catalytic process; that is, to include in the physiochemical description the important effect of the sorbate upon the surface structure of the solid itself. Several examples of this kind of interaction have already been discussed, either from the point of view of the reacting molecules or the electronic energy distribution of the solid. H. A. Taylor and Thon[192] have noted in a less specific manner the possibility that the activity of the surface is produced by the adsorption itself, thus separating the energetics of the sorption process from that of the reaction proper. Basing their discussion on the general applicability of the Elovich equation[49] for the rate of chemisorption of a gas, they consider the consequences of assuming an immediate production of active sites upon contact of gas with surface, and the bimolecular decay of the surface concentration of these sites as the chemisorption process continues. The same authors[205] also discuss the result of applying this model to surface reactions. Here it is stated as a general rule that (1) the centers of activity upon the surface are "dissociatively chemisorbed particles of one reactant only," and (2) the rate of reaction is determined by the number of such centers present on a given area. The reaction proceeds then by interaction between free gaseous molecules of one reactant and the fragments of the other which form the active centers upon the surface. As before, these active sites may disappear bimolecularly, but in general will be regenerated through some chain mechanism which will maintain their surface density. Such a kinetic treatment of the catalytic process helps greatly in organizing the data in this field but does not attack the detailed mechanism of the catalyst-adsorbate interactions. There may also be some question as to whether any single set of principles can be expected to be applicable to so wide a field as is here being considered.

It has already been remarked that the formalism of statistical mechanics particularly recommends itself to the treatment of problems of this kind, in that the nature of the model under consideration may be specified through the partition functions used in its development. Horiuti[104] has recently considered the general problem of interactions between particles from this point of view and has derived a systematic method of treating such problems through the introduction of certain functions which are closely related to the activities of the various components. In connection with this treatment he also introduces the "stoichiometric number"[105], a parameter which is determined by the sequence of elementary reactions in the over-all process. When the stoichiometric number can be obtained for each such elementary reaction, it should be possible experimentally to determine the course of a catalytic reaction through that complex of reactions of which it is made up. In its present form, however, it does not appear possible to apply the treatment of Horiuti because of the lack of specific information about the partition functions involved. This is, of course, the same difficulty which has already been discussed on pp. 292–293, and only a greater knowledge of the structure of the surface and of the adsorbate complex will permit its resolution.

References

1. Adam, N. K., "The Physics and Chemistry of Surfaces," 3rd Ed. p. 404, London, Oxford University Press, 1941.
2. Allmand, A. J., and Chaplin, R., *Trans. Faraday Soc.*, **28,** 223 (1931).
3. Anderson, R. B., and Emmett, P. H. *J. App. Phys.*, **19,** 367 (1948).
4. Balaceanu, J. C., and Jungers, J. C., *Bull. Soc. Chim. Belg.*, **60,** 476 (1951).
5. Anderson, R. B., *J. Am. Chem. Soc.*, **68,** 686 (1946).
6. Balandin, A. A., *Z. physik. Chem.*, **B2,** 289 (1929).
7. Balandin, A. A., *ibid.*, **B3** 167 (1929).
8. Balandin, A. A., *Acta Physicochim. U.R.S.S.*, **22,** 80 (1947).
9. Beeck, O., "Advances in Catalysis," Vol. II, p. 151, New York, Academic Press, Inc., 1950.
10. Beeck, O., *Discussions Faraday Soc.*, **8,** (1950).
11. Beeck, O., and Ritchie, A. W., *Rev. Mod. Phys.*, **17,** 61 (1945).
12. Beeck, O., Ritchie, A. W., and Wheeler, A., *Colloid Sci.*, **3,** 504 (1948).
13. Beeck, O., Smith, A. E., and Wheeler, A., *Proc. Roy. Soc. (London)*, **A177,** 62 (1940).
14. Beeck, O. and Wheeler, A., *J. Chem. Phys.*, **7,** 631 (1939).
15. Benton, A. F., and White, T. A., *J. Am. Chem. Soc.*, **52,** 2325 (1930).

16. Berkman, S., Morrell, J. C., and Egloff, G., "Catalysis," New York, Reinhold Publishing Corp., 1940.
17. Bethe, H., *Proc. Roy. Soc. (London)*, **A150,** 552 (1935).
18. Bevan, D. J. M., and Anderson, J. S., *Discussions Faraday Soc.*, **8,** 238 (1950).
19. Born, M., and Weisskopf. V., *Z. physik. Chem.*, **B12,** 206 (1931).
20. Bosworth, R. C. L., and Rideal, E. K., *Physica*, **4,** 925 (1937).
21. Boudart, M., *J. Am. Chem. Soc.*, **74,** 1531 (1952).
22. Boudart, M., *ibid.*, **74,** 3556 (1952).
23. Boyd, C. A., Ph.D. Thesis, University of Wisconsin (1948).
24. Breger, A. K., and Zhukhovitskii, A. A., *J. Phys. Chem. S. S. S. R.*, **21,** 423 (1947).
25. Bremner, J. G. M., *Discussions Faraday Soc.*, **8,** 79 (1950).
26. Brunauer, S., Emmett, P. H., and Teller, E., *J. Am. Chem. Soc.*, **60,** 309 (1938).
27. Cernuschi, F., and Eyring, H., *J. Chem. Phys.*, **7,** 547 (1939).
28. Colburn, C. B., Wallenstein, M. B., Parlin, R. B., and Zwolinski, B. J., *Some Aspects of Catalytic Hydrogenation III. Ethylene*, XII International Congress of Pure and Applied Chemistry, New York, Sept., 1951 (unpublished).
29. Cook, M. A., and Oblad, A. G., unpublished work.
30. Cook, M. A., Pack, D. H., and Oblad, A. G., *J. Chem. Phys.*, **19,** 367 (1951).
31. Cook, M. A., *J. Am. Chem. Soc.*, **70,** 2925 (1948).
32. Coulson, C. A., *Research*, **4,** 307 (1951).
33. Couper, A., and Eley, D. D., *Discussions Faraday Soc.*, **8,** 172 (1950).
34. Cremer, E., *J. chim. phys.*, **46,** 411 (1949).
35. Daniels, F., Boyd, C. A., and Saunders, D. F., *Science*, **117,** 343 (1953).
36. de Bruijn, H., *Discussions Faraday Soc.*, **8,** 69 (1950).
37. Dole, M., *J. Chem. Phys.*, **16,** 25 (1948).
38. Dowden, D. A., *Ind. Eng. Chem.*, **44,** 977 (1952).
39. Dowden, D. A., *J. Chem. Soc.*, **1950,** 242–65.
40. Dowden, D. A., *Research*, **1,** 239 (1948).
41. Dowden, D. A., and Reynolds, P. W., *Discussions Faraday Soc.*, **8,** 184 (1950).
42. Ehrenfest, F., *Ann. Physik*, **51,** 327 (1915).
43. Eischens, R. P., and Selwood, P. W., *J. Am. Chem. Soc.*, **69,** 1590 (1947).
44. Eischens, R. P., and Selwood, P. W.; *ibid.*, **69,** 2698 (1947).
45. Eischens, R. P., and Selwood, P. W., *ibid.*, **70,** 2271 (1948).
46. Eley, D. D., *Discussions Faraday Soc.*, **8,** 34 (1950).
47. Eley, D. D., *et al.*, *Discussions Faraday Soc.*, **8,** 195–211 (1950).
48. Eley, D. D., and Rideal, E. K., *Proc. Roy. Soc. (London)*, **A178,** 429 (1941).
49. Elovich, S. Yu., and Zhabrora, G. M., *Zhur. Fiz. Khim.*, **13,** 1761, 1775 (1939).
50. Emmett, P. H., "Advances in Catalysis," Vol. I, New York, Academic Press, Inc., 1948.
51. Emmett, P. H., and Brunauer, S., *J. Am. Chem. Soc.*, **59,** 1553, 2682 (1937).
52. Emmett, P. H., and DeWitt, T., *Ind. Eng. Chem. (Anal. Ed.)*, **13,** 28 (1941).
53. Emmett, P. H., and Kummer, J. T., *J. chim. phys.*, **47,** 67 (1950).
54. Emmett, P. H., and Kummer, J. T., *Colloque sur l'Adsorption et la Cinetique Heterogene* (Lyon, Sept. 1949).
55. Emmett, P. H., and Podgurski, H., *J. Phys. Chem.*, **57,** 159 (1953).
56. Emmett, P. H., and Brunauer, S., *J. Am. Chem. Soc.*, **56,** 35 (1934).
57. Emmett, P. H., and Teller, E., "12th Report of Committee on Catalysis," p. 68, New York, National Research Council, 1940.
58. Emmett, P. H., and Skau, K., *J. Am. Chem. Soc.*, **65,** 1029 (1943).
59. Eucken, A., *Discussions Faraday Soc.*, **8,** 128 (1950).

60. Eucken, A., *Z. Electrochem.*, **53,** 285 (1949).
61. Eucken, A., *ibid.*, **54,** 108 (1950).
62. Eucken, A., *Naturwiss.*, **36,** 74 (1949).
63. Everett, D. H., *Trans. Faraday Soc.*, **46,** 453 (1950).
64. Eyring, H., and Polanyi, M., *Z. physik. Chem.*, **B12,** 279 (1931).
65. Eyring, H., Parlin, R. B., Wallenstein, M. B., and Zwolinski, B. J., "L. Farkas Memorial Volume," p. 152, Research Council of Israel, Jerusalem, (1952).
66. Eyring, H., Colburn, C. B., and Zwolinski, B. J., *Discussions Faraday Soc.*, **8,** 39 (1950).
67. Eyring, H., Hulburt, H. M., and Harman, R. A., *Ind. Eng. Chem.*, **35,** 511 (1943).
68. Eyring, H., and Wallenstein, M. B., *Proc. Natl. Acad. Sci.*, **39,** 138 (1953).
69. Eyring, H., Wallenstein, M. B., Everton, J. K., and Wylie, C. R., *Proc. Natl. Acad. Sci.* (in Press).
70. Faraday, M., "On the Power of Metals and Other Solids to Induce the Combination of Gaseous Bodies," 30 November 1833.
71. Farkas, A., *Trans. Faraday Soc.*, **35,** 906 (1939).
72. Fowler, R. H., *Proc. Cambridge Phil. Soc.*, **32,** 144 (1936).
73. Fowler, R. H., "Statistical Mechanics," England, Cambridge University Press, 1936.
74. Fowler, R. H., and Guggenheim, E. A., "Statistical Thermodynamics," Chapter X, London, Cambridge University Press, 1939.
75. Fricke, H., *Z. Electrochem.*, **53,** 264 (1949).
76. Garner, W. E., *Discussions Faraday Soc.*, **8,** 211 (1950).
77. Garner, W. E., Gray, T. J., and Stone, F. S., *Discussions Faraday Soc.* **8,** 246 (1950).
78. Garner, W. E., Stone, F. S., and Tiley, P. F., *Proc. Roy. Soc.* (*London*), **A211,** 472 (1952).
79. Gauger, A. W., and Taylor, H. S., *J. Am. Chem. Soc.*, **45,** 920 (1923).
80. Glasstone, S., Laidler, K. J., and Eyring, H., "The Theory of Rate Processes," New York, McGraw-Hill Book Company, Inc., 1941.
81. Griffith, R. H., Chapman, P. R., and (Miss) P. R. Lindars, *Discussions Faraday Soc.*, **8,** 258 (1950).
82. Griffith, R. H., "Advances in Catalysis," Vol. I, p. 107, New York, Academic Press, Inc. 1948.
83. Guggenheim, E. A., *Trans. Faraday Soc.*, **36,** 397 (1940).
84. Guggenheim, E. A., "Thermodynamics," p. 35, New York, Interscience Publishers, Inc., 1949.
85. Guggenheim, E. A., "Modern Thermodynamics," Chap. XII, London, Methuen and Co., Ltd., 1933.
86. Guggenheim, E. A., *Trans. Faraday Soc.*, **33,** 607 (1937).
87. Halsey, G. D., "Advances in Catalysis," Vol. IV, p. 259, New York, Academic Press, Inc., 1952.
88. Halsey, G. D., *J. Phys. & Colloid Chem.*, **55,** 21 (1951).
89. Halsey, G. D., *Discussions Faraday Soc.*, **8,** 54 (1950).
90. Halsey, G. D., and Taylor, H. S., *J. Chem. Phys.*, **15,** 624 (1947).
91. Harkins, W. D., and Jura, G., *J. Am. Chem. Soc.*, **66,** 1366 (1944).
92. Herington, E. F. G., and Rideal, E. K., *Trans. Faraday Soc.*, **40,** 505 (1944).
93. Hill, T. L., *J. Chem. Phys.*, **14,** 263 (1946).
94. Hill, T. L., *ibid.*, **17,** 507, 520 (1949).
95. Hill, T. L., *ibid.*, **17,** 520 (1949).

96. Hill, T. L., *ibid.*, **17,** 772, 775 (1949).
97. Hill, T. L., *ibid.*, **17,** 762 (1949).
98. Hill, T. L., *ibid.*, **18,** 246 (1950).
99. Hill, T. L., *Trans. Faraday Soc.*, **47,** 376 (1951).
100. Himmler, W., *Z. physik. Chem.*, **195,** 244 (1950).
101. Hinshelwood, C. N., "Kinetics of Chemical Change," Third Ed., Oxford, 1933.
102. Hirschfelder, J., Eyring, H., and Topley, B., *J. Chem. Phys.*, **4,** 170 (1936).
103. Horiuti, J., and Polanyi, M., *Trans. Faraday Soc.*, **30,** 1164 (1934).
104. Horiuti, J., *J. Res. Inst. Catalysis (Hokkaido Univ.)*, **1,** 8 (1948).
105. Horiuti, J., *Proc. Japan Acad.*, **29,** 160, 164 (1953).
106. Hulburt, H. M., and Hirschfelder, J. O., *J. Chem. Phys.* **17,** 964 (1949).
107. Hüttig, G. F., *Discussions Faraday Soc.*, **8,** 215 (1950).
108. Isenberg, I. *Phys. Rev.*, **79,** 737 (1950).
109. Ipatieff, V. N., "Catalytic Reactions at High Pressures and Temperatures," New York, The Macmillan Company, 1936.
110. Kimball, G. E., *J. Chem. Phys.*, **3,** 560 (1935).
111. Kimball, G. E., *ibid.*, **6,** 447 (1938).
112. Kington, G. L., and Aston, J. G., *J. Am. Chem. Soc.*, **73,** 1929 (1951).
113. Kramers, H. A., *Physica*, **7,** 284 (1940).
114. Laidler, K. J., "Chemical Kinetics," Chap. VI, New York, McGraw-Hill Book Company, Inc., 1950.
115. Laidler, K. J., *J. Phys. Chem.*, **53,** 712 (1948).
116. Laidler, K. J., *Trans. Faraday Soc.*, **47,** 47 (1951).
117. Laidler, K. J., Glasstone, S., and Eyring, H., *J. Chem. Phys.*, **8,** 667 (1940).
118. Laidler, K. J., Glasstone, S., and Eyring, H., *ibid.*, **8,** 659 (1940).
119. La Mer, V. K., *Science*, **86,** 614 (1937).
120. Langmuir, I., *J. Am. Chem. Soc.*, **38,** 2221 (1916).
121. Langmuir, I., *ibid.*, **40,** 1361 (1918).
122. Langmuir, I., *ibid.*, **54,** 2798 (1932).
123. Langmuir, I., *Trans. Faraday Soc.*, **17,** 641 (1922).
124. Lennard-Jones, J. E., *Trans. Faraday Soc.*, **28,** 333 (1932).
125. Lewis, G. N. and Randall, M., "Thermodynamics," McGraw-Hill Book Company, New York, 1923.
126. London, F., "Probleme der Modernen Physik," Summerfeld-Testachrift, p. 104, Leipzig, 1928.
127. Long, J. H., Frazer, J. C. W., and Ott, E., *J. Am. Chem. Soc.*, **56,** 1101 (1934).
128. Marcelin, A., *Ann. Phys.* **3,** 158 (1915).
129. Markham, W. C., Wall, M. C., and Laidler, K. J., *J. Chem. Phys.*, **21,** 949 (1953).
130. Markham, W. C., Wall, M. C., and Laidler, K. J., *ibid.*, **20,** 1331 (1952).
131. Maxted, E. B., "Advances in Catalysis," Vol. III, Academic Press, New York, 1951.
132. Maxted, E. B., *J. Chem. Soc.*, **1949,** 1987.
133. Maxted, E. B., and Hassid, N., *J. Chem. Soc.*, **1932,** 1532.
134. Maxted, E. B., and Moon, K. L., *J. Chem. Soc.*, **1949,** 2171.
135. McBain, J. W., "The Sorption of Gases and Vapours by Solids," London, Routledge (1932).
136. McGeer, J. P., and Taylor, H. S., *J. Am. Chem. Soc.*, **73,** 2743 (1951).
137. McMillan, W. G., and Teller, E., *J. Phys. & Colloid Chem.*, **55,** 17 (1951).
138. Mignolet, J. C. P., *Discussions Faraday Soc.*, **8,** 105 (1950).
139. Miller, A. R., "The Adsorption of Gases on Solids," London, Cambridge University Press, 1949.

140. Miller, A. R., *Discussions Faraday Soc.*, **8,** 57 (1950).
141. Miller, A. R., *J. Chem. Phys.*, **16,** 841 (1948).
142. Miller, A. R., *Proc. Cambridge Phil. Soc.*, **42,** 292 (1946).
143. Mills, G. A., Boedeker, E. R., and Oblad, A. G., *J. Am. Chem. Soc.*, **72,** 1554 (1950).
144. Mott, N. F., *Proc. Cambridge Phil. Soc.*, **32,** 281 (1936).
145. Nyrop, J. E., "Catalytic Action of Surfaces," Williams and Norgate, Ltd., London, 1937.
146. Ono, S., *Mem. Faculty Eng., Kyushu Imp. University, Japan*, **121,** 9 (1950).
147. Ono, S., *J. Phys. Soc.*, (*Japan*), **5,** 232 (1950).
148. Owen, J. R., *J. Am. Chem. Soc.*, **69,** 2559 (1947).
149. Palmer, W. G., *Proc. Roy. Soc.* (*London*), **A110,** 133 (1926).
150. Parlin, R. B., and Eyring, H., *Chem. Rev.*, **44,** 47 (1949).
151. Parravano, G., *J. Am. Chem. Soc.*, **75,** 1448 (1953).
152. Parravano, G., *J. Chem. Phys.*, **20,** 342 (1952).
153. Parravano, G., *J. Am. Chem. Soc.*, **75,** 1452 (1953).
154. Pauling, L., "Nature of the Chemical Bond," New York, Cornell University Press, 1939.
155. Pauling, L., *Proc. Roy. Soc.* (*London*), **A196,** 343 (1949).
156. Peierls, R., *Proc. Cambridge Phil. Soc.*, **32,** 477 (1936).
157. Peierls, R. *ibid.*, **32,** 471 (1936).
158. Polanyi, M., *Z. Electrochem.*, **35,** 584 (1929).
159. Prigogine, I., and Mahieu, M., *Physica*, **16,** 51 (1950).
160. Rienäcker, G., *Z. anorg. Chem.*, **236,** 252 (1938).
161. Rideal, E. K., and Trapnell, B. M. W., *J. chim. phys.*, **47,** 126 (1950).
162. Rideal, E. K., *Chemistry & Industry*, **62,** 335 (1943).
163. Roberts, J. K., *Nature*, **135,** 1037 (1935).
164. Roberts, J. K., *Proc. Roy. Soc.* (*London*), **A152,** 445 (1935).
165. Roberts, J. K., *Proc. Cambridge Phil. Soc.*, **34,** 399 (1938).
166. Roberts, J. K., *ibid.*, **35,** 293 (1939).
167. Roberts, J. K., *Proc. Roy Soc.* (*London*), **A161,** 141 (1937).
168. Rodin, T. N., *J. Am. Chem. Soc.*, **72,** 569 (1950).
169. Roginskii, S. Z., *J. Phys. Chem.*, *U.S.S.R.*, **21,** 1143 (1947).
170. Roginskii, S. Z., *Doklady Akad. Nauk. S. S. S. R.*, **67,** 97 (1949).
171. Roginskii, S. Z., and Levin, V. I., *Bull. acad. sci., U. R. S. S. Classe sci. chim.*, 137–51 (1950).
172. Rushbrooke, G. S., and Coulson, C. A., *Proc. Cambridge Phil. Soc.*, **36,** 248 (1940).
173. Sadek, H., and Taylor, H. S., *J. Am. Chem. Soc.*, **72,** 1168 (1950).
174. Schuit, G. C. A., *Discussions Faraday Soc.*, **8,** 126 (1950).
175. Schuler, K. E., and Laidler, K. J., *J. Chem. Phys.*, **17,** 1212 (1949).
176. Schwab, G. M., *Discussions Faraday Soc.*, **8,** 166 (1950).
177. Schwab, G. M., *Trans. Faraday Soc.*, **42,** 689 (1946).
178. Schwab, G. M., *Z. Electrochem.*, **35,** 585 (1929).
179. Schwab, G. M., Taylor, H. S., and Spence, R., "Catalysis," New York, D. van Nostrand Co., Inc., 1937.
180. Selwood, P. W., "Advances in Catalysis," Vol. III, p. 28, New York, Academic Press, Inc., 1951.
181. Selwood, P. W., *Bull. soc. chim.* (*France*), (*D*), 489 (1949).
182. Selwood, P. W., Hill, F. N., and Boardman, H., *J. Am. Chem. Soc.*, **68,** 2055 (1946).
183. Sherman, A., and Eyring, H., *J. Am. Chem. Soc.*, **54,** 2661 (1932).

184. Sherman, A., Sun, C. E., and Eyring, H., *J. Chem. Phys.*, **3,** 49 (1935).
185. Shockley, W., "Electrons and Holes in Semi-conductors," Chap. XVI, New York, D. van Nostrand Co., Inc., 1950.
186. Sips, R., *J. Chem. Phys.*, **16,** 490 (1948).
187. Stearn, A. E., Johnston, H. P., and Clark, C. R., *J. Chem. Phys.*, **7,** 970 (1939).
188. Steinhardt, J., *Kgl. Danske Videnskab. Selskab, Mat.-fys. Medd.*, **14,** (11) (1937).
189. Steinhardt, J., *Nature*, **138,** 74 (1936).
190. Stock, F., and Bodenstein, M., *Ber.* **40,** 570 (1907).
191. Takayanagi, K., *Progress of Theoretical Physica* (*Japan*), **6,** 486 (1951).
192. Taylor, H. A., and Thon, N., *J. Am. Chem. Soc.*, **74,** 4169 (1952).
193. Taylor, H. S., "Advances in Catalysis," Vol. I, p. 19 ff., New York, Academic Press, Inc., 1948.
194. Taylor, H. S., *Colloque sur l'Adsorption et la Cinetique Heterogene* (Lyon, September, 1949).
195. Taylor, H. S., *J. Am. Chem. Soc.*, **53,** 578 (1931).
196. Taylor, H. S., and Lewis, J. R., *J. Am. Chem. Soc.*, **60,** 877 (1938).
197. Taylor, H. S., and Liang, S. C., *J. Am. Chem. Soc.*, **69,** 1306 (1947).
198. Taylor, H. S., and McKinney, P. V., *J. Am. Chem. Soc.*, **53,** 3604 (1931).
199. Taylor, H. S., and Williamson, A. T., *J. Am. Chem. Soc.*, **53,** 813 (1931).
200. Taylor, H. S., and Williamson, A. T., *ibid.*, **53,** 2168 (1931).
201. Taylor, T. I., and Dibeler, V. H., *J. Phys. & Colloid Chem.*, **55,** 1036 (1951).
202. Temkin, M., *Acta Physicochim., U.R.S.S.*, **8,** 141 (1938).
203. Temkin, M., and Pyzhev, W., *Zhur. Fiz. Khim.*, **31,** 851 (1939).
204. Thiele, E. W., *Ind. Eng. Chem.*, **31,** 916 (1939).
205. Thon, N., and Taylor, H. A., *J. Am. Chem. Soc.*, **75,** 2747 (1953).
206. Toyama, O., *Rev. Phys. Chem. Japan*, **11,** 153 (1933).
207. Toyoma, O., *ibid.*, **14,** 86 (1940).
208. Trapnell, B. M. W., "Advances in Catalysis," Vol. III, p. 1, New York, Academic Press, Inc., 1951.
209. Twigg, G. H., *Discussions Faraday Soc.*, **8,** 152 (1950).
210. Verschaffelt, J. E., *Acad. Roy. Belg., Bull. classe sci.*, **22,** (no. 4) 373, 390, 402, (1936).
211. Volkenstein, F. F., *Levin Uspekki Khimii*, **17,** 174 (1948).
212. Volkenstein, F. F., *Zhur. Fiz. Khim.*, **22,** 311 (1948).
213. Volkenstein, F. F., *ibid.*, **24,** 1068 (1950).
214. Wagner, C. D., Wilson, J. N., Otvos, J. W., and Stevenson, D. P., *J. Chem. Phys.*, **20,** 338 (1952).
215. *Ibid.*, **20,** 1331 (1952).
216. Wallenstein, M. B., Colburn, C. B., Zwolinksi, B. J., and Parlin, R. B., *Some Aspects of Catalytic Hydrogenation II. Propylene.* XIIth International Congress of Pure and Applied Chemistry, New York, Sept., 1951 (unpublished).
217. Ward. A. F. H., *Trans Faraday Soc.*, **28,** 229 (1931).
218. Wheeler, A., "Advances in Catalysis," Vol. III, p. 250, New York, Academic Press, Inc., 1951.
218a. Yates, D. J. C., *Proc. Roy. Soc.* (*London*), **A224,** 526 (1954).
219. Zeldowitch, J., *Acta Physicochim.*, **1,** 961 (1934).
220. Zwietering, P., and Roukens, J. J., *Trans. Faraday Soc.*, **50,** 178 (1954).
221. Zwolinski. B. J., and Eyring, H., *J. Am. Chem. Soc.*, **69,** 2702 (1947).

CHAPTER 6

CATALYSIS IN HOMOGENEOUS REACTIONS IN A LIQUID PHASE

Edward L. King

Department of Chemistry, University of Wisconsin, Madison, Wis.

In this chapter catalysis of chemical reactions occurring in a liquid phase will be considered. The subject is an important one, both from a practical point of view and from the fundamental point of view that such phenomena are worth considering in an effort to make the chemical behavior of substances better understood.

Some desirable purposes might be served if a cleancut definition of catalysis could be presented. Various authors have from time to time proposed slightly different definitions. W. Ostwald defined a catalyst as any substance which alters the velocity of a chemical reaction without appearing in the end products[241]. A definition which includes some types of phenomena which are not included in the definition of Ostwald is that due to Bredig: "... the so-called catalysts can remain unaltered or also become altered themselves, but in the latter case they are still only to be considered as catalysts, when no stoichiometric whole number relationship exists between the amount of the so-called catalyst eventually changed and the amount of the other substances, the so-called substrate, that are converted"[47]. Some of the subjects to be discussed in this chapter are not within the bounds of the first definition but do conform to this second one. The definition offered by Bell[19]: "A substance is said to be a catalyst for a reaction in a homogeneous system when its concentration occurs in the velocity expression to a higher power than it does in the stoichiometric equation," does not seem particularly fundamental since only the relative values of the coefficients in a stoichiometric equation are of physical significance.

A strict definition of a catalyzed reaction is necessarily arbitrary and is not particularly useful. If the rate of a chemical reaction is increased by the presence of some particular substance, that substance is a part of the activated complex for the reaction. If the reaction or reactions which follow the rate-determining step regenerate this substance, it is not consumed during the reaction, and it *would not* appear as a reactant in the equation for the over-all reaction; this substance would qualify as a catalyst according to most definitions. On the other hand, if this substance were not regenerated in a reaction which followed the rate-determining step, it *would* appear as a reactant in the equation for the over-all reaction and would not be considered to be a catalyst. Yet the role which this substance plays in the formation of the activated complexes for these two reactions might be quite similar. It would be unfortunate if an arbitrary definition prevented the consideration, side by side, of reactions believed to have similar mechanisms.

The field of catalysis, even when limited to homogeneous reactions in a liquid phase, is an extremely large one. As the discussion in the preceding paragraph makes clear, a catalyzed reaction is essentially one in which a substance taking part in the rate-determining step is regenerated after the rate-determining step. Emphasis in this chapter is placed upon the mechanisms of the catalyzed reactions and upon the extent to which kinetic data can elucidate these mechanisms. The first two sections of the chapter deal with background material for the discussion of the mechanisms of catalyzed reactions; these sections are on "Theories of Reaction Kinetics" and "Rate Laws and Reaction Mechanisms." There follow sections on "Medium Effects" (a type of catalysis), "Acid and Base Catalysis" (certainly the field of homogeneous catalysis which has been most widely studied), "The Influence of Complexing Agents Upon Reaction Velcity," "Catalysis in Oxidation-Reduction Reactions," "Miscellaneous Examples of Catalysis," and "Negative Catalysis."

THEORIES OF REACTION KINETICS

Most kinetic studies are currently discussed in terms of either of two theories: the collision theory or the theory of absolute reaction rates. Recent books which discuss reactions in solution from these two points of view are by Moelwyn-Hughes, who discusses reactions in the nomenclature of the collision theory[224] and by Glasstone, Laidler and Eyring[93], and Laidler[177], who approach the question from the point of view of the theory of absolute reaction rates. For a detailed discussion of these theories, the reader is referred to these works. Since any theory which enjoys an appreciable lifetime must have some success in explaining or rationalizing experimental facts, it is not surprising that each of these approaches leads to a similar conclusion with respect to certain observable quantities. Thus, the theoretical expression for the frequency factor in a bimolecular reaction of two atoms A and B in the gas phase is the same in the two theories[94]. It is worthwhile to consider briefly some of the equations used in the two theories.

If temperature-coefficient data for a reaction rate are available, the calculation of the apparent energy of activation of the reaction is possible. This is defined by the equation

$$E_A = -R\,\frac{d \ln k}{d(1/T)} \tag{1}$$

in which k is the rate constant for the reaction. The value of E_A, also referred to as the Arrhenius energy of activation, is clearly determined directly by experiment and does not depend upon any particular theory of reaction kinetics. The temperature range over which the kinetics of most chemical reactions has been studied is limited; it has been observed that associated with most chemical reactions, both in solution and in the gas phase, there is for each reaction a relatively constant value of this apparent activation energy. For some reactions, on the other hand, the value of E_A varies with temperature. The two theories of chemical kinetics deal with the dependence of E_A upon temperature in different ways.

The rate constant in the collision theory is given by the equation

$$k = PZ\,\frac{(E/RT)^F}{F!}\,e^{-E/RT} \qquad (2)^{225}$$

in which $E = E_A + (F - \frac{1}{2})RT$, Z is the collision frequency, and P is a probability factor. The letter F stands for the number of degrees of freedom among which the activation energy is shared. (The term $-\frac{1}{2}RT$ arises because of the temperature dependence of the collision frequency.) The collision frequency is generally calculated using an equation derived from the kinetic theory of gases; such an approximation appears to be reasonable in view of the many simple reactions in solution with P values close to unity[226]. There are, however, many reactions which have P values that are very different from unity, both larger and smaller[227]. At first sight, it may appear unreasonable that this probability factor can exceed unity. In some cases, values of P greater than one may merely indicate a true collision frequency appreciably greater than that calculated using the kinetic theory equation. In others, the large values of P may result from a treatment of temperature coefficient data under the tacit assumption that $F = 1$, while it is really greater than unity. Moelwyn-Hughes suggests that the simple collision theory will fail in predicting the rate of a reaction involving molecules which exert strong forces, attractive or repulsive, upon one another[228].

The basic postulates of the theory of absolute reaction rates may be stated rather briefly. In going from the initial state of relative stability to the final state of greater stability, the reactants pass through a succession of configurations. Of all of the possible independent reaction paths, there are at most a few by which the actual system will be transformed from reactants to products. Along each of these favorable reaction paths, there is a configuration of maximum instability. Such configurations are the activated complexes for the reaction. It is assumed that each activated complex is in equilibrium with the reactants and that the rate of the reaction via each reaction path is determined by the equilibrium concentration of that particular activated complex and the specific rate at which the activated complex decomposes. The rate constant in the theory of absolute reaction rates is given by the equation

$$k^0 = \mathrm{K}\,\frac{kT}{h}\, e^{\Delta S^{\ddagger}/R}\, e^{-\Delta H^{\ddagger}/RT}$$ (3)[95, 178]

where K is the transmission coefficient, k is the Boltzmann constant, T is the absolute temperature, h is Planck's constant, and R is the gas constant (i.e., the product of k and Avogadro's number). The quantities $\Delta S^{\ddagger}$ and $\Delta H^{\ddagger}$ are the standard entropy and enthalpy changes accompanying the activation process. (With these quantities defined as the standard changes, the k given by Eq. (3) is that for the ideal solution. The modification which this equation undergoes in order to account for medium effects will be discussed later.) The value of $\Delta H^{\ddagger}$ is very close to the experimental activation energy, $E_A : E_A = \Delta H^{\ddagger} + RT$. Changes in the measured activation energy with temperature would, in this theory, be due to the fact that $\Delta C_P{}^{\ddagger}$ is not equal to zero; the thermodynamic relationships pertaining to the activation process are the same as those relating to ordinary chemical reactions[88a]. The $\Delta S^{\ddagger}$ of this theory and the P factor of the collision theory are loosely associated. Thus an abnormally slow reaction is one with a low value of $P (P \ll 1)$ and a negative value of $\Delta S^{\ddagger}$; an abnormally fast reaction is one with a large value of $P (P \gg 1)$ and a positive value of $\Delta S^{\ddagger}$. The rigorous application of the absolute rate theory to reactions in solution is not possible. It is convenient, however, to discuss chemical reactions occurring in solution in the nomenclature of this theory. Various factors alter reaction rates; if a rationalization of these influences in terms of their effect on $\Delta H^{\ddagger}$ and $\Delta S^{\ddagger}$ is fruitful, the approach is of considerable value.

Rate Laws and Reaction Mechanisms

Much of the discussion of catalysis which is presented in this chapter deals with details of the rate laws of catalyzed reactions and with the mechanisms consistent with these rate laws. It is, therefore, of interest to deal briefly with the question of how much one can learn regarding a mechanism from the form of the rate law for a reaction. It is first a necessity to know the formulas of the predominant forms of the reactants and products which exist in the solutions in which the kinetic studies are carried out.

For example, the conclusions to be drawn from an observation of first power dependence of a reaction rate on the concentration of an acid, HX, depend upon whether HX exists in the reaction medium predominately as H^+ and X^- or predominantly as unionized HX. Knowledge of the predominant forms in which the products exist is necessary if a correctly balanced equation for the net reaction is to be written. Quite obviously, correct interpretation of rate data to yield a rate law may depend upon the precise stoichiometry of the reaction.

If the rate law for a chemical reaction is a linear equation of several independent terms, each term corresponds to a different reaction path. The stoichiometric formula of the activated complex for each of these reaction paths is given by the form of the term in the rate law which is associated with that reaction path. Thus, if a term in a rate law has the form: $k(A)(B)^2$, the formula of the activated complex for that reaction path is AB_2S_n, where S represents a solvent molecule. In studies in dilute solution, it is impossible to determine the order of the reaction with respect to the solvent; thus, the number of solvent molecules in the activated complex is not derivable from the form of the rate law. A simple inverse dependence of the rate upon the concentration of some substance indicates that this species is split out of the reactants before forming the activated complex. Thus, the activated complex for a reaction path which corresponds to a rate law $k(A)(B)(C)^{-1}$ contains one molecule of C less than the sum of one molecule each of A and B and of course an undeterminable number of solvent molecules. A mechanism which is consistent with such a term in a rate law is

$$A \rightleftarrows D + C$$

$$B + D \rightarrow \quad ;$$

the first reaction is a rapidly established equilibrium which lies far to the left, and the second reaction is rate-determining. The activated complex has the composition BD which is the same as AB minus C. While the form of the rate law establishes the composition of the activated complex, it does not determine the mechanism uniquely. Other mechanisms might be suggested which are consistent with such a rate law; each of these would show C being split out of A, B, or a species made up by combination of A and B before the rate-determining step.

In order to illustrate clearly the indistinguishability of mechanisms with activated complexes of the same composition, the second order reaction of HX, a weak acid, and BOH, a weak base, will be considered. (The reaction is not merely one of neutralization.) The rate of the reaction is given by a rate law

$$\text{Rate} = k(\text{HX})(\text{BOH})$$

if the experiments are carried out in a pH range where both HX and BOH are the dominant species of these two substances. The form of this rate law leads to the conclusion that the activated complex has the composition $BX(H_2O)_n$. Two of the possible mechanisms which are consistent with this rate law are:

(1) $HX + BOH \xrightarrow{k_1}$ product or substance which is rapidly converted to the product, in which case k, defined by the rate equation, is equal to k_1, and

(2) $HX \rightleftarrows H^+ + X^-$ a rapid equilibrium
$BOH \rightleftarrows B^+ + OH^-$ a rapid equilibrium
$H_2O \rightleftarrows H^+ + OH^-$ a rapid equilibrium
$B^+ + X^- \xrightarrow{k_2}$ product or substance which is rapidly converted to product, in which case k, defined by the rate equation, is equal to the product $k_2K_{HX}K_{BOH}K_w^{-1}$, where K_{HX}, K_{BOH}, and K_w are the equilibrium constants for the ionization of HX, BOH, and H_2O.

It is seen that in each of the two mechanisms, the activated complex has the composition $BX(H_2O)_n$. This activated complex is in equilibrium with the dominant form of the reactants, HX and BOH; whether or not the activated complex is actually formed by the union of these two species or by the union of the species B^+ and X^-, species which are also in equilibrium with the dominant BOH and HX, clearly cannot be answered from the kinetic data.

Studies of the kinetics of some reactions indicate that the order of the reaction with respect to the stoichiometric concentration of one or more substances changes as the concentrations are altered. If the order of the reaction with respect to a particular substance increases with an increase in concentration of that substance, a rate law which involves two or more independent terms is suggested. Thus, the order of the reaction of hydrogen peroxide and iodide ion with respect to hydrogen ion increases from zero order to first order as the acidity is increased. The rate law for the reaction is[195] $-d(H_2O_2)/dt = k_1(H_2O_2)(I^-) + k_2(H_2O_2)(H^+)(I^-)$. This is interpreted to mean that two independent reaction paths exist; the activated complexes have the compositions

$$(H_2O_2I^-) \pm n(H_2O) \text{ and } (H_3O_2I) \pm m(H_2O).$$

If the order of the reaction with respect to a particular substance decreases with an increase in concentration of that substance, the cause may be a change in the dominant form of one or more of the reactants which is brought about by this change of concentration. A decrease in the order with respect to the concentration of hydrogen ion with an increase in the acidity is often observed for reactions involving weak acids. Referring again to the second order reaction between the weak acid HX and the weak base BOH which proceeds by the way of a single activated complex with the composition $BX(H_2O)_n$, it can be shown that the rate law, written in terms of the total concentration of HX and BOH, which is valid at all acidities is:

$$\text{Rate} = k[\text{HX}][\text{BOH}]\left\{\frac{(\text{H}^+)}{(\text{H}^+) + K_{\text{HX}}}\right\}\left\{\frac{K_{\text{W}}/K_{\text{BOH}}}{(\text{H}^+) + K_{\text{w}}/K_{\text{BOH}}}\right\},$$

where [HX] and [BOH] are the total concentrations of HX and BOH, respectively, and the quantity in the first bracket is the fraction of the X-containing species which is HX and the quantity in the second bracket is the fraction of the B-containing species which is BOH. At very low concentrations of hydrogen ion, where (H^+) is small compared to both K_{HX} and K_w/K_{BOH}, the reaction rate is proportional to the first power of the concentration of hydrogen ion; at high concentrations of hydrogen ion where (H^+) is large compared to both K_{HX} and K_w/K_{BOH}, the reaction rate is *inversely* proportional to the concentration of hydrogen ion. Thus the order of the reaction with respect to the concentration of hydrogen ion decreases from +1 to −1 as the hydrogen ion concentration increases. This change in the order of the reaction with respect to the concentration of hydrogen ion is due to the changes in the dominant forms of the reactants; there is but a single activated complex over the entire range of acidity.

In the mechanisms discussed thus far, a single step for each reaction path is slow compared to all of the rest of the steps in that path. That is, it can be said that *one* of the steps in each path is the rate-determining step. It is also of interest to examine the sort of rate law which is obtained if two of the reaction steps have comparable velocities. A rate law of the form

$$\text{Rate} = \frac{k(\text{A})(\text{B})(\text{E})}{k'(\text{D}) + (\text{E})}$$

is consistent with a mechanism,

$$\text{A} + \text{B} \underset{k_{-1}}{\overset{k_1}{\rightleftharpoons}} \text{C} + \text{D}$$

$$\text{C} + \text{E} \xrightarrow{k_2} \text{product or intermediates which rapidly yield the products,}$$

if the intermediate C is thermodynamically unstable and cannot exist at appreciable concentrations. (The constants of the rate equation and the mechanism are related: $k = k_1$ and $k' = k_{-1}/k_2$). The rate law was derived from the mechanism by a method commonly referred to as the method of the stationary state or unstable intermediate[40, 64, 267]. In this method an expression for the concentration of the unstable intermediate C is derived by equating $d(\mathrm{C})/dt$ to zero. Of course, $d(\mathrm{C})/dt$ does not exactly equal zero, but it is extremely small if the maximum concentration at which C can exist is very low. If $k_2(\mathrm{E}) \gg k_{-1}(\mathrm{D})$, the rate law becomes Rate $= k_1(\mathrm{A})(\mathrm{B})$, and it would be correct to say that the first step was rate-determining; if $k_{-1}(\mathrm{D}) \gg k_2(\mathrm{E})$, the rate law becomes: Rate $= \dfrac{k_2K(\mathrm{A})(\mathrm{B})(\mathrm{E})}{(\mathrm{D})}$, $(K = k_1/k_{-1})$, and it would be correct to say that the second step was rate-determining. The order of the reaction with respect to both D and E depends upon the concentration conditions; in both cases, the order decreases with an increase in the concentration of the substance being considered (i.e., D or E). The two extreme situations correspond to the two extremes in the possible fate of the unstable intermediate C. On the one hand practically every C which forms reacts with E, in which case equilibrium in the first reaction is not established. On the other hand, if practically every C reacts with D to reform the reactants, equilibrium in the first reaction is established, and the rate-determining step is the second reaction. It is to be noted that fundamental distinction exists between this type of mechanism and those discussed in the preceding sections. The discussion in this paragraph concerns mechanisms in which more than one step may be rate-determining; two different possible activated complexes exist along the one reaction path and which one of these is the activated complex depends upon the concentration conditions.

An interesting question regarding reaction mechanisms in which one or more intermediate steps is postulated is the following: Under what conditions must the reverse of each of the postulated steps be taken in account in the rate law? Consider a chemical change for which the net reaction is

$$\mathrm{A} + 3\mathrm{B} = \mathrm{C} + 3\mathrm{D},$$

and for which the mechanism is

$$\mathrm{A} + \mathrm{B} \rightleftarrows \mathrm{X} + \mathrm{D}$$

$$\mathrm{X} + \mathrm{B} \rightleftarrows \mathrm{Y} + \mathrm{D}$$

$$\mathrm{Y} + \mathrm{B} \rightarrow \mathrm{C} + \mathrm{D},$$

in which X and Y are unstable intermediates. Three limiting cases exist; the rate-determining step may be step 1, step 2 or step 3. In these three limiting cases, the rate laws are:

$$\text{Rate} = k_1(\text{A})(\text{B}),$$

$$\text{Rate} = \frac{k_1k_2}{k_{-1}} \frac{(\text{A})(\text{B})^2}{(\text{D})},$$

and

$$\text{Rate} = \frac{k_1k_2k_3}{k_{-1}k_{-2}} \frac{(\text{A})(\text{B})^3}{(\text{D})^2}.$$

It is seen that the rate constants for the reverse of all of the reactions which occur before the rate-determining step appear in the rate equation. The reason for this is straightforward enough. If account were not taken of the reverse of those steps which precede the rate-determining step, a situation would exist in which the concentrations of the unstable intermediates could build up to values in excess of their maximum value possible in equilibrium with A and B. Such a situation is obviously impossible. The measured rate constant for a reaction includes the equilibrium constants for all of the steps which precede the rate-determining step. This is shown in the rate laws presented in this paragraph for $k_1/k_{-1} = K_1$, and $k_2/k_{-2} = K_2$, where K_1 and K_2 are the equilibrium constants for the first two reactions (i.e., those leading to the unstable intermediates X and Y). The general expression for the rate of this reaction is

$$\text{Rate} = \frac{k_1k_2k_3(\text{A})(\text{B})^3}{k_2k_3(\text{B})^2 + k_{-1}k_3(\text{B})(\text{D}) + k_{-1}k_{-2}(\text{D})^2}.$$

The three limiting cases are given if each of the three terms in the denominator is large compared to the remaining two. This general expression can be conveniently derived using the formulation devised by Christiansen.[64, 130]

No allowance has yet been made in the discussion of reaction mechanisms for reversibility of the over-all reaction. If a reaction is studied under concentration conditions such that equilibrium is approached, it is necessary to take into consideration the diminution of the observed rate of the forward reaction because of the simultaneous occurrence of the reverse reaction. A mechanism for the forward reaction is also a mechanism for the reverse reaction; the reverse reaction proceeds by the reverse of each step via which the forward reaction proceeds. If the rate law for the forward reaction consists of several independent terms which, as we have seen, correspond to several independent reaction paths, there will be the same number of independent terms in the rate law for the reverse reaction. At equilibrium, not only is the total rate of the forward reaction equal to the total rate of the reverse reaction, but the rate of the forward reaction by each particular path is equal to the rate of the reverse reaction by the reverse of that particular path. This is the "principle of microscopic reversibility." It will be seen in the next section (Medium Effects: Activity Coefficients in Rate Equations) that the form of the rate law for the reverse reaction has a definite relationship to the form of the rate law for the forward reaction if the rate law has one independent term. If the rate law is one which involves several independent terms, the form of each term in the rate law for the reverse reaction is related to the form of the corresponding term in the rate law for the forward reaction.

The principles discussed in this section have been general in nature. Applied to catalytic reactions, nothing fundamentally different is introduced Of course, the order of the reaction with respect to a true catalyst is not determined in a single run since its concentration does not change during the course of a single run. It may be determined by observing the dependence of the reaction rate upon the catalyst concentration in a number of runs. The order of the reaction with respect to the catalyst concentration will disclose the number of catalyst molecules in the activated complex.

MEDIUM EFFECTS

Activity Coefficients in Rate Equations

Certain simple considerations make clear the necessity that some function of the activity coefficients of the reactants and/or products appear in the rate equation for a chemical reaction. The subject may be discussed in terms of a reversible reaction which is represented by the equation

$$\mathrm{A} + \mathrm{B} \rightleftarrows \mathrm{C} + \mathrm{D}.$$

This reaction has associated with it an equilibrium constant, K, which has the form $K = (\mathrm{C})(\mathrm{D})y_\mathrm{C}y_\mathrm{D}/(\mathrm{A})(\mathrm{B})y_\mathrm{A}y_\mathrm{B}$, where the symbol enclosed in parentheses stands for the concentration of the substance and y is the activity coefficient based on the particular concentration units and standard states which are being used. This equilibrium constant has a definite value at a given temperature; the value of K is related to the value of the standard free energy change in the reaction $\Delta F^\circ = -RT \ln K$.

The rates of the forward and reverse reactions are given by the equations:

$$\text{Forward reaction: Rate} = k_f(\mathrm{A})^a(\mathrm{B})^b(\mathrm{C})^c(\mathrm{D})^d(\mathrm{F})^f$$

$$\text{Reverse reaction: Rate} = k_r(\mathrm{A})^{a'}(\mathrm{B})^{b'}(\mathrm{C})^{c'}(\mathrm{D})^{d'}(\mathrm{F})^{f'};$$

the rate constants k_f and k_r which are defined by these equations are not independent of the composition of the medium in which the reaction occurs. At equilibrium, the rates of the forward and reverse reactions are equal, and therefore

$$\frac{(\mathrm{C})^{c'-c}(\mathrm{D})^{d'-d}(\mathrm{F})^{f'-f}}{(\mathrm{A})^{a-a'}(\mathrm{B})^{b-b'}} = \frac{k_f}{k_r}.$$

If medium effect upon the value of k_f/k_r is to be accounted for by the incorporation of an activity coefficient factor, the following relationships must be true: $c' - c = 1$, $d' - d = 1$, $f' = f$, $a - a' = 1$ and $b - b' = 1$ (since F is a catalyst, f' must equal f). This follows since two functions (of the type being discussed) of the concentrations of A, B, C and D can both be constant over a range of the values of the concentrations of A, B, C and D only if these two functions are equal to one another or are rational powers of one another. Since only the relative values of the coefficients of substances in the chemical equation are of significance, these coefficients may be chosen such that the two functions of the concentrations ($Ky_\mathrm{A}y_\mathrm{B}/(y_\mathrm{C}y_\mathrm{D})$ and k_f/k_r) are equal. That is,

$$\frac{(\mathrm{C})(\mathrm{D})}{(\mathrm{A})(\mathrm{B})} = K\frac{y_\mathrm{A}y_\mathrm{B}}{y_\mathrm{C}y_\mathrm{D}}$$

and

$$\frac{(\mathrm{C})(\mathrm{D})}{(\mathrm{A})(\mathrm{B})} = \frac{k_f}{k_r},$$

which leads to:

$$\frac{k_f}{k_r} = K\frac{y_\mathrm{A}y_\mathrm{B}}{y_\mathrm{C}y_\mathrm{D}}.$$

What, then, is the relationship between the two rate constants k_f and k_r and two rate constants k_f^0 and k_r^0, which are independent of medium composition (i.e., which are truly constant) and are related to the equilibrium constant by the equation $k_f^0/k_r^0 = K$?

A number of possibilities exist; they include relationships such as $k_f = k_f^0 y_\mathrm{A}y_\mathrm{B}$ and $k_r = k_r^0 y_\mathrm{C}y_\mathrm{D}$, or $k_f = k_f^0(y_\mathrm{C}y_\mathrm{D})^{-1}$ and $k_r = k_r^0(y_\mathrm{A}y_\mathrm{B})^{-1}$. The first possibility, which is consistent with the requirement that $k_f^0/k_r^0 = K$ is equivalent to the statement that the rate of a chemical reaction is proportional to the product of the activities of the reactants; this has been referred to as the activity rate theory and was first proposed by van't Hoff[150]. The kinetics of a number of reactions have been discussed in terms of this theory[132, 133, 134, 135, 156, 217, 239, 258]. Since the activity coefficients of ions are lowered by the addition of an inert salt if the total concentration of salt is low, the rates of all ionic reactions should be decreased by the addition of an inert salt if the activity rate theory is valid. It is actually observed that reactions between ions of like charge sign are accelerated by the addition of an inert salt. Thus the activity rate theory is not consistent with some experimental observations. In addition, if this theory were valid, there would be available a technique for the measurement of the activity coefficient of a single ion. This information is believed to be impossible to acquire[109]. Although the activity rate theory is consistent with the thermodynamic requirement that $k_f^0/k_r^0 = K$, it does not appear to be valid.

The second possibility ($k_f = k_f^0(y_C y_D)^{-1}$ and $k_r = k_r^0(y_A y_B)^{-1}$) was suggested by v. Halban[115]. If this formulation were correct, the kinetic salt effect in an ionic reaction would be determined by the charge type of the substances which influence the rate of the reverse reaction. No such correlation has been observed.

The Bronsted Equation. In 1922, J. N. Bronsted pointed out that the effect of an inert salt on the rate of an ionic reaction is one of three types[49]. Reactions between two ions of like charge sign are accelerated by the addition of inert salt. Reactions between ions of unlike charge sign proceed more slowly upon the addition of an inert salt, while those between an ion and a neutral molecule are, in general, not subject to large salt effects. He suggested the quantitative relationship

$$k_f = k_f^0 y_A y_B / y_X \, , \tag{4}$$

in which y_X is the activity coefficient of the critical complex in the reaction. This critical complex was pictured as the least stable configuration involving A and B of all of the configurations through which these molecules pass in the actual path they follow in being converted to the products. If, as Bronsted proposed, the rate of a chemical reaction is determined by the difference between the chemical potential of this critical complex and the reactants, the effect of medium changes would be determined by changes in the value of the activity coefficient factor. Since the critical complexes for the forward and reverse reactions are the same, the formulation presented by Bronsted is consistent with the requirement $k_f^0/k_r^0 = K$.

This equation $k_f = k_f^0 y_A y_B / y_X$ was also developed by Bjerrum who postulated that an unstable collision complex, in equilibrium with the reactants, decomposes at a rate proportional to its concentration[37]. Since the concentration of this complex, S, is given by the expression (S) $\propto$ (A) (B) $\dfrac{y_A y_B}{y_S}$, it is clear that this set of assumptions leads to the equation presented earlier by Bronsted.

The Medium Effect in the Absolute Rate Theory[96]. In the theory of absolute reaction rates, the dependence of the concentration rate constant upon activity coefficients is the same as that which appears in the Bronsted equation, $k_f = k_f^0 y_A y_B / y_X$. In this theory, the rate of the reaction is assumed to be equal to the product of the concentration of the activated complex and a universal frequency $\dfrac{kT}{h}$ (if the transmission coefficient is unity). It is assumed that the activated complex is in equilibrium with the reactants. The derivation leading to the equation $k_f = k_f^0 y_A y_B / y_X$* is straightforward and resembles that of Bjerrum although the exact nature of X was viewed differently by Bjerrum than it is in the absolute rate theory.

The Bronsted Equation and Ionic Reactions. The validity of the Bronsted equation is most easily investigated in studies of ionic reactions because in such systems the property of the activated complex which is of primary importance in establishing its activity coefficient is known. This property is the charge and it is the algebraic sum of the charges on the reactants which come together to form the activated complex. The activity coefficients of ionic substances in dilute solution may be calculated using the equation developed by Debye and Huckel[79]. A first approximation for the calculation of the activity coefficient of an ion is the Debye-Huckel limiting law,

$$\log y_i = -\alpha Z_i^2 \sqrt{\Gamma} \tag{5}$$

where y_i is the activity coefficient of the i ion, α is a constant at a particular temperature (see reference 136, Chapter 5 for a tabulation of values of constants which are related to this constant), Z_i is the charge on the i ion and Γ is the ional concentration which is defined by the equation $\Gamma = \sum c_i Z_i^2$, in which the summation is taken over all of the ions in the solution, and c_i is the molar concentration of the i ion. The ional concentration differs from the ionic strength, which is also frequently used in equations for activity coefficients; the ionic strength is defined, $\mu = \frac{1}{2} \sum m_i Z_i^2$, where m_i is the molal concentration of the i ion. The expression for the dependence of the rate constant for a rate law, Rate $= k(\mathrm{A}^{Z_A})(B^{Z_B})$, upon the ional concentration is derived by combining equations of 4 and 5:

$$\begin{aligned} \log k/k_0 = \log \frac{y_A y_B}{y_{AB}} &= -\alpha\sqrt{\Gamma}(Z_A^2 + Z_B^2 - (Z_A + Z_B)^2) \\ &= +2Z_A Z_B \alpha \sqrt{\Gamma}. \end{aligned} \tag{6}$$

This equation leads to the conclusion that reactions between ions of like charge sign are accelerated and those between ions of unlike charge sign proceed more slowly in media of higher ionic strength. These predictions are consistent with the generalizations which Bronsted made regarding the salt effect on ionic reactions. In the more general case where the re-

---

* The value of k_f^0 is given by the equation $k_f^0 = \frac{kT}{h} K_0^\ddagger$ where $K_0^\ddagger$ is the true thermodynamic equilibrium constant for the reaction A + B ⇄ X.

action is not second order, e.g., where

$$\text{Rate} = k\,\frac{(\text{A})(\text{B})(\text{E})}{(\text{D})},$$

the equation for the rate constant is

$$\log\frac{k}{k_0} = \log\frac{y_{\text{A}}y_{\text{B}}y_{\text{E}}}{y_{\text{X}}y_{\text{D}}} = \alpha\Delta Z^2\sqrt{\Gamma} \tag{6'}$$

where $\Delta Z^2 = Z_{\text{X}}^2 + Z_{\text{D}}^2 - Z_{\text{A}}^2 - Z_{\text{B}}^2 - Z_{\text{E}}^2$ (with, of course, $Z_{\text{X}} = Z_{\text{A}} + Z_{\text{B}} + Z_{\text{E}} - Z_{\text{D}}$). The comparison of experimentally determined salt effects and the quantitative predictions of the Bronsted-Debye and Huckel equation will be examined later.

Another approach to the subject of the effect of environment upon reaction rate is that developed by Christiansen[61] and Scatchard[260]; this is most easily discussed with reference to reactions involving ions. The essential idea in this formulation is that the concentration of the activated complex made up of an A ion and a B ion is proportional to the bulk concentration of A multiplied by the average concentration of B at a distance of r from A, where r is the distance of approach of A and B in the activated complex. The Debye and Huckel theory provides an expression for the value of this concentration. This leads to an equation for the value of $\log\frac{(X)}{(\text{A})(\text{B})} - \log\frac{(X)_0}{(\text{A})_0(\text{B})_0}$, (the concentrations with zero subscripts refer to the standard state which is the hypothetical solution of unit activity), which is also equal to the activity coefficient factor. The resulting equation for the activity coefficient factor is

$$\log\frac{y_{\text{A}}y_{\text{B}}}{y_{\text{X}}} = 2.303\,\frac{\epsilon^2 Z_{\text{A}}Z_{\text{B}}}{DkTr}\left\{1 - \frac{e^{-\kappa r}e^{\kappa a}}{1+\kappa a}\right\} \tag{7},$$

where κ is defined by the equation[139]

$$\kappa^2 = \frac{4\pi\epsilon^2}{DkT}\sum_i n_i Z_i^2$$

in which ϵ is the electronic charge, D is the dielectric constant of the medium, k is the Boltzmann constant, and n_i is the number of i ions per cubic centimeter; a is the distance of closest approach of the ions. If r and a are approximately equal, Eq. (7) is simplified to the form

$$\log\frac{y_{\text{A}}y_{\text{B}}}{y_{\text{X}}} = 2.303\,\frac{\epsilon^2 Z_{\text{A}}Z_{\text{B}}}{DkT}\,\frac{\kappa}{1+\kappa a}. \tag{8}$$

This equation becomes, for the conditions of very low concentrations, the same as the expression which results from a substitution of the Debye-Huckel limiting law expression for activity coefficients into the Bronsted equation.

In order to consider the salt effect in the concentration region in which the Debye and Huckel limiting law is not valid, one or another of the extensions of this limiting equation must be used. In some of these extensions, the distance of closest approach of the ions appears as a parameter; in solutions containing several ions of different sizes the meaning of this parameter becomes somewhat obscure. In general, some sort of a mean value is used[260]. In the more detailed theories which should be valid to higher values of the ionic strength, some assumptions must be made regarding the size and shape of the activated complex[99]. The equation developed by Scatchard[259, 260], which has already been presented (Eq. 7), is based on a double sphere model of the activated complex. Laider and Eyring have derived an equation based upon a spherical activated complex[176]. The difference between this equation and the one derived by Scatchard using the double sphere model is not very significant; they become identical if, in the equation derived by Laidler and Eyring, one assumes the radii of A, B and the activated complex are equal.

The Activity Coefficients of Electrolytes and Nonelectrolytes in Aqueous Solution

The medium effect upon reaction velocity is determined by the value of the activity coefficient factor $(\pi_i y_i^{\alpha_i})/y^{\ddagger}$, where the activity coefficient product is taken over all the i substances the concentrations of which, raised to the α_i power, appear in the rate law. If an alteration in the medium (e.g., addition of a new solvent species, "inert" salt, etc.) has a large enough effect upon the rate, the rate law may be expanded to include new terms which involve the concentration of the added substance which so markedly influences the rate[259]. On the other hand, the quantitative allowance for the influence may be made in the activity coefficient factor, the reaction being formulated as before. As background material for a discussion of kinetic salt effects, consideration of the experimental values of activity coefficients of electrolytes is worthwhile. Activity coefficients of many nonelectrolytes have been measured in electrolytic solutions; a discussion of this will also be presented because of its relevance to the salt effect upon reactions of an ion and a neutral molecule.

Activity Coefficients of Electrolytes. The experimental values of the mean activity coefficient of the strong electrolytes: hydrochloric acid, sodium chloride, potassium chloride, calcium chloride, and lanthanum chloride are presented in Figure 1[266]. It is to be noted that the data ap-

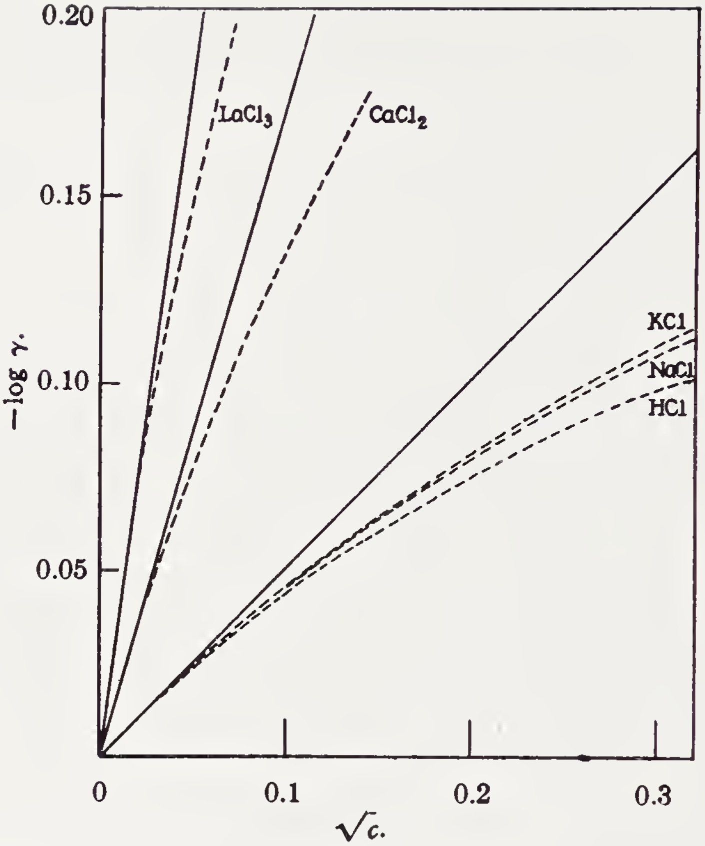

FIG. 1. The activity coefficient of various strong electrolytes. (Reproduced from Ref. 266 with the permission of the Editor of the *Journal of the American Chemical Society*).

proach the limiting law rather closely at low values of the concentration. At an ionic strength of 0.02 the approximate percentage difference between the experimental values of the mean activity coefficient and those calculated using the Debye-Huckel limiting law are: hydrochloric acid, 3 per cent; sodium chloride, 2 per cent; potassium chloride, 2 per cent; calcium chloride, 7 per cent; and lanthanum chloride, 13 per cent. If the product of the charge on an ion involved in a reaction as a reactant or an activated complex and the charge on an oppositely charged ion in the solution is not in excess of three, the Bronsted-Debye and Huckel limiting law should be obeyed within the precision suggested by this agreement. At greater concentrations, larger discrepancies between the observed values of activity coefficients and the values calculated using the limiting law will be expected. Extensions of the limiting law which are useful in evaluating the activity coefficients of electrolytes are also useful in correlation of kinetic salt effects. Among the most useful extensions of the limiting law is that suggested by Guggenheim[111],

$$\log y_i = -\alpha Z_i^2 \sqrt{\Gamma}/(1 + \sqrt{\Gamma/2}) + \sum_j B_{ij}C_j \qquad (9),$$

in which the summation is taken over all of the j ions which have a charge that is opposite in sign to the charge on the i ion; the B values are empirical and are assumed to be independent of C, the concentration. More recently, Glueckauf has modified this equation in a useful way by assuming that the B_{ij} values are not constant but depend upon the ionic strength[101]. The basis for taking the summation over only the concentrations of the ions of charge which is opposite that of the ion under consideration is Bronsted's principle of specific interaction of ions which has as a fundamental postulate that "in dilute salt solutions of constant total concentration, ions will be uniformly influenced by ions of like sign"[48].

At higher concentrations, the activity coefficients of many strong electrolytes have a minimum value and then increase at still higher concentrations. This behavior is rather typical of strong electrolytes and has been explained on the basis of ion hydration by Stokes and Robinson[273] in an extension of a theory proposed by Bjerrum[36]. Among the electrolytes which show no pronounced minimum in the value of $y_\pm$ are the alkali metal sulfates, most divalent metal sulfates, the alkali metal nitrates (except lithium nitrate) and silver nitrate. On the basis of values of the conductance of solutions of these substances, they are often considered to be incompletely ionized[140]. The values of the dissociation constants of some salts and complex ions of this type are presented in Table 1.

It is clear that the rates of reactions in which ionic substances of this type participate, either as a reactant or as an added "inert" salt, will be influenced by electrolyte concentration changes in a way which reflects this abnormality in the activity coefficient.

TABLE 1. DISSOCIATION CONSTANTS OF SALTS AND COMPLEX IONS IN WATER AT 18°C (Estimated from Conductance Data)

	K	Ref.		K	Ref.
$KClO_3$	1.4	73	$LiSO_4^-$	0.23	74
KNO_3	1.4	73	$NaSO_4^-$	0.20	74
$AgNO_3$	1.2	73	KSO_4^-	0.15	74
$TlNO_3$	0.52	73	$AgSO_4^-$	0.05	74
$TlCl$	0.30	73	$TlSO_4^-$	0.05	74
$CdNO_3^+$	0.39	74	$MgSO_4$	0.008	76
$CdCl^+$	0.010	74	$CaSO_4$	0.005	75
$PbNO_3^+$	0.065	74	$CuSO_4$	0.005	76
$PbCl^+$	0.030	74	$ZnSO_4$	0.005	76
$CaNO_3^+$	0.52	74	$CdSO_4$	0.005	76
$SrNO_3^+$	0.15	74			
$BaNO_3^+$	0.12	74			

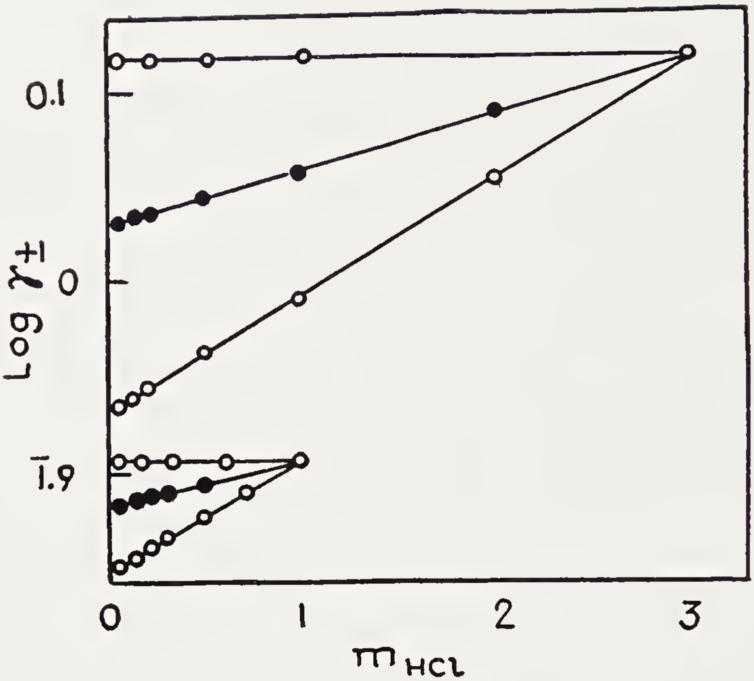

Fig. 2. Linear variation of log γ of hydrochloric acid in 1-1 chloride solutions at constant total molality. The three upper plots at 3M, the three lower plots at 1M. The upper curve of each series of three refers to lithium chloride; the center dots to chloride, and the lower to potassium chloride. (Reproduced from Ref. 136)

In studies of reaction kinetics in which the concentrations of ionic substances are varied over a wide range, it has often been the practice to maintain the ionic strength constant with some "inert" salt. It is of interest to look into the question of how much variation is shown by the activity coefficient of an electrolyte in a medium of constant ionic strength but varying composition[138]. The mean activity coefficient of hydrochloric acid in hydrochloric acid-alkali metal chloride solutions of constant ionic strength is shown in Figure 2. While the activity coefficient of hydrochloric acid is relatively constant in hydrochloric acid-lithium chloride solutions, it is far from constant in hydrochloric acid-potassium chloride solutions. Both the experimental data now available and the equation presented by Glueckauf[101], as an extension of Guggenheim's earlier equation[110], lead to the conclusion that the activity coefficient of AX, in a solution of AX and MX of constant ionic strength, is more nearly constant with changing composition the more nearly the activity coefficient of MX in solutions of MX approaches the activity coefficient of AX in solutions of AX of the same ionic strength. The parallel nature of the curves, in Figure 2, for a given added electrolyte but different values of the total ionic strength is of practical importance. Since the lines are parallel, the relative change of the activity coefficient of an electrolyte in media of constant ionic strength depends upon the change of the concentration of that electrolyte and not upon the total ionic strength. Therefore, it serves no useful purpose to use an ionic strength in excess of the maximum value furnished by the reactants at their highest concentrations other than to demonstrate the kinetic salt effect.

Even the use of potassium chloride to maintain a constant ionic strength in a solution of varying hydrochloric acid concentration serves to keep the activity coefficient of the hydrochloric acid approximately constant if the concentration of hydrochloric acid changes by no more than 0.1 molar. A change in the concentration of 0.1 molar results in a change of the mean activity coefficient of only 1.4 per cent. On the other hand, the change in the mean activity coefficient of hydrochloric acid in going from 0 molar to 0.1 molar in a solution containing no added salts is 20 per cent.

The necessity of assigning dissociation constants as low as those presented in Table 1 to electrolytes which involve two ions of multiple charge indicates that the activity coefficient of an electrolyte involving a polyvalent ion is influenced abnormally by polyvalent ions of the opposite charge sign. This is brought out clearly in Figure 3, which shows that data obtained by LaMer and Mason for the solubility of the 1–3 salt, $[Co(NH_3)_6][Co(NH_3)_2(NO_2)_2C_2O_4]_3$, in various salt solutions at 25°C[179].

A significant advance in the field of dilute solutions of polyvalent electrolytes has been made by Scatchard[263], who uses Mayer's[218] theory of ionic

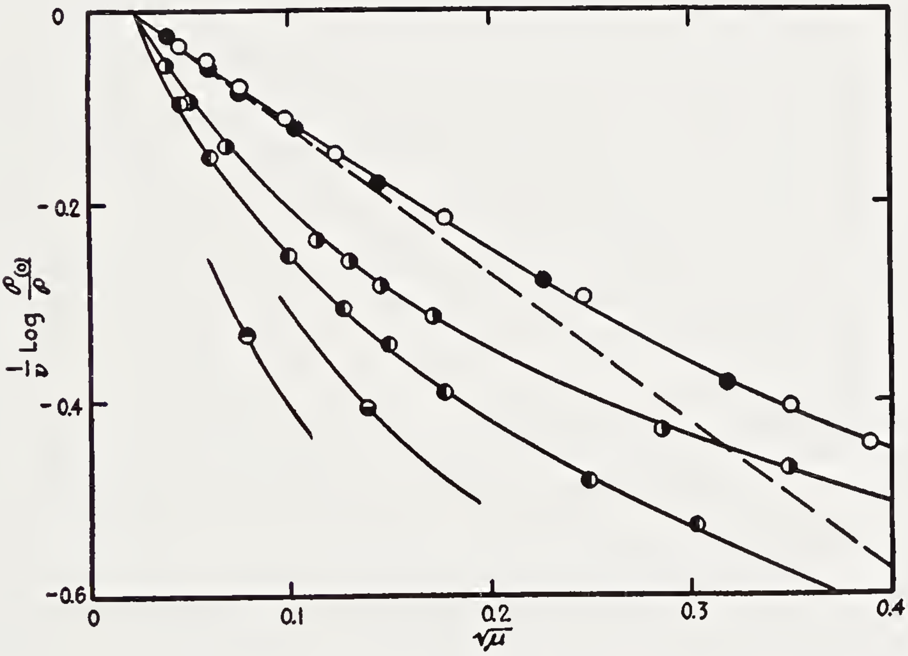

FIG. 3. The influence of various salts upon the solubility of $[Co(NH_3)_6]Co(NH_3)_2(NO_2)_2C_2O_4]_3$ in water at 25°C. ● = KNO_3 ; ○ = $BaCl_2$; ◐ = K_2SO_4 ; ◑ = $MgSO_4$; ◒ = $K_3Fe(CN)_6$; ◓ = $K_4Fe(CN)_6$. The broken line represents the limiting law. (Reproduced from Ref. 136)

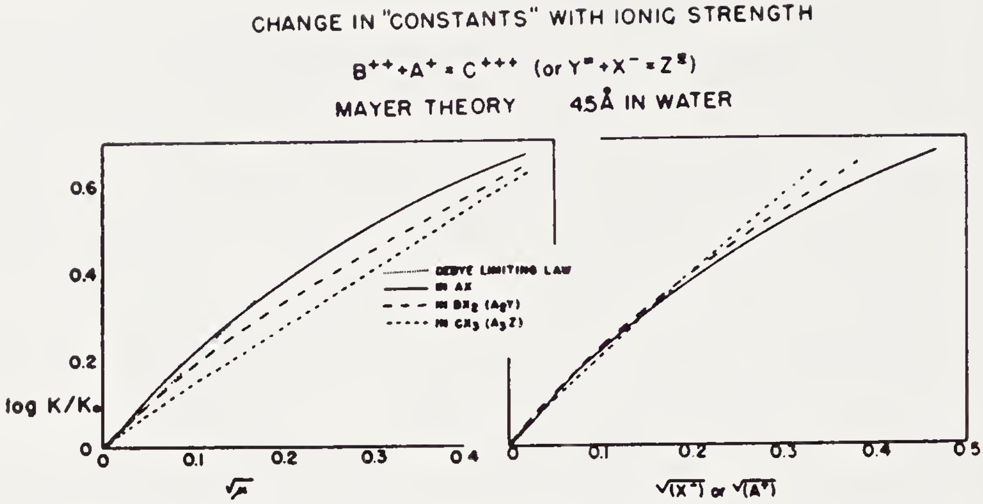

FIG. 4. The dependence of the "constant" (rate or equilibrium) for the reaction $B^{++} + A^{+} = C^{+++}$ (or $Y^{=} + X^{-} = Z^{\equiv}$) upon the composition of the solution. (Reproduced from Ref. 263 with the permission of the National Bureau of Standards)

solutions in the calculation of the value of log k/k_0 for a reaction $B^{++} + A^{+} = C^{+++}$ (or $Y^{=} + X^{-} = Z^{\equiv}$) as a function of the concentration and valence type of the salt which contributes the ionic environment. The quantity k/k_0 is equal to $y_{B^{++}}y_{A^{+}}/y_{C^{+++}}$; the calculations apply to both the rate constant and the equilibrium constant for a reaction of species of these charge types. A parameter, the distance of closest approach, occurs in the equations; the value of log k/k_0 is particularly sensitive to the magnitude of this parameter if multivalent ions of the charge opposite the charge on the reactants are present. The calculated curves using 4.5Å as the value of this parameter are presented as Figures 4 and 5. On the basis of these calculations, it appears that the value of the quantity $y_{B^{++}}y_{A^{+}}/y_{C^{+++}}$ in solutions containing salts with univalent anions is determined primarily by the concentration of the anions and not by the ionic strength. It is also to be concluded that multivalent ions of the charge opposite that of the reactants have an enormous effect upon the activity coefficient factor. As was mentioned, this effect is very sensitive to the value chosen for the distance of approach. A value of 7Å for the case of a 3-1 salt causes the curve to fall to that for the 2-1 salt in Figure 5. It is of interest to note that this theory leads to the expectation that the rate constant for a reaction $B^{++} + A^{+} = C^{+++}$ would decrease with increasing concentration of A_3Z at ionic strength values greater than ~0.01. This emphasizes the necessity of extending measurement of rate "constants" or equilibrium "constants" to very low values of the ionic strength if a reliable extrapolation to zero ionic strength is to be made.

The qualitative features of the theoretical curve of log k/k_0 vs. $\sqrt{\mu}$ for

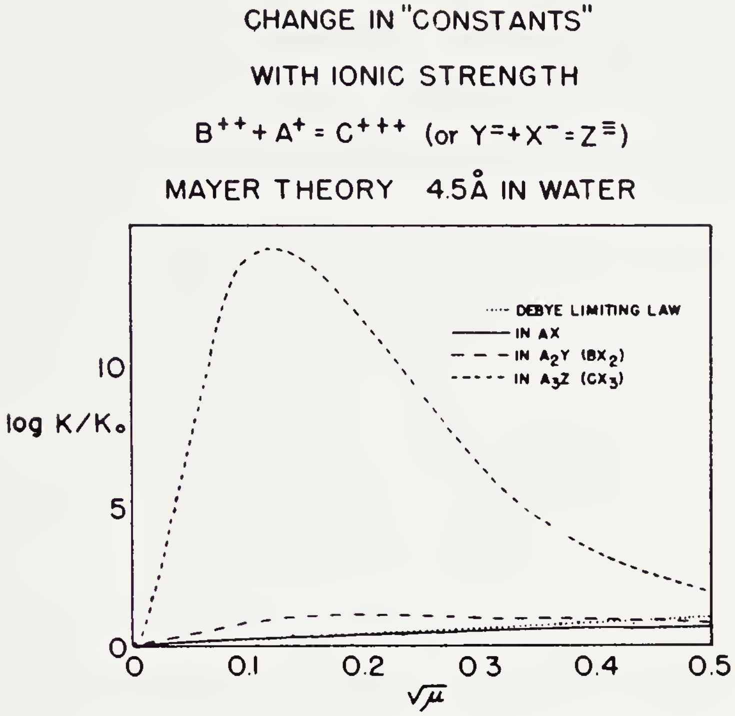

FIG. 5. The dependence of the "constant" (rate or equilibrium) for the reaction $B^{++} + A^{+} = C^{+++}$ (or $Y^{=} + X^{-} = Z^{\equiv}$) upon the composition of the solution. (Reproduced from Ref. 263 with the permission of the National Bureau of Standards)

the reaction $B^{++} + A^{+} = C^{+++}$ in the presence of trivalent anions are consistent with a scheme involving ion-pair complexes of $Z^{\equiv}$ and the three species B^{++}, A^{+} and C^{+++} (if the k is a rate "constant," C^{+++} is the activated complex). In order to rationalize the shape of the theoretical curve, it is merely necessary that the rate by way of the activated complex CZ is much greater than the rate by the way of C^{+++}, and that at a high enough concentration of $Z^{\equiv}$, the species BZ^{-} and $AZ^{=}$ are the predominant forms of B^{II} and A^{I}. The qualitative description of salt effects upon rates or equilibria involving polyvalent ions in terms of ion-pair formation is convenient. The quantitative treatment in terms of ion-pair complex formation is relatively straightforward, particularly if data on the complexes involving the reactants have been obtained in studies which are independent of the kinetic studies. Nevertheless, the activity coefficients of the several species must be taken into account in such a treatment. Generally, it appears more reasonable, therefore, to describe the kinetic salt effect completely in terms of the activity coefficient factor when dealing with slightly weak electrolytes.

The Activity Coefficients of Nonelectrolytes in Aqueous Salt Solutions. A considerable number of experimental studies have been carried out in which the salt effect upon the rate of a reaction of an ion and a neutral molecule has been investigated. The activity coefficient factor of the rate equation for such a reaction, $y_{A^+}y_B/y_{X^+}$, involves the activity coefficient of a nonelectrolyte in the salt solution. It seems worthwhile, therefore, to discuss briefly the activity coefficients of nonelectrolytes in salt solutions. Discussions of this subject have been presented by Randall and Failey[253], Harned and Owen[142], and Long and McDevit[203]. It is not the purpose here to consider at length detailed theories which have been developed but rather to make brief note of the experimental values of the activity coefficients of various non-electrolytes in aqueous salt solution. (This solvent has been the most investigated and is of the greatest interest to us in connection with existing kinetic studies.) At constant temperature and at low concentrations of salt and nonelectrolyte, the activity coefficient of the nonelectrolyte, y_n, can be expressed as a function of the molar concentrations of the nonelectrolyte, C_n, and the normal concentration of salt, C_s, by the equation

$$\log y_n = B_sC_s + k_nC_n \tag{10}$$

where B_s and k_n are constants which depend upon the nature of the nonelectrolyte and the salt. The molarity (moles/liter) concentration scale is widely used in kinetic studies, and plots of log y_n versus C_s are usually linear to higher salt concentrations than are those of the logarithm of the molal activity coefficient versus salt molality[203]. For these reasons, the data in this section will be presented as plots of logarithm y_n versus C_s, and the B_s values which are tabulated are those defined by the equation using molarity or normality concentration units. Although our interest at this point is primarily focused on B_s, it is to be noted that the activity coefficient of the nonelectrolyte may also be a function of the concentration of the nonelectrolyte (i.e., the nonelectrolyte may not obey Henry's law).

Values of B_s for the nonpolar species: hydrogen, oxygen and benzene all show the approximate trend $B_{\mathrm{NaOH}} \cong B_{\mathrm{KOH}} \cong B_{\mathrm{Na_2SO_4}} \cong B_{\mathrm{K_2SO_4}} > B_{\mathrm{NaCl}} > B_{\mathrm{KCl}} > B_{\mathrm{NaBr}} > B_{\mathrm{LiCl}} > B_{\mathrm{KNO_3}} > B_{\mathrm{CsCl}} > B_{\mathrm{HCl}} > B_{\mathrm{HNO_3}} > B_{\mathrm{HClO_4}} > B_{\mathrm{Me_4NBr}}$.* Long and McDevit point out that the similarity of the order of the B values for the several salts in the case of each of these three nonelectrolytes is strong evidence that the interaction of the electrolyte and water plays an important role in determining the value of B_s[203]. Although the B_s values show this similarity in trend, the actual magnitude of the values depends upon which nonelectrolyte we are considering. This is shown in Table 2. Consideration of the magnitude of the several B values leads to the conclusion that the effect of a salt is the sum of the effects of the constituent ions.

If the nonelectrolyte under consideration is a polar substance, it is, in general, salted into an aqueous phase to a greater extent (or salted out to a

---

* Most but not all of these salts have been studied for each of the three nonelectrolytes.

TABLE 2. LIMITING VALUES OF B_s FOR SEVERAL NONPOLAR NONELECTROLYTES*

Salt	Nonelectrolyte		
	Hydrogen	Oxygen	Benzene
NaOH	0.140	0.179	0.255
KOH	0.130	0.175	
Na_2SO_4†	0.139		0.274
K_2SO_4†		0.172	
NaCl	0.114	0.141	0.195
KCl	0.102	0.132	0.166
NaBr		0.110	0.155
LiCl	0.076	0.100	0.141
KNO_3	0.070	0.100	
CsCl			0.088
HCl	0.030	0.031	0.048
HNO_3	0.022	0.019	
$HClO_4$			−0.041
Me_4NBr			−0.24

* These data are taken from Figures 1, 2 and 3 of the review paper by F. A. Long and W. F. McDevit[203].

† Note that the concentration of these salts is expressed in equivalents per liter in the equation defining B_s.

lesser extent) than is an otherwise similar nonelectrolyte which is nonpolar. (Another way of stating this is to say that the values of B_s are, in general, more negative for polar nonelectrolytes.) The trend in the order of the values of B_s for the polar nonelectrolytes is very similar to that already discussed in connection with the nonpolar nonelectrolytes. Some important exceptions, the effects of salts containing small ions on the activity coefficients of acidic and basic nonelectrolytes, have been discussed by Long and McDevit. These effects seem to be quite consistent with the localized hydrolysis theory presented by Harned and Owen in connection with their discussion of activity coefficients of strong electrolytes[141]. Considering lithium ion and sulfate ion as examples of ions for which this localized hydrolysis is important, the following statements can be made:* (1) The values of B_s for lithium salts are more positive for acidic nonelectrolytes and more negative for basic nonelectrolytes than expected from the trends observed for nonpolar nonelectrolytes. (2) The values of B_s for metal sulfates are more negative for acidic nonelectrolytes and more positive for basic nonelectrolytes than expected from the trends observed for nonpolar nonelectrolytes. The rationalization of these observations is straightforward; a

---

* It is to be noted that the trend of the values of the activity coefficients of lithium and sodium sulfate is the same as for the chlorides, bromides and iodides. This probably indicates that localized hydrolysis is not dominant in establishing the order of the activity coefficients.

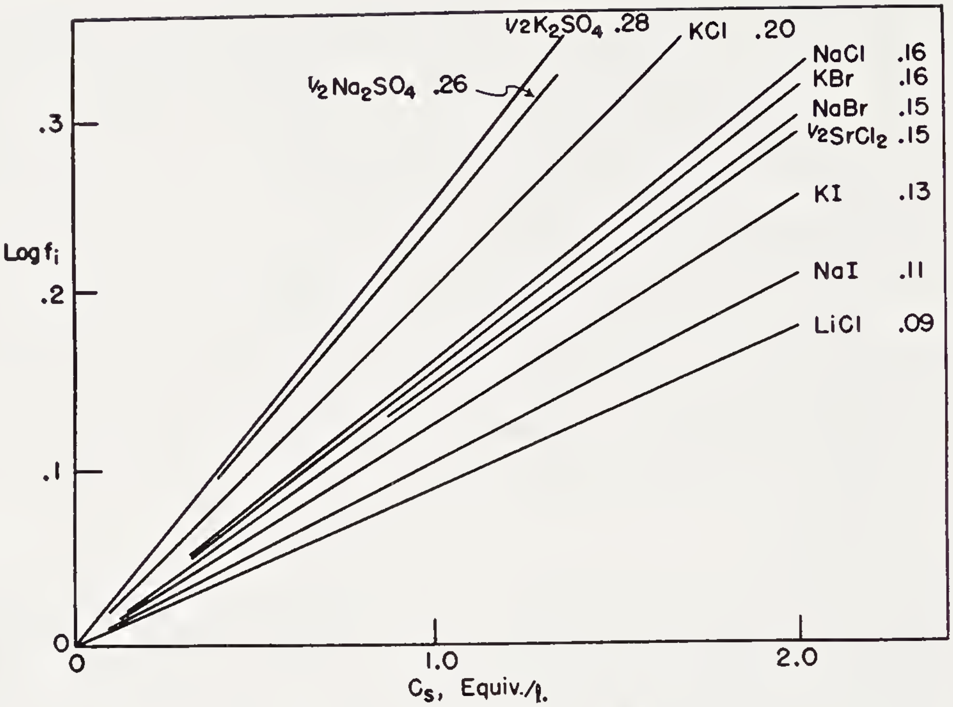

FIG. 6. The activity coefficient of trimethylamine in aqueous salt solution as a function of the salt concentration. The numbers are the B values (equation 10) for the various electrolytes. (Reproduced from Ref. 203 with the permission of the Editor of *Chemical Reviews*)

hydrogen of a water molecule coordinated to the small lithium ion is more positive in character than is the hydrogen atom on the average water molecule. Basic substances are attracted to these hydrated cations while acidic substances are repelled. The opposite sort of reasoning applies to solutions containing anions which strongly attract water molecules; such water molecules are oriented with the oxygen end out, and this oxygen is more negative than the oxygen of an average water molecule. The contrasting trends in the values of B_s for acidic and basic nonelectrolytes are shown in Figures 6 and 7 in which data for trimethylamine and benzoic acid are presented. In Figure 7, the salting-in effect of salts with large ions is clearly shown; this is also observed for such salts in cases where the nonelectrolyte is nonpolar.

The magnitude of the salt effect is also very dependent upon the effect which the nonelectrolyte has upon the dielectric constant of the aqueous medium. This is shown by the data of Gross[105, 106] on the salt effect on the activity coefficients of acetone and hydrocyanic acid in aqueous solution. Acetone decreases the dielectric constant of an aqueous solution while hydrocyanic acid increases it. The contrasting effect of salts on the activity coefficients of these two substances is shown in Figure 8. This influence which the effect of the nonelectrolyte upon the dielectric constant of the

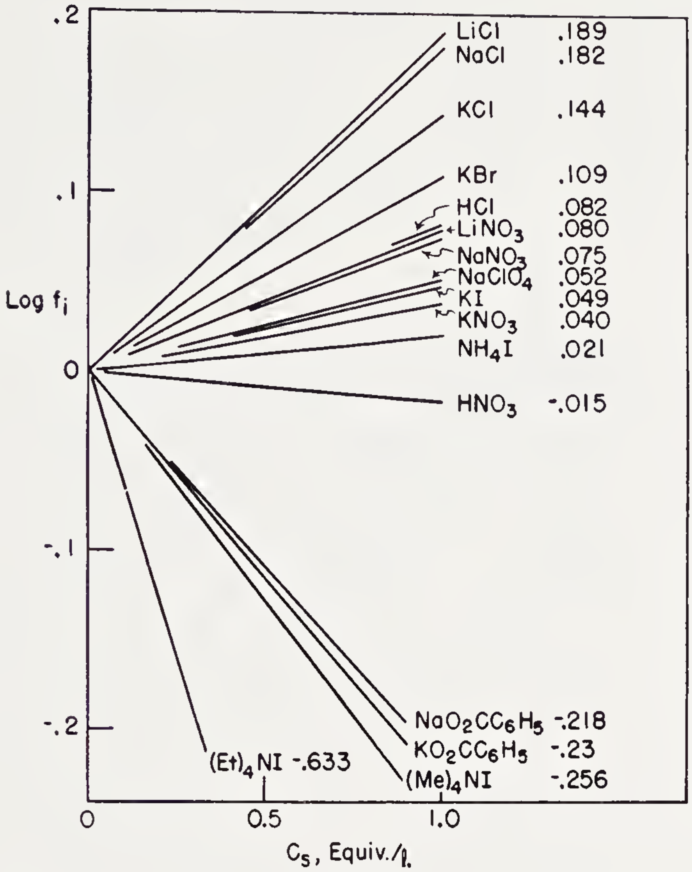

Fig. 7. The activity coefficient of benzoic acid as a function of electrolyte concentration. The numbers are the B values (equation 10) for the various electrolytes. (Reproduced from Ref. 203 with the permission of the Editor of *Chemical Reviews*)

solution has upon the value of B_s is predicted by the theories of Debye and McAulay[80], and Debye[81].

The activity coefficients of nonelectrolytes vary over wide limits in aqueous salt solutions. Considering only uni-univalent electrolytes, the values of B_s range between 0.256 for the effect of sodium hydroxide on the activity coefficient of benzene[257] and -0.633 for the effect of tetraethylammonium iodide on the activity coefficient of benzoic acid[39]. In a 0.5 normal salt solution these values of B_s lead to values of y_n of 1.34 and 0.48, respectively. Thus, the presence of salts in solution may influence the activity coefficients of nonelectrolytes markedly. The extent to which this factor influences the kinetic salt effect in a reaction involving nonelectrolytes will be discussed.

The Kinetic Salt Effect Upon Ionic Reactions

Ion-Ion Reactions. The actual determination of the rate law for an ionic reaction is complicated by the existence of the inert salt effect. Thus, an increase from 0.05 to 0.10 molar in the initial concentration of a strong

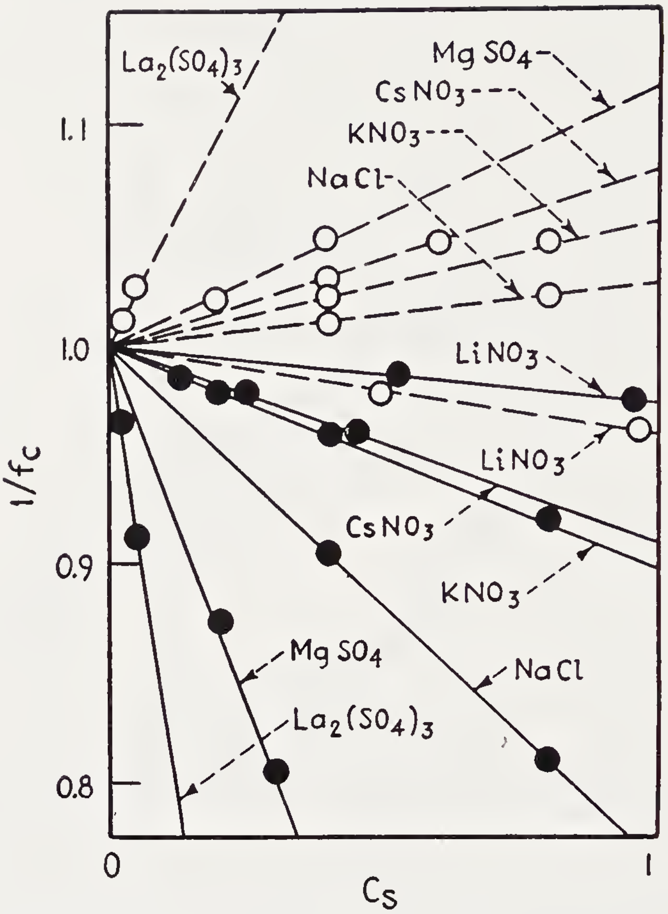

FIG. 8. The contrasting effect of salts upon the activity coefficient of hydrocyanic acid and acetone. ● acetone; ○ hydrocyanic acid. (Reproduced from Ref. 136)

electrolyte AB, which undergoes a reaction that is first order in A^+ and first order in B^-, increases the initial rate by a factor of 3.55 instead of 4.00.* While this effect is not large enough to lead to an erroneous conclusion regarding the form of the rate law, it is an effect which must be recognized. In the course of a single run, the ionic strength of the reaction mixture changes if the ionic charges of the products differ from those of the reactants. The treatment of data obtained in the study of a reaction in a changing environment has been discussed by Scatchard[259]. In some studies designed to establish the form of the rate equation, the ionic strength of the reaction medium is maintained constant with an inert salt, the concentration of which is varied as the concentrations of the reactants are varied. As already mentioned, maintenance of constant ionic strength

---

* This calculation is based upon the assumption that the activity coefficient of the electrolyte AB is equal to that of potassium chloride, and the activity coefficient of the neutral activated complex is unity.

does not insure constancy of the activity coefficients of the various solutes present in the solution.

The purpose of this section is the presentation of a comparison of experimentally observed kinetic salt effects with the predictions of the Bronsted equation. It is desirable, however, to consider an additional point before proceeding. It has been pointed out that a number of mechanisms may often be proposed which are consistent with a given rate law. For ionic reactions, these several mechanisms may differ in the charges on the ions which are suggested as coming together in the rate-determining step. The several mechanisms differ because different equilibria are postulated as preceding the rate-determining step. All lead, however, to an activated complex of the same stoichiometric composition. The question which is raised at this time is this: Will a study of the salt effect upon the reaction velocity tell us anything regarding which of these several mechanisms is correct? The empirical rate equation expresses the rate as a function of the concentrations of the reactants in the forms which predominate in the reaction medium. The corresponding apparent rate constant is then a product of the rate constant for the postulated rate-determining step and the one or more equilibrium constants for the equilibria which precede it. The over-all activity coefficient factor has a form determined by the composition of the activated complex (which, of course, establishes its charge) and the formulae of the predominant forms of the reactants. The over-all activity coefficient factor does not depend upon which of the several mechanisms, all consistent with the rate law, is correct; the activity coefficient factor is determined by the rate law, not by the mechanism. This is really a direct consequence of the activated complex being in equilibrium with the predominant forms of the reactants. The salt effect upon a reaction velocity is the salt effect upon this equilibrium, and it is in no way influenced by the existence, at very low concentrations, of other species which are also in equilibrium with the reactants, and from which, it is postulated, the activated complex forms. Although some confusion regarding this point has existed in various papers, the subject is correctly and clearly discussed by Weil and Morris[299a].

The salt effect upon the velocity of a number of ionic reactions is presented in Figure 9. This figure was first presented by Livingston[199] and has been widely published to show the general validity of the Bronsted-Debye and Huckel equation.

We have already seen, however, that the Debye-Huckel limiting law is valid only at low electrolyte concentrations, and further, that many electrolytes commonly considered to be strong have conductances or activity coefficients which are anomalous enough to warrant the assignment of finite concentration ionization constants to these salts. It is not too

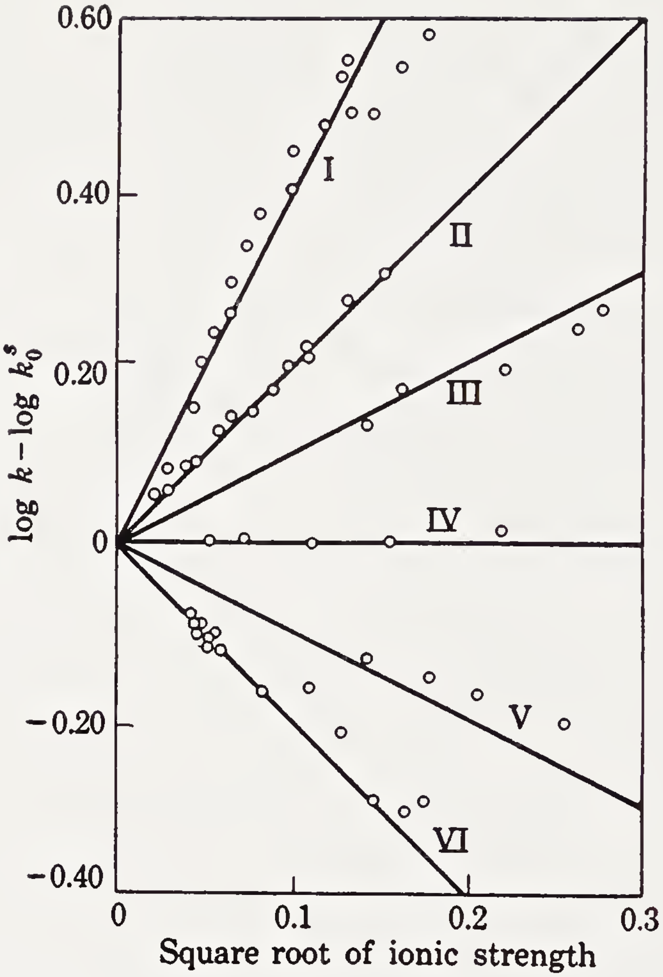

FIG. 9. The Livingston diagram; the kinetic salt effect upon the reactions:

I. $Co(NH_3)_5Br^{++} + Hg^{++} = (Co(NH_3)_5BrHg^{++++}) \rightarrow$

II. $S_2O_8^{=} + I^- = (S_2O_8I^{\equiv}) \rightarrow$

III. $O_2NNCO_2C_2H_5^- + I^- = (O_2NNCO_2C_2H_5I^{=}) \rightarrow$

IV. $CH_3CO_2C_2H_5 + OH^- = (CH_3CO_2C_2H_5OH^-) \rightarrow$

V. $H_2O_2 + H^+ + Br^- = (H_3O_2Br) \rightarrow$

VI. $Co(NH_3)_5Br^{++} + OH^- = (Co(NH_3)_5BrOH^+) \rightarrow$

(Reproduced from Ref. 180a with the permission of the Editor of *Chemical Reviews*)

surprising, then, to find anomalies in the kinetic salt effects for some reactions.

It appears that the rate of a reaction between two ions of like charge sign is determined primarily by the concentration and character of the ions of the opposite charge sign. This is shown by the data of Table 3. The rates of the reactions in the presence of salts of different valence types are very nearly equal in solutions of the same salt normality and containing the same ion of the charge type opposite that of the reactants. With the

TABLE 3. KINETIC SALT EFFECT IN REACTIONS OF IONS OF LIKE CHARGE SIGN

(A)[169] $BrCH_2CO_2^- + S_2O_3^= = (S_2O_3CH_2BrCO_2^{\equiv}) \rightarrow$
Reactants concentration: 0.00125M each
Temperature: 25°C

(Na^+) moles/l	k (in $NaNO_3$ soln.)	k (in Na_2SO_4 soln.)
0.01	0.412	0.432
0.05	0.580	0.577
0.10	0.678	0.682
0.25	0.875	0.886
0.50	1.05	1.10

(B)[240] $BrCH_2CO_2^- + S_2O_3^= = (S_2O_3CH_2BrCO_2^{\equiv}) \rightarrow$
Reactant concentration: 0.00100M each
Salt concentration: 0.020N
Temperature: 25°C

Salt	k	Ionic Strength
KNO_3	0.472	0.0240
K_2SO_4	0.472	0.0340
$K_3Co(CN)_6$	0.462	0.0440

(C)[240] $Co(NH_3)_5Br^{++} + Hg^{++} = (Co(NH_3)_5BrHg^{++++}) \rightarrow$
Concentrations: Cobalt amine 5.0×10^{-6} molar
$Hg(ClO_4)_2$ 2.5×10^{-4} molar
$HClO_4$ 1.0×10^{-3} molar
Temperature: 15.0°C

(ClO_4^-) moles/l	k (in $NaClO_4$ soln.)	k (in $La(ClO_4)_3$ soln.)
8.56×10^{-3}	145.0	146.7
13.20×10^{-3}	162.2	164.2
25.06×10^{-3}	200.4	200.4

salts chosen as they were, these solutions of the same salt normality have the same concentration of the ion of charge opposite to the charge on the reacting ions; such solutions have different values of the ionic strength. These data would be considered highly anomalous if the only theoretical guide to their interpretation were the Bronsted equation coupled with the Debye-Huckel limiting law. The fact that the charges on the activated complexes in the two reactions are −3 and +4 should be warning enough that agreement between the limiting law and experimental values cannot be expected. The recent work of Scatchard[263], which has already been mentioned, indicates that this behavior is not anomalous but is to be expected. It is seen in Figure 4 that the several curves for log k/k_0 in the pres-

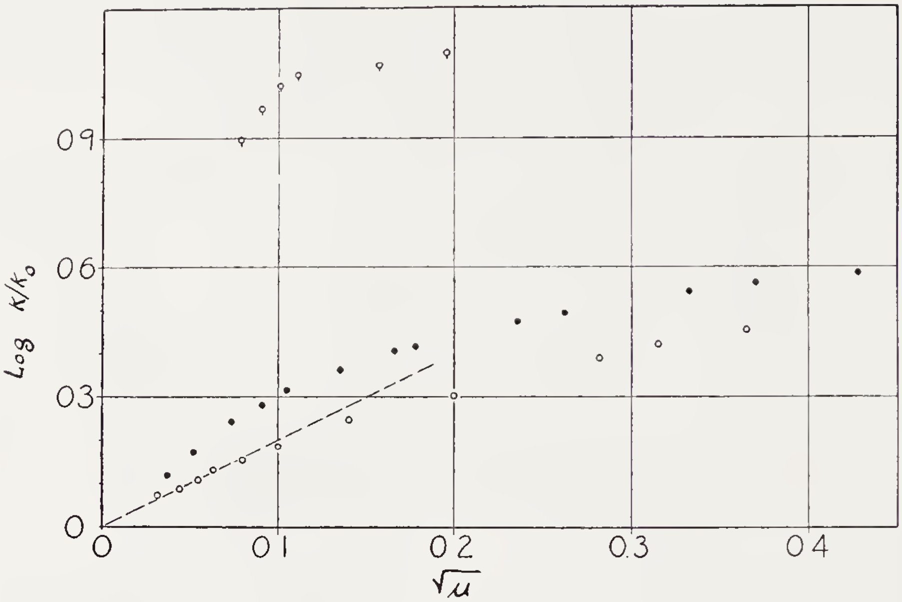

Fig. 10. The kinetic salt effect upon the reaction: $BrAcO^- + S_2O_3^= = S_2O_3AcO^= + Br^-$. ○ = reactants, present as potassium salts; ● reactants present as calcium salts; ♀ = ionic strength due largely to lanthanum chloride[180].

ence of different inert salts of varying charge type fall close to one another when plotted as a function of the concentration of the ion of charge type which is opposite that of the reactants.

Multivalent ions of the charge type opposite that of the reactants have an abnormal effect upon reactions of ions of like charge. The effects of potassium ion, calcium ion, and lanthanum ion upon the rate of the reaction of bromacetate and thiosulfate ions have been studied by LaMer and Fessenden[180]. The results are presented in Figure 10. It is seen that the dependence of the reaction rate upon ionic strength is consistent with the Bronsted-Debye and Huckel equation if the only cation in the solution is potassium ion (sodium ion behaves similarly); if calcium ion or lanthanum ion is present, however, the rate is much greater at any given ionic strength. This may be interpreted in a qualitative way as indicating an abnormally greater collision frequency of ions of like charge in a solution containing multivalent ions of the opposite charge sign. The results may also be attributed to a tendency for the reaction to proceed by the way of an activated complex which involves the multivalent cation[183, 261]. Quantitative calculations which proceed from this assumption necessitate knowledge of the extent to which the multivalent cations and the anionic reactants are associated into ion-pairs. The association constants for calcium ion and barium ion with thiosulfate and bromacetate ions have been determined by Davies and Wyatt[77]. Using these data, Wyatt and Davies have shown that the salt effect upon the rate of the reaction of bromacetate ion and thiosulfate ion in the presence of calcium ions and barium ions is consistent with the reaction proceeding by the way of two activated complexes, one of charge −3 and the other of charge −1 (i.e., one containing no alkaline earth metal ion and the other containing one alkaline earth metal ion)[78]. Presumably the large effect of lanthanum ion would be attributed to the introduction of the reaction path with the activated complex (LaS_2O_3BrAcO). The small variation of the rate constant with the concentration of lanthanum ion in the range 0.0014 − 0.0034 moles per liter is consistent with the sum of the average number of lanthanum ions associated with thiosulfate and bromacetate ions being one if the activated complex also involves one lanthanum ion.

The calculations of Scatchard[263], using the electrolyte theory developed by Mayer[218], indicate that a multivalent ion of charge opposite that of the reactants will exert a large influence upon the rate of such an ionic reaction. In this calculation, there is no specific suggestion that lanthanum ion is associated in the activated complex. Thus, there are two points of view: (1) the "anomalous" salt effect is due to the participation of a multivalent ion in an important activated complex, and (2) the effect is not "anomalous"; the effect is just what one would expect on the basis of the more refined theoretical treatment of electrolytic solutions.

Although both the Debye-Huckel theory and the Mayer theory of electrolytic solutions assume spherical ions, many reactions which are of interest involve nonspherical ions, if not as reactants, then certainly as the activated complex. It is of interest to note that some reactions involving nonspherical ions have kinetic salt effects very close to the values predicted by the use of the Bronsted-Debye and Huckel equation. Nielsen has studied the rate of the reactions[231]

$$C_2H_5OOCCO_2^- + OH^- = C_2H_5OH + C_2O_2^=$$

$$C_2H_5OOCCH_2CO_2^- + OH^- = C_2H_5OH + CH_2(CO_2)_2^=$$

$$C_2H_5OOC(CH_2)_2CO_2^- + OH^- = C_2H_5OH + C_2H_4(CO_2)_2^=$$

$$C_2H_5OOC(CH_2)_4CO_2^- + OH^- = C_2H_5OH + C_4H_8(CO_2)_2^=$$

as a function of the ionic strength. The data are presented in Figure 11. Since the solid lines shown in this figure have slopes 77 per cent, 70 per cent, 66 per cent, and 64 per cent of the values expected on the basis of the Bronsted-Debye and Huckel equation, one would conclude that the equation does not break down altogether when applied to reactions of nonspherical ions.

When account is taken of the abnormalities in activity coefficients which are expected in solutions containing multivalent ions, it appears that the kinetic salt effect which is observed for most ionic reactions is consistent

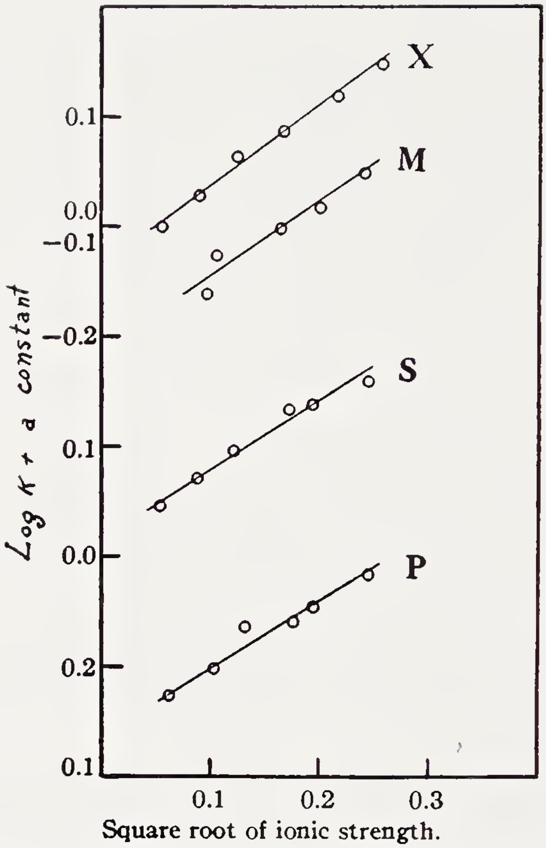

FIG. 11. The kinetic salt effect for the hydrolysis of the ester ions:

X = monoethyloxalate ion
M = monoethylmalonate ion
S = monoethylsuccinate ion
P = monoethyladipate ion

(Reproduced from Ref. 231 with permission of the Editor of the *Journal of the American Chemical Society*)

with the Bronsted equation. There do exist, however, some data on reaction rates in media of high ionic strength which are, at first sight, surprising. The salt effect upon the rate constant k_2 of the rate law for the reaction of hydrogen peroxide and iodide ion,

$$\frac{d(I_2)}{dt} = k_1(H_2O_2)(I^-) + k_2(H_2O_2)(H^+)(I^-)$$

is negligible from an ionic strength of 0.15 to 3.6 (furnished by sodium or barium perchlorate)[196]. At ionic strength values below approximately 0.15, however, the value of k_2 shows the dependence upon ionic strength which would be expected on the basis of the Bronsted equation[318]. The activity coefficient factor for k_2 is $y_{H^+}y_{I^-}y_{H_2O_2}/y_{H_3O_2I}$. Is it reasonable that this should be independent of ionic strength in the range 0.15 to 3.6? The activity coefficient product $y_{H^+}y_{I^-}$ in solutions containing predominantly sodium or barium perchlorate may be calculated using the approach suggested by Glueckauf[101]. The value of $y_{H^+}y_{I^-}$, so calculated, varies from 0.59 in a solution of the composition 0.07 molar hydrogen iodide, 0.23 molar sodium perchlorate to 1.44 in a solution of the composition 0.07 molar hydrogen iodide, 2.93 molar sodium perchlorate. The ratio of these numbers, which is 2.4, would be the ratio of the values of k_2 in these two solutions if $y_{H_2O_2}/y_{H_3O_2I}$ were constant over this range of the concentration. Therefore, if k_2 is to be independent of the electrolyte concentration over this concentration range, the value of $y_{H_2O_2}/y_{H_3O_2I}$ must change by a factor of 2.4. Is a change of this magnitude reasonable? The calculations indicate that the difference between the B values (Eqs. 10 and 11) for the two neutral species, H_2O_2 and the activated complex H_3O_2I, would not be constant over this concentration range. Therefore, the activity coefficient of one or both of these neutral species is not consistent with Eq. (10) if this kinetic salt effect conforms to the Bronsted equation. The activated complex, H_3O_2I, may be rather polar and a lack of conformity of its activity coefficient to equation 10 may be reasonable.

While the unusual nature of the kinetic salt effect upon k_2 in media of high ionic strength may be due to failure of the Bronsted theory[196b], our present knowledge of the activity coefficients of polar nonelectrolytes in concentrated salt solutions is too incomplete to warrant the citing of these data as proof of such a failure. At the present time, it might be better to forego any discussion of the general validity of the Bronsted theory applied to concentrated electrolyte solutions.

The Kinetic Salt Effect on Reactions of an Ion and a Neutral Molecule. Since the activity coefficient of an ion depends upon factors in addition to the charge of the ion, and the activity coefficient of a neutral molecule is influenced in a specific way by the presence of electrolytic solutes, the rate of a reaction of an ion and a neutral molecule has associated with it a kinetic salt effect. In a reaction of this type,

$$A + H^+ = (AH^+) \rightarrow$$

the charge on the activated complex is the same as that on the ionic reactant and therefore the Bronsted equation for such a reaction is

$$k = k^0 y_A y_{H^+}/y_{AH^+}.$$

The conclusion which may be drawn from the discussion of activity coefficients of electrolytes and non-electrolytes (pp. 351–361) is that the primary salt effect on a reaction of an ion and a neutral molecule is given approximately by the equation

$$\log k/k_0 = \sum B_j C_j \tag{11}$$

TABLE 4. SUMMARY OF B VALUES FOR ELECTROLYTE EFFECTS UPON ACID-CATALYZED REACTIONS

$$B = \frac{\log k_{H_3O^+} - \log k^\circ_{H_3O^+}}{C}$$

Reaction	HCl	HClO₄	HNO₃	pC₆H₄CH₃SO₃H
Hydration of isobutene*[163, 206]	0.44	0.47	0.21	0.30
Hydrolysis of ethylal[161]	0.35			
Inversion of sucrose[113]	0.28	0.38	0.30	
Hydrolysis of ethyl acetate[287]	0.078			

* It has been suggested by Taft[281a] that the rate of hydration of isobutene is proportional to the acidity of the solution as measured by the Hammett acidity function, h_0. The problem of distinguishing between the two possibilities, Rate α h_0, and Rate α (H_3O^+) with a significant medium effect, is discussed elsewhere in this chapter.

where $B_j = (B_A + B_{H^+} - B_{AH^+})_j$ and the summation is taken over all of the ions in the solution, both reactant ions and "inert" salt ions. This equation is derived from empirical equations (Eqs. 9 and 10) for the activity coefficients of electrolytes and non-electrolytes in electrolytic solution. (The B quantities are defined by these equations.) This equation is expected to be valid in the concentration range in which these empirical equations are valid. The wide range in the magnitude of the observed salt effects on this type of reaction is illustrated by the data of Table 4. It is seen that the electrolyte effect upon a particular reaction depends upon the nature of the electrolyte, and for a given electrolyte, it differs from one reaction to another. At a concentration of 0.2 molar, the correspondence between a B value and a percentage increase in rate is: $B = 0.50:26$ per cent, $B = 0.35:17$ per cent, $B = 0.20:10$ per cent, $B = 0.05:2$ per cent. Clearly, one cannot assume that a reaction between an ion and a neutral molecule is subject to only an inappreciable salt effect at concentrations of electrolyte of a few tenths molar.

The B values for the hydrolysis of sucrose which are presented in Table 4 were determined in experiments on solutions of a single acid without added salt. Guggenheim and Wiseman[113] present these B values as corresponding to the anion of the acid; it is observed that the medium effect in solutions containing more than one acid or an acid-alkali metal salt mixture conforms to equation 11 with the summation taken over the anions only. The basis for ignoring the nature of the cation is Bronsted's principle of specific interaction of ions[48]. Since the activated complex and the ionic reactant, hydronium ion, are both positively charged, the nature of the cation is not important in determining the medium effect. This ignores, of course, the electrolyte effect upon the activity coefficient of the nonelectrolyte; since acids and the corresponding alkali metal salts influence the activity coefficients of nonelectrolytes to different extents (see Table 2), the approximation of omitting from consideration the nature of the cation cannot be completely correct. Guggenheim finds that the nature of the cation does have an effect if the cation is multivalent. This may be due to the failure of Bronsted's principle of specific interaction of ions, or to the effect of these polyvalent cations on the activity coefficient of the sucrose. The effect of the polyvalent cation is to depress the rate, a trend which is expected if polyvalent cations have a smaller salting-out effect or a greater salting-in effect upon sucrose than do univalent cations.

If measurements are extended to a greater concentration of electrolyte, the specific effect of the electrolyte upon the activity coefficient of the nonelectrolyte becomes so appreciable that large errors would be made in taking the summation in Eq. (11) over only those ions of charge opposite that of the ionic reactant. Such is true in the case of the hydroxide ion catalyzed decomposition of diacetone alcohol, $CH_3COCH_2C(OH)(CH_3)_2 = 2CH_3COCH_3$. The rate of this reaction in $0.1N$ NaOH $-$ $1.9N$ NaX or $0.1N$ KOH $-$ $1.9N$ KX depends very markedly upon the nature of X[3]. In both sets of experiments, the effect of the anions was in the order: nitrate > chloride > bromide > iodide > thiocyanate (the rate being greatest in the presence of the first named anion). It is significant that the activity coefficient of diacetone alcohol in sodium or potassium salt solutions shows this trend: chloride > bromide > iodide > thiocyanate (the activity coefficient being greatest in the presence of the first named anion)[4]. Thus, the fact that the activity coefficient of the nonelectrolyte reactant is influenced in a marked and specific way by electrolytes is reflected by the manner in which electrolytes influence the rate of the reaction of the nonelectrolyte.

The acid catalyzed hydrolysis of diethyl acetal,

$$CH_3CH(OC_2H_5)_2 + H_2O = CH_3CHO + 2C_2H_5OH$$

is subject to rather large kinetic salt effects[54, 159, 239]. Equation (11) does not hold in the case of this reaction; the values of B for a number of salts were determined in experiments in which a single salt furnishes essentially all of the electrolyte. The results are presented in Figure 12. It is seen that the value of B is not independent of the concentration of the electrolyte. Since the activity coefficient of a nonelectrolyte can be evaluated independently, the value of (y_{H^+}/y_{HA^+}) may be obtained from the kinetic data. This has been done by Olson and Tong, who found that the activity coefficient of diethyl acetal in aqueous sodium chloride conforms to equation 10 ($B = 0.260$ at 25°C)[239]. Much of the salt effect upon the rate constant for this reaction can be attributed to the variation in the activity coefficient of the diethyl acetal. The variation of the value of y_{H^+}/y_{HA^+} (which is equal

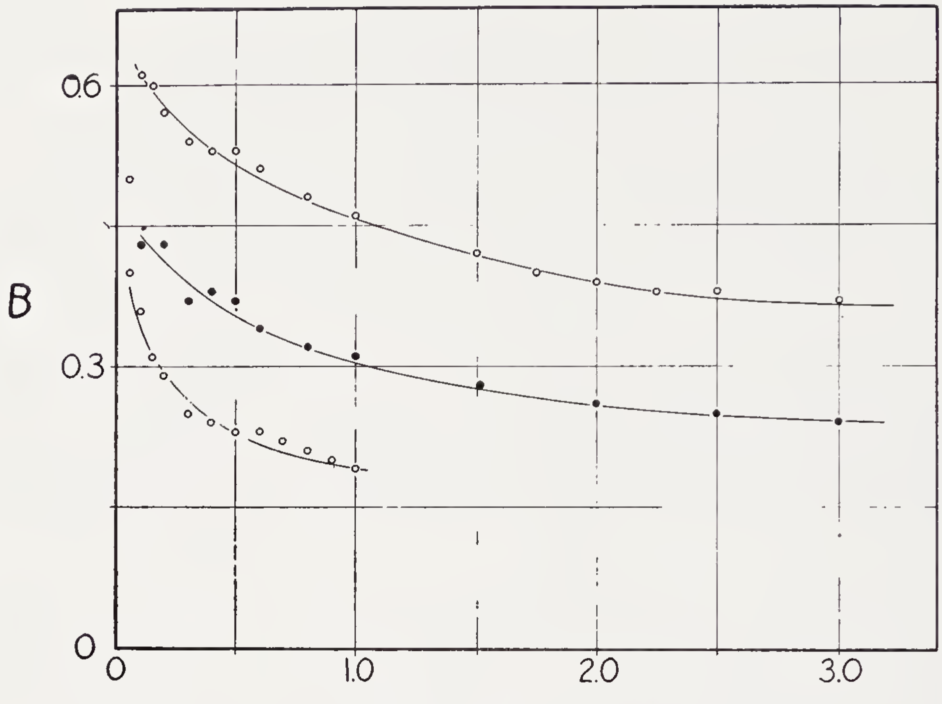

FIG. 12. Values of B (Eq. 11) for the hydrolysis of acetal.
Upper curve—sodium perchlorate
Middle curve—sodium nitrate
Lower curve—sodium p-toluenesulfonate
(Data from compilation in Ref. 159)

to the experimentally determined quantity $k/(k_0y_A))$ with electrolyte concentration was considered to be abnormally large by Olson and Tong[239] who point out that the value of this ratio of the activity coefficients of two univalent cations is larger than the value of the ratio y_{Li^+}/y_{K^+} at the same ionic strength. It has been pointed out that this activity coefficient ratio y_{H^+}/y_{HA^+} is smaller than the activity coefficient ratio y_{H^+}/y_{Cs^+}, and therefore not abnormal[202]. (These comparisons are open to some question, however; the activity coefficients in the ratio y_{H^+}/y_{HA^+} correspond to the same medium, while the ratios y_{Li^+}/y_{K^+} and y_{H^+}/y_{Cs^+} are obtained from values of the mean activity coefficients of the halides of each of these elements in media in which the ionic strength is furnished exclusively by each particular electrolyte.) Although the experimentally determined values of the activity coefficient ratio y_{H^+}/y_{HA^+} for the hydrolysis reactions of acetals and formals are large, they do not appear to be so large as to constitute proof that the Bronsted equation is not valid.

The specific nature of the salt effects upon a reaction of the type being discussed is clearly indicated in the acid-catalyzed hydrolysis of γ-butyro-

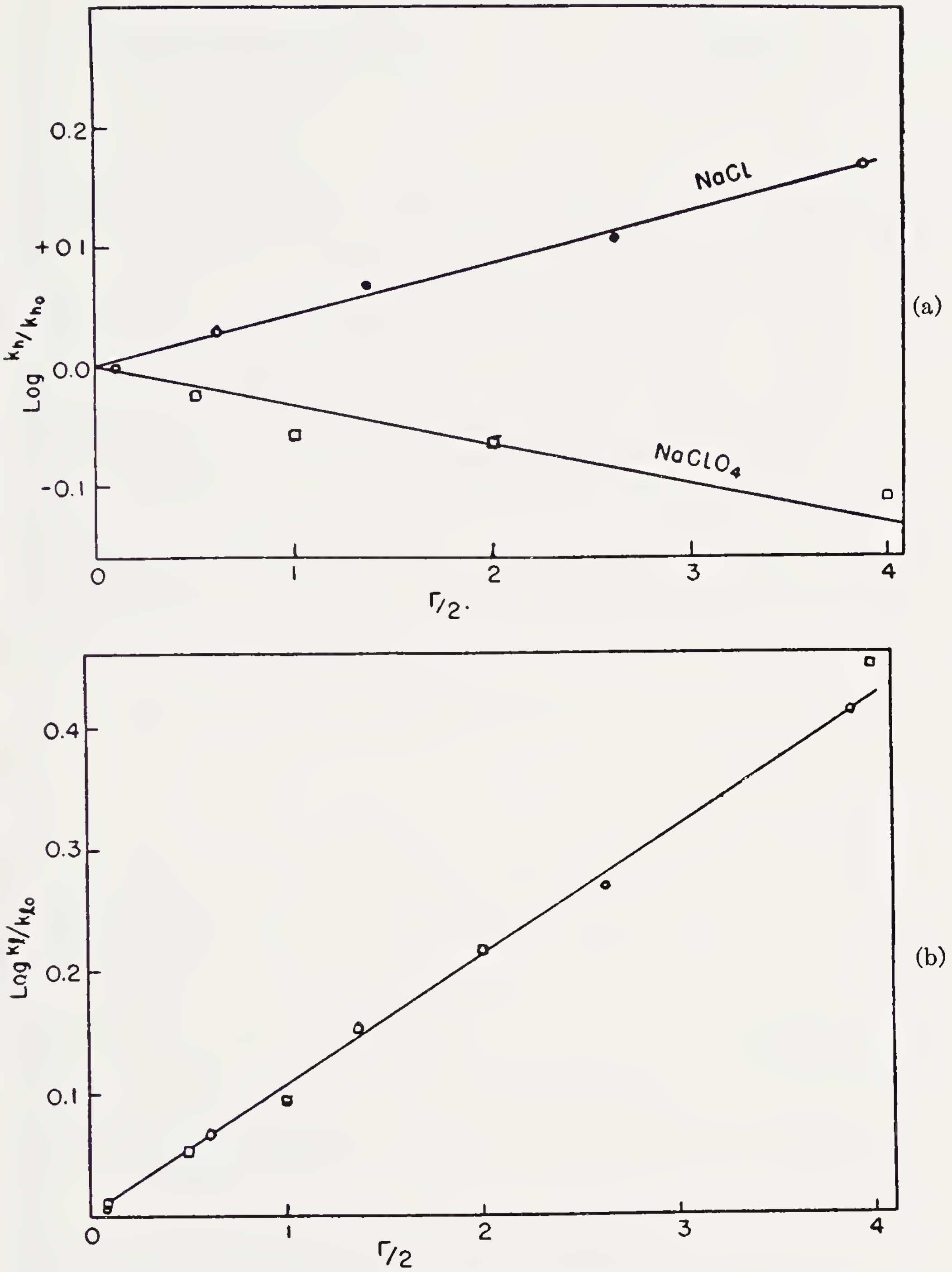

FIG. 13. The kinetic salt effect for (a) the hydrolysis of γ-butyrolactone, (b) the formation of γ-butyrolactone from γ-hydroxybutyric acid; □ = sodium perchlorate, ○ = sodium chloride.
(Reproduced from Ref. 202 with the permission of the Editor of the *Journal of Physical & Colloid Chemistry*)

lactone:

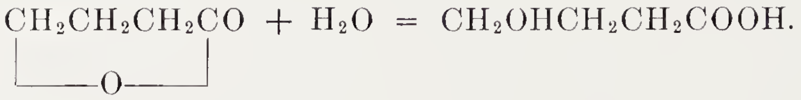

$$\underbrace{CH_2CH_2CH_2CO}_{O} + H_2O = CH_2OHCH_2CH_2COOH.$$

(The activity coefficient of the lactone is known in a number of salt solutions including sodium chloride and sodium perchlorate, the salts which were used in the kinetic runs[201]. A large range in the values of B (equation 10) is found; sodium sulfate and sodium chloride ($B_{NaCl} \cong 0.065$) cause definite salting-out of the lactone while sodium iodide, sodium perchlorate ($B_{NaClO_4} \cong -0.12$) and potassium iodide have a salting-in effect on the lactone.) The values of $\log k/k_0$ for both the forward and reverse reaction are presented in Figure 13. It is seen that sodium chloride and sodium perchlorate influence the rate of the forward reaction in different ways while these two salts have very nearly identical effects upon the rate of the reverse reaction. The value of y_{H^+}/y_{HA^+} is the same for the forward and reverse reactions since the activated complexes for the forward and reverse reactions are identical. The value of y_{H^+}/y_{HA^+} as a function of salt concentration is presented in Figure 14. Since the effect of sodium chloride and sodium perchlorate upon the activity coefficient of hydrogen ion is expected

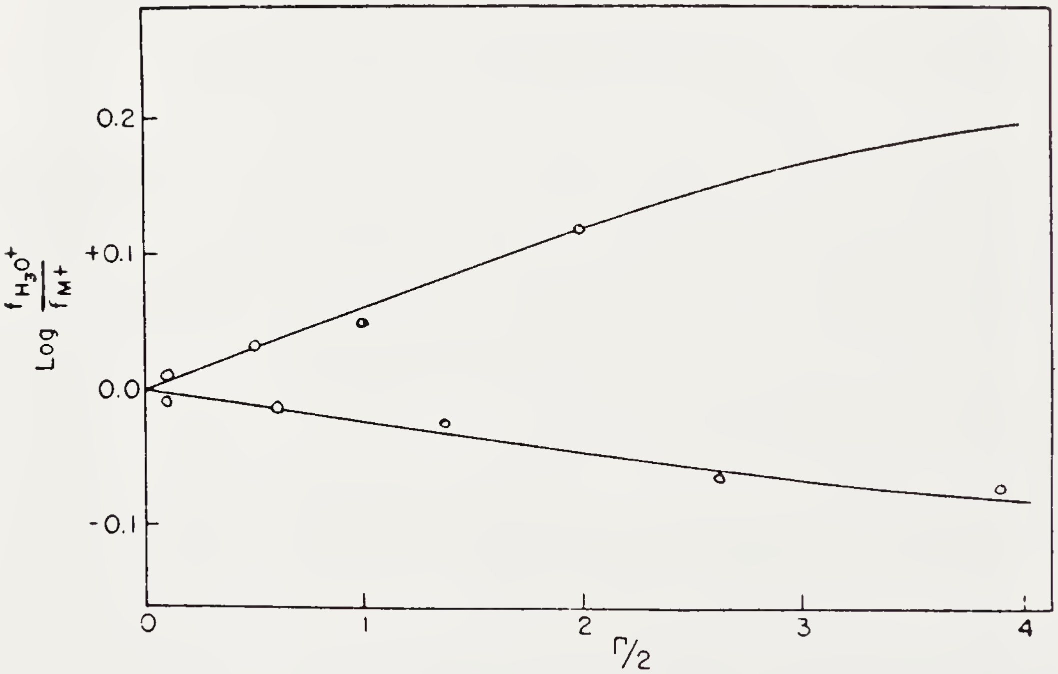

FIG. 14. Calculated values of $y_H{}^+/y_{HA}{}^+$ for the hydrolysis of γ-butyrolactone as a function of ionic strength. Upper curve for sodium perchlorate; lower curve for sodium chloride.
(Reproduced from Ref. 202 with the permission of the editor of the *Journal of Physical & Colloid Chemistry*)

to be very similar, the difference in the trend in y_{H^+}/y_{HA^+} with sodium chloride and sodium perchlorate must be due to the difference in the effect of the two salts upon y_{HA^+}. The value of $(y_{HA^+})_{NaCl}/(y_{HA^+})_{NaClO_4}$ must, therefore, be greater than unity; this is quite reasonable since both $(y_{\text{lactone}})_{NaCl}/(y_{\text{lactone}})_{NaClO_4}$ and $(y_{\text{hydroxy-acid}})_{NaCl}/(y_{\text{hydroxy-acid}})_{NaClO_4}$ are greater than unity[201]. This confirms the reasonable expectation that the activity coefficient of an activated complex made up of an ion and a neutral molecule may depend upon the nature of the inert salt which is present in approximately the same way that the activity coefficient of the reactant neutral molecule depends upon the nature of the inert salt.

Reactions of an ion and a neutral molecule may be subject to large kinetic salt effects. This arises because the activity coefficient of a neutral substance is influenced in a marked and specific way by the presence of an inert salt. However, the activity coefficient of the activated complex is also influenced in a specific way by the nature of the salt, and in those cases where this parallels in magnitude the effect upon the activity coefficient of the neutral molecule, the salt effect upon the rate constant may not depend to any noticeable extent upon the nature of the salt. This follows from these relationships:

if

$$(y_A)_1/(y_A)_2 = (y_{HA^+})_1/(y_{HA^+})_2$$

$$\therefore\ (k/k_0)_1 \cong (k/k_0)_2$$

since

$$(y_{H^+})_1/(y_{H^+})_2 \cong 1,$$

where the subscripts 1 and 2 refer to different inert salts. This is the state of affairs which exists in the reaction of γ-hydroxybutyric acid to yield γ-butyrolactone[202].

The Influence of Dielectric Constant upon Reaction Velocity

The discussion of medium effects in ionic reactions has been confined, thus far, to consideration of medium alterations consisting of ionic strength changes. It is clear from equation 7 that the dielectric constant influences the effect of ionic strength upon the velocity of a reaction involving ions. The influence of the dielectric constant upon the velocity of a reaction involving ions should be evaluated by a comparison of the rate constants which have been extrapolated to zero ionic strength.*

---

* If the extrapolation in a log k versus $\sqrt{\Gamma}$ plot is uncertain, an extrapolation in a plot of $(\log k - \alpha Z_A Z_B \sqrt{\Gamma})$ versus Γ may be more certain. This type of plot is suggested if the activity coefficient of an ion is given by

$$\log y_i = -\alpha Z_i^2 \sqrt{\Gamma} + \beta\Gamma \tag{12}$$

This extrapolation has been used by F. H. Westheimer, W. A. Jones and R. A. Lad[306].

An equation which relates the rate constant for the reaction in the infinitely dilute solution to the rate constant for the reaction in a dilute gas, and which was first presented by Scatchard[260] is

$$\ln k_0^s = \ln k_0 + \frac{\epsilon^2 Z_A Z_B}{kTr}\left\{1 - \frac{1}{D}\right\}^* \tag{13}$$

This equation predicts a variation of the rate constant of an ionic reaction with dielectric constant

$$\frac{d \ln k_0^s}{d(1/D)} = -\frac{\epsilon^2 Z_A Z_B}{kTr} \tag{15}$$

thus, an increase of the dielectric constant increases the velocity of a reaction between ions of like sign and decreases the velocity of a reaction between ions of unlike sign.

It is desired to present certain data which are relevant to the question of the validity of this equation, but it is first necessary to discuss certain limitations of the equation. Perhaps the most important of these is the possibility that changing the medium brings about important changes in the nature of the reactants in addition to the changes in solvation which necessarily occur. This is particularly important when one is studying ionic reactions in media of low dielectric constant. In such media, salts considered to be strong electrolytes in water may exist as associated ion-pairs or more complex aggregates[137]. Such changes may alter the form of the rate law, either because the stoichiometric composition of the activated complex changes, or because there are changes in the predominant forms of the reactants (such changes alter the form of the rate law even though the activated complex has the same stoichiometric composition). Thus, the form of the rate law and the predominant forms in which the reactants and products exist should be known in each solvent which is under consideration.

The numerical magnitude of the rate constant depends upon the concentration units which are used. In comparing the rate constants for a reaction carried out in different pure solvents or mixed solvents, the practice has been to calculate rate constants based upon volume concentration units. It appears to be a more sound procedure from a theoretical point of view to use mole fraction concentration units[185, 261]. The correlation between ex-

---

* It is clear that a combination of this equation and Eq. (8) leads to

$$\ln k = \ln k_0 + \frac{\epsilon^2 Z_A Z_B}{DkT}\left\{\frac{\kappa}{1 + \kappa a}\right\} + \frac{\epsilon^2 Z_A Z_B}{kTr}\left\{1 - \frac{1}{D}\right\} \tag{14}$$

an equation which relates the rate constant in a liquid medium of ionic strength given by the κ value and dielectric constant D to the rate constant of the infinitely dilute gas.

perimentally observed rate constants and the predictions of Eq. (15) is shown in Figure 15. It is seen that the correlation with theory is much better when the rate constants have been calculated on the basis of the mole fraction concentration scale.

When the dielectric constant of a solvent is altered by mixing pure substances, the question of how homogeneous the solvent is in the presence of the ionic solute is an important one. The sorting of mixed solvents by ions has been discussed from a theoretical point of view by Scatchard[262]. This calculation predicts that in an ethyl alcohol-water solvent, the molecules in contact with an ion are water molecules even though the solvent is 99 per cent alcohol. The theory does not yield adequate quantitative agreement with experimental observations; as Scatchard points out, the neglect of the discrete structure of the solvent is undoubtedly an important reason for the failure of the theory. The qualitative conclusion is an important one, however; in a mixed solvent, the solvent molecules will be sorted with the more polar molecules congregating around the ions.

The conversion of ammonium cyanate into urea has been studied as a function of the dielectric constant of the solvent in a number of solvent mixtures and pure solvents.* The effect of the dielectric constant of the medium upon this reaction is approximately that expected for a reaction between two univalent ions of opposite charge. Just as a study of the dependence of the rate constant upon ionic strength does not distinguish the mechanisms involving the rate-determining steps

$$NH_4^+ + OCN^- \rightarrow, \qquad \text{and}$$

$$NH_3 + HOCN \rightarrow,$$

neither will a study of the influence of the dielectric constant of the medium. If the activated complex has the composition NH_4OCN and the dielectric

---

* A serious question regarding the interpretation of studies of this reaction has been raised by the work of Wyatt and Kornberg[316a] who show that in aqueous solutions at 70°C, the reaction

$$OCN^- + 2H_2O = HCO_3^- + NH_3$$

occurs to a significant extent. The total rate of disappearance of cyanate ion in solutions containing initially equivalent amounts of ammonium ion and cyanate ion is approximately proportional to the square of the concentration of cyanate ion and therefore the existence of this side reaction was not detected by the workers who measured the reaction rate by determining the concentration of cyanate ion as a function of time[294, 295]. At this temperature the rate constant in the rate equation $-d(OCN^-)/dt = k''(OCN^-)^2$ is 40 per cent higher than the rate constant for the rate equation $+d(CO(NH_2)_2)/dt = k(NH_4^+)(OCN^-)$, and thus the side reaction is quite important. The extent to which this side reaction occurs in mixed solvents which contain water is not known.

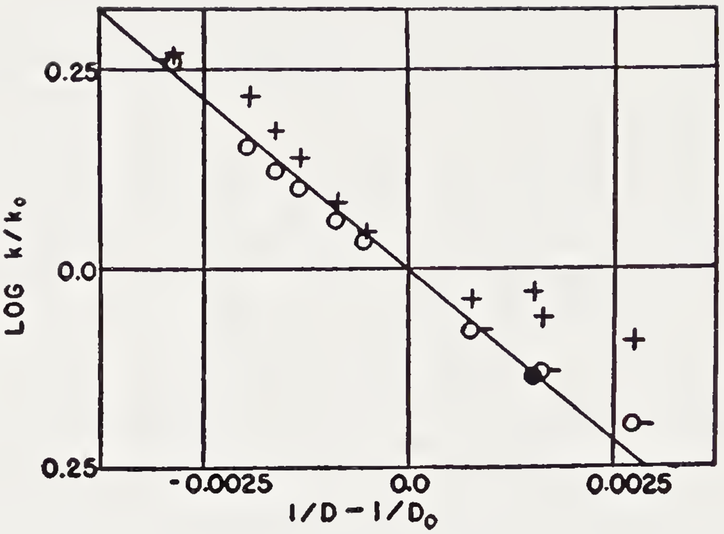

Fig. 15. Relative rate constants (mole fraction concentration units) for the bromacetate-thiosulfate reaction at 250°C.

● sucrose-water; -○ glycine-water; ○ urea-water; ○- ethanol-water. The crosses are the corresponding values if the molar concentration scale is used. (Reproduced from Ref. 261 with the permission of the Editor of the *Journal of Chemical Physics.*)

constant is high enough that ammonium cyanate is a strong electrolyte, the medium effect will be that expected for the equilibrium between the ions and the neutral activated complex even though the activated complex is formed from the neutral species NH_3 and HOCN. On the basis of the equation derived by Scatchard, log k_0 plotted versus $1/D$ should give a straight line. The slope of the line is influenced by the solvent only if the distance of approach of the ions in the activated complex is influenced by the solvent. The results of some measurements by Warner, Svirbely and co-workers are presented in Figure 16. It is seen that the points do not fall on straight lines; the value of $d \ln k_0/d(1/D)$ becomes smaller the lower the dielectric constant becomes. Further, the rate depends upon the nature of the solvent as well as upon the dielectric constant.* One may attribute this to a difference in the distance of closest approach, but this is not a completely satisfactory answer. Some specific properties of the solvent are undoubtedly playing an important role in determining the reaction velocity. It is to be noted, however, that the qualitative effect of changing the di-

---

* That specific properties of the solvent other than the dielectric constant are important in determining the extent of interaction of ions is shown very strikingly by the relative values of the dissociation constants for *o*-chlorophenyltrimethylammonium perchlorate in the solvents ethylidene chloride and ethylene chloride. Although these solvents are isomeric and have dielectric constant values which are the same within one per cent, the dissociation constant of this salt is ten fold greater in ethylene chloride than it is in ethylidene chloride[252].

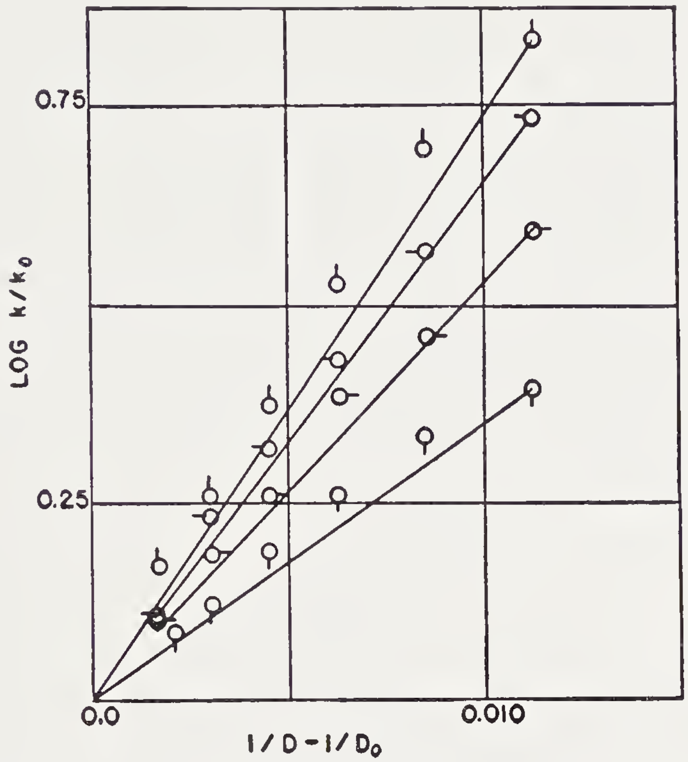

Fig. 16. The relative rates of the ammonium cyanate reaction at 50°C. ⫰ methanol-water; ⊸ ethanol-water; ⟜ propanol-water; ⫯ glycol-water. (Reproduced from Ref. 261 with the permission of the Editor of the *Journal of Chemical Physics*)

electric constant upon the rate is that predicted by equation 15; this reaction between two ions of unlike charge sign proceeds more rapidly the lower the dielectric constant of the solvent.

Since a possible cause of the curvature may be the sorting of the solvent molecules[261], it is desirable to examine data which have been obtained in pure solvents. Svirbely and Petersen have studied this same reaction in the pure solvents: methanol, ethanol, isopropanol, glycol and glycerol[275]. Their results are presented in Figure 17. It is seen that the points do not fall on a straight line regardless of which concentration scale is used. The type of curvature in the figure is the same as is observed in Figure 16, in which data for the mixed solvents are presented. Therefore, the curvature cannot be attributed to a sorting of the solvent molecules.

A more reasonable explanation of the trend toward a lower value of $d \ln k_0/d(1/D)$ at low D values is to be found in the nature of the reactants in such media. While ammonium cyanate is a strong electrolyte in water, it is very unlikely that it is completely ionized in isopropanol, a solvent with a dielectric constant of 18.6 at 20°C[5]. The work of Fuoss and Kraus[175] on tetraisoamylammonium nitrate in water-dioxane mixtures indicates

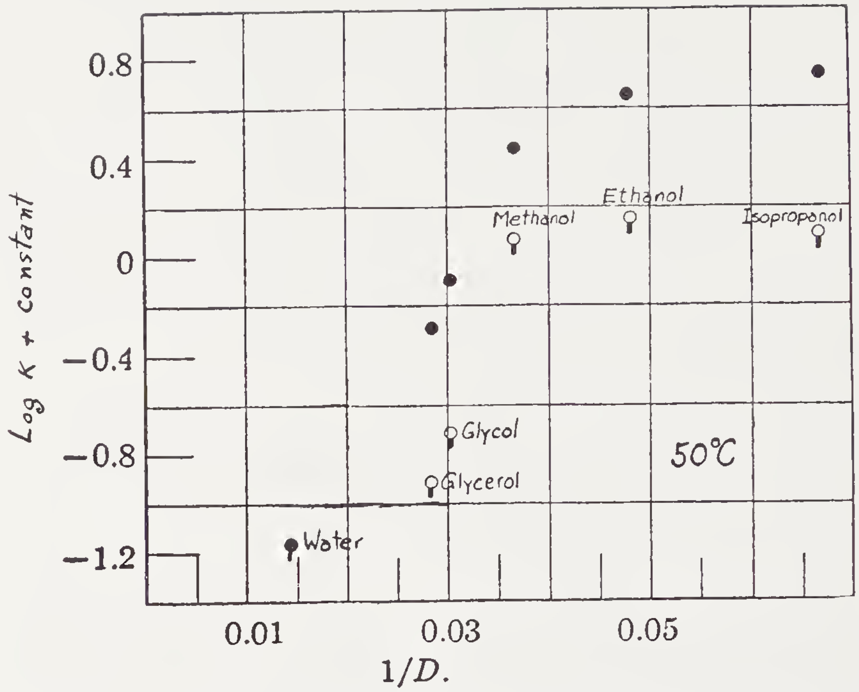

FIG. 17. The rate constant for the ammonium cyanate reaction.
♀ Data based on mole fraction concentration units.
● Data based on volume concentration units.
(Reproduced from Ref. 275 with the permission of the Editor of the *Journal of the American Chemical Society*)

that appreciable ion association occurs in media with a dielectric constant greater than that of isopropanol. Because of the size of the ions, it is expected that ammonium cyanate is a weaker electrolyte than the salt studied by Fuoss and Kraus.* The possibility that some association of ammonium ion and cyanate does occur in solvents of low dielectric constant was recognized by Svirbely and Lander[274]. Under conditions which lead to a significant fraction of the ammonium cyanate being associated as ion-pairs, the treatment of the data should be different. If, in such media, the activated complex has the composition NH_4CNO, the order of the reaction will become first, rather than second, as medium changes lead to complete association of ammonium ion and cyanate ion.

Other reactions between ions of unlike charge sign which have been studied as a function of the dielectric constant include the acid-catalyzed decomposition of azodicarbonate ion[165], and the acid-catalyzed decomposition of ethyl xanthate ion[166]. In both of these studies, the slope of the curve of log k versus $1/D$ decreases at low values of D. This is the same trend as

---

* Kraus and Bray have given a value of 4.5×10^{-3} as the dissociation constant of sodium iodide in propyl alcohol at 18°C[174].

is observed in the ammonium cyanate reaction, a trend which it seems reasonable to ascribe, in part, to ion association.

The effect of varying the dielectric constant upon the rate of a reaction between ions of like charge sign is in the opposite direction. On the basis of Eq. (15), it is expected that such a reaction would proceed more slowly the lower the dielectric constant. Reactions of this type which have been studied in media of varying dielectric constant include the reaction of bromacetate ion and thiosulfate ion (data already presented in Figure 15), and the alkaline fading of brom phenol blue[184] (a reaction between an ion of charge -1 and an ion of charge -2). In reactions of this type, deviations from the straight line relationship between log k_0 and $1/D$ are also observed. Ion association may again be the cause. In this case, the reacting ions are not associated with one another but with oppositely charged ions in the solution. The rate of reaction of such ion pairs would not be influenced by changes of dielectric constant to as great an extent as is the rate of the reaction between the unassociated ions.

It is seen that data on the variation of the rates of reactions involving ions are in reasonable agreement with Scatchard's equation (Eq. 15) with certain reservations. The straight line relationship does not persist at low dielectric constant values. It is suggested that ion association occurs in these solutions. Under such conditions, it is expected that the reaction rate will depend less strongly upon the dielectric constant since the average charge on the reactants is lower. For a given value of $Z_A Z_B$, the only parameter in equation 15 which may be altered is r, the distance of approach of the ions in the activated complex. The experimental results require the assignment of different values of r to the same reaction in two different solvent mixtures. This is surprising, but not impossible to rationalize in view of the one important assumption underlying the whole theory. This assumption, which is questionable, is that a polar solvent can be looked upon as a continuous medium with properties which can be correlated with the value of a single property, the dielectric constant of the solvent.

The Energy of Activation in Ionic Reactions

As has already been pointed out (p.339), the apparent energy of activation, E_A, is defined by the equation $E_A = -R\, d \ln k/d(1/T)$. Certain questions of interpretation arise when values of E_A for ionic reactions are considered. If E_A has been determined from the variation of the rate constant in media of constant composition, this variation in the rate constant can be looked upon as arising from two causes: the pure temperature effect and the change due to the change in the dielectric constant of the medium brought about by the change of temperature. This very fundamental point was first discussed by Warner and Svirbely[296], who suggested that the energy of activation which is of more fundamental significance is that determined in media of constant dielectric constant[298]. It is of considerable interest that the value of E_A for the reaction of ethylene chlorohydrin and hydroxide ion is a function of temperature if it is determined in water, but is independent of the temperature, if it is determined in ethyl alcohol-water or dioxane-water mixtures of constant dielectric constant[297].

If one assumes that the rate constant at zero ionic strength is a function of only the temperature and the dielectric constant, one obtains[296]

$$\frac{d \ln k^0}{dT} = \left\{\frac{\partial \ln k^0}{\partial T}\right\}_D + \left\{\frac{\partial \ln k^0}{\partial D}\right\} \frac{dD}{dT} \tag{16}$$

which leads to

$$(E^0)_C = (E^0)_D + 2.3\ RT^2 \left\{\frac{\partial \log k^0}{\partial D}\right\} \frac{dD}{dT} \qquad (17).$$

The apparent energy of activation measured in media of constant composition and the apparent energy of activation measured in media of constant dielectric constant are related by this equation which also involves the dependence of the rate constant upon the dielectric constant and the dependence of the dielectric constant upon temperature. The observed and calculated values of the difference between $(E^0)_C$ and $(E^0)_D$ are in good agreement for the conversion of ammonium cyanate into urea[296].

The use of solvents of different compositions at different temperatures in order to eliminate the variation of the dielectric constant with temperature is an interesting approach, but it is not without its flaws. The possibility that the molecules of a mixed solvent are sorted in the presence of solute ions or molecules has already been discussed. This is a complication which renders uncertain the interpretation of data obtained in mixed solvents. In addition, numerous observations, already discussed, make clear that "inert" solvents exert specific influences upon rates and equilibria in chemical reactions.

The kinetic salt effect upon ionic reactions has already been discussed. No mention was made, however, of the manner in which the addition of an inert salt influences the apparent energy of activation and the "temperature independent" factor of the Arrhenius equation. In the case of the reaction of bromacetate ion and thiosulfate ion, the addition of inert salt increases the rate of the reaction. This is particularly pronounced in the presence of multivalent positively charged ions[180]. In view of this positive kinetic salt effect, it is surprising that the apparent energy of activation for this reaction is increased in the presence of barium chloride or lanthanum chloride[181]. The explanation of this situation is the marked influence of these salts upon the "temperature independent" factor. In the presence of $0.18M$ sodium chloride to give a total ionic strength of 0.20, the value of E_A is 15,950 cal and the value of A is 3.9×10^{11}. In the presence of 0.03 molar lanthanum chloride to give a solution of the same total ionic strength, the value of E_A is 17,730 cal and the value of A is 2.9×10^{13}. The net increase in the rate of this reaction which is brought about by the addition of an inert salt is due to the preponderance of the effect of ionic strength upon A compared to its effect upon E_A.

The Bronsted-Debye and Huckel theory provides a means of calculating the expected effect of ionic strength upon the apparent activation energy and the "temperature independent" factor. The limiting slopes in graphs in which the experimental quantities $\log A$ and $E_A/2.3RT$ are plotted against $Z_A Z_B \sqrt{\mu}$ should be 1.52 and 0.51, respectively[181]. Since $\log k = \log A - E_A/2.3RT$, the limiting law predicts an increase in k with increasing ionic strength despite the fact that E_A increases with increasing ionic strength. This follows from the magnitude of the slopes of the graphs of $\log A$ and $E_A/2.3RT$ versus $Z_A Z_B \sqrt{\mu}$.

Medium Effects in Nonionic Reactions

A discussion of medium effects in nonionic reactions is not as exact as the corresponding discussion for reactions involving ions. The charge on an ionic activated complex is known, and while the charge does not establish with certainty the activity coefficient of this species in a medium of a certain ionic strength and dielectric constant, the theories which relate the activity coefficient of an ion to its charge and the known properties of the solvent are moderately successful. Correlations of the activity coefficients of neutral molecules with measurable properties of the pure substances, solvent and solute, are not as straightforward.* Even if a theory were available which would allow the calculation of the activity coefficient of a neutral molecule of a certain structure and polarity in a particular solvent, it would not allow a calculation of the medium effect upon a reaction rate, for the exact structure of the activated complex is but a subject of speculation. It has been suggested that in a reaction of the type

$$A + B \rightarrow AB,$$

which is first order in A and first order in B, the activated complex resembles the reaction product, AB[92]. In general, it seems reasonable to picture the activated complex in a bimolecular reaction as having properties intermediate between the properties of the reactants and products. Therefore the activated complex in a reaction of two nonpolar molecules to give a

---

* The most complete reference on this subject is the book by J. H. Hildebrand and R. L. Scott[145].

polar product (or products) is probably more polar than the reactants. The converse is true also; a reaction in which the reactants are polar and the products are nonpolar will be expected to have an activated complex which is less polar than the reactants. Although the activity coefficient factor, $y_A y_B / y_X$, does not involve the activity coefficients of the products, the preceding generalizations indicate the manner in which knowledge of the nature of the products is helpful in a qualitative discussion of medium effects upon the activity coefficient factor, and, therefore, upon the rate.

Empirical correlations which relate the nature of the reactants, the products, and the solvents to the rate of reaction were suggested by Richardson and Soper: "If the reaction is one where the products are of greater cohesion than the reagents, it is accelerated by solvents of high cohesion, whilst if the products are of lower cohesion than the reagents, the reaction is retarded by such solvents. When products and reagents are substances of like cohesion, the solvent has relatively little effect"[255]. Richardson and Soper present a resume of the results of several workers which conform to these generalizations. Reactions of the Menshutkin type, which involve the formation of a quaternary ammonium salt from a tertiary amine and an alkyl halide, are reactions for which the activated complex probably has a greater cohesion than the reactants. Such reactions are, quite generally, accelerated in solvents of high cohesion or high internal pressure. Esterification reactions, on the other hand, are reactions for which the activated complex has, undoubtedly, a lower cohesion than the reactants. Such reactions are, quite generally, accelerated in solvents of low cohesion or low internal pressure.

An enormous amount of work has been done on reactions of the alkyl halides, in which the halide is replaced by another group or atom; in addition to the formation of quaternary ammonium salts, the formation of an alcohol (from the halide and water) and an ether (from the halide and alcohol) are reactions of this type. Many discussions of the mechanisms of these reactions and the relation between the mechanism and the solvent effect upon the rate have been presented[127, 128, 153, 314, 315]. Only a few points

TABLE 5. SOLVENT EFFECTS IN THE REPLACEMENT OF HALOGENS IN ALKYL HALIDES

Reactants	Activated Complex	Effect upon Rate of Increasing the Solvent Polarity
$R - X$	$\overset{\delta+}{R} - \overset{\delta-}{X}$	Acceleration
$Y^- + R - X$	$\overset{\delta-}{Y} - R - \overset{\delta-}{X}$	Slight retardation
$Y: + R - X$	$\overset{\delta+}{Y} - R - \overset{\delta-}{X}$	Acceleration

of interest will be mentioned here. The relationship between the type of mechanism and the solvent effect, as presented by Hughes[153], is given in Table 5. In the first type of reaction listed, the rate-determining step is pictured as being a unimolecular reaction; the role of solvent is discussed in terms of its ionizing power. Grunwald and Winstein[314] have established a quantitative scale which is alleged to be a measure of the "ionizing power" of the solvent. This quantity is determined by the rate at which tertiary butyl chloride, a compound which is believed to react by the first type of mechanism (in Table 5), undergoes solvolysis in the solvent under consideration. The "ionizing power," which is so defined, correlates the rates of solvolysis of a number of similar type compounds. While a correlation such as this is interesting and of value, it is not certain that this approach, in which the specific participation of the solvent molecules in the activated complex is ignored, gives the clearest picture of the actual reaction mechanism.

In some studies, evidence for active participation of solvent molecules in the activated complex has been obtained. The rate of the reaction of benzhydryl chloride with ethyl alcohol in ethyl alcohol solvent to yield benzhydryl ethyl ether is markedly increased by the addition of water[123]. The role of the water is a catalytic one since the reaction product is predominantly the ether and not benzhydrol. These authors suggest that several molecules, water or alcohol, take part in the reaction; the role of these molecules is to solvate the halide ion which is being formed. Water catalyzes the reaction since it solvates the halide ion more effectively than ethyl alcohol.

The order of the reaction with respect to the substance which is reacting with the alkyl halide is most readily established in studies in solutions which are dilute with respect to this substance. The concentration of this substance can then be varied under conditions which do not lead to large medium changes. Such an approach has been used by Swain[276, 277], who studied the reaction of triphenylmethyl chloride with methyl alcohol and with phenol in benzene, and the reaction of methyl bromide and pyridine in benzene. The reaction of triphenylmethyl chloride is third order, first order in the halide and second order in the hydroxy compound. It is of interest that in the presence of both phenol and methyl alcohol, the rate of disappearance of the halide is much greater than it is in the presence of either hydroxy compound alone, and the product is exclusively the methyl ether. The reaction under these conditions is still third order: first order in the halide, first order in methyl alcohol, and first order in phenol. The phenol is acting as a true catalyst under these conditions for it is not consumed. These results, as well as those obtained in the reaction of methyl bromide and pyridine, lead Swain to propose that these reactions occur by a termolecular push-pull mechanism. The three molecules in the activated complex are the substrate, a reagent which solvates the halogen atom which is in the process of becoming a halide ion, and a reagent which attacks the carbon atom which is electron deficient because of the electrons which the halogen is taking with it. When these substances, which are proved part of the activated complex in the dilute solutions in an inert solvent, are present at high concentrations, it is no longer possible to prove their presence in the activated complex. Instead, one may discuss the reaction in terms of the "ionizing power" of the solvent. It seems very reasonable, however, to picture solvent molecules participating in the activated complex in these polar solvents just as they did in the inert solvents.

A quantitative relationship between the rates of reactions involving polar molecules and the dielectric constant of the solvent can be derived. Kirkwood[167] has developed equations which make possible the calculation of the activity coefficient of a spherical molecule of radius r and dipole moment μ in a medium of dielectric constant D[97]. The equation is

$$\log \alpha = -\frac{\mu^2}{2.3kTr^3} \times \frac{D - 1}{2D + 1} \qquad (18),$$

where α is the activity coefficient with reference to the dilute gas ($D = 1$) as the standard state. Use of this equation and the Bronsted equation leads to

$$\log k/k_0 = -\frac{1}{2.3kT} \times \frac{D - 1}{2D + 1} \left\{ \frac{\mu_A^2}{r_A^3} + \frac{\mu_B^2}{r_B^3} - \frac{\mu_X^2}{r_X^3} \right\} \qquad (19),$$

which predicts a straight line if $\log k$ is plotted versus $(D - 1)/(2D + 1)$. Correlations of the rates of various reactions in terms of this equation have been made[98]. The uncertainties involved in studies in mixed solvents (pp 377–379) exist in systems involving polar neutral molecules, just as they did in solutions of electrolytes. Therefore one would not expect the dependence of the rate constant upon the dielectric constant of the solution to be given by this equation, if sorting of the molecules of the mixed solvent by the polar solute molecules occurs. Similarly, if nonelectrostatic interaction of solute and solvent is important, or if specific complexing of the reactants by the solvent species occurs, the predictions of Eq. (19) will fail. It is noted, however, that the qualitative predictions of the equation are those which have already been discussed. If the activated complex is more polar than the reactants, the rate will be increased in solvents of higher dielectric constant; if the activated complex is less polar than the reactants, the rate will be decreased in solvents of higher dielectric constant.

TABLE 6. DECOMPOSITION OF NITROGEN PENTOXIDE AT 20°C[68, 69]

Solvent	D	$k \times 10^5$	E_A (kcal.)
Gas phase	1	1.65	24.7
Nitromethane	35.9*	1.53	24.5
Bromine	3.1	2.15	24.0
Pentachlorethane	3.7	2.20	25.0
Carbon tetrachloride	2.2	2.35	24.2
Ethylene chloride	10.7	2.38	24.4
Chloroform	4.8	2.74	24.6
Ethylidine chloride	10.0	3.22	24.9
Nitrogen tetroxide	2.6	3.44	25.0

* D at 30°.

A first order reaction which has been studied in the gas phase[68] and in a number of solvents[69] is the decomposition of nitrogen pentoxide

$$N_2O_5 = 2NO_2 + \tfrac{1}{2}O_2 .$$

Although the reaction is accurately first order in the several solvents which were studied, the first order rate constant increases with increasing initial concentration of nitrogen pentoxide. It appears that a slight medium effect is produced by the nitrogen pentoxide, and that nitrogen oxides (NO_2 and N_2O_4), which are the products, exert a similar medium effect. A comparison of the first order rate constants for this reaction in the several solvents is presented in Table 6. It appears that the variation in the rate constant cannot be attributed to an effect of the dielectric constant of the medium. The high value of k which is observed in nitrogen tetroxide as the solvent is in the direction expected on the basis of the effect of this substance upon the rate in dilute solution, where it must have a positive catalytic effect in order to account for the first order nature of the reaction in spite of the effect of the initial concentration of nitrogen pentoxide upon the rate.

The manner in which trends in the rate constant for a nonionic reaction with a change of medium are related to changes of the activation energy is of interest. The apparent energy of activation in the reaction of pyridine and methyl iodide has been determined in a number of solvents: isopropyl ether, carbon tetrachloride, mesitylene, toluene, benzene, chloroform, chlorobenzene, dioxane, bromobenzene, anisole, iodobenzene, benzonitrile, and nitrobenzene (the value of the rate constant for the reaction increases as one goes from isopropyl ether to nitrobenzene)[147]. A graph showing the relationship of the rate constant at 100°C and the value of E_A is presented as Figure 18. It is seen that the change in the rate constant is predominantly

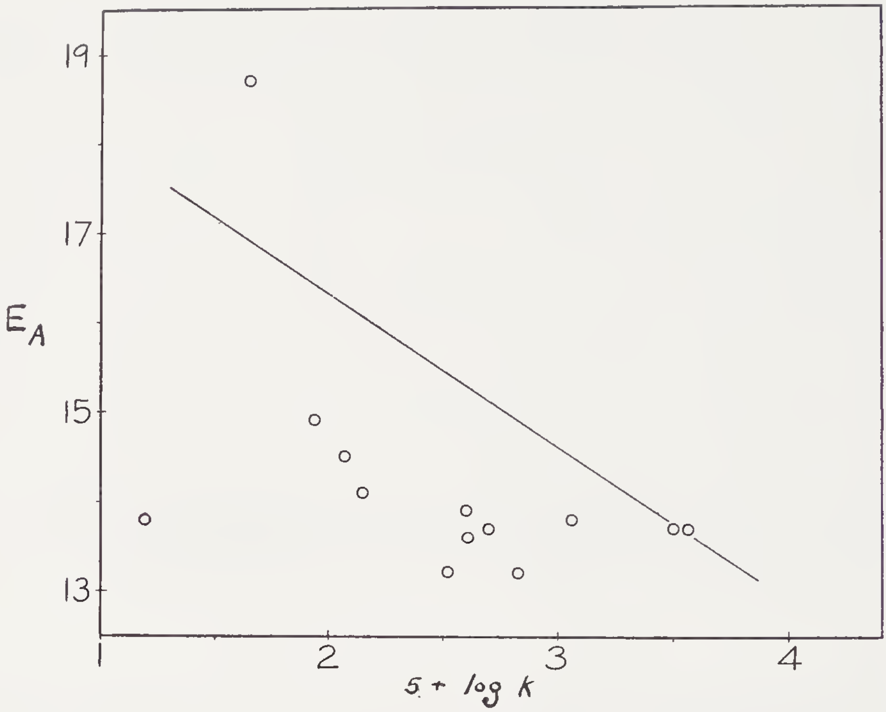

FIG. 18. The activation energy for the reaction of pyridine and methyl iodide in various solvents (see text). If change in k were due exclusively to change in E_A, the points should fall on a line of the indicated slope. (Data from Ref. 147)

due to a change in the value of the "temperature independent" factor. The authors of this work point out that a rough parallelism exists between the dipole moment of the solvent and the rate constant in those solvents for which the change in rate is due to a change of the "temperature independent" factor. This increase in rate at an approximately constant activation energy as one goes to more polar solvents is also observed in the condensation of cyclopentadiene with benzoquinone[148], a reaction in which the product, cyclopentadienebenzoquinone, has a low polarity[299]. The effect of increasing the polarity of the solvent is not as pronounced in this case as in the reaction which leads to the formation of methylpyridinium iodide, a reaction in which the product (and presumably the activated complex) is quite polar.

Unusual trends in the apparent energy of activation for the reaction of triethylamine and methyl iodide with solvent composition are observed in benzene-nitrobenzene mixtures as solvents[149]. On the basis of considerations which have already been discussed, it is expected that this reaction would proceed more rapidly in the solutions of higher dielectric constant (i.e., those solutions which are relatively rich in nitrobenzene). The values of the rate constant at 25°C and the apparent activation energy as a function of solvent composition are presented in Figure 19. (The value of the

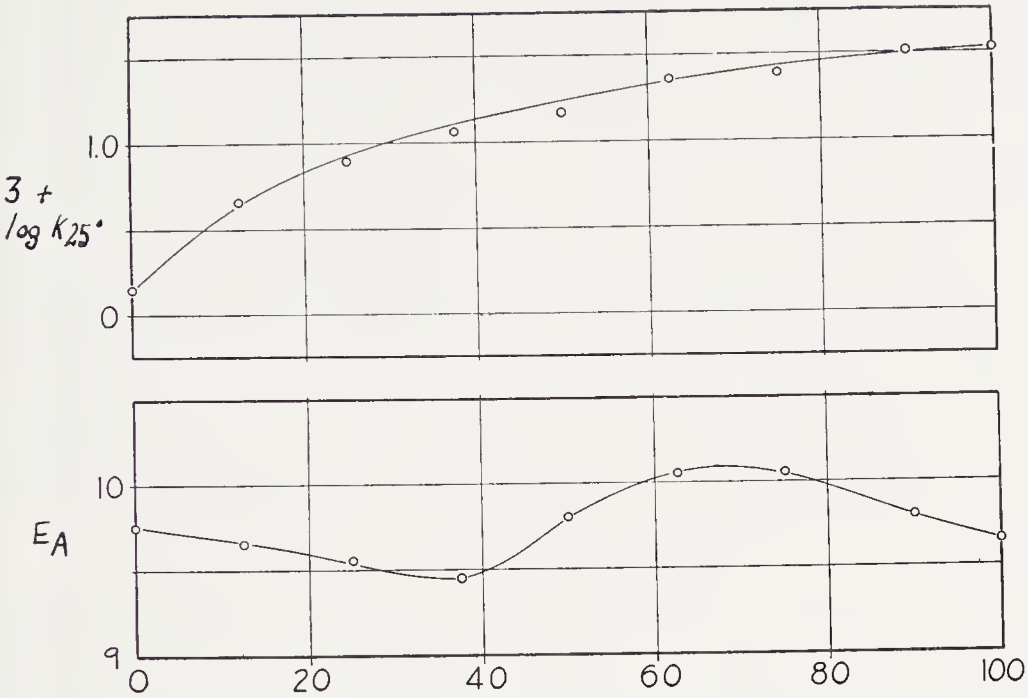

Per cent Nitrobenzene in Solvent

FIG. 19. The rate constant and activation energy for the reaction of methyl iodide and triethylamine in benzene-nitrobenzene solutions. (Data from Ref. 149)

dielectric constant for these media show a monotonic trend from 2.19 for pure benzene to 27.6 for pure nitrobenzene at 70°C[216].) It is seen that the activation energy has the same value in two different solutions containing benzene that it has in pure nitrobenzene. A rationalization of the unusual trend in E_A with solvent composition is not immediately obvious. The temperature dependence of the dielectric constant varies with solvent composition; this effect has been considered important in the determination of the energy of activation for ionic reactions. It is unlikely that this alone could account for the observed trends. The rationalization of the observations may be found in a combination of this effect and other effects, such as the sorting of the polar and nonpolar solvent molecules by the solute molecules.

ACID AND BASE CATALYSIS

The rates of many chemical reactions in solution are increased in the presence of an acid or a base. Such reactions do not fit into a single category but include isomerization reactions, decomposition reactions, displacement reactions and addition reactions. Although the terms acid and base are used in this initial statement in their most general sense, it is useful to open the discussion in terms of reactions in aqueous solution, and the acid

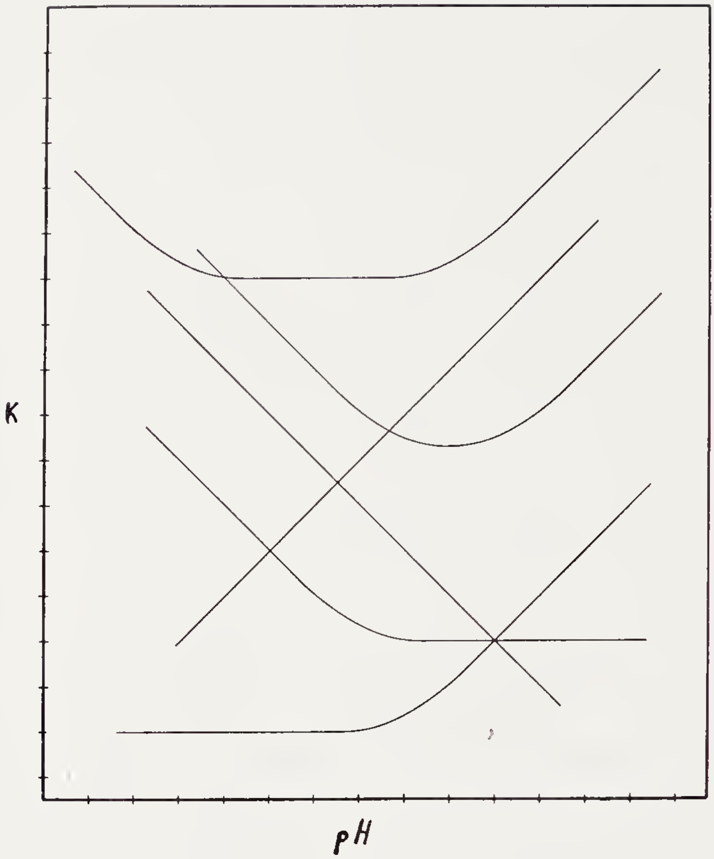

Fig. 20. The possible ways in which the pseudo- first order rate constant for a reaction which is catalyzed by hydronium ion and/or hydroxide ion may vary with pH.

and base, H_3O^+ and OH^-. If a reaction Y → Z is first order in (Y) and is catalyzed by hydronium ion and hydroxide ion, the first order rate constant is given by the equation

$$k = -\frac{d \ln (Y)}{dt} = (k_0 + k_{H_3O^+}(H_3O^+) + k_{OH^-}(OH^-)),$$

and depending upon the relative magnitude of k_0 (the rate constant for the so-called spontaneous reaction), $k_{H_3O^+}$, and k_{OH^-}, the rate constant varies in different ways with the pH of the solution. This is illustrated in Figure 20. Early work on acid and base catalysis by Bronsted[51, 52] and others[70, 71] demonstrated that the rates of reactions catalyzed by hydronium ion and/or hydroxide ion were in some cases dependent upon the actual concentrations of the buffer constituents HB and NaB, and not only upon the value of the ratio $(HB)/(B^-)$; this quantity determines the pH of the solution and, therefore, the rate if the equation already presented is a complete equation for k. Therefore, it was necessary to ascribe catalytic activity to the undissociated acid molecules and to bases other than hydroxide ion. These substances, HB and B^-, which are capable of catalyzing reactions which are also catalyzed by hydronium ion and hydroxide ion conform to the general definitions of an acid and a base which were proposed by Bronsted[50] and Lowry[204]. These definitions are simply: *An acid is a substance which has a tendency to lose a proton*, and *a base is a substance which has a tendency to add a proton.* Reactions which are catalyzed only by hydronium ion and hydroxide ion are said to be subject to specific hydrogen ion (or hydronium ion) catalysis, and specific hydroxide ion catalysis, respectively, while the term general acid and base catalysis refers to catalysis by all of the substances conforming to the Bronsted definitions of acids and bases.

If, as is generally true, the catalyzed reaction is first order with respect to the acid or base, a more general expression for the rate constant is

$$k = k_0 + \sum_i k_{ai}(HB_i) + \sum_j k_{bj}(B_j) \qquad (20),$$

where the first summation is taken over all i of the acids in the solution and the second summation is taken over all j of the bases in the solution. (The charges are not shown with the formulas in this equation; there is no limitation on the charge type of the acid and base.) The evaluation of the k_a's and k_b's is more easily accomplished if there exists a wide pH range in which k_0 is large compared to both $k_{H_3O^+}(H_3O^+)$ and $k_{OH^-}(OH^-)$. Within such a pH range, studies may be carried out at variable (HB) with constant (B), and also at variable (B) with constant (HB); under these conditions no ambiguity in the interpretation arises in spite of the change in the concentrations of hydronium ion and hydroxide ion. The pH range in which catalysis by hydronium ion or hydroxide ion is negligible may be such as to eliminate the possibility of studying the catalysis by particular acids or bases in such a pH region. Thus, in general, it is not convenient to determine the catalytic effect of an aliphatic carboxylic acid, which has a pK value of approximately 5, in measurements upon solutions of pH greater than 8. There are cases, however, in which the value of the catalytic coefficient for a weak acid (or base) is so very great compared to the value of k_0 that the catalysis by the weak acid (or base) is readily determined in solutions in which the catalyst acid (or base) are present predominantly as the conjugate base (or conjugate acid).

It is possible to determine the values of k_{HB} and k_B even though the simplified approach just mentioned is not feasible (e.g., the study of the depolymerization of dimeric dihydroxyacetone by Bell and Baughan[14a]). In solutions containing a single buffer constituent, the equation for the rate constant is

$$k = k_0 + k_{H_3O^+}(H_3O^+) + k_{OH^-}(OH^-) + k_{HB}(HB) + k_{B^-}(B^-)$$

which becomes:

$$k = k_0 + k_{H_3O^+}K_{HB}\frac{(HB)}{(B^-)} + k_{OH^-}\frac{K_w}{K_{HB}}\frac{(B^-)}{(HB)} + k_{HB}(HB) + k_{B^-}(B^-)$$

upon making the appropriate substitutions for (H_3O^+) and (OH^-) in terms of the equilibrium quotients: $K_{HB} = \dfrac{(H_3O^+)(B^-)}{(HB)}$, and $K_w = (H_3O^+)(OH^-)$. If a series of experiments are carried out in media of constant total ionic strength in which the ratio $(HB)/(B^-)$ is kept at a constant value r, this equation becomes

$$k = k_r + (HB)\{k_{HB} + k_B r^{-1}\}.$$

The value of k_r is a constant in any one series of experiments at constant r if the medium effect upon K_{HB} and K_w is negligible. The results of series of experiments at two different values of r allow the evaluation of both k_{HB} and k_B ; it is desirable, of course, to use the results of more than two such series in the evaluation of the two constants k_{HB} and k_B .

If studies which involve a number of weak acids and bases fail to reveal catalysis by these substances, the reaction which has already been shown to be catalyzed by hydronium ion and/or hydroxide ion is said to be subject to specific hydronium ion and/or hydroxide ion catalysis. The rate equation for a reaction which is subject to general acid or base catalysis is consistent with proton transfer occurring in the rate-determining step. Does this mean that reactions which are apparently subject only to specific hydronium ion and/or hydroxide ion catalysis involve a rate-determining step which is not a proton transfer? Further, does it mean that all reactions which are subject to general acid and/or base catalysis involve a proton transfer in the rate-determining step? These are questions which are intimately connected with the correlation of the catalytic efficiency of an acid or a base and the strength of the substance as an acid or a base; this subject will now be discussed.

The Bronsted Relationship

In their investigation of the decomposition of nitramide,

$$O_2NNH_2 \rightarrow N_2O + H_2O,$$

a reaction which is subject to general base catalysis, Bronsted and Pedersen[51] observed a quantitative relationship between the catalytic coefficient for a base and the strength of the substance as a base. The relationship is

$$k_B = G_B K_B^{\beta} = G_B K_A^{-\beta} \qquad (21)$$

where k_B is the catalytic coefficient of the base B, K_B is a measure of the strength of the catalyst as a base (this is conveniently expressed as the reciprocal of the dissociation constant of the conjugate acid), and β and G are constants for a particular reaction being studied in a particular solvent at a particular temperature. A similar relationship,

$$k_A = G_A K_A^{\alpha} \qquad (21')$$

is valid for reactions catalyzed by acids. The first well-studied example of this was the mutarotation of glucose[52, 205a].

Although attempts have been made to "derive" the Bronsted equation[25], it is really an empirical equation. Guggenheim believes that such "derivations" involve assumptions which are essentially equivalent to the relationship itself[112].

The data correlating the catalytic activity of various bases in the nitramide decomposition with the base strength are given in Figure 21. It is seen that bases with different net charges are correlated with Bronsted equations having different parameters. This indicates but one of the types of structural change in an acid or a base which alter the relationship between the catalytic activity and the acid or base strength.

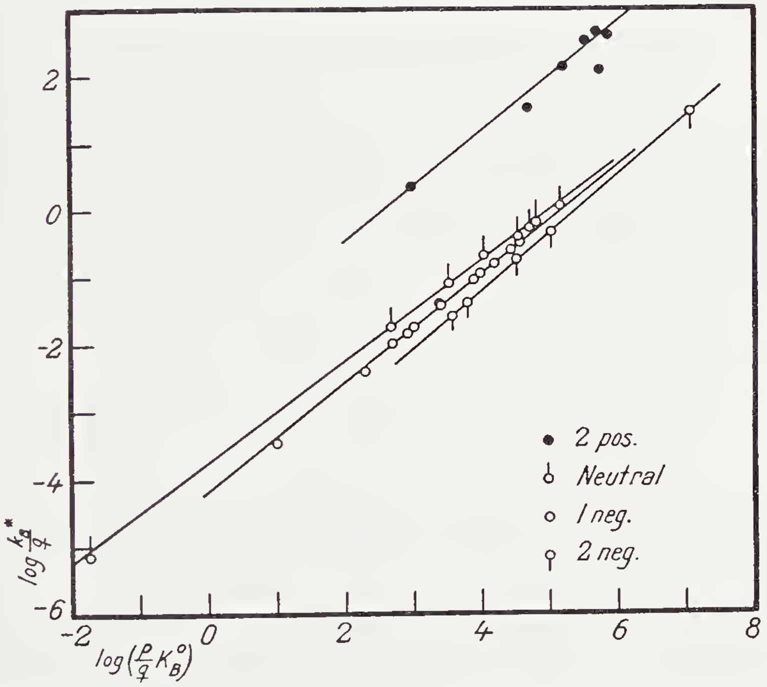

Fig. 21. The correlation of the rate constant for the decomposition of nitramide with the base strength constant of the basic catalyst. The several curves are for bases with varying charge. (Reproduced from Ref. 244 with permission of the Editor of the *Journal of Physical Chemistry*)

In the activated complex for a proton transfer reaction, the proton is shared between the catalyst and the substrate; the one bond is being broken as the other is being formed. The Bronsted relationship indicates that there is a correlation between the free energy of formation of such an activated complex and the standard free energy change for the reaction in which a proton is *completely* transferred from an acid molecule to a solvent molecule. There is a fundamental difference between the two processes for which the free energy values are being compared. In the one case, the proton transfer is complete, while in the other case, it is not. The Bronsted equation does not, in general, correlate the catalytic activity of acids (or bases) of rather different structure. The dissociation constant of an acid is determined by a number of factors including the distribution of charge in the acid molecule and the conjugate base, the number of equivalent ionizable protons and the number of equivalent positions in the conjugate base at which a proton may associate, the relative values of the resonance energy in the acid and the conjugate base, and the relative values of the entropy and energy of solvation of the acid and the conjugate base[41, 146, 168, 173]. Some of these factors are more important in one type of acid than in another, and the relative contribution of these several factors in determining the value of $\Delta F^\circ_{\text{ionization}}$ and $\Delta F^\ddagger$ will be different for different types of acids.

Attempts have been made to take into account one of the factors which influences the relationship between the acid strength and the catalytic coefficient of an acid catalyst. This is the statistical effect, the effect arising because the acids which are being compared have different numbers of equivalent ionizable protons and the conjugate bases have different numbers of equivalent points at which a proton may associate[53]. The Bronsted equations modified to take the statistical factor into account are

$$\frac{k_B}{q} = G_B\left(\frac{p}{q}K_B\right)^\beta \qquad (21'')$$

$$\frac{k_A}{p} = G_A\left(\frac{q}{p}K_A\right)^\alpha \qquad (21''')$$

where p is the number of equivalent dissociable protons, and q is the number of equivalent positions in the base at which a proton can associate. Ambiguity arises in the assignment of the statistical factor when several ionizable protons are bonded to the same atom. Should the value of p for ammonium ion be chosen as four or one[20, 244]? It is generally chosen as one. On the basis of a comparison of the rates of the base-catalyzed bromination of various ketones, it has recently been suggested that the factor should be chosen in the opposite way; it is observed that bromobenzoylacetone brominates one half as fast as does benzoylacetone[30]. (It is assumed

TABLE 7. DEHYDRATION OF ACETALDEHYDE HYDRATE: DEVIATIONS FROM THE BRONSTED RELATION

Catalyst	Dev. (log units)
Negative Deviations	
Benzoylacetone enol	−1.4
1,3 diketo-5,5-dimethylcyclohexane enol	−1.1
Nitromethane	−1.4
1-nitropropane	−1.5
Nitroethane	−1.7
2-nitropropane	−1.9
Nitrourethan	−0.4
Positive Deviations	
Benzophenone oxime	+1.2
Acetophenone oxime	+1.4
Diethyl ketoxime	+2.1
Chloral hydrate	+0.7
Water	+1.6

that this change in structure does not alter the tendency for the proton to ionize.) It is seen that the quantitative correction for the statistical factor, which has been made in many studies, does not appear to be free from ambiguity.

Some types of structural change cause marked deviations of the activity of a catalyst from the expectations of the Bronsted relationship which has been established for a series of catalysts which are structurally similar to one another but different from the catalyst under consideration. The so-called pseudo acids are catalysts which are abnormal in this respect. This has been shown in the acid-catalyzed dehydration of acetaldehyde hydrate[29, 33]. Forty-five carboxylic acids and phenols obey the Bronsted relationship with a mean deviation of 0.1 logarithm unit. Acids of different structural types deviate much more than this as is shown in Table 7. These data are rationalized in terms of the extent to which the negative charge on the base, which results from the ionization of the proton, distributes itself over the entire anion. Those substances which show a positive deviation are acids in which the negative charge is largely localized at the point of proton dissociation. In the acids used in establishing the Bronsted relationship for this reaction, there is some redistribution of charge, and in the acids which show a negative deviation, the negative charge is redistributed in the ion to a greater extent than it is in the carboxylic acids or phenols. These trends are reasonable since the acids which yield conjugate bases with the negative charge widely distributed over the ion probably have larger dissociation constants than would be expected on the basis of the strength of the bond by which the proton is held. In the activated complex, however, this effect of the distribution of the negative charge has not come into play completely, and the catalytic activity is lower than would be expected on the basis of the acid strength. Other facets of this situation are discussed by Bell[33], and are included in the paper on the relationship between the rate of ionization of pseudo acids and their acid strength by Pearson and Dillon[249a].

In reactions in aqueous solution, the acids H_3O^+ and H_2O and bases OH^- and H_2O occupy rather special positions. Using the conventional dissociation constant of an acid:

$$K_A = K(H_2O) = \frac{(H_3O^+)(B)}{(HB)},$$

the value of K_A is 55.5 for H_3O^+, and 1.1×10^{-16} for H_2O. It has been suggested that the correlation of the catalytic activity of these species would be better if different K_A values were used[26]. This procedure is somewhat arbitrary; it seems preferable to omit these species from correlations with the Bronsted equation. It is important, however, to recognize certain qualitative conclusions regarding the catalytic activity of these species in reactions which are subject to general acid or base catalysis. If the α or β value of the appropriate Bronsted equation approaches one, the maximum possible value[23], the much greater strength of H_3O^+ as an acid or OH^- as a base makes it unlikely that catalysis by any other acid or base are detectable. Therefore, it is possible that a reaction which shows specific hydronium ion or hydroxide ion catalysis is a reaction in which the rate-determining step is a proton transfer. On the other hand, if the value of α or β approaches zero, the much greater concentration of water make it the most active catalytic species despite the small magnitude of its strength as an acid or a base. Therefore a reaction in water may show no catalysis by acids or bases and yet be a reaction in which the rate-determining step is a proton transfer[21].

It is desirable at this point to indicate that nonprotolytic reactions are known in which the reactivity parallels the base strength of the reactant, thus indicating that such a parallelism does not necessarily prove that a proton transfer is involved in the rate-determining step. Chlor- and bromacetate ions, in dilute aqueous solution, are unstable with respect to the reaction

$$CH_2XCO_2^- + H_2O \rightarrow CH_2OHCO_2H + X^-.$$

The reaction is catalyzed by basic anions, B^-, with the intermediate formation of $CH_2BCO_2^-$ through the reaction

$$CH_2XCO_2^- + B^- \rightarrow CH_2BCO_2^- + X^-;$$

the species $CH_2BCO_2^-$ then undergoes a reaction which converts it into the hydroxy-acid. Dawson and co-workers have studied this reaction extensively; although complications exist, these authors were able to evaluate the rate constants for the terms in the rate law which have the form $k(CH_2XCO_2^-)\ (B^-)$[72]. It is observed that the Bronsted equation

$$k/q = 8.13 \times 10^{-7} \left\{\frac{K_b p}{q}\right\}^{0.203}$$

correlates the rate constant for the reaction of chloracetate ion with thirty-one bases with the value of K_b for these bases, where K_b is the reciprocal of the dissociation constant of the conjugate acid[270]. (Water, thiosulfate, and sulfite do not conform to this relationship.) Since the base strength varies over about thirteen powers of ten, it is clear that the relationship is being adequately tested.

In this reaction, a proton transfer does not occur. It seems reasonable that a Walden inversion occurs with the base B^- entering as the chloride ion leaves[128, 238]. The base B^- is attracted to the carbon atom at the positively charged region which is diametrically opposite the chlorine atom. Thus, this can be pictured as an acid-base reaction in which the proton no longer holds the central role. It therefore conforms more nearly to the general picture of acids and bases which Lewis suggested[191]. It is not surprising that a parallelism exists between the standard free energy change in a series of reactions in which bases share a pair of electrons with a proton, taking the proton away from a hydronium ion, and the free energy of activation for the series of reactions being discussed. If the Walden inversion mechanism is correct, the activated complex is a species in which the base is partially sharing a pair of electrons with the carbon atom which is electron deficient because the halide ion is in the process of leaving with a pair of electrons which the carbon had shared.

The Determination of the Degree of Ionization of Weak Acids and Bases from Reaction-Kinetic Studies

A reaction which is subject to specific hydronium ion or hydroxide ion catalysis provides a tool for the determination of hydronium ion and hydroxide ion concentration in solution. Unfortunately, many reactions which would otherwise be suitable are subject to rather large kinetic salt effects (see Table 4). It is possible to make appropriate corrections for the salt effect by studying also the reaction in salt solutions containing a strong acid of known concentration. If the calculated value of the dissociation constant is independent of the concentration of the weak acid, it indicates that catalysis by the undissociated acid is not important. This general subject has been reviewed by Kilpatrick[164].

The extents of ionization of the ion-pair complexes $CaOH^+$, $BaOH^+$ and TlOH have been determined in a study of the hydroxide ion catalyzed decomposition of diacetone alcohol by a comparison of the catalytic effect of calcium hydroxide, barium hydroxide and thallium hydroxide with the catalytic effect of the alkali metal hydroxides[27]. Certain assumptions, which have been discussed by the authors of this work, must be made in order to evaluate the equilibrium constant for the ionization of these ion-pair complexes. A similar determination of the dissociation constant of $CaOH^+$ has been made in a study of the hydroxide ion catalyzed hydrolysis of carbethoxymethyltriethylammonium ion[31]. The values of the $CaOH^+$ dissociation constant determined in the kinetic studies are very close to the value determined in solubility studies. It is of interest that calcium ion does not retard the hydroxide ion catalyzed hydrolysis of ethyl acetate[31]. Therefore, in this reaction calcium ion must also be associated in the activated complex to some extent.

Kinetic studies are in some cases useful for elucidating equilibria. There will be, in general, *at least as much uncertainty* in interpreting the kinetic data as there is in the interpretation of equilibrium studies (e.g., emf determination, solubility determination, etc.). For this reason, it appears preferable to avoid the use of kinetic methods of studying an equilibrium if other techniques are available.

Mechanisms of Prototropic Isomerizations[24, 129, 244, 317]

In a prototropic isomerization, a hydrogen atom is transferred from one position in a molecule to another position. A common reaction which falls into this class is the enolization of ketones. The enolization reaction is generally not studied directly since for many ketones the amount of enol which can exist at equilibrium is very small. The observation that an isolable enol reacts rapidly with halogens while the keto form does not, coupled with the fact that the rate of the acid- or base-catalyzed halogenation of ketones is zero order in the halogen has lead to the conclusion that the observed rate of halogenation of a ketone is its rate of enolization. This reaction is subject to general acid and base catalysis. It will first be discussed from the point of view that the reaction consists of bimolecular steps and proceeds through intermediates which are either the conjugate acid or conjugate base of the substrate. (Another way of looking at these reactions will be discussed in the following section.) Since the prototropic isomerization involves the transfer of a proton from one place to another, it clearly involves the action of both an acid and a base. In the case of acid catalysis, the proton transfer *to* the substrate occurs first and the intermediate is a cation (or a complex of the weak acid HB and the substrate); in the case of base catalysis, the proton transfer *from* the substrate occurs first and the intermediate is an anion (or a complex of the base B and the substrate).

The prototropic isomerization may simply be represented:

$$\mathrm{HM} \rightarrow \mathrm{MH}.$$

If this reaction is subject to general acid catalysis, there are terms in the rate law which have the form $k_{\mathrm{HX}}(\mathrm{HM})(\mathrm{HX})$, and the conclusion which follows from this is that one particular path for this reaction has associated with it an activated complex of the stoichiometric composition $\mathrm{H_2MX}$ (plus or minus solvent molecules). The mechanism

$$\mathrm{HM} + \mathrm{HX} \underset{k_{-1}}{\overset{k_1}{\rightleftarrows}} \mathrm{HMH^+} + \mathrm{X^-}$$

$$\mathrm{X^-} + \mathrm{HMH^+} \xrightarrow{k_2} \mathrm{MH} + \mathrm{HX}$$

is consistent with this if HM is weak enough as a base that the usual steady-state approximation regarding the concentration of $\mathrm{HMH^+}$ is valid. The rate equation derived on the basis of this assumption is

$$\frac{d(\mathrm{MH})}{dt} = \left\{\frac{k_1k_2}{k_{-1} + k_2}\right\}(\mathrm{HM})(\mathrm{HX}).$$

Whether the rate-determining step for the reaction is the first step or the second step, the rate law has this same form; an examination of the mechanism indicates that the activated complexes for the two steps have identical stoichiometric compositions. Of course, these activated complexes differ; they have different geometric configurations. In the one, the proton is being transferred from the acid HX to an unshared electron pair in the substance HM, and in the other a different proton from the intermediate $\mathrm{HMH^+}$ is being transferred to the base $\mathrm{X^-}$. Regardless which of these possibilities is the activated complex, the rate-determining step is a proton transfer reaction. The question of which of these configurations is actually the activated complex is an interesting one, but not one which can be answered by consideration of the form of the rate law.

It is sometimes possible to bring other types of information to bear on the question of which of these steps is rate-determining. An interesting example of this is provided in the enolization of acetone. A possible scheme of reaction steps corresponding to general acid catalysis in this reaction is that outlined, with 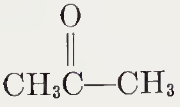 $\mathrm{CH_3\overset{\overset{\displaystyle O}{\|}}{C}{-}CH_3}$ represented by HM, 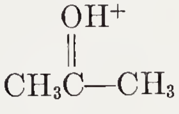 $\mathrm{CH_3\overset{\overset{\displaystyle OH^+}{\|}}{C}{-}CH_3}$

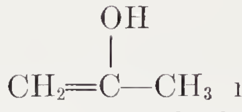

represented by HMH^+ and $CH_2{=}\overset{\overset{OH}{|}}{C}{-}CH_3$ represented by MH. The enolization can be studied by following the halogenation of the ketone; the rate of this reaction is independent of the concentration of the halogen. The exchange of O^{18} between water and acetone is also subject to general acid catalysis and the first step in the reaction is pictured as being the same as that in the enolization reaction[290]. It is observed that the oxygen exchange reaction proceeds at a rate which is several orders of magnitude larger than the enolization reaction. This leads to the conclusion that the first step in the enolization reaction can't be rate-determining. If it were and if the first step were common to the two reactions (enolization and oxygen transfer), the oxygen exchange could proceed no faster than the enolization. While this establishes the fact that the first step in this proposed mechanism for enolization cannot be the rate-determining one, it does not establish whether or not the first step in the oxygen exchange reaction is the rate-determining step.

Other evidence which indicates that the second step of the proposed mechanism for enolization is the rate-determining step is furnished by the work of Zucker and Hammett[124]. If the first step were rate-determining, there would be a correlation between the observed rate constant and the base strength of the ketone in a series of experiments using a common catalyst with different ketones, the base strengths of which are measur-

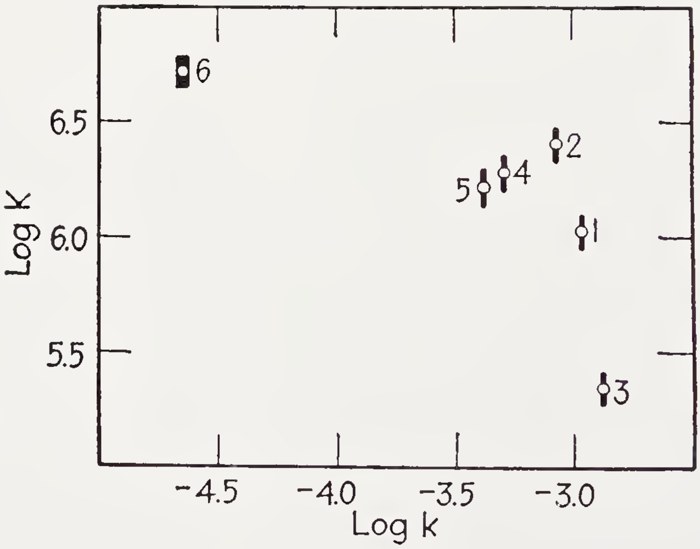

Fig. 22. The base strength constant for various ketones versus the rate constant for their hydronium ion catalyzed enolization reactions.

1. Acetophenone; 2. *p*-bromoacetophenone, 3. *p*-methylacetophenone; 4. propiophenone; 5. *n*-butyrophenone; 6. isobutyrophenone. (Reproduced from Ref. 124 with the permission of the Editor of the *Journal of the American Chemical Society*.

able.* On the other hand, if the second step were rate-determining, the observed rate constant would be the product of the equilibrium constant for the first step (k_1/k_{-1}) and the rate constant for the second step (k_2). While the first quantity (k_1/k_{-1}) depends upon the base strength of the ketone, the second (k_2) does not. The proton which is removed in the second step is not the one which is added in the reaction which gives a ketone its basic character. The results of Zucker and Hammett, which are shown in Figure 22, show no correlation between the observed rate constant and the base strength of the ketone; this is good evidence that it is the second step which is the rate-determining one. It is worth noting explicitly that if the rate-determining step in the acid-catalyzed halogenation of acetone is the reaction of a base and the conjugate acid of acetone, no information regarding the mechanism of formation of the conjugate acid of acetone is provided by the kinetic data.

A mechanism for prototropic isomerization consisting of consecutive bimolecular steps which is consistent with general base catalysis is

$$HM + B \underset{k_{-1}}{\overset{k_1}{\rightleftarrows}} HB^+ + M^-$$

$$M^- + HB^+ \xrightarrow{k_2} MH + B.$$

The rate law corresponding to this mechanism is

$$\frac{d(MH)}{dt} = \left\{\frac{k_1k_2}{k_{-1} + k_2}\right\}(HM)(B)$$

regardless of which step is rate-determining. As was true for the case of acid catalysis, the form of the rate law does not allow one to decide which of the two steps is the rate-determining one. It seems reasonable, however, to picture the first step as the slow one; the second step is really the reaction of a strong primary base, M^-, and a substance which is a primary acid, although perhaps not too strong an acid.† In the case of the enolization of ketones followed by means of the halogenation reaction, the halogenation could occur after the first step. That is, the ion 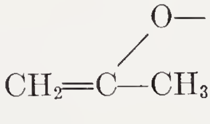 $CH_2{=}\overset{O-}{C}{-}CH_3$ may react rapidly with X_2.

The Termolecular Mechanism for Acid-Base Catalysis

The mechanisms for acid- and base-catalyzed prototropic isomerizations which have already been discussed consist of two bimolecular steps. The

---

* It is generally not possible to investigate the correlation between the rate of an acid- (or base-) catalyzed reaction with the base (or acid) strength of the substrate since these substances are generally extremely weak bases or acids.

† The terms primary acid and primary base are used here in the sense suggested by Lewis[191].

possibility that these two steps: the transfer of a proton from the substrate and the transfer of a proton to the substrate, occur simultaneously was suggested by Lowry and Faulkner[205]. These authors observed that the mutarotation of 2, 3, 4, 6-tetramethylglucose proceeds very much more rapidly in a mixed solvent consisting of pyridine and cresol than it does in pure pyridine or pure cresol. Thus, a solvent containing both an acidic and a basic substance is a very much more effective medium for this isomerization reaction than is a solvent which is predominantly acidic (cresol) or one which is very predominantly basic (pyridine). A more quantitative description of the rate of this reaction is provided by the work of Swain and Brown[279]. These authors have observed that in a solution of phenol and pyridine in benzene the important term in the rate law for the mutarotation of tetramethylglucose is: $k(G)(C_5H_5N)(C_6H_5OH)$ (G stands for tetramethylglucose). The third order term does not prove that a termolecular concerted mechanism is the actual path for the reaction. The third order kinetic law is equally consistent with a reversible association of any two of the three species followed by a rate-determining bimolecular reaction of this binary complex with the third molecule. The demonstration of the third order nature of this reaction in a solvent possessing relatively little acidic or basic character is important and of great significance; whether the mechanism is termolecular or a reversible equilibrium followed by a bimolecular rate-determining step is less important and of less significance.

In aqueous solution, there is present at a high, approximately constant concentration a substance, water, which is capable of acting both as an acid and a base. Because of its much greater concentration, water may act as the acid or base in the formation of the ternary activated complex in preference to other stronger acids or bases which are necessarily present at much lower concentrations. The general failure, then, to detect a third order term in the rate laws for reactions subject to general acid and base catalysis cannot necessarily be viewed as evidence against ternary activated complexes being important. Dawson and Spivey[71] have detected a third order term, k (acetone) (HOAc)(OAc^-), in their study of the rate of iodination of acetone in water solution, and this has been confirmed by Bell and Jones[33a]. The equation for the pseudo first order rate constant as determined by Bell and Lidwell[17a] and Bell and Jones is:

$$k\ (\text{in min}^{-1}) = \frac{\text{Rate}}{(\text{acetone})} = 2.78 \times 10^{-8} + 1.64 \times 10^{-3}(H_3O^+)$$

$$+ 15.0(OH^-) + 5.0 \times 10^{-6}(HOAc)$$

$$+ 15.1 \times 10^{-6}(OAc^-) + 20.4 \times 10^{-6}(HOAc)(OAc^-)$$

The corresponding data from the work of Dawson and Spivey were cited by Pedersen[244] as evidence that the termolecular mechanism could not be the major path by which this reaction and, presumably, other similar reactions proceed. If the reaction proceeds by termolecular paths exclusively, the terms in the rate law of order less than third correspond to reaction paths involving one or two water molecules. At first sight, one would associate the term $k(\mathrm{OAc}^-)$ with the path which involves acetate ion as the base and water as the acid, and the term $k(\mathrm{HOAc})$ with the path which involves water as the base and acetic acid as the acid. If the effectiveness of a particular acid (base) is independent of the base (acid) which is also acting in the concerted termolecular step, one would expect a definite relationship between the coefficient of the third order term and the coefficients of the second order terms involving (AcO^-) and (HOAc). Pedersen concluded that the third order term was 220-fold smaller than would be expected on the basis of the Lowry picture coupled with the above stated assumption regarding relative reactivities. An important error which Pedersen made was the assumption that the term $k(\mathrm{AcO}^-)$ necessarily corresponds to acetate ion acting as the base and water acting as the acid, and that the term $k(\mathrm{HOAc})$ necessarily corresponds to acetic acid acting as the acid and water acting as the base. Swain[278] points out that the term $k(\mathrm{AcO}^-)$ could equally well correspond to acetic acid acting as the acid and hydroxide ion acting as the base, and the term $k(\mathrm{HOAc})$ could correspond to hydronium ion acting as the acid and acetate ion acting as the base. This is merely proper recognition of the fact that the rate law does not establish the reactants in the rate-determining step, but only the stoichiometric composition of the activated complex. Swain shows that the rate equation for this reaction conforms approximately to an equation of the form:

$$k = k_0'(\sum r_\mathrm{A}(\mathrm{A}))(\sum r_\mathrm{B}(\mathrm{B})) \tag{22}$$

where k_0' is the coefficient for the term involving an arbitrarily chosen standard acid and base, and r_A and r_B are the catalytic reactivities of the acid A and the base B relative to the standard acid and base. This treatment depends, of course, upon the relative reactivity of the acid and base being independent of the identity of the other reagent (base or acid) which is taking part in the reaction. Since there are five parameters in equation 22 (k_0', $r_{\mathrm{H_3O^+}}$, r_{HOAc}, $r_{\mathrm{OH^-}}$, and $r_{\mathrm{OAc^-}}$) and six rate constants in the experimentally determined rate equation, the possibility of representing the rate of iodination of acetone by equation 22 was viewed by Swain[278] as evidence for the termolecular mechanism being generally valid for reactions subject to general acid and base catalysis. Bell and Jones[33a] point out that a wide range of values of r_{HOAc} would fit the observed rate data, and therefore the data are not a stringent test of the validity of equation 22. It has further been observed by Bell and Clunie[32] that a third order term is not required in the equation for the rate of hydration of acetaldehyde under concentration conditions which demand its presence if equation 22 is valid. Bell and Jones[33a] also present other arguments which strongly suggest that equation 22 is not valid. Although Swain was correct in his criticism of Pedersen's argument regarding the validity of the termolecular mechanism, it appears that the experimental data now available for reactions in aqueous solution do not substantiate his suggestion that the termolecular path is the mechanism by which acid *and* base catalyzed reactions occur.

Since the mutarotation of tetramethylglucose requires the action of both an acid and a base, there is the possibility that a single molecule containing both acidic and basic functional groups would be an effective catalyst. Swain and Brown observed that 2-hydroxypyridine is an extremely effective catalyst for the mutarotation reaction in benzene solution[280]. The reaction is first order in tetramethylglucose and *first* order in 2-hydroxypyridine. In order to be effective, the acidic and basic functional groups in a polyfunctional catalyst must have the proper geometrical configuration. It is observed that 3- or 4-hydroxypridine is very much poorer as a catalyst than 2-hydroxypridine. Structural models indicate that the nitrogen and hydroxyl groups are too far apart in the 3- and 4-hydroxypyridine to fulfill the required role with the sugar molecule. These authors suggest a resemblance between the polyfunctional catalysis as demonstrated in this reaction and the action of enzymes.

Acid and Base Catalysis in Nonaqueous Solvents

Various complications arise in the study of acid- and base-catalyzed reactions in non-aqueous solvents. Some solvents, like water, are amphiprotic; equilibria of the type:

$$2HB \rightleftarrows H_2B^+ + B^-$$

exist in these solvents. The lyonium ion, H_2B^+, and lyate ion, B^-, are analogous to hydronium ion and hydroxide ion in water solution[38]. The value of the equilibrium constant for the solvent ionization reaction, the autoprotolysis constant for the solvent, determines the range of acidity which can be realized in the solvent[131]. In amphiprotic solvents, there is the possibility of both general acid and base catalysis and specific lyonium ion and lyate ion catalysis. Among the amphiprotic solvents are the alcohols, amines and various acids. The association of ions in these solvents depends upon the dielectric constant of the solvent and also upon specific properties of the solvent which are so important in determining the solvation of ions and polar molecules. Much that is relevant to this subject has already been discussed in the section on the effect of the dielectric constant upon the rate of ionic reactions.

The base-catalyzed decomposition of nitramide has been studied in a number of non-aqueous solvents. As is the case in water, the catalytic constants for this reaction in isoamyl alcohol[56], cresol[57], and anisole[28] conform to the Bronsted relationship. In the studies in isoamyl alcohol and cresol, it was found that Bronsted equations with two different sets of parameters are required; one set of parameters correlates the negatively charged bases while another one correlates the neutral bases. The neutral base catalysts which were studied in anisole fall into four groups: pyridine and quinoline bases, tertiary aromatic amines, secondary aromatic amines, and primary aromatic amines. The points for each of these groups fall on four parallel lines when log k is plotted versus log K_a, the acid constant of the conjugate acid in water. If, however, the correlation of the rate constants is made with the value of K_a determined in *m*-cresol, the catalytic coefficients of the six bases, for which such K_a values were known, belonging to three of the groups all fall on the same straight line in a plot of log k versus log K_a. Because of this, it has been suggested that the base strength of the amines in water is anomalous[289]. A comparison of the catalytic coefficients for a number of catalysts in the several solvents in which this reaction has been studied is presented in Table 8. It is of interest to note that the catalytic efficiencies of the neutral bases decrease as the dielectric constant of the solvent decreases; the trend observed with the anionic bases is the reverse. These trends seem reasonable. In the case of catalysis by neutral bases, the activated complex, in which a proton is partially transferred to the neutral base from the neutral substrate, is more polar than the reactants and it, therefore, is stabilized in solvents of high dielectric constant. In the case of catalysis by anionic bases, the activated complex is relatively more stable in solvents of low dielectric constant since the charge is more widely distributed in the activated complex than it is in the reactant ion.

TABLE 8. CATALYTIC CONSTANTS FOR THE DECOMPOSITION OF NITRAMIDE IN VARIOUS SOLVENTS AT 20°C[18]

Catalyst	Water $D = 80$	*m*-Cresol $D = 13$	Isoamyl alcohol $D = 5.7$	Anisole $D = 4.4$
p-Chloraniline	0.38	0.045	0.0092	0.00076
Aniline	0.97	0.146	0.033	0.0019
p-Toluidine	2.1	0.33	0.098	—
Dichloracetate ion	0.0010	0.0118	0.063	—
Salicylate ion	0.038	0.41	2.02	—
Benzoate ion	0.36	5.4	17.0	—

Acid-catalyzed reactions in aprotic solvents are of interest because the catalysis can only be of the general type; there is no lyonium or lyate ion in such a solvent. Because of the low dielectric constant of the solvents which are most generally used in such studies, there is no possibility of ions being present at appreciable concentrations, and there is even a tendency for the polar solutes, substrate or catalyst, to associate. This introduces complications in the interpretation of the observed order of the reaction in terms of the reaction mechanism. In a number of studies of acid-catalyzed reactions in aprotic solvents, it has been observed that the catalytic coefficient for the acid is not independent of the acid concentration[15, 16, 55, 117, 302, 303]. The first order rate constant is, in some cases, expressible by an equation of the form: $k = \alpha C_A^2 + \beta C_A$, and in other cases by an equation of the form: $k = \beta C_A + \gamma \sqrt{C_A}$ (where C_A is the stoichiometric concentration of the acid). In the case of the inversion of menthone, it is observed that the rate constant also depends upon the menthone concentration[15, 303]. Clearly, the situation is a complex one. Weissberger[303] interprets the data in terms of the activated complex involving two molecules of trichloroacetic acid and one molecule of menthone. The order of the reaction with respect to acid and ketone is not simple since there is present in the solution not only the dimeric form of the acid but also a complex formed by the association of one molecule of acid and one molecule of menthone. It is expected that complications of this sort exist in all systems involving polar molecules in non-polar solvents. If the reaction occurs predominately by a path involving an activated complex of *one* particular composition, the equilibria in the solution can probably be elucidated by a determination of the order of the reaction with respect to all of the reactants over a wide range of composition. If activated complexes of several different compositions are important, an attempt to obtain both the formulae of the activated complexes and the nature of the equilibria involving the reactants in the solution is really a complicated task. If possible, the nature of the equilibria should be established independently.

In spite of the complex nature of the results obtained in studies of acid-catalyzed reactions in aprotic solvents, a correlation of the catalytic efficiency of an acid and the strength of the acid is observed. Bell and Lidwell have studied the acid-catalyzed rearrangement of N-bromobenzanilide in chlorobenzene[17]. They find that the catalytic coefficients of eight acids (extrapolated to zero acid concentration) are related to the strengths of these acids in *water* by the Bronsted relationship: $k_A = 0.0078\ K_A^{0.51}$. It is a common practice to correlate the catalytic coefficient of an acid in an aprotic solvent with the dissociation constant of the acid in water[22]. It has been suggested that this dissociation constant is a better measure of the "intrinsic strength" of the acid than is the value of the dissociation constant which is measured in a less polar solvent.

The Correlation of Reaction Rate and the Hammett Acidity Function

A useful measure of the acidity of a concentrated solution of acid is the acidity function H_0[118, 122, 126]. This is measured using an indicator which exists in the form of a neutral base and in the conjugate acid form, a cation of charge +1; the value of the acidity function for a particular medium is a measure of the tendency for a proton to be transferred to any neutral base in that medium. The equations which define H_0 and h_0 are:

$$\begin{aligned} H_0 &= -\log h_0 \\ &= -\log \frac{a_{\mathrm{H}^+} y_{\mathrm{B}}}{y_{\mathrm{BH}^+}} \end{aligned} \qquad (23).$$

Since it is observed that the rates of some acid-catalyzed reactions are proportional to h_0 while others are more closely proportional to the concentration of hydronium ion, it is desirable to correlate these two relationships (i.e., $k \propto h_0$ and $k \propto (\mathrm{H_3O^+})$) with possible reaction mechanisms. Of course, one can distinguish between these two correlations only in the concentration region in which h_0 is not proportional to $(\mathrm{H_3O^+})$[125].

Within the limitations of a reasonable assumption regarding an activity coefficient factor, the reactions for which the rate is proportional to h_0 appear to be those in which the rate is proportional to the concentration of the conjugate acid of the substrate[121]. If the rate-determining step is the *unimolecular* decomposition of this cation, the rate is given by

$$\text{rate} = k(\mathrm{SH^+}) \frac{y_{\mathrm{SH}^+}}{y_{\mathrm{X}^+}} = kK(\mathrm{S}) a_{\mathrm{H}^+} \frac{y_{\mathrm{S}}}{y_{\mathrm{X}^+}},$$

where y_{X^+} is the activity coefficient of the activated complex and K is the thermodynamic equilibrium constant for the reaction

$$\mathrm{S} + \mathrm{H^+} \rightleftarrows \mathrm{SH^+}.$$

If a substitution for a_{H^+} is made in terms of h_0, the equation becomes

$$k_{\mathrm{obs.}} = \frac{\text{rate}}{(\mathrm{S})} = kKh_0 \frac{y_{\mathrm{S}} y_{\mathrm{BH}^+}}{(y_{\mathrm{X}^+})(y_{\mathrm{B}})},$$

and $k_{\mathrm{obs}} \propto h_0$, if $\dfrac{y_{\mathrm{S}} y_{\mathrm{BH}^+}}{(y_{\mathrm{X}^+})(y_{\mathrm{B}})}$ = a constant. Since the substrate and the activated complex differ from one another in the same way that the indicator

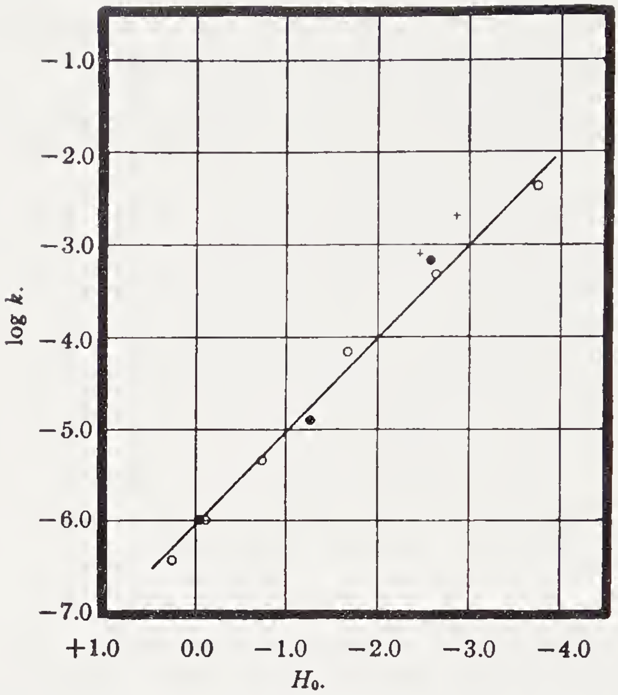

FIG. 23. Log k_0 versus H_0 for the acid-catalyzed decomposition of trioxane: ○ = H_2SO_4 in water; ● = HCl in water; + = H_2SO_4 in glacial acetic acid. (Reproduced from Ref. 242 with the permission of the Editor of the *Journal of the American Chemical Society*)

base differs from its conjugate acid, it is reasonable that a change in the medium will alter the activity coefficient ratios $\frac{y_S}{y_{X^+}}$ and $\frac{y_B}{y_{BH^+}}$ to the same extent.

A reaction which shows a striking correlation between k and h_0 is the decomposition of trioxane, the cyclic trimer of formaldehyde[242]. This correlation is shown in Figure 23. An approximately sixteen fold change in the concentration of hydronium ion ($0.5M$ H_2SO_4 to $8.0M$ H_2SO_4) gives rise to a change in both k and h_0 by a factor of 10,000. It has also been observed that a marked salt effect upon H_0 in perchloric acid-sodium perchlorate solutions is paralleled by an equivalent salt effect upon the rate of this reaction[242].

Other reactions which have rates closely proportional to h_0 are: the hydrolysis of sucrose[121], the hydrolysis of cyanamide in nitric acid[107, 108], the hydrolysis of β-propiolactone in perchloric, sulfuric and nitric acids[200], the conversion of γ-hydroxybutyric acid to γ-butyrolactone in hydrochloric acid or perchloric acid[202], and the deacylation of aromatic ketones[264]. These are reactions, then, in which the activated complex has the same stoichiometric composition as the conjugate acid of the substrate. The conjugate acid decomposes unimolecularly without the specific participation of a solvent molecule. The activated complex and the substrate may be solvated. The correlation of the rate of reaction and the acidity function will exist if the relative solvation of X^+ and S is the same as the relative solvation of BH^+ and B (the indicator used in the establishment of H_0). This has already been implied in the assumption that $\frac{y_S y_{BH^+}}{(y_{X^+})(y_B)}$ is a constant as the medium changes, for the change of medium involves a change in the activity of the solvent species.

Another possibility is a reaction mechanism in which the activated complex has the stiochiometric composition SH_3O^+. (The rate-determining step could be the proton transfer from hydronium ion to the substrate, or the proton transfer from the conjugate acid of the substrate to a water molecule). The rate equation in this case is

$$\text{rate} = k(\text{S})(\text{H}_3\text{O}^+)\,\frac{y_S y_{H_3O^+}}{y_{X^+}},$$

and the rate is proportional to the concentration of hydronium ion only if $\frac{y_S y_{H_3O^+}}{y_{X^+}}$ is relatively constant with a change of medium. The medium effect upon an activity coefficient factor of this form has already been discussed (pp. 346–348). The question which exists is this: will a medium effect of reasonable magnitude vitiate the expected correlation of k and the concentration of hydronium ion? Some numerical data which aid in answer-

TABLE 9. DATA PERTAINING TO THE CORRELATION OF REACTION RATES WITH (H_3O^+) OR h_0

Acid Conc. (molar)	$h_0/(h_0)_{1\text{ molar}}$			Assumed B value (Eq. 11)			
				$B = 0.10$		$B = 0.30$	
	$HClO_4$[119]	HCl[120]	HNO_3[120]	$\frac{y_{H_3O^+}\,y_S}{y_{X^+}}$	k/k_1	$\frac{y_{H_3O^+}\,y_S}{y_{X^+}}$	k/k_1
1.0	1.00	1.00	1.00	1.26	1.00	2.00	1.00
1.5	2.14	1.82	1.74	1.41	1.68	2.82	2.12
2.0	3.63	2.95	2.88	1.58	2.51	3.98	3.98
4.0	29.5	15.9	13.3	2.51	7.97	15.8	31.6
6.0	363.	75.9	43.6	3.98	19.0	63.1	189.3
$(h_0)_{1\text{ molar}}$	1.2_3	1.2_0	1.2_3				

NOTE: The k/k_1 ratio is equal to $(H_3O^+)\,\frac{y_{H_3O^+}\,y_S}{y_{X^+}}$ at the stated concentration relative to that at one molar acid.

ing this question are presented in Table 9. A kinetic salt effect of the magnitude corresponding to a B value (equation 11) of 0.10 would result in the product $(H_3O^+) \times \frac{y_{H_3O^+}y_S}{y_{X^+}}$ varying about one-half as much as h_0 between one and six molar nitric acid. If the kinetic salt effect is of a larger magnitude, for example $B = 0.30$, the rate of a chemical reaction which is proportional to the hydronium ion concentration will actually undergo a greater change between one and six molar hydrochloric or nitric acid than will a reaction for which the rate is proportional to h_0. It is clear that the electrolyte effect upon the reaction velocity should be elucidated before any conclusion regarding which of the correlations: rate $\propto (H_3O^+)$, or rate $\propto h_0$ is valid. Since equation 11 is often valid to high concentrations of electrolyte (4 molar in the case of the hydrolysis of γ-butyrolactone), the B value established in studies at low acid concentrations ($< \sim 1.0$ molar), where $h_0 \propto (H_3O^+)$, may be used to predict the value of $y_{H_3O^+}y_S/y_{X^+}$ at a higher electrolyte concentration. An alternate procedure would be the use of a B value determined for a salt at high concentration, the assumption then being made that the ratio $y_{H_3O^+}y_S/y_{X^+}$ is influenced in the same way by acid as by the salt chosen as a model.

It is reasonable to conclude that those reactions for which the rate is nicely correlated with the concentration of hydronium ion at high acidity are reactions with an activity coefficient factor $\frac{y_{H_3O^+}y_S}{y_{X^+}}$ which is not markedly influenced by the composition of the medium. This has been found in the case of the enolization of acetophenone in perchloric acid solution[125], and the hydrolysis of γ-butyrolactone in perchloric or hydrochloric acid[202]. In the case of the latter reaction, the kinetic salt effect due to sodium chloride or perchlorate is known. A slight trend in $k_{H_3O^+} = \frac{k}{(H_3O^+)}$ is such that the medium effect due to hydrochloric acid or perchloric acid appears to be in the same direction as the medium effect due to the corresponding salts.

Acid Catalysis in Very Concentrated Acid Solution

Many substances which are predominantly acidic in dilute aqueous solution do exhibit some basic properties in concentrated acid solution. The acetyl cation, CH_3CO^+, or the species formed by the union of this with an acetic acid molecule, acetic anhydridium, $(CH_3CO)_2OH^+$, are believed to exist in solutions containing perchloric acid and acetic acid[58, 211]. (Since some water is present in the perchloric acid reagent, acetic anhydride is used to react with this water.) If the cationic species formed in these strongly acidic media are particularly effective in certain reactions, the catalysis by acids which are strong enough to donate a proton to an acetic anhydride molecule to form $(CH_3CO)_2OH^+$ or to remove an hydroxide ion from an acetic acid molecule to form CH_3CO^+ is rationalized. Burton and Praill[58] have found that the acylation involved in the conversion of anisole into *p*-methoxyacetophenone goes readily in media in which the cations CH_3CO^+ or $(CH_3CO)_2OH^+$ are present but not in those media which contain sufficient water to favor the formation of $CH_3C(OH)_2^+$. This reaction is also brought about by the use of acetyl perchlorate[59], which is prepared from acetyl chloride and silver perchlorate, and by the use of zinc chloride and acetyl chloride or zinc chloride and acetic anhydride as the sources of CH_3CO^+ [60]. Another reaction in which the active species appears to be the acetyl cation is the acylation of benzoquinone (the "Thiele acylation"); this reaction is catalyzed by strong acids in acetic anhydride[211]. In acetic acid as a solvent, the difference in strength of the acids, which are considered to be completely ionized in dilute aqueous solution is considerable[116], and therefore perchloric acid may be effective when less strong acids are not effective.

An important class of reactions which is accelerated in strongly acidic media is the aromatic nitration reaction[91]. Extensive recent work by Hughes, Ingold and their associates has elucidated this subject considerably[152]. The greater rate of nitration in strongly acidic media (sulfuric acid or perchloric acid[256]) is equally consistent with $H_2NO_3^+$ or NO_2^+ acting as the nitrating agent. The observation that the rate of nitration of reactive aromatic compounds, in nitromethane or acetic acid as a solvent, is zero order in the aromatic compound suggests strongly that NO_2^+ is the reactive nitrating agent in these solvents[152]. The lack of dependence of the rate upon the concentration of the aromatic compound indicates that it is not a part of the activated complex. Since the species $H_2NO_3^+$ is expected to be in rapid equilibrium with the predominant form of nitric acid, the slow step which involves only nitric acid (and possibly the solvent) is pictured as

$$H_2NO_3^+ \rightarrow NO_2^+ + H_2O.$$

In the more strongly acidic solvents (e.g., sulfuric acid or nitric acid), the rate does depend upon the concentration of the aromatic compound. The authors interpret this to mean that the rate of formation of NO_2^+ is enough greater in these solvents to make the step involving the aromatic compound the rate-determining one. If the rate under such conditions depends upon the equilibrium concentration of NO_2^+, the rate should be greater the more acidic the solvent (as measured by h_0) and the lower the activity of water in the solvent.

If a reactant in a chemical reaction is an exceedingly weak base and if the reactivity of its conjugate acid is greater than the reactivity of this weakly basic reactant, the catalysis by acid becomes noticeable only in media of high acidity. It is worth keeping in mind, therefore, that a reaction may show acid catalysis in concentrated acids although it does not in dilute acidic solution; a reaction may proceed in concentrated perchloric or sulfuric acid which does not proceed in concentrated hydrochloric acid.

The Dependence of the Activation Energy of Acid- and Base-Catalyzed Reactions Upon Temperature, Environment, and the Nature of the Catalyst[162].

In the preliminary discussion of the theories of reaction kinetics, it was mentioned that the apparent energy of activation of a reaction may vary with temperature. This is true even though the reaction under consideration proceeds by a simple bimolecular mechanism. In addition, a variation of E_A with temperature, over a certain temperature range, is to be expected if the mechanism is not a simple one. If the rate law involves two or more independent terms or is of the type with a sum of terms in the denominator (see pages 343–346), the apparent activation rnergy will change with temperature under the conditions of concentrations and temperature such that more than one of the terms in the rate law are important; in addition, for E_A to vary with temperature because of this, the temperature coefficients of the rate constants must be different. Since the rate law for a chemical reaction should be completely elucidated before the significance of the activation energy is discussed, the variations of E_A with temperature which arise because the mechanism does not consist of a single simple step should not be considered anomalous. The complexities of the mechanism are not always apparent from the form of the rate law, however. If, for example, a reactant forms more than one solvated species with the solvent molecules and if these species have different reactivities, the existence of these several species will escape detection in kinetic runs at constant temperature in dilute solutions in the pure solvent. This complexity may lead, however, to a large variation of E_A with temperature if the equilibria between the several solvated species shift appreciably with temperature[194].

Not only is E_A a function of the temperature, but the "temperature independent" factor, A, of the Arrhenius equation is not really independent of the temperature. This has one important consequence with regard to the experimental evaluation of E_A. If both E_A and A vary with temperature in a manner such that

$$RT \frac{d \ln A}{dT} \cong \frac{dE_A}{dT},$$

TABLE 10. THE VARIATION OF E_A WITH T FOR ACID-CATALYZED HYDROLYSIS OF ACETALS AND FORMALS

Substance	$\Delta E_A/\Delta T$	Ref.
Diethyl formal	+31 cal/deg.	161
Dimethyl acetal	~0	162
Diethyl acetal	−33	162
Ethylene acetal	−7	162

the usual plot of ln k versus $1/T$ gives a straight line even though $dE_A/dT \neq 0$[162]. If accurate values of the rate constant are known at several temperatures which are not too widely spaced, the integrated form of the Arrhenius equation:

$$E_A = \frac{RT_1T_2}{(T_1 - T_2)} \ln \frac{k_{T_1}}{k_{T_2}}$$

may be used with data at successive temperatures[162]. A trend in E_A with temperature will generally be exposed by this method.

Among acid-catalyzed reactions, there are several which show a marked dependence of E_A upon temperature. A summary of the findings of Kilpatrick and co-workers regarding the acid-catalyzed hydrolysis reactions of acetals and formals is presented in Table 10. On the basis of these data, no generalizations can be made regarding the magnitude or even the sign of $\Delta E/\Delta T$; in this group of related reactions, $\Delta E_A/\Delta T$ varies from −33 to +30.

The value of E_A for the inversion of sucrose decreases with increasing temperature[160, 222]; at the low end of the temperature range studied by Leininger and Kilpatrick[160], the value of $\Delta E_A/\Delta T$ is approximately −70 cal/deg. It is interesting that the hydrolysis reactions of methyl chloride, methyl bromide and methyl iodide all have associated with them values of $\Delta E_A/\Delta T = -67$ cal/deg.[223], while the reactions of these same alkyl halides with hydroxyl ion or thiosulfate ion have associated with them values of E_A which are approximately constant[229].

The temperature dependence of the rate constant for the hydroxide ion catalyzed dealdolization of diacetone alcohol has been studied by LaMer and Miller[182]. In both water and 18.5 per cent methyl alcohol, the apparent energy of activation and the "temperature independent" factor show a variation with temperature. In water solution, both of these quantities have maximum values at a temperature of ~35°C.

These several reaction studies, in which the variation of E_A with temperature was determined, were carried out in media of constant composition, and therefore one factor which causes the rate to change with changing temperature is the change of dielectric constant of the medium with temperature. In general, one would not expect as large a variation in the rate with changing dielectric constant for these reactions involving an ion and a neutral molecule as was true for ion-ion reactions.

It is apparent that not all reactions conform to the Arrhenius equation. Some reactions which now appear to conform to this equation will undoubtedly be shown to have values of E_A which depend upon temperature if more careful measurements are made over a wider range of temperature. It has been suggested that the deviations from the Arrhenius equation are most marked in reactions involving the solvent[223]. Certain points regarding the equilibrium between the activated complex and the reactants are clarified if one adopts the point of view that this equilibrium is in many respects like an ordinary chemical equilibrium. Thus, it is perfectly reasonable that $\Delta C_p^\ddagger$ should have a value not identically equal to zero. The values of ΔC_p for the most widely studied equilibria in aqueous solution, the ionization equilibria involving weak acids and bases, are very different than zero. The association reactions of a hydrogen ion and a negatively charged base have ΔC_p values of approximately +40 cal./mole[250], while the formation of a positively charged acid from a hydrogen ion and a neutral base (i.e., an ammine) leads to ΔC_p values ranging from 0 (ammonia) to −41 (trimethylammine)[88]. Therefore, it is reasonable that the formation of an activated complex could have associated with it a $\Delta C_p^\ddagger$ value of this magnitude. It has been suggested that values of $\Delta E_A/\Delta T$ as large as 100 cal/deg. are quite amenable to a kinetic or statistical interpretation[170]. Values of $\Delta E_A/\Delta T$ much larger than this may arise in the case of parallel reaction paths or complex mechanisms; in such cases the value of E_A changes with a change of temperature because the apparent rate constant is a composite of several rate constants (and possibly equilibrium constants) which have different temperature coefficients. The surprising thing is not so much the exceptions to the Arrhenius equation as the great number of reactions which appear to conform.

From both an empirical and a theoretical point of view, the rate constant of a chemical reaction may be viewed as depending upon the value of two factors. In the Arrhenius equation, these two factors are the apparent energy of activation, E_A, and the "temperature independent" factor, A. In the collision theory, these two factors, upon which the magnitude of k depends, are P, the probability factor, and E, the activation energy, while in the absolute rate theory, $\Delta S^\ddagger$ and $\Delta H^\ddagger$, the change in entropy and enthalpy associated with the activation process, determine the magnitude of the rate constant. The question of which of these two factors is influenced to the greater extent by changing the catalyst is an interesting one. The answer to the question is not clean cut. It is desirable to examine some data which show the unpredictable nature of the trends.

TABLE 11. VARIATION OF E_A AND A WITH HYDROCHLORIC ACID CONCENTRATION AT 25°C

	Concentration of Hydrochloric Acid		
	0 molar	1 molar	2 molar
E_A (cal)	25,960	25,350	24,740
A (sec.$^{-1}$ mole^{-1} l.)	1.25×10^{15}	7.13×10^{14}	4.28×10^{14}

It is first worthwhile to point out that the energy of activation of a reaction may depend upon the concentrations of the reactants, both catalyst and substrate. Such trends are often overlooked; it is only rather careful work which brings out this concentration effect if it exists. The study of the inversion of sucrose in aqueous solution by Leininger and Kilpatrick brings out trends of E_A and A with hydrochloric acid concentration[160]. At 25°C, the rate constant ($k_{H_3O^+} = k/(H_3O^+)$) depends upon the concentration of hydrochloric acid in a manner given by the equation

$$\log k_{H_3O^+} = \bar{3}.8793 + 0.1992\ (H_3O^+).$$

The manner in which E_A and A depend upon the concentration of hydrochloric acid is shown in Table 11. It is clear that the increase in the rate constant with an increasing concentration of hydrochloric acid is due to the decrease in E_A since the effect of acid concentration upon A is in the direction which would produce the opposite effect. Another acid-catalyzed reaction for which the value of E_A has been found to decrease with increasing concentration of catalyst (hydrochloric acid) is the hydrolysis of ethylal ($CH_2(OC_2H_5)_2$)[161]. On the other hand, the apparent energy of activation for the hydrolysis of diethyl acetal does not depend upon the electrolyte concentration within the experimental error[159]; salt concentrations as high as 3 molar were studied.

The acid- and base-catalyzed reactions which have been studied as a function of the temperature are not numerous. They include the acid- and base-catalyzed iodination of acetone[268], the base-catalyzed decomposition of nitramide[14], the mutarotation of glucose catalyzed by both acids and bases[158, 269], and the base-catalyzed bromination of acetoacetic ethyl ester[245]. In the case of the acetone-iodine reaction and the mutarotation of glucose, the variation in the rate brought about by the use of different catalysts is predominantly due to the changes in the "temperature independent" factor of the Arrhenius equation. It is of interest to note that the apparent energy of activation in the mutarotation reaction is the same for acidic catalysts (average: 17,800 cal for three catalysts) as it is for basic catalysts (average: 17,900 cal for six catalysts). In the case of the iodination of acetone, the activation energy is appreciably greater (2000 to 3500 cal) for the two basic catalysts studied than it is for the acid catalysts. If the mechanism of the acid-catalyzed iodination consists of two bimolecular reactions, the second of which is rate-determining, the apparent activation energy is really the energy of activation for the rate-determining step plus the ΔH of the preceding equilibrium. (See pages 402–404 for a discussion of this mechanism.)

Both the values of E_A and A for the base-catalyzed decomposition of nitramide depend upon the identity of the catalyst; most of the trend in k is due to changes of E_A.

The rate-determining step in most reactions subject to general acid or base catalysis is a proton transfer. The greater the strength of the catalyzing acid, the greater is the rate of this proton transfer. The relationship between the catalytic constant and the strength of the catalyst as an acid (or base) is the familiar Bronsted equation

$$k = GK^{\alpha} \tag{21},$$

which has already been discussed. Because this empirical relationship correlates the rate constant and the dissociation constant of the acidic or basic catalyst so very well, one might expect a correlation of the change of the equilibrium constant with temperature and the change of the catalytic constant with temperature[245]. No general parallelism is to be found for the reactions which have been studied. The ionization equilibria of weak electrolytes in aqueous solution is an interesting and complicated subject[88, 143, 166a, 212, 250]. Until this subject is better understood, it is premature to expect a neat correlation between the trends in k and K with temperature.

The Arrhenius equation parameters may be altered by a change in the medium brought about by the addition of "inert" nonelectrolytes. Rice and Kilpatrick[254] studied the acetone iodination catalyzed by hydrochloric acid in the presence of the nonelectrolytes: sucrose, glycerol, methyl acetate, methyl alcohol, and acetic acid (which is essentially unionized at the hydrogen ion concentration under consideration). The nonelectrolyte concentration was as high as 30 per cent by weight and the rate constant was altered as much as 100 per cent. The temperature coefficient was not influenced by these changes.

THE INFLUENCE OF COMPLEXING AGENTS UPON REACTION VELOCITY

The effect of varying the solvent or the concentration of an *"inert"* salt upon a reaction velocity is generally discussed in terms which do not involve specific interactions of solvent molecules or the *"inert"* electrolyte ions with the reactant molecules. What might be called the chemical nature of these substances (solvent or *"inert"* salt) is largely ignored. On this basis, the effect of a solvent may be correlated with its dielectric constant or internal pressure, and the effect of an ionic solute may be correlated with the ionic strength or possibly the concentration. It is obvious, however, that this simple approach is not valid for all systems. The possibility of a solvent effect or a salt effect being quite specific has been mentioned in some of the discussion already presented.

Those effects which are more conveniently discussed in terms of specific interactions involving the added solutes will now be considered. If the velocity of a reaction is influenced in a relatively large and specific way by the addition of some substance, the role which the added substance plays is often discussed in terms of the complexing of this substance with the reactants and/or the activated complex. If the added solute (the complexing agent) and one or more of the reactants interact to form relatively stable complexes, these complexes should be studied by a means which is independent of the kinetic study. This is not always possible, but it is desirable, nevertheless. Its importance has already been commented upon; the formulae of the predominant forms of the reactants and products, which exist in the solutions in which the kinetic studies are to be made, should be known.

This point can be made clear by the discussion of an example. If A and B react by a reaction path with an activated complex AB, the reaction rate is decreased by the addition of a reagent, C, which unites with A to form a complex AC. In media in which AC is the dominant A-containing species, the rate is inversely proportional to the concentration of C, for the concentration of A is determined by the equilibrium

$$\mathrm{AC} \rightleftarrows \mathrm{A} + \mathrm{C}.$$

If, on the other hand, there is an important activated complex with the composition ABC, the rate constant defined by the equation

$$\text{Rate} = k[\mathrm{A}](\mathrm{B}),$$

where [A] is the total concentration of A-containing species, changes with a change in the concentration of C; it, however, does not show an inverse dependence upon the concentration of C at high concentrations of C. The complete rate law is:

$$\text{Rate} = \frac{(k_1 + k_2K(\mathrm{C}))}{1 + K(\mathrm{C})}\,[\mathrm{A}](\mathrm{B}),$$

where K is the equilibrium quotient for the reaction

$$\mathrm{A} + \mathrm{C} \rightleftarrows \mathrm{AC}.$$

Whether the presence of C increases the rate or decreases the rate clearly depends upon the relative values of k_1 and k_2. An activated complex which involves C may be important even though no complex of A and C (or B and C) has appreciable stability. The reaction, in this case, is third order, and while the data may be interpreted in terms of a sequence of two steps: the unfavorable equilibrium giving AC, and the reaction of AC and B, the data do not prove the existence of the complex AC. The rate law merely establishes the composition of the activated complex, in this case ABC.

The Specific Anion Catalysis in Reactions of Positive Ions

A sharp boundary cannot be drawn between the type of catalysis which is to be discussed in this section and the kinetic salt effect which is exerted upon a reaction between ions of like charge sign. In some reactions between positive ions, it is undoubtedly difficult to say whether or not the catalyzing anion is incorporated into the activated complex. There are reactions, however, for which little doubt exists regarding this point. In particular, some oxidation-reduction reactions which involve two cations are subject to catalysis by specific anions over and above any reasonable kinetic salt effect.

An example of a reaction between two ions of like charge sign which proceeds very much more rapidly in the presence of specific ions of the opposite charge sign is the reaction of iron (III) and tin (II). In solutions of perchloric acid, the rate of this reaction is very low, and it decreases as the acidity is increased[102]. This trend is consistent with a greater rate being associated with reaction paths involving activated complexes in which hydroxyl ions are incorporated. Since various types of experimental evidence (e.g., activity coefficients and absorption spectra) indicate that metal ions and perchlorate ions have little tendency to associate to form ion-pairs or complex ions in dilute aqueous solution, it does not appear reasonable to assume that the activated complexes in cation-cation reactions involve perchlorate ion.* The rate of the reaction of iron (III) and tin (II) is greatly enhanced in the presence of chloride ion; the rate law in such solutions is[87]

$$\text{Rate} = k(\text{Fe}^{\text{III}})(\text{Sn}^{\text{II}}),$$

where k is a function of the concentration of chloride ion, and (Fe^{III}) and (Sn^{II}) represent the stoichiometric concentrations of iron (III) and tin (II). The dependence of k upon the actual concentration of chloride ion is greater than third power in the concentration range 0.04 to 0.48 molar. This chloride ion dependence gives the average number of chloride ions which are in the activated complexes in *addition* to those associated in the pre-

---

* Some reactions are known in which activated complexes involving perchlorate ion are indicated to be important. These include the mercuration of benzene[310] and the exchange of iodine and iodate[157].

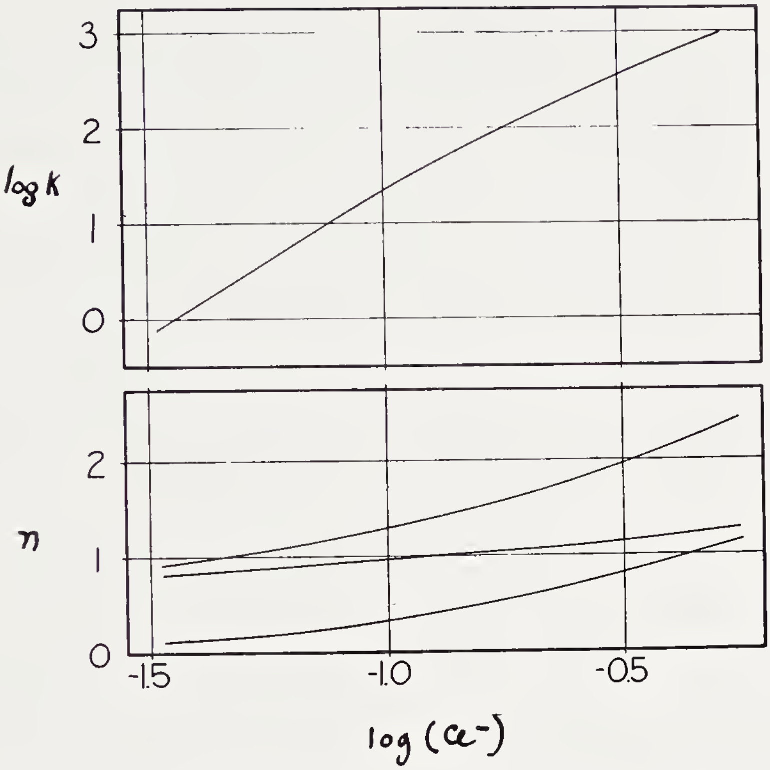

FIG. 24. Quantities pertaining to the iron (III)—tin (II) reaction as a function of the chloride ion concentration. Upper figure: log k versus log (Cl^-). Lower figure: The average number of chloride ions per iron (III) (lowest curve), per tin (II) (middle curve), and the sum of these values (uppermost curve). (Data from Ref. 87)

dominant forms of iron (III) and tin (II) at the same chloride ion concentration. Since the equilibrium quotients for the formation of the iron (III)[251] and tin (II)[56] complex ions: $FeCl^{++}$, $FeCl_2^+$, $FeCl_3$, $SnCl^+$, $SnCl_2$ and $SnCl_3^-$ are known, the average number of chloride ions associated with iron (III) and tin (II) is known as a function of the chloride ion concentration. This information is presented as part of Figure 24. This figure also presents the dependence of k upon (Cl^-).

Although it has frequently been emphasized that the slowness of reactions between ions of like charge may be primarily a matter of the electrostatic repulsion between the reacting ions[300], this factor does not exert the controlling influence on the iron (III)-tin (II) reaction. There is no indication of any contribution to the observed rate by the reaction of Fe^{+++} and $SnCl_2$. Activated complexes involving three or more chloride ions seem to be important and those with the largest number are most important. One factor which would make the reaction paths involving the largest number of chloride ions the most favorable is the probable greater stability of those chloride complexes of tin (III) which involve a large number of chloride ions. If the reaction proceeds by an electron transfer, the tin (III) which is formed as an intermediate (which then rapidly reacts with another iron (III)) will probably have associated with it only those chloride ions which were associated with the tin (II) in the activated complex. This is a consequence of the Franck-Condon principle which leads to the conclusion that the atoms involved in the activated complex are not going to move to an appreciable extent in the time required for an electron transfer. If the activated complex involves a chlorine bridge between the iron (III) and tin (II), this chlorine atom which was originally associated with iron (III) may stay with the tin upon rupture of the activated complex to give iron (II) and tin (III); the process in this case may more appropriately be called a chlorine atom transfer. Duke and Pinkerton suggest this possibility of halogen atom transfer and cite the greater catalytic effect of bromide than chloride as evidence supporting this view. Even though the halogen atom transfer mechanism does not necessitate the production, in the solution, of halogen atoms, it would be expected that a bromine atom would be more easily transferred than a chlorine atom.

Other oxidation-reduction reactions involving metal ions which have been studied quantitatively, and which show catalysis by anions include the thallium (III)-iron (II) reaction in which activated complexes involving hydroxyl ion are important[155]. The reaction of neptunium (IV) and iron (III) to form neptunium (V) and iron (II) is inversely proportional to the third power of the hydrogen ion concentration[154]. This indicates that the activated complex has three more hydroxide ions than to the predominant forms of neptunium (IV) and iron (III) over the hydrogen ion concentration range studied (0.5–1.0M).

A type of reaction which has been much studied in recent years is the exchange of two different oxidation states of the same element. Even though no net chemical reaction occurs when the two different oxidation states of the same element are together in solution; the question of the frequency with which the oxidation state associated with a *particular* atom changes is of interest. This change may be accomplished by a transfer of one (or more if necessary) electron from the one atom to the other. It will be seen that the exchange may also be accomplished by the transfer of an atom in some cases. The usual technique for studying these exchange reactions involves the use of a sample of the element in the one oxidation state which does not have the normal isotopic composition. The difference from the normal isotopic composition may be in the presence, at trace concentrations, of a radioactive isotope, or merely in there being different relative amounts of the stable isotopes of the element. The rate of the exchange is related to the rate at which the isotopic composition of both oxidation states acquire the same value[89]. The dependence of the exchange rate upon the various concentration variables is determined in several runs since the

TABLE 12. THE EXCHANGE OF IRON (II) AND IRON (III) AT 0°C[85, 293]
(ionic strength = 0.50 or 0.55)

Iron (III) Complex	k (l. moles^{-1} sec^{-1})
Fe^{+++}	0.87
$FeOH^{++}$	1010
$FeCl^{++}$	9.7
$FeCl_2^+$	15
FeF^{++}	9.7
FeF_2^+	2.5
FeF_3	0.5

k—the specific rate constant for the reaction of Fe^{++} and the listed iron (III) complex.

concentrations of all chemically distinguishable species remain constant during the course of a particular run.

In general, it is found that the rate of exchange of two cationic species is influenced in a specific way by anions, particularly by those which tend to form complex ions with metal ions (e.g., the halide ions). The exchange of iron (II) and iron (III) has been studied in the presence of perchlorate[85], chloride[85] and fluoride[293] ions. Under all of the conditions studied, the exchange is first order in iron (II) and iron (III). The influence of hydrogen ion, chloride ion and fluoride ion upon the exchange rate can be interpreted in terms of the existence of activated complexes for the exchange reaction which involve hydrated iron (II) and (III) ions alone, and with one hydroxyl, one chloride, two chlorides, one fluoride, two fluorides and three fluorides. Since the equilibrium constants for the association of iron (III) and hydroxyl[251], chloride[251] and fluoride[82, 293] are known, it is convenient to express the rate of the exchange reaction as a rate of the reaction of the particular iron (III) complex and uncomplexed iron (II). Such rate constants are presented in Table 12. An examination of these data clearly indicate that no general statement can be made regarding the relative rates of the reactions involving the complexes with one and two halide ions. The difluoro-complex reacts less rapidly than the monofluoro-complex while the reverse is true for the chloro-complexes.

The following must be kept in mind, however. The rate law tells us only the composition of the activated complex. The activated complex involving one chloride could equally well be formed by the collision of $FeCl^+$ and Fe^{+++}; this possibility is not as appealing as the collision of $FeCl^{++}$ and Fe^{++} since iron (II) chloride appears to be a strong electrolyte[272]. If, however, the exchange proceeds by an electron transfer, the reaction of $FeCl^+$ and Fe^{+++} must proceed at the same rate as the reaction of $FeCl^{++}$ and Fe^{++}. This is a consequence of the principle of microscopic reversibility since an electron transfer from Fe^{++} to $FeCl^{++}$ leads to Fe^{+++} and $FeCl^{+}$. On the other hand, the exchange may proceed by a halogen atom transfer from $FeCl^{++}$ to Fe^{++}; this process leads to $FeCl^{++}$ and Fe^{++}, and the principle of microscopic reversibility would not impose any limitation upon the rate of the reaction of $FeCl^{+}$ and Fe^{+++}. This argument regarding microscopic reversibility was first discussed in connection with exchange reactions by Silverman and Dodson[85]. It appears to be a strong argument for the exchange proceeding by atom transfer in some systems. In some cases an electron transfer between two rather reasonable species leads to highly improbable species (e.g., $FeF_3 + Fe^{++} \rightleftarrows FeF_3^- + Fe^{+++}$). The exchange must, then, also proceed by the path involving the highly improbable species at this same rate. Where this rate can be shown to be impossible on the basis of any reasonable collision frequency, it is probable that the exchange is accomplished by atom transfer rather than by electron transfer.

The exchange reactions of other cationic species which have been shown to proceed by paths involving anions in the activated complex include europium (II)-europium (III) (catalysis by chloride)[90], cerium (III)-cerium (IV) (catalysis by fluoride[192] and hydroxide[84]), and thallium (I)-thallium (III) (catalysis by chloride[83], hydroxide[83, 292] and nitrate[292]).

On the basis of existing data, it seems reasonable to expect a specific effect of anions upon the rate of exchange of the different cationic forms of an element. Such effects do not always correspond to an increase in the rate compared to the rate of exchange of the simple hydrated species. It does appear reasonable, in some systems, to describe the exchange mechanism as an atom transfer rather than as an electron transfer.

The Reactions of Organic Bases Which Are Influenced by the Presence of Metal Ions

A hydrated metal ion is an acid in the Bronsted sense and a metal ion which is not hydrated (or otherwise solvated) is an acid in the Lewis sense. The interaction of such species and organic compounds with unshared electrons is to be expected. Because of such interaction, metal ions play an important catalytic roll in many organic reactions.

An interesting example of a reaction which is influenced by metal ions through complex ion formation is the decarboxylation of nitroacetic acid. In the absence of metal ions other than the alkali metals, this substance reacts by way of a path involving an activated complex of charge −1 as shown by the dependence of the rate upon pH[144, 243]. The mechanism which is strongly suggested is:

$$O_2NCH_2CO_2H \rightleftarrows O_2NCH_2CO_2^- + H^+$$

$$O_2NCH_2CO_2^- \rightarrow O_2NCH_2^- + CO_2\,.$$

The first step is a rapid reversible equilibrium with an equilibrium constant of 0.021 at 18°C. The rates of decarboxylation of the uncharged acid and the ion of charge -2, which is formed in alkaline solution (K_2 for nitroacetic acid is 10^{-9}), are not appreciable compared to the rate of the reaction involving the ion of charge -1. Pedersen has studied the effect of various metal ions upon the rate of this reaction[248]. The data are consistent with the formation of complex ions involving the metal ion and nitroacetate ion which have an inappreciable tendency to decarboxylate. On the basis of this assumption, it is possible to calculate the value of the association equilibrium quotient, $K = (MX^{+n-1})/(M^{+n})(X^-)$. The values of K calculated by Pedersen for a number of metal ions are: Al^{+++}: 3.05, Cu^{++}: 2.77, Be^{++}: 1.82, Cd^{++}: 1.54, Pb^{++}: 1.39, Ni^{++}: 1.14, Zn^{++}: 1.08, Co^{++}: 1.00, Mg^{++}: 0.65, Ca^{++}: 0.50. It appears that the coordination of a metal ion to the carboxylate group renders the nitroacetate ion inactive in the same way that the association of hydrogen ion does.

The bromination of some keto esters, a reaction which is subject to general base catalysis, is influenced by the presence of metal ions. Since the reaction is zero order in bromine, the rate-determining step appears to be the removal of a proton from the carbon which is alpha to the carbonyl group. Ethyl acetoacetate with two hydrogen atoms on the alpha carbon atom brominates in two consecutive first order reactions. Pedersen has studied this reaction in the presence of copper ions, which exert a pronounced catalytic effect upon the first step of the bromination but not the second[246]. The first order rate constant for the reaction in solutions containing acetic acid, sodium acetate and copper (II) is given by the expression

$$k = 0.043\ (1 + 145\ (Cu^{++})) + 19\ (Ac^-)\ (1 + 139\ (Cu^{++})).$$

It is of interest to note that copper ion catalyzes both the reaction path involving water as the base and that involving acetate as the base to the same extent compared to the corresponding reaction paths which are not catalyzed by copper (II). This fact has been cited by Swain as evidence that the mechanism is a termolecular one involving the substrate, an acid (water or copper (II)) and a base (water or acetate ion)[278]. For a similar reaction, the bromination of 2-carbethoxycyclopentanone, however, copper (II) and nickel (II) increase the rate of the reaction by the acetate catalyzed path 3.1 and 2.4 fold, respectively, greater than they increase the uncatalyzed (i.e., water-catalyzed) path[247]. This trend, a greater catalytic activity of the positively charged ion in the path which involves a negatively charged base, is to be expected on the basis of a more favorable entropy of activation.* Thus, the results in the case of 2-carbethoxycyclopentanone are really more reasonable than are the results for ethyl acetoacetate. Very

---

* The association of a positive ion and a negative ion in aqueous solution is generally accompanied by an increase of entropy[166a].

reasonable factors, such as the effect of the charge type of the acid and base upon the entropy and energy of activation, lead to the expectation that the catalytic efficiency of an acid (base) is not independent of the base (acid) which is also present in the activated complex. This, of course, makes uncertain any assertion that approximate agreement of kinetic data with equation 22 proves the termolecular mechanism to be the predominant reaction path.

Since the complexing of copper (II) ion in aqueous solution by nonenolic ketones has not been observed, the catalytic role of copper (II) ion in this reaction is predominantly due to its stabilization of the activated complex. There is no way of using the kinetic data to prove or disprove the existence, at a low concentration, of a complex of copper (II) and the ketone. A copper (II) ion coordinated to the oxygen undoubtedly makes easier the shift of electrons which occurs in the activated complex as the α-hydrogen is removed.

Another example of the role of metal ions in the reactions of organic bases is the catalysis of the decarboxylation of dimethyloxaloacetate ion by copper(II)[309]. Since the decarboxylation of the monethyl ester ($C_2H_5O_2CCOC(CH_3)_2COOH$) is not influenced by metal ions, it appears reasonable that the role which the metal ion plays is the coordination of the carboxylate group which is not being lost as CO_2. A chelate type complex involving both the carboxylate group and the oxygen on the adjacent carbon is suggested by Steinberger and Westheimer[309]. This type of complex is also suggested by Pedersen, who investigated the copper (II)- and zinc (II)-catalyzed decomposition of oxaloacetic acid[249]. The complex involving copper (II) and oxaloacetate ion is sufficiently stable with respect to ionization that the equilibrium constant for the reaction: $Cu^{++} + Ox^{=} = CuOx$ can be evaluated from the kinetic data; the zinc (II) complex is less stable and only the product of the equilibrium constant for its formation and the rate constant for its decarboxylation can be evaluated. The complete rate law for the decarboxylation of oxaloacetic acid in the presence of copper ions is:

$$\begin{aligned}\text{Rate} = k_0(H_2Ox) + k_1(HOx^-) + k_2(Ox^=) + k_3(CuOx)\\ + k_4K_4(Cu^{++})(HOx^-),\end{aligned}$$

where $K_4 = (CuOxH^+)/(Cu^{++})(HOx^-)$. (The complex of copper ion and HOx^- is not the predominant species under any of the concentration conditions studied and therefore only the product k_4K_4 can be evaluated.) It is of interest to note that copper (II) ion exerts a net catalytic effect even though those complexes in which copper (II) is coordinated at the acetate carboxylate group would be expected to be inactive. (This expectation is based upon the observed effect of metal ions upon the rate of decarboxylation of nitroacetic acid.)

CATALYSIS IN OXIDATION-REDUCTION REACTIONS

It is not possible to make any broad statement which correlates the rates of all oxidation-reduction reactions with the free energy changes of the overall reaction. Catalysis in oxidation-reduction reactions is of several types; it will be seen that specific properties of the oxidized and reduced forms of a half-reaction couple are important in establishing the rate of an oxidation-reduction reaction.

Some oxidation-reduction reactions are accelerated markedly by the presence, at a low concentration, of a substance which exists in more than one oxidation state. The catalysis may be due to a special combination of relative rates of reaction. The three chemical reactions:

$$\text{(a)}\quad \mathrm{AO + B = BO + A}$$

$$\text{(b)}\quad \mathrm{AO + C = CO + A}$$

$$\text{(c)}\quad \mathrm{BO + C = CO + B}$$

will all proceed essentially to completion if the oxidizing power of the oxidized species shows this trend: AO $>$ BO $>$ CO. The relevant half reactions are

$$(\alpha)\quad \mathrm{A = AO} + a e^-$$

$$(\beta)\quad \mathrm{B = BO} + b e^-$$

$$(\gamma)\quad \mathrm{C = CO} + c e^-$$

and the oxidizing power may be discussed in terms of the oxidation potentials, which would be: E^0_γ more positive than E^0_β, and E^0_β more positive than E^0_α.* (It is to be noted that the formulas AO, BO, and CO denote the oxidized forms of A, B, and C, and not necessarily a species containing one oxygen atom.) If reaction (b) proceeds at a very low rate while reactions (a) and (c) are much more rapid, it would be observed that the oxidation of C by AO is subject to catalysis by BO and/or B. The increase in the overall rate of reaction (b), and the value of the ratio (BO)/(B) during the reaction depend upon the relative rates of reactions (a) and (c). If reaction (a) proceeds much more rapidly than reaction (c), the value of the ratio (BO)/(B) will be high during the course of the reaction, and the overall rate of reaction (b) will depend upon the concentration of C but not on the concentration of AO. If reaction (c) proceeds much more rapidly than reaction (a), the value of the ratio (BO)/(B) will be low during the course of the reaction, and the overall rate of reaction (b) will depend upon the con-

---

* The sign of the oxidation potentials corresponds to the convention used by W. M Latimer[188]. The more negative the half-reaction potential, the greater is the oxidizing power of the oxidized form of the couple.

centration of AO but not upon the concentration of C. These reaction schemes are simple because each element which is involved exists in only two oxidation states. The point of importance in this scheme is the possibility that a substance which exists in more than one oxidation state can, by being successively oxidized and reduced at a relatively large rate, act as a catalyst for a slower oxidation-reduction reaction. A catalyst may act in this way even though the oxidation potentials are such that AO cannot convert a large fraction of the catalyst (B) to its oxidized form (BO). The couple (B-BO) will still act as a catalyst if reactions (a) and (c) are relatively rapid.

Actual reactions which correspond closely to this general scheme are the reactions of oxidation of a great number of reducing agents by peroxydisulfate ion catalyzed by silver (I). The oxidation of chromium (III)[319], vanadium (IV)[320], hydrazine[321], and cerium (III)[65] by peroxydisulfate ion are all catalyzed by silver (I). The reaction rate in each case is independent of the concentration of the reducing agent and is proportional to the first power of the concentration of peroxydisulfate and silver (I). The rate constants for each of these reactions are the same within experimental error. Therefore, activated complexes for each of these reactions are identical and have the composition $AgS_2O_8^-$. The lack of dependence of the reaction rate upon the concentration of the reducing agent indicates that the product (or products) of the decomposition of the activated complex oxidizes the reducing agent at a relatively large rate. Yost has suggested that the products of the rate determining step are Ag^{+++} and $SO_4^=$, and he has shown that silver (III) oxide may be precipitated from a solution prepared by the interaction of silver (I) and peroxydisulfate ion[319]. This is not, of course, direct proof that silver (III) is the primary product of the decomposition of the activated complex. The products might be Ag^{++}, $SO_4^=$ and SO_4^-.* Both silver (II) and silver (III) are present in the reaction mixture, regardless of which is formed initially, since evidence exists that the equilibrium

$$2Ag^{II} \rightleftarrows Ag^{III} + Ag^{I}$$

is established relatively rapidly[235]. This equilibrium is shifted predominantly to the left in concentrated nitric acid[233 234]. It is obvious that the form of the rate law furnishes no information regarding the exact identity of the products of the rate-determining step or the nature of the following reaction steps.

Quantitative studies of the catalysis of reactions in which peroxydisulfate

---

* Since silver exists in two different oxidation states greater than +1, and the sulfate radical SO_4^- may be formed in this reaction mixture, this system is not as simple as the general one outlined in the introduction.

ion is the oxidizing agent are most numerous for silver (I) acting as the catalyst. Other reducing agents do catalyze these reactions, however. Copper (II) is a better catalyst for the peroxydisulfate oxidation of oxalate than silver (I)[6]. The catalysis by copper (II) is so great that its presence at very low concentrations (10^{-7} molar) markedly increases the rate of this reaction. It is suggested that copper (III) and the sulfate radical are produced in the initial kinetic step; this oxidation state of copper is known[213] and has been postulated as an intermediate in a number of other oxidation-reduction reactions[282, 286]. The polymerization of ethylinic compounds is initiated by peroxydisulfate[10, 230]. The addition of certain reducing agents has two major effects upon the reaction: the induction period is shortened and the rate of polymerization is increased. Silver (I) and copper (II) are among the reducing agents which were found to be effective.

Since ozone oxidizes silver (I) to silver (III) at a convenient rate[232], silver (I) should be a catalyst for the oxidation of various reducing agents by ozone. Silver (I) has been used as a catalyst for the ozone oxidation of manganese (II)[313].

Many oxidation-reduction reactions which are of importance in analysis are subject to catalysis by small amounts of substances which exist in more than one oxidation state. In many of these systems, the catalysis is probably due to the type of oxidation-reduction cycle already discussed. From the point of view of simplicity in the calculation of the results of the analysis, it is an advantage to add the catalyst in the form in which it will exist at the endpoint. During the course of the reaction, the relative concentrations of the catalyst in its several oxidation states depend upon the reagent concentrations and the relative rates of the several reactions.

Because they exist in several oxidation states, the halogens and their compounds are effective catalysts for many oxidation-reduction reactions. Iodine compounds are catalysts for a number of cerium (IV) oxidation reactions[271, 322]. In the presence of hydrochloric acid at a concentration of one molar or greater, cerium (IV) oxidizes iodide to ICl_2^-[281], and therefore iodine monochloride is the most convenient iodine compound to use as a catalyst in cerium (IV) oxidation reactions. The oxidation reactions of oxalate[311], arsenic (III)[312], and antimony (III)[312] by cerium (IV) are catalyzed by iodine monochloride. This catalytic action does not appear to be due to an oxidation-reduction cycle involving ICl_2^- and iodine in a lower oxidation state since Willard and Young[311] have observed that ICl_2^- does not oxidize oxalate in hydrochloric acid solution. This suggests that the catalysis may be through an oxidation-reduction cycle involving ICl_2^- and a higher oxidation state of iodine. Halide catalysis of the permanganate oxidation of arsenic (III) has been discussed by Lang[186].

Osmium exists in a number of oxidation states, the range extending to

+8. Osmium tetroxide catalyzes the oxidation of arsenic (III) by cerium (IV) or permanganate[100]. The chlorate oxidation of fumaric and maleic acids to racemic and mesotartaric acids is catalyzed by osmium tetroxide[151, 221]. Kinetic studies indicate that the activated complex does not contain chlorate[323]. Presumably a lower oxidation state of osmium is formed in the rate-determining or some following step; this is then rapidly reoxidized to the higher oxidation state by chlorate. The oxidation of bromide ion by perchlorate ion is catalyzed by osmium (IV) in a reaction which is zero order in bromide ion in its initial stages[67]. Presumably the rate-determining step is a reaction in which osmium (IV) is oxidized to a species which oxidizes bromide at a relatively large rate. Ruthenium salts also catalyze the oxidation of bromide by perchlorate ion[66].

If two adjacent, stable oxidation states of an element differ in oxidation number by two units, it is to be concluded that the oxidation state which is intermediate between these two extremes is unstable with respect to disproportionation. Such intermediate oxidation states may be of so low an order of stability as to completely escape detection under all concentration conditions, or they may be dominant in solution only under some narrow range of concentration conditions. It is clear from the preceding discussion that such intermediates may be extremely important in catalysis. A group of organic substances which are analogous to the element with the two stable oxidation states differing by two units is the quinone-hydroquinone type of substance. The unstable intermediate in this case is the semiquinone[219, 220]. By taking part in a one electron change oxidation-reduction cycle, a quinone or hydroquinone type substance is converted to the corresponding semiquinone and back again:

$$\begin{array}{lllcll}
 & \mathrm{AO} & + \mathrm{H_2Q} & = & \mathrm{A} & + \mathrm{HQ} \\
 & \mathrm{HQ} & + \mathrm{B} & = & \mathrm{BO} & + \mathrm{H_2Q} \\ \hline
\text{Net:} & \mathrm{AO} & + \mathrm{B} & = & \mathrm{BO} & + \mathrm{A}
\end{array}$$

$$\begin{array}{lllcll}
\text{or} & \mathrm{B} & + \mathrm{Q} & = & \mathrm{HQ} & + \mathrm{BO} \\
 & \mathrm{AO} & + \mathrm{HQ} & = & \mathrm{A} & + \mathrm{Q} \\ \hline
\text{Net:} & \mathrm{AO} & + \mathrm{B} & = & \mathrm{BO} & + \mathrm{A}.
\end{array}$$

If either of these sequences of reactions occurs at a greater rate than the overall reaction in the absence of quinone or hydroquinone, the reaction is subject to catalysis by the quinone or hydroquinone. In addition to the possibilities of catalysis by these two paths, two successive one electron oxidations (reductions) by a one electron oxidizing agent (reducing agent) place the catalytic species in a state where it can take part in a two electron oxidation (reduction) of the reducing agent (oxidizing agent):

$$\begin{array}{lllll} & AO + H_2Q & = & HQ + A \\ & AO + HQ & = & Q + A \\ & Q + D & = & DO + H_2Q \\ \hline \text{Net:} & 2AO + D & = & DO + 2A \end{array}$$

Therefore, substances of the quinone or hydroquinone type may catalyze a reaction in which a one electron reagent *and* a two electron reagent are the reactants. The form of the rate law will not necessarily allow a decision regarding which of these mechanisms is correct. The substances which are called two electron reagents are those for which the intermediate oxidation state is of so low a stability as to have escaped detection.

Catalysis of a simple inorganic reaction by organic substances of this type occurs in the reaction of titanium (III) and iodine in acid solution[265, 316]. Johnson and Winstein have studied a number of catalysts and have found a variety of types of behavior[316]. With pyocyanine and α-hydroxyphenazine, the rate of the catalyzed reaction is *independent* of the iodine concentration and is first order in titanium (III). The rate of the catalyzed reaction with indigo carmine acting as the catalyst is independent of the titanium (III) concentration and is first order in iodine (triiodide is actually the dominant species). For some other catalysts, there appear to be two terms in the rate law for the catalyzed reaction

$$\text{Rate} = k(\text{Ti}^{\text{III}})(\text{I}_3^-) + k'(\text{Ti}^{\text{III}});$$

although this was not checked thoroughly, the dependence of k and k' upon the concentration of catalyst seems to be first order. A possible reaction path corresponding to the third order term (pseudo-second order) involves a rate-determining step in which titanium (III) reacts with the oxidized form of the catalyst, which is in equilibrium with the reduced form of the catalyst (which is the dominant form), triiodide, and iodide. (The inverse dependence of the rate upon iodide ion concentration which is required by this mechanism is suggested by the relevant data.)

Induced Reactions

Reactions Involving Simple Coupling. When the substances which are involved in an oxidation reduction reaction exist in more than two oxidation states, the mechanism of catalysis may be more complex than is possible when each reactant and catalyst exists in two oxidation states. If only elements which have two oxidation states are involved, the E value (at 25°C),

$$E = E^0 - \frac{0.059}{n} \log \frac{(\mathrm{Ox})}{(\mathrm{Red})},$$

for any couple in the system cannot be more negative than the value which corresponds to the ratio of the concentrations of the oxidized and reduced forms of the *oxidizing agent* at that time if all other substances (reactants or catalysts) were initially present in the reduced forms. That is, there will not be produced in such a reaction system any oxidizing agent with a more negative oxidation potential (E not E^0) than that potential produced by the original oxidizing agent. This is not necessarily true when elements which exist in several oxidation states take part in the reactions. Consider, for example, the reactions which can occur in a solution containing A^{+++} and B^+, A^{+++} and C^+, and A^{+++}, B^+ and C^+, if the relevant values of the oxidation potentials are given by the potential diagrams:*

$$\underbrace{A^+ \;\underline{\;-1.40\;}\; A^{++} \;\underline{\;-0.60\;}\; A^{+++}}_{-1.00}$$

$$B^+ \;\underline{\;-0.45\;}\; B^{++}$$

$$C^+ \;\underline{\;-1.25\;}\; C^{++}.$$

At equilibrium, solutions containing these substances cannot contain an appreciable concentration of A^{++}, or C^{++} and B^+ together, or C^{++} and A^+ together, or A^{+++} and B^+ together. It might seem unlikely that any combination of relative rates of reaction would lead to a situation in which the concentration of C^{++} could build up to a relatively high value. It can, however; the concentration of C^{++} can build up from an initial value of zero to a higher concentration than corresponds to its equilibrium value in a solution prepared by adding A^{+++} to a mixture of B^+ and C^+ if the rates of the several reactions are:

Relatively fast reactions:

(a) $A^{+++} + B^+ \rightarrow A^{++} + B^{++}$

(b) $A^{++} + C^+ \rightarrow C^{++} + A^+$

---

* These potential diagrams are of the type used by W. M. Latimer[188]. The potential is the E^0 value for the half reaction:

$$\mathrm{Red} = \mathrm{Ox} + ne^-$$

with the sign convention which has already been mentioned.

Relatively slow reactions:

(c) $2A^{++} \rightarrow A^{+} + A^{+++}$

(d) $C^{++} + B^{+} \rightarrow C^{+} + B^{++}$

(e) $C^{++} + A^{+} \rightarrow C^{+} + A^{++}$

(f) $C^{++} + A^{++} \rightarrow C^{+} + A^{+++}$

(g) $A^{++} + B^{+} \rightarrow B^{++} + A^{+}$.

Strictly speaking, it is *incorrect* to say that B^{+} has catalyzed the oxidation of C^{+} by A^{+++}; the amount of C^{+} which is oxidized can in no case exceed the amount of B^{+} which is oxidized. Since no reaction regenerates B^{+}, it is effective only at a relatively high concentration. The net chemical change which occurs, before an appreciable reduction of the C^{++} formed in reaction (b) takes place, may be expressed by the combinations of the two chemical reactions:

$$A^{+++} + 2B^{+} = 2B^{++} + A^{+}$$

and

$$A^{+++} + B^{+} + C^{+} = A^{+} + B^{++} + C^{++}.$$

Eventually the concentration of C^{++} decreases toward its equilibrium value because of its reaction by steps (d), or (e) plus (f), or (e) plus (c). If the relative rates were those indicated but the potential of the $C^{+} - C^{++}$ couple were -0.85 volts, the concentration ratio $(C^{++})/(C^{+})$ would be high at equilibrium in the presence of excess A^{+++}. In both of these situations (i.e., $E^0_{C^+-C^{++}} = -1.25$ and $E^0_{C^+-C^{++}} = -0.85$), the oxidation of C^{+} has been induced by the $A^{+++} - B^{+}$ reaction. In the one case ($E^0_{C^+-C^{++}} = -1.25$), the reaction would not have occurred in the absence of B^{+}; in the other case ($E^0_{C^+-C^{++}} = -0.85$), the reaction would have occurred, but at a lower rate on the basis of the assigned relative rates.

An example of a system in which the first possibility is realized is the induction of the chromium (VI)-manganese (II) reaction by the chromium (VI)-isopropyl alcohol reaction[307]. As the concentration of manganese (II) is raised relative to the isopropyl alcohol concentration, the fraction of the total oxidation state change of chromium (VI) which leads to manganese (II) oxidation approaches one-third. This may also be expressed in terms of the induction factor, which is defined:

$$\text{I.F.} = \frac{\text{equivalents of reducing agent oxidized}}{\text{equivalents of inductor oxidized}}.$$

The reducing agent in this case is the manganese (II), the inductor is the isopropyl alcohol, and the induction factor has the limiting value of 0.5. The usual convention is to use the term reducing agent for the substance which reacts only slowly or not at all; the inductor, which is also a reducing agent, reacts more rapidly. It is possible, in principle, that neither of the reducing agents (B^+ or C^+ in the general discussion) react rapidly with the oxidizing agent in the absence of the other substance. In such a case, the induction factor would have to be more explicitly defined. A mechanism which is consistent with this observed induction factor (and with other observations on the kinetics of this reaction) is:

$$Cr^{VI} + (CH_3)_2CHOH \rightarrow Cr^{IV} + (CH_3)_2CO$$

$$Cr^{IV} + Mn^{II} \rightarrow Cr^{III} + Mn^{III}$$

$$2Mn^{III} \rightarrow Mn^{++} + MnO_2 .$$

The manganese dioxide which is produced is not stable; it is capable of oxidizing chromium (III) to chromium (VI). Therefore, this is an example of an induced reaction which is thermodynamically unfavorable in the absence of the inductor. Although the reaction

$$3Mn^{++} + Cr_2O_7^{=} + 2H^+ = 2Cr^{+++} + 3MnO_2 + H_2O$$

does not go, the reactions with a stoichiometry given by the equations:

$$Cr_2O_7^{=} + 8H^+ + 3(CH_3)_2CHOH = 2Cr^{+++} + 3(CH_3)_2CO + 7H_2O$$

and $$Cr_2O_7^{=} + Mn^{++} + 2(CH_3)_2CHOH + 6H^+ = 2Cr^{+++} + MnO_2 + 2(CH_3)_2CO + 5H_2O$$

do go.*

Induced reactions involving chromium (VI) are numerous; the subject has been reviewed by Westheimer[308]. An oxidation state change of 3 occurs when chromium (VI) is reduced to chromium (III). Therefore, one would expect limiting induction factors of 0.5 or 2 to be observed depending upon whether one-third or two-thirds of this total oxidation state change leads to

---

* In general, it is not desirable to show the oxidation of two reducing agents by a single oxidizing agent in a single chemical equation. Such a chemical equation is the sum of the equations for two independent reactions. The situation existing here is an unusual one however; one of the independent chemical equations, which goes to make up the composite equation, is for a reaction which does not occur independently. Under such circumstances, it actually seems preferable to write, as one chemical equation, the equation which shows the most favorable stoichiometry as far as the number of equivalents of reducing agent oxidized per equivalents of inductor oxidized is concerned.

oxidation of the reducing agent. This expectation is realized; the oxidation of iodide by chromium (VI) induced by iron (II)[34, 214], arsenious acid[207], vanadium (IV)[210], vanadium (III)[210], vanadium (II)[210], and titanium (III)[215] all give induction factors of about 2. The chromium (VI) oxidation of manganese (II) induced by arsenious acid[187] or isopropyl alcohol[307] give induction factors which approach 0.5 at a high value of the concentration ratio (reducing agent)/(inductor). These values are approached at a high value of this concentration ratio because the reducing agent and inductor are competing for the intermediates, Cr^{V} or Cr^{IV}. The value 2 is approached if Cr^{V} is the intermediate which reacts with the reducing agent, and the value 0.5 is approached if Cr^{IV} is the intermediate which reacts with the reducing agent.

This type of induced reaction has been referred to as a simple coupling by Bray and Ramsey[46] instead of the longer term "coupling due to a single intermediate compound"[208]. Under the conditions which are most favorable, the induction factor for induced reactions of this type approaches a definite small value such as ½, 1 or 2. The discussion of the induced reactions involving chromium (VI) makes clear the reason for the induction factor having such simple values.

Induced Catalysis. In some systems the induction factor rises to very large values under the most favorable circumstances. In such a system, the situation corresponds closely to catalysis in the strictest sense of the word. The inductor is consumed, however, and therefore a given amount of inductor will bring about only a finite amount of the induced reaction. A reaction which is induced with a large induction factor must be a reaction which has associated with it a decrease in free energy. The failure of such a reaction to go in the absence of the inductor is a consequence of unfavorable rates and not because the equilibrium is unfavorable. A chain mechanism can account for these extremely large values of the induction factor.

The oxygen oxidation of many reducing agents proceeds very slowly. This has been attributed to the fact that the reaction proceeds through the species, HO_2 (for a one electron reduction) and H_2O_2 (for a two electron reduction)[103, 265]. The potential scheme

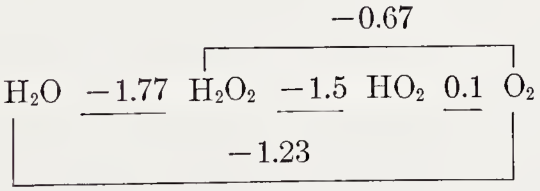

indicates clearly that the thermodynamic tendency for oxygen to be reduced in a reaction step involving a change of oxidation state of one or two per oxygen molecule is much less than its over-all thermodynamic tendency to be reduced to water. If, in the course of an oxidation-reduction reaction which involves a substance that reduces oxygen very slowly, there is produced an intermediate which is rapidly oxidized by oxygen, a chain reaction may be initiated. As an example the oxygen oxidation of A^+, which normally is a slow reaction, is induced by the reaction

$$2C^{++} + A^+ = A^{+++} + 2C^+$$

if the mechanism is:

(a) $C^{++} + A^+ \rightarrow A^{++} + C^+$

(b) $A^{++} + O_2 \rightarrow O_2^- + A^{+++}$

(b′) $H^+ + O_2^- \rightleftarrows HO_2$

(c) $HO_2 + A^+ \rightarrow HO_2^- + A^{++}$

(c′) $HO_2^- + H^+ \rightleftarrows H_2O_2$

(d) $C^{++} + A^{++} \rightarrow A^{+++} + C^+$

(e) $2H^+ + H_2O_2 + A^+ = A^{+++} + 2H_2O$ (a relatively rapid reaction).

The induction factor could have very large values if the chain-breaking step (d) is relatively slow compared to those steps (b and c) which propagate the chain. The induced catalysis of oxygen reactions has been discussed by Bray and Ramsey[46].

In what fundamental way does this reaction scheme differ from the type of catalysis existing in the system: peroxydisulfate, silver (I) ion and reducing agent? As outlined, this reaction scheme does not provide for the regeneration of C^{++}; therefore, the oxidation of A^+ by oxygen will proceed only as long as some C^{++} persists. If the oxidation of C^+ by oxygen were relatively rapid, the catalysis of the reaction:

$$4H^+ + O_2 + 2A^+ = 2A^{+++} + 2H_2O$$

by the couple $C^{++} - C^+$ would differ in no fundamental way from the type of catalytic mechanism by which the couple $Ag^+ - Ag^{++}$ catalyzes oxidations by peroxydisulfate.

The reaction of chlorine and oxalic acid proceeds slowly at ordinary temperatures by a path involving an activated complex of the stoichiometric composition $(ClC_2O_4^- + nH_2O)$[104]. The rate of this reaction is greatly enhanced during the course of the iron (II)-chlorine reaction. The mechanism suggested by Taube[282], which is completely consistent with the experimental observations is:*

Chain Initiating Step:

(a) $Fe^{++} + Cl_2 \rightarrow Fe^{+++} + Cl_2^-$

Chain Carrying Steps:

$H_2C_2O_4 \rightleftarrows H^+ + HC_2O_4^-$

(b) $Cl_2^- + HC_2O_4^- \rightarrow H^+ + 2Cl^- + C_2O_4^-$

(c) $C_2O_4^- + Cl_2 \rightarrow Cl_2^- + 2CO_2$

Chain Breaking Steps:

(d) $Cl_2^- + C_2O_4^- \rightarrow 2Cl^- + 2CO_2$

(e) $Cl_2^- + Cl_2^- \rightarrow 2Cl^- + Cl_2$

The form of the rate law depends upon which of the chain-breaking steps is dominant; at relatively high values of $(Cl_2)/(H_2C_2O_4)$, step (e) is the dominant chain-breaker, while at lower values of this ratio, step (d) becomes the chain-breaking step. Chain lengths as great as 100 are observed under the conditions which favor step (e) as the chain-breaker. A number of substances inhibit the induced reaction. These include vanadium (IV), cerium (III), manganese (II) and ammonium ion. The action of vanadium (IV) is interpreted quantitatively in terms of the steps:†

$$Cl_2^- + VO^{++} \rightarrow 2Cl^- + VO^{+++}$$

and $$VO^{+++} + Fe^{++} \rightarrow VO^{++} + Fe^{+++}$$

or $$VO^{+++} + C_2O_4^- \rightarrow 2CO_2 + VO^{++};$$

the action of VO^{++} is the breaking of chains. Other metal ions have a positive catalytic effect upon the induced reaction; these species are copper (II), nickel (II), praseodymium (III), and cobalt (II). The positive catalysis results because the sequence of two steps,

$$Cl_2^- + Co^{++} \rightarrow Co^{+++} + 2Cl^-$$

$$Co^{+++} + HC_2O_4^- \rightarrow Co^{++} + H^+ + C_2O_4^-\,,$$

---

* The one-electron oxidizing agent which is produced in the reduction of chlorine by iron (II) could equally well be represented as a chlorine atom.

† The species of vanadium (V) is shown as VO^{+++} for convenience; the data do not allow the identification of the species.

proceeds more rapidly than step (b), which accomplishes the same end. In addition, the second of these two steps must be more important than the reaction of cobalt (III) with the chain-carriers, Cl_2^- or $C_2O_4^-$, since its reaction with either of these species would terminate a chain.

The chlorine-oxalic acid reaction is also induced by the manganese (III)-oxalate oxidation-reduction reaction[283]. The sequence of steps which accounts for the action is:

$$Mn^{+++} + nH_2C_2O_4 \rightleftarrows Mn(C_2O_4)_n^{+3-2n} + 2nH^+ \qquad (n = 1, 2 \text{ or } 3)$$

$$\text{(a)}\ MnC_2O_4^+ \rightarrow Mn^{++} + C_2O_4^-$$

$$\text{(b)}\ C_2O_4^- + Cl_2 \rightarrow Cl_2^- + 2CO_2$$

$$\text{(c)}\ Cl_2^- + Mn^{++} \rightarrow Mn^{+++} + 2Cl^-$$

$$\text{(d)}\ C_2O_4^- + Mn(C_2O_4)_n^{+3-2n} \rightarrow 2CO_2 + Mn^{++} + nC_2O_4^{=}.$$

Steps (b) and (c) carry the chain while (a) initiates the chains and (d) breaks them. Other studies which relate to the decomposition of the manganese (III)-oxalate complex ion include the study by Launer[189], in which it is shown that the oxygen oxidation of oxalate is induced by the manganese (III)-oxalate reaction, and the two studies by Taube, in one of which the manganese (III)-oxalate complex ion equilibria are studied and the rate of decomposition of each of the complex ions is determined[284], and in the other of which the role of manganese (III) in the bromine-oxalic acid reaction is studied[285].

Autocatalysis in Oxidation-Reduction Reactions

A chemical reaction may show an induction period under a number of circumstances. If the rate of the reaction is increased markedly by increasing the concentration of a product, autocatalysis will be observed; if the other paths for the reaction are exceptionally slow compared to the autocatalytic path, an induction period, during which the rate is negligible, will be observed.

An interesting type of autocatalysis arises in certain oxidation-reduction reactions in which one or both of the reactants change oxidation state by two or more units. In its simplest form, the scheme is:

Over-all Reaction:

$$A^+ + 2C^{++} = A^{+++} + 2C^+$$

Relatively Slow Reaction:

$$\text{(a)}\ A^+ + C^{++} \rightarrow A^{++} + C^+$$

Relatively Fast Reaction:

$$\text{(b)}\quad A^{++} + C^{++} \rightarrow A^{+++} + C^{+}$$

$$\text{(c)}\quad A^{+++} + A^{+} \rightarrow 2A^{++}$$

The important point in this reaction scheme is merely that the totally oxidized product, A^{+++}, reacts with A^{+} more rapidly than the reactant, C^{++}, does. Even with as simple a scheme as this one, the course of the reaction will depend upon the magnitude of the relative rate constants. The dependence of the rate upon the concentration of C^{++} will be between zero order and first order. If A^{+++} has built up to a concentration such that reaction (c) is faster than reaction (a), and if, in addition, step (b) is very fast compared to step (c), the rate of the reaction will be independent of the concentration of C^{++}. The first power dependence of the rate upon the concentration of C^{++} is realized under two different sets of conditions: (1) in the early stages of the reaction when $k_a(A^{+})(C^{++})$ is large compared to $k_c(A^{+})(A^{+++})$, and (2) under conditions which correspond to the equilibrium in step (c) being maintained and with step (b) as the rate-determining step. Under these conditions, the rate would also be proportional to $\{(A^{+})(A^{+++})\}^{1/2}$ if the equilibrium in step (c) is displaced to the left.

Actual chemical reactions which correspond to the one just outlined are the oxidation of hydroquinones, α-ketols (—CHOHCO—), α-aminoketones (—$CHNH_2CO$—) and enediols (—COH═COH—). In these systems, the species corresponding to the intermediate A^{++} is the semiquinone radical which has already been mentioned in connection with the catalysis of various oxidation-reduction reactions by substances of this type. The oxidation of such substances by oxygen has been widely investigated, in particular by Weissberger and co-workers. The reaction schemes which apply to these actual systems are, in general, more complicated than the simple one which has been outlined because (a) side reactions may occur, (b) a dimeric species made up of two semiquinone radicals may exist and may be formed from the monomeric semiquinone or directly from the hydroquinone and the quinone, and (c) association between the quinone and semiquinone may occur. A detailed discussion of the rate behavior which is expected in the many limiting situations is presented by LuValle and Weissberger[304]. These oxidation reactions are subject to catalysis and inhibition by other substances[305].

A reaction of importance in analysis which proceeds autocatalytically is the permanganate-oxalate reaction. A review of the kinetics of this reaction has been presented recently[236]. The reaction occurs in two stages; in the initial stage, manganese (VII) reacts with manganese (II) to produce oxalate complexes of manganese (III), and in the second stage, the oxalate complexes of manganese (III) decompose to yield manganese (II) and substances which are rapidly converted to carbon dioxide. The discussion of the second stage of this reaction has already been mentioned in connection with the induction of the chlorine-oxalate reaction by the manganese (III)-oxalate reaction[284, 285]. The direct reaction of manganese (VII) and oxalate is extremely slow if it occurs at all. The important reaction step in the initial stage of the reaction is one in which manganese (II) is oxidized by manganese (VII); therefore the reaction is an autocatalytic one. Since manganese (VII) reacts much more rapidly with a solution containing manganese (II) and oxalate than with one containing only manganese (II), it has been suggested that a complex ion of manganese (II) and oxalate reacts with manganese (VII)[237]. Although considerably more complicated than the simple scheme which was outlined for autocatalysis in oxidation-reduction reactions, the fundamental cause for autocatalysis in this system is analogous to that in the simple one: the rate of reduction of the oxidizing agent by a reduced form of the oxidizing agent is considerably greater than the rate of the direct reaction.

The Catalyzed Decomposition of Hydrogen Peroxide

If a substance contains an element in an oxidation state intermediate between the maximum and minimum values possible for that element, the substance may be unstable with respect to disproportionation. In some systems, the rate of the disproportionation reaction is so low that the substance containing the element in the intermediate oxidation state, although thermodynamically unstable, may be kept for long periods of time.

Such a substance is hydrogen peroxide; in the absence of a catalyst, this compound persists for long periods of time although the reaction

$$2H_2O_2\ (aq) = 2H_2O\ (1.) + O_2\ (g)$$

is accompanied by an enormous decrease in free energy ($\Delta F^0 = -50{,}440$ cal). The homogeneous catalysis of this reaction by some substances is due to the thermodynamic feasibility of hydrogen peroxide oxidizing the reduced form of the catalyst and also reducing the oxidized form of the catalyst[45a]. Substances capable of acting as catalysts through such reaction paths are those for which the value of the oxidation potential is between the values of the oxidation potentials for the hydrogen peroxide half reactions

$$H_2O_2 = O_2 + 2H^+ + 2e^- \qquad E^0 = -0.68$$

$$2H_2O = H_2O_2 + 2H^+ + 2e^- \qquad E^0 = -1.77.$$

In such a case, both of the reactions

$$\text{(a)}\ H_2O_2 + AO = O_2 + A$$

$$\text{(b)}\ H_2O_2 + A = 2H_2O + AO$$

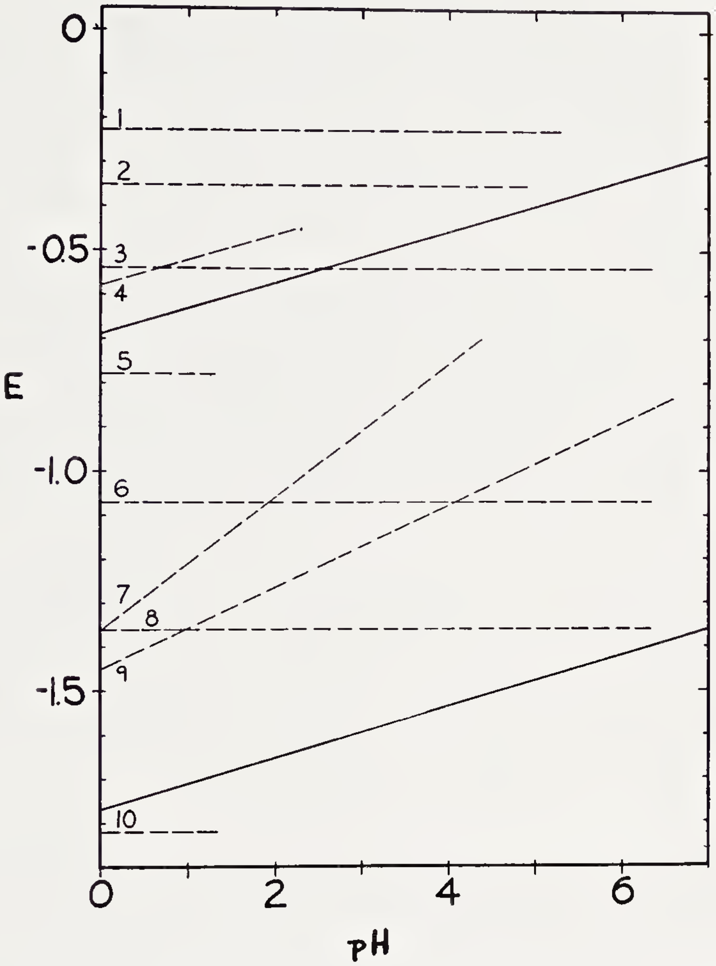

FIG. 25. Values of the formal potential for various couples as a function of pH. Upper solid line: $H_2O_2 = O_2 + 2H^+ + 2e^-$. Lower solid line: $2H_2O = H_2O_2 + 2H^+ + 2e^-$.

1. $Ag(S) + Cl^- = AgCl + e^-$
2. $Cu = Cu^{++} + 2e^-$
3. $3I^- = I_3^- + 2e^-$
4. $H_3ASO_3 + H_2O = H_3AsO_4 + 2H^+ + 2e^-$
5. $Fe^{++} = Fe^{+++} + e^-$
6. $2Br^- = Br_2 + 2e^-$
7. $2Cr^{+++} + 7H_2O = Cr_2O_7^{=} + 14H^+ +. 6e^-$
8. $2\ Cl^- = Cl_2 + 2e^-$
9. $Mn^{++} + 4H_2O = MnO_4^- + 8H^+ + 5e^-$
10. $Co^{++} = Co^{+++} + e^-$

are thermodynamically possible. The dependence of the oxidation potential of the couple involving AO, the oxidized form, and A, the reduced form, upon the concentration of hydrogen ion may be such that both of these reactions are possible over only a limited range of hydrogen ion concentration. Figure 25 shows the oxidation potential values for a number of half reactions. All of those falling between the solid lines, which correspond to the potentials for the half reactions involving hydrogen peroxide, are capable of undergoing reactions (a) and (b). Thermodynamic considerations alone do not allow a prediction of what happens when AO or A is added to a solution containing hydrogen peroxide. The rates of the two reactions exert a controlling influence upon what actually occurs. The concentrations of AO and A change as one or both of these reactions proceed. If the rate of the one reaction is enormously greater than the rate of the other, the final state of the system will be that which is expected on the basis of only the faster of the two reactions occurring. Such is the case of hydrogen peroxide reacts with either of the oxidizing agents cerium (IV) in dilute sulfuric acid[286], or permanganate in dilute acid[171]. In both of these systems, the rate of reduction of hydrogen peroxide by the reduced form of the couple is negligible compared to the rate of oxidation of hydrogen peroxide by the oxidized form of the couple.

Those systems for which the rates of these two reactions are comparable are of considerable interest. In this case, the concentrations of AO and A will be comparable when the two reactions (a and b) are proceeding at the same rate. At this point a steady state will exist; the concentrations of AO and A will undergo no further change, and the net change occurring in the system will be the reaction

$$2H_2O_2 = 2H_2O + O_2 .$$

The substances AO and A are, under such conditions, catalysts for the decomposition of hydrogen peroxide.

The AO-A oxidation-reduction couples which catalyze the decomposition of hydrogen peroxide by a steady state mechanism of this type include: $Br_2 - Br^-$[42a, 43, 104a, 196a, 198], $Cl_2 - Cl^-$[46a, 65a, 197, 212a], $I_3^- - I^-$[1, 47a, 193a, 193b, 196, 294a, 318], and $I_2 - IO_3^-$[42, 44, 45, 193].

It is clear that this steady state is not an equilibrium. These two reactions which are proceeding at the same rate are not the reverse of one another; they have been called compensating reactions by Abel[1], and Bray and Livingston[43]. Their net result leaves the concentrations of all substances except hydrogen peroxide and oxygen constant. Equating the rates of the two compensating reactions, as expressed by the two rate laws, leads to an equation in which a function of the concentrations is equal to a constant. In the case of the $Br_2 - Br^-$ system, the two rate laws are:

$$d(Br_2)/dt = k_1 \, (H_2O_2)(Br^-)(H^+),$$

and

$$-d\,(Br_2)/dt = k_2 \, (H_2O_2)(Br_2)(Br^-)^{-1}(H^+)^{-1},$$

and the steady state quotient is

$$R = \frac{k_1}{k_2} = \frac{(Br_2)}{(H^+)^2(Br^-)^2}$$

Livingston[198] found that the value of R/y^4 is 1.7 ± 0.2 at 25° (y is the mean activity coefficient of hydrobromic acid). (It is to be noted, however, that Griffith and McKeown[104a] have presented data which suggest that a true steady state is not realized; this is a point which deserves further attention.)

Catalysis of the decomposition of hydrogen peroxide may also proceed by the way of a mechanism involving species containing hydrogen peroxide and the catalyst. Hydrogen peroxide does form complex species with iron (III)[87a], chromium (VI)[266a, 266b], molybdenum (VI)[266c] and tungsten (VI)[266c], and these elements *do* catalyze the decomposition of hydrogen peroxide. The role which the complex species plays in the catalytic decomposition of hydrogen peroxide is not easily established, however. The catalysis in the iron (II)-(III) system will be discussed in the next section of this chapter, and catalysis by chromium, molybdenum, and other elements is discussed in the recent review by Baxendale[13a].

Reactions Involving Hydrogen Peroxide and Iron in Oxidation States (II) or (III)

The oxidation potential for the iron (II)-iron (III) couple has a value which falls in the range qualifying this couple to catalyze the hydrogen peroxide decomposition by a steady state mechanism of the type already discussed; the actual situation is very complex. The reactions involving these substances have been studied by many workers; recent reviews on this subject include those by Abel[2], Medalia and Kolthoff[172], Uri[291], Baxendale[13a], and Weiss[301a]; recent experimental studies which shed considerable light upon the mechanisms of these reactions are those by Barb, Baxendale, George and Hargrave[11, 12], and Cahill and Taube[286].

The reactions which occur when hydrogen peroxide, iron (II) and/or iron (III) are brought together in an acid solution depend upon the relative concentrations of these substances. It is convenient to first discuss the reaction of iron (II) and hydrogen peroxide in solutions containing approximately equivalent amounts of iron (II) and hydrogen peroxide or an excess of iron (II). Under such conditions, the chemical change corresponds to the stoichiometric equation[11],

$$H_2O_2 + 2Fe^{++} + 2H^+ = 2Fe^{+++} + 2H_2O,$$

and the rate is given by the rate law:

$$-d(Fe^{++})/dt = k_0\ (Fe^{++})(H_2O_2).$$

An unstable intermediate must result from the decomposition of an activated complex with the composition $H_2O_2Fe^{++}$; it may be OH or a species involving iron (IV). In the medium under discussion (i.e., one containing excess iron (II)), these intermediates are rapidly reduced by iron (II).

either directly or through other intermediates which result from the interaction of the OH or iron (IV) and hydrogen peroxide. Since the formation of either iron (IV) or hydroxyl is consistent with the form of the rate law, other types of information must be used in an effort to decide between these possibilities. Extremely useful information in elucidating this problem has been obtained by Cahill and Taube[286] in the study of the relative rates of reduction of the isotopic species $HOO^{18}H$ and HOOH by a number of reducing agents including iron (II).* The ratio of the relative rates of the reactions involving $HOO^{18}H$ and HOOH is called the isotope fractionation factor and its value is characteristic of the process which leads to the reduction of the hydrogen peroxide. The fractionation factors for the reducing agents, iron (II), copper (I), tin (II), and chromium (II), are essentially the same while that for titanium (III) is significantly different. This suggests that the mechanism in the case of the titanium (III) reaction is different than the mechanism of the reactions of the other reducing agents. The magnitude of the observed fractionation factors indicates that the reducing agents other than titanium (III), a reducing agent which is oxidized only by a one-electron change, react by a two-electron change. It is suggested by Cahill and Taube that the observed *greater* discrimination between the isotopic peroxide species by the two-electron reducing agents is due to the absence of vibration of the oxygen-oxygen bond in the activated complex; the magnitude of the fractionation factor for these reducing agents is just about the value expected on the basis of the difference of the zero point vibrational energies of the isotopic hydrogen peroxide molecules. Thus, this is evidence that iron (IV) is formed in the decomposition of the activated complex $H_2O_2Fe^{++}$ (step 2 of suggested mechanism).

At a higher concentration of hydrogen peroxide relative to iron (II), oxygen is evolved; that is, hydrogen peroxide decomposes in a reaction catalyzed by iron (II), or the hydrogen peroxide decomposition is induced by the iron (II)-hydrogen peroxide reaction. The value of the ratio $(H_2O_2)/(Fe^{++})$ at which the oxygen evolution becomes important depends upon the concentrations of iron (III) and hydrogen ion. A relatively high concentration of iron (III) and a relatively high pH value favor oxygen evolution. The observed dependence upon the iron (III) concentration suggests that iron (III) is a reactant in the step leading to oxygen production; this point is incorporated in recently suggested mechanisms[11, 12] but it was not in the earlier mechanism suggested by Haber and Weiss[114].† The observation regarding the hydrogen ion concentration dependence suggests that a reactant in the reactions leading to oxygen production involves

---

* Unlabeled oxygen atoms have mass number sixteen.

† Modifications of this mechanism have been suggested by J. Weiss[301, 301a] and N. Uri[291].

OH^- or is a species containing fewer hydrogen ions than the dominant form of that particular substance. A very significant point in the elucidation of the reaction mechanism is the observation that the amount of oxygen evolved concurrent with the reduction of a certain amount of iron (II) increases with an increase in the hydrogen peroxide concentration but approaches a maximum value (which depends upon the pH) and does not increase further with an extended increase in the hydrogen peroxide concentration. Therefore the reaction step which gives rise to oxygen doesn't involve hydrogen peroxide. This observation indicates that some facets of the original Haber-Weiss mechanism are incorrect.

A single rate law cannot be written for the rate at which oxygen is produced in the decomposition of hydrogen peroxide catalyzed by iron (III). At high values of $(H_2O_2)/(Fe^{III})$, the observed rate is given by the equation[12]

$$-d(H_2O_2)/dt = k(H_2O_2)(Fe^{+++})(H^+)^{-1}.$$

When the value of $(H_2O_2)/(Fe^{III})$ is diminished, the observed rate is given by the equation

$$-d(H_2O_2)/dt = k'(H_2O_2)^{3/2}(Fe^{+++})(H^+)^{-n}$$

where n was not determined exactly.

It is significant that the isotope fractionation factor in the *reduction* of hydrogen peroxide during its catalytic decomposition in the presence of iron (III) is the same as in the *reduction* of hydrogen peroxide by iron (II). This suggests strongly that the process by which hydrogen peroxide is reduced is the same in the two cases. Since the process leading to hydrogen peroxide reduction in the reaction of hydrogen peroxide and iron (II) involves the activated complex $H_2O_2Fe^{++}$, it is reasonable to believe that the same process is important in reduction in the catalytic decomposition. Iron (II) has been shown to exist in solution during the decomposition of H_2O_2 catalyzed by iron (III)[12]. The postulated intermediate HO_2 (or O_2^-) has been widely accepted as the reducing agents in the catalytic decomposition without any real proof of its role in the reaction[114]. These observations by Cahill and Taube using this new technique suggest that HO_2 (or O_2^-) is *not* the important reducing agent in the iron (III)-catalyzed decomposition of hydrogen peroxide.

To be considered satisfactory, a mechanism must account for all of these observations as well as many pertaining to the induction of other reactions by the iron (II) or (III)-hydrogen peroxide system. Because it is consistent with the isotope fractionation factor data and the observed first order dependence of the rate of hydrogen peroxide decomposition upon the concentration of iron (III) at low values of $(H_2O_2)/(Fe^{III})$, the mechanism suggested by Cahill and Taube is being presented[286].*

Equilibria which are not shifted predominantly to the right:

(a) $Fe^{+++} + H_2O_2 \rightleftarrows FeOOH^{++} + H^+$

(b) $Fe^{IV} + H_2O_2 \rightleftarrows FeOOH^{+++} + nH^+$

Rapid reactions which go essentially to completion:

(α) $Fe^{III} + HO_2 = Fe^{++} + O_2 + H^+$

(β) $Fe^{++} + OH = Fe^{+++} + OH^-$ (or $FeOH^{++}$)

Rate Determining Steps:

Chain Initiation:

(1) $FeOOH^{++} \rightarrow Fe^{++} + HO_2$ (Fe^{III} reaction)

(2) $Fe^{++} + H_2O_2 \rightarrow Fe^{IV} + 2OH^-$ (Fe^{II} reaction)

Chain Carrying:

(2) $Fe^{++} + H_2O_2 \rightarrow Fe^{IV} + 2OH^-$

(3) $FeOOH^{+++} \rightarrow Fe^{+++} + HO_2$

(4) $Fe^{++} + FeOOH^{++} \rightarrow FeO^{++} + FeOH^{++}$

Chain Breaking:

(5) $Fe^{++} + H_2O_2 \rightarrow Fe^{+++} + OH^- + OH$

(6) $Fe^{++} + Fe^{IV} \rightarrow 2Fe^{III}$

(7) $Fe^{++} + HO_2 \rightarrow Fe^{+++} + HO_2^-$

In this scheme, the chain carriers are iron (II) and iron (IV). The observations in the various concentration regions are consistent with this scheme. For the concentration conditions $((Fe^{II})/(H_2O_2) \geqq 1))$ which lead to a reaction conforming to the stoichiometry

$$2Fe^{++} + 2H^+ + H_2O_2 = 2Fe^{+++} + 2H_2O,$$

---

* The number of hydrogen ions appearing in the reactions which involve Fe^{III} or Fe^{IV} is not certain since the degree of hydrolysis of the particular species which are involved is unknown.

a reaction path consisting of (2) and (6), or (2), (b), (3) and (7) dominates. At relatively higher concentrations of hydrogen peroxide, oxygen evolution accompanies the oxidation of iron (II). The reaction path which becomes important under these conditions consists of (2), (b), (3), (α) and (7); the sequence (2), (b), (3) and (α) propagates the chain. In the solutions containing excess iron (III), two possible paths exist. At high $(H_2O_2)/(Fe^{III})$, the path consists of steps (a), (1), (α), (2), (b), (3), (α), (5), (β); the sequence (2), (b), (3) and (α) propagates the chain just as it did in the iron (II) reaction. At lower concentrations of hydrogen peroxide the steps (4) and (6) replace (2) and (5), (β), respectively. Rather long chains are known to be propagated in this system; under conditions of high $(H_2O_2)/(Fe^{III})$, about 10^3 molecules of peroxide are decomposed per initiation.

The details of the reactions of hydrogen peroxide and iron (II) or (III) are of interest not only because of the many facets of this system, which at first sight might be expected to behave simply, but also because other reactions are induced by these reactions. Many organic compounds which are oxidized very slowly by hydrogen peroxide are readily oxidized by hydrogen peroxide in the presence of iron (II). Such a reaction is generally called a Fenton reaction.* A simple example is the oxidation of ethyl alcohol to acetaldehyde which is accomplished by the steps:

$$CH_3CH_2OH + Fe^{IV} \rightarrow Fe^{+++} + H^+ + CH_3\dot{C}HOH$$

$$CH_3\dot{C}HOH + Fe^{+++} \rightarrow Fe^{++} + H^+ + CH_3CHO.$$

In addition to the chain breaking steps already discussed, the reaction of the organic radical and iron (II) will break a chain.

The polymerization of vinyl compounds is promoted by the iron (II)-hydrogen peroxide reaction[13]. Under these conditions, the stoichiometric relationship between the iron (II) and hydrogen peroxide becomes one to one rather than two to one. In this reaction, the organic radicals propagate the chains. It has also been reported that polymerization reactions may be induced by the iron (III)-hydrogen peroxide reaction[12].

Miscellaneous Examples of Catalysis

The Isomerization of Cis and Trans Ethylinic Compounds. The catalysis of the isomerization of cis and trans ethylinic compounds by iodine is of interest. The rate of the conversion of cis-cinnamic acid into the trans isomer in benzene solution is proportional to the square root of the iodine concentration and the first power of the cinnamic acid concentration[81a]. This indicates that the activated complex contains *one* iodine atom and one

---

* The Fenton reaction is discussed by Medalia and Kolthoff[172].

molecule of the ethylinic compound. A similar rate law is observed for the isomerization of dichloroethylene[81b] and diiodoethylene[81c] and for the exchange of iodine atoms between iodine and diiodoethylene. Although the activated complexes for the isomerization of diiodoethylene and for the exchange reaction have the same composition, they are not identical because the observed activation energy for the catalyzed isomerization is approximately 4 kcal greater than the activation energy for the exchange reaction. The exchange reaction, with a rate approximately 100 fold higher than the rate of the isomerization, cannot proceed by the way of an intermediate radical in which there is free rotation of the CHI_2 group around the carbon-carbon bond. The authors of this work suggest that the 4 kcal difference in the activation energies of the two reactions is a reasonable value for the barrier opposing internal rotation in the intermediate $C_2H_2I_3$.

Catalysis in Reactions Involving Molecular Hydrogen in Solution. Of interest because it is the simplest reaction of the simplest molecule as well as because of its relationship to other important reactions of hydrogen is the ortho-para hydrogen conversion. It has been observed that various paramagnetic copper (II) complex ions and chromium (III) complex ions catalyze the ortho-para hydrogen conversion in aqueous solution[313b]. The rate is proportional to the concentration of the ionic catalyst indicating that one copper (II) ion or one chromium (III) is present in the activated complex for the reaction. These authors correlate the catalytic efficiency of the chromium (III) complexes with distance of approach of the hydrogen molecule and the central chromium (III) ion.

Wilmarth and Barsh[313c] have observed that the ortho-para hydrogen conversion is catalyzed in quinoline solution by copper (I) acetate. The reaction is second order in copper (I) acetate and first order in hydrogen. This catalysis by copper (I) acetate is of particular interest since the reduction of copper (II) acetate by hydrogen in quinoline solution is catalyzed by copper (I) acetate (i.e., the reaction is autocatalytic)[313a].

Chloride Catalysis of the Cerium (IV) Oxidation of Bromide Ion. In sulfate media, in which cerium (IV) is predominantly present as the complex ion $Ce(SO_4)_3^{=}$, the rate of oxidation of bromide ion by cerium (IV) follows the rate law:

$$\frac{d(\mathrm{Ce^{IV}})}{dt} = \frac{(\mathrm{Ce^{IV}})}{(\mathrm{SO_4^{=}})} \ \{k_{12}(\mathrm{Br^-})^2 + k_{11}(\mathrm{Br^-})\},$$

where (Ce^{IV}) is the total concentration of cerium (IV) species[166b]. A mechanism consistent with this rate law is:

$$\text{(a)}\ \mathrm{Ce(SO_4)_3^{=} + Br^- \rightleftarrows Ce(SO_4)_2Br^- + SO_4^{=}}$$

$$\text{(b)}\ \mathrm{Ce(SO_4)_2Br^- + Br^- \rightarrow Ce(SO_4)_2^- + Br_2^-}$$

$$\text{(c)}\ \mathrm{Ce(SO_4)_2Br^- + aq \rightarrow Ce(SO_4)_2^- + Br(aq)}.$$

The first reaction is a rapidly established equilibrium which lies far to the left, and the second and third reactions are the rate-determining steps corresponding to the two terms in the rate law. The bromine species Br_2^- and Br(aq) produced in the rate-determining steps are converted to bromine relatively rapidly. In the presence of chloride ion, the rate is greatly enhanced. A reaction path which is first order in chloride ion *and* first order in bromide ion accounts for the catalysis. A mechanism analogous to that consisting of reactions (a) and (b), with one chloride ion substituted for one *or* the other of the two bromide ions, leads to the observed concentration dependences of the catalytic path. The kinetic data do not allow one to say in which of the steps the chloride ion takes part. In any case, the data suggest the formation of the intermediate $BrCl^-$, which would be rapidly converted to bromine and chloride ion.

NEGATIVE CATALYSIS

As was true in the case of positive catalysis, certain difficulties arise in attempting to define negative catalysis. A useful definition, which excludes from consideration examples of retardation of reactions which are brought about by large changes in the concentration conditions, is the following: "A substance will be said to act as a negative catalyst if it decreases the rate of the reaction significantly, when it is present at a concentration which is low compared to the concentration of the least concentrated reactant." It does not seem reasonable to consider a retardation brought about by a major change of the medium as negative catalysis. If the rate of a reaction in a particular solvent is lower than it is in a solvent which can be considered inert, it is reasonable to ascribe this lowering of the rate to the formation of one or more complexes between the reactant molecules and the solvent molecules. In such a case, an appreciable decrease in the rate will result only if an appreciable fraction of the reactant molecules are so complexed; this does not correspond to our definition of negative catalysis. The addition of other solutes may lower the rate of a reaction because they convert a reactant to some less reactive form. This is the situation which exists in the case of the decarboxylation of nitroacetic acid[144, 243] (see pp. 422–423); the addition of hydrogen ion or various metal ions to a solution containing nitroacetic acid or nitroacetate ion diminishes the rate of this reaction because these ions tie up the reactive species, nitroacetate ion. The rate of the reaction can be lowered by no more than a factor of two if one-half of the nitroacetate ions are so tied up; this limiting condition is approached if activated complexes involving the metal ion or hydrogen ion are completely unimportant. Under the concentration conditions which lead to considerable retardation caused by the presence of a metal ion, it would be proper to express the net reaction by an equation which involves the metal ion-nitroacetate complex; it does not seem reasonable to consider this as negative catalysis.

Under what conditions, then, does one observe a retardation of a chemical reaction which *does* correspond to the definition of negative catalysis which has been presented? It appears that a substance which is present at a relatively low concentration may diminish the rate of a chemical reaction in solution for either of two reasons: (1) the substance may act as a chain-breaker in a chain reaction[8, 9, 62, 63], or (2) the substance may be effective in diminishing the catalytic activity of a positive catalyst which is present at relatively low concentrations[209].

The chain reaction in solution which was among the first shown to be subject to negative catalysis is the oxygen oxidation of sulfite ion which proceeds by a chain mechanism[7, 8, 35, 209, 288]. Various alcohols inhibit this oxidation; in the process of acting as an inhibitor, the alcohol is oxidized. Although the inhibitor in a reaction such as this is rendered inactive in its action as an inhibitor, it may be effective at relatively low concentrations if the chain length is quite long. Valuable information regarding the role of the inhibitor may be obtained by a study of the rate at which it disappears in a reaction mixture in which it is acting as an inhibitor. Alyea and Backstrom[7], studying the sulfite oxidation reaction, showed that, at a high enough concentration of inhibitor, the rate of oxidation of the inhibitor was approximately independent of the concentration and the nature of the inhibitor. This limiting situation arises when *every* chain is broken by reaction involving an inhibitor; the more effective an inhibitor is, the lower is the concentration at which this limiting rate is realized.

It has already been pointed out (p. 434) that various oxidizable species inhibit the induced reaction of chlorine and oxalic acid[282]. In the "ideal" inhibitory role played by vanadium (IV), the vanadium (IV) is regenerated in the sequence of steps, the net result of which is the breaking of a chain.

It seems reasonable to call by the term negative catalysis that inhibition which results because a positive catalyst is converted to an inactive form by a complexing agent. In this role, a negative catalyst may exert an enormous influence upon the rate, even though it is present at a very low concentration. Of course, the complexing of a positive catalyst does not necessarily lead to negative catalysis because this complex may also be an active catalyst. An example of negative catalysis, which appears to be due to an interaction of the negative catalyst and a positive catalyst is the fluoride ion inhibition of the manganese (VII)-oxalate reaction[190]. The manganese (III) fluoride complexes do not react with manganese (VII) at a rate which is appreciable compared to the rate of reduction of manganese (VII) by the uncomplexed or oxalate complexed lower oxidation states of manganese. Negative catalysis of this type is possible in the oxidation-reduction reactions which are catalyzed by metal ions which exist in several oxidation states; the metal ion which is a positive catalyst may form relatively stable complex ions which are not as active kinetically as were the simple hydrated ions.

References

1. Abel, E., *Z. Elektrochem.*, **14,** 598–607 (1908); *Z. physik Chem.*, **96,** 1–179 (1920); *Monatsh.*, **41,** 405–21 (1920); *Z. physik Chem.*, **136,** 161–82 (1928).
2. Abel, E., *Oestrr. Chem.-Ztg.*, **49,** 79 (1948).
3. Akerlof, G., *J. Am. Chem. Soc.*, **49,** 2955 (1927).
4. Akerlof, G., *ibid,* **51,** 984 (1929).
5. Akerlof, G., *ibid,* **54,** 4125 (1932).
6. Allen, T. L., *J. Am. Chem. Soc.*, **73,** 3589 (1951).
7. Alyea, H. N., and Backstrom, H. L. J., *J. Am. Chem. Soc.*, **51,** 90 (1929).
8. Backstrom, H. L. J., *J. Am. Chem. Soc.*, **49,** 1460 (1927).
9. Backstrom, H. L. J., *Trans. Faraday Soc.*, **24,** 601 (1928).
10. Bacon, R. G. R., *Trans. Faraday Soc.*, **42,** 140 (1946).
11. Barb, W. G., Baxendale, J. H., George, P., and Hargrave, K. R., *Trans. Faraday Soc.*, **47,** 462 (1951).
12. Barb, W. G., Baxendale, J. H., George, P., and Hargrave, K. R., *Trans. Faraday Soc.*, **47,** 591 (1951).
13. Baxendale, J. H., Evans, M. G., and Park, G. S., *Trans. Faraday Soc.*, **42,** 155 (1946).

13a. Baxendale, J. H., "*Advances in Catalysis*," Vol. IV., pp. 31–86, New York, Academic Press Inc., 1952.

14. Bell, R. P., and Baughan, E. C., *Proc. Roy. Soc. (London)*, **158,** 464–78 (1937).

14a. Bell, R. P., and Baughan, E. C., *J. Chem. Soc.*, **1937,** 1947.

15. Bell, R. P., and Caldin, E. F., *J. Chem. Soc.*, **1938,** 382.
16. Bell, R. P., Lidwell, O. M., and Wright, J., *J. Chem. Soc.*, 1861 (1938).
17. Bell, R. P., and Lidwell, O. M., *J. Chem. Soc.*, 1096 (1939).

17a. Bell, R. P., and Lidwell, O. M., *Proc. Roy. Soc. (London)*, **A176,** 88 (1940).

18. Bell, R. P., "Acid and Base Catalysis," Oxford University Press (1941).
19. Bell, R. P., *ibid.*, p. 3.
20. Bell, R. P., *ibid.*, p. 85.
21. Bell, R. P., *ibid.*, pp. 93–95.
22. Bell, R. P., *ibid.*, pp. 107–111.
23. Bell, R. P., *ibid.*, p. 117.
24. Bell, R. P., *ibid.*, Chap. VII.
25. Bell, R. P., *ibid.*, Chap. VIII.
26. Bell, R. P., *Trans. Faraday Soc.*, **39,** 253 (1943).
27. Bell, R. P., and Prue, J. E., *J. Chem. Soc.*, **1949,** 362.
28. Bell, R. P., and Trotman-Dickenson, A. F., *J. Chem. Soc.*, **1949,** 1288.
29. Bell, R. P., and Higginson, W. C. E., *Proc. Roy. Soc. (London)*, **A197,** 141 (1949).
30. Bell, R. P., Gelles, E., and Moller, E., *Proc. Roy. Soc.*, **A198,** 308 (1949).
31. Bell, R. P., and Waind, G. M., *J. Chem. Soc.*, **1950,** 1979.
32. Bell, R. P., and Clunie, J. C., *Proc. Roy. Soc. (London)*, **A212,** 33 (1952).
33. Bell, R. P., *J. Phys. Colloid Chem.*, **55,** 885 (1951).

33a. Bell, R. P., and Jones, P., *J. Chem. Soc.*, **1953,** 88.

34. Benson, C., *J. Phys. Chem.*, **7,** 1 (1903).

35. Bigelow, S. L., *Z. physik. Chem.*, **26,** 493 (1898).
36. Bjcrrum, N., *Z. anorg. Chem.*, **109,** 275 (1920).
37. Bjerrum, N., *Z. physik Chem.*, **108,** 82 (1924).
38. Bjerrum, N., *Chem. Rev.*, **16,** 287 (1935).
39. Bockris, J. O'M., Bowler-Reed, J., and Kitchener, J. A., *Trans. Faraday Soc.*, **47,** 184 (1951).
40. Bodenstein, M., *Z. Elektrochem.*, **38,** 911 (1932).
41. Branch, G. E., and Calvin, M., "The Theory of Organic Chemistry," New York, Prentice-Hall, Inc., 1941.
42. Bray, W. C., *J. Am. Chem. Soc.*, **43,** 1262 (1921).
42a. Bray, W. C., and Livingston, R. S., *J. Am. Chem. Soc.*, **45,** 1251, 2048 (1923).
43. Bray, W. C., and Livingston, R. S., *J. Am. Chem. Soc.*, **50,** 1654–65 (1928).
44. Bray, W. C., and Liebhafsky, H. A., *J. Am. Chem. Soc.*, **53,** 38 (1931).
45. Bray, W. C., and Caulkins, A. L., *J. Am. Chem. Soc.*, **53,** 44 (1931).
45a. Bray, W. C., *Chem. Rev.*, **10,** 161 (1932).
46. Bray, W. C., and Ramsey, J. B., *J. Am. Chem. Soc.*, **55,** 2279 (1933).
46a. Bray, W. C., and Makower, B., *J. Am. Chem. Soc.*, **55,** 4765 (1933).
47. Bredig, G., *Ulmann's Enzyke techn. Chem.*, **6,** 670 (1909).
47a. Brode, J., *Z. physik Chem.*, **49,** 208 (1904).
48. Bronsted, J. N., *J. Am. Chem. Soc.*, **42,** 761 (1920); **44,** 877 (1922); **44,** 938 (1922); **45,** 2898 (1923).
49. Bronsted, J. N., *Z. physik. Chem.*, **102,** 169 (1922); **115,** 337 (1925).
50. Bronsted, J. N., *Rec. trav. chem.*, **42,** 718 (1923).
51. Bronsted, J. N., and Pedersen, K. J., *Z. physik. Chem.*, **108,** 185 (1923).
52. Bronsted, J. N., and Guggenheim, E. A., *J. Am. Chem. Soc.*, **49,** 2554 (1927).
53. Bronsted, J. N., *Chem. Rev.*, **5,** 322 (1928).
54. Bronsted, J. N, and Wynne-Jones, W. F. K., *Trans. Faraday Soc.*, **25,** 59 (1929).
55. Bronsted, J. N., and Bell, R. P., *J. Am. Chem. Soc.*, **53,** 2478 (1931).
56. Bronsted, J. N., and Vance, J. E., *Z. physik. Chem.*, **163A,** 240 (1933).
57. Bronsted, J. N., Nicholsen, A. L., and Delbanco, A., *Z. physik. Chem.*, **169A,** 379 (1934).
58. Burton, H., and Praill, P. F. G., *J. Chem. Soc.*, **1950,** 1203.
59. Burton, H., and Praill, P. F. G., *ibid.*, **1950,** 2034.
60. Burton, H. and Praill, P. F. G., *ibid.*, **1951,** 726.
61. Christiansen, J. A., *Z. physik Chem.*, **113,** 35 (1924).
62. Christiansen, J. A., *J. Phys. Chem.*, **28,** 145 (1924).
63. Christiansen, J. A., *Trans. Faraday Soc.*, **24,** 596 (1928).
64. Christiansen, J. A., *Z. physik. Chem.*, **28B,** 303 (1935).
65. Cone, W. H., *J. Am. Chem. Soc.*, **67,** 78 (1945).
65a. Connick, R. E., *J. Am. Chem. Soc.*, **69,** 1509 (1947).
66. Crowell, W. R., Yost, D. M., and Carter, J. M., *J. Am. Chem. Soc.*, **51,** 786 (1929).
67. Crowell, W. R., Yost, D. M., and Roberts, J. D., *J. Am. Chem. Soc.*, **62,** 2176 (1940).
68. Daniels, F., and Johnston, E. H., *J. Am. Chem. Soc.*, **43,** 53 (1921).
69. Daniels, F., and Eyring, H., *J. Am. Chem. Soc.*, **52,** 1472 (1930).
70. Dawson, H. M., *et al.*, *J. Chem. Soc.*, **1926,** 2282; *ibid.*, **1928,** 2844; *ibid.*, **1929,** 1884.
71. Dawson, H. M., and Spivey, E., *J. Chem. Soc.*, **1930,** 2180.
72. Dawson, H. M., Pycock, E. R., and Smith, G. F., *J. Chem. Soc.*, **1943,** 517.
73. Davies, C. W., *Trans. Faraday Soc.*, **23,** 351 (1927).

74. Davies, C. W., and Righellato, E. C., *Trans. Faraday Soc.*, **26,** 592 (1930).
75. Davies, C. W., and Money, R. W., *Trans. Faraday Soc.*, **28,** 609 (1932).
76. Davies, C. W., *J. Chem. Soc.*, **1938,** 2093.
77. Davies, C. W., and Wyatt, P. A. H., *Trans. Faraday Soc.*, **45,** 770 (1949).
78. Davies, C. W., and Wyatt, P. A. H., *ibid.*, **45,** 774 (1949).
79. Debye, P., and Huckel, E., *Physik. Z.*, **24,** 185 (1923).
80. Debye, P., and McAulay, J., *ibid.*, **26,** 22 (1925).
81. Debye, P., *Z. physik Chem.*, **130,** 56 (1927).
81a. Dickinson, R. G., and Lotzkar, H., *J. Am. Chem. Soc.*, **59,** 472 (1937).
81b. Dickinson, R. G., and Wood, R. E., *J. Am. Chem. Soc.*, **61,** 3259 (1939).
81c. Dickinson, R. G., Noyes, R. M., and Schomakèr, V., *J. Am. Chem. Soc.*, **67,** 1319 (1945).
82. Dodgen, H. W., and Rollefson, G. K., *J. Am. Chem. Soc.*, **71,** 2600 (1949).
83. Dodson, R. W., and Harbottle, G., *J. Am. Chem. Soc.*, **73,** 2442 (1951).
84. Dodson, R. W., and Gryder, J. W., *J. Am. Chem. Soc.*, **73,** 2890 (1951).
85. Dodson, R. W., and Silverman, J., *J. Phys. Chem.*, **56,** 846 (1952).
86. Duke, F. R., and Courtney, W. G., *Iowa State J. Sci.* **24,** 397 (1950).
87. Duke, F. R., and Pinkerton, R. C., *J. Am. Chem. Soc.*, **73,** 3045 (1951).
87a. Evans, M. G., George, P., and Uri, N., *Trans. Faraday Soc.*, **45,** 230 (1949).
88. Everett, D. H. and Wynne-Jones, W. F. K., *Trans. Faraday Soc.*, **35,** 1384 (1939).
88a. Eyring, H. and Smith, R. P., *J. Phys. Chem.*, **56,** 972 (1952).
89. Friedlander, G. and Kennedy, J. W., "Introduction to Radiochemistry," Chap. XIIIB, New York, John Wiley & Sons, Inc., 1949.
90. Garner, C. S., and Meier, D. J., *J. Phys. Chem.*, **56,** 853 (1952).
91. Gillespie, R. J., and Millen, D. J., *Quart. Revs.*, **2,** 277 (1948).
92. Glasstone, S., *J. Chem. Soc.*, 723 (1936).
93. Glasstone, S., Laidler, K. J., and Eyring, H., "The Theory of Rate Processes," New York, McGraw-Hill Book Company, 1941.
94. Glasstone, S., Laidler, K. J., and Eyring, H., *ibid.*, pp. 16-17.
95. Glasstone, S., Laidler, K. J., and Eyring, H., *ibid.*, p. 196.
96. Glasstone, S., Laidler, K. J., and Eyring, H., *ibid.*, pp. 403-410.
97. Glasstone, S., Laidler, K. J., and Eyring, H., *ibid.*, p. 419.
98. Glasstone, S., Laidler, K. J., and Eyring, H., *ibid.*, pp. 419-423.
99. Glasstone, S., Laidler, K. J., and Eyring, H., *ibid.*, p. 427.
100. Gleu, K., *Z. anal. Chem.*, **95,** 305 (1933).
101. Glueckauf, E., *Nature*, **163,** 414 (1949).
102. Gorin, M., *J. Am. Chem. Soc.*, **58,** 1787 (1936).
103. Gorin, M., *Trans. N. Y. Acad. Sci.*, **40,** 123 (1940).
104. Griffith, R. O., and McKeown, A., *Trans. Faraday Soc.*, **28,** 518 (1932).
104a. Griffith, R. O., and McKeown, A., *J. Am. Chem. Soc.*, **58,** 2555 (1936).
105. Gross, P., and Schwarz, K., *Monatsh.*, **55,** 287 (1930).
106. Gross, P., and Iser, M., *Monatsh.*, **55,** 329 (1930).
107. Grube, G., and Motz, G., *Z. physik. Chem.*, **118,** 145 (1925).
108. Grube, G., and Schmid, G., *Z. physik. Chem.*, **119,** 29 (1926).
109. Guggenheim, E. A., *J. Phys. Chem.*, **33,** 842 (1929); **34,** 1540 (1930).
110. Guggenheim, E. A., *Phil. Mag.*, **19,** 606 (1935).
111. Guggenheim, E. A., *ibid.*, [7], **19,** 588 (1935); **22,** 322 (1936).
112. Guggenheim, E. A., *Trans. Faraday Soc.*, **34,** 263 (1938).
113. Guggenheim, E. A., and Wiseman, L. A., *Proc. Roy. Soc.* (*London*), **A203,** 17 (1950).

114. Haber, F., and Weiss, J., *Proc. Roy. Soc.*, **A147,** 332 (1934).
115. Halban, H. v., *Z. physik Chem.*, **67,** 129 (1909).
116. Hall, N. F., *Chem. Rev.*, **8,** 191 (1931).
117. Hartman, R. J., Hochanadel, C. J., and Bobalek, E. G., *J. Am. Chem. Soc.*, **68,** 2071–4 (1946).
118. Hammett, L., and Deyrup, A. J., *J. Am. Chem. Soc.*, **54,** 2721 (1932).
119. Hammett, L., and Deyrup, A. J., *ibid.*, **54,** 2734 (1932).
120. Hammett, L., and Paul, M., *J. Am. Chem. Soc.*, **56,** 827 (1934).
121. Hammett, L. P., and Paul, M. A., *ibid.*, **56,** 830 (1934).
122. Hammett, L., *Chem. Rev.*, **16,** 67 (1935).
123. Hammett, L. P., and Farinacci, N. T., *J. Am. Chem. Soc.*, **59,** 2542 (1937).
124. Hammett, L. P., and Zucker, L., *J. Am. Chem. Soc.*, **61,** 2779, 2785 (1939).
125. Hammett, L. P., and Zucker, L., *ibid.*, **61,** 2791 (1939).
126. Hammett, L. P., "Physical Organic Chemistry," New York, McGraw-Hill Book Company, 1940.
127. Hammett, L. P., *ibid.*, Chap. 5.
128. Hammett, L. P., *ibid.*, Chap. 6.
129. Hammett, L. P., *ibid.*, Chap. 8.
130. Hammett, L. P., *ibid.*, pp. 107–109.
131. Hammett, L. P., *ibid.*, pp. 255-256.
132. Harned, H. S., *J. Am. Chem. Soc.*, **40,** 1461 (1918).
133. Harned, H. S., and Seltz, H., *J. Am. Chem. Soc.*, **44,** 1475 (1922).
134. Harned, H. S., and Pfanstiel, R., *J. Am. Chem. Soc.*, **44,** 2193 (1922).
135. Harned, H. S., and Akerlof, G., *Trans. Faraday Soc.*, **24,** 666 (1928).
136. Harned, H. S., and Owen, B. B., "The Physical Chemistry of Electrolytic Solutions," 2nd Ed., New York, Reinhold Publishing Corp., 1950.
137. Harned, H. S., and Owen, B. B., *ibid.*, Chap 7.
138. Harned, H. S., and Owen, B. B., *ibid.*, Chap. 14.
139. Harned, H. S., and Owen, B. B., *ibid.*, p. 26.
140. Harned, H. S., and Owen, B. B., *ibid.*, pp. 145-8.
141. Harned, H. S., and Owen, B. B., *ibid.*, p. 385.
142. Harned, H. S., and Owen, B. B., *ibid.*, pp. 397–405.
143. Harned, H. S., and Owen, B. B., *ibid.*, pp. 508–516, 529–536.
144. Heuberger, J. F., *Svensk. Kem. Tid.*, **38,** 340, 378 (1926).
145. Hildebrand, J. H., and Scott, R. L., "The Solubility of Nonelectrolytes," New York, Reinhold Publishing Corp., 1950.
146. Hill, T. L., *J. Chem. Phys.*, **11,** 545, 552 (1943); **12,** 147 (1944).
147. Hinshelwood, C. N., and Pickles, N. J. T., *J. Chem. Soc.*, **1936,** 1353.
148. Hinshelwood, C. N., and Fairclough, R. A., *J. Chem. Soc.*, **1938,** 236.
149. Hinshelwood, C. N., and Raine, H. C., *J. Chem. Soc.*, **1939,** 1378.
150. Hoff, J. H. Van't, *Vorlesungen*, **1,** 219 (1898).
151. Hoffman, K. A., Ehrhart, O., and Schneider, O., *Ber.*, **46,** 1657 (1913).
152. Hughes, E. D., Ingold, C. K., and Reed, R. I., *J. Chem. Soc.*, **1950,** 2400.
153. Hughes, E. D., *Quart. Rev.*, **5,** 245 (1951).
154. Huizenga, J. R., and Magnusson, L. B., *J. Am. Chem. Soc.*, **73,** 3202 (1951).
155. Johnson, C. E., *J. Am. Chem. Soc.*, **74,** 959 (1952).
156. Jones, C. M., and Lewis, W. C. McC., *J. Chem. Soc.*, **1920,** 1120.
157. Kennedy, J. W., and Myers, O. E., *J. Am. Chem. Soc.*, **72,** 897 (1950).
158. Kilpatrick, M., and Kilpatrick, M. L., *J. Am. Chem. Soc.*, **53,** 3698 (1931).
159. Kilpatrick, M., and Riesch, L. C., *J. Phys. Chem.*, **39,** 561 (1935).

160. Kilpatrick, M., and Leininger, P. M., *J. Am. Chem. Soc.*, **60,** 2891 (1938).
161. Kilpatrick, M., and Leininger, P. M., *ibid.*, **61,** 2510 (1939).
162. Kilpatrick, M., in "Handbuch der Katalyse", Bd II. Katalyse in Losungen. Edited by G. M. Schwab. J. Springer, Vienna.
163. Kilpatrick, M., and Ciapetta, F. G., *J. Am. Chem. Soc.*, **70,** 639 (1948).
164. Kilpatrick, M., *Trans. N. Y. Acad. Sci.*, **51,** 673 (1949).
165. King, C. V., and Josephs, J. J., *J. Am. Chem. Soc.*, **66,** 767 (1944).
166. King, C. V., and Chatenever, A., *J. Am. Chem. Soc.*, **71,** 3587 (1949).
166a. King, E. L., *J. Chem. Ed.* **30,** 71 (1953).
166b. King, E. L., and Pandow, M. L., *J. Am. Chem. Soc.*, **75,** 3063 (1953).
167. Kirkwood, J. G., *J. Chem. Phys.*, **2,** 351 (1934).
168. Kirkwood, J. G., and Westheimer, F. H., *J. Chem. Phys.*, **6,** 506, 513 (1938).
169. Kiss, A. von, and Vass, P., *Z. anorg. allgem. Chem.*, **217,** 305 (1934).
170. Kistiakowsky, G. B., and Lumry, R., *J. Am. Chem. Soc.*, **71,** 2006 (1949).
171. Kolthoff, I. M., and Sandell, E. B., "Textbook of Quantitative Inorganic Analysis," p. 604, New York, The Macmillan Company, 1948.
172. Kolthoff, I. M., and Medalia, A. I., *J. Polymer Sci.*, **4,** 377 (1949).
173. Kossiakoff, A., and Harker, D., *J. Am. Chem. Soc.*, **60,** 2047 (1938).
174. Kraus, C. A., and Bray, W. C., *J. Am. Chem. Soc.*, **35,** 1383 (1913).
175. Kraus, C. A., and Fuoss, R. M., *J. Am. Chem. Soc.*, **55,** 1019 (1933).
176. Laidler, K. J., and Eyring, H., *Ann. N. Y. Acad. Sci.*, **39,** 303 (1940).
177. Laidler, K. J., "Chemical Kinetics," New York, McGraw-Hill Book Company, 1950.
178. Laidler, K. J., *ibid.*, p. 75.
179. LaMer, V. K., and Mason, C. F., *J. Am. Chem. Soc.*, **49,** 410 (1927).
180. LaMer, V. K., and Fessenden, R. W., *J. Am. Chem. Soc.*, **54,** 2351 (1932).
180a. LaMer, V. K., *Chem. Rev.*, **10,** 185 (1932).
181. LaMer, V. K., and Kamner, M. E., *J. Am. Chem. Soc.*, **57,** 2662 (1935).
182. LaMer, V. K., and Miller, M. L., *J. Am. Chem. Soc.*, **57,** 2674 (1935).
183. LaMer, V. K., *J. Franklin Inst.*, **225,** 709 (1938).
184. LaMer, V. K., and Amis, E. S., *J. Am. Chem. Soc.*, **61,** 905 (1939).
185. LaMer, V. K., and Davis, H. G., *J. Chem. Phys.*, **10,** 585 (1942).
186. Lang, R., *Z. anorg. Chem.*, **152,** 197 (1926).
187. Lang, R., and Zwerina, J., *Z. anorg. Chem.*, **170,** 389 (1928).
188. Latimer, W. M., "Oxidation Potentials," New York, Prentice-Hall, 1952.
189. Launer, H. F., *J. Am. Chem. Soc.*, **55,** 865 (1933).
190. Launer, H. F., and Yost, D. M., *J. Am. Chem. Soc.*, **56,** 2571 (1934).
191. Lewis, G. N., *J. Franklin Inst.*, **226,** 293 (1938).
192. Libby, W. F., and Hornig, H. C., *J. Phys. Chem.*, **56,** 869 (1952).
193. Liebhafsky, H. A., *J. Am. Chem. Soc.*, **53,** 896, 2074 (1931); *Z. physik Chem.*, **155A,** 289 (1931).
193a. Liebhafsky, H. A., *J. Am. Chem. Soc.*, **54,** 1792 (1932).
193b. Liebhafsky, H. A., *ibid.*, **54,** 3499 (1932).
194. Liebhafsky, H. A., *Chem. Rev.*, **17,** 89 (1933).
195. Liebhafsky, H. A., and Mohammed, A., *J. Am. Chem. Soc.*, **55,** 3977 (1933).
196. Liebhafsky, H. A., and Mohammed, A., *J. Phys. Chem.*, **38,** 857 (1934).
196a. Liebhafsky, H. A., and Mohammed, A., *J. Am. Chem. Soc.*, **56,** 1680 (1934).
196b. Liebhafsky, H. A., private communication (1952).
197. Livingston, R., and Bray, W. C., *J. Am. Chem. Soc.*, **47,** 2069–82 (1925); **48,** 405 (1926).

198. Livingston, R., *J. Am. Chem. Soc.*, **48,** 53 (1926).
199. Livingston, R., *J. Chem. Ed.*, **7,** 2887 (1930).
200. Long, F. A., and Purchase, M., *J. Am. Chem. Soc.*, **72,** 3267 (1950).
201. Long, F. A., McDevit, W. F., and Dunkle, F. B., *J. Phys. & Colloid Chem.*, **55,** 813 (1951).
202. Long, F. A., Dunkle, F. B., and McDevit, W. F., *J. Phys. & Colloid Chem.*, **55,** 829 (1951).
203. Long, F. A., and McDevit, W. F., *Chem. Rev.* **51,** 119–169 (1952).
204. Lowry, T. M., *Chem. & Ind.*, **1,** 43 (1923).
205. Lowry, T. M., and Faulkner, I. J., *J. Chem. Soc.*, **127,** 2883 (1925).
205a. Lowry, T. M., and Smith, G. F., *J. Chem. Soc.*, **1927,** 2539.
206. Lucas, H. J., and Eberz, W. F., *J. Am. Chem. Soc.*, **56,** 460 (1934).
207. DeLury, R. E., *J. Phys. Chem.*, **11,** 54 (1907).
208. Luther, R., and Schilow, N., *Z. physik Chem.*, **46,** 777 (1903).
209. Luther, R., *Z. angew. Chem.*, **19,** 2049 (1906).
210. Luther, R., and Rutter, T. F., *Z. anorg. Chem.*, **54,** 1 (1907).
211. MacKenzie, H. A. E., and Winter, E. R. S., *Trans. Faraday Soc.*, **44,** 159, 171, 243 (1948).
212. Magee, J. L., Ri, T., and Eyring, H., *J. Chem. Phys.*, **9,** 419 (1941).
212a. Makower, B., *J. Am. Chem. Soc.*, **56,** 1315 (1934).
213. Malatesta, L., *Gazz. chim. ital.*, **71,** 467 (1941).
214. Manchot, W., and Wilhelms, O., *Ann.*, **325,** 105, 125 (1902).
215. Manchot, W., and Richter, P., *Ber.*, **39,** 488 (1906).
216. Martin, A. R., *Trans. Faraday Soc.*, **33,** 191 (1937).
217. Moran, T., and Lewis, W. C. McC., *J. Chem. Soc.*, **1922,** 1613.
218. Mayer, J. E., *J. Chem. Phys.*, **18,** 1426 (1950).
219. Michaelis, L., *Chem. Rev.*, **16,** 243 (1935).
220. Michaelis, L., and Schubert, M. P., *Chem. Rev.*, **22,** 437 (1938).
221. Milas, N. A., and Terry, E. M., *J. Am. Chem. Soc.*, **47,** 1412 (1925).
222. Moelwyn-Hughes, E. A., *Z. physik Chem.*, **B26,** 281 (1934).
223. Moelwyn-Hughes, E. A., *Proc. Roy. Soc. (London)*, **A164,** 295 (1938).
224. Moelwyn-Hughes, E. A., "Kinetics of Reactions in Solution," Oxford Press, 1947.
225. Moelwyn-Hughes, E. A., *ibid.*, pp. 53–66.
226. Moelwyn-Hughes, E. A., *ibid.*, p. 71
227. Moelwyn-Hughes, E. A., *ibid.*, pp. 73-74.
228. Moelwyn-Hughes, E. A., *ibid.*, pp. 75-76.
229. Moelwyn-Hughes, E. A., *Proc. Roy. Soc. (London)*, **A196**, 540, (1949).
230. Morgan, L. B., *Trans. Faraday. Soc.*, **42,** 169 (1946).
231. Nielsen, R. F., *J. Am. Chem. Soc.*, **58,** 206 (1936).
232. Noyes, A. A., Hoard, J. L., and Pitzer, K. S., *J. Am. Chem. Soc.*, **57,** 1221 (1935).
233. Noyes, A. A., Pitzer, K. S., and Dunn, C. L., *J. Am. Chem. Soc.*, **57,** 1229 (1935).
234. Noyes, A. A., and Kossiakoff, A., *J. Am. Chem. Soc.*, **57,** 1238 (1935).
235. Noyes, A. A., Coryell, C. D., Stitt, F., and Kossiakoff, A., *J. Am. Chem. Soc.*, **59,** 1316 (1937).
236. Noyes, R. M., *Trans. N. Y. Acad. Sci.*, [2], **13,** 314 (1951).
237. Noyes, R. M., and Malcolm, J. M., *J. Am. Chem. Soc.*, **74,** 2769 (1952).
238. Olson, A. R., *J. Chem. Phys.*, **1,** 418 (1933).
239. Olson, A. R., and Tong, L. K. J., *J. Am. Chem. Soc.*, **66,** 1555 (1944).
240. Olson, A. R., and Simonson, T. R., *J. Chem. Phys.*, **17,** 1167 (1949).
241. Ostwald, W., *Physik. Z.*, **3,** 313 (1902).

242. Paul, M. A., *J. Am. Chem. Soc.*, **72,** 3813 (1950); **74,** 141 (1952).

243. Pedersen, K. J., *Trans. Faraday Soc.*, **23,** 316 (1927).

244. Pedersen, K. J., *J. Phys. Chem.*, **38,** 581 (1934).

245. Pedersen, K. J., *ibid.*, **38,** 601 (1934).

246. Pedersen, K. J., *Acta Chem. Scand.*, **2,** 252 (1948).

247. Pedersen, K. J., *ibid.*, **2,** 385 (1948).

248. Pedersen, K. J., *ibid.*, **3,** 676 (1949).

249. Pedersen, K. J., *ibid.*, **6,** 285 (1952).

249a. Pearson, R. G., and Dillon, R. L., *J. Am. Chem. Soc.* **75,** 2439 (1953).

250. Pitzer, K. S., *J. Am. Chem. Soc.*, **59,** 2365 (1937).

251. Rabinowich, E., and Stockmeyer, W. H., *J. Am. Chem. Soc.*, **64,** 335 (1942).

252. Ramsey, J. B., and Colichman, E. L., *J. Am. Chem. Soc.*, **69,** 3041 (1947).

253. Randall, M., and Failey, C. F., *Chem. Rev.*, **4,** 271, 285, 291 (1927).

254. Rice, F. O., and Kilpatrick, M., *J. Am. Chem. Soc.*, **45,** 1401 (1923).

255. Richardson, M., and Soper, F. G., *J. Chem. Soc.*, **1929,** 1873.

256. Robinson, R., *J. Chem. Soc.*, 238 (1941).

257. Saylor, J. H., Whitten, A. I., Claiborne, I., and Gross, P. M., *J. Am. Chem. Soc.*, **74,** 1778 (1952).

258. Scatchard, G., *J. Am. Chem. Soc.*, **43,** 2387 (1921).

259. Scatchard, G., *ibid.*, **52,** 52 (1930).

260. Scatchard, G., *Chem. Rev.*, **10,** 229 (1932).

261. Scatchard, G., *J. Chem. Phys.*, **7,** 657 (1939).

262. Scatchard, G., *ibid.*, **9,** 34 (1941).

263. Scatchard, G., *Natl. Bur. Standards Circular* **524,** 185–92 (1953).

264. Schubert, W. M., and Latourette, H. K., *J. Am. Chem. Soc.*, **74,** 1829 (1952).

265. Shaffer, P. A., *J. Phys. Chem.*, **40,** 1021 (1936).

266. Shedlovsky, T., *J. Am. Chem. Soc.*, **72,** 3680 (1950).

266a. Sidgwick, N. V., "*Chemical Elements and Their Compounds*," Oxford Press (1950).

266b. Sidgwick, N. V., *ibid.*, pp. 1006-07.

266c. Sidgwick, N. V., *ibid.*, p 1045.

267. Skrabal, A., *Monatsh.*, **64,** 289 (1934).

268. Smith, G. F., *J. Chem. Soc.*, **1934,** 1744.

269. Smith, G. F., and Smith, M. C., *J. Chem. Soc.*, **1937,** 1413.

270. Smith, G. F., *J. Chem. Soc.*, **1943,** 521.

271. Smith, G. F., "Cerate Oxidimetry," G. F. Smith Chem. Co., Columbus, Ohio, 1942.

272. Stokes, R. H., and Robinson, R. A., *Trans. Faraday Soc.*, **37,** 419 (1941).

273. Stokes, R. H., and Robinson, R. A., *J. Am. Chem. Soc.*, **70,** 1870 (1948).

274. Svirbely, W. J., and Lander, G., *J. Am. Chem. Soc.*, **61,** 3538 (1939).

275. Svirbely, W. J., and Petersen, S., *J. Am. Chem. Soc.*, **65,** 166 (1943).

276. Swain, C. G., *J. Am. Chem. Soc.*, **70,** 1119 (1948).

277. Swain, C. G., and Eddy, R. W., *J. Am. Chem. Soc.*, **70,** 2989 (1948).

278. Swain, C. G., *J. Am. Chem. Soc.*, **72,** 4578 (1950).

279. Swain, C. G., and Brown, J. F., *J. Am. Chem. Soc.*, **74,** 2534 (1952).

280. Swain, C. G., and Brown, J. F., *ibid.*, **74,** 2538 (1952).

281. Swift, E. H., *J. Am. Chem. Soc.*, **52,** 894 (1930).

281a. Taft, R. W., *J. Am. Chem. Soc.*, **74,** 5372 (1952).

282. Taube, H., *J. Am. Chem. Soc.*, **68,** 611 (1946).

283. Taube, H., *ibid.*, **69,** 1418 (1947).

284. Taube, H., *ibid.*, **70,** 1216 (1948).

285. Taube, H., *ibid.*, **70,** 3928 (1948).
286. Taube, H., and Cahill, A. E., *J. Am. Chem. Soc.*, **74,** 2312 (1952).
287. Taylor, H. S., *Medd. Vetenskapsakad-Nobelinst.* **2,** No. 37 (1913).
288. Titoff, A., *Z. physik. Chem.*, **45,** 641 (1903).
289. Trotman-Dickenson, A. F., *J. Chem. Soc.*, **1949,** 1293.
290. Urey, H. C., and Cohn, M., *J. Am. Chem. Soc.*, **60,** 679 (1938).
291. Uri, N., *Chem. Rev.* **50,** 375 (1952).
292. Wahl, A. C., and Prestwood, R. J., *J. Am. Chem. Soc.*, **71,** 3137 (1949).
293. Wahl, A. C., and Hudis, J., *J. Am. Chem. Soc.*, **75,** 4153 (1953).
294. Walker, J., and Hambly, F. J., *J. Chem. Soc.*, **67,** 746 (1895).
294a. Walton, J. H., *Z. physik. chem.*, **47,** 185 (1904).
295. Warner, J. C., and Stitt, F. B., *J. Am. Chem. Soc.*, **55,** 4807 (1933).
296. Warner, J. C., and Svirbely, W. J., *J. Am. Chem. Soc.*, **57,** 1883 (1935).
297. Warner, J. C., and Winstrom, L. O., *J. Am. Chem. Soc.*, **61,** 1205 (1939).
298. Warner, J. C., *Trans. N. Y. Acad. Sci.*, **39,** 345 (1940).
299. Wasserman, A., *J. Chem. Soc.*, **1935,** 828.
299a. Weil, I., and Morris, J. C., *J. Am. Chem. Soc.*, **71,** 1664 (1949).
300. Weiss, J., *J. Chem. Soc.*, **1944,** 309.
301. Weiss, J., *Experientia*, **7,** 135 (1951).
301a. Weiss, J., "*Advances in Catalysis*," Vol. IV, pp. 343–364, New York, Academic Press Inc., 1952.
302. Weissberger, A., and Hogen, J., *Z. physik. Chem.*, **A156,** 321 (1931).
303. Weissberger, A., *J. Am. Chem. Soc.*, **65,** 102 (1943).
304. Weissberger, A., and LuValle, J. E., *J. Am. Chem. Soc.*, **69,** 1567 (1947).
305. Weissberger, A., and LuValle, J. E., *ibid.*, **69,** 1821 (1947).
306. Westheimer, F. H., Jones, W. A., and Lad, R. A., *J. Chem. Phys.*, **10,** 478 (1942).
307. Westheimer, F. H., and Watanabe, W., *J. Chem. Phys.*, **17,** 61 (1949).
308. Westheimer, F. H., *Chem. Rev.*, **45,** 419 (1949).
309. Westheimer, F. H., and Steinberger, R., *J. Am. Chem. Soc.*, **73,** 429 (1951).
310. Westheimer, F. H., Schramm, R. M., and Klapproth, W., *J. Phys. & Colloid Chem.*, **55,** 843 (1951).
311. Willard, H. H., and Young, P., *J. Am. Chem. Soc.*, **50,** 1322 (1928).
312. Willard, H. H., and Young, P., *J. Am. Chem. Soc.*, **50,** 1372 (1928); **55,** 3260 (1933).
313. Willard, H. H., and Merritt, L. L., *Ind. Eng. Chem., Anal. Ed.*, **14,** 486 (1942).
313a. Wilmarth, W. K., Ph.D. thesis, University of California, Berkeley (1942).
313b. Wilmarth, W. K., and Baes, C. F., *J. Chem. Phys.*, **20,** 116 (1952).
313c. Wilmarth, W. K., and Barsh, M. K., *J. Am. Chem. Soc.*, **75,** 2237 (1953).
314. Winstein, S., and Grunwald, E., *J. Am. Chem. Soc.*, **70,** 846 (1948).
315. Winstein, S., Grunwald, E., and Jones, H. W., *J. Am. Chem. Soc.*, **73,** 2700 (1951).
316. Winstein, S., and Johnson, C. E., *J. Am. Chem. Soc.*, **74,** 755 (1952).
316a. Wyatt, P. A. H., and Kornberg, H. L., *Trans. Faraday Soc.*, **48,** 454 (1952).
317. Wynne-Jones, W. F. K., *Trans. Faraday Soc.*, **34,** 245 (1938).
318. Wynne-Jones, W. F. K., Bell, F., Gill, R., and Holden, D., *J. Phys. & Colloid Chem.*, **55,** 874 (1951).
319. Yost, D. M., *J. Am. Chem. Soc.*, **48,** 152 (1926).
320. Yost, D. M., and Claussen, W. H., *J. Am. Chem. Soc.*, **53,** 3349 (1931).
321. Yost, D. M., Dekker, A. O., and Levy, H. A., *J. Am. Chem. Soc.*, **59,** 2129 (1937).
322. Young, P., *Anal. Chem.*, **24,** 152 (1952).
323. Zelikoff, M., and Taylor, H. A., *J. Am. Chem. Soc.*, **72,** 5039 (1950).

AUTHOR INDEX

SUBJECT INDEX

Date Due

MAY - 9			
MAR [illegible]			